# STEREOSELECTIVE SYNTHESIS OF AZIRIDINOLS AND THEIR ELABORATION TOWARDS PYRROLIDINE AND PIPERIDINE CONTAINING NATURAL PRODUCTS

By

Aman Kulshrestha

A DISSERTATION

Submitted to
Michigan State University
in partial fulfillment of the requirements
for the degree of

DOCTOR OF PHILOSOPHY

Chemistry

2011

## ABSTRACT

STEREOSELECTIVE SYNTHESIS OF AZIRIDINOLS AND THEIR ELABORATION TOWARDS PYRROLIDINE AND PIPERIDINE CONTAINING NATURAL PRODUCTS

By

Aman Kulshrestha

Aziridinols can be synthesized in moderate to excellent diastereoselective fashion via the addition of organometallic reagents to aziridine-2-carboxaldehydes. The CHO moiety strongly prefers bifurcated geometries relative to the ring, with the oxygen oriented either *endo* or *exo*. The aziridine nitrogen remains strongly pyramidalized; invertomeric alternative conformations therefore must be considered. For Bn protected aziridine-2-carboxaldehydes, selectivity originates from chelation. Excellent *syn* addition selectivity is achieved for *N*-Bn *cis* aziridine-2-carboxaldehydes while *trans* substrates undergo almost completely unselective addition. For this case, as well as the *N*-Boc protected *cis* and 2,3-disubstituted systems, the low selectivity seems to be due to the substrates' conformational ambiguity, both between aldehyde *endo*/*exo* rotamer and N-invertomer structures. However, for the *N*-Boc *trans* substrates, extremely high *syn* selectivity is observed, which is unaffected by chelation modifiers. This strong stereopreference appears to be dictated by the chelation-like favorable interaction between the aldehyde carbonyl and the *syn*-Boc group's carbon. For the *N*-Ts protected series, diastereoselectivity is largely understandable in terms of the systems' conformational preferences. Though *cis* substrates do not enjoy

any kind of selectivity, their *trans* analogues afford the product with moderate to high *syn* selectivity, while exceptional stereospecificity is achieved in the case of *N*-Ts-2,3-disubstituted aziridine-2-carboxaldehyde.

The assembly of appropriately stereo-defined aziridinols has paved the way to our discovery of a one-pot tandem aza-Payne/hydroamination reaction; a process that yields highly functionalized densely substituted pyrrolidines. A number of transformations have been revealed to derive a diverse range of interesting scaffolds, which can be used as advanced intermediates toward the synthesis of natural products. The total synthesis of salinosporamide A, currently underway, is an example of the latter point.

Scope of such transformation is not limited only to the pyrrolidine rings, piperidines can also be accessed via exploiting a similar concept. Replacement of the alkyne functionality with an $\alpha,\beta$-unsaturated carbonyl tethered in a stereodefined aziridinol allows entry to six member heterocyclic rings. These modified aziridinols can be accessed via a highly stereoselective Baylis-Hillman reaction of *N*-Ts 2,3-substituted aziridine-2-carboxaldehydes.

Outcome of the tandem aza-Payne/hydroamination can also be altered via trapping the aza-Payne intermediate with $CO_2$, leading to a latent nucleophile that yields *N*-Ts enamide carbonates upon intramolecular hydroamination of the pendant alkyne. The latter can be elaborated towards the synthesis of biologically interesting 3,4-dihydroxy pyrrolidinones.

To my family and teachers.

## TABLE OF CONTENTS

LIST OF TABLES ..... x

LIST OF FIGURES ..... xiii

LIST OF SCHEMES ..... xvii

LIST OF SYMBOLS AND ABBREVIATIONS ..... xxxiv

Chapter 1 Aziridine: Ring strain and its exploitation in organic synthesis.
- 1.1 General introduction to aziridines ..... 1
- 1.2 Properties of aziridines ..... 3
- 1.3 Activated *vs* unactivated aziridines ..... 5
- 1.4 Ring opening reactions and their applications. ..... 7
  - 1.4.1 Ring opening of aziridines and their application in the synthesis of amino acid derivatives. ..... 9
  - 1.4.2 Ring expansion of aziridines into synthetically useful compounds. ..... 11
  - 1.4.3 Application of ring opening of aziridine in natural product synthesis. ..... 15
- 1.5 An overview of methods available for the synthesis of aziridines. ..... 16
  - 1.5.1 From epoxides. ..... 17
  - 1.5.2 Additions to alkenes via nitrenes. ..... 18
  - 1.5.3 Additions to imine. ..... 23
  - 1.5.4 Other miscellaneous methods. ..... 26
- 1.6 References. ..... 29

Chapter 2 Stereochemical Induction Controlled By Aziridine Ring.
- 2.1. Introduction. ..... 32
- 2.2. Addition of organometallic reagents to epoxy-2-carboxaldehydes. ..... 33
- 2.3 Conformational preference of cyclopropyl-2-carboxaldehydes and ketones and its effect on the resulting selectivity achieved during nucleophilic additions. ..... 38
- 2.4 Precedence on nucleophilic additions to aziridine carbonyl compounds. ..... 39
- 2.5 Selectivity in Additions of Organometallic Reagents to Aziridine-2-Carboxaldehydes: Effects of Protecting Groups and Substitution Patterns. ..... 41
  - 2.5.1 Results and discussion of computational studies. ..... 42

2.5.2 Results and discussion of experimental studies. ..... 53
2.5.2.1 *N*-Bn protected aziridine-2-carboxaldehydes. ..... 53
2.5.2.2 *N*-Boc protected aziridine-2-carboxaldehydes ..... 61
2.5.2.3 *N*-Ts protected aziridine-2-carboxaldehydes. ..... 70
2.6 Conclusions. ..... 80
2.7 Experimental procedures. ..... 83
2.8 References. ..... 136

Chapter 3 Elaboration Of The Tetrasubstituted Pyrrolidine Moieties, Obtained Via Tandem Aza-Payne/Hydroamination Methodology.
3.1. Introduction to hydroamination chemistry ..... 142
3.2. Introduction to aza-Payne rearrangement ..... 146
3.3. From one carbon homologative relay ring expansion of 2,3-aziridin-1-ols to tandem aza-Payne/hydroamination ..... 148
3.3.1 Significance of *syn* v *anti* isomer on hydroamination reactions ..... 153
3.4. Synthetic potential of the *N*-Ts enamide nucleus and its elaboration ..... 156
3.4.1 Challenges and preliminary attempts on the ring opening reactions of the epoxide present in *N*-Ts enamide ..... 157
3.4.2 Elaboration of enamine functionality in *N*-Ts enamide ... 165
3.4.2.1 Stereoselective access to *E* and *Z* vinyl bromide intermediates ..... 165
3.4.2.2 Functionalization of vinylbromide compounds via Suzuki cross coupling reactions ..... 170
3.4.2.3 Functionalization of vinylbromide compounds via carbonylation reactions ..... 172
3.4.3 Elaboration to lactam and its functionalization ..... 174
3.4.3.1 Attempts at epoxide opening reactions at lactam stage ..... 175
3.4.3.1.1 Intramolecular epoxide ring opening in lactam: Future Direction ..... 181
3.5 Attempts toward screening alternative protecting groups on nitrogen ..... 182
3.6 Attempts toward detosylation of the pyrrolidine. ..... 195
3.7 Experimental procedures. ..... 197
3.8 References ..... 221

Chapter 4 Progress towards the total synthesis of salinosporamide A via tandem aza-Payne/hydroamination methodology.
4.1 Introduction ..... 225
4.2 The Proteasome: Target in Cancer Chemotherapy ..... 227
4.3 Anti cancer activity of salinosporamide A *vs* other lactam based proteasome inhibitors ..... 230

4.4 A glance through previous syntheses. ..... 232
4.4.1 Total synthesis of salinosporamide A by Corey and coworkers. ..... 232
4.4.2 Synthesis by Endo and Danishefsky..... 235
4.4.3 Pattenden's synthesis. ..... 237
4.4.4 Biomimetic synthesis by Romo and coworkers. ..... 238
4.4.5 Total synthesis toward salinosporamide A by Nereus pharmaceuticals. ..... 241
4.4.6 Indium catalyzed Conia-ene approach towards the synthesis of salinosporamide A. ..... 242
4.4.7 Synthesis by Omura and coworkers. ..... 243
4.4.8 Discussion of other syntheses reported in the literature. ..... 246
4.5 Retrosynthetic analysis using tandem aza-Payne/hydroamination methodology..... 249
4.6 Racemic route toward the synthesis of salinosporamide. ..... 251
4.6.1 Diasteroselective synthesis of trisubstituted aziridinol **4.93** and construction of *N*-Ts enamide intermediate **4.92**. ... 251
4.6.2 Ring opening of the epoxide and elaboration to a-bromo hydroxylactam intermediate **4.107**. ..... 253
4.6.3 Attempts at C-3 alkylation of a-bromo hydroxylactam.. .. 256
4.6.3.1 Rationale for the selectivity achieved under non-Lewis acid radical conditions. ..... 265
4.6.3.2 Rationale for the selectivity observed under Lewis acid radical conditions ..... 266
4.6.4 Epimerization: Thermodynamic equilibrium towards the desired C-3 epimer ..... 268
4.6.5 Successful attempt at detosylation.... ..... 269
4.6.6 Attempts at C-5 alkylation and b-lactonization ..... 272
4.6.6.1 Attempts at O-carbonylation ..... 273
4.6.7 Re-visiting previous C-5 alkylation strategies; challenges associated, solution and future endeavors.. ..... 299
4.6.7.1 C-5 alkylation on masked C-2 carbonyl intermediates. ..... 302
4.6.7.2 Scope of C-5 alkylation at earlier stages during synthesis..... 306
4.6.7.3 Scope of C-5 alkylation via palladium chemistry 307
4.6.7.4 Scope of C-5 alkylation via radical chemistry..... 308
4.6.7.5 Scope of C-5 alkylation via Steven's rearrangement. ..... 310
4.6.8 Conclusion ..... 311
4.8 Experimental procedures ..... 313
4.9 References ..... 344

Chapter 5 One-pot Baylis-Hillman/aza-Payne/Conjugate addition reaction: Novel entry to iminosugars.
5.1 Introduction to iminosugars and their biological significance.....351
5.2 Previous approaches for the syntheses of piperidine based iminosugars..... 353
5.3 Pyrrolidines to piperidines; via extension of tandem aza-Payne/hydroaminaiton methodology..... 358
5.3.1 Synthesis of aziridinols substituted with activated olefins..... 360
5.3.1.1 Precedence of Baylis-Hillman (B-H) reactions with aziridine -2-carboxaldehydes..... 361
5.3.1.2 Unprecedented diastereoselective Baylis-Hillman reactions with *N*-Ts protected aziridine-2-carboxaldehydes..... 367
5.3.1.2.1 Effects of ring substitution and *N*-protecting group on *syn*/*anti* ratios of adducts in the Baylis-Hillman reactions. ..... 371
5.3.2 Cyclization of diastereomerically pure Baylis-Hillman products..... 379
5.3.3 Efforts toward a one-pot Baylis-Hillman/aza-Payne/conjugate addition protocol..... 384
5.3.4 Challenges toward elaboration of dehydropiperidines toward iminosugars and future directions..... 385
5.3.4.1 Attempts at epoxidation of $\alpha,\beta$-unsaturated olefin present in dehydropiperidine..... 386
5.3.4.2 Epoxide formation via activation of $\alpha,\beta$-unsaturated ester..... 388
5.3.4.3 Attempts at detosylation. ..... 390
5.3.4.4 Future directions toward elaboration of piperidine compounds toward 7-member nitrogen containing rings..... 391
5.4 Experimental procedures..... 393
5.5 References..... 418

Chapter 6 Polyhydroxylated alkaloids via modification of the tandem aza-Payne/hydroamination reaction
6.1 Polyhydroxylated alkaloids and their biological significance.... 422
6.2 General approaches to install polyhydroxylated pyrrolidines... 424
6.3 Modification of the tandem aza-Payne/hydroamination reaction towards functionalized pyrrolidines. ..... 426
6.4 Evidence of Intermediates and mechanistic studies..... 433
6.5 Elaboration of *N*-Ts enamide carbonates toward Iminosugars 443

6.6 Prospect of other latent nucleophiles in modified tandem aza-Payne chemistry..... 444
6.7 Experimental procedures. ..... 447
6.8 References ..... 455

## LIST OF TABLES

Table 1.1 Effect of N-protective groups on the barrier to inversion .... 4

Table 1.2 Stereoselectivity achieved in nucleophilic ring opening of aziridine-2-carboxylates ..... 9

Table 2.1 Addition of organometallic reagents to epoxy-2-carboxaldehydes ..... 34

Table 2.2 *Anti*-selective addition of lithium enolates to epoxy-2-carboxaldehydes ..... 36

Table 2.3 Lewis acid mediated addition of allyltributyl tin to epoxy-2-carboxaldehydes ..... 37

Table 2.4 Computationally calculated energy for truncated model systems ..... 43

Table 2.5 B3LYP/6-31G*/SM8 $CH_2Cl_2$ vs. G3(MP2)/SM8 $CH_2Cl_2$ relative energies compared ..... 47

Table 2.6 Addition of organometallic reagents to Bn protected *cis*-2-aziridine carboxaldehydes ..... 54

Table 2.7 Addition of organometallic reagents to Bn protected *trans*-2-aziridine carboxaldehydes ..... 58

Table 2.8 Addition of organometallic reagents to Boc protected *trans*-2-aziridine carboxaldehydes ..... 62

Table 2.9 Addition of organometallic reagents to Boc protected *cis*-2-aziridine carboxaldehyde ..... 65

Table 2.10 Addition of organometallic reagents to Boc protected 2,3-disubstituted-2-aziridine carboxaldehydes ..... 68

Table 2.11 Addition of organometallic reagents to Ts protected *cis*-2-aziridine carboxaldehydes ..... 71

Table 2.12 Addition of organometallic reagents to Ts protected *trans*-2-aziridine carboxaldehydes ..... 72

Table 2.13 Addition of organometallic reagents to Ts protected 2,3-disubstituted-2-aziridine carboxaldehyde ..... 74

Table 2.14 Summarized results of selectivity (*syn/anti*) observed in addition of organometallic reagents to aziridine carboxaldehydes ..... 81

Table 3.1 Effect of substituents present on nitrogen and oxygen on the aza-Payne rearrangement equilibrium ..... 146

Table 3.2 Diastereoselective 2,3-disubstituted pyrrolidines obtained via tandem aza-Payne/hydroamination ..... 151

Table 3.3 Substrate scope of tandem aza-Payne/hydroamination chemistry..... 154

Table 3.4 Site-selective reduction of vinyl epoxides..... 162

Table 3.5 Desilylation of TBS ether of aziridine alcohol ..... 185

Table 3.6 Effective Lewis acids for the rearrangement of 2,3-aziridinols ..... 189

Table 3.7 Nosylation of aziridine alcohol 6.8..... 191

Table 3.8 Attempts at detosylation of N-Ts enamide substrate..... 195

Table 3.9 Attempts at detosylation of lactam 6.8 ..... 196

Table 4.1 Lactam-based inhibitors and their bioactivity ..... 231

Table 4.2 Radical mediated alkylation under various conditions.... 264

Table 4.3 Mono and bis-protection achieved under different conditions..... 278

Table 4.4 Different de-silylating conditions tried on TBS ether ..... 280

Table 4.5 Various oxidation methods to obtain aldehyde intermediate ..... 296

Table 4.6 Attempts at imidate synthesis ..... 303

Table 5.1 Substrate scope of *N*-Tr protected aziridine-2-carboxaldehydes in Baylis-Hillman reactions ..... 363

Table 5.2 Aza-Michael/Aldol reactions of aziridine-2-carboxaldehyde dimmers ..... 365

Table 5.3 Scope of 2,3-disubstituted aziridine-2-carboxaldehydes utilized in Baylis-Hillman reactions ..... 369

Table 5.4 Scope of different activated olefins used in the Baylis-Hillman reaction ..... 371

Table 5.5 Baylis-Hillman reaction using *trans* substituted aziridine-2-carboaxaldehydes ..... 374

Table 5.6 Efforts at epoxidation ..... 387

Table 6.1 Optimization of reaction towards the synthesis of *N*-Ts enamide carbonate compound **6.19** ..... 431

## LIST OF FIGURES

Figure 1.1 Natural products containing aziridine functionalities ..... 1

Figure 1.2 Activation of the nitrogen via oxygenated N-protective group under Lewis acidic conditions ..... 8

Figure 2.1 a. Felkin-Ahn control. b. Chelation control addition to epoxy-2-carboxaldehydes ..... 35

Figure 2.2 **a.** Walsh model. **b.** Conformational preferences of a cyclopropyl ring adjacent to p-system. **c.** Conformation allowing maximum overlap between p-system and cyclopropyl orbitals 38

Figure 2.3 Preferred bisected conformations of cyclopropyl-2-carboxaldehyde ..... 39

Figure 2.4 a Felkin-Ahn model. b Chelation control model ..... 40

Figure 2.5 (a) Bisected *exo* (*s-trans*) and *endo* (*s-cis*) conformations of cyclopropyl carbonyl systems. (b) B3LYP/6-31+G* optimized TS structures ..... 45

Figure 2.6 B3LYP/6-31+G* optimized TS structures (relative energies) for chelation-controlled attack on the *AN* conformer of the model compound **Me_*H3*** ..... 51

Figure 2.7 a) Proposed *syn* selective attack on *N*-benzyl-*cis*-3-ethylaziridine-2-carboxaldehyde **2.7** under chelation control. b) RHF/3-21G optimized structure of **2.7** chelating $Zn(CH_3)_2$ ..... 55

Figure 2.8 a) Energy-minimized conformers of Bn protected *trans* substrate **2.9**. Among these forms, both *pro-syn* and *pro-anti* faces are equally available ..... 59

Figure 2.9 Dipole interactions between the Bn-N and CHO moieties in **2.9**, proposed to explain the relative order of stabilities of the conformers ..... 60

Figure 2.10 Comparison of the crystal structure of **2.11** (a) with its energy minimized model (b) illustrates excellent similarity ..... 63

Figure 2.11 a) Chelated *AN* conformation of the Boc protected *cis*-aziridine would favor *syn* selective addition (pictured with

MeMgCl). b) The *exo* isomer (*AX*) is not capable of chelations and would favor the *pro-anti* approach of the nucleophile ..... 66

Figure 2.12 Low energy conformers of **2.15** showing near isoenergetic (a) *SX* (0.23 kcal/mol) and (b) *SN* (0 kcal/mol) -CHO rotamers ..... 69

Figure 2.13 The lower energy *SX* conformation of **2.21** is *syn* selective due to steric blocking afforded by the Ts protecting group. The *AX* conformer exhibits less steric bias and thus would reduce the overall stereoselectivity. The modest selectivity in Ts protected *trans*-aziridine-2-carboxaldehyde could arise from the energetically close lying *SX* and *AX* conformers 73

Figure 2.14 Comparison of the molecular structure of **2.25** as determined by X-ray diffraction with the lowest energy B3LYP/6-31G* optimized aziridine conformer of **2.25**. The **Ts_*23Di*** model structure shows an analogous *SX*-type lowest conformation .... 75

Figure 2.15 a) N-Invertomers of Ts protected 2,3-disubstituted-2-aziridine carboxaldehyde. b) N-Invertomers of Ts protected *trans* aziridine aldehyde ..... 76

Figure 2.16 Aldehydic resonance of **2.25** at a) -12 ºC and b) -76 ºC. Aldehydic resonance of **2.21** at c) -12 ºC, expansion shown in the inset, and d) -76 ºC. e) Simulated of **2.21** at -12 ºC, expansion shown in the inset. f) Simulated spectrum of **2.21** at -76 ºC ..... 78

Figure 3.1 Thermodynamics of aza-Payne chemistry of unprotected aziridinol ..... 147

Figure 3.2 Thermodynamics of aza-Payne chemistry of activated aziridines ..... 148

Figure 3.3 Natural products with highly functionalized pyrrolidine nuclei in skeletal frameworks ..... 155

Figure 3.4 Potential functionalization feasible at C-3 and C-4 under various conditions ..... 157

Figure 3.5 X-ray structure of *Z*-bromo olefin **3.21** ..... 166

Figure 3.6 Sterically less demanding conformations lead to the formation of *E*-bromo olefin **3.23** ..... 167

Figure 3.7 Challenging oxidative addition step in case of sterically demanding *Z*-olefin ..... 172

Figure 3.8 X-ray structure of bromolactam **3.37** ..... 180

Figure 3.9 Hypothesized transition state involved in the semi-pinacol rearrangement of TBS ether of aziridinols ..... 188

Figure 3.10 Possible products of the tandem aza-Payne/hydroamination reaction of N-*Ns* aziridinol ..... 193

Figure 4.1 Salinosporamide A and structurally related proteasome inhibitors ..... 225

Figure 4.2 Novel natural products isolated from marine actinomycetes of the genus *Salinispora*: cyanosporamide A **4.5**, saliniketal **4.6** and sporolide A **4.7** ..... 226

Figure 4.3 Homologues of salinosporamide and lactacystin ..... 227

Figure 4.4 X-Ray structure of $\alpha$-bromo hydroxylactam intermediate **4.107** ..... 254

Figure 4.5 Origin of regio- and stereoselectivity established during epoxide ring opening reaction ..... 255

Figure 4.6 Intramolecular transfer of R would establish the desired stereochemistry at C-3 position ..... 258

Figure 4.7 Radical intermediates for TBS and Bn ether substrates 266

Figure 4.8 Stereochemical explanation of favored attack at $\beta$-face under Lewis acid conditions ..... 267

Figure 4.9 X-ray structure of detosylated lactam **4.113** ..... 271

Figure 4.10 Severe steric clash between groups substituted at C-3 and C-4 leads to epimerization in bis-protected **4.115** only ..... 276

Figure 4.11 Structural features responsible for the undesired elimination pathways ..... 282

Figure 4.12 X-ray structure of lactone **4.132**..... 294

Figure 4.13 Structural analysis of precursors to perform the C-5 alkylation..... 302

Figure 5.1 Iminosugars compounds..... 351

Figure 5.2 Naturally occurring iminosugars..... 352

Figure 5.3 X-ray structure of *syn* Baylis-Hillman adduct **5.30** ..... 368

Figure 5.4 X-ray structure of dehydropiperidine **5.63**..... 382

Figure 5.5 X-ray structure of dehydropiperidine **5.64**..... 383

## LIST OF SCHEMES

Scheme 1.1 Various 1,2-difunctional compounds can be derived via ring opening of the aziridine ring ..... 2

Scheme 1.2 **a**. Activated aziridine where nitrogen is stabilized in the transition state **b.** non-activated aziridine ..... 5

Scheme 1.3 Resonance between amide and amidate like isomers ... 6

Scheme 1.4 Regioselectivity obtained in ring opening of aziridine under nucleophilic conditions ..... 8

Scheme 1.5 Excellent regio and stereospecificity obtained with 3-phenylaziridine-2-carboxylic ester ..... 10

Scheme 1.6 Synthesis of amino acids via reductive ring opening of aziridines ..... 11

Scheme 1.7 Ring expansion of activated aziridine-2-carboxylic esters yield imidazolines that can be hydrolyzed to a,b-diaminocarboxylic acid derivatives ..... 11

Scheme 1.8 a) Ring expansion via Heine reaction. b) Ring expansion with *N*-acyl aziridine-2-carboxylate occurs with net retention of the stereochemistry ..... 12

Scheme 1.9 Aza-[2,3]-Wittig reaction of vinyl aziridine yields tetrahydropyridine ..... 13

Scheme 1.10 Distinct transition states explain different stereochemical results obtained for **a**) *trans* and **b**) *cis* di-substituted vinyl aziridines ..... 14

Scheme 1.11 Aza-[3,3]-Claisen rearrangement of *N*-acyl vinyl aziridines yield 7-member lactams ..... 15

Scheme 1.12 Ring opening of chiral aziridines applied in the total syntheses ..... 15

Scheme 1.13 Application of ring opening of tricyclic aziridines in total synthesis ..... 16

Scheme 1.14 Synthesis of aziridines from epoxides ..... 17

Scheme 1.15 Enantioselective synthesis of aziridines via Jacobsen's modified HKR ..... 18

Scheme 1.16 Decomposition of alkoxycarbonylazides leads to the generation of nitrenes ..... 19

Scheme 1.17 Reagents upon oxidation with $Pd(OAc)_4$ generate aziridinating species ..... 20

Scheme 1.18 Reaction with nitrene-generated *in-situ* from hydrazine derivatives provide high stereoselective aziridination ..... 20

Scheme 1.19 $Q^1$-NHOAc is an active aziridinating species ..... 21

Scheme 1.20 Mechanism of aziridination with $Q^1$-NHOAc ..... 21

Scheme 1.21 Mechanism of (diimine)-copper catalyzed aziridination ..... 22

Scheme 1.22 Aziridination via rhodium-based catalyst ..... 23

Scheme 1.23 Addition of chiral carbenes to iminium ..... 23

Scheme 1.24 Diastereo and enantioselective synthesis of *cis*-aziridines ..... 24

Scheme 1.25 Universal asymmetric aziridination catalyzed by chiral polyborate based Bronsted acid..... 25

Scheme 1.26 Stereoselective synthesis of aziridines via iodonium ylide..... 26

Scheme 2.1 Ts protected aziridine aldehydes serve as precursors for tandem Aza-Payne/hydroamination methodology..... 32

Scheme 3.1 Hydroamination process..... 142

Scheme 3.2 a. Hydroamination of olefins catalyzed by lanthanide–amides via intramolecular insertions of alkenes into an M–amide bond. b) Catalyzed by group IV complexes via [2 + 2] cycloaddition..... 144

Scheme 3.3 Base catalyzed hydroamination of alkenes..... 145

Scheme 3.4 Thermodynamic equilibrium of aza-Payne under Lewis acidic conditions..... 147

Scheme 3.5 Ylide mediated one carbon homologative ring expansion of 2,3-aziridin-1-ols to 2,3-disubstituted pyrrolidines..... 149

Scheme 3.6 Use of ylide as a latent electrophile limits the scope of functionalization at C-5..... 149

Scheme 3.7 Use of an electron sink would allow room to achieve further functionalization at C-5..... 150

Scheme 3.8 Tandem aza-Payne/hydroamination of *syn* aziridinols yield highly functionalized pyrrolidines..... 152

Scheme 3.9 Fate of *syn* vs *anti* isomer in tandem aza-Payne/hydroamination reactions..... 153

Scheme 3.10 Synthesis of tetrasubstituted pyrrolidine ..... 156

Scheme 3.11 Grignard addition to the *N*-Ts enamide epoxide..... 158

Scheme 3.12 Excess of Grignard reagent leads to undesired product ..... 158

Scheme 3.13 Proposed elimination and isomerization generates undesired pyrrole compound..... 159

Scheme 3.14 Addition of organo-copper leads to isomerized product ..... 160

Scheme 3.15 Attempt to protect the in-situ generated tertiary alcohol also leads to undesired aromatic compound..... 160

Scheme 3.16 Addition of organo-copper to *N*-Ts enamide containing di-substituted epoxide also lead to isomerization..... 161

Scheme 3.17 Palladium mediated ring opening of vinyl epoxide. a) Takemura's protocol. b) Modified conditions..... 163

Scheme 3.18 Palladium mediated vinyl epoxide opening reaction yields an unexpected ring opened product..... 163

Scheme 3.19 Mechanistic hypothesis for the unexpected product observed during Pd mediated reductive ring opening reaction 164

Scheme 3.20 Two step-protocol to obtain *Z*-bromoolefin **3.21**..... 165

Scheme 3.21 Synthesis of (*E*)-vinyl bromide **3.23** and its mechanistic rationalization..... 167

Scheme 3.22 Tandem aza-Payne/hydroamination yields *Z*-isomer selectively ..... 168

Scheme 3.23 Mechanistic explanation for the generation of *Z*-bromo olefin ..... 169

Scheme 3.24 Failed attempt at dibromination..... 170

Scheme 3.25 *E*-vinylbromide successfully participates in Suzuki reaction ..... 170

Scheme 3.26 *Z*-vinylbromide shows poor reactivity in coupling reaction ..... 171

Scheme 3.27 Attempt at the carbonylation via lithium-halogen exchange leads to β-elimination..... 173

Scheme 3.28 Palladium mediated carbonylation of vinyl bromide . 173

Scheme 3.29 Oxidation of enamine to lactam **3.30** ..... 174

Scheme 3.30 Epoxide ring opening at lactam stage..... 175

Scheme 3.31 Addition of lithtiumcuprate to lactam ..... 176

Scheme 3.32 Attempt at epoxide opening via addition of cyanocuprate under Lewis acidic conditions ..... 177

Scheme 3.33 Failed attempts at epoxide ring opening via non-carbon based nucleophiles ..... 178

Scheme 3.34 Reported opening of oxiranes by Bonini and coworkers..... 178

Scheme 3.35 Regio and stereocontrolled opening of the epoxide. 179

Scheme 3.36 Epoxide ring opening using amberlyst 15 as an additive..... 180

Scheme 3.37 Proposed activation of the epoxide and intramolecular opening ..... 181

Scheme 3.38 De-nosylation occurs in the presence of strong nucleophiles ..... 183

Scheme 3.39 Synthesis of *N*-Ns protected aziridinol ..... 184

Scheme 3.40 Semi-pinacol rearragement utilized by Cha and coworkers during the synthesis of asteltoxin..... 186

Scheme 3.41 Lewis acid promoted rearrangement of 2,3-aziridino alcohols..... 187

Scheme 3.42 Mechanistic insight to the semi-Pinacol rearrangement..... 188

Scheme 3.43 Synthesis of *N*-Ns protected aziridine alcohol..... 190

Scheme 3.44 Reported selective *N*-tosylation ..... 191

Scheme 3.45 Tandem aza-Payne/hydroamination reaction of *N*-Ns protected substrate ..... 192

Scheme 3.46 Synthesis of trichloroethylsulfate reagent ..... 192

Scheme 3.47 Failed attempt at the synthesis of N-*Tces* protected aziridinol..... 193

Scheme 3.48 Successful protection of aziridinol..... 194

Scheme 3.49 Subjection of aziridinol **3.46** to basic conditions..... 194

Scheme 4.1 Mechanism of protein degradation by ubiquitin-proteasome system..... 229

Scheme 4.2 Proposed mechanism of action in proteolytic sites .... 231

Scheme 4.3 Total synthesis of salinosporamide by Corey et al..... 234

Scheme 4.4 Kulinchovik reaction: An alternative route to install γ-lactam ..... 235

Scheme 4.5 Synthesis by Endo and Danishefsky..... 236

Scheme 4.6 Pattenden's biosynthetically inspired synthesis of *rac*-salinosporamide A..... 237

Scheme 4.7 $A^{1,3}$-strain in β-keto tertiary amide leads to optically defined bis-cyclized product..... 239

Scheme 4.8 Enantioselective synthesis of salinosporamide A by Romo et al..... 240

Scheme 4.9 Synthetic route reported by Nereus Pharmaceuticals 242

Scheme 4.10 Total synthesis of salinosporamide A by Hatakeyama and coworkers..... 243

Scheme 4.11 Total synthesis by Omura and coworkers..... 245

Scheme 4.12 Formal synthesis by Chida and coworkers ..... 246

Scheme 4.13 Formal synthesis by Langlois et al ..... 246

Scheme 4.14 Formal synthesis reported by Tepe and coworkers . 247

Scheme 4.15 Formal synthesis reported by Lam et al ..... 248

Scheme 4.16 Formal synthesis by Bode et al ..... 249

Scheme 4.17 Disconnective approach for the synthesis of salinosporamide A ..... 249

Scheme 4.18 Proposed route for the synthesis of chiral trisubstituted aziridinol ..... 250

Scheme 4.19 Schematic route for the construction of *N*-Ts enamide **4.105** ..... 252

Scheme 4.20 Elaboration of *N*-Ts enamide to 3-bromo hydroxylactam **4.107** ..... 254

Scheme 4.21 Competing dehydration upon treatment with freshly generated $MgBr_2 \cdot OEt_2$ ..... 256

Scheme 4.22 Alternative procedure to perform ring opening of the epoxide ..... 256

Scheme 4.23 Attempt at enolate mediated intermolecular alkylation reaction ..... 257

Scheme 4.24 An attempt at O-silylation of the tertiary alcohol ..... 259

Scheme 4.25 Proposed plan to execute allyl transfer intramolecularly ..... 259

Scheme 4.26 Attempts at O-allylation..... 260

Scheme 4.27 Palladium mediated conversion of allyloxycarbonyls to allylether..... 260

Scheme 4.28 Palladium mediated decarboxlyation and generation of allyl ether from allyloxycarbonyl compounds..... 261

Scheme 4.29 Various attempts at O-protection ..... 262

Scheme 4.30 Radical mediated C-3 alkylation of bromo hydroxylactam **4.107** ..... 263

Scheme 4.31 Allylation under non-Lewis acid conditions ..... 265

Scheme 4.32 Allylation achieved under Lewis acid type conditions..... 266

Scheme 4.33 Hypothesized mnemonic to predict stereochemical outcome at C-3 position in radical mediated alkylation reactions ..... 268

Scheme 4.34 Thermodynamic equilibrium towards the desired C-3 epimer..... 268

Scheme 4.35 Epimerization of the C-3 center ..... 269

Scheme 4.36 Detosylation under sodium-naphthlenide conditions 270

Scheme 4.37 Mg-MeOH mediated detosylation reaction..... 271

Scheme 4.38 Strategy to install β-lactone via O-carbonylation ..... 272

Scheme 4.39 C-5 alkylation and b-lactonization required to proceed to the advanced precursor to salinosporamide A ..... 273

Scheme 4.40 An attempt at O-carbonate formation via treatment with phosgene ..... 273

Scheme 4.41 An attempt at carbonate formation at C-4 hydroxyl group ..... 274

Scheme 4.42 Carbonate and carbamate formation ..... 275

Scheme 4.43 Acylation leads to both mono and bis protected compounds ..... 276

Scheme 4.44 Li$O^{t}$Bu mediated acylation ..... 277

Scheme 4.45 Successful protection of both N and O..... 279

Scheme 4.46 Failed silyl deprotection of the TBS ether ..... 279

Scheme 4.47 Mechanistic hypothesis for the elimination reaction observed during de-silylation conditions ..... 281

Scheme 4.48 TBAF mediated desilylation of TBS ether ..... 282

Scheme 4.49 Failed N-carbamate formation under mild conditions..... 283

Scheme 4.50 *N*-Boc migration observed in lactam ..... 283

Scheme 4.51 *N*-Boc protection and desilylation ..... 284

Scheme 4.52 Failed de-silylation with TBAF..... 285

Scheme 4.53 HF-pyridine assisted de-silylation of TBS ether ..... 285

Scheme 4.54 DMP oxidation to yield aldehyde..... 286

Scheme 4.55 Enolate mediated C-5 alkylation and β-lactonization attempt..... 286

Scheme 4.56 Aldehyde exhibited instability under basic conditions..... 287

Scheme 4.57 Cyclization attempted via enamine-catalysis ..... 287

Scheme 4.58 Attempts to form enamine..... 288

Scheme 4.59 Cyclization attempted via enol ether-catalysis ..... 288

Scheme 4.60 Synthesis of the ester intermediate..... 289

Scheme 4.61 C-5 alkylation suffered by β-elimination pathway..... 290

Scheme 4.62 β-elimination predominates during C-5 alkylation conditions..... 291

Scheme 4.63 Failed synthesis of lactol with exposed C-5 primary alcohol..... 292

Scheme 4.64 Ozonolysis of the TBS ether compound..... 292

Scheme 4.65 Formation of lactone and TBS removal to reveal alcohol..... 293

Scheme 4.66 Failed oxidation of alcohol by DMP ..... 294

Scheme 4.67 An attempt at ruthenium mediated oxidation of alcohol ..... 296

Scheme 4.68 Jones oxidation yields carboxylic acid ..... 297

Scheme 4.69 Esterification of the lactam acid ..... 298

Scheme 4.70 Synthesis of N-methoxycarbonyl imdizaole ..... 298

Scheme 4.71 Failed attempt at C-5 alkylation ..... 298

Scheme 4.72 C-5 alkylation with reactive electrophile gave mixture of undesired products ..... 299

Scheme 4.73 β-elimination foils attempt at one-pot C-5 alkylation and β-lactonization under various conditions ..... 300

Scheme 4.74 Proposed pathways for elimination ..... 301

Scheme 4.75 Synthesis of O-methyl imidate ..... 304

Scheme 4.76 Planned precursor for future C-5 alkylation studies . 305

Scheme 4.77 Disconnective approach proposed with C-2 masked carbonyl intermediates ..... 305

Scheme 4.78 Schematic outline for early stage C-5 functionalization ..... 306

Scheme 4.79 Tandem aza-Payne/hydroamination on precursor with pre-installed C-5 quaternary center ..... 307

Scheme 4.80 Pd catalyzed $\alpha$-vinylation of ketones. **a.** Literature precedence **b.** proposed plan ..... 308

Scheme 4.81 Endocyclic $\alpha$-aminonitriles resulting from DCA-photosensitization of alkylpiperideines ..... 309

Scheme 4.82 Proposition of $\alpha$-cyanation to pyrrolidine using photoinduced electron transfer ..... 309

Scheme 4.83 Intramolecular cyclization of iminium generated via SET by oxygen nucleophile ..... 310

Scheme 4.84 $\alpha$-allylation to nitrogen via Steven's rearrangement. 311

Scheme 4.85 Elaboration to aldehyde precursor and remaining challenges towards salinosporamide ..... 312

Scheme 5.1 Synthesis of azido lactone, a common precursor employed in iminosugar syntheses ..... 353

Scheme 5.2 Proposed route to synthesize FNJ derivatives ..... 354

Scheme 5.3 Route for the synthesis of iminosugars from glucopyranose ..... 356

Scheme 5.4 Retrosynthetic disconnections to access iminosugars starting from non-carbohydrate type starting material ..... 357

Scheme 5.5 Route to iminosugars using 2-aminofuran derivatives 357

Scheme 5.6 Alkynes serve as latent electrophiles in tandem aza-Payne/hydroamination ..... 359

Scheme 5.7 Proposed plan for the synthesis of piperidine rings ... 360

Scheme 5.8 Epoxy-2-carboxaldehydes as electrophiles in Baylis-Hillman reactions..... 362

Scheme 5.9 Monomer-dimer equilibrium for amphoteric amino-aldehydes..... 364

Scheme 5.10 Mechanistic explanation for domino aza-Michael/Aldol reactions ..... 366

5.11 Highly diastereoselective Baylis-Hillman reactions of aziridine-2-carboxaldehyde..... 367

Scheme 5.12 Synthesis of 2,3-disubstituted aziridine-2-carboxaldehyde..... 370

Scheme 5.13 Synthesis of *N*-Ts protected *trans* aziridine-2-carboxaldehyde **5.41**..... 372

Scheme 5.14 Synthesis of aziridine-2-carboxaldehyde **5.42** ..... 373

Scheme 5.15 Failed attempt to detosylate *N*-Ts protected aziridinol..... 375

Scheme 5.16 Successful synthesis of desoylated azirdine alcohol 376

Scheme 5.17 Synthesis of *N*-Boc protected aziridine-2-carboxaldehyde..... 377

Scheme 5.18 Alternate route to synthesize *N*-Boc protected aziridine-2-carboxaldehyde..... 378

Scheme 5.19 **a**) Unreactive *N*-Boc proctected substrate **b**) *N*-Tr protected azirdine-2-carboxaldehyde yields Baylis-Hillman product successfully..... 378

Scheme 5.20 Failed cyclization under tandem aza-Payne/hydroamination ..... 379

Scheme 5.21 Baylis-Hillman adduct degrades under the aza-Payne rearrangement conditions ..... 380

Scheme 5.22 Successful cyclization of Baylis-Hillman adduct with catalytic base ..... 380

Scheme 5.23 Postulated mechanism for the tandem aza-Payne/aza-Michael addition reaction ..... 381

Scheme 5.24 Successful participation of nitrile compound in tandem aza-Payne/conjugate addition reaction ..... 383

Scheme 5.25 Synthesis of dehydropiperidines via Baylis-Hillman/aza-Payne/conjugate addition reactions in one pot..... 384

Scheme 5.26 Planned elaboration of dehydropiperidines toward iminosugars and other piperidine containing natural products 386

Scheme 5.27 Attempt at oxa-Michael addition and formation of epoxide ..... 389

Scheme 5.28 Attempt at Lewis acid mediated oxa-Michael addition and epoxide formation..... 390

Scheme 5.29 Detosylation of *N*-Ts dehydropiperidine compound . 390

Scheme 5.30 Ring expansions to azepanes ..... 391

Scheme 6.1 Polyhydroxylated alkaloids with significant biological activity ..... 422

Scheme 6.2 General approach towards the synthesis of imino-D-galactitol derivatives ..... 424

Scheme 6.3 Synthesis of imino-D-galactitol derivatives ..... 425

Scheme 6.4 Retrosynthetic approach for the synthesis of polyhydroxylated pyrrolidines ..... 426

Scheme 6.5 Tandem aza-Payne/hydroamination yields tetrasubstituted pyrrolidines ..... 427

Scheme 6.6 Comparatively long-lived alkoxide intermediate leads to the semi-Pinacol rearranged aldehyde product ..... 428

Scheme 6.7 Trapping latent nucleophile such as $CO_2$ by alkoxide intermediate would deliver functionalized enamides ..... 429

Scheme 6.8 Initial attempt to trap *in-situ* generated alkoxide with $CO_2$ ..... 430

Scheme 6.9 The unmasked alcohol does not undergo aza-Payne/hydroamination reaction ..... 434

Scheme 6.10 Putative mechanism for the formation of *N*-Ts enamide carbonate **6.19** ..... 434

Scheme 6.11 Treatment of *N*-Ts enamide epoxide under conditions that lead to the carbonate product does not yield the *N*-Ts carbonate **6.19** ..... 435

Scheme 6.12 Postulated mechanism for the formation of *N*-Ts enamide carbonate compound ..... 436

Scheme 6.13 Hydroamination of aziridinol **6.22** does not yield the hydroaminated product ..... 437

Scheme 6.14 Silylation of aziridine alcohol ..... 437

Scheme 6.15 Substrate incapable of undergoing the hydroamination reaction yields the elusive carbonate amide intermediate ..... 438

Scheme 6.16 Mechanistic rationale for the synthesis of enamide epoxide and carbonate compounds ..... 441

Scheme 6.17 Failed attempt at trapping the vinyl lithium with $CO_2$ ..... 442

Scheme 6.18 Elaboration of the *N*-Ts enamide carbonate to lactam ..... 443

Scheme 6.19 Hydrolysis of the lactam carbonate to 3,4-dihydoxylactam ..... 443

Scheme 6.20 Potential exploitable latent nucleophiles ..... 445

Scheme 6.21 Potential products via intramolecular aziridine ring opening via azacarbonate intermediate ..... 446

## LIST OF SYMBOLS AND ABBREVIATIONS

| | |
|---|---|
| Å | angstrom |
| [α] | specific rotation |
| δ | chemical shift |
| *μ*W | microwave |
| Ac | acetyl |
| APCI | atmospheric pressure chemical ionization |
| aq | aqueous |
| Ar | aryl |
| atm | atmospheres |
| BBN | 9-borabicyclo[3.3.1]nonane |
| Bn | benzyl |
| Boc | *tert*-butyloxycarbonyl |
| BOM | (benzyloxy)methyl |
| br | broad (spectral peak) |
| Bu | butyl |
| CI | chemical ionization |
| Cy | cyclohexyl |
| d | doublet (spectral peak) |
| dba | dibenzylideneacetone |
| DCM | dichloromethane |
| DME | 1,2-dimethoxyethane |

| | |
|---|---|
| DMF | dimethylformamide |
| DMSO | dimethyl sulfoxide |
| dppf | 1,1'-bis(diphenylphosphino) ferrocene |
| EI | electron ionization |
| ESI | electrospray ionization |
| eV | electron volt |
| EWG | electron withdrawing group |
| GC | gas chromatography |
| HRMS | high-resolution mass spectrometry |
| LiHMDS | lithium hexamethyldisilazide |
| mCPBA | *m*-chloroperbenzoic acid |
| MHz | megahertz |
| MOM | methoxymethyl |
| mp | melting point |
| ms | molecular sieves |
| MS | mass spectrometry |
| *n*Bu | *n*-butyl |
| NMR | nuclear magnetic resonance |
| NuH | nucleophile |
| Ns | nosyl |
| OAc | acetate |
| Ph | phenyl |

| | |
|---|---|
| PMB | *p*-methoxybenzyl |
| ppm | parts per million |
| R | substituent |
| RCM | ring-closing metathesis |
| rt | room temperature |
| SAR | Structure-activity relationship |
| $^{t}$Bu | *tert*-butyl |
| THF | tetrahydrofuran |
| TIPS | triisopropylsilyl |
| TLC | thin-layer chromatography |
| TOF | time of flight |
| Trt | triphenylmethyl, trityl |
| Ts | tosyl |
| TSE | trimethylsilylethyl |
| UV | ultraviolet |

# Chapter 1

## Aziridine: Ring Strain and Its Exploitation In Organic Synthesis.

### 1.1 General introduction to aziridines.

Ethyleneimines **1.1** generally known as aziridines are three-member nitrogen containing rings. History of this class of heterocyclic compounds dates back to 1888 when the parent member was first synthesized by Gabriel.[1]

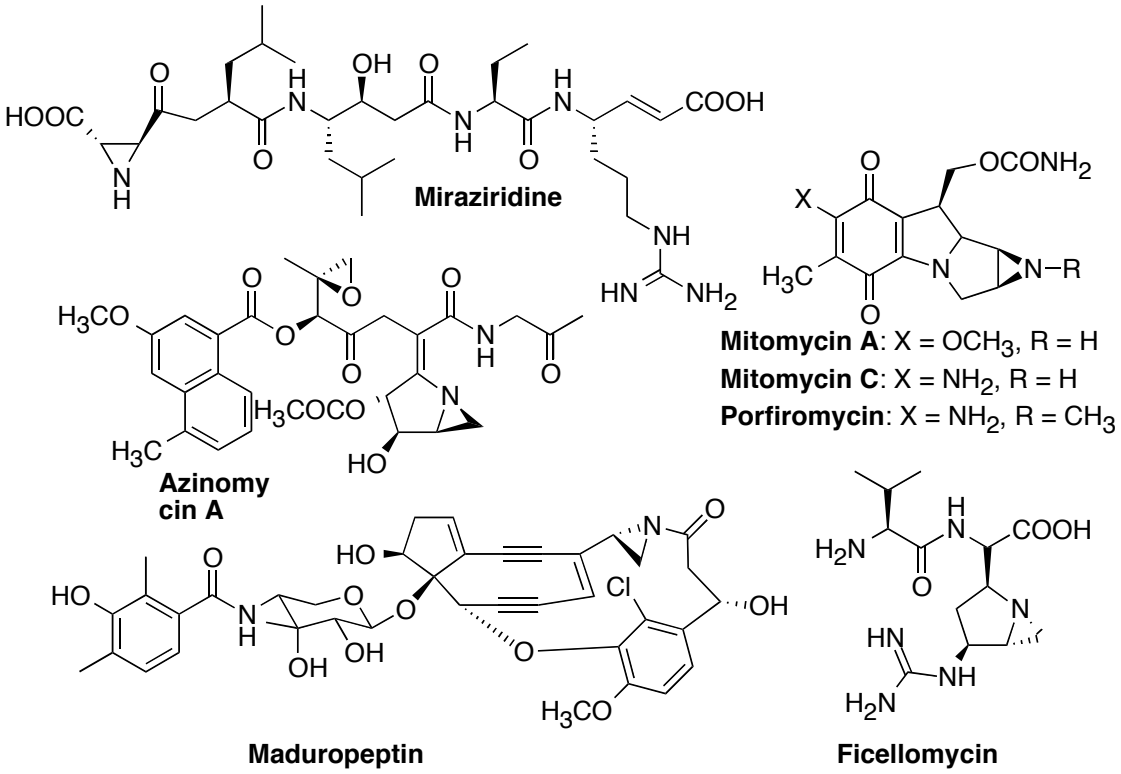


**Figure 1.1** Natural products containing aziridine functionalities.

Less prevalent than the corresponding oxygen analogs, aziridines also occur as constituents in several biologically important natural products such as azinomycins, mitomyins, ficellomycin, miraziridine and maduropeptin (Figure 1.1). Like other three member rings such as cyclopropanes and epoxides, aziridines are also highly strained compounds. Baeyer's strain worth 26.5 Kcal/mol associated with the ring is quite comparable to that present in case of epoxides.[2] As a result, ring opening reactions can be achieved in relatively mild conditions under both nucleophilic and electrophilic conditions.[3]

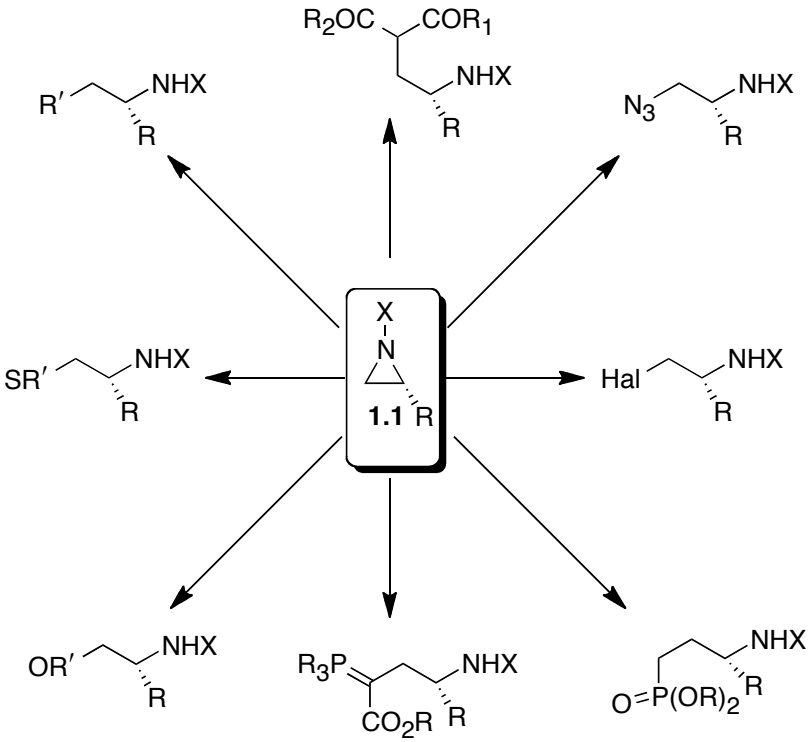


**Scheme 1.1** Various 1,2-difunctional compounds can be derived via ring opening of the aziridine ring.

Ring opening of aziridine with various nucleophiles affords a large variety of 1,2-difunctional compounds, which serve as versatile intermediates (Scheme 1.1).[2] The ring strain inherited in these compounds has been exploited, thereby establishing these heterocycles as useful and versatile building blocks in organic synthesis and medicinal chemistry.[4]

**1.2 Properties of aziridines.**

Aziridines exhibit weaker basicity than alkyl amines but stronger than aromatic amines. The aziridinium ion has $pK_a$ of 7.98.[5] They react with alkylating reagents in a fashion similar to that exhibited by secondary amines.

It has been known that the energy barrier of inversion at nitrogen in case of non-cyclic amines is 6-7 Kcal/mol. The geometric constraint of the trigonal ring makes this barrier to N-inversion higher for aziridine rings. For instance enthalpy of activation for the inversion at nitrogen for 2-methylaziridine is approximately 16.7 Kcal/mol, although not enough to restrict it at room temperature.[5] A substituent (protective group) at the nitrogen however, modifies the geometric constraints and therefore reactivity associated with these compounds. This adds to the complexity associated with these heterocycles compared to epoxides. Park and Kang have investigated the N-inversion energies for aziridine rings substituted with various N-protecting groups using B3LYP/6-31+G* methods.[6] Table 1.1 illustrates some of the energies calculated for various commonly used protective groups on nitrogen. Noticeably, for most cases the energy lies close to 16 Kcal/mol. In the case where either an ester or a ketone is present as the protective

group, the energy is remarkably lowered to 5.48 and 5.75 Kcal/mol (entries 6 and 7). These energies are even smaller than most of the acyclic amines. The lowered barrier for inversion has been rationalized as a result of the dominance of the planar-shaped transition states.

**Table 1.1** Effect of N-protective groups on the barrier to inversion.

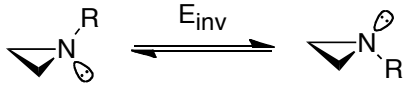


| entry | R | $E_{inv}$ (Kcal/mol) |
|---|---|---|
| 1 | H | 16.65 |
| 2 | Me | 16.98 |
| 3 | Ph | 8.91 |
| 4 | Bn | 16.71 |
| 5 | CHMePh | 17.06 |
| 6 | $CO_2Me$ | 5.48 |
| 7 | COPh | 5.75 |
| 8 | $SO_2Ph$ | 12.19 |
| 9 | Cl | 25.10 |

Carbonyl groups present on nitrogen can lower the barrier of inversion by incorporation of the lone pair of electrons on the N into the planar shaped transition state. The carbonyl groups are more effective in accommodating aziridine ring towards coplanarity than the sulfone group (entries 6, 7 *vs* 8). Presence of an electron-withdrawing group

such as chlorine on the nitrogen, on the other hand substantially increases the barrier to inversion (entry 9).

### 1.3 Activated *vs* unactivated aziridines.

In 1964 Ham reported the classification of aziridines into two categories based on their reactivity towards nucleophiles and other related properties.[7] Aziridines that contain a N-substituent capable of stabilizing a negative charge, generated on the nitrogen in the transition state when they undergo nucleophilic ring opening, are known as activated aziridines. 1-Acetyl aziridine **1.2** is of one such example (Scheme 1.2a). The activation energy to attain the transition state in this case is reduced due to the stabilization of the negative charge generated on the nitrogen via participation of the neighboring acetyl group.

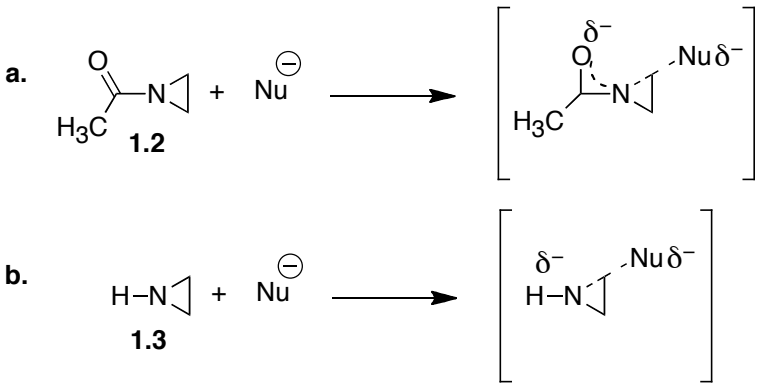


**Scheme 1.2 a**. Activated aziridine where nitrogen is stabilized in the transition state **b.** non-activated aziridine.

Sulfonyl, sulfinyl, phosphoryl and phosphinyl are some other examples which serve as activating N-substituents.

Ring strain in the three member ring does not allow an efficient overlap between nitrogen non-bonded pair and that of C=O $\pi^*$. Therefore, kinetic activation provided by these substituents is mostly based on inductive effects.[2] This augments the polarization of the C-N bond, stabilizing the developed negative charge on the more electronegative nitrogen. The thermodynamic effect on the other hand, is realized after ring cleavage via stabilization of the amide like anion (Scheme 1.3). The latter is much more pronounced in cases when a carbonyl substituent is present on the nitrogen. The stabilization achieved in most of the other cases is primarily controlled by inductive effect. These activated aziridines undergo ring opening reactions with a variety of nucleophiles without the need for an acid catalyst. Although, when a more electrophilic carbonyl group is attached to the nitrogen, ring-cleavage often does not result specially with the use of carbon based nucleophiles and instead competing attack on the acyl group leads to acyl-transfer reactions.

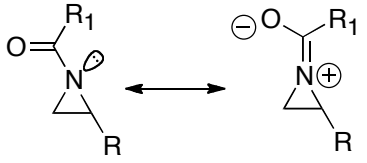


**Scheme 1.3** Resonance between amide and amidate like isomers.

Aziridine **1.3** (Scheme 1.2b) on the other hand, lacks such interaction and leads to an energetically high transition state and belong to unactivated class of aziridines. Unlike the activated aziridines, opening of the ring with nucleophiles only occur when aziridine is protonated, quaternized or complexes with a Lewis-acid.

### 1.4 Ring opening reactions and their applications.[3,8]

Aziridines have often been exploited in organic synthesis by virtue of their reactivity originating from ring strain. Consequently many regio- and stereoselective ring-opening reactions on aziridines have been reported till date. Due to the reduced electronegativity of the nitrogen compared to oxygen, ring opening is not as facile as observed in the case of epoxides. The cleavage via a nucleophilic attack however, occurs in an analogous fashion. Ring opening of an unsymmetrically substituted aziridine **1.4** can lead to products of either 3-substitution **1.5a** or 2-substitution **1.5b**. The ratio of the two products is mostly governed by the conditions employed in the reaction. For example under strictly nucleophilic conditions, attack is usually favored at the stericaly more available position resulting in the predominance of the 3-substituted **1.5a** product (Scheme 1.2). The latter effect however, can be perturbed by the presence of a neighboring group such as aryl systems that can stabilize the positive charge generated at C-2 leading to the prevalence of 2-substituted product **1.5b**.

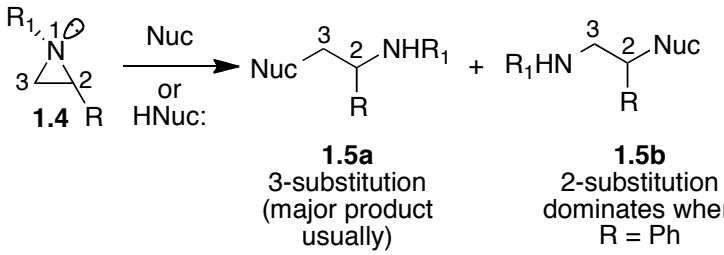


**Scheme 1.4** Regioselectivity obtained in ring opening of aziridine under nucleophilic conditions.

In case of epoxides where reactivity can easily be tuned by the interaction of the Lewis acid with the non-bonded lone pair of electrons on oxygen (thereby weakening the C-O bond), such effect is less pronounced for aziridines and occurs only when a non-oxygenated protective group is substituted on the ring nitrogen. The possibility of coordination between the oxygenated N protective groups however, allows major activation achieved in these cases via coordination of the lone pairs of oxygen with the Lewis acid (Figure 1.2)

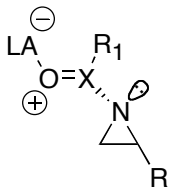


**Figure 1.2** Activation of the nitrogen via oxygenated N-protective group under Lewis acidic conditions.

### 1.4.1 Ring opening of aziridines and their application in the synthesis of amino acid derivatives.

Ring opening in aziridines has been vastly exploited for the synthesis of amino acids,[9] aza-sugars,[10-12] chiral auxiliaries and ligands,[13] biologically active compounds and natural product syntheses. Amino acids can be prepared starting from aziridine-2-carboxylic esters. Regioselectivity obtained in the nucleophilic ring opening reactions on aziridine-2-carboxylate is often governed by the conditions employed or the substituents present on the aziridine ring.

**Table 1.2** Stereoselectivity achieved in nucleophilic ring opening of aziridine-2-carboxylates.

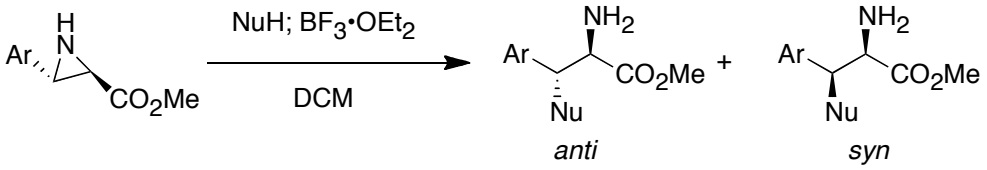


| entry | Ar | NuH | *syn*/*anti* | Yield (%) |
|---|---|---|---|---|
| 1 | *p*-$MeOC_6H_4$ | PhSH | 60/40 | 65 |
| 2 | Ph | PhSH | *anti* only | 80 |
| 3 | *p*- $O_2NC_6H_4$ | PhSH | *anti* only | 65 |
| 4 | *p*-$MeOC_6H_4$ | indole | 55/45 | 68 |
| 5 | Ph | indole | *anti* only | 53 |
| 6 | *p*-$O_2NC_6H_4$ | indole | *anti* only | 60 |

High stereo and regiospecific ring-opened products are obtained when these compounds contain aryl-substitution. Table 1.2 illustrates some examples. Noteworthy regio and stereospecificity is obtained when the 3-aryl substituent was either phenyl or *p*-nitrophenyl group. Amino acid derivatives are obtained in high enantioselectivity upon treatment of chirally pure 3-phenyl-aziridine-2-carboxylate **1.6** with nucleophiles under Lewis acidic conditions (Scheme 1.5).[14]

Reductive ring opening of un-activated aziridine-2-carboxylic esters also enables the convenient preparation of amino acid derivatives. Treatment of aziridine-2-carboxylic esters with Pearlman's catalyst affords amino acids in high yield and enantioselectivity (Scheme 1.6).

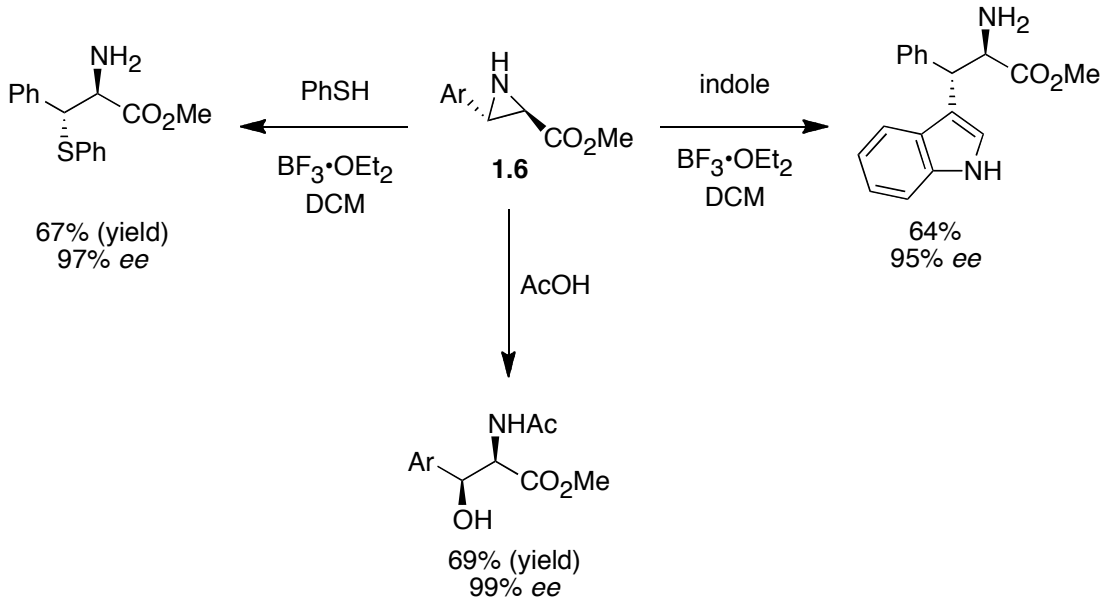


**Scheme 1.5** Excellent regio and stereospecificity obtained with 3-phenylaziridine-2-carboxylic ester.

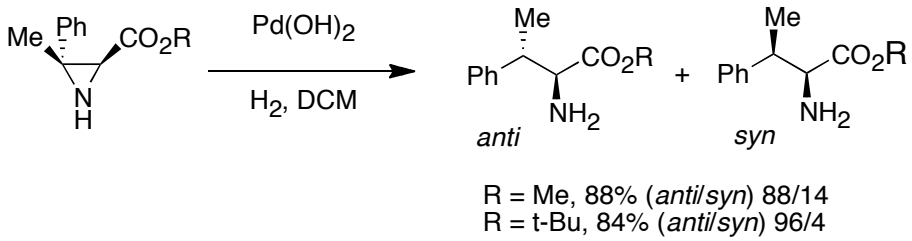


**Scheme 1.6** Synthesis of amino acids via reductive ring opening of aziridines.

### 1.4.2 Ring expansion of aziridines into synthetically useful compounds.

Treatment of activated aziridine-2-carboxylates with acetonitrile in the presence of $BF_3$•$OEt_2$ furnishes ring expanded products.[15] Under modified Ritter type conditions, nitrile opening of the ring is followed by intramolecular nucleophilic attack by the aziridine nitrogen (Scheme 1.7). This leads to the inversion of the C-3 position. Thus *trans* substituted starting materials deliver imidazolines with C-2 and C-3 substituents disposed in *cis* fashion. At this stage, both of the nitrogen atoms are differentially masked with a protecting group, which eases further elaboration of these compounds. For instance resulting imidazolines can be hydrolyzed to furnish α,β-diaminocarboxylic acid derivatives.

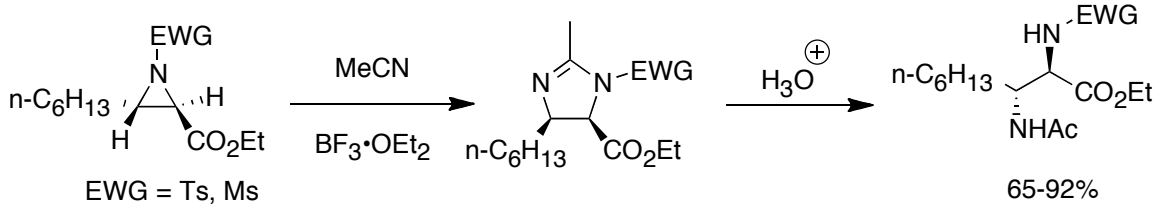


**Scheme 1.7** Ring expansion of activated aziridine-2-carboxylic esters yield imidazolines that can be hydrolyzed to α,β-diaminocarboxylic acid derivatives.

The Heine reaction has also been elegantly applied to demonstrate the scope of ring expansion of aziridines toward the synthesis of oxazolines (Scheme 1.8**a**).[16] Using a slight variation, expansion can be accomplished using *N*-acyl aziridine-2-carboxylic esters as the starting material.[17] In this case, nitrile attacks the aziridine ring, inverting the C-3 center and later intramolecular attack via the newly generated imidate, leads to the formation of oxazolines with a second inversion at the same position (Scheme 1.8**b**). The stereochemistry of the starting material is retained since inversion occurs twice unlike in the previous case (compared to Scheme 1.7) where C-3 inversion was observed.

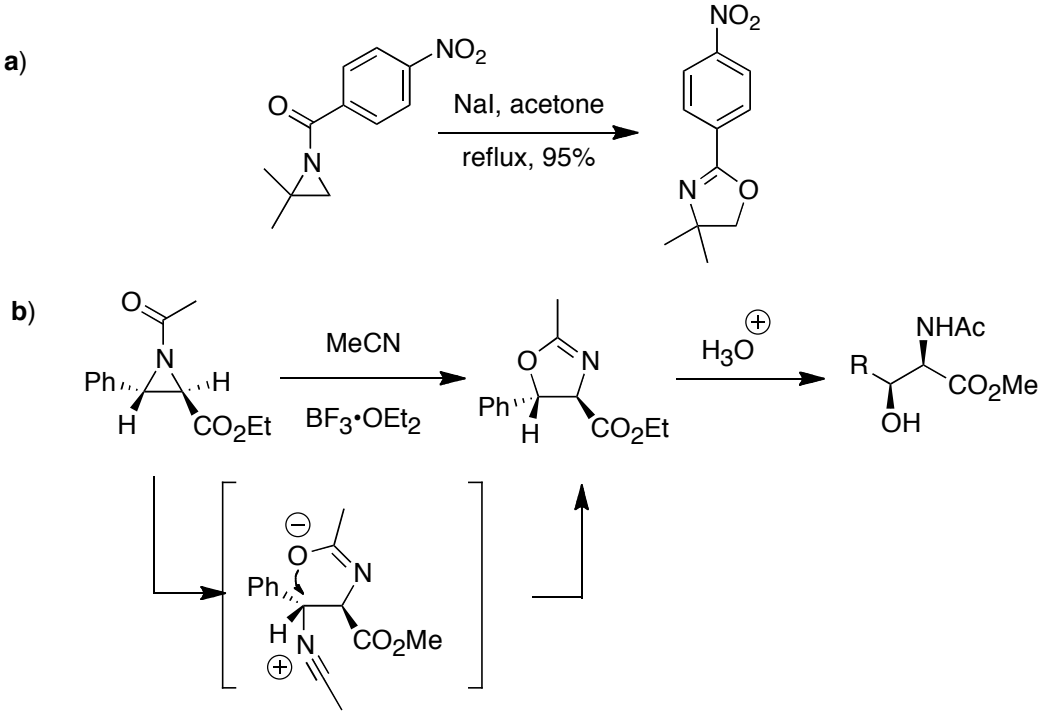


**Scheme 1.8 a**) Ring expansion via Heine reaction. **b**) Ring expansion with *N*-acyl aziridine-2-carboxylate occurs with net retention of the stereochemistry.

The resulting oxazolines can be hydrolyzed to yield synthetically useful α-amino alcohols. Similar expansion on *N*-Boc protected aziridine-2-carboxylic esters led to oxazolidinones.[18] Thus judicious choice of *N*-protective groups allows for the preparation of a variety of compounds taking advantage of the ring expansion chemistry.

Somfai et al. have elegantly demonstrated the aza-[2,3]-Wittig reaction of vinyl aziridines to yield tetrahydropyridine derivatives.[19] Although *trans* substituted vinyl aziridines afford *cis*-2,6-disubstituted tetrahydropyridines, *cis* substitution results in a mixture of geometric isomers (Scheme 1.9).

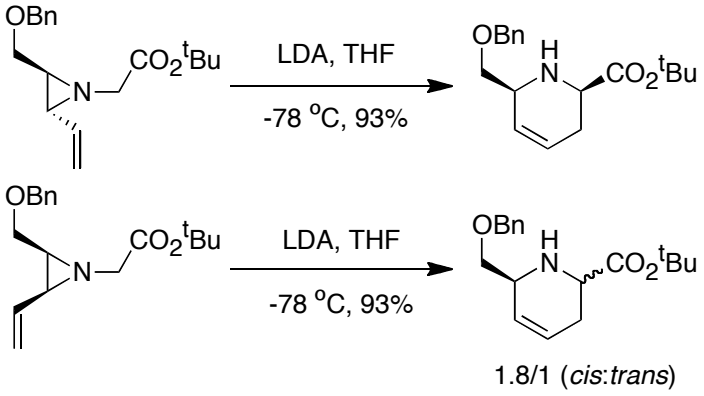


**Scheme 1.9** Aza-[2,3]-Wittig reaction of vinyl aziridine yields tetrahydropyridine.

The mechanistic rationalization invokes a six-member pseudo-chair like transitions state. Notably, the t-butyl group locks the conformation, being preferred in a pseudo-equatorial position. Bond formation between the rearrangement origin to the terminus (carbon 1 to 2, Scheme 1.10 **a**) along with the ring opening of the aziridine then yields the product with the observed stereochemistry. In case of the *cis* substituted vinyl

aziridines the stable invertomer bears the protective group *trans* relative to the substituents present on the ring. The latter arrangement places the reactive ends (1 and 2, Scheme 1.10**b**) far away to reach for an efficient orbital overlap.

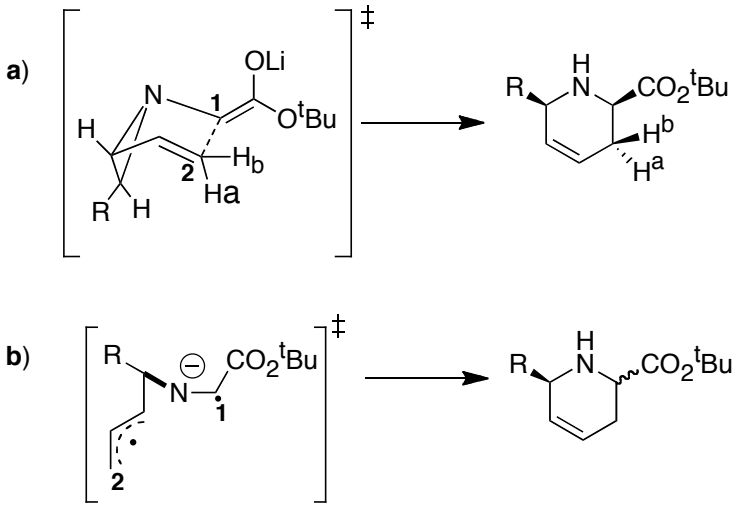


**Scheme 1.10** Distinct transition states explain different stereochemical results obtained for **a**) *trans* and **b**) *cis* di-substituted vinyl aziridines.

Thus in the latter case, cleavage of the initially formed anion generates a diradical species, which would explain the resulting mixture of isomerized products. Corresponding aza-[3,3]-Claisen rearrangement of vinylaziridines however, have been shown to furnish seven-member lactams via ring expansion reactions.[20] Treatment of *N*-acyl vinylaziridines with LiHMDS therefore provides tetrahydroazepin-2-ones via undergoing stereoselective rearrangement (Scheme 1.11).

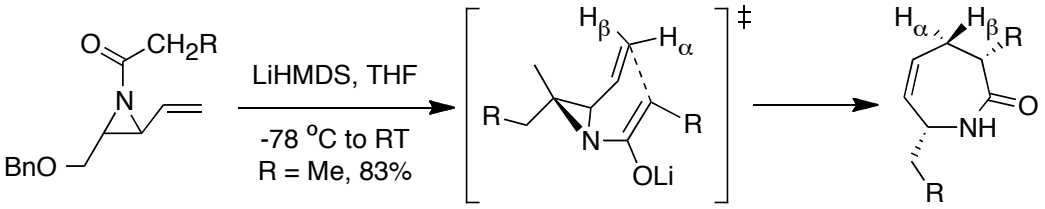


**Scheme 1.11** Aza-[3,3]-Claisen rearrangement of *N*-acyl vinyl aziridines yield 7-member lactams.

### 1.4.3 Application of ring opening of aziridine in natural product synthesis.

Oppolzer and Flaskamp have elegantly applied ring opening of aziridine rings using organometallic reagents for the total synthesis of pumiliotoxin-C (Scheme 1.12).[21] Similiar openings have been featured in the total syntheses of several other molecules such as verruculotoxin,[22] and pseudoconhydrine.[23]

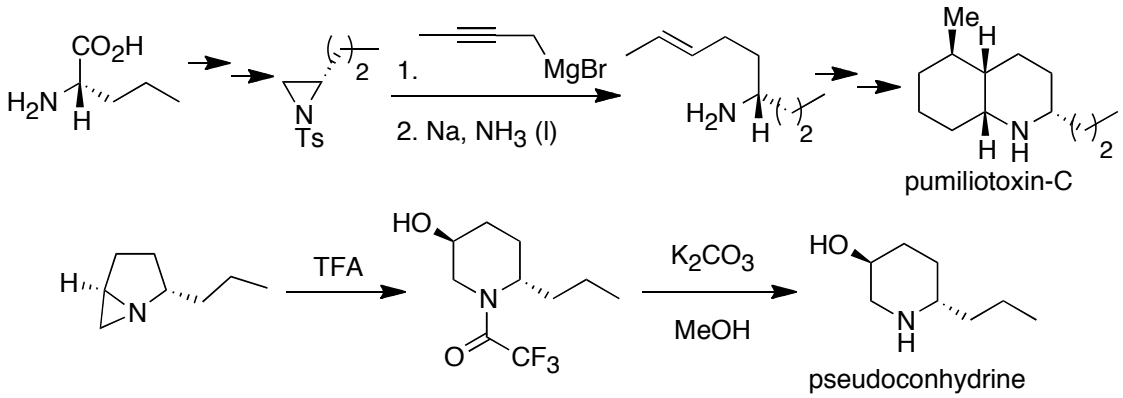


**Scheme 1.12** Ring opening of chiral aziridines applied in the total syntheses.

Several routes to complex spirocyclic molecules that belong to the family of histrionicotoxin have also been developed relying on the ring opening of tricyclic

aziridines or aziridinium ions (Scheme 1.13).[24-26] Hudlicky and coworkers have developed an enantioselective route toward the synthesis of pyrrolizidine alkaloid trihydroxyheliotridane.[27] The route involves the thermal rearrangement of chiral vinyl aziridines.

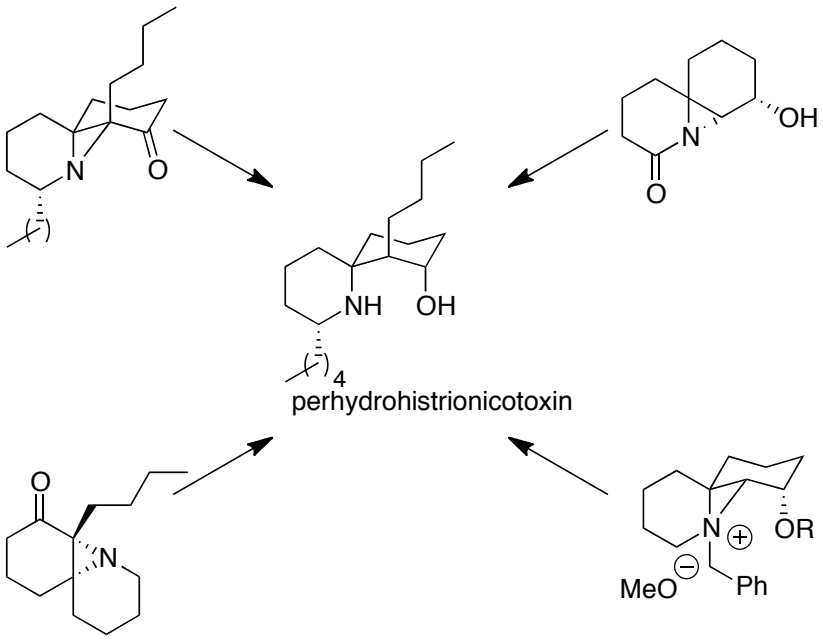


**Scheme 1.13** Application of ring opening of tricyclic aziridines in total synthesis.

### 1.5 An overview of methods available for the synthesis of aziridines.

Not surprisingly, due to their diverse applications in organic synthesis, various chiral and racemic syntheses of aziridines have been reported.[28,29]

### 1.5.1 From epoxides.

One of the most conventional ways to prepare aziridines relies on the ring opening of easily available epoxides. Innumerable methods are precedent in the literature that allows for the asymmetric syntheses of epoxides. Sharpless asymmetric epoxidation is one of the most extensively utilized protocols for the preparation of chiral epoxides. Elaboration of asymmetric epoxides provides access to optically active aziridines.[30] For example opening of epoxide **1.7** with sodium azide leads to a regioisomeric mixture of azido alcohols **1.8a** and **1.8b**. Phosphine mediated ring closure (Staudinger reaction) then provides the aziridine ring **1.10** via reduction of the oxazaphospholidine **1.9a** and **1.9b** intermediates (Scheme 1.14). For the cases where synthesis of the chiral precursor is problematic, the racemic compound can be treated with doubly protected amine in the presence of Jacobsen's catalyst (an extension of hydrolytic kinetic resolution: **HKR**).[31]

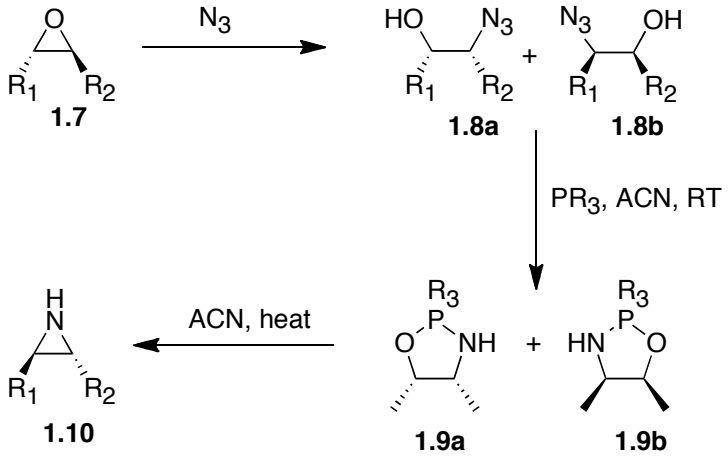


**Scheme 1.14** Synthesis of aziridines from epoxides.

Initial HKR on racemic substrate **1.11** in the presence of catalyst **1.12**, followed by nucleophilic ring opening of the mismatched case (unopened epoxide) with amine **1.13** leads to the generation of the highly enantioenriched amino alcohol **1.14**.[32] Routine functional manipulation then provides the chiral aziridine compound **1.15** (Scheme 1.15).

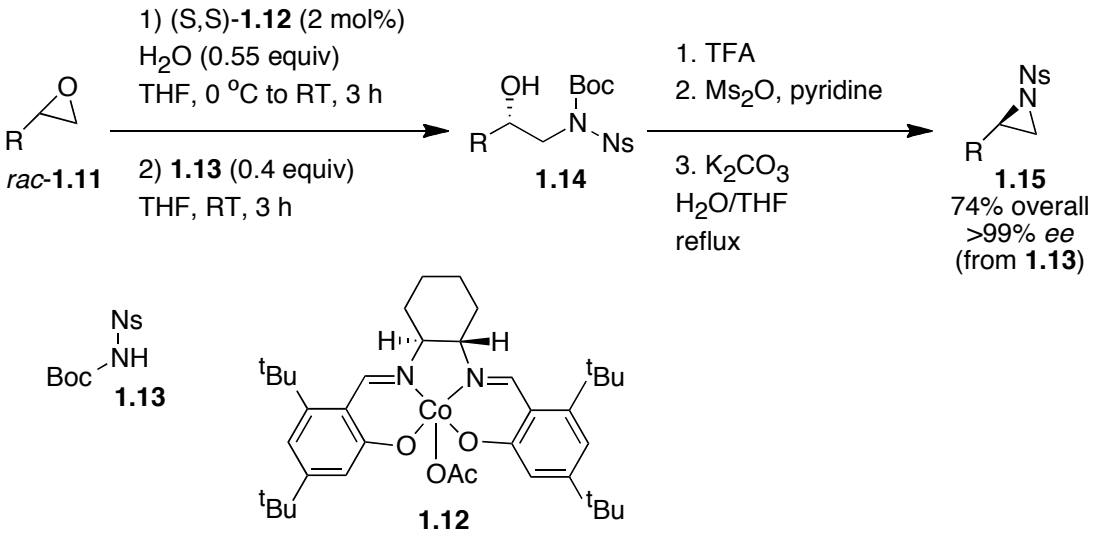


**Scheme 1.15** Enantioselective synthesis of aziridines via Jacobsen's modified HKR.

### 1.5.2 Additions to alkenes via nitrenes.[33]

Unlike the previous step-wise approaches, addition of nitrogen across the double bond can proceed in one step. Addition of nitrenes is a well investigated process particularly using alkoxycarbonylnitrenes. Nitrenes **1.16** are reactive intermediates in which the nitrogen atom bears one substituent, a lone pair and two other electrons to the unsaturated partner. Nitrenes are conventionally generated by the thermal or photochemical decomposition of the alkoxycarbonylazide **1.15**. Unfortunately these

methods often lead to a mixture of more reactive singlet nitrene species **1.16a** and more stable triplet species **1.16b**. The singlet species nitrogen bears its non bonded electrons in two orbitals (each containing an antiparallel electron set), the latter arrangement allows formation of both the C-N bonds with the olefin in one concerted fashion.

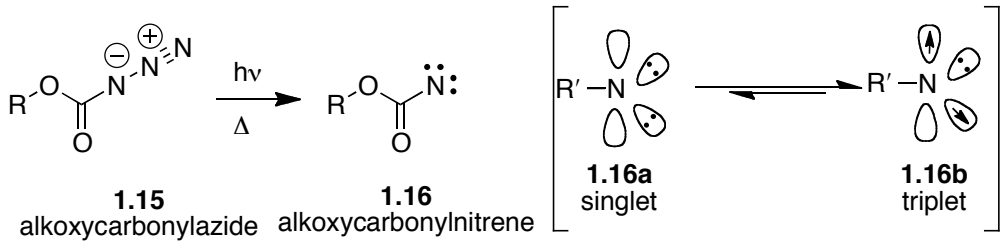


**Scheme 1.16** Decomposition of alkoxycarbonylazides leads to the generation of nitrenes.

The reaction of an olefin with the singlet nitrene **1.16a** occurs with complete stereospecificity. The more stable triplet species **1.16b** holds non bonded electrons in three orbitals (one filled with antiparrallel set and the other two semi filled with one electron each, of parallel spin), which allows C-N bond formation with the alkene in two steps. Since the diradical can undergo bond rotation, reactions with triplet nitrene are not stereospecific.

Harsh conditions to generate nitrenes, competing insertions into C-H bond and loss of streospecificity with triplet state nitrenes limit the scope of these processes. The nature of the N-substituent in the nitrene source however, alters the reactivity. When non-acyl azides were subjected under similar conditions, reaction with olefin instead occurs via cycloaddition step.

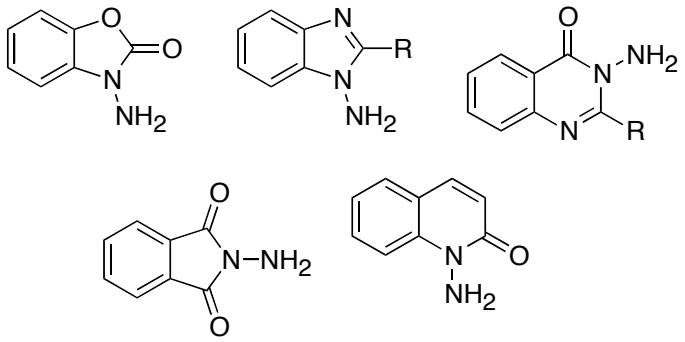

**Scheme 1.17** Reagents upon oxidation with $Pd(OAc)_4$ generate aziridinating species.

Several N-amino species were developed by Rees and coworkers, where aziridinating species was generated via oxidation with $Pb(OAc)_4$ (Scheme 1.17). Later Atkinson and coworkers also investigated the scope and the application of these reagents.[34] Reaction of the olefin substrates with hydrazine derivatives in the presence of an oxidant, provides aziridines with comparatively high stereoselectivity, which implies that mostly singlet nitrenes are generated under these conditions.

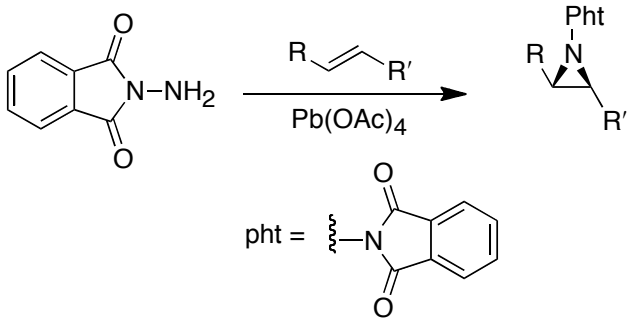

**Scheme 1.18** Reaction with nitrene-generated *in-situ* from hydrazine derivatives provide high stereoselective aziridination.

Atkinson and coworkers have later demonstrated that these reactions do not proceed via involvement of nitrene species.[35] The active source of aziridinating species in the reaction involving N-aminoquinazolinones **1.17** (Q-$NH_2$) is N-(acetoxyamino) quinazolinone **1.18** ($Q^1$-NHOAc) (Scheme **1.19**).

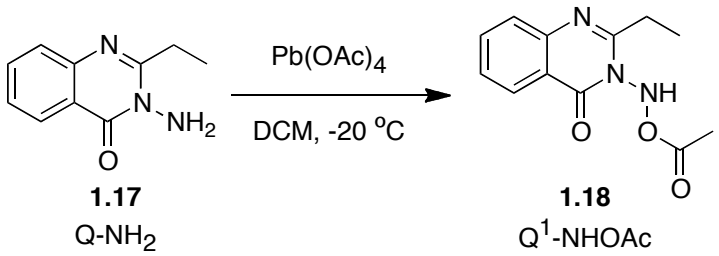


**Scheme 1.19** $Q^1$-NHOAc is an active aziridinating species.

It was proposed that during the reaction, nitrogen electron pair is directed towards the more electron-deficient side of the alkene, whereas the acetate group lies *anti* to the electron rich site, facilitating the attack in an $S_N2$ manner (Scheme 1.20).[36]

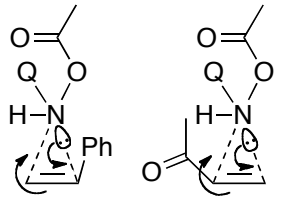


**Scheme 1.20** Mechanism of aziridination with $Q^1$-NHOAc.

Later, metal based nitrene sources were also introduced using porphyrin and salen catalysts. These catalysts could aziridinate the olefin substrates in the presence of a

nitrene precursor such as N-tosyliminophenyliodinane. The concept was later extended with the incorporation of an asymmetric metal catalyst to install the aziridine ring in high enantioselective fashion. Evans,[37] Jacobsen,[38] and Katsuki illustrated the use of chiral bis-oxazolines and 1,2-diamines in chiral aziridination processes.[39] Jacobsen demonstrated that the reaction proceeds via a copper-nitrene complex and not radical (Scheme 1.21).

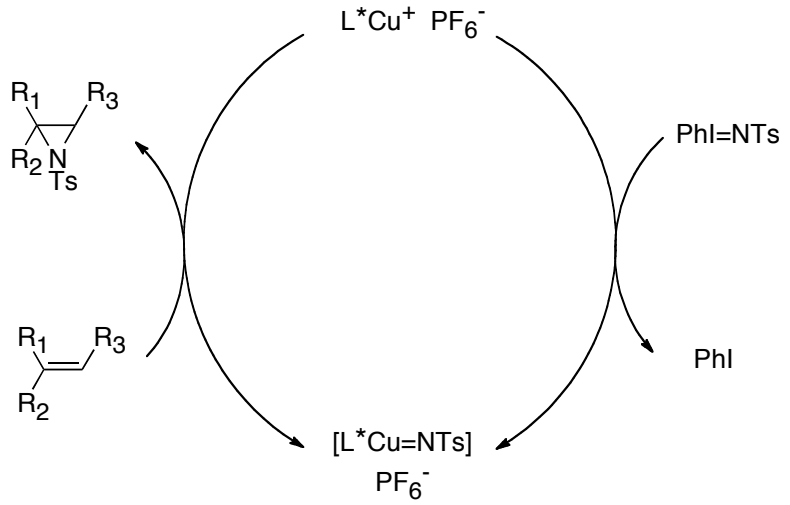


**Scheme 1.21** Mechanism of (diimine)-copper catalyzed aziridination.

Du Bois and coworkers have recently reported an alternative route for the aziridination with rhodium carboxamide catalyst **1.20**, using a sulfamate ester **1.19**, and an inexpensive terminal oxidant.[40] The tetratrifluoroacetamide rhodium catalyst is optimally tuned for aziridination process since it is selective for $\pi$-bond functionalization as opposed to $\sigma$ C-H insertion pathway (Scheme 1.22). The sulfate ester can easily be cleaved under milder conditions using Zn-amalgam reagent.

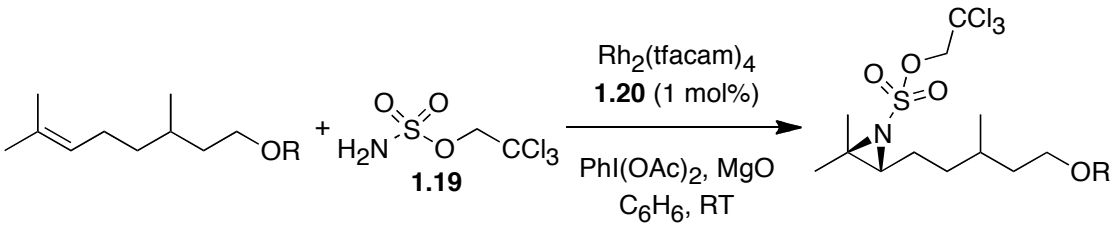


**Scheme 1.22** Aziridination via rhodium-based catalyst.

### 1.5.3 Additions to imine.

Methods to install aziridine via nitrene precursors involve two C-N bond formation. In an analogous manner one can imagine the formation of an aziridine using a carbene precursor to an imine, the latter would require formation of one C-N and one C-C bond. Such a strategy has recently been investigated. Aggarwal and coworkers reported tosylhydrazone as a successful source of carbene by demonstrating their application in the enantioselective aziridination reaction.[41]

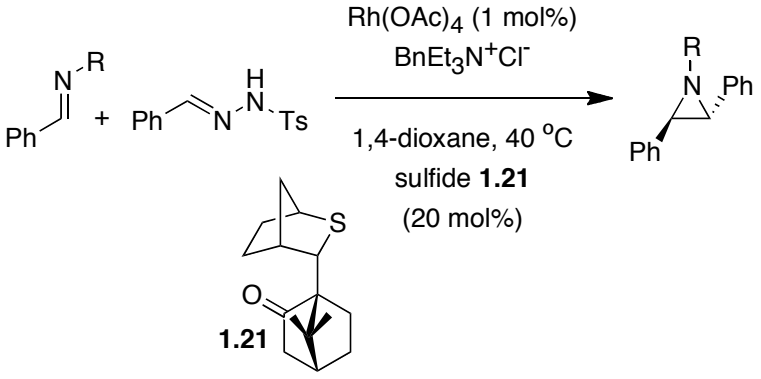


**Scheme 1.23** Addition of chiral carbenes to iminium.

Initially generated metal-carbenoid transfers the carbene to the chiral sulfide **1.21** which eventually serve as a chiral source of carbene and executes the nucleophilic attack on the imine substrate (Scheme 1.23). The process provides high enantioselectivity but suffers from low level of diastereoselection (approximately 2:1) for most of the substrates. Wulff and coworkers demonstrated asymmetric aziridination utilizing axially chiral Bronsted acids to perform addition of ethyldiazoacetate to imines (Scheme 1.24).[42,43] The method utilizes a mixed aryl borate catalyst derived from either VANOL and VAPOL.

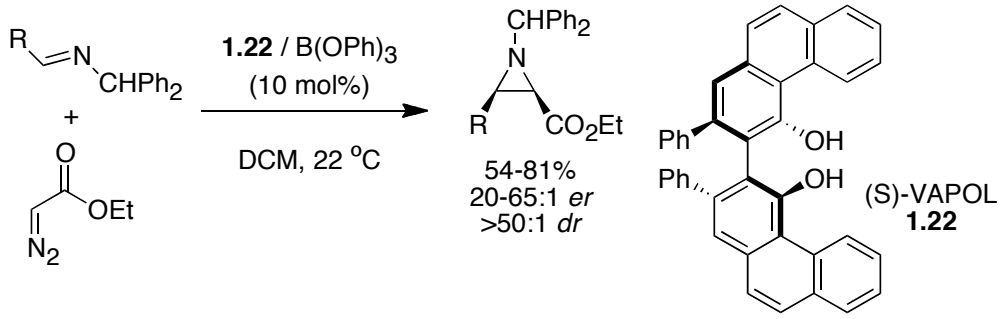


**Scheme 1.24** Diastereo and enantioselective synthesis of *cis*-aziridines.

Wulff et al. have recently reported a universal catalytic asymmetric aziridination process.[44] A chiral Bronsted acid **1.25** that assembles as a boroxinate core is known to catalyze the reaction of the same imines with diazoacetamide **1.24** to furnish *trans* aziridines and with diazoacetate **1.23** to yield *cis* aziridines.[45] Both transformations occur remarkably with excellent diastereo and enantioselectivity. The opposite stereochemical outcomes obtained with ethyl diazoacetate and that with

diazoacetamide were explained by the difference in the specific non-covalent interactions involved in the stereochemistry determining transitions states.[46] For the latter case, an extra H-bond interaction between the amidic H of **1.24** and the oxygen of the chiral counterion present in **1.25** was invoked, explaining the reversed selectivity resulting into the *trans* selective aziridination pathway.

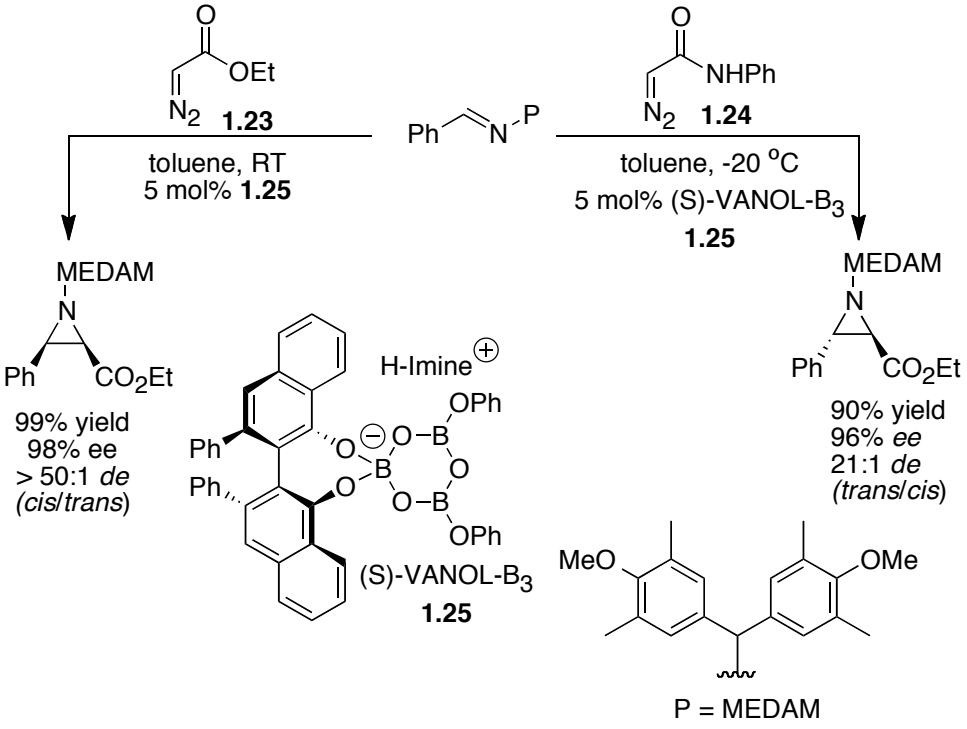


**Scheme 1.25** Universal asymmetric aziridination catalyzed by chiral polyborate based Bronsted acid.

Other than carbenes, sulfur and iodine ylides can also add across the imines. Ylides react with imines initially to form β-iodonium and β-sulfonium amide anions, which are reactive and undergo ring closure yielding aziridine rings. Ochiai et al. have shown the

reaction of monocarbonyl ylide **1.27** with the activated imines for the stereoselective synthesis of both *cis* and *trans* aziridine-2-ketones.[47] These ylides in turn, are generated from *Z*-(2-acetoxy-1-alkyl)(phenyl) iodonium bromide **1.26** upon treatment with lithium ethoxide.

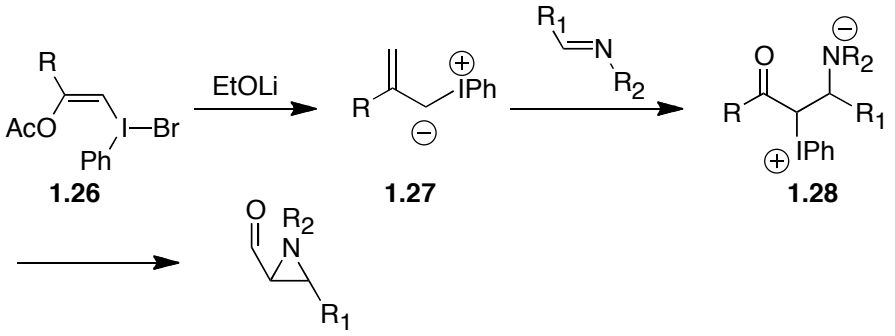


**Scheme 1.26** Stereoselective synthesis of aziridines via iodonium ylide.

Hou and coworkers have reported the preparation of $\alpha$-unsaturated substituted aziridines in high *cis*-selective fashion via a transformation involving aryl imines and partially stabilized sulfonium ylides in the presence of $BF_3 \cdot OEt_2$.[48]

### 1.5.4 Other miscellaneous methods.

Several other studies have been reported for aziridination reactions. Michael addition reactions to $\alpha$-bromo-$\alpha,\beta$-unsaturated ketones also yield aziridine rings via the Gabriel-Cromwell reaction.[49] Reduction of azirines also allows for the synthesis of aziridines. The former can in turn be easily prepared via the Neber reaction.[50] Chiral sulfinimine and a metal enolate have successfully shown to undergo Darzen reactions to yield

aziridine rings.[51] Aza version of Corey Chaykowsi reaction has also been utilized for a similar purpose.[52] Stereoselective route to aziridines by using different chloramine salts in the presence of a catalyst has also been extensively studied.[53-56] Factors such as low cost, commercial availability, non-toxicity and easy handling associated with the use of latter reagents make them highly utilizable reagents in the aziridination methods. Several methodologies have been developed over the years that rely on exploiting the ring strain of these heterocycles in the preparation of important synthetic intermediates. As a result their application has tremendously increased over the years in several areas. A large number of approaches has been reported and is still under study for the synthesis of aziridines. A large amount of progress has been made in the development of enantioselective routes; nevertheless considerable improvement is still required especially in case of the trisubstituted aziridines. Easy availability of epoxidizing reagents such as *m*-CPBA and t-BuOOH has significantly helped popularize the utility of epoxides in the field of organic synthesis. Lack of analogous reagents however, in case of aziridination, still hampers their utility. Presence of a nitrogen substituent tremendously affects both the nature and properties of these compounds and therefore contributes towards the complexity found in such systems. Tuning the reactivity of aziridines via modifying the protective groups might seem like a daunting task, it nevertheless broadens the horizon of the field and scope of these compounds towards obtaining a diverse range of products.

# REFERENCES

## REFERENCES


1. Gabriel, S. *Berichte der deutschen chemischen Gesellschaft,* **1888**, *21*, 1049-1057.
2. Sweeney, J. B. *Chem. Soc. Rev.,* **2002**, *31*, 247-258.
3. Hu, X. E. *Tetrahedron,* **2004**, *60*, 2701-2743.
4. Florio, S.; Luisi, R. *Chemical Reviews*, **2010**,*110*, 5128-5157.
5. Ono, N. *The nitro group in organic synthesis*; Wiley-VCH: New York, 2001.
6. Park, G.; Kim, S.-C.; Kang, H.-Y. *Bull. Korean Chem Soc,* **2005**, *26*, 1339.
7. Ham, G. E. *Journal of Organic Chemistry,* **1964**, *29*, 3052-3055.
8. McCoull, W.; Davis, F. A. *Synthesis-Stuttgart,* **2000**, 1347-1365.
9. Cardillo, G.; Gentilucci, L.; Tolomelli, A. *Aldrichimica Acta,* **2003**, *36*, 39-50.
10. Depezay, J. C. *Synthesis of Enantiopure Azasugars from D-Mannitol: Carbohydrate and Peptide Mimics*; Wiley-VCH Verlag GmbH & Co. KGaA, 2005.
11. Dhavale, D. D.; Kumar, K. S. A.; Chaudhari, V. D.; Sharma, T.; Sabharwal, S. G.; PrakashaReddy, J. *Org. Biomol. Chem.,* **2005**, *3*, 3720-3726.
12. McCort, I.; Dureault, A.; Depezay, J. C. *Tetrahedron Lett.,* **1996**, *37*, 7717-7720.
13. McCoull, W.; Davis, F. A. *Synthesis,* **2000**, *2000*, 1347,1365.
14. Metz, P.; Zwanenburg, B.; ten Holte, P. In *Stereoselective Heterocyclic Synthesis III*; Springer Berlin / Heidelberg: 2001; Vol. 216, p 93-124.
15. Legters, J.; Willems, J.; Thijs, L.; Zwanenburg, B. *Recl. Trav. Chim Pays-Bas,* **1992**, *111*, 59.
16. Heine, H. W.; Kaplan, M. S. *The Journal of Organic Chemistry,* **1967**, *32*, 3069-3074.
17. Legters, J.; Thijs, L.; Zwanenburg, B. *Recl. Trav. Chim Pays-Bas,* **1992**, *111*, 75.
18. Tomasini, C.; Vecchione, A. *Org. Lett.,* **1999**, *1*, 2153-2156.
19. Aahman, J.; Somfai, P. *J. Am. Chem. Soc.,* **1994**, *116*, 9781-9782.
20. Lindstr√∂m, U. M.; Somfai, P. *J. Am. Chem. Soc.,* **1997**, *119*, 8385-8386.

21. Oppolzer, W.; Flaskamp, E. *Helv. Chim. Acta,* **1977**, *60*, 204-207.

22. Martens, J. r.; Scheunemann, M. *Tetrahedron Lett.,* **1991**, *32*, 1417-1418.

23. Harding, K. E.; Burks, S. R. *The Journal of Organic Chemistry,* **1984**, *49*, 40-44.

24. Corey, E. J.; Balanson, R. D. *Heterocyles,* **1976**, *5*, 445-470.

25. Aratani, M.; Dunkerton, L. V.; Fukuyama, T.; Kishi, Y.; Kakoi, H.; Sugiura, S.; Inoue, S. *The Journal of Organic Chemistry,* **1975**, *40*, 2009-2011.

26. Sha, C. K.; Ouyang, S. L.; Hsieh, D. Y.; Chang, R. C.; Chang, S. C. *The Journal of Organic Chemistry,* **1986**, *51*, 1490-1494.

27. Hudlicky, T.; Luna, H.; Price, J. D.; Rulin, F. *The Journal of Organic Chemistry,* **1990**, *55*, 4683-4687.

28. Bisol, T. B.; Sa, M. M. *Quim. Nova,* **2007**, *30*, 106-115.

29. Zwanenburg, B.; ten Holte, P. *Stereoselective Heterocyclic Synthesis Iii,* **2001**, *216*, 93-124.

30. Tanner, D. *Angewandte Chemie International Edition in English,* **1994**, *33*, 599-619.

31. Larrow, J. F.; Schaus, S. E.; Jacobsen, E. N. *J. Am. Chem. Soc.,* **1996**, *118*, 7420-7421.

32. Kim, S. K.; Jacobsen, E. N. *Angewandte Chemie International Edition,* **2004**, *43*, 3952-3954.

33. Atkinson, R. S. *Tetrahedron,* **1999**, *55*, 1519-1559.

34. Atkinson, R. S.; Rees, C. W. *Journal of the Chemical Society C: Organic,* **1969**, 772-778.

35. Atkinson, R. S.; Grimshire, M. J.; Kelly, B. J. *Tetrahedron,* **1989**, *45*, 2875-2886.

36. Atkinson, R. S.; Williams, P. J. *Journal of the Chemical Society, Perkin Transactions 1,* **1996**, 1951-1959.

37. Evans, D. A.; Bilodeau, M. T.; Faul, M. M. *J. Am. Chem. Soc.,* **1994**, *116*, 2742-2753.

38. Li, Z.; Quan, R. W.; Jacobsen, E. N. *J. Am. Chem. Soc.,* **1995**, *117*, 5889-5890.

39. Nishikori, H.; Katsuki, T. *Tetrahedron Lett.,* **1996**, *37*, 9245-9248.

40. Guthikonda, K.; Du Bois, J. *J. Am. Chem. Soc.,* **2002**, *124*, 13672-13673.

41. Aggarwal, V. K.; Alonso, E.; Fang, G.; Ferrara, M.; Hynd, G.; Porcelloni, M. *Angewandte Chemie International Edition,* **2001**, *40*, 1433-1436.

42. Antilla, J. C.; Wulff, W. D. *Angew. Chem., Int. Ed.,* **2000**, *39*, 4518-4521.

43. Antilla, J. C.; Wulff, W. D. *J. Am. Chem. Soc.,* **1999**, *121*, 5099-5100.

44. Desai, A. A.; Wulff, W. D. *J. Am. Chem. Soc.,* **2010**, *132*, 13100-13103.

45. Hu, G.; Huang, L.; Huang, R. H.; Wulff, W. D. *J. Am. Chem. Soc.,* **2009**, *131*, 15615-15617.

46. Vetticatt, M. J.; Desai, A. A.; Wulff, W. D. *J. Am. Chem. Soc.,* **2010**, *132*, 13104-13107.

47. Ochiai, M.; Kitagawa, Y. *Tetrahedron Lett.,* **1998**, *39*, 5569-5570.

48. Wang, D.-K.; Dai, L.-X.; Hou, X.-L. *Chemical Communications,* **1997**, 1231-1232.

49. Garnet, P.; Dogan, O.; Pillai, S. *Tetrahedron Lett.,* **1994**, *35*, 1653-1656.

50. Verstappen, M. l. M. H.; Ariaans, G. J. A.; Zwanenburg, B. *J. Am. Chem. Soc.,* **1996**, *118*, 8491-8492.

51. Davis, F. A.; Liu, H.; Zhou, P.; Fang, T.; Reddy, G. V.; Zhang, Y. *The Journal of Organic Chemistry,* **1999**, *64*, 7559-7567.

52. Saito, T.; Sakairi, M.; Akiba, D. *Tetrahedron Lett.,* **2001**, *42*, 5451-5454.

53. Minakata, S. *Journal of Synthetic Organic Chemistry Japan,* **2009**, *67*, 1001-1011.

54. Karabal, P. U.; Chouthaiwale, P. V.; Shaikh, T. M.; Suryavanshi, G.; Sudalai, A. *Tetrahedron Lett.,* **2010**, *51*, 6460-6462.

55. Minakata, S.; Murakami, Y.; Tsuruoka, R.; Kitanaka, S.; Komatsu, M. *Chemical Communications,* **2008**, 6363-6365.

56. Kolvari, E.; Ghorbani-Choghamarani, A.; Salehi, P.; Shirini, F.; Zolfigol, M. A. *Journal of the Iranian Chemical Society,* **2007**, *4*, 126-174.

# Chapter 2

## Stereochemical Induction Controlled By Aziridine Ring.

### 2.1 Introduction.

Aziridines are important as subunits in chiral auxiliaries, pharmaceutical intermediates, and biologically active natural products.[1-6] Available via several recently developed stereo- and enantioselective syntheses,[3,7-13] these compact and robust heterocycles are endowed with controllable reactivity due to their three-membered ring strain and their acid- and substituent-governed activation. Thus, via modern regio- and stereoselective ring opening methods, aziridine building blocks offer efficient, versatile access to structurally complex targets. Significance of aziridines and their vast application in organic synthesis essentially as a result of their ring opening reactions has been briefly discussed in Chapter 1.

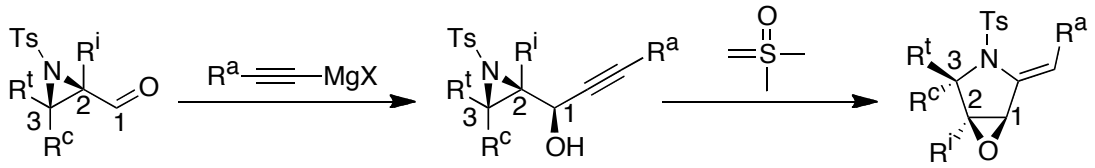


**2.1** **2.2** **2.3**

**Scheme 2.1** Ts protected aziridine aldehydes serve as precursors for tandem Aza-Payne/hydroamination methodology.

However, strategies to install a new chiral center thereby taking advantage of ring's inherent stereochemistry have been less examined. For example, we have recently reported that *N*-tosyl-2,3-disubstituted aziridine-2-carboxaldehydes undergo addition with Grignard reagents to form *syn* adducts **2.2** ($R^i$ = $CH_3$, $R^t$ = alkyl, $R^c$ = H) with excellent diastereoselectivity (>99:1) (Scheme 2.1). Use of these products as starting materials enabled our discovery of a one-pot tandem aza-Payne/hydroamination reaction, a process that yields highly functionalized densely substituted pyrrolidines **2.3** (Scheme 2.1).[14] Notably, it is the newly generated carbinol stereocenter that is the key to the success of these reactions.

Addition of nucleophiles to aziridine-2-carboxaldehydes and ketones enables installation of a stereocenter adjacent to and guided by the rigid, stereochemically defined aziridine ring. This chapter will expand greatly on the literature precedence, which admittedly is lacking in this area. Such chemistry has proven useful with epoxides, the oxygen analogues of aziridines, where additions of organometallic reagents to epoxy-2-carboxaldehydes have been extensively studied and exploited in syntheses of natural products.[15-17]

**2.2 Addition of organometallic reagents to epoxy-2-carboxaldehydes.**

The addition of an organometallic nucleophile to epoxy-2-carboxaldehyde **2.4** leads to the generation of a new stereogenic center. The transformation resulting into the formation of either *anti* **2.5a** or *syn* **2.5b** adduct depending on the choice of the metal employed in the reaction. Note in Table 2.1, $R^c$, $R^t$ and $R^i$ represent substituents that

are *cis*, *trans* and *ipso* to the aldehyde. $R^a$ denotes the nucleophile added to the carbonyl. Metals that are strong coordinators of oxygen favor *syn* selectivity, as rationalized by a chelation-based transition state model (Figure 2.1b).[16] On the other hand, metals that coordinate poorly or conditions that suppress chelation favor the *anti* adduct as predicted by the Felkin-Ahn model (Figure 2.1a).[18-20]

**Table 2.1** Addition of organometallic reagents to epoxy-2-carboxaldehydes.

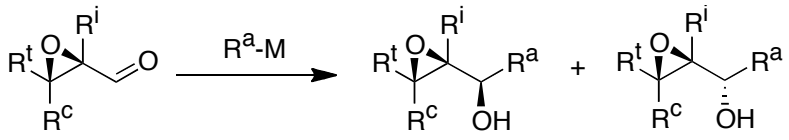


**2.4** epoxy aldehyde | **2.5b** *syn* | **2.5a** *anti*

| entry | $R^t$ | $R^c$ | $R^i$ | $R^a$-M | *syn*/*anti* | yield (%) |
|---|---|---|---|---|---|---|
| 1 | $Me_3Si$ | H | H | $Et_2Zn$ | 93:7 | 70 |
| 2 | $C_6H_{13}$ | H | H | $Et_2Zn$ | 93:7 | 78 |
| 3 | H | $C_5H_{11}$ | H | $Et_2Zn$ | 63:37 | 59 |
| 4 | H | H | $C_9H_{19}$ | $Et_2Zn$ | 50:50 | 11 |

Sato and coworkers have studied addition of diethyl zinc reagents to epoxy-2-carboxaldehydes.[16] The affects of substitution pattern of the epoxide ring on *syn*:*anti* selectivity has been investigated. For the entries where addition occurs with high *syn*-selectivity, the outcome has been explained by invoking a chelation between the

epoxide oxygen and the aldehydic carbonyl moiety with the metal (Figure 2.1 b). Remarkably high *syn*-selectivity is observed when *trans* substituted epoxy aldehydes (entries 1 and 2) were subjected to the addition. Selectivity on the other hand, deteriorated to an equimolar mixture of two adducts in case of the *ipso* substituted compound (entry 4).

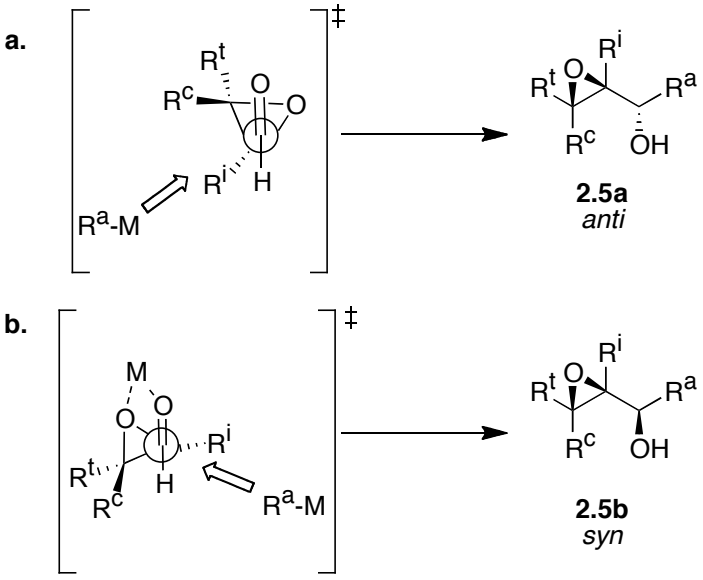


**Figure 2.1** a. Felkin-Ahn control. b. Chelation control addition to epoxy-2-carboxaldehydes.

Gorrichon et al. have examined the stereoselective addition of lithioenolates to epoxy-2-carboxaldehydes (Table 2.2).[21,22] Moderately high *anti* selectivity was observed with both *cis* and 2,3-disubstituted epoxy-2-carboxaldehyde substrates, which has been explained on the basis of Felkin-Ahn control. Author suggests that the oxygen atom of the epoxide is the largest susbtituent and leads to a transition state where the incoming

nucleophile is antiperiplanar with the C-O bond of the epoxide (analogous to Figure 2.1a). Howe and Proctor examined the additions of methyl lithium, methyl magnesium halides and allyl stannanes to epoxy-2-carboxaldehydes.[23] Non-chelation *anti* adducts were favored during the transformation.

**Table 2.2** *Anti*-selective addition of lithium enolates to epoxy-2-carboxaldehydes.

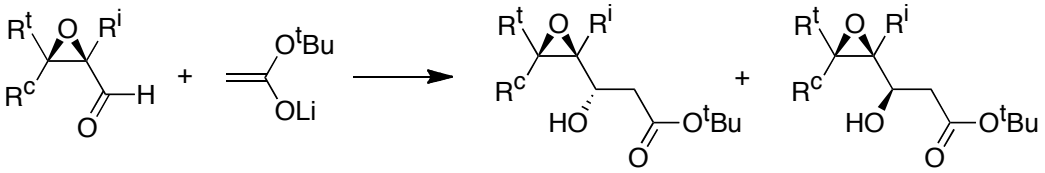

| entry | $R^1$ | $R^2$ | $R^3$ | *anti*/*syn* | yield (%) |
|---|---|---|---|---|---|
| 1 | H | H | $CH_2OBn$ | 82:18 | 87 |
| 2 | H | H | $CH_2OTBDPS$ | 80:20 | 90 |
| 3 | Ph | Me | H | 71:29 | 75 |

Righi and coworkers have studied addition of boron enolates to *trans* substituted epoxy-2-carboxaldehydes.[24] The reaction proceeded with excellent *anti*-selectivity, as predicted via the Felkin-Ahn transition state. Kalinowski et al. have examined the addition of allyltributyl tin and trimethylsilyl chloride to epoxy-2-carboxaldehydes in the presence of Lewis acids (Table 2.3).[25] High *syn*-selectivity was observed when addition of allyltributyl tin was carried out in the presence of $LiClO_4$. A similar stereochemical outcome was observed upon addition of trimethylsilyl chloride. The chelation control model was invoked to justify both of the resulting stereochemical outcomes.

Interestingly, reverse selectivity was observed when addition of allyltributyltin was carried out with $BF_3$•$OEt_2$ instead of $LiClO_4$ (Table 2.3, entries 3 *vs* 2; 5 *vs* 4), which lies in agreement with the observation made by Howe and Proctor during the addition of allyl stannanes in the presence of $BF_3$•$OEt_2$.

**Table 2.3** Lewis acid mediated addition of allyltributyl tin to epoxy-2-carboxaldehydes.

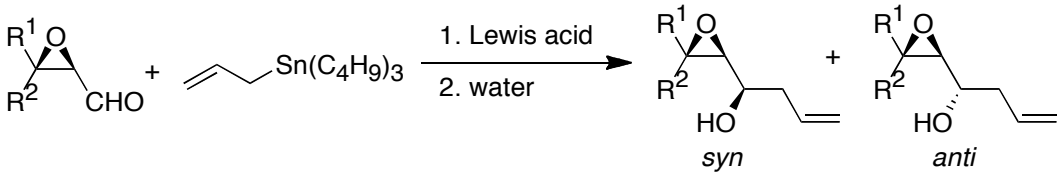


| entry | $R^1$ | $R^2$ | Lewis acid | *syn*/*anti* | yield (%) |
|---|---|---|---|---|---|
| 1 | $C_3H_7$ | H | $LiClO_4$ | 90:10 | 95 |
| 2 | $CH_2OBn$ | H | $LiClO_4$ | 87:13 | 90 |
| 3 | $CH_2OBn$ | H | $BF_3$•$OEt_2$ | 18:82 | 60 |
| 4 | H | $CH_2OBn$ | $LiClO_4$ | 86:14 | 97 |
| 5 | H | $CH_2OBn$ | $BF_3$•$OEt_2$ | 12:88 | 55 |

To conclude, several studies have aimed to report the stereochemical outcomes observed upon addition of various nucleophiles to epoxy-2-carboxaldehydes. Nucleophiles that are capable of forming an efficient chelate with both the aldehyde and epoxide oxygens are known to afford adducts with high *syn*-selectivity. Whereas selectivity in the cases where nucleophiles lack the latter ability, are governed by a Felkin-Ahn based transition state. The effect of the nature of the nucleophile, the

substitution pattern of the epoxide ring and presence of various additives has been extensively investigated and mode of asymmetric induction is well understood.

**2.3 Conformational preference of cyclopropyl-2-carboxaldehydes and ketones and its effect on the resulting selectivity achieved during nucleophilic additions.**

An understanding of the conformational preference of simple carbon analogs is essential in order to comprehend the origin of selectivity encountered during addition of the nucleophiles to heterocyclic carbonyls.

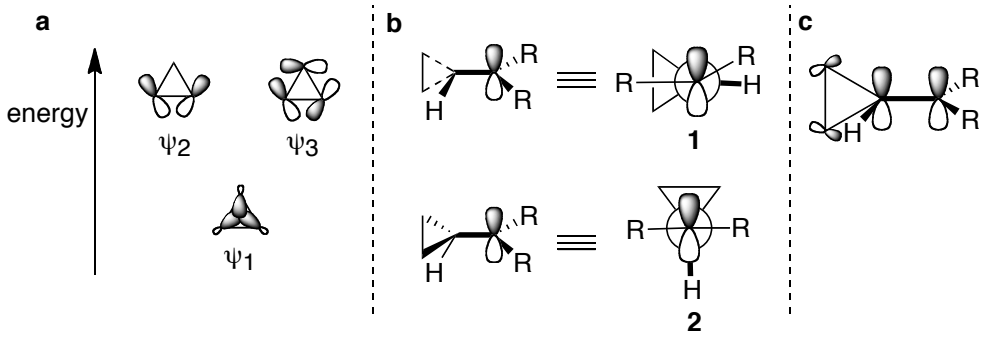


**Figure 2.2 a.** Walsh model. **b.** Conformational preferences of a cyclopropyl ring adjacent to π-system. **c.** Conformation allowing maximum overlap between π-system and cyclopropyl orbitals.

Cyclopropane consists of three $sp^2$ hybridized carbons atoms as represented by Walsh's model.[26] Molecular orbital diagram is illustrated in Figure 2.2a.[27] When attached to a π-system, a cyclopropyl ring behaves as a strong π-donor. The interaction between $\psi_2$ and $\psi_3$ with the adjacent π-system is maximized when the cyclopropyl ring

adopts a bisected conformation (1, Figure 2.2b) rather than a symmetrical arrangement (2, Figure 2.2b) with respect to the adjacent π-system. The bisected conformation allows for maximum overlap between the p-orbital on the cyclopropyl carbon and that of the adjacent π-system (Figure 2.2c).[27] In symmetric conformation (2, Figure 2.2b) on the other hand, the two orbitals are orthogonal. Thus, cyclopropyl ketones or aldehydes (Figure 2.3) preferentially exist in the bisected s-*trans* **2.6a** and s-*cis* **2.6b** conformations.[28]

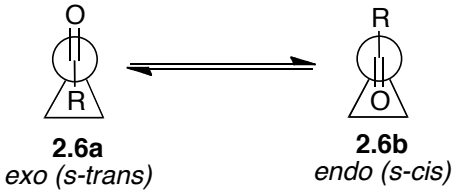


**Figure 2.3** Preferred bisected conformations of cyclopropyl-2-carboxaldehyde.

Nucleophilic additions to cyclopropyl carbonyl compounds have been systematically investigated[28-31] and the resulting selectivity during these transformations is shown to be governed by the more stable bisected conformation.[29,32]

**2.4 Precedence on nucleophilic additions to aziridine carbonyl compounds.**

A limited number of reports have explored reactions of organometallic reagents with aziridine carbonyl species. Addition of boron enolates to *N*-Boc *trans*-substituted aziridine-2-carboxaldehydes proceeds with superior *anti* selectivity.[33] Reductions of aziridine ketones with various reagents have led to similar results, i.e., the nucleophile

attacks via the *pro-anti* approach.[34,35] In both cases, the stereochemical outcomes were rationalized in terms of Felkin-Ahn transition states for attack on the carbonyl site (Figure 2.4a). It should be noted, however, that the latter precedent is not universally applicable; others have found the *pro-syn* approach to predominate under certain conditions.[36]

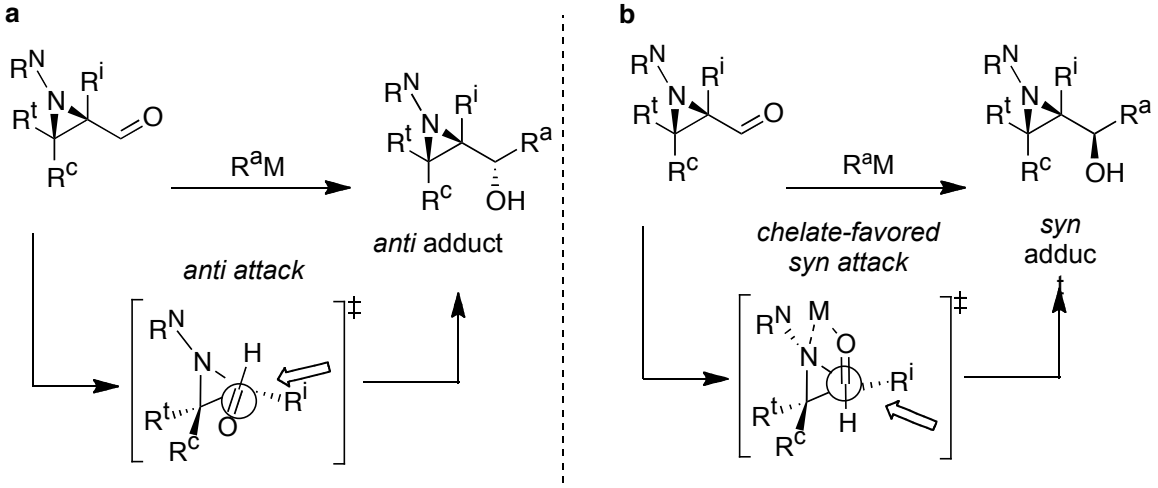


**Figure 2.4** a Felkin-Ahn model. b Chelation control model.

Investigating the addition of Grignard reagents to *N*-Boc-protected aziridine-2-carboxaldehydes, Righi and coworkers reported excellent *syn* selectivity with *trans* substrates, a result they attributed to N-centered chelation control (Figure 2.4b).[37] This selectivity was completely lost in the case of *cis* substrates, whose cyclic chelate intermediates the authors judged to be unfavorably strained. Contrarily, in a related study of Bn protected aziridine aldehydes,[38] Andres and coworkers observed high *syn* selectivity specifically in the case of *cis* substrates and invoked chelation control to

justify the selectivity. These two reports appear contradictory; more precisely, taken together, they suggest that chelation control and the resulting product selectivities are a function of both N-protecting group and substitution geometry.

## 2.5 Selectivity in Additions of Organometallic Reagents to Aziridine-2-Carboxaldehydes: Effects of Protecting Groups and Substitution Patterns.

Noting the limited number of studies on stereoselective additions of carbon nucleophiles to aziridine-2-carboxaldehydes, and intrigued by the widely varying diastereoselectivity in our own study of *N*-tosyl protected systems (Scheme 2.1), we recognized the need for a set of principles to rationalize observations and guide synthetic decisions. We therefore undertook a combined theoretical and experimental study of nucleophilic reagent additions to *cis*- and *trans*-substituted aziridine-2-carboxaldehydes with various N-substituents.

To establish a common reference framework, an initial set of detailed quantum chemical studies were carried out on truncated model systems. By exploring the ground state conformational preferences of the various substitution patterns, our aim was to develop not only useful insights, but also a simple procedure to routinely predict reactions' stereochemical outcomes.

To map the effects of electronic variations at nitrogen on reaction selectivity, we chose the common N-protecting groups: alkyl, alkoxycarbonyl, and alkylsulfonyl. In the abbreviated models used to simplify the theoretical analysis, these were methyl (Me), methoxycarbonyl (Moc), and methanesulfonyl (Ms) groups; the corresponding

experimental systems employed benzyl (Bn), *tert*-butoxycarbonyl (Boc) and toluenesulfonyl (Ts) groups. A simple alkyl or Bn group leaves the nitrogen comparatively electron rich and amine-like; Boc's moderate capacity as a π-acceptor and strong conformational preferences offer intermediate activation; and Ts is the most electron withdrawing but is less conformationally defined than Boc. The results of our study provide intuitive insight and a working model for controlling selective addition of organometallic reagents to aziridine-2-carboxaldehydes. Identified are the unique combinations of nitrogen protecting groups and aziridine substitution patterns that yield the highest stereoselectivity; interestingly, these are different for each of the N-protecting groups.

### 2.5.1 Results and discussion of computational studies:

To develop an understanding of the relevant conformational preferences and to set the stage for analysis of experimental results, fifteen model substituted aziridine-2-carboxaldehydes were studied via quantum chemical modeling.

**Table 2.4** Computationally calculated energy for truncated model systems.

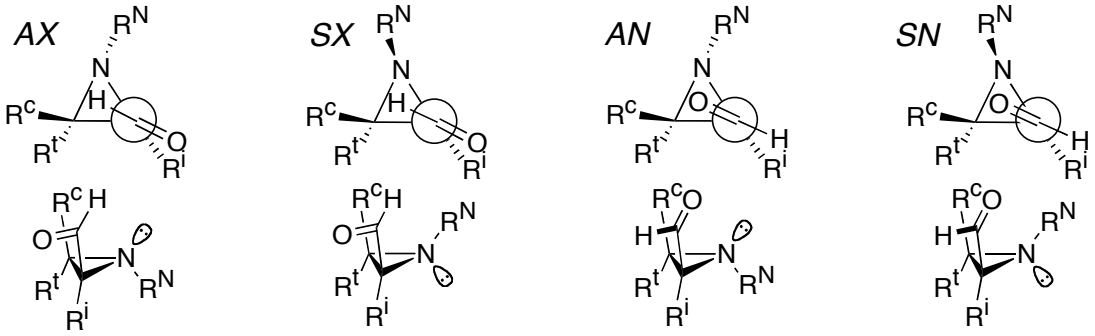


| Name | $R^N$ | $R^i$ | $R^t$ | $R^c$ | Lowest $E_a$ | $\Delta E_a$ to 2nd | 2nd Lowest $E_a$ | *AX*[b] | *SX*[b] | *AN*[b] | *SN*[b] |
|---|---|---|---|---|---|---|---|---|---|---|---|
| Me_*H3* | Me | H | H | H | *AX* | 1.42 | *AN* | **0.00** | 2.60 | 1.42 | 2.53 |
| Me_*Ipso* | Me | Me | H | H | *AX* | 0.44 | *SX* | **0.00** | 0.44 | 2.59 | 0.95 |
| Me_*Trans* | Me | H | Me | H | *SN* | 0.30 | *AX* | 0.30 | 0.31 | 1.66 | **0.00** |
| Me_*Cis* | Me | H | H | Me | *AX* | 0.48 | *AN* | **0.00** | 5.47 | 0.48 | 4.03 |
| Me_*23Di* | Me | Me | Me | H | *SX* | 0.19 | *SN* | 1.80 | **0.00** | 4.22 | 0.19 |
| Moc_*H3* | $CO_2Me$ | H | H | H | *SN* | 0.53 | *AX* | 0.53 | 0.93 | 1.76 | **0.00** |
| Moc_*Ipso* | $CO_2Me$ | Me | H | H | *SX* | 0.01 | *SN* | 0.28 | **0.00** | 2.37 | 0.01 |
| Moc_*Trans* | $CO_2Me$ | H | Me | H | *SN*[c] | 1.20 | *SX* | 1.32 | 1.20 | 2.32 | **0.00** |
| Moc_*Cis* | $CO_2Me$ | H | H | Me | *AX* | 0.21 | *AN* | **0.00** | 1.77 | 0.21 | 0.26 |
| Moc_*23Di* | $CO_2Me$ | Me | Me | H | *SN* | 0.23 | *SX* | 1.97 | 0.23 | 3.69 | **0.00** |
| Ms_*H3* | $SO_2Me$ | H | H | H | *AX* | 1.30 | *AN* | **0.00** | 2.06 | 1.30 | 4.72 |
| Ms_*Ipso* | $SO_2Me$ | Me | H | H | *SX* | 0.18 | *AX* | 0.18 | **0.00** | 2.23 | 3.35 |
| Ms_*Trans* | $SO_2Me$ | H | Me | H | *SX* | 0.50 | *AX* | 0.50 | **0.00** | 1.37 | 2.45 |
| Ms_*Cis* | $SO_2Me$ | H | H | Me | *AX* | 0.42 | *AN* | **0.00** | 5.84 | 0.42 | 6.66 |
| Ms_*23Di* | $SO_2Me$ | Me | Me | H | *SX* | 3.14 | *SN* | 4.03 | **0.00** | 5.95 | 3.14 |

[a]All energies shown in kcal/mol; [b]*AX*, *SX*, *AN*, and *SN* label the conformers as *Anti* or *Syn* (relationship of $R^N$ to CHO) and *eXo* or *eNdo* (orientation of CHO group relative to aziridine ring); [c]An *SN* conformation like that here in **Moc_*Trans*** is seen in the X-ray structure of related *trans N*-Boc analogue **2.11** (vide infra); [d]An *SX* conformation like that in **Ms_*23Di*** is seen in the X-ray structure of related *trans N*-Ts-2,3-disubstituted-2-carboxaldehyde analogue **2.25**.

Specifically, (a) Gas-phase DFT simulations of substrates' ground state conformations were run in hopes that the preferences uncovered would offer simple explanations for the experimental stereochemical outcomes; (b) Solvation effects of the $CH_2Cl_2$ reaction medium were simulated via single point SM8 calculations on the minima computed; (c) The validity of the gas-phase DFT energetic analyses was verified via comparison of a subset of the systems studied with G3(MP2) composite thermochemistry calculations; (d) Selected potential energy functions for aldehyde rotation and nitrogen inversion were also explored in several model aziridine-2-carboxaldehydes.

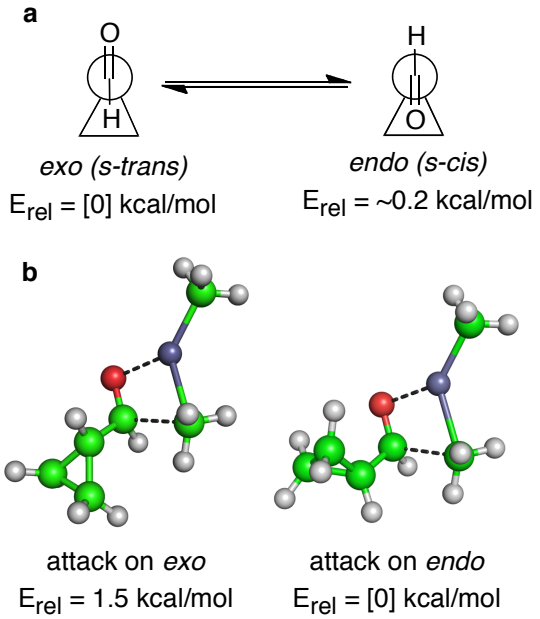


**Figure 2.5** (a) Bisected *exo* (*s-trans*) and *endo* (*s-cis*) conformations of cyclopropyl carbonyl systems. (b) B3LYP/6-31+G* optimized TS structures (relative energies with vibrational, thermal, and solvent corrections) for attack of $(CH_3)_2Zn$ on *endo* and *exo* conformations of cyclopropane-carboxaldehyde. For interpretation of the references to color in this and all other figures, the reader is referred to the electronic version of this dissertation.

All calculations were performed with the Spartan 08[39,40] software package, using the B3LYP functional,[41] the 6-31G* basis set,[42] and the SM8 solvation modeling scheme[43] to account for the effects of the $CH_2Cl_2$ solvent environment. To check on the performance of this DFT-based method, the G3(MP2) composite scheme was used; this method offers near-experimental accuracy for heats of formation and reaction energetics of small gas-phase organic molecules.[44]

*Conformational analysis of ground state aziridine-2-carboxaldehydes:* The model systems considered are shown in Table 2.4, together with energetic information on their preferred conformations and the energy gap (in kcal/mol) that separates each compound's lowest energy minimum from its next lowest conformation of a different category. Two binary choices define the four categories of conformations listed; these are (a) the relationship (*anti* or *syn*) between the N-substituent ($R^N$) and the aldehyde moiety; and (b) the rotamer orientation of the aldehyde carbonyl oxygen (*exo*, with hydrogen over the ring, or *endo*, with oxygen over the ring). This latter choice deserves comment here; the conjugation of carbonyl groups with adjacent cyclopropyl rings in the bisected *endo* (*s-cis*) and *exo* (*s-trans*) conformations has long been known (Figure 2.5a).[26,45,46] Like cyclopropane, the aziridine ring favors bisected conformations for attached carbonyl groups, leading to this simple *exo*/*endo* choice. This conjugative preference is surprisingly insensitive to the replacement of carbon with a heteroatom, in terms of preferred rotameric angle.[47] The $tH^iCCH^{CHO}$ dihedral angle values deviate only by ±15˚ relative to the 0˚ and 180˚ seen in cyclopropane carboxaldehyde. Nucleophilic additions to cyclopropyl carbonyl compounds have also been systematically investigated[28-31] and show selectivity often governed by the more stable bisected conformation.[28,29]

The above conformational choices are coded *A* vs. *S* (*Anti* vs. *Syn*), and *X* vs. *N* (*eXo* vs. *eNdo*), respectively, leading to the four categories *AX*, *AN*, *SX*, and *SN*. Where more

than four conformers exist due to $R^N$ rotations, the listed energies in the table represent the lowest energy conformer in each category.

**Table 2.5** B3LYP/6-31G*/SM8 $CH_2Cl_2$ vs. G3(MP2)/SM8 $CH_2Cl_2$ relative energies compared.

| Name | ***AX*** | | ***SX*** | | ***AN*** | | ***SN*** | |
|---|---|---|---|---|---|---|---|---|
| | DFT | (G3) | DFT | (G3) | DFT | (G3) | DFT | (G3) |
| Me_*H3* | **0.00** | ***0.00*** | 2.60 | *2.98* | 1.42 | *1.79* | 2.53 | *3.54* |
| Me_*Ipso* | **0.00** | ***0.00*** | 0.44 | *0.82* | 2.59 | *2.87* | 0.95 | *1.89* |
| Me_*Trans* | 0.30 | ***0.00*** | 0.31 | *0.26* | 1.66 | *1.80* | **0.00** | *0.75* |
| Me_*Cis* | **0.00** | ***0.00*** | 5.47 | *5.56* | 0.48 | *0.98* | 4.03 | *5* |
| Me_*23Di* | 1.80 | *1.32* | **0.00** | ***0.00*** | 4.22 | *4.08* | 0.19 | *1.01* |

As noted above, the model $R^N$ groups $CH_3$, $COOCH_3$, and $SO_2CH_3$ were chosen to simulate Bn, Boc, and Ts substituents, respectively. Even without inspecting the full conformer list, including $R^N$ rotamers, it is immediately evident that relatively few of the model substrates considered here have a strong structural bias toward a particular conformation. However, it is noteworthy that *the structures calculated to be most conformationally defined correspond to analogues with strong experimental stereoselectivities.* Also, in cases where it is low enough in relative energy, the *AN* conformation allows for chelation to exert further directing effects with Grignard and organozinc nucleophiles. Before delving into the significance of the conformational

findings in Table 2.4, several checks on the appropriateness of this level of calculation should be discussed. The 1.42 kcal/mol *AX* preference computed for **Me_*H3*** is consistent with the conformation assigned to *N*-*t*-butylaziridine-2-carboxaldehyde by Pierre, *et al.* on the basis of variations in the H-C-C(=O)-H $^1$H NMR coupling constant with temperature and solvent polarity.[48] Likewise, the close-lying energies calculated for **Me_*Trans*** conformations are consistent both with the invertomer distribution of 2-acetyl-*N*,3-dimethyl aziridine observed previously, and with our own findings for the closely related *trans*-*N*-benzyl-3-ethylaziridine-2-carboxaldehyde **2.9** discussed below.[49] As noted in Table 2.4, X-ray structures of *N*-Boc-*trans*-3-cyclohexylaziridine-2-carboxaldehyde **2.11** and *N*-Ts-*trans*-3-benzyloxymethyl-2-methylaziridin-2-carboxaldehyde **2.25**, the experimental analogues to **Moc-*Trans*** and **Ms-*23Di***, confirm the calculated minimum energy conformational assignments. Broader support is found in the G3(MP2) calculations on the *N*-methyl series of model substrates. As noted above, this level of calculation is designed to provide energetics comparable to experiment in quality. Table 2.5 compares their "$CH_2Cl_2$ solvated" enthalpies as calculated at the DFT and G3(MP2) levels. Although not a perfect match, the energy variations seen in the DFT results generally mirror the G3(MP2) data.

To translate the conformational preferences computed above into predictions regarding nucleophilic attack stereochemistry, some estimate of the intrinsic reactivities and stereoselectivities of the *exo* vs. *endo* CHO rotamer conformations must first be made. Then directing effects due to the roles of chelation and sterically interfering substituents can be explored.

*Carbonyl conformation: endo vs. exo:* Focusing on the steric demands of a carbon nucleophile alone, it might be expected that an *endo*-oriented carboxaldehyde conformer should be more reactive than *exo*, as attack along the Bürgi-Dunitz angle would be likely to encounter more interference approaching the *exo* conformer. However, an organometallic such as a Grignard or organozinc reagent likely follows a less open trajectory as its metal component coordinates to the increasingly negative carbonyl oxygen. Nonetheless, the above assumption is supported by B3LYP/6-31+G* calculations on the transition states for dimethylzinc attacking cyclopropane carboxaldehyde (Figure 2.5b). Although the substrate's ground state conformation is found to prefer the *exo* geometry by 0.1-0.2 kcal/mol (0.27 experimental),[50] the *endo* attack TS is favored over the *exo* by 1.7 kcal/mol (1.5 with vibrational, thermal, and solvation corrections), enough to create a >10:1 preference for the *endo* path at relevant reaction temperatures. Though further skewed by the aziridine nitrogen's own chelation and conformational dynamics, this steric bias toward attack on *endo* aldehyde conformations remains true for aziridine-2-carboxaldehydes where the substituent *ipso* to the aldehyde is hydrogen.

As is evident from Table 2.4, replacement of the *ipso* hydrogen with an alkyl group in the $R^i$ site has two notable effects on ground state conformations: (a) it adds steric bulk on the *trans* face which, in turn, decreases the *anti-syn* energy gap by shifting *anti* up in energy relative to the *syn* invertomers at nitrogen regardless of the nature of $R^N$; and (b) it adds a stereoelectronic preference for the *exo* over the *endo* aldehyde rotamer. Although the rational for the latter preference is not understood, the added invertomer

bias can be as large as 2-3 kcal/mol, while the aldehyde rotamer preference is in the 0.5-1 kcal/mol range. To illustrate, comparison of **Me_*H3*** vs. **Me_*Ipso*** models, both of which have *AX* lowest conformers, is instructive: (a) The energy changes for *N*-$CH_3$ inversion from *syn* to *anti* are shifted to favor the *syn* isomer upon adding the methyl group to go from **Me_*H3*** ($\Delta E_{SX \rightarrow AX}$ = -2.60 and $\Delta E_{SN \rightarrow AN}$ = -1.11) to **Me_*Ipso*** ($\Delta E_{SX \rightarrow AX}$ = -0.44 and $\Delta E_{SN \rightarrow AN}$ = +1.64). Thus the *ipso* $CH_3$ groups adds 2.16 and 2.75 kcal/mol, respectively, to the steric cost for the *N*-$CH_3$ to be on the *trans* face, balancing (but not completely overcoming) the preference for the *anti* forms. Analogous numbers for **Ts** model (**Ms** series) are 2.24 and 2.30 kcal/mol, quite similar to those seen for the **Me** set; in this case the *anti* preference is overcome, moving *SX* to the lowest energy spot. Interestingly, the **Moc** series is only shifted by 0.68 and 0.60, consistent with **Moc**'s strong preference (due to N-conjugation) for orientating its thinnest dimension toward vicinal substituents. (b) Comparisons analogous to those above, but comparing aldehyde rotamers are shifted as follows: $\Delta E_{AN \rightarrow AX}$ = -1.42 and $\Delta E_{SN \rightarrow SX}$ = +0.07 for **Me_*H3*** vs. $\Delta E_{AN \rightarrow AX}$ = -2.59 and $\Delta E_{SN \rightarrow SX}$ = -0.51 in **Me_*Ipso***. Thus, the *ipso* $CH_3$ group favors the *exo* rotamer by 1.17 and 0.58 kcal/mol, respectively; analogous value pairs for Moc and Ts systems are 0.86/0.94 and 0.75/0.67 kcal/mol.

But what of transition states? How does addition of an *ipso* alkyl group affect the relative energetics of the *endo* vs. *exo* attacks? As illustrated in Figure 2.5b, attack on the *endo* rotamer is favored over *exo* by 1.5 kcal/mol when the *ipso* substituent is hydrogen. But just as methyl substitution adds a bias favoring *exo* aldehyde rotamers in the ground

state structures, it also stabilizes the *exo* relative to the *endo* attack TS, leaving the two paths essentially equal in energy. Thus, *ipso* substitution is expected to both enhance the proportion of *exo* conformations and lower the barrier to attack on such forms, favoring product formation via *AX* and *SX* forms. Herein, we will refer to the latter phenomena as the '*ipso* effect' during our discussions.

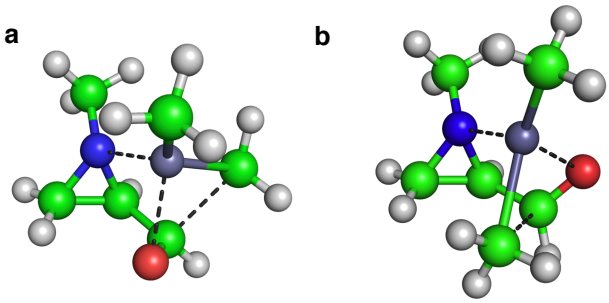


**Figure 2.6.** B3LYP/6-31+G* optimized TS structures (relative energies) for chelation-controlled attack on the *AN* conformer of the model compound **Me_*H3***. Notably, the *pro-anti* path (a) is calculated to be 1.9 kcal/mol higher in energy than the *pro-syn* path (b).

*Chelation effects:* Chelation between the aldehyde carbonyl and the organometallic's metal center may drastically alter the conformational energy landscape by selectively favoring the *AN* conformation (the only conformation of the four that is able to support chelation of the nitrogen with the aldehyde) provided that *AN* is not too much higher in energy than other rotamers. Meanwhile, the polarization further activates the carbonyl in this already reactive *endo* rotamer for *pro-syn* attack (Figure 2.6). Because of the

intimate involvement of solvent and reagent aggregation, it is difficult for theory to directly compare energies of chelating and non-chelating paths on an equal footing. However, between the competing *pro-syn* and *pro-anti* chelating paths calculated for dimethyl zinc attack on **Me_*H3*** in $CH_2Cl_2$ (Figure 2.6), the *pro-syn* is substantially favored, as its transition structure (TS) is closer to the ground state *AN* conformation with the CHO moiety bisecting the aziridine ring. In contrast, the CHO group in the *pro-anti* TS appears nearly perpendicular to either of the ground state bisecting conformers of the aldehyde. Noting that the aziridine-CHO rotational barrier in isolation is calculated to be 6 kcal/mol, this difference in conformations represents a substantial extra energy cost for the *pro-anti* attack. This finding concurs with the previously reported experiments and analysis of Pierre, *et al.* in which $CH_3Li$ and PhLi additions to *N-t*-butyl-aziridine-2-carboxaldehyde showed a strong preference for the *pro-syn* attack, despite the absence of any perturbing *cis* substituents.[36] As the experiments below illustrate, specific chelation effects are easily revealed by simple competition with multidentate ligands such as TMEDA.

*Steric effects of cis substituents:* It seems obvious that a *cis*-related substituent (either the group on C3 or the nitrogen invertomer with the protecting group *syn* to the aldehyde) should hinder approach of nucleophiles to the blocked face of the aldehyde carbonyl. However, such steric reasoning does not include the effects of polarity in the N-protecting groups, which may interact with the carbonyl group's dipole, orienting it and potentially modifying its reactivity. Such effects have been clearly observed in infrared studies focusing on the carbonyl group's resonance as a probe of conformational

preferences.[39] Similarly, in the case of the Moc substituent in **Moc_*Trans***, the favorable electrostatic interaction between the aldehyde's carbonyl oxygen and the Moc group's electrophilic center plays a role akin to metal chelation by the aziridine nitrogen, inducing a substantial preference for the strongly *pro-syn* selective *SN* conformation. The 'electronically chelated' Moc/aldehyde group (see Figure 2.10 for an illustration of the aforementioned interaction) places the Moc substituent *syn* to the aldehyde, which is in contrast to the benzyl protected aziridines that necessarily have the protecting group *anti* to the aldehyde as the result of the chelating arrangement of the nitrogen lone pair and the carbonyl group. This orientation effect is also seen in a related X-ray structure of the Boc-protected aziridine **2.11** described below. In the analogous framework, but with the negatively polarized Ts group in **Ts_*Trans***, the aldehyde carbonyl orients away, weakly favoring the *SX* conformation. When that conformation is more strongly preferred, as in **Ts_*23Di*** where the *ipso* substituent exerts extra *exo*-preference, *SX* dominates, the Ts group effectively blocks approach to the *pro-anti* face, and the resulting *pro-syn* addition yields *syn* products exclusively.

### 2.5.2 Results and discussion of experimental studies.

#### 2.5.2.1 *N*-Bn protected aziridine-2-carboxaldehydes:

Addition of ethylmagnesium bromide to *N*-benzyl-*cis*-3-ethylaziridin-2-carboxaldehyde **2.7** (Table 2.6, entry 1**)** provided the *syn*[34] adduct **2.8a** exclusively. The corresponding zinc reagent afforded a cleaner reaction with improved yield and similarly high *syn*:*anti* ratios (entry 2). However, addition of TMEDA, a strong chelator of magnesium ions,

lowered the *syn*-selectivity (entry 3). Thus, chelation of the organometallic's metal center by the electron rich nitrogen and the carbonyl oxygen appears likely to be the key to the selectivity (Figure 2.7a). To avoid eclipsing steric interactions, the *N*-Bn substituent in the *cis*-substituted substrate is expected to prefer the *anti* conformations, with the nitrogen atom lone pair on the same face as the aldehyde (the *AN* conformation). This arrangement ideally sets the stage for chelation to control the aldehyde carbonyl group's orientation.

**Table 2.6.** Addition of organometallic reagents to Bn protected *cis*-2-aziridine carboxaldehydes.

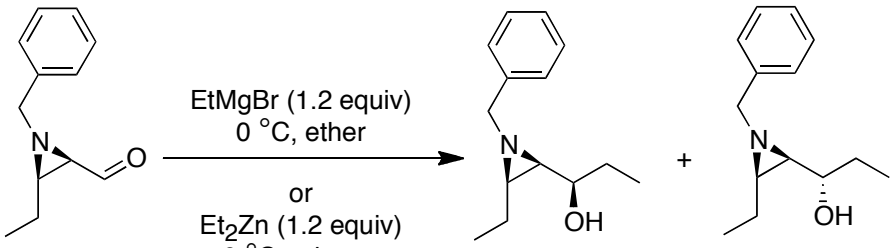


**2.7** **2.8a *syn*** **2.8b *anti***

| entry | reagent | additive | **a**:**b**[a] | yield |
|---|---|---|---|---|
| 1 | EtMgBr | --- | >99:1[b] | 75 |
| 2 | $Et_2Zn$ | --- | >99:1[b] | 85 |
| 3 | EtMgBr | TMEDA[c] | 62:38 | 65 |

[a]Diastereomeric ratios were determined by NMR. [b]Only *syn* compound was observed by NMR. [c]10 equiv of TMEDA was used.

In the resulting chelate, the *anti* approach should be blocked by the *cis* ethyl substituent leaving *syn* addition as the dominant path, consistent with the strong *syn* preference seen in these reactions (Figure 2.7b). It should be noted that chelation offsets the intrinsic preference for the *AX* conformer, which is favored by only ~0.5 kcal/mol in the modeled **Me_*Cis*** system. This line of reasoning is exactly how Pierre, *et al.* rationalized the strong stereoselectivity they observed for $LiAlH_4$ reductions of aziridinyl ketones in ether.[36]

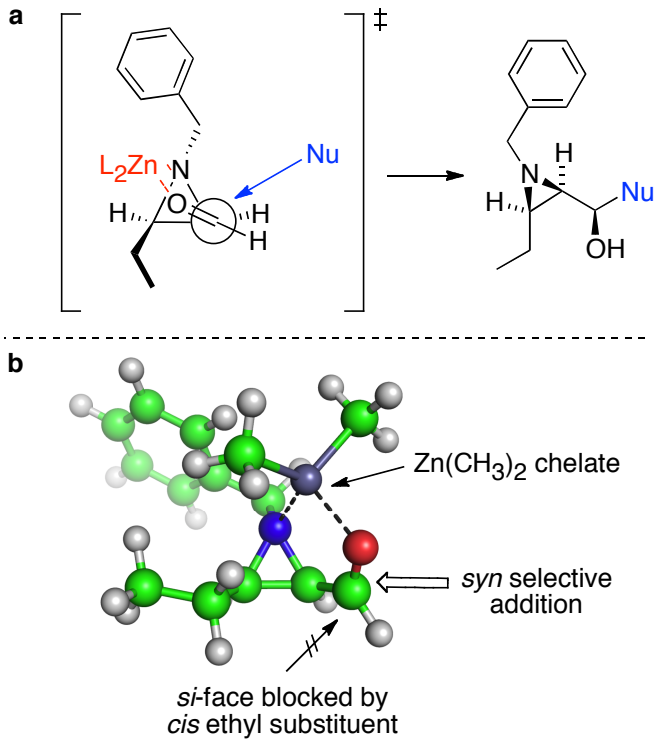


**Figure 2.7**. a) Proposed *syn* selective attack on *N*-benzyl-*cis*-3-ethylaziridine-2-carboxaldehyde **2.7** under chelation control. b) RHF/3-21G optimized structure of **2.7** chelating $Zn(CH_3)_2$. The structure rationalizes the observed high *syn* selectivity, as the *anti* approach is blocked by the *cis*-ethyl substituent.

Although the *cis* substituent clearly augments the observed selectivity,[38] it is not the only directing factor; even *N*-*t*-butylaziridine-2-carboxaldehyde, with no additional substituents and the *t*-butyl group oriented *trans* to the aldehyde, prefers *syn* reaction with $CH_3Li$ and PhLi, yielding products in *syn*:*anti* ratios of 4:1 and 2.5:1, respectively.[36] In related work, Noh, *et al.* reported a similar chelation-controlled strong preference for *syn* products in organometallic additions to an *N*-alkylated aziridine-2-carboxaldimine lacking any additional substituents on the ring.[51] Similarly, Hou *et al.* have reported additions of phosphite ions to *N*-benzyl-2-aziridinesulfinimines; as expected for a chelation controlled process, more Lewis acidic metal ions favored *syn* selectivity, which fell off when less coordinating ions such as $Na^+$ were used.[52]

Added TMEDA destroys the reaction's selectivity, presumably by blocking chelation in the Grignard reaction of **2.7** (Table 2.6, entry 3). Thus, an uncomplexed neutral aldehyde apparently has little intrinsic selectivity. Computational modeling on **Me_*Cis***, the model analogue (see Table 2.4) of **2.7**, shows a small energy difference between *endo* and *exo* –CHO rotamers for the *anti* series (the *syn* series are not considered here since they are energetically inaccessible). Thus, an incoming nucleophile could react with *pro*-*syn* and *pro*-*anti* faces of the aldehyde with nearly equal probability, even as it avoids the face shielded by the *cis* oriented ethyl group. But interestingly, despite the (presumably *anti*-selective) *AX* conformation being lower in energy (see Table 2.4) and thus prevalent, a 62:38 preference for *syn* addition is still seen; evidently the smaller population of *AN* outcompetes *AX*, supporting the notion that *endo* conformations are more reactive.

With chelation's observably important role in stereochemical control, it was natural to attempt a direct study of the chelating properties of the *N*-benzyl aziridine-2-carboxaldehydes by NMR. Unfortunately, the *cis* substituted *N*-benzylaziridine-2-carboxaldehyde **2.7** uniformly formed precipitates when combined with $MgBr_2$, $MgCl_2$, or $ZnCl_2$ in $CDCl_3$ or toluene-$d_8$. Evidently, association does occur with these Lewis acidic $MX_2$ species. However, in the Grignard reactions of **2.7**, no precipitates were noted. Perhaps when the X (Cl or Br) on the metal is small and polar, the resulting complex is also polar enough to aggregate and precipitate, whereas with an organic group in place of simple halide, the complexes remain soluble. In contrast to the *cis* case, the *trans* aziridine carboxaldehyde **2.9** (Table 2.7) was found to exist as a mixture of two invertomers in a 1:1.2 ratio. Structural assignments based on $^1$H NMR (NOE analysis) suggest that the favored invertomer is *syn* with benzyl and aldehyde substituents on the same side of the aziridine ring (e.g. structures *SX* or *SN* in Figure 2.8). This finding is in accord with conventional notions of steric demand that suggest the aldehyde should be smaller than the ethyl group (their respective A values are 0.56-0.8 and 1.79).[53] Furthermore, in *trans*-1,3-dimethyl-2-acetyl aziridine, Pierre *et al.* found a 3:1 preference for the *syn* conformation.[39] Also, the results stand in agreement with our DFT results for the model aziridine **Me_*Trans*** in simulated $CH_2Cl_2$, where for the respective *syn* and *anti* analogues of **2.9**, the *SN* conformer lies 0.3 kcal/mol lower than *AN*.

**Table 2.7.** Addition of organometallic reagents to Bn protected *trans*-2-aziridine carboxaldehydes.

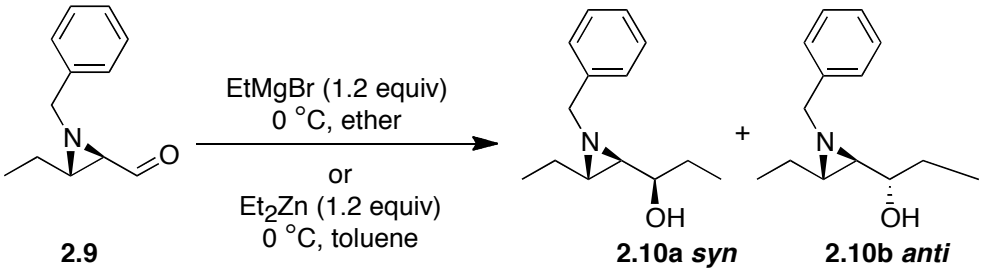


**2.9** **2.10a *syn*** **2.10b *anti***

| entry | reagent | additive | **a**:**b**[b] | yield |
|---|---|---|---|---|
| 1 | EtMgBr | --- | 55:45[c] | 75 |
| 2 | EtMgBr | TMEDA[d] | 55:45[c] | 85 |

[a]Exists as 55:45 mixture of invertomers at N on NMR time scale. [b]Diastereomeric ratios were determined by NMR. [c]S*yn* and *anti* compounds could not be separated. NMR analysis of product mixtures showed 55:45 mixture of unassigned stereoisomers. [d] 10 equiv of TMEDA was used.

Perhaps even more important for the reaction's stereochemical outcome is that the calculated energy difference between the model *endo* and *exo* aldehyde rotamers *SN* and *SX* (see Table 2.4) in **Me_*Trans*** is also quite small, suggesting little differentiation between access to the two faces of the aldehyde carbonyl. One might expect chelate formation to offer stereocontrol via the *AN* conformation of **2.9**. However, upon addition of ethyl magnesium bromide to compound **2.9**, an almost equimolar mixture of *syn* and *anti* adducts **2.10a** and **2.10b** was obtained (Table 2.7**,** entry 1).

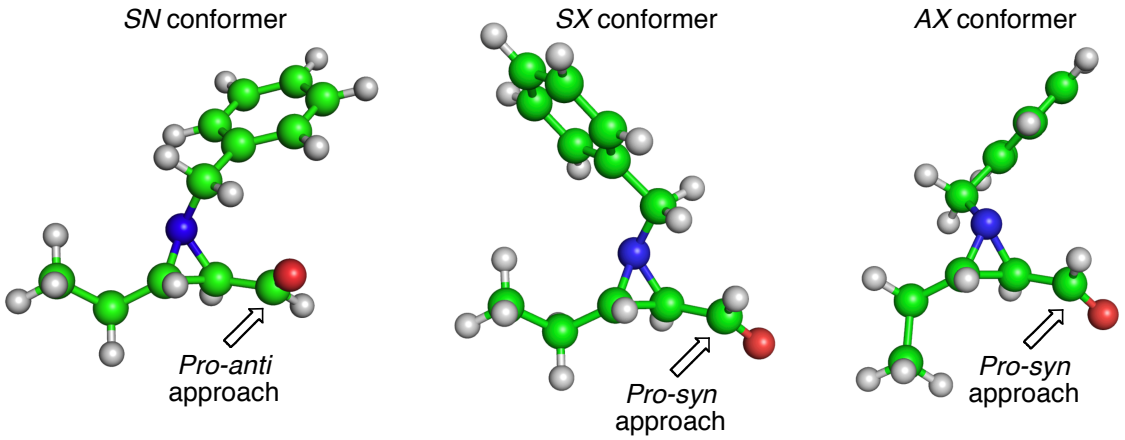


**Figure 2.8**. a) Energy-minimized conformers of Bn protected *trans* substrate **2.9**. Among these forms, both *pro-syn* and *pro-anti* faces are equally available. Of the **Me_*Trans*** model structures, the *SX* and *AX* conformers lie only 0.3 kcal/mol above the lowest energy *SN* form; B3LYP/6-31G*/SM8 energies of the actual structures above space them more widely but still compress their overall energy range to ca. 1 kcal/mol. In contrast, the potentially chelating *AN* conformer lies and additional 1.3 kcal/mol higher, which explains the apparent lack of chelation in additions to **2.9**.

Notably, this diastereomeric ratio was unaffected by addition of TMEDA (entry 2); thus, it appears that such complexation is unimportant in reactions with this substrate. This finding makes sense in light of the high relative energy calculated for the *AN* conformer, a significant point of contrast with the chelation-capable *cis* substrate **2.7**. There, chelation locks the carbonyl rotamer in the *AN* geometry, and the ethyl substituent offers strong stereo-differentiation by blocking one face of the aldehyde. We were thus surprised at first to find that, as with **2.7**, addition of Lewis acidic $MX_2$ to **2.9** quantitatively precipitated complexed aldehyde, removing it from solution in both toluene

and chloroform; evidently, these systems are capable of strong monodentate complexation, a conclusion supported by the structural studies of Bartnik, *et al.*[54]

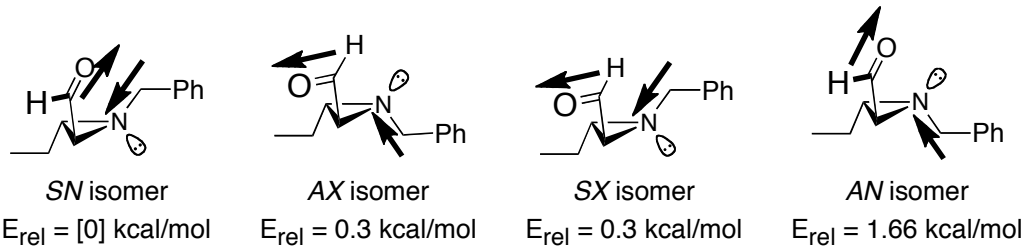


**Figure 2.9**. Dipole interactions between the Bn-N and CHO moieties in **2.9**, proposed to explain the relative order of stabilities of the conformers. Relative energies shown are those calculated for the model system **Me_*Trans***. Based on the simple steric size order CHO < Et, the *syn* systems *SN* and *SX* should be favored. But the added dipole repulsion in *AN* and attractions in *AX* and *SN* ultimately disfavor chelation in this system by pushing *AN* to relatively high energy. Presumably, the sterically unfavored *AX* isomer lies close in energy to *SX* as a result of *AX*'s favorable dipole interaction that counterbalances *SX*'s less than ideal dipole arrangement.

Notably, in the X-ray crystal structure of a $ZnBr_2$ complex of 2-benzoyl aziridine, [54] the heterocycle only serves as a monodentate ligand via nitrogen, despite the carbonyl group being in an *endo* conformation. This finding suggests that chelation in the aziridine-2-carbonyl framework is at most capable of modest energy lowering, on the same energy scale as conformational variations. For substrate **2.9**, our analysis points to the *SN* conformation (Figure 2.8) as the lowest energy form. Here, a favorable dipole-

dipole interaction between the Bn-N and aldehyde C=O moieties favors the *endo* orientation of the aldehyde carbonyl (Figure 2.9). This conformation itself would be expected to have a modest *syn* preference, but two low-lying *exo* forms (*SX* and *AX*) that are only a fraction of a kcal/mol higher in energy offer reactivity favoring the *anti* product. This equilibrating mix of conformations explains the unselective additions found both in the presence and absence of TMEDA additive (Table 2.7, entry 2). Thus, for *N*-benzyl-protected *trans* substrates, almost no *de* is seen in the mixture of *syn* and *anti* adducts as neither chelation nor a single strong candidate among free conformers is available to control Grignard addition stereochemistry.

#### 2.5.2.2 *N*-Boc protected aziridine-2-carboxaldehydes:

In contrast to the *N*-benzyl cases discussed above, where the *cis* substituted system was most selective, in the *N*-Boc series, it is the *trans* substrates that show the greatest selectivity. Addition of methyl magnesium bromide to Boc-protected *trans* 3-cyclohexylaziridine-2-carboxaldehyde **2.11** led exclusively to the formation of *syn*[55] alcohol **2.12a** (Table 2.8, entry 1).

**Table 2.8.** Addition of organometallic reagents to Boc protected *trans*-2-aziridine carboxaldehydes.

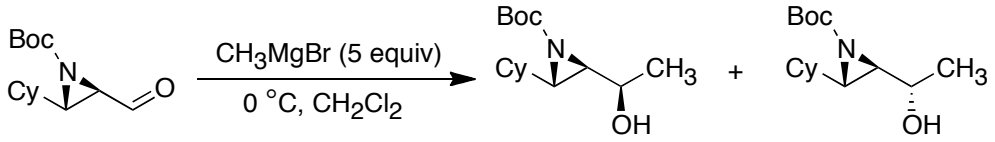


**2.11** **2.12a** *syn* **2.12b** *anti*

| entry | additive | **a**:**b**[a] | yield |
|---|---|---|---|
| 1 | --- | >99:1[b] | 85 |
| 2 | --- | >99:1[b,c] | 83 |
| 3 | TMEDA[d] | >99:1[b] | 80 |
| 4 | $MgBr_2 \cdot OEt_2$[e] | >99:1[b] | 78 |

[a]Diastereomeric ratios were determined by NMR. [b] Only *syn* compound was observed by NMR. [c]Reaction was carried out at -78 ºC. [d]10 equiv of TMEDA was used. [e]2.5 equiv of freshly prepared $MgBr_2 \cdot OEt_2$ was used.

To our surprise, despite the N-activation expected from the Boc group, ring opened products were not observed during these additions even near ambient temperatures; comparable yields and selectivities of product **2.12a** were obtained at 0 ºC and at -78 ºC (Table 5, entry 2). Addition of strong chelating reagents such as TMEDA or Lewis acids such as $MgBr_2 \cdot OEt_2$ had no effect on the product isomer distribution; in fact, the *anti* addition compound **2.12b** was never seen in any of the reaction conditions studied, as confirmed via independent Mitsunobu conversion of **2.12a** to **2.12b** (see the supporting information) and spectroscopic analysis. Thus, in contrast to the *N*-benzyl series, for the

*N*-Boc aziridine-2-carboxaldehydes, it is the *trans* substrates that shows excellent *syn* selectivity in a non-chelation controlled Grignard addition (Table 2.8, entries 3 and 4). This finding is at odds with a previous report[37] where a chelate is suggested between the nitrogen lone pair, the aldehyde carbonyl oxygen and the magnesium atom.

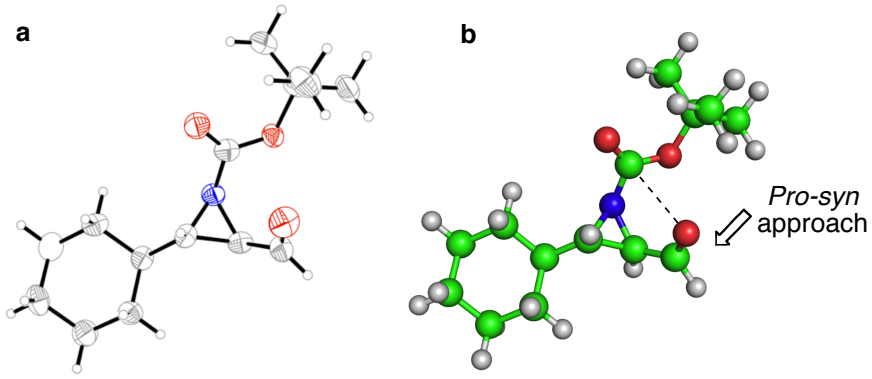


**Figure 2.10**. Comparison of the crystal structure of **2.11** (a) with its energy minimized model (b) illustrates excellent similarity. Both structures indicate the *SN* isomer as the most stable conformation. The dotted line highlights the favorable electrostatic arrangement of the aldehyde with the Boc carbonyl (electrostatically chelated).

However, the observed failure of additives to alter selectivity ratios argues against such a scenario. Though the Boc group's carbonyl oxygen could possibly offer a coordination site to participate in chelation, the unfavorable 7-membered ring size and the Boc group's strong preference for conformations that maintain conjugation between the N lone pair and the Boc carbonyl make chelation appear unlikely.

This issue is further illuminated by the X-ray crystal structure of Boc-protected *trans* substrate **2.11** (Figure 2.10a), in which the Boc and carboxaldehyde moieties are in the

*SN* conformation. Interpretation of crystal structures as models for relevant solution conformations of reactive species must be approached skeptically,[56] due to crystal packing interactions and the absence of solvation effects. But this relatively rigid and hydrophobic compound is only capable of modest dipole-dipole and van der Waals interactions in the lattice, so its internal structural preferences would likely dominate the conformation that crystallizes. Also, for both the actual substrate **2.11** and, more rigorously, on our model system **Moc_*Trans***, calculations find a strong preference for the same conformation that is found in the X-ray structure, as shown in Figure 2.10b. The contact distance (2.8 and 2.9 Å for X-ray and calculated structures, respectively) between the aldehyde oxygen and the Boc carbonyl carbon is substantially below van der Waals contact (3.2 Å), suggesting a favorable interaction. This notion is reinforced by the observation of pyramidalization at the Boc carbon; the N-C=O-O torsion angle is compressed (172˚ exp.; 173˚ theory) from the expected 180˚, suggesting the beginning of a Bürgi-Dunitz-like attack trajectory and the corresponding electrophilic activation of the aldehyde carbonyl.[57] The effect of this aldehyde-Boc dipole-dipole attraction is to favor both the *endo* orientation of the aldehyde and the N-invertomer with the Boc group *cis* to the aldehyde moiety; i.e. the *SN* conformation. Like the chelate structure invoked for addition to *cis*-Bn system **2.7**, this *SN* form favors attack on the more accessible and reactive *pro-syn* face of the aldehyde yielding the observed high selectivity (compare Figures 2.7b and 2.10b to note similarities in conformation and the resulting face selectivity).

**Table 2.9.** Addition of organometallic reagents to Boc protected *cis*-2-aziridine carboxaldehyde.

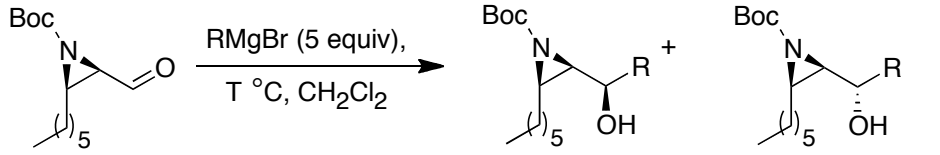


**2.13**

**2.14a-$C_2$H** *syn*
**2.14a-Ph** *syn*

**2.14b-$C_2$H** *anti*
**2.14b-Ph** *anti*

| entry | R | T | additive | **a**:**b**[a] | yield |
|---|---|---|---|---|---|
| 1 | $C_2$H | 0 | --- | 59:41[b] | 53 |
| 2 | $C_2$H | 0 | TMEDA[c] | 50:50[b] | 51 |
| 3 | $C_2$H | 0 | $ZnCl_2$[d] | 70:30[b] | 60 |
| 4 | $C_2$H | -78 ºC | --- | 52:48[b] | 50 |
| 5 | Ph | 0 | --- | 90:10 | 55 |
| 6 | Ph | 0 | TMEDA[c] | 61:39 | 52 |
| 7 | Ph | -78 ºC | --- | 88:12 | 49 |

[a]Diastereomeric ratios were determined by NMR. [b]Stereochemistry of *anti* alcohol was confirmed by X-ray crystallography. [c]10 equiv of TMEDA was used. [d]2.5 equiv of anhydrous $ZnCl_2$ was used.

The case of Boc protected *cis* aziridine-2-carboxaldehyde is less clearcut than the *trans* in terms of selectivity; here, addition of Grignard reagents resulted in moderate yields with variable low to high *syn* selectivity (Table 2.9). Ring opening products were frequently observed when the reaction was initiated at room temperature. As a result,

Grignard additions were run at 0 ºC and then slowly warmed to room temperature. Notably, *syn*-selectivity improved as the size of the nucleophile increased (compare entries 1 vs. 5).

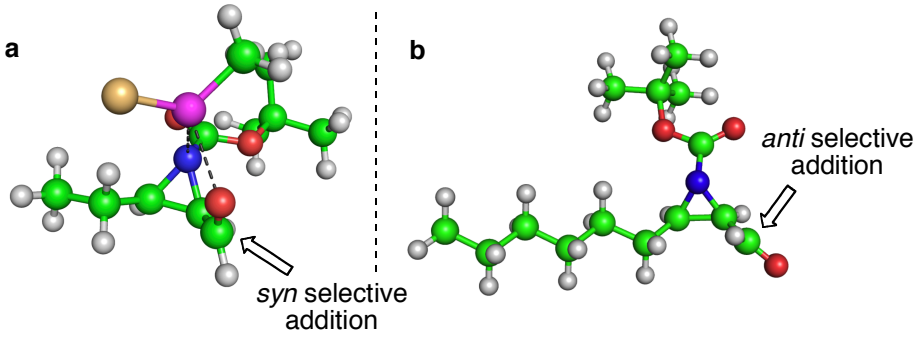


**Figure 2.11**. a) Energy minimized chelated *AN* conformation of the Boc protected *cis*-aziridine would favor *syn* selective addition (pictured with MeMgCl). b) The energy minimized *exo* isomer (*AX*) is not capable of chelations and would favor the *pro-anti* approach of the nucleophile.

Chelation appears to exert weak effects on this addition; formation of the Lewis acidic dialkyl zinc[15,58] reagent (Table 2.9, entry 3) led to a modest increase in *syn*-selectivity, while addition of TMEDA decreased it (entries 2 and 6). Simple steric arguments suggest that the Boc protecting group should be situated *trans* to the aziridine substituents. Our modeling studies agree, but find only small energy differences (0.1-0.5 kcal/mol) among the *AX*, *AN*, and *SN* conformers for the **Moc_*Cis*** model system. Though the *AX* conformer is lowest, *AN* and *SN* are only 0.2-0.3 kcal/mol higher in energy. Thus, two factors seem to be relevant in this system: (a) Weak chelation

between CHO and N in the *AN* conformer shifts the proportions of nearly equienergetic conformers toward those that favor the *syn* products. (b) Larger nucleophiles discriminate more strongly against *exo* conformers (*AX* in this case) than smaller nucleophiles, since presumably the *exo* rotamer is harder to attack, as discussed above (Figure 2.6b). Thus, the greater selectivity seen with the larger nucleophile suggests that the *endo* conformers *AN* and *SN* dominate those additions. Interestingly, the favorable dipole-dipole interaction between the aldehyde carbonyl and the Boc group appears almost completely to offset the steric effects of the *cis* hexyl sidechain, placing the *SN* invertomer only 0.3 kcal/mol above *AX* in the **Moc_*Cis*** model, and 0.4 kcal/mol higher in **2.13** itself. This last finding highlights the favorable aldehyde-Boc dipole-dipole interaction seen above in the *trans* case to control both ground state conformation and addition stereochemistry.

Formation of a cyclic chelate (Figure 2.11a) with the metal of methylmagnesium chloride coordinated between nitrogen and the aldehydic oxygen might explain the modest preference towards *syn* addition product. But here, though it remains pyramidalized due to being in a three-membered ring, the somewhat delocalized carbamate nitrogen would only be capable of weak binding at best, unlike the case in the *N*-Bn *cis* substrate **2.7**, where chelation is clearly controlling.

**Table 2.10.** Addition of organometallic reagents to Boc protected 2,3-disubstituted-2-aziridine carboxaldehydes.

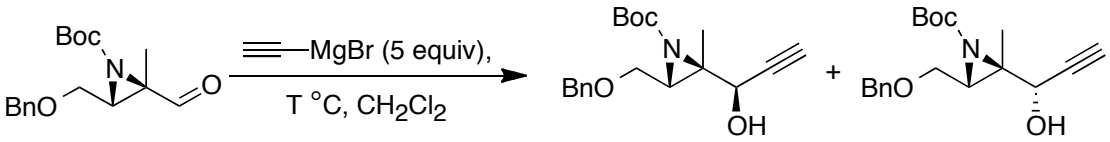


**2.15** **2.16a** *syn* **2.16b** *anti*

| entry | T | additive | **a**:**b**[a] | yield |
|---|---|---|---|---|
| 1 | 0 ºC | --- | 85:15[b] | 85 |
| 2 | 0 ºC | TMEDA[d] | 85:15[b] | 72 |
| 3 | -78 ºC | --- | 60:40[b] | 51[c] |
| 4 | -78 ºC | TMEDA[d] | 71:29[b] | 48 |

[a]Diastereomeric ratios were determined by NMR. [b]Stereochemistry was determined as discussed in SI; [c]Conversion = 79%; for all other entries, conversion = 100%. [d]10 equiv of TMEDA was used.

As a result, transition states based on the *AX* conformation of the aldehyde may compete; with the *cis* substituent blocking approach from the *pro-syn* face, these conformations should lead to predominantly *anti* addition (Figure 2.11b). Thus the opposing effects of weak chelation-favored *endo*, aldehyde-Boc attraction, and energetically close-lying *exo* aldehyde orientations may explain the limited selectivity found in these additions. In the case of Boc-protected 2,3-disubstituted aziridine-2-carboxaldehyde **2.15**, the reaction occurred with moderate to good *syn* selectivity. Both reactivity and conversion rates were found to drop off at lower temperature as seen with

the *cis* substrates (Table 2.10, entries 3, 4). Addition of TMEDA also showed temperature dependent selectivity effects, enhancing *syn* adduct formation at -78 ºC (Table 2.10, entry 4) but not at 0 ºC (entry 2).

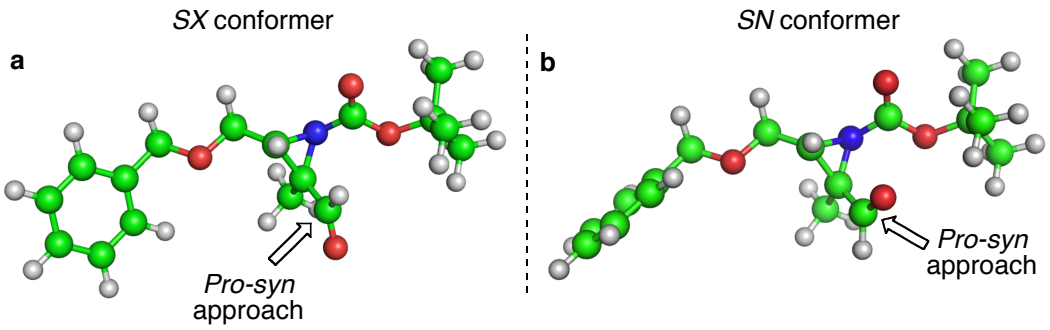


**Figure 2.12.** Low energy conformers of **2.15** showing near isoenergetic (a) *SX* (0.23 kcal/mol) and (b) *SN* (0 kcal/mol) -CHO rotamers [note these energies are for the **Moc-*23Di*** modeled *SX* and *SN* isomers].

The lowest energy calculated conformation of **2.15** has both the Boc and aldehyde groups disposed on the same side of the ring, but between the competing effects of the alpha substituent, which favors the *exo* rotamer (Figure 2.12a), and the dipole-dipole interaction with the Boc group, which favors the *endo* rotamer (Figure 2.12b), there is little ground state conformational preference. The temperature effect disclosed in Table 2.10 seems counterintuitive. We speculate, however, that the higher *syn*/*anti* ratio at higher temperatures might be due to an increase in population of the highly *syn*-selective *SX* isomer with increasing temperature. Based on the energetics of the model **Moc-*23Di*** system, the slightly lower energy *SN* isomer should predominate (Figure 2.12). But if the *SX* isomer had both higher reactivity and strong *syn*-selectivity (as

expected due to the Boc group's shielding the *pro-anti* approach), its contribution to product formation would grow quickly with increasing temperature. As noted earlier, *ipso* alkyl substitution enhances the reactivity of *exo* vs. *endo* aldehyde rotamers; thus *SX* reactivity would be enhanced by the methyl substitution at the *ipso* position (see discussion of *ipso* effect above). At -78 ºC the less *syn* selective *SN* isomer would dominate a) due to the decreased temperature and b) due potentially to Lewis acid amplification of the Boc group's pseudo-chelating interaction with the aldehyde.[25] The latter notion is further supported by the results for TMEDA addition at -78 ºC, which increases the *syn*:*anti* product ratio, presumably by disrupting the above proposed *SN*-supporting complexation.

#### 2.5.2.3 *N*-Ts protected aziridine-2-carboxaldehydes:

Grignard addition to Ts protected *cis*-2-aziridine carboxaldehyde was accompanied by the undesired nucleophilic aziridine ring opening. In order to suppress such reactions, it was crucial to carry out the addition at -78 ºC. The *cis* substrate **2.17** exhibited poor reactivity towards nucleophilic addition at the aldehyde carbonyl at this temperature. Conversion was low even after adding excess (10 equiv) Grignard reagent. In all cases, the desired alcohol was either impossible to isolate, or if isolable, was recovered in low yield (Table 2.11, entry 2). In an attempt to promote reaction by Lewis acid activation, $MgBr_2 \cdot OEt_2$ was added. In this case, higher yields of the alcohol products were isolated (entry 4), but no higher selectivity between *syn* and *anti* adducts was observed than in all the other cases.

**Table 2.11.** Addition of organometallic reagents to Ts protected *cis*-2-aziridine carboxaldehydes

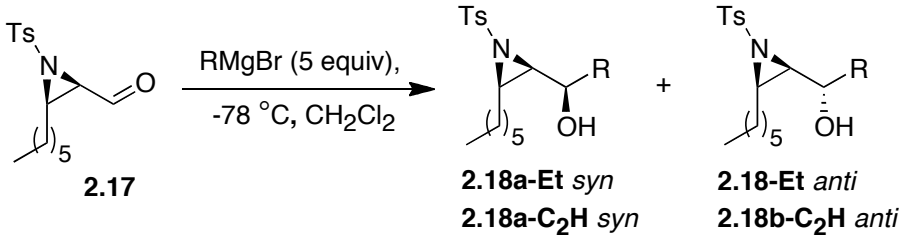


**2.17**

**2.18a-Et** *syn*
**2.18a-$C_2$H** *syn*

**2.18-Et** *anti*
**2.18b-$C_2$H** *anti*

| entry | R | additive | **a**:**b**[a] | yield |
|---|---|---|---|---|
| 1 | Et | --- | 50:50 | ND[b] |
| 2 | $C_2$H | --- | 56:43 | 20 |
| 3 | $C_2$H | TMEDA[c] | 50:50 | ND[b] |
| 4 | $C_2$H | $MgBr_2$•$OEt_2$[d] | 50:50 | 85 |

[a]Diastereomeric ratios were determined by NMR. [b]Ratios and yield could not be determined due to undesired side reaction products. [c]10 equiv of TMEDA was used. [d]2.5 equiv of freshly prepared $MgBr_2$•$OEt_2$ was used.

The product ratios were not altered under chelating or non-chelating conditions, which clearly argues against the involvement of a chelated transition state. As observed previously with Boc protected *cis*-aziridine-2-carboxaldehydes, only one invertomer needs to be considered, as the protecting group is situated *trans* to the substituent. Though the lowest energy calculated conformation is *exo*, multiple *exo* and *endo* conformations lie within 0.5 kcal/mol of the lowest form, differing only in the rotameric orientations of ethyl and tosyl groups. Thus both faces of the carbonyl are expected to

be equally prone towards nucleophilic attack, which explains the lack of diastereoselectivity.

**Table 2.12.** Addition of organometallic reagents to Ts protected *trans*-2-aziridine carboxaldehyde.

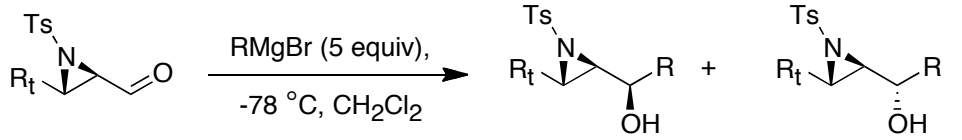


**2.19**, $R_t$ = *n*-hexyl
**2.21**, $R_t$ = *n*-propyl
**2.23**, $R_t$ = $CH_2OBn$

**2.20a** *syn* **2.20b** *anti*
**2.22a** *syn* **2.22b** *anti*
**2.24a-$C_2$H** *syn* **2.24b-$C_2$H** *anti*
**2.24a-Ph** *syn* **2.24b-Ph** *anti*

| entry | substrate | R | additive | **a**:**b**[a] | yield |
|---|---|---|---|---|---|
| 1 | **2.19** | $C_2H$ | --- | 70:30 | 76 |
| 2 | **2.19** | $C_2H$ | TMEDA[c] | 70:30 | 73 |
| 3 | **2.19** | $C_2H$ | $MgBr_2$•$OEt_2$[d] | 69:31 | 75 |
| 4 | **2.21** | $C_2H$ | --- | 70:30 | 81 |
| 5 | **2.21** | $C_2H$ | $MgBr_2$•$OEt_2$[d] | 72:28 | 69 |
| 6 | **2.23** | $C_2H$ | --- | 67:33 | 71 |
| 7 | **2.23** | Ph | --- | >99:1 | 85 |

[a]Diastereomeric ratios were determined by NMR. [b]Freshly prepared $MgBr_2$•$OEt_2$ was used. [c]10 equiv of TMEDA was used. [d]2.5 equiv of freshly prepared $MgBr_2$•$OEt_2$ was used.

Addition of Grignard reagents to *trans* substituted *N*-Ts-aziridine-2-carbaldehydes proceeded with moderate to excellent *syn* selectivity and good yields (Table 2.12**,** entries 1-7). Nucleophilic ring-opening reactions in this case were completely suppressed at -78 ºC. Chelation appears to play no role in these reactions as addition of $MgBr_2$•$OEt_2$ (entry 3) or TMEDA (entry 2) had no remarkable effect either on selectivity or yield. In the calculated minimum energy conformation of **2.21** (Figure 2.13) the aldehyde moiety has a strong preference for the *exo* orientation. The **Ms-*Trans*** models indicate that the *SX* isomer is 0.5 kcal/mol more stable than the *AX* isomer. As such, the bulky tosyl group in the *SX* isomer blocks one face of the carbonyl and directs the nucleophile to approach from the opposite direction, thus yielding the *syn* addition product.

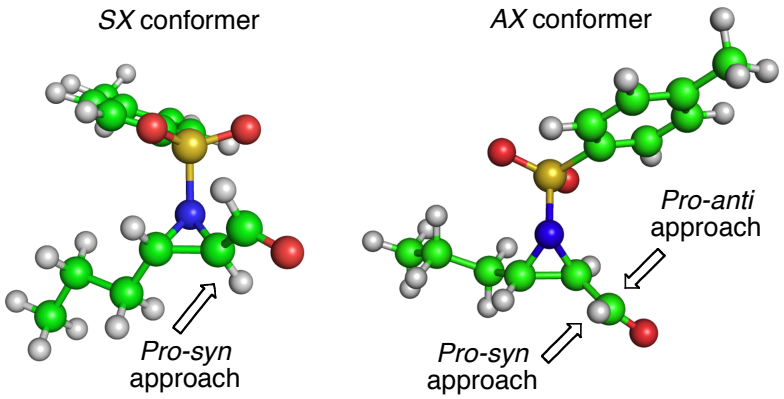


**Figure 2.13.** The lower energy *SX* conformation of **2.21** is *syn* selective due to steric blocking afforded by the Ts protecting group. The *AX* conformer exhibits less steric bias and thus would reduce the overall stereoselectivity. The modest selectivity in Ts protected *trans*-aziridine-2-carboxaldehyde could arise from the energetically close lying *SX* and *AX* conformers.

On the other hand, the *AX* isomer is less *syn* selective, owing to the fact that the Ts group is on the opposite face of the aziridine ring. This is presumably the cause for the lowered overall *syn/anti* product ratios. With this in mind, we hypothesized that increasing the size of the incoming nucleophile should increase the stereo-differentiation since the *pro-anti* approach of the *AX* isomer would be sterically retarded. Indeed, addition of phenyl magnesium bromide to substrate **2.23** afforded exclusively the *syn* adduct **2.24a-Ph** in good yield (Table 2.12, entry 7).

**Table 2.13.** Addition of organometallic reagents to Ts protected 2,3-disubstituted-2-aziridine carboxaldehyde.

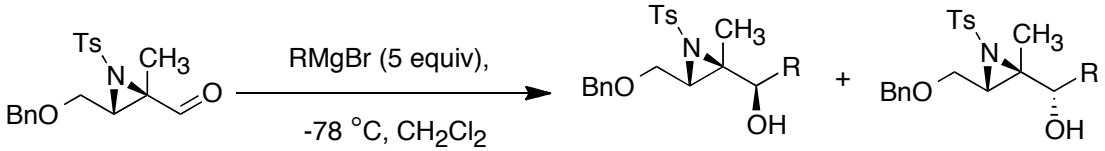


**2.25**

**2.26a-$C_2H$** *syn*
**2.26a-Ph** *syn*

**2.26b-$C_2H$** *anti*
**2.26b-Ph** *anti*

| entry | R | additive | **a**:**b**[a] | yield |
|---|---|---|---|---|
| 1 | $C_2H$ | --- | >99:1[b,c] | 92 |
| 2 | $C_2H$ | $MgBr_2 \cdot OEt_2$[d] | >99:1[b,c] | 81 |
| 3 | $C_2H$ | TMEDA[e] | >99:1[b,c] | 79 |
| 4 | Ph | --- | >99:1[b,c] | 85 |

Diastereomeric ratios were determined by NMR. [b]Only *syn* isomer was seen by NMR. [c]Stereochemistry was confirmed by X-ray. [d]2.5 equiv of freshly prepared $MgBr_2 \cdot OEt_2$ was used. [e]10 equiv of TMEDA was used.

Both high yield and exceptional *syn*-selectivity were achieved with 2,3-disubstituted 2-aziridine carboxaldehyde **2.25** (Table 2.13). Similar to the *trans* system, selectivity was not at all affected by TMEDA (entry 3) or $MgBr_2 \cdot OEt_2$ (entry 2) addition. As in the *trans* case, the energy-minimized conformation (Figure 2.14a) orients the aldehyde carbonyl *exo*, such that the tosyl group blocks the *pro-anti* face of the carbonyl, favoring the *syn*-selective approach of the nucleophile. Based on **Ms-*23Di*** models, the *SX* isomer is by far the most stable conformation.

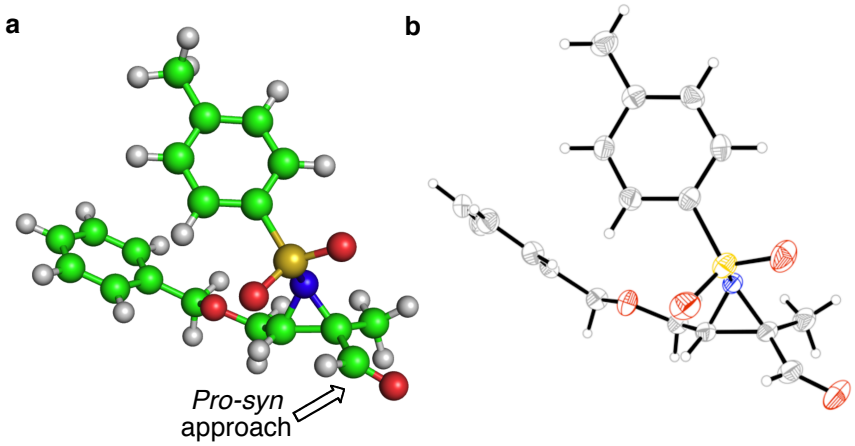


**Figure 2.14.** Comparison of the molecular structure of **2.25** as determined by X-ray diffraction with the lowest energy B3LYP/6-31G* optimized aziridine conformer of **2.25**. The **Ts_*23Di*** model structure shows an analogous *SX*-type lowest conformation.

The high *exo* tendency is not only due to the Ts protecting group, but also, as described above, the result of the *ipso* methyl substitution. The highly favored *syn* orientation, as expected, originated from the nitrogen atom adopting the necessary invertomer to avoid steric clash with the two substituents on the *anti* face of the aziridine ring. The crystal

structure obtained for aziridine-2-carboxaldehyde **2.25** (Figure 2.14b) is in close agreement with our optimized structures, supporting the above rationalization of this substrate's strong conformational preference and reaction stereospecificity.

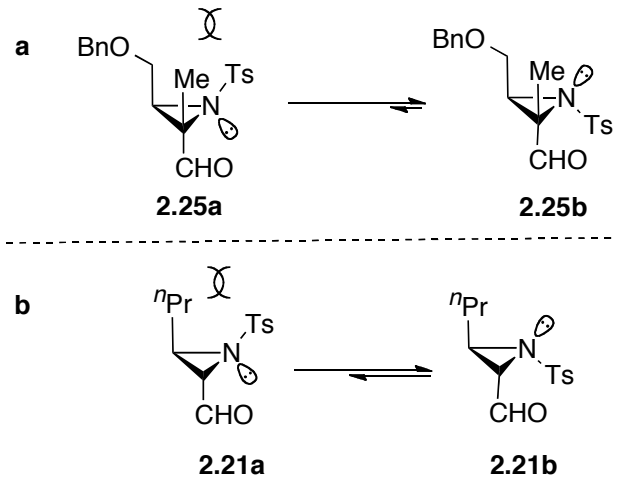


**Figure 2.15**. a) N-Invertomers of Ts protected 2,3-disubstituted-2-aziridine carboxaldehyde. b) N-Invertomers of Ts protected *trans* aziridine aldehyde.

The structural similarity between the most stable ground state conformations calculated for *trans* aziridines **2.19-2.23** and 2,3-disubstituted aziridine-2-carboxaldehyde **2.25** does not entirely justify the exceptional *syn*-selectivity observed in the case of 2,3-disubstituted aziridine-2-carboxaldehyde. The extra methyl substituent at the alpha position clearly makes a large difference in yield and level of stereoselection. A careful analysis of energy minimized conformations for **2.21** and **2.25** suggests that the difference in stereoselectivity is a result of two factors, both of which favor a more defined ground state conformation in **2.25** as compared to **2.21**. These factors are that (a) the tosyl group is sterically limited to a *syn* relationship with the aldehyde by the two

alkyl substituents on the opposite ring face; and (b) the methyl group alpha to the aldehyde favors the *exo* aldehydic rotamer. Figure 2.15 illustrates the expected invertomer equilibria for **2.21** and **2.25**, based on the energies calculated for the *syn* and *anti* (specifically, *SX* and *AX*) conformations of model compounds **Ms_*Trans*** and **Ms_*23Di*** respectively. As expected, *syn* invertomers are favored in both cases, but the *AX*-*SX* ΔG difference is significantly larger (4.1 vs. 0.58 kcal/mol; see Table 2.4) for **Ms_*23Di*** than for **Ms_*Trans***, and hence by analogy for **2.25** vs. **2.21**. While the steric bias toward *syn* (Figure 2.15a) in **2.25** is straightforward, that in **2.21** results from a delicate balance between *n*-alkyl and CHO groups as substituents *cis* to the Ts group. The 0.58 kcal/mol calculated *anti*-*syn* energy difference calculated for **Ms-*Trans*** predicts an invertomer ratio of 2.3:1 at 23 ºC. Because the barrier to nitrogen inversion is higher in aziridines than in other pyramidal nitrogen heterocycles, their invertomer spectra can readily be resolved in low-temperature NMR studies.[59-66] We therefore resorted to dynamic $^{1}$H NMR measurements to explore the conformational behaviors of the *trans* and 2,3-disubstituted aziridine-2-carboxaldehydes **2.21** and **2.25** at different temperatures (Figure 2.16). In the case of **2.25**, resonances displayed essentially identical line shapes at temperatures from 25 to -70 ºC, confirming the exclusive presence of one conformation (presumably **2.25**-*SX* in Figure 2.15a), which is expected (see Figure 2.16a vs. 2.16b for NMR spectra). In contrast, **2.21** showed broadening of most peaks as a function of lowering the temperature (Figure 2.16c vs. 2.16d). Of particular interest is the aldehydic resonance, which showed considerable broadening upon cooling and eventually exhibited decoalescence below -64 °C.

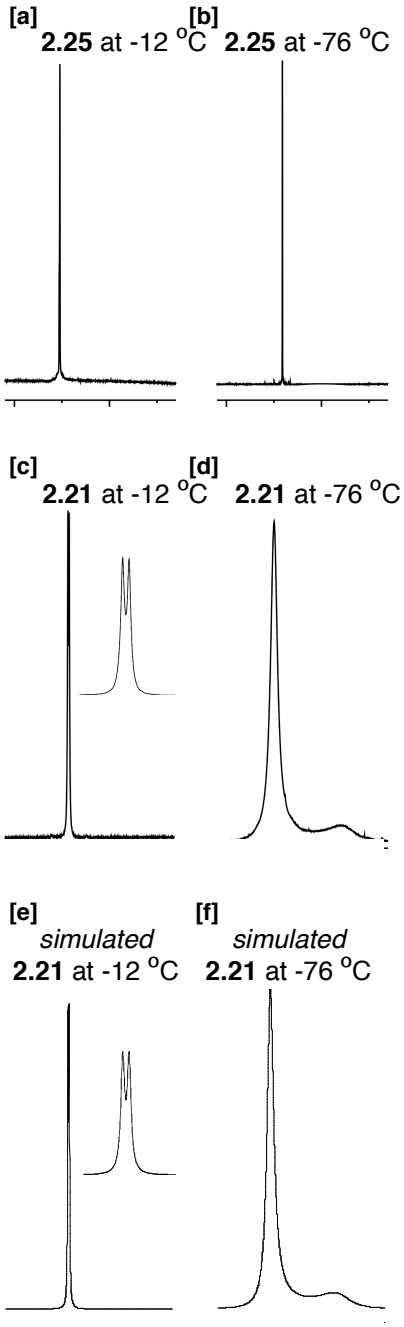


**Figure 2.16**. Aldehydic resonance of **2.25** at a) -12 ºC and b) -76 ºC. Aldehydic resonance of **2.21** at c) -12 ºC, expansion shown in the inset, and d) -76 ºC. e) Simulated of **2.21** at -12 ºC, expansion shown in the inset. f) Simulated spectrum of **2.21** at -76 ºC.

At the lowest temperature observed, -70 °C, two distinct broad peaks were visible in a ratio of 88:12 (integrated ratio); this translates into a ΔΔG° of 0.80 kcal/mol. Confirming the **Ms-*Trans*** model system's calculated 0.58 kcal/mol free energy difference, a detailed conformational search and optimization of **2.21** at the B3LYP/6-31G* level with single-point SM8 "$CH_2Cl_2$" solvation calculations yielded a calculated ΔΔE of 0.63 kcal/mol between the invertomers **2.21**-*SX* and **2.21**-*AX*; the resulting predicted 4.8:1 invertomer ratio is in reasonably good agreement with the ~7:1 value observed. Full line shape analysis of the aldehydic resonance (Figure 2.16e/f),[46] used to determine the activation parameters, leads to the calculation of the energy barrier for nitrogen inversion of **2.21** ($\Delta G^{\ddagger}$ = 10.7 ± 1.4 kcal/mol, $\Delta H^{\ddagger}$ = 7.99 ± 0.3 kcal/mol, and $\Delta S^{\ddagger}$ = -8.94 ± 0.3 cal/mol/K, data from Eyring plot, see Supporting Information). The corresponding B3LYP/6-31G*/SM8-$CH_2Cl_2$ calculation for **Ms_*Trans*** finds an inversion $\Delta G^{\ddagger}$ of 10.2 kcal/mol, quite similar to the experimental value for **2.21**.[67] With this modest inversion barrier, both invertomers would be available throughout the reaction with the organometallic nucleophile. Presumably, this mix of substrate conformers also leads to the observed moderate selectivity observed in addition of organometallic reagents to Ts-protected *trans*-aziridine-2-carboxyaldehyde **2.21**, in contrast to the exclusive *syn* selectivity seen with the *SX*-dominated 2,3-disubstituted aziridine-2-carboxaldehyde **2.25**.

## 2.6 Conclusions.

The selectivity of organometallic addition to N-protected *cis*, *trans*, and 2,3-disubtituted aziridine-2-carboxaldehydes is governed by multiple intimately coupled factors. Most important are the rotameric orientations of the aldehyde functionality and invertomeric preferences of the nitrogen protective group. As with cyclopropane carboxaldehydes, the CHO moiety strongly prefers bifurcated geometries relative to the ring, with the oxygen oriented either *endo* or *exo*; rotation to other orientations can cost as much as 6 kcal/mol. Also, though conjugation might have been expected to oppose it, the aziridine nitrogen remains strongly pyramidalized regardless of which substituent it carries; invertomeric alternative conformations therefore must be considered. These aspects are further modulated by the N-substituents' electronic nature, and by the steric environment set by the other substituents on the aziridine ring (see Table 2.14 for summary). Additional variation arises from use of different metal and alkyl components of the organometallic nucleophiles. For Bn protected aziridine aldehydes, selectivity originates from chelation, consistent with findings in the literature. Excellent *syn* addition selectivity (>99:1 *syn*/*anti*) is achieved for *N*-Bn *cis* aziridine aldehydes while *trans* substrates undergo almost completely unselective (55/45 *syn*/*anti*) addition. For this case, as well as the *N*-Boc protected *cis* and 2,3-disubstituted systems, the low selectivity seems to be due to the substrates' conformational ambiguity, both between aldehyde *endo*/*exo* rotamer and N-invertomer structures. However, for the conformationally well-defined *N*-Boc *trans* substrates, extremely high *syn* selectivity (>99:1 *syn*/*anti*) is observed which is unaffected by chelation modifiers. This strong

stereopreference appears to be dictated by the chelation-like favorable interaction between the aldehyde carbonyl and the *syn*-Boc group's electrophilic carbon.

**Table 2.14.** Summarized results of selectivity (*syn/anti*) observed in addition of organometallic reagents to aziridine carboxaldehydes.

| | *N*-protecting group (R) | | |
|---|---|---|---|
| substitution pattern | Bn | Boc | Ts |
| *cis* | **excellent** | poor | poor |
| *trans* | poor | **excellent** | moderate |
| *2,3-Di* | --- | moderate | **excellent** |

Because of amide resonance, the Boc substituent adopts a tangential rotameric orientation relative to the aziridine 3-membered ring; this is the opposite of the bifurcated geometry preferred by the C-bonded aldehyde, and leads to their meshing in this complementary manner, effecting mild Lewis Acid activation of the aldehyde specifically in the *SN* conformation.

For the *N*-Ts protected series, diastereoselectivity is again largely understandable in terms of the systems' conformational preferences. Though *cis* substrates do not enjoy any kind of selectivity, their *trans* analogues afford the addition product with moderate to high *syn* (70:30 *syn*/*anti*) selectivity, while exceptional stereospecificity is achieved in the case of *N*-Ts-2,3-disubstituted aziridine-2-carboxaldehyde **2.25** (>99:1 *syn*/*anti*). In the *trans* case, the *SX* (i.e. *syn* N-invertomer and *exo* aldehyde rotamer) conformer

dominates, but only weakly; in the 2,3-disubstituted cast, the additional methyl substituent alpha to the carbonyl more definitively locks in the *SX* conformer, enforcing *syn*-selective addition by attack on the aldehyde face away from the Ts group. Thus, in conclusion, extremely high *syn*-selectivity can be achieved with *cis* substrates utilizing Bn, *trans* substrates using Boc, and 2,3-disubstituted aziridine-2-carboxaldehyde substrates bearing Ts as nitrogen protective groups. The corresponding *anti* adducts can easily be accessed by Mitsunobu inversion, or by complementary hydride reduction of the related ketones, guided by the early conformational and synthetic analyses of Pierre et al., augmented by the more detailed conformational insights developed here with the aid of quantum chemical modeling.

**2.7 Experimental Procedures.**

All glassware was dried in an oven at 150 °C prior to use. All air/moisture sensitive experiments were carried out under a slight static pressure of dry Nitrogen unless indicated otherwise. Anhydrous toluene, $CH_2Cl_2$ were dried over $CaH_2$ and THF, $Et_2O$ were dried over sodium and benzophenone and were freshly distilled prior to use. DMSO was dried over $CaH_2$ and distilled under high vacuum at temperature < 60 °C and stored over molecular sieves. TMSOI was dried under high vacuum at 30 °C overnight prior to use. Chloramine-T was dried at 60 ºC under the vacuum overnight prior to use. N-Bromosuccinimide was re-crystallized from hot water and dried over $P_2O_5$ under vacuum using the established procedure[68]. All the commercially available chemicals were used as received unless indicated otherwise. Commercial grade solvents were used for routine purposes without further purification. Pyridine and TEA was distilled from $CaH_2$ under $N_2$ atmosphere prior to use. All NMR spectra were recorded on a 300 MHz Inova or 500 MHz Varian NMR spectrometers. Column chromatography was performed using Silicycle (40 – 60 μm) silica gel. Precoated silica gel 60 F254 plates were used for analytical TLC and visualized using UV light/ p-anisaldehyde/ PMA as the stain. Chemical shifts are reported in parts per million (ppm) from internal tetramethylsilane or the residual solvent signal of $CDCl_3$. NMR spectra were obtained using either and referenced using deuterated chloroform or DMSO. Infrared spectra were taken on a Nicolet IR/42 spectrometer using thin neat film deposition on NaCl plates and peaks are reported in wave numbers ($cm^{-1}$). All the ultra

sonic reactions were performed using FS30 Fisher Scientific ultrasonicator. High-resolution mass spectra (HRMS) were taken on a Micromass Q-TOF Ultima. Hewlett Packard HPLC instrument, Zorbax SIL (9.4 mm X 25 cm, 5 μ) preparative column and HPLC grade hexane and isopropanol solvents were used for the separation done by HPLC.

**Preparation of *N*-Bn protected aziridine substrates:**

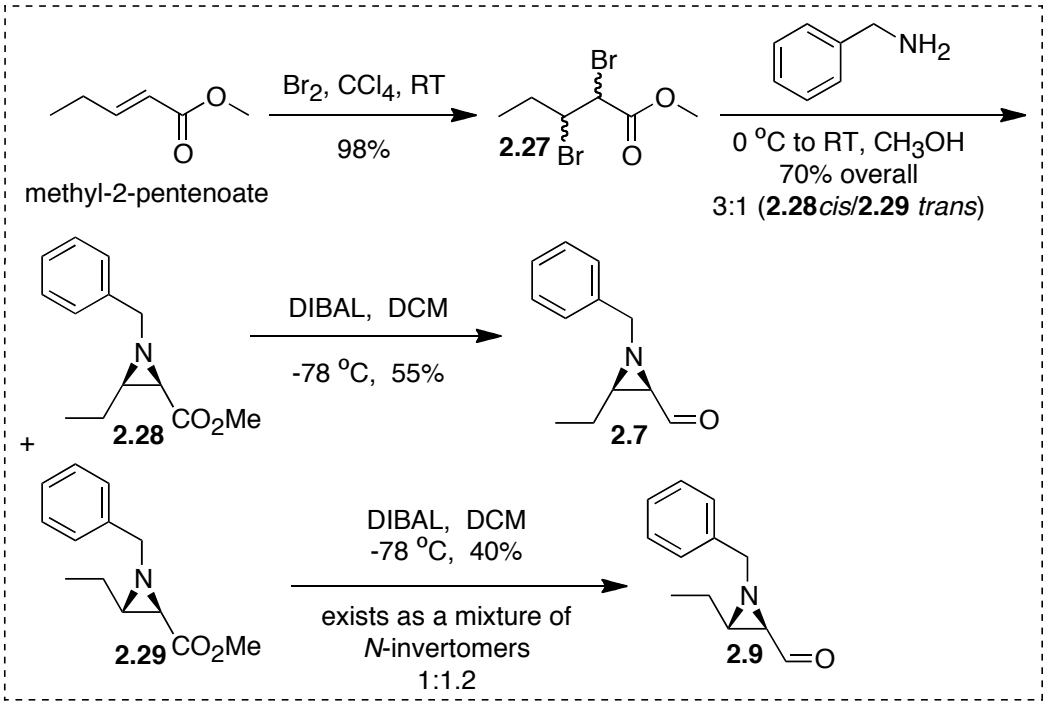


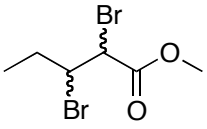

**2.27**

**Preparation of 2,3-dibromopentanoate 2.27.**[69] Bromine (5 mL, 100.23 mmol) was

added drop wise to the solution of commercially available methyl 2-pentenoate (8.75 g, 77.09 mmol) in carbon tetrachloride (350 mL) at room temperature. After reflux for 2.5 h, the solution was cooled and evaporated which afforded methyl 2,3-dibromopentanoate **2.27** (20.5 g, 98% yield) as sweet scented oil, which was taken to the next step without further purification.

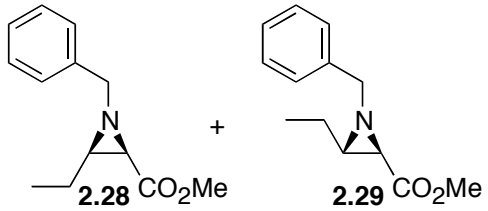


**Preparation of *cis* and *trans* aziridine-2-methylcarboxylates 2.28 and 2.29.**[69,70]

Methyl 2,3 - dibromopentanoate **2.27** (18 g, 65.71 mmol) was dissolved in methanol (164 mL) and slowly added at 0 ºC to a stirred solution of commercially available benzylamine (29 g, 271.4 mmol) in methanol (472 mL). The reaction mixture was slowly warmed to room temperature and stirred overnight. After completion, solvent was removed via rotary evaporation. The residue left, was dissolved in ethyl ether (100 mL), washed with water (100 mL) and the aqueous phase was extracted with ethyl ether (3 x 100 mL), dried over magnesium sulfate and concentrated to give a brownish yellow oil. The crude compound was purified by column chromatography (6:1 petroleum ether:ether) to afford a 3:1 mixture of *cis* aziridine-2-methylcarboxylate **2.28** (8 g) and *trans* aziridine-2-methylcarboxylate **2.29** (2.7 g) as yellow oil in 70% overall yield. *Cis* aziridine ester **2.28**: $R_F$ = 0.14 (6:1 petroleum ether:ether). Spectral data: $^1$H-NMR (300 MHz, $CDCl_3$) $\delta$ 7.29 (m, 5H), 3.69 (s, 3H), 3.55 (m, 2H), 2.24 (d, 1H, *J* = 6.8 Hz), 1.86

(dd, 1H, *J* = 13.3, 6.7 Hz), 1.62 (m, 1H), 1.49 (m, 1H), 0.85 (t, 3H, *J* = 7.4 Hz); $^{13}$C NMR (125 MHz, $CDCl_3$) δ 169.7, 137.5, 127.8, 127.6, 126.7, 63.5, 51.4, 47.7, 42.0, 20.7, 11.0; *Trans* aziridine ester **2.29**: Found as a mixture of 75:25 invertomers at nitrogen. $R_F$ = 0.25 (6:1 petroleum ether:ether). Spectral data: Major invertomer: $^1$H-NMR (500 MHz, $CDCl_3$) δ 7.32 (m, 5H), 4.00 (d, 1H, *J* = 13.4 Hz), 3.92 (d, 1H, *J* = 13.4 Hz), 3.68 (s, 3H), 2.51 (d, 1H, *J* = 3.0 Hz), 2.27 (m, 1H), 1.52 (m, 1H), 1.45 (m, 1H), 0.88 (t, 3H, J = 7.8 Hz); $^{13}$C NMR (125 MHz, $CDCl_3$) δ 170.0, 139.2, 128.2, 127.5, 126.8, 54.2, 51.9, 48.7, 46.8, 40.0, 25.5, 10.9; Minor invertomer: $^1$H-NMR (300 MHz, $CDCl_3$) δ 7.25 (m, 5H), 3.92 (d, 1H, *J* = 13.4 Hz), 3.70 (d, 1H, *J* = 12.3 Hz), 3.68 (s, 3H), 2.27 (m, 1H), 2.06 (m, 1H), 1.74 (m, 1H), 1.67 (m, 1H), 1.09 (t, 3H, J = 7.5 Hz); $^{13}$C NMR (125 MHz, $CDCl_3$) δ 171.5, 138.6, 128.4, 128.1, 126.8, 126.6, 54.8, 46.8, 43.1, 18.9, 12.3.

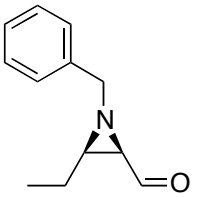


**2.7**

**Preparation of *N*-Bn protected *cis* aziridine-2-carboxaldehyde 2.7.**[69] 2.5 M solution of Dibal-H in toluene (7.6 mL, 19 mmol) was carefully added drop wise to the stirred solution of *cis* aziridine ester **2.28** (2 g, 9.12 mmol) in anhydrous DCM (30 mL) at -78˚C, under nitrogen. After 0.5 h, NaF (8 g, 190 mmol) was added followed by water (6 mL). The white inorganic precipitates were filtered off and washed with ether (50 mL).

The aqueous phase was extracted with ethyl ether (3 x 100 mL), dried over magnesium sulfate and concentrated to give transparent oil, which was purified by column chromatography (4:1 Petroleum ether:ether) to afford *cis* aziridine-2-carboxaldehyde **2.7** (1.1 g, 55%) as a colorless oil. $R_F$ = 0.26 (4:1 petroleum ether:ether). Spectral data: $^1$H-NMR (300 MHz, $CDCl_3$) $\delta$ 9.32 (d, 1H, *J* = 5.8 Hz), 7.32 (m, 5H), 3.63 (d, 1H, *J* = 13.1 Hz), 3.47 (d, 1H, *J* = 13.1 Hz), 2.16 (dd, 1H, *J* = 6.8, 6.0 Hz), 1.99 (dd, 1H, *J* = 13.7, 7.0 Hz), 1.66 (m, 1H), 1.55 (m, 1H), 0.89 (t, 3H, *J* = 7.8 Hz); $^{13}$C NMR (125 MHz, $CDCl_3$) $\delta$ 200.6, 137.7, 128.2, 127.9, 127.1, 63.5, 49.7, 49.1, 22.4, 11.5; IR (neat, $cm^{-1}$) 2956, 2932, 1714, 1672, 1495, 1454, 1265, 1072; HRMS (ESI) (m/z): $[M + H]^+$ calculated for $[C_{12}H_{16}NO]^+$ 190.1232, found 190.1230.

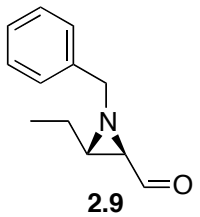


**2.9**

**Preparation of *N*-Bn protected *trans* aziridine-2-carboxaldehyde 2.9.**[69] 2.5 M solution of Dibal-H in toluene (6.27 mmol, 2.53 mL) was added drop wise to a solution of *trans* aziridine-2-methylcarboxylate **2.29** (0.66 g, 3 mmol) dissolved in anhydrous DCM (10 mL) at -78˚C, under inert atmosphere. After 1 h, NaF (1.26 g, 30 mmol) and water (1 mL) was added. The white inorganic precipitates were filtered off and washed with ether (5 mL). The aqueous phase was extracted with ethyl ether (3 x 10 mL), dried over magnesium sulfate and concentrated to give a transparent oil. The crude compound

was purified by column chromatography (3:1 petroleum ether:ether) to afford *trans* aziridine-2-carboxaldehyde **2.9** (0.22 g, 40%), which was found to exist as 55:45 mixture of invertomers at nitrogen as a colorless oil. $R_F$ = 0.5 (1:1 petroleum ether:ether). Spectral data: Major invertomer: $^1$H-NMR (300 MHz, $CDCl_3$) δ 9.62 (d, 1H, *J* = 4.36 Hz), 7.34 – 7.23 (m, 5H), 4.08 (d, 1H, *J* = 13.6 Hz), 3.98 (d, 1H, *J* = 13.6 Hz), 2.60 (m, 1H), 2.41 (m, 1H), 1.78 (m, 1H), 1.66 (m, 1H), 0.88 (t, 3H, *J* = 7.2 Hz); $^{13}$C NMR (125 MHz, $CDCl_3$) δ 200.6, 138.6, 128.4, 128.0, 127.7, 127.3, 57.0, 51.0, 47.4, 29.6, 25.9, 11.0. Minor invertomer: Spectral data: $^1$H-NMR (300 MHz, $CDCl_3$) δ 8.95 (d, 1H, *J* = 5.91 Hz), 7.34 – 7.23 (m, 5H), 3.87 (d, 1H, *J* = 14.2 Hz), 3.67 (d, 1H, *J* = 14.0 Hz), 2.45 (m, 1H), 2.03 (m, 1H), 1.53 (m, 2H), 1.05 (t, 3H, *J* = 7.7 Hz); $^{13}$C NMR (125 MHz, $CDCl_3$) δ 198.8, 138.6, 128.4, 128.0, 127.7, 127.3, 54.5, 51.0, 45.2, 18.9, 12.3; IR (neat, $cm^{-1}$) 2969 (m), 2870 (m), 1720 (s), 1603 (w), 1454 (m); HRMS (ESI) (m/z): $[M + H]^+$ calculated for $[C_{12}H_{16}NO]^+$ 190.1232, found 190.1230.

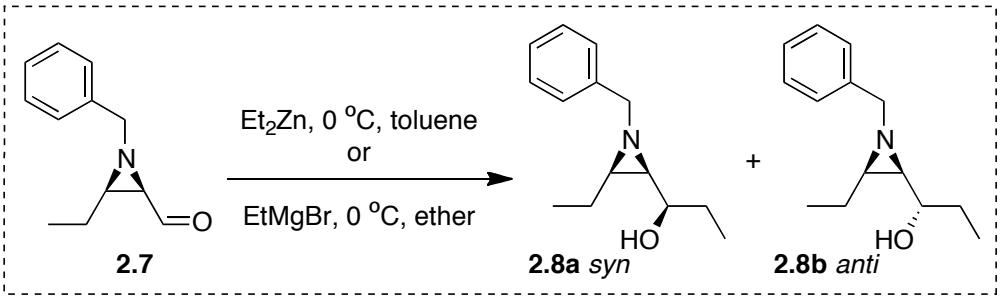


**2.7** **2.8a** *syn* **2.8b** *anti*

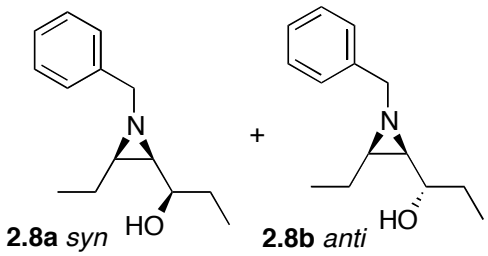


**2.8a** *syn* **2.8b** *anti*

**Procedure for alkylation of *N*-Bn protected cis aziridine-2-carboxaldehyde 2.7 by diethylzinc addition**.[38] An oven-dried flask was charged with *cis* aziridine aldehyde **2.7** (135.4 mg, 0.715) and anhydrous toluene (1.43 mL). To this was added 1M solution of commercially available diethylzinc solution in toluene (1.43 mL, 1.43 mmol) drop wise at 0 ºC (ice bath). The mixture was stirred at that temperature until all the starting material was consumed as analyzed by TLC. The reaction was quenched with sat. $NH_4Cl$ (15 mL). The organic layer was separated and the aqueous layer was extracted with ethyl ether (3 x 20 mL). The combined organic layers were washed with brine (20 mL), dried over anhydrous sodium sulfate. The solvent was removed via rotary evaporation. The the residue was purified with column chromatography using 1:1 (petroleum ether:ether) to afford the alcohol **2.8a**[1] (117.6 mg, 75%) as a yellow oil. $R_F$ = 0.26 (1:1 petroleum ether:ether). Spectral data: $^1$H-NMR (300 MHz, $CDCl_3$) $\delta$ 7.35 -7.24 (m, 5H), 3.55 (d, 1H, J = 13.1 Hz), 3.36 (d, 1H, *J* = 13.7 Hz), 3.31 (bs, 1H), 3.24 (dd, 1H, *J* = 13.7, 7.0 Hz), 1.59 (m, 2H), 1.47 – 1.39 (m, 4H), 0.90 (t, 3H, *J* = 7.7 Hz), 0.85 (t, 3H,

[1] Identity of the *syn* isomer was made by comparison of its $^1$H-NMR spectrum to that of a similar compound reported in Ref 4 (*N*-benzyl *cis*-3-methyl aziridine-2-carboxaldehyde was used in Ref 4 as compared to *N*-benzyl *cis*-3-ethyl aziridine-2-carboxyaldehyde used here).

$J$ = 7.6 Hz); $^{13}$C NMR (125 MHz, $CDCl_3$) δ 138.9, 128.4, 128.2, 127.1, 69.4, 64.8, 49.3, 46.2, 28.7, 21.5, 12.0, 9.6; IR (neat, $cm^{-1}$) 3329, 2966, 2930, 2876, 1454; HRMS (ESI) (m/z): $[M + H]^+$ calculated for $[C_{14}H_{22}NO]^+$ 220.1701, found 220.1705.

**Alkylation of *N*-Bn protected *cis* aziridine-2-carboxaldehyde 2.7 by Grignard addition.**[38] *Cis* aziridine carboxaldehyde **2.7** (0.13 g, 0.71) was dissolved in anhydrous ethyl ether (1.8 mL), to which was added 2.2 M solution of ethyl magnesium bromide solution in THF (0.5 mL, 0.86 mmol) at 0 ºC (ice bath). The mixture was stirred at that temperature for 1 h. The reaction was quenched with sat. $NH_4Cl$ (15 mL). The organic layer was separated and the aqueous layer was extracted with ethyl ether (3 x 20 mL). The combined organic layers were washed with brine (20 mL), dried over anhydrous sodium sulfate. The solvent was removed via rotary evaporation and the residue was purified with column chromatography (1.5:1 Hex:EtOAc) to afford the alcohol **2.8a** (0.98 g, 55%) as a yellow oil. $R_F$ = 0.26 (1:1 petroleum ether:ether). Spectral data: $^1$H-NMR (300 MHz, $CDCl_3$) δ 7.35 – 7.24 (m, 5H), 3.55 (d, 1H, $J$ = 13.1 Hz), 3.36 (d, 1H, $J$ = 13.7 Hz), 3.31 (bs, 1H), 3.24 (dd, 1H, $J$ = 13.7, 7.0 Hz), 1.59 (m, 2H), 1.47 – 1.39 (m, 4H), 0.90 (t, 3H, $J$ = 7.7 Hz), 0.85 (t, 3H, $J$ = 7.6 Hz); $^{13}$C NMR (125 MHz, $CDCl_3$) δ 138.9, 128.4, 128.2, 127.1, 69.4, 64.8, 49.3, 46.2, 28.7, 21.5, 12.0, 9.6; IR (neat, $cm^{-1}$) 3379, 3030, 2966, 1604, 1454, 1309, 1115, 970; HRMS (ESI) (m/z): $[M + H]^+$ calculated for $[C_{14}H_{22}NO]^+$ 220.1701, found 220.1705.

**Alkylation of *N*-Bn protected *cis* aziridine-2-carboxaldehyde 2.7 by Grignard addition in the presence of TMEDA.**[38] *Cis* aziridine aldehyde **2.7** (126.9 mg, 0.67) was dissolved in anhydrous ethyl ether (0.7 mL) and freshly distilled TMEDA (0.24 mL, 1.6 mmol), to which was added 2.2 M solution of ethyl magnesium bromide solution in THF (0.4 mL, 0.80 mmol) at 0 ºC (ice bath). The mixture was stirred at that temperature for 1 h (or until no more starting material was observed as analyzed by TLC). The reaction was quenched with sat. $NH_4Cl$ (1.6 mL). The organic layer was separated and the aqueous layer was extracted with ethyl ether (3 x 20 mL). The combined organic layers were washed with brine (10 mL), dried over anhydrous sodium sulfate. The solvent was removed via rotary evaporation and the residue was purified with column chromatography (1.5:1 Hex:EtOAc) to afford a mixture of *syn* and *anti* aziridine alcohol **2.8a** and **2.8b** as a mixture of 1:1.2 as a yellow oil (0.98 g, 54%). *Syn* **2.8a**: $R_F$ = 0.23 (1.5:1 Hex:EtOAc). Spectral data: $^1$H-NMR (300 MHz, $CDCl_3$) δ 7.35 –7.24 (m, 5H), 3.55 (d, 1H, J = 13.1 Hz), 3.36 (d, 1H, *J* = 13.7 Hz), 3.31 (bs, 1H), 3.24 (dd, 1H, *J* = 13.7, 7.0 Hz), 1.59 (m, 2H), 1.47 – 1.39 (m, 4H), 0.90 (t, 3H, *J* = 7.7 Hz), 0.85 (t, 3H, *J* = 7.6 Hz); $^{13}$C NMR (125 MHz, $CDCl_3$) δ 138.9, 128.4, 128.2, 127.1, 69.4, 64.8, 49.3, 46.2, 28.7, 21.5, 12.0, 9.6; IR (neat, $cm^{-1}$) 3379, 3030, 2966, 1604, 1454, 1309, 1115, 970; HRMS (ESI) (m/z): $[M + H]^+$ calculated for $[C_{14}H_{22}NO]^+$ 220.1701, found 220.1705; *Anti* **2.8b**: $R_F$ = 0.14 (1.5 :1 Hex:EtOAc). Spectral data: $^1$H-NMR (300 MHz, $CDCl_3$) δ 7.30 – 7.24 (m, 5H), 3.51 (d, 1H, *J* = 13.1 Hz), 3.46 (m, 1H), 3.45 (d, 1H, *J* = 13.1 Hz), 1.56 – 1.43 (m, 6H), 0.92 (t, 3H, *J* = 7.4 Hz), 0.90 (t, 3H, *J* = 6.9 Hz); $^{13}$C NMR (125

MHz, $CDCl_3$) δ 138.9, 128.5, 128.3, 127.2, 70.9, 64.9, 47.5, 46.1, 28.4, 21.7, 12.3, 9.8; IR (neat, $cm^{-1}$) 3350, 3030, 2970, 2876, 1496, 1377, 1115, 970; HRMS (ESI) (m/z): $[M + H]^+$ calculated for $[C_{14}H_{22}NO]^+$ 220.1701, found 220.1699.

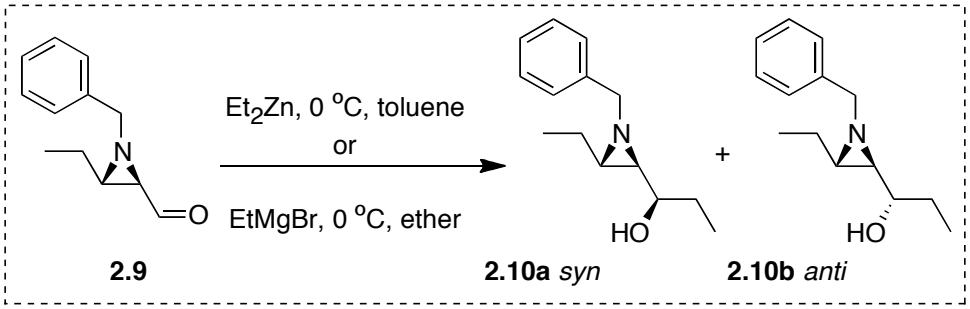


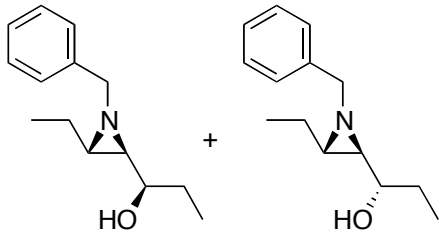


**Alkylation of *N*-Bn *trans* aziridine-2-carboxaldehyde 2.9 by Grignard addition.**[38]

*Trans* aziridine aldehyde **2.9** containing a mixture of N-invertomers (44.5 mg, 0.24 mmol) was dissolved in anhydrous ethyl ether (0.5 mL), to which was added 3.0 M solution of commercially available ethyl magnesium bromide (0.1 mL, 0.29 mmol) solution in THF at 0 °C (ice bath). An extra equivalent of ethyl magnesium bromide (0.08 mL, 0.24 mmol) was added at this point. The mixture was stirred at this temperature until no more starting material was found as analyzed by TLC. The reaction was quenched with sat. $NH_4Cl$ (0.6 mL). The organic layer was separated and

the aqueous layer was extracted with ethyl ether (3 x 5 mL). The combined organic layers were washed with brine (5 mL), dried over anhydrous sodium sulfate. The solvent was removed via rotary evaporation and the residue was purified with column chromatography using 1:1 (Hex:EtOAc) to afford 1:1.2 mixture of *syn* and *anti* aziridine alcohols **2.10a** and **2.10b** (27 mg, 54%) as a colorless oil. $R_F$ = 0.23 (1.5:1 Hex:EtOAc). *Major isomer*: Spectral data: $^1$H-NMR (300 MHz, $CDCl_3$) δ 7.32 – 7.26 (m, 5H), 3.84 (d, 1H, *J* = 13.8 Hz), 3.45 (d, 1H, *J* = 12.4 Hz), 3.14 (dd, 1H, *J* = 12.4, 6.4 Hz), 1.99 (m, 1H), 1.73 – 1.40 (m, 5H), 1.04 (t, 3H, *J* = 7.3 Hz), 0.88 (t, 3H, *J* = 7.3 Hz); $^{13}$C NMR (125 MHz, $CDCl_3$) δ 128.2, 127.1, 126.8, 73.0, 55.3, 49.4, 43.3, 28.4, 19.4, 12.7, 9.9; *Minor isomer*: Spectral data: $^1$H-NMR (300 MHz, $CDCl_3$) δ 7.32 – 7.26 (m, 5H), 3.89 (d, 1H, *J* = 13.8 Hz), 3.60 (m, 1H), 3.59 (d, 1H, *J* = 13.8 Hz), 2.78 (bs, 1H), 2.06 (m, 1H), 1.74 – 1.43 (m, 5H), 1.04 (t, 3H, *J* = 7.8 Hz), 0.94 (t, 3H, *J* = 7.8 Hz); $^{13}$C NMR (125 MHz, $CDCl_3$) δ 128.4, 127.7, 126.9, 68.8, 54.5, 48.1, 40.1, 27.5, 19.3, 12.7, 9.8, IR (neat, $cm^{-1}$) 3362, 2964, 1736, 1454; HRMS (ESI) (m/z):$[M + H]^+$ calculated for $[C_{14}H_{22}NO]^+$ 220.1701, found 220.1700.

**Alkylation of *N*-Bn aziridine carboxaldehydes by Grignard addition in the presence of TMEDA.**[38] Refer to the procedure used for the similar reaction in case of *N*-Bn protected *cis* aziridine-2-carboxaldehyde **2.7**.

**Preparation of *N*-Boc protected aziridine substrates:**

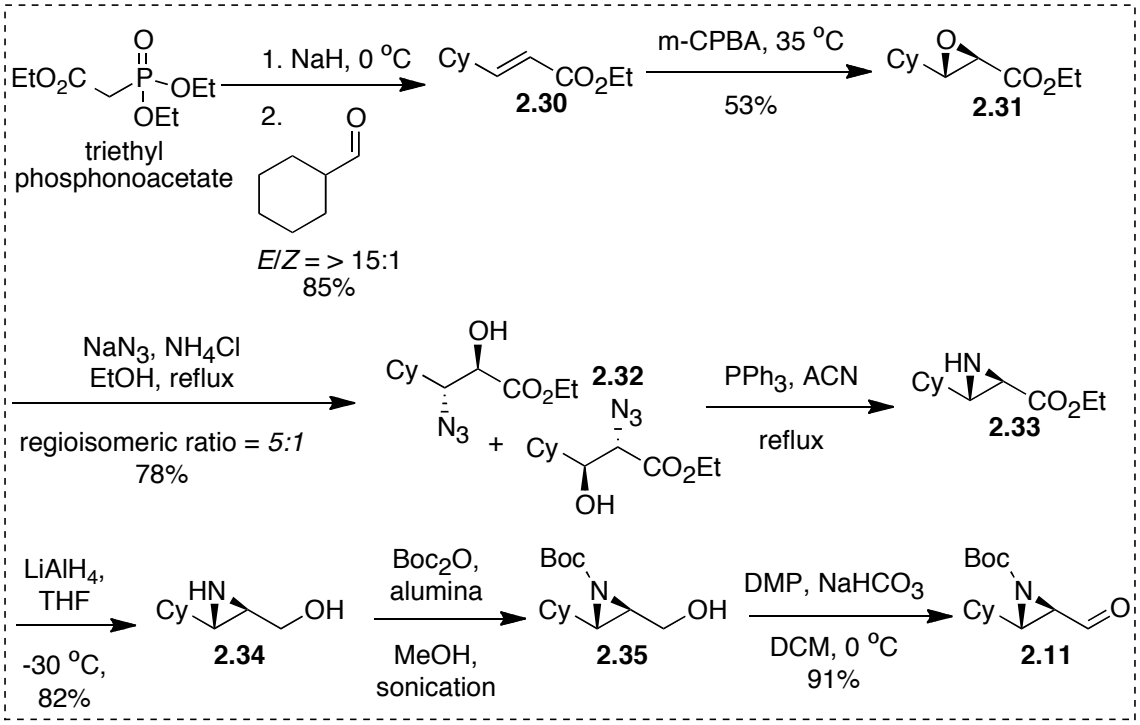


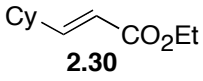


**Preparation of ethyl ester 2.30.**[71] To a cooled solution of sodium hydride (2.18 g, 54.4 mmol) in dimethoxyethane (84 mL) at 0 ºC was added triethylphosphonoacetate (13.3 g, 59.4 mmol) drop wise. The reaction mixture was stirred at the same temperature for 30 min and then allowed to warm to room temperature. Freshly distilled cyclohexylcarboxaldehyde (5.6 g, 49.9 mmol) was added and the reaction mixture was stirred for 4 h. Reaction was quenched with water (50 mL), the aqueous phase was extracted with EtOAc (3 x 100 mL). The organic layer was dried over anhydrous sodium sulfate and the solvent was removed by rotary evaporation. The crude material was

purified by column chromatography using 10% EtOAc in hexane to afford the ester **2.30** as an oil (7.6 g, 85%) (*E*:*Z* > 15:1). $R_F$ = 0.74 (10% EtOAc in Hex). Spectral data: $^1$H-NMR (300 MHz, $CDCl_3$) δ 6.92 (dd, 1H, *J* = 7.2 Hz), 5.76 (d, 1H, J = 15.9 Hz), 4.18 (q, 2H, *J* = 7.2 Hz), 2.14 (m, 1H), 1.78 – 1.74 (m, 5H), 1.29 (t, 3H, *J* = 7.2 Hz), 1.23 – 1.14 (m, 5H); $^{13}$C NMR (125 MHz, $CDCl_3$) δ 168.2, 153.9, 118.5, 60.0, 39.8, 30.1, 25.6, 13.8.

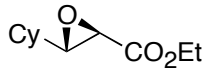


**2.31**

**Preparation of epoxide 2.31.**[72] To a solution of alkene **2.30** (6.5 g, 35.7 mmol) in anhydrous DCM (36 mL) was added commercially available 3-chloroperbenzoic acid (77%) (4.82 g, 44.2 mmol). The solution was refluxed at 35 ºC under nitrogen for 24 h. Solution was washed with sat. $NaHCO_3$ (20 mL). The aqueous solution was extracted with DCM (3 x 50 mL). Organic layer was dried over anhydrous sodium sulfate and the solvent was removed under vacuum. The crude material was purified by column chromatography (Hex to 3:1 Hex:EtOAc) to afford the epoxide **2.31**[2] as an oil (3.74 g, 53%). $R_F$ = 0.71 (3:1 Hex:EtOAc). Spectral data: $^1$H-NMR (300 MHz, $CDCl_3$) δ 4.19 (m, 2H), 3.22 (m, 1H), 2.93 (m, 1H), 1.8 – 1.66 (m, 5H), 1.26 (t, 3H, *J* = 7.5 Hz), 1.19 – 1.10 (m, 6H); $^{13}$C NMR (125 MHz, $CDCl_3$) δ 169.4, 62.4, 61.4, 52.0, 39.4, 29.2, 28.7, 26.0, 25.5, 25.3, 14.0.

---

[2] Epoxidation of *trans* olefin by m-CPBA is assumed to deliver the *trans* epoxide as the major product. We believe that the data for *cis vs. trans* epoxy compounds has been mislabeled in Ref 6.

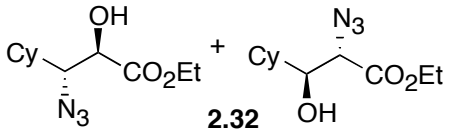


**2.32**

**Preparation of azido alcohol 2.32.** A solution of epoxy ester **2.31** (3.74 g, 18.86 mmol) in absolute ethanol (42 mL) was added to a mixture of ammonium chloride (3.1 g, 56.58 mmol) and sodium azide (3.7 g, 56.58 mmol). The solution was slowly warmed to reflux over 1 h, heated for another 1 h, then solution was cooled to room temperature. Reaction mixture was filtered, solid residue was washed with ethanol (20 mL), solvent was removed via rotary evaporation and the crude was purified (3:1 Hex:EtOAc) to afford a 5:1 isomeric mixture of azido alcohol **2.32** as colorless oil (3.56 g, 78%). $R_F$ = 0.76 (3:1 Hex:EtOAc). Spectral data: Major isomer: $^1$H-NMR (300 MHz, $CDCl_3$) $\delta$ 4.27 (m, 2H), 3.91 (dd, 1H, $J$ = 6.1, 2.5 Hz), 3.66 (m, 1H), 2.39 (m, 1H), 1.76 – 1.57 (m, 5H), 1.31 (m, 3H), 1.26 – 1.03 (m, 6H); $^{13}$C NMR (125 MHz, $CDCl_3$) $\delta$ 169.5, 76.0, 63.4, 62.0, 29.4, 27.1, 26.2, 26.1, 25.8, 14.0; IR (neat, $cm^{-1}$) 2930, 2855, 2110, 1738, 1450, 1264, 1196, 1026; HRMS (ESI) (m/z): $[M + H]^+$ calculated for $[C_{11}H_{19}N_3Na]^+$ 264.1324, found 264.1327.

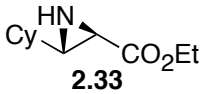


**2.33**

**Preparation of aziridine 2.33.** To a solution of isomeric mixture of azido alcohol **2.32** (3.16 g, 13.09 mmol) in acetonitrile (57 mL) was added triphenyl phosphine (3.78 g, 14.39 mmol) over a period of 30 minutes. The reaction mixture was slowly brought to

reflux and heated for 3 h. After completion, solvents were evaporated and the residue was dissolved in ethyl ether (50 mL). Hexane was added (20 mL), the precipitates were filtered off and the solvent was removed via rotary evaporation. The crude was taken to next step without further purification. $R_F$ = 0.6 (3:1 Hex:EtOAc); Spectral data: $^1$H-NMR (300 MHz, $CDCl_3$) δ 4.16 (m, 2H), 2.27 (dd, 1H, *J* = 7.1, 2.2 Hz), 1.99 (m, 1H), 1.83 (d, 1H, *J* = 12 Hz), 1.70 – 1.60 (m, 4H), 1.26 (t, 3H, *J* = 7.2 Hz), 1.15 – 0.93 (m, 7H); $^{13}$C NMR (75 MHz, $CDCl_3$) δ 170.9, 61.1, 44.0, 37.0, 34.2, 31.6, 30.8, 26.0, 25.4, 25.4, 14.

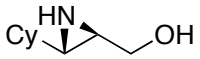


**2.34**

**Preparation of aziridine alcohol 2.34.**[69] To a 1 M solution of lithium aluminium hydride (0.75 g, 18.7 mmol) in anhydrous THF (19 mL) was added solution of aziridine ester **2.33** (1.85 g, 9.38 mmol) in anhydrous THF (47 mL) through a funnel under inert atmosphere at -30 ºC. The reaction mixture was stirred at the same temperature. After 6 h reaction was quenched with 0.5 N sodium hydroxide solution (0.75 mL) and water (0.75 mL). The reaction mixture was filtered and filter cake was washed with ether (5 x 25 mL) to get the aziridine **2.34** as an off white solid (mp 66 - 67 ºC) (1.19 g, 82%), which was taken to next step without further purification. Spectral data: $^1$H-NMR (300 MHz, $CDCl_3$) δ 3.76 (dd, 1H, *J* = 12.0, 3.5 Hz), 3.33 (dd, 1H, *J* = 12.0, 6.1 Hz), 2.14 (bs, 1H), 1.97 (m, 1H), 1.78 (d, 1H, *J* = 13.0 Hz), 1.68 – 1.62 (m, 5H), 1.15 – 1.05 (m, 5H),

0.86 (m, 1H); $^{13}C$ NMR (125 MHz, $CDCl_3$) δ 63.2, 41.8, 40.4, 37.3, 31.0, 30.7, 26.2, 25.8, 25.7.

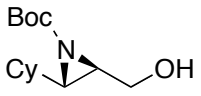


**2.35**

**Preparation of *N*-Boc protected aziridine alcohol 2.35.**[73] Aziridine **2.34** (1.13 g, 7.32 mmol) was dissolved in a small amount of anhydrous DCM (~ 2 mL). To this was added basic alumina (Activity – 1, Brokman, 60 – 325 mesh) (1.12 g, 10.99 mmol) and $Boc_2O$ (1.76 g, 8.06 mmol). The reaction mixture was stirred at room temperature until the starting material was completely disappeared as analyzed by TLC. EtOAc (3 mL) was added and the solution was filtered. The solvent was removed under vacuum and the product taken to next step without further purification.

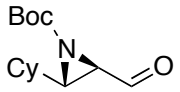


**2.11**

**Preparation of *N*-Boc protected *trans* aziridine-2-carboxaldehyde 2.11.** To a solution of aziridine alcohol **2.35** (1 g, 3.91 mmol) in anhydrous DCM (43 mL) at 0 ºC was added sodium bicarbonate (0.5 g, 5.86 mmol) and DMP (2.32 g, 5.48 mmol). The reaction mixture was stirred, allowing the temperature to warm up to room temperature by itself until no more starting material was found as analyzed by TLC. After completion the solution was washed with sat. sodium thiosulfate (8 mL), sat. $NaHCO_3$ solution (8

mL) and water (8 mL) and stirred for another 20 minutes. The aqueous solution was extracted with DCM (3 x 50 mL). The organic layer was dried over anhydrous sodium sulfate and solvent was removed under vacuum. The crude material was purified by column chromatography (4:1 Hex:EtOAc) to afford the aldehyde **2.11** as a yellow crystalline solid (mp = 52 - 55 ºC) (0.99 g, 91%). $R_F$ = 0.46 (4:1 Hex:EtOAc). Spectral data: $^1$H-NMR (300 MHz, $CDCl_3$) δ 9.05 (d, 1H, *J* = 5.1 Hz), 2.94 (dd, 1H, *J* = 5.1, 2.7 Hz), 2.62 (dd, 1H, *J* = 6.8, 2.7 Hz), 1.71 (m, 6H), 1.42 (s, 9H), 1.17 (m, 5H); $^{13}$C NMR (125 MHz, $CDCl_3$) δ 195.4, 159.8, 82.3, 48.7, 45.8, 39.3, 30.2, 29.7, 27.8, 26.0, 25.5, 25.4; IR (neat, $cm^{-1}$) 2928, 1726, 1450, 1369, 1315, 1159, 1045; HRMS (ESI) (m/z): [M + H]$^+$ calculated for $[C_{14}H_{24}NO_3]^+$ 254.1756, found 254.1758.

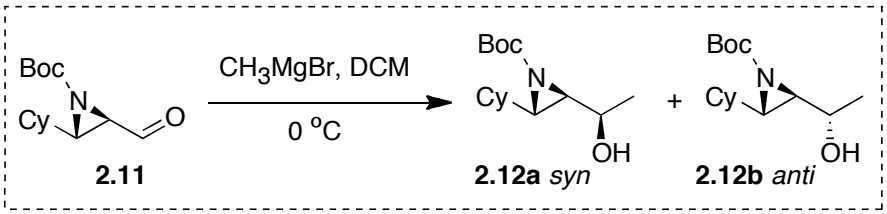


**2.11** **2.12a** *syn* **2.12b** *anti*

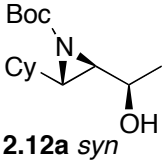


**2.12a** *syn*

**Alkylation of *N*-Boc protected *trans* aziridine-2-carboxaldehyde 2.11 by addition of Grignard reagent.**[37] To a solution of aziridine-2-carboxaldehyde **2.11** (97 mg, 0.383 mmol) in anhydrous DCM (14 mL) at room temperature, (3 M solution in THF) methyl

magnesium bromide (0.64 mL, 1.91 mmol) was added drop wise. The solution was stirred until no more starting material was observed as analyzed by TLC. The reaction was quenched with sat. $NH_4Cl$ (8 mL). The organic layer was washed with brine (2 mL), aqueous layer was extracted with EtOAc (2 x 15 mL). The combined organic layer was dried over sodium sulfate and then evaporated in vacuum. The crude mixture was purified by column chromatography (5:1 Hex:EtOAc) to afford product **2.12a** as a pale oil (87 mg, 85%), whose spectroscopic data matches with that of the reported compound in literature and thus confirms the *syn* stereochemistry of the only compound obtained under these conditions.[37] $R_F$ = 0.68 (3:1 Hex:EtOAc). Spectral data: $^1$H-NMR (300 MHz, $CDCl_3$) $\delta$ 3.34 (dq, 1H, $J$ = 8.2, 6.1 Hz), 2.3 (dd, 1H, $J$ = 8.2 Hz), 2.00 – 1.95 (m, 1H), 1.93 (bs, 1H), 1.81 – 1.50 (m, 11H), 1.46 (s, 9H), 1.30 (d, 3H, $J$ = 6.2 Hz); $^{13}$C NMR (125 MHz, $CDCl_3$) $\delta$ 160.6, 81.9, 69.8, 48.5, 46.8, 39.6, 30.6, 29.8, 28.0, 26.2, 25.7, 25.5, 20.2.

**Alkylation of *N*-Boc protected *trans* aziridine-2-carboxaldehyde 2.11 by the addition of Grignard reagent in the presence of various additives:** Similar procedure as reported above was used. In case of Grignard addition in presence of TMEDA, 5 equivalents of freshly distilled TMEDA reagent were added; for the reaction in presence of $MgBr_2 \cdot OEt_2$, 2.5 equivalents of freshly prepared reagent were used and for the reaction in presence of $ZnCl_2$, 2.5 equivalents of the dried reagent was used.

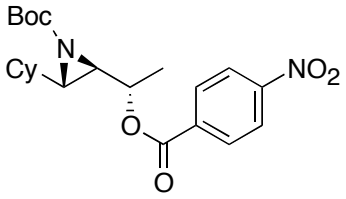


**Preparation of 2.36.**[74] A round bottom flask was charged with *syn*-aziridinol **2.12a** (37.2 mg, 0.14 mmol), 4-nitrobenzoic acid (92.71 mg, 0.55 mmol), triphenylphosphine (0.144 g, 0.55 mmol) and anhydrous THF (1 mL). The flask was maintained at 0 ºC using an ice bath. DIAD (0.1 mL, 0.55 mmol) was added drop wise at such a rate that the reaction temperature was maintained below 10 ºC. After completion of the reaction excess solvent was removed under vacuum. The resulting thick syrup was dissolved in ether (20 mL) and the solution was allowed to stand at room temperature whereupon precipitates were formed. Hexane (10 mL) was added slowly. The white solid was then vacuum filtered and filter cake was washed with 1:1 Hex:EtOAc (50 mL). Solvent was removed under vacuum and the crude compound was taken to the next step without further purification.

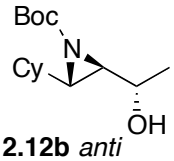

**2.12b** *anti*

**Preparation of *anti* aziridine alcohol 2.12b.**[74] The crude ester **2.36** (40 mg, 0.1 mmol) was dissolved in methanol (5 mL) and anhydrous THF (0.5 mL). The mixture was stirred at 0 ºC for 5 min, after which $LiBH_4$ (3 mg, 0.12 mmol) was added at the

same temperature. Reaction was stirred until no more starting material was found as analyzed by TLC. Upon completion the reaction was quenched with sat. $NH_4Cl$ (0.1 mL), water (0.1 mL) and glycerol (0.1 mL) and was left stirring overnight. The organic phase was separated and the aqueous layer was extracted with EtOAc (3 x 10 mL). The solvent was removed via rotary evaporation and the crude compound was purified by column chromatography (100% Hex to 6:1 Hex:EtOAc) afforded the *anti* alcohol **2.12b** as a white crystalline solid (mp = 59 – 60 ºC) (34.5 mg, 86.2%) $R_F$ = 0.60 (3:1 Hex:EtOAc). Spectral data: $^1$H-NMR (300 MHz, $CDCl_3$) $\delta$ 4.12 (m, 1H), 2.33 (m, 2H), 2.11 (m, 1H), 1.76 – 1.62 (m, 6H), 1.48 (s, 9H), 1.27 (d, 3H, $J$ = 7.4 Hz), 1.23 – 1.04 (m, 4H); $^{13}$C NMR (125 MHz, $CDCl_3$) $\delta$ 161.4, 81.0, 64.0, 46.2, 44.7, 39.4, 31.2, 30.6, 28.0, 26.2, 25.8, 25.5, 20.3; IR (neat, $cm^{-1}$) 2925, 2855, 1739, 1456, 1371, 1280, 1164; HRMS (ESI) (m/z): $[M+H]^+$ calculated for $[C_{15}H_{27}NO_3]^+$ 270.2069, found 270.2070.

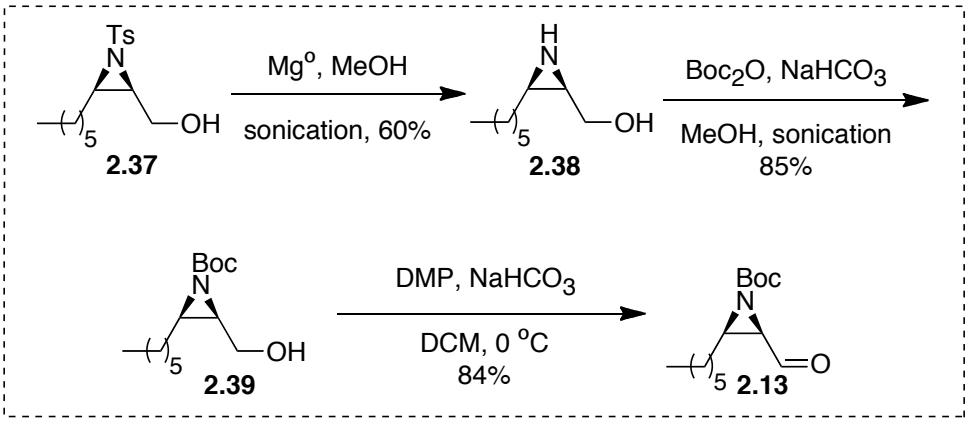

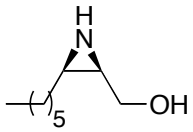


**2.38**

**Preparation of aziridine alcohol 2.38.** *N*-Ts aziridine alcohol **2.37** (0.3 g, 1.26 mmol) was placed in methanol (1.2 mL). To this grounded magnesium powder (0.18g, 7.56 mmol) was added. The solution was sonicated for 2 h, upon completion; reaction was diluted with sat. $NH_4Cl$ (20 mL). The aqueous phase was extraction with EtOAc (3 x 30 mL). Combined organic layer was dried over sodium sulfate and solvent was removed under vacuum. Crude material was purified by column chromatography using a gradient solvent system (1:1 to 100% EtOAc) to afford the detosylated product **2.38** (90.8 mg, 60%) as a yellow solid (mp = 46 – 48 ºC): $R_F$ = 0.06 (3:1 EtOAc:Hex). Spectral data: $^1$H-NMR (500 MHz, $CDCl_3$) $\delta$ 3.71 (dd, 1H, *J* = 11.6, 4.4 Hz), 3.42 (dd, 1H, *J* = 11.5, 7.8 Hz), 2.43 (bs, 1H), 2.28 (m, 1H), 2.09 (dd, 1H, *J* = 12.7, 6.2 Hz), 1.42-1.21 (m, 10H), 0.83 (t, 3H, *J* = 7.1 Hz); $^{13}$C NMR (125 MHz, $CDCl_3$) $\delta$ 60.7, 36.1, 35.0, 31.6, 28.9, 28.5, 27.8, 22.4, 13.9; IR (neat, $cm^{-1}$) 3285, 2957, 2926, 1595, 1468, 1041; HRMS (ESI) (m/z): $[M + H]^+$ calculated for $[C_9H_{20}NO]^+$ 158.1545, found 158.1543.

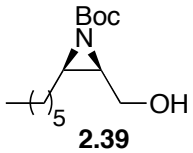


**2.39**

**Preparation of *N*-Boc protected *cis* aziridine alcohol 2.39.** To a solution of aziridine

alcohol **2.38** (83.3 mg, 0.53 mmol) in methanol (2 mL) was added sodium bicarbonate (0.13 g, 1.6 mmol) and $Boc_2O$ (0.19 mL, 0.8 mmol. The solution was sonicated for 2 h. The crude compound was directly dry loaded for purification by column chromatography using 5:1 (Hex:EtOAc) to afford the *N*-Boc protected aziridine alcohol **2.39** (116 mg, 85%) as a colorless oil: $R_F$ = 0.4 (3:1 Hex:EtOAc). Spectral data: $^1$H-NMR (500 MHz, $CDCl_3$) δ 3.62 (m, 2H), 2.81 (bs, 1H), 2.57 (dd, 1H, *J* = 12.4, 6.7 Hz), 2.40 (m, 1H), 1.44 (m, 2H), 1.38 (s, 9H), 1.16-1.33 (m, 6H); $^{13}$C NMR (125 MHz, $CDCl_3$) δ 162.6, 81.1, 60.2, 42.6, 42.3, 31.6, 28.7, 27.7, 27.6, 27.3, 22.4, 13.9; IR (neat, $cm^{-1}$) 3395, 2928, 2856, 1722, 1599, 1369, 1304, 1159, 1043; HRMS (ESI) (m/z): $[M + H]^+$ calculated for $[C_{14}H_{28}NO_3]^+$ 304.1889, found 304.1886.

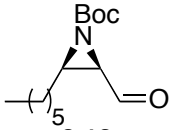


**2.13**

**Preparation of *N*-Boc protected *cis* aziridine-2-carboxaldehyde 2.13.** To a solution of aziridine alcohol **2.39** (0.33 g, 1.28 mmol) in anhydrous DCM (14 mL) was added sodium bicarbonate (0.16 g, 1.92 mmol) and DMP (0.76 g, 1.8 mmol) at 0 ºC. The solution was stirred for 4 h. Upon completion the reaction was quenched with sat. sodium thiosulfate (17 mL), sat. $NaHCO_3$ (17 mL) and water (17 mL). The crude compound was directly dry loaded for purification by column chromatography using 5:1 (Hex:EtOAc) to afford the aziridine aldehyde **2.13** (0.25 g, 84%) as a colorless oil: $R_F$ =

0.75 (3:1 Hex:EtOAc). Spectral data: $^{1}$H-NMR (500 MHz, $CDCl_3$) δ 9.32 (d, 1H, *J* = 5.4 Hz), 2.96 (dd, 1H, *J* = 6.8, 5.3 Hz), 2.69 (m, 1H), 1.62 – 1.49 (m, 4H), 1.44 (s, 9H), 1.37 – 1.27 (m, 6H), 0.86 (t, 3H, *J* = 7 Hz); $^{13}$C NMR (125 MHz, $CDCl_3$) δ 198.2, 160.5, 82.3, 45.7, 44.7, 31.6, 28.7, 28.6, 27.8, 27.3, 22.5, 14.0; IR (neat, $cm^{-1}$) 3363, 2959, 2931, 2864, 1712, 1510, 1460, 1395, 1247, 1171, 1073; HRMS (ESI) (m/z): $[M+H]^+$ calculated for $[C_{14}H_{26}NO_3]^+$ 256.1913, found 256.1934.

**General procedure for the alkylation of aziridine-2-carboxaldehydes by addition of Grignard reagent:**[37] To a solution of aziridine aldehyde (1 mmol) in anhydrous DCM (0.027M) at appropriate temperature, Grignard reagent (5 mmol) was added. For the case when TMEDA was used as additive, 10 equivalents of freshly distilled reagent was added to the reaction mixture. For the case where $MgB_2{\bullet}OEt_2$ was used as additive, 2.5 equivalents of the freshly prepared reagent was added to the reaction mixture. For the case, where $ZnCl_2$ was added, 2.5 equivalents of dried reagent were used. The solution was stirred at the same temperature until no more starting material was observed as analyzed by TLC. The reaction was quenched at the same temperature with sat. $NH_4Cl$ (10 mL) drop wise. The organic layer was washed with brine, the aqueous layer was extracted with EtOAc (3 x 10mL). The combined organic layer was dried over sodium sulfate and then evaporated in vacuum. The crude mixture was purified by column chromatography using an appropriate solvent system.

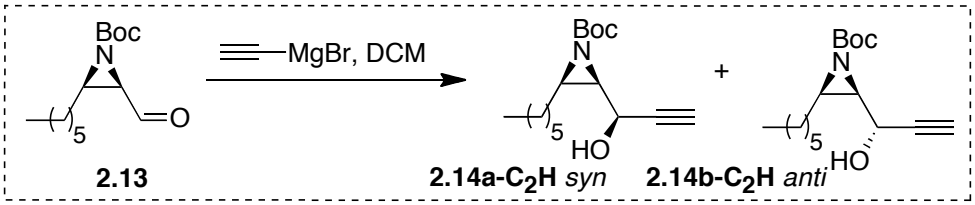


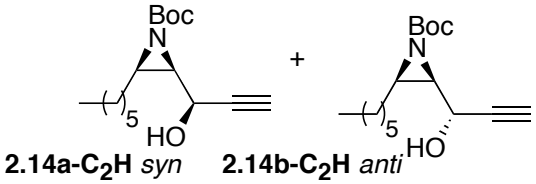


Alkylation of aziridine-2-carboxaldehyde **2.13** was carried out using the representative procedure as discussed above. A mixture of *syn* and *anti* diastereomers was obtained in all the cases; separation was achieved by preparative HPLC in all the cases. $R_F$ (both the isomers) = 0.50 (3:1 Hex:EtOAc). **2.14a-$C_2$H** *syn*: colorless oil. Spectral data: $^1$H-NMR (500 MHz, $CDCl_3$) $\delta$ 4.15 (m, 1H), 2.71 (dd, 1H, *J* = 7.8, 6.6 Hz), 2.53 (d, 1H, *J* = 2.13 Hz), 2.39 (m, 1H), 1.50 (m, 3H), 1.43 (s, 9H), 1.35 – 1.25 (m, 8H), 0.86 (t, H, 6.9 Hz); $^{13}$C NMR (75 MHz, $CDCl_3$) $\delta$ 161.8 81.7, 81.3, 74.4, 60.9, 46.4, 42.6, 31.7, 28.8, 28.0, 27.8, 27.3, 22.5, 14.1; IR (neat, $cm^{-1}$) 3400, 3314, 2955, 2928, 1723, 1456, 1369, 1305, 1159; HRMS (ESI) (m/z): $[M + H]^+$ calculated for $[C_{16}H_{27}NO_3Na]^+$ 304.1889, found 304.1892. **2.14b-$C_2$H** *anti*: white crystalline (stereochemistry was confirmed by X-ray crystallography, see the attached supporting information): Spectral data: $^1$H-NMR (500 MHz, $CDCl_3$) $\delta$ 4.30 (m, 1H), 2.70 (dd, 1H, *J* = 7.6, 6.4 Hz), 2.54 (d, 1H, *J* = 2.19 Hz), 2.46 (m, 1H), 2.10 (d, 1H, *J* = 4.6 Hz), 1.57 – 1.27 (m, 19H), 0.86 (t, 3H, *J* = 7.0

Hz); $^{13}$C NMR (125 MHz, $CDCl_3$) δ 161.9, 82.2, 81.4, 74.1, 60.4, 44.9, 42.7, 31.7, 28.9, 27.8, 27.6, 27.4, 22.6, 14.1; IR (neat, $cm^{-1}$) 3429, 3314, 2957, 2930, 1722, 1456, 1305, 1236, 1159, 1047, 849; HRMS (ESI) (m/z): $[M + H]^+$ calculated for $[C_{16}H_{27}NO_3Na]^+$ 304.1889, found 304.1886;

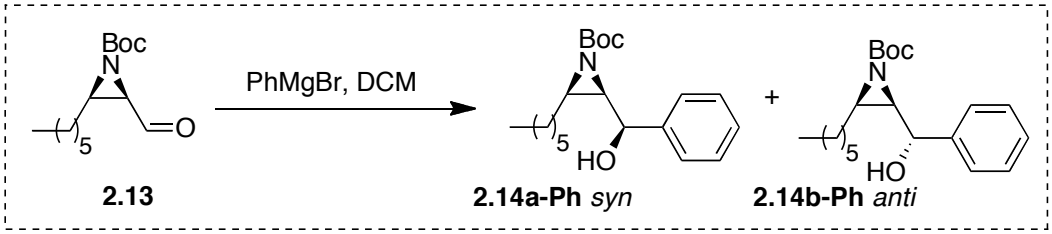


**2.13** **2.14a-Ph** *syn* **2.14b-Ph** *anti*

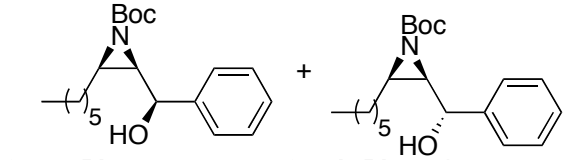


**2.14a-Ph** *syn* **2.14b-Ph** *anti*

Alkylation of aziridine-2-carboxaldehyde **2.13** was carried out using the representative procedure as discussed above. The product was obtained as a mixture of *syn* and *anti* diastereomers. $R_F$ (both the isomers) = 0.71 (3:1 Hex:EtOAc). Purification was achieved by preparative HPLC. **2.14a-Ph** *syn*: colorless oil; Spectral data: $^1$H-NMR (500 MHz, $CDCl_3$) δ 7.41 (d, 1H, J = 8.2 Hz), 7.36 (t, 3H, *J* = 7.1 Hz), 7.29 (t, 1H, *J* = 7.5 Hz), 4.48 (dd, 1H, *J* = 7.8, 2.7 Hz), 2.66 (d, 1H, *J* = 2.8 Hz), 2.62 (d, 1H, *J* = 2.8 Hz), 2.52 (m, 1H), 163 – 1.52 (m, 3H), 1.45 (s, 9H), 1.37 – 1.27 (m, 6H), 0.87 (t, 3H, *J* = 6.9 Hz); $^{13}$C NMR (125 MHz, $CDCl_3$) δ 162.2, 140.9, 128.6, 128.0, 126.3, 81.5, 71.6, 48.3, 43.2, 31.7, 28.9, 28.3, 27.9, 27.6, 22.6, 14.0; IR (neat, $cm^{-1}$) 3422, 2955, 2928, 2856,

1722, 1454, 1369, 1302, 1159; HRMS (ESI) (m/z):[M + H]$^+$ calculated for $[C_{20}H_{32}NO_3]^+$ 334.2382, found 334.2384. **2.14b-Ph** *anti*: colorless oil; Spectral data: $^1$H-NMR (500 MHz, $CDCl_3$) δ 7.49 (d, 2H, *J* = 7.3 Hz), 7.36 – 7.29 (m, 3H), 4.60 (dd, 1H, *J* = 7.8, 3.0 Hz), 2.68 (dd, 1H, *J* = 7.8, 6.3 Hz), 2.48 (m, 1H), 1.96 (d, 1H, *J* = 3.6 Hz), 1.69 – 1.38 (m, 5H), 1.30 (s, 9H), 1.28 (m, 4H), 0.88 (t, 3H, *J* = 6.6 Hz); $^{13}$C NMR (125 MHz, $CDCl_3$) δ 162.2, 141.7, 128.5, 128.4, 127.8, 127.6, 126.5, 126.2, 80.9, 71.9, 46.4, 43.0, 31.8, 29.0, 28.1, 27.7, 27.6, 22.6, 14.1; IR (neat, cm$^{-1}$) 3410, 2928, 2858, 1722, 11697, 1454, 1369, 1305, 1159; HRMS (ESI) (m/z): [M + Na]$^+$ calculated for $[C_{20}H_{31}NO_3Na]^+$ 356.2202, found 356.2206.

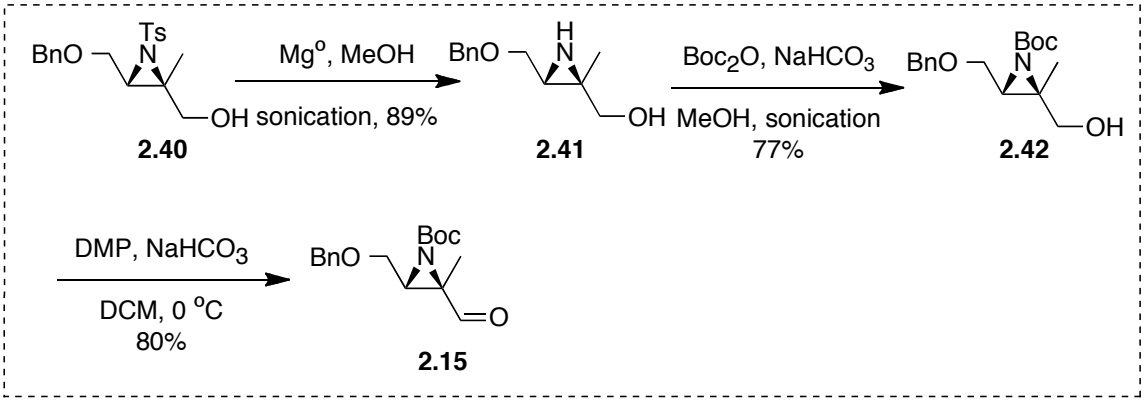


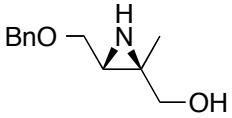


**2.41**

**Preparation of detosylated aziridine alcohol 2.41.**[14,75] To a solution of *N*-Ts aziridine alcohol **2.40** (1.0 g, 3.32 mmol) in methanol (13 mL) was added powdered

magnesium metal (0.4 g, 16.6 mmol). The solution was stirred at 0 ºC for an hour and then warmed to room temperature. The solution was stirred till no more starting material was observed as analyzed by TLC. Upon completion sat. $NH_4Cl$ (10 mL) was added. The aqueous layer was extracted with EtOAc (3 x 50 mL), the combined organic layers were washed with brine and dried over sodium sulfate. The solvent was removed via rotary evaporation and the crude compound was purified by column chromatography (3:1 to 1:1, Hex:EtOAc) to afford detosylated aziridine alcohol **2.41** as an oil (0.79 g, 89%) as a colorless oil: $R_F$ = 0.26 (1:1 Hex:EtOAc). Spectral data: $^1$H-NMR (300 MHz, $CDCl_3$) δ 7.36 (m, 5H), 4.60 (d, 1H, *J* = 12 Hz), 4.53 (d, 1H, *J* = 11.9 Hz), 3.60 (m, 1H), 3.53 (s, 2H), 2.37 (t, 1H, *J* = 6.2 Hz), 1.20 (s, 3H); $^{13}$C NMR (125 MHz, $CDCl_3$) δ 137.7, 128.2, 127.6, 127.5, 126.0, 74.1, 73.1, 68.6, 66.2, 37.1, 14.3; IR (neat, $cm^{-1}$) 3289, 2924, 2862, 1728, 1652, 1601, 1454, 1074; HRMS (ESI) (m/z): $[M + H]^+$ calculated for $[C_{12}H_{18}NO_2]^+$ 208.1338, found 208.1334.

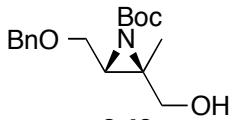


**2.42**

**Preparation of *N*-Boc protected aziridine alcohol 2.42.**[33,76] To a solution of aziridine alcohol **2.41** (87.2 mg, 0.42 mmol) in methanol (2 mL) was added sodium bicarbonate (0.10 g, 1.26 mmol) and $Boc_2O$ (0.15 mL, 0.63 mmol. The solution was sonicated for 1.5 h. The crude compound was directly dry loaded for purification by column

chromatography using 5:1 (Hex:EtOAc) to afford *N*-Boc aziridine alcohol **2.42** (100 mg, 77%) as a colorless oil. $R_F$ = 0.24 (3:1 Hex:EtOAc). Spectral data: $^1$H-NMR (500 MHz, $CDCl_3$) δ 7.33 – 7.26 (m, 5H), 4.65 (d, 1H, *J* = 11.8 Hz), 4.51 (d, 1H, *J* = 11.8 Hz), 3.89 (dd, 1H, *J* = 12.35, 9.9 Hz), 3.68 (dd, 1H, *J* = 10.7, 5.6 Hz), 3.48 (dd, 1H, *J* = 11.0, 6.4 Hz), 3.36 (dd, 1H, *J* = 12.9, 3.3 Hz), 2.87 (dd, 1H, *J* = 10.1, 3.5 Hz), 2.61 (dd, 1H, *J* = 6.5, 5.8 Hz), 1.45 (s, 9H), 1.29 (s, 3H); $^{13}$C NMR (125 MHz, $CDCl_3$) δ 161.6, 137.9, 128.3, 127.7, 81.8, 72.8, 67.8, 66.9, 46.8, 42.7, 27.9, 14.8; IR (neat, $cm^{-1}$) 3420, 3306, 2978, 2930, 2868, 1741, 1454, 1369, 1222, 1163, 1093; HRMS (ESI) (m/z): $[M + H]^+$ calculated for $[C_{17}H_{26}NO_4]^+$ 308.1862, found 308.1863.

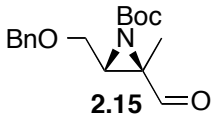

**2.15**

**Preparation of *N*-Boc protected aziridine-2-carboxaldehyde 2.15.** Aziridine alcohol **2.42** (75.3 mg, 0.25 mmol) was dissolved in anhydrous DCM (2.8 mL) and cooled to 0 ºC by ice bath. Sodium bicarbonate (31.5 mg, 0.38 mmol) and DMP (148.5 mg, 0.35 mmol) were added and the reaction was stirred for approximately 4 h. The reaction was quenched with sat. sodium thiosulfate (1.2 mL), sat. $NaHCO_3$ (1.2 mL) and water (1.2 mL). The aqueous layer was extracted with EtOAc (3 x 20 mL) and the combined organic layers were washed with brine and dried over anhydrous sodium sulfate. The crude upon purification by column chromatography afforded the aldehyde **2.15** (59.8 mg, 80%) as a white solid (mp = 32 ºC): $R_F$ = 0.33 (4:1, Hex:EtOAc). Spectral data: $^1$H-

NMR (300 MHz, $CDCl_3$) δ 8.75 (s, 1H), 7.32-7.27 (m, 5H), 4.64 (d, 1H, *J* = 11.8 Hz), 4.51 (d, 1H, *J* = 11.8 Hz), 3.75 (dd, 1H, *J* = 11.1, 5.5 Hz), 3.47 (dd, 1H, *J* = 10.9, 6.6 Hz), 3.07 (dd, 1H, *J* = 6.6, 5.4 Hz), 1.42 (s, 9H), 1.39 (s, 3H); $^{13}C$ NMR (125 MHz, $CDCl_3$) δ 196.0, 158.7, 137.5, 128.6, 128.5, 127.9, 82.6, 73.1, 67.1, 49.6, 44.4, 27.8, 11.1; IR (neat, $cm^{-1}$) 2980, 2936, 2868, 1728, 1456, 1369, 1280, 1159; HRMS (ESI) (m/z): $[M + H]^+$ calculated for $[C_{17}H_{24}NO_4]^+$ 306.1705, found 306.1699.

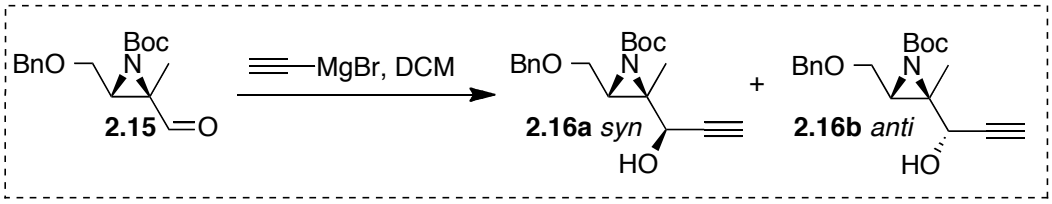


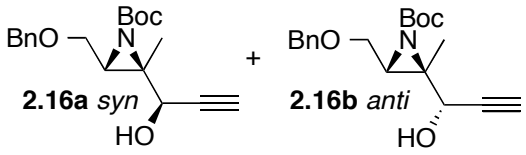


Grignard addition was carried out in a similar fashion as discussed earlier.[38] The product was obtained as a mixture of isomers and separation was achieved by preparative HPLC. $R_F$ (both of the isomers) = 0.34 (4:1 Hex:EtOAc); **2.16a** *syn*: Spectral data: $^1H$-NMR (300 MHz, $CDCl_3$) δ 7.33 – 7.28 (m, 5H), 4.63 (d, 1H, *J* = 11.7 Hz), 4.55 (d, 1H, *J* = 11.8 Hz), 3.98 (dd, 1H, *J* = 3.2, 2.2 Hz), 3.72 (d, 1H, *J* = 3.4 Hz), 3.67 (dd, 1H, *J* = 11.5, 5.9 Hz), 3.55 (dd, 1H, *J* = 11.5, 6.1 Hz), 2.65 (t, 1H, *J* = 6.6 Hz), 2.51 (dd, 1H, *J* = 2.2, 0.8 Hz), 1.50 (s, 9H), 1.42 (s, 3H); $^{13}C$ NMR (125 MHz, $CDCl_3$) δ 161.5,

128.4, 127.7, 127.6, 82.7, 74.6, 72.5, 68.1, 67.2, 43.7, 29.7, 27.9, 12.1; IR (neat, $cm^{-1}$) 3390, 3294, 2932, 1711, 1496, 1392, 1315, 1251; HRMS (ESI) (m/z): $[M + H]^+$ calculated for $[C_{19}H_{26}NO_4]^+$ 332.1862, found 332.1865; **2.16b** *anti*: Spectral data: $^1$H-NMR (300 MHz, $CDCl_3$) δ 7.33 – 7.28 (m, 5H), 4.66 (d, 1H, *J* = 10.2, 2.3 Hz), 4.54 (d, 1H, *J* = 11.9 Hz), 3.93 (d, 1H, *J* = 10.4 Hz), 3.67 (d, 1H, *J* = 10.9, 5.6 Hz), 3.51 (dd, 1H, *J* = 11.1, 6.3 Hz) , 3.11 (t, 1H, *J* = 5.9 Hz), 2.52 (d, 1H, *J* = 2.4 Hz), 1.46 (s, 9H), 1.38 (s, 3H); $^{13}$C NMR (125 MHz, $CDCl_3$) δ 161.0, 128.6, 128.0, 82.3, 73.1, 68.1, 66.1, 43.7, 28.2, 16.1; IR (neat, $cm^{-1}$) 3420, 3289, 2980, 2932, 1689, 1454, 1369, 1315, 1161; HRMS (ESI) (m/z): $[M + H]^+$ calculated for $[C_{19}H_{26}NO_4]^+$ 332.1862, found 332.1860. Stereochemistry of **2.16a** *syn* was confirmed by carrying out the following transformation:

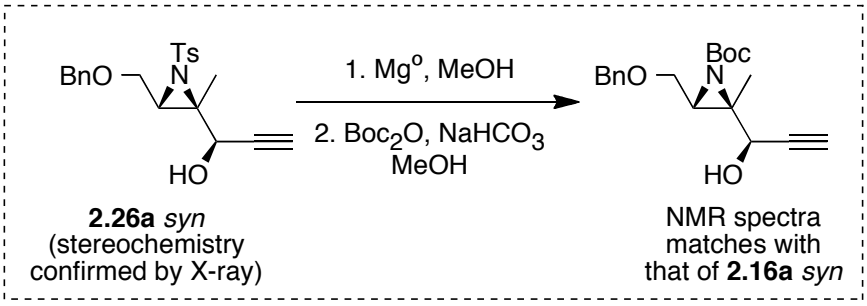

**Preparation of *N*-Ts aziridine substrates:**

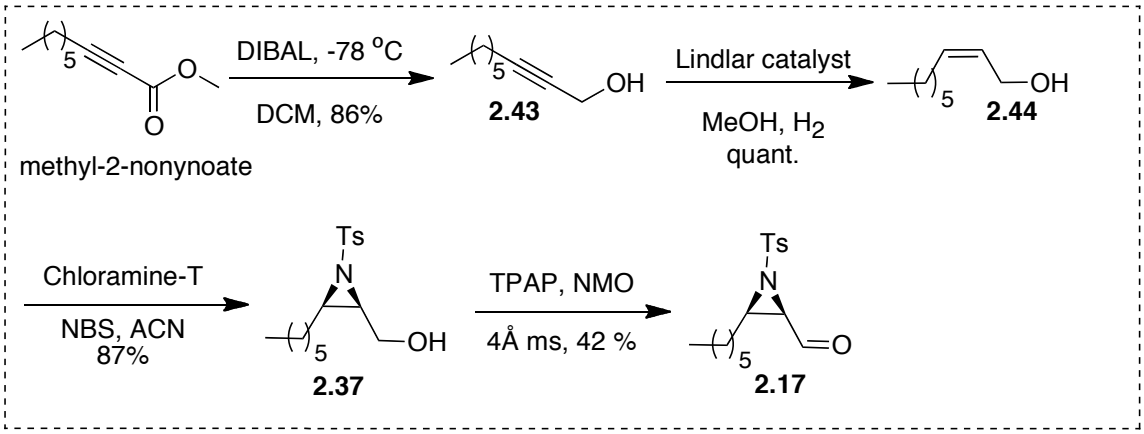


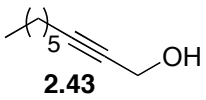

**2.43**

**Preparation of propargylic alcohol 2.43.**[14,77] Methy-2-nonynoate (2.5 g, 14.9 mmol) was dissolved in anhydrous DCM (75 mL) and the solution was cooled to -78 °C. 1 M solution of DIBAL in toluene (32.7, 32.7 mmol) was added drop wise and allowed to stir for 15 min and then warmed to room temperature. Saturated solution of Rochelle's salt (10 mL) was carefully added, followed by glycerol (0.5 mL). The biphasic system was stirred at room temperature for 6 h. Water (50 mL) was added and the aqueous phase was extracted with EtOAc (3 x 100 mL). Combined organic layers were washed with brine (10 mL) and dried over sodium sulfate. The crude product was purified via column chromatography (4:1 Hex/EtOAc) to afford alcohol **2.43** as a colorless oil (1.79 g, 86%). $R_F$ = 0.71 (4:1 Hex:EtOAc). Spectral data: $^1$H NMR (500 MHz, $CDCl_3$) $\delta$ 4.25 (dt, 2H, *J* = 3.0, 2.1 Hz), 2.60 (br s, 1H), 2.20 (m, 2H), 1.50 (m, 2H), 1.2-1.45 (m, 6H), 0.78 (t, 3H,

$J$ = 6.6 Hz); $^{13}$C NMR (125 MHz, $CDCl_3$) δ 86.0, 78.0, 51.0, 31.2, 28.5, 28.4, 22.4, 18.6, 13.9.

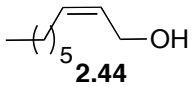


**2.44**

**Preparation of allylic alcohol 2.44.**[14] Propargylic alcohol **2.43** (2.2 g, 11.6 mmol) was dissolved in methanol (120 mL) and 5 drops of chloroform. Lindlar catalyst (550 mg, 5% Pd by wt, 0.25 mmol) was added. The flask was evacuated and filled with 1 atmosphere of hydrogen (using a balloon filled with hydrogen gas). The suspension was stirred at room temperature for 5 h, the catalyst was removed via filtration through a pad of celite and the filtrate was then evaporated under reduced pressure. The crude product was obtained as an oil with a quantitative yield and was taken to the next step without further purification. $R_F$ = 0.69 (4:1 Hex:EtOAc). Spectral data: $^1$H NMR (300 MHz, $CDCl_3$) δ 5.55 (m, 2H), 4.17 (d, 1H, $J$ = 5.7 Hz), 2.05 (dd, 2H, $J$ = 13.2, 6.9 Hz), 1.33 –1.2 (m, 8H), 0.88 (t, 3H, $J$ = 6.6 Hz); $^{13}$C NMR (75 MHz, $CDCl_3$) δ 85.3, 78.5, 51.1, 30.9, 29.0, 28.1, 22.7, 19.1, 14.1.

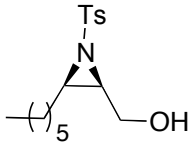


**2.37**

**Preparation of 2.37.**[14] Allylic alcohol **2.44** (1.23 g, 6.45 mmol) was dissolved in

acetonitrile (30 mL). Anhydrous chloramine-T (1.47 g, 6.45 mmol) and N-bromosuccinimide (0.23g, 1.29 mmol) were successively added and allowed to stir overnight. The reaction mixture was quenched with water (30 mL). The aqueous phase was extracted with EtOAc (3 X 15 mL), the combined organic layers were washed with brine and dried over sodium sulfate. The crude product was purified via column chromatography (3:1 Hex:EtOAc) to give aziridine alcohol **2.37** (2.34 g, 87%) as a yellow syrup. $R_F$ = 0.54 (3:1 Hex:EtOAc). Spectral data: $^1$H NMR (300 MHz, $CDCl_3$) $\delta$ 7.8 (d, 2H, *J* = 8.2 Hz), 7.3 (d, 2H, *J* = 8.0 Hz), 3.7 (m, 1H), 3.55 (m, 1H), 3.0 (dd, 1H, *J* = 7.5, 5.1 Hz), 2.7 (dd, 1H, *J* = 7.8, 5.7 Hz), 2.4 (s, 3H), 1.4 (m, 2H), 1.3 – 1.0 (m, 8H), 0.8 (t, 3H, *J* = 6.8 Hz); $^{13}$C NMR (75 MHz, $CDCl_3$) $\delta$ 144.5, 134.5, 129.6, 128.0, 59.2, 44.9, 31.4, 28.6, 27.1, 26.7, 22.3, 21.5, 13.9.

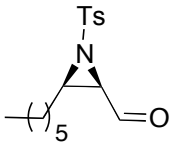

**2.17**

**Preparation of *N*-Ts protected aziridine-2-carboxaldehyde 2.17.**[78] Aziridine alcohol **2.37** (3.0 g, 9.65 mmol) was dissolved in dry acetonitrile (19.3 mL). TPAP (0.17 g, 0.48 mmol), NMO (1.75 g, 14.47 mmol) and activated 4Å molecular sieves (500 mg/mmol) were added to the above solution. The reaction mixture was stirred at room temperature. After completion of the reaction as analyzed by TLC, the crude product was purified via column chromatography (5:1 Hex:EtOAc) to give aldehyde **2.17** (1.25 g, 42%) as a white solid (mp= 55 ºC); $R_F$ = 0.75 (3:1 Hex:EtOAc). Spectral data: $^1$H NMR

(300 MHz, $CDCl_3$) δ 9.33 (d, 1H, *J* = 5.1 Hz), 7.88 (d, 2H, *J* = 8.4 Hz), 7.38 (d, 2H, *J* = 8.4 Hz), 3.24 (dd, 1H, *J* = 8.1, 5.7 Hz), 3.09 (dt, 1H, *J* = 7.8, 5.7 Hz), 2.44 (s, 3H), 1.6 – 1.2 (m, 10H), 0.88 (m, 3H); $^{13}C$ NMR (125 MHz, $CDCl_3$): δ 195.4, 146.0, 134.1, 130.1, 128.5, 47.0, 46.0, 31.7, 28.7, 27.9, 27.5, 22.6, 21.9, 14.2; IR (neat) 2926, 2857, 1728, 1599, 1460, 1329, 1101, 1092, 912; HRMS (ESI) (m/z): $[M+H]^+$ calculated for $[C_{16}H_{24}NO_3S]^+$ 310.1477, found 310.1473.

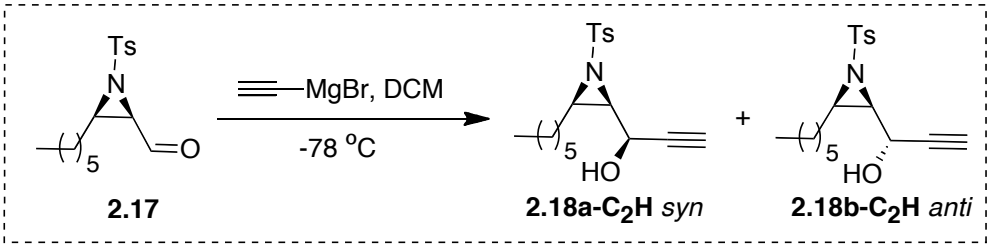


**2.17** **2.18a-$C_2$H** *syn* **2.18b-$C_2$H** *anti*

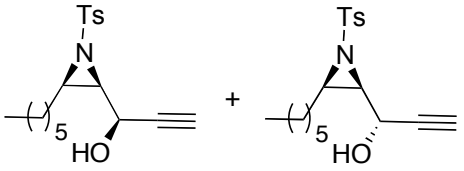


**2.18a-$C_2$H** *syn* **2.18b-$C_2$H** *anti*

**General procedure for the alkylation by the addition of Grignard reagent to *N*-Ts protected aziridine-2-carboxaldehydes.** The aldehyde (0.69 mmol, 1.0 equiv) was dissolved in dry DCM (0.027 M) and cooled to -78 °C. Alkylmagnesium bromide (3.5 mL of 1 M solution in THF, 5.0 equiv) was added drop wise over 10 min. For the case where TMEDA was used, 10 equivalents of the freshly distilled reagent were used. For the case where $Mg.Br_2{\cdot}OEt_2$ was used, 2.5 equivalents of freshly prepared reagent were added. The reaction was stirred till all the starting material was consumed as

analyzed by TLC. The reaction mixture was quenched with saturated ammonium chloride at -78 °C and extracted three times with DCM. Combined organic layers were washed with brine and dried over sodium sulfate. The crude products were purified via column chromatography and further ratios of *syn* vs *anti* were determined by analyzing the integrations of crude NMR (in some cases preparative HPLC).

**Alkylation of aziridine-2-carboxaldehyde 2.17**. A mixture of **2.18a-$C_2$H** *syn* and **2.18b-$C_2$H** *anti* adducts was obtained, which was separated by preparative HPLC. $R_F$ (both the isomers) = 0.36 (3:1 Hex:EtOAc). *Major diastereomer*: colorless oil; Spectral data: $^1$H-NMR (300 MHz, $CDCl_3$) δ 7.82 (d, 2H, *J* = 8.2 Hz), 7.33 (d, 2H, *J* = 8.3 Hz), 4.16 (m, 1H), 3.07 (dd, 1H, *J* = 8.07, 7.53 Hz), 2.87 (m, 1H), 2.52 (d, 1H, *J* = 2.2 Hz), 2.42 (s, 3H), 1.93 (d, 1H, *J* = 5.1 Hz), 1.57 – 1.25 (m, 9H), 0.86 (t, 3H, *J* = 7.3 Hz); $^{13}$C NMR (125 MHz, $CDCl_3$) δ 144.8, 134.7, 129.5, 128.5, 81.4, 75.1, 60.1, 48.4, 44.7, 31.5, 29.7, 28.7, 27.3, 27.1, 14.0; IR (neat) 3460, 3283, 2955, 2858, 1599, 1460, 1325, 1101, 1091, 874; HRMS (ESI) (m/z): $[M+H]^+$ calculated for $[C_{18}H_{26}NO_3S]^+$ 336.1633, found 336.1630; *Minor diastereomer*: colorless oil; Spectral data: $^1$H-NMR (300 MHz, $CDCl_3$) δ 7.83 (d, 2H, *J* = 8.3 Hz), 7.31 (d, 2H, *J* = 8.4 Hz), 4.22 (m, 1H), 3.02 (d, 1H, *J* = 7.2, 7.22 Hz), 2.88 (m, 1H), 2.42 (s, 3H), 2.26 (d, 1H, *J* = 2.2 Hz), 1.91 (d, 1H, *J* = 5.4 Hz), 1.24 – 1.17 (m, 9H), 0.84 (t, 3H, *J* = 7.4 Hz); $^{13}$C NMR (125 MHz, $CDCl_3$) δ 144.6, 134.3, 129.5, 128.5, 80.4, 74.5, 60.0, 47.0, 44.6, 31.5, 28.8, 27.2, 26.7, 22.4, 21.6, 14.0; IR

(neat) 3304, 2928, 2850, 1604, 1402, 1355, 1101; HRMS (ESI) (m/z): $[M+H]^+$ calculated for $[C_{18}H_{26}NO_3S]^+$ 336.1633, found 336.1634.

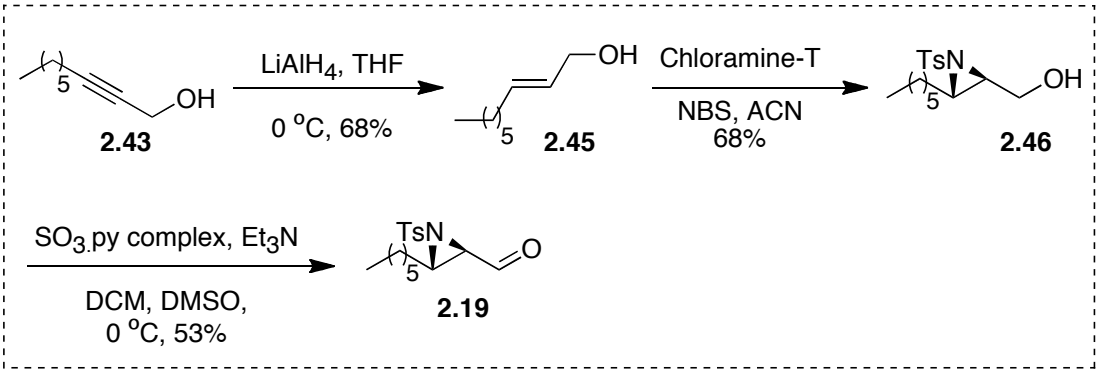


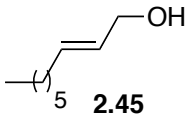


**Preparation of allylic alcohol 2.45**.[79] To a suspension of lithium aluminium hydride (0.7 g, 17.86 mmol) at 0 °C in dry THF (10 mL) was added compound propargylic alcohol **2.43** (2.27 g, 16.25 mmol) dissolved in dry THF (2 mL) via cannula. The reaction was stirred at 0 °C for 10 min before it was allowed to warm to room temperature and allowed to stir for 12 hrs. Upon completion, the reaction was carefully quenched at 0°C by the addition of water (0.7 mL) and 3 M NaOH (0.7 mL) followed by water (3X 0.7 mL). The mixture was carefully filtered and the filter cake was washed repeatedly with diethyl ether (5 X 10 mL) and DCM (2 mL). Concentration in vacuo and purification by column chromatography provided allylic alcohol **2.45** (0.48 g, 68%) as an oil. $R_F$ = 0.21 (3:1 Hex:EtOAc). Spectral data: $^1$H NMR (300 MHz, $CDCl_3$) $\delta$ 5.62 (m,

2H), 7.83 (d, 2H, *J* = 8.4 Hz), 7.33 (d, 2H, *J* = 8.4 Hz), 3.24 (m, 1H), 3.09 (m, 1H), 2.44 (s, 3H), 1.2 (m, 10H), 0.86 (m, 3H); $^{13}$C NMR (75 MHz, $CDCl_3$) δ 131.3, 129.1, 69.2, 33.7, 31.9, 29.9, 29.4, 14.1.

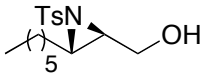


**2.46**

**Preparation of aziridine alcohol 2.46.** Allylic alcohol **2.45** (1.5 g, 10.55 mmol) was dissolved in acetonitrile (21 mL). Anhydrous chloramine-T (1.88 g, 10.55 mmol) and *N*-bromosuccinimide (0.48g, 2.11 mmol) were successively added and allowed to stir overnight. The reaction mixture was then diluted with water (10 mL). The reaction was extracted with EtOAc (3 X 10 mL). The combined organic layers were washed with brine (5 mL) and dried over sodium sulfate. The crude product was purified via column chromatography (9:1 Hex:EtOAc) to give aziridine alcohol **2.46** (2.2 g, 68%) as a colorless oil. $R_F$ = 0.39 (3:1 Hex:EtOAc). Spectral data: $^1$H NMR (300 MHz, $CDCl_3$) δ 7.82 (d, 2H, *J* = 9 Hz), 7.30 (d, 2H, *J* = 9 Hz), 4.14 (m, 1H), 3.83 (m, 1H), 2.93 (m, 2H), 2.65 (bm, 1H), 2.42 (s, 3H), 1.63 -1.45 (m, 2H), 1.2 (m, 8H), 0.84 (m, 3H); $^{13}$C NMR (125 MHz, $CDCl_3$) δ 144.2, 137.2, 129.6, 127.3, 60.9, 51.8, 46.5, 31.5, 29.7, 28.6, 27.1, 22.4, 21.6, 14.0; IR (neat) 3510, 2958, 2870, 1458, 1321, 1020; HRMS (ESI) (m/z): $[M+H]^+$ calculated for $[C_{16}H_{25}NO_3SH]^+$ 312.1633, found 312.1630.

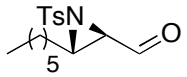


**2.19**

**Preparation of *N*-Ts protected *trans* aziridine-2-carboxaldehyde 2.19.** Aziridine alcohol **2.46** (1.15 g, 3.7 mmol) was dissolved in dry DCM (28 mL) and cooled to 0 °C. Triethylamine (1.5 g, 14.8 mmol) was added followed by $SO_3$.Pyridine complex (1.8 g, 11.1 mmol) dissolved in dry DMSO (11 mL). The reaction was stirred for 30 min and diluted with a 2:1 mixture of Hex/diethyl ether (50 mL). The organic layer was washed with sat. $NaHCO_3$ (10 mL) and the aqueous layer was back-extracted with more Hex/diethyl ether. The combined organic layer was then washed with a 1 M solution of sodium phosphate monobasic (10 mL) then brine (10 mL) and the organics were dried over sodium sulfate. The crude product was purified via column chromatography (7:1 Hex/EtOAc) to give aziridine-2-carboxaldehyde **2.19** (0.61 g, 53%) as an oil. $R_F$ = 0.45 (3:1 Hex:EtOAc). Spectral data: $^1$H NMR (300 MHz, $CDCl_3$) δ 9.42 (d, 1H, *J* = 6.6 Hz), 7.83 (d, 2H, *J* = 8.4 Hz), 7.34 (d, 2H, *J* = 8.4 Hz), 3.35 (m, 1H), 3.09 (m, 1H), 2.43 (s, 3H), 1.6 (m, 2H), 1.23 (m, 8H), 0.85 (m, 3H); $^{13}$C NMR (75 MHz, $CDCl_3$) δ 194.4, 145.0, 136.0, 129.8, 127.7, 52.4, 46.9, 31.5, 30.0, 28.5, 27.0, 22.4, 21.6, 14.0; IR (neat) 3068, 2926, 2857, 1719, 1597, 1458, 1329, 1161; HRMS (ESI) (m/z): $[M+H]^+$ calculated for $[C_{16}H_{23}NO_3SH]^+$ 310.1477, found 310.1470.

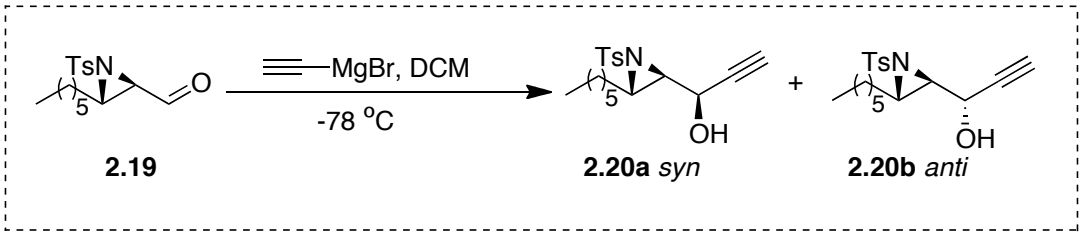


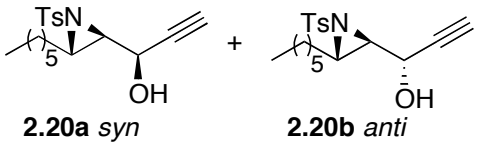


**Alkylation of carboxaldehyde 2.19 by the addition of Grignard reagent:** Refer to the general procedure as described previously. **2.20a** *syn*: Spectral data: $^{1}$H NMR (300 MHz, $CDCl_3$) δ 7.80 (d, 2H, *J* = 8.1 Hz), 7.25 (d, 2H, *J* = 8.1 Hz), 4.47 (m, 1H), 3.30 (dd, 1H, *J* = 4.5 Hz, 0.1 Hz), 2.89 (m, 1H), 2.42 (s, 3H), 1.75 - 1.62 (m, 2H), 1.33 - 1.16 (m, 8H), 0.84 (t, 3H, *J* = 4.5 Hz); $^{13}$C NMR (125 MHz, $CDCl_3$) δ 144.7, 137.2, 129.8, 127.8, 80.7, 74.8, 61.5, 53.2, 47.3, 31.8, 29.5, 28.9, 27.5, 22.7, 21.9, 14.3; IR (neat) 3310, 2926, 1599, 1460, 1159; HRMS (ESI) (m/z): $[M+H]^+$ calculated for $[C_{18}H_{26}NO_3S]^+$ 336.1633, found 336.1633. **2.20b** *anti*: Spectral data: $^{1}$H NMR (300 MHz, $CDCl_3$) δ 7.83 (d, 2H, *J* = 8.1 Hz), 7.30 (d, 2H, *J* = 8.0 Hz), 4.50 (m, 1H), 3.1 (t, 1H, *J* = 2.9 Hz), 2.40 (s, 3H), 2.05 (m, 1H), 1.86 (m, 1H), 1.18-1.31 (m, 8H), 0.87 (t, 3H, *J* = 4.5 Hz). $^{13}$C NMR (125 MHz, $CDCl_3$) δ 129.6, 127.6, 74.8, 60.3, 49.9, 48.0, 31.6, 29.7, 28.7, 27.8, 22.5, 21.6, 14.0; IR (neat) 3341, 2924, 1595, 1423, 1120 ; HRMS (ESI) (m/z): $[M+H]^+$ calculated for $[C_{18}H_{26}NO_3S]^+$ 336.1633, found 336.1637.

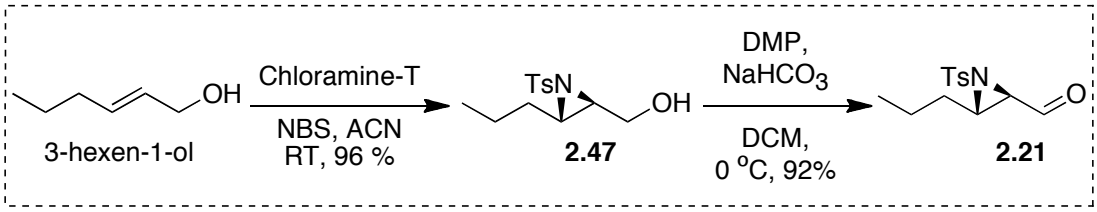


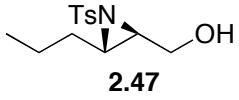


**2.47**

**Preparation of aziridine alcohol 2.47.** To a solution of 3-hexen-1-ol (2.53 g, 25.25 mmol) in acetonitrile (126 mL) was added chloramine-T (5.75 g, 25.25 mmol) and NBS (0.9 g, 5.05 mmol). The reaction mixture was stirred at room temperature for 12 h, which upon completion was diluted with water (80 mL). The aqueous phase was extracted with EtOAc (3 X 25 mL), concentrated and purified over silica to afford aziridine alcohol **2.47** (6.5 g, 96%) as a yellow syrupy oil. $R_F$ = 0.34 (3:1 Hex:EtOAc). Spectral data: $^1$H NMR (500 MHz, $CDCl_3$) $\delta$ 7.82 (d, 2H, $J$ = 8.3 Hz), 7.31 (d, 2H, $J$ = 8.2 Hz), 4.07 (m, 1H), 3.88 (m, 1H), 2.93 (m, 2H), 2.63 (dd, 1H, $J$ = 9.2, 5.3 Hz), 2.42 (s, 3H), 1.58 – 1.51 (m, 3H), 1.27 (m, 2H), 0.85 (t, 3H, $J$ = 7.4 Hz); $^{13}$C NMR (125 MHz, $CDCl_3$) $\delta$ 144.2, 137.3, 129.6, 127.3, 60.9, 51.7, 46.2, 32.2, 21.6, 20.4, 13.4; IR (neat) 3515, 2961, 2874, 1458, 1321, 1159, 1020; HRMS (ESI) (m/z): $[M+H]^+$ calculated for $[C_{13}H_{20}NO_3S]^+$ 270.1164, found 270.1167.

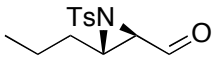


**2.21**

**Preparation of *N*-Ts protected aziridine-2-carboxaldehyde 2.21.** The aziridine alcohol **2.47** (1.4 g, 5.2 mmol) was dissolved in dry DCM (58 mL) and cooled to 0 °C. The solution was treated with sodium bicarbonate (0.66 g, 7.8 mmol) and DMP (3.1 g, 7.28 mmol) and stirred for 3 h. The reaction mixture was quenched with a mixture of 1:1:1 saturated sodium bicarbonate/sodium *m*-bisulfite/water (2.3 mL each) and extracted with DCM (3 X 10 mL). Combined organic layers were washed brine (5 mL) and dried over sodium sulfate. The crude product was purified via column chromatography (8:2 Hex/EtOAc) to give aldehyde **2.21** (1.28 g, 92%) as a yellow oil. $R_F$ = 0.6 (3:1 Hex:EtOAc). Spectral data: $^1$H NMR (500 MHz, $CDCl_3$) $\delta$ 9.40 (d, 1H, *J* = 6.8 Hz), 7.81 (d, 2H, *J* = 8.3 Hz), 7.32 (d, 2H, *J* = 8.3 Hz), 3.35 (m, 1H), 3.05 (dd, 1H, *J* = 6.8, 3.4 Hz), 2,42 (s, 3H), 1.68 -1.60 (m, 2H), 1.34 (m, 2H), 0.87 (t, 3H, *J* = 7.3 Hz); $^{13}$C NMR (125 MHz, $CDCl_3$) $\delta$ 194.4, 144.9, 135.8, 129.8, 129.6, 129.5, 127.6, 52.3, 46.7, 31.8, 21.6, 21.5, 20.3, 13.4; IR (neat, $cm^{-1}$) 2956, 2936, 2876, 1720, 1599, 1329, 1163, 912; HRMS (ESI) (m/z): $[M + H]^+$ calculated for $[C_{13}H_{18}NO_3S]^+$ 268.1010, found 268.1007.

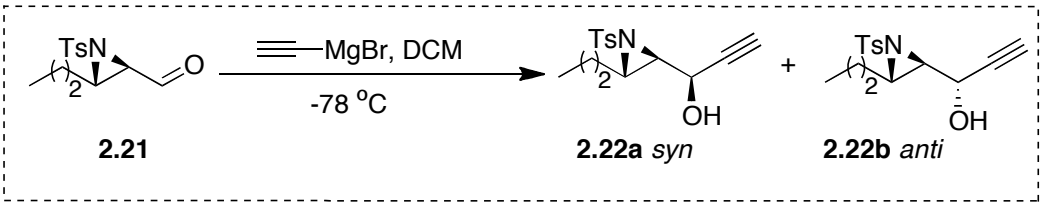


**2.21** **2.22a** *syn* **2.22b** *anti*

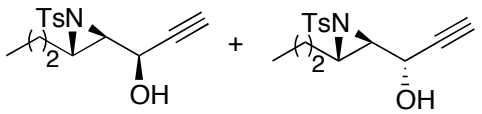


**2.22a** *syn* **2.22b** *anti*

**Alkylation of *N*-Ts protected trans aziridine-2-carboxaldehyde 2.21 by addition of Grignard reagent**: Refer to the general procedure as described previously. Compound **2.22a** *syn*: Spectral data: $^{1}$H NMR (300 MHz, $CDCl_3$):δ 7.84 (d, 2H, *J* = 8.4 Hz), 7.31 (d, 2H, *J* = 8.3 Hz), 4.53 (m, 1H), 3.04 (dd, 1H, *J* = 7.0, 4.3 Hz), 2.90 (m, 1H), 2.73 (d, 1H, *J* = 5.5 Hz), 2.45 (d, 1H, *J* = 2.2 Hz), 2.42 (s, 3H), 1.77 (m, 1H), 1.67 (m, 1H), 1.38 (m, 2H), 0.91 (t, 3H, *J* = 7.4 Hz); $^{13}$C NMR (125 MHz, $CDCl_3$):δ 144.4, 137.0, 129.6, 127.6, 80.6, 74.5, 61.3, 52.9, 46.8, 31.3, 21.6, 13.6; IR (neat, $cm^{-1}$) 3481, 3279, 2963, 2876, 1599, 1450, 1321, 1159; HRMS (ESI) (m/z): $[M + H]^+$ calculated for $[C_{15}H_{20}NO_3S]^+$ 294.1164, found 294.1167; Compound **2.22b** *anti*: Spectral data: δ 7.84 (d, 2H, *J* = 8.3 Hz), 7.31 (d, 2H, *J* = 8.0 Hz), 4.50 (m, 1H), 3.11 (t, 1H, *J* = 4.2 Hz), 2.94 (dt, 1H, *J* = 8.3, 5.1 Hz), 2.42 (s, 3H), 2.40 (dd, 1H, *J* = 2.2, 0.5 Hz), 2.07 (m, 2H), 1.95 (d, 1H, *J* = 6 Hz), 1.85 (m, 2H), 0.97 (t, 3H, *J* = 4.6 Hz); $^{13}$C NMR (125 MHz, $CDCl_3$):δ 144.4, 137.3, 129.6, 127.6, 80.3, 74.8, 60.3, 49.9, 47.8, 29.9, 21.6, 21.1, 13.6; IR (neat, $cm^{-1}$) 3285, 2934, 1602, 1496, 1091, 1159; HRMS (ESI) (m/z): $[M + H]^+$ calculated for $[C_{15}H_{20}NO_3S]^+$ 294.1164, found 294.1160. The stereochemistry of **2.22a** *syn* was established on the basis of its successful participation in one-pot tandem aza-Payne hydroamination protocol as shown below (note the *anti* isomer is incapable of undergoing the following transformation):[14]

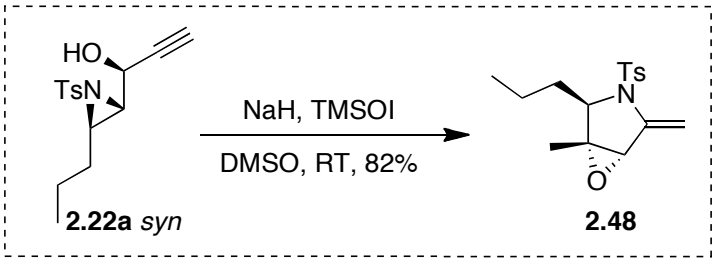


**2.22a** *syn* **2.48**

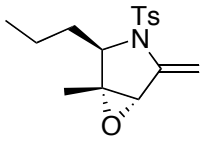


**2.48**

**Preparation of N-Ts enamide 2.48.** NaH (60% dispersion in oil) (23 mg, 0.57 mmol) was suspended in anhydrous freshly distilled DMSO (2.9 mL). This was treated with trimethylsulfoxonium iodide (0.126 g, 0.57 mmol). The reaction was stirred at room temperature for 30 min. Aziridine alcohol **2.22a** (84 mg, 0.29 mmol) dissolved in small amount of anhydrous DMSO (~ 0.2 mL) was added to the above solution. The reaction was stirred at room temperature overnight. After completion, the reaction was quenched with sat. $NH_4Cl$ (1 mL). The aqueous phase was extracted with EtOAc (3 X 2 mL). The combined organic layers were washed with brine (1 mL) and dried over anhydrous sodium sulfate and solvent was removed via rotary evaporation. Upon purification with silica gel chromatography (9:1 Hex:EtOAc) compound **2.48** (68.5 mg, 82%) was obtained as a white solid (mp = 110- 112 ºC). $R_F$ = 0.37 (5:1 Hex:EtOAc). Spectral data: $^1$H-NMR (500 MHz, $CDCl_3$) $\delta$ 7.65 (d, 2H, $J$ = 8.6 Hz), 7.24 (d, 2H, $J$ = 7.9 Hz), 5.42 (s, 1H), 4.85 (s, 1H), 4.11 (m, 1H), 3.59 (d, 1H, $J$ = 3.2 Hz), 3.50 (d, 1H, $J$ = 2.9 Hz), 2.38 (s, 3H), 1.72 (m, 3H), 1.46 (m, 2H), 0.97 (t, 3H, $J$ = 7.5 Hz); $^{13}$C NMR (125

MHz, $CDCl_3$) δ 143.9, 141.5, 134.6, 129.2, 128.0, 100.3, 63.2, 56.6, 56.1, 35.2, 21.6, 18.2, 14.0; IR (neat) 2951, 2872, 1657, 1344, 1165, 1032; HRMS (ESI) (m/z): $[M+H]^+$ calculated for $[C_{15}H_{20}NO_3S]^+$ 294.1164, found 294.1163.

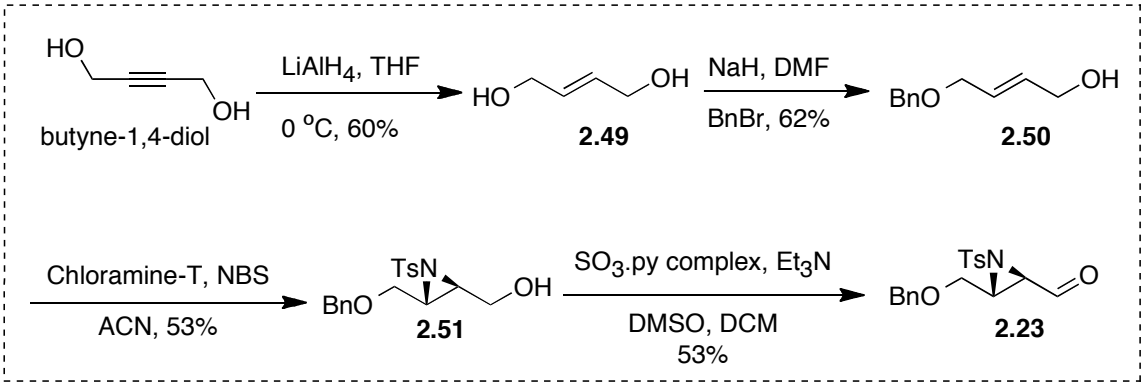


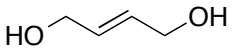


**2.49**

**Preparation of allylic alcohol 2.49.**[80] To a suspension of lithium aluminium hydride (13.49 g, 348 mmol) in dry THF (1000 mL) at 0 ºC was added 1,4-butyne-diol (25 g, 290 mmol) dissolved in dry THF (260 mL) via cannula. The reaction was stirred at 0 °C for 10 min before it was allowed to warm to room temperature and allowed to stir for 12 h. Upon completion, the reaction was cooled to 0 °C and celite (6 g) was added. The mixture was carefully hydrolyzed by the addition of saturated $(NH_4)_2SO_4$ (32 mL) and filtered through celite, where the filter cake was washed repeatedly with diethyl ether and DCM. Concentration at reduced pressure and purification by distillation provided allylic alcohol **2.49** (14.7 g, 60%) (bp ≈ 105 °C, 2 torr) as a viscous oil. Spectral data: $^1H$

NMR (300 MHz, $CDCl_3$) δ 5.88 (dt, 2H, *J* = 2.4, 1.2 Hz), 4.16 (dd, 4H, *J* = 2.4, 1.2 Hz); $^{13}C$ NMR (75 MHz, $CDCl_3$) δ 130.5, 62.8.

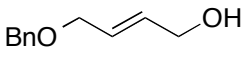


**2.50**

**Preparation of benzyl ether 2.50.**[81] NaH (0.227 g, 5.68 mmol) was washed two times with cyclohexane and suspended in dry DMF (7.88 ml). To this stirred suspension under $N_2$ at room temperature was added diol **2.49** (1 g, 11.35 mmol) drop wise over 20 min. After stirring for 2 h, benzyl bromide (0.449 ml, 3.78 mmol) was added and stirred for 16 h. The resulting mixture was carefully poured onto crushed ice (21 g), and the solution was extracted with $Et_2O$ (3 x 20 mL). The ethereal solutions were combined, washed with water (2 X 5 mL) and once with brine (2 mL), dried over sodium sulfate, filtered, concentrated under vacuum and distilled to give benzyl ether **2.50** (1.25 g, 62%) as a yellow oil; bp = 130-133 °C (0.05 torr). Spectral data: $^1H$ NMR (300 MHz, $CDCl_3$) δ 7.2 (m, 5H), 5.7 (m, 2H), 4.4 (s, 2H), 4.0 (d, 2H, *J* = 4.2 Hz), 3.85 (d, 2H), 1.9 (br s, 1H); $^{13}C$ NMR (75 MHz, $CDCl_3$) δ 138.0, 132.3, 128.3, 127.7, 127.6, 127.5, 72.2, 70.0, 62.7.

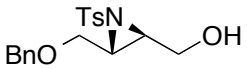


**2.51**

**Preparation of 2.51.**[14] The allylic alcohol **2.50** (10 g, 56.1 mmol) was placed in dry acetonitrile (50 mL) and treated with chloramine T (9.99 g, 56.1 mmol) and N-

bromosuccinimide (2.55 g, 11.22 mmol). The light yellow slurry was stirred at room temperature overnight, upon completion, diluted with water (25 mL) and extracted with EtOAc (3 X 20 mL). Combined organic layers were washed with brine (10 mL), dried over sodium sulfate and the volatiles removed by rotary evaporation. The residue was purified via column chromatography (4:1 Hex:EtOAc) to give aziridine alcohol **2.51** (10.3 g, 53%) as a white syrup. $R_F$ = 0.17 (3:1 Hex:EtOAc). Spectral data: $^1$H NMR (300 MHz, $CDCl_3$) δ 7.8 (d, 2H, *J* = 8.2), 7.1-7.4 (m, 7H), 4.4 (s, 2H), 4.1 (m, 1H), 3.9 (m, 1H), 3.7 (dd, 1H, *J* = 11.0, 4.1 Hz), 3.5 (dd, 1H, *J* = 11.0, 6.6 Hz), 3.2 (dt, 1H, *J* = 6.6, 4.4 Hz), 3.0 (m, 1H), 2.8 (br s, 1H), 2.4 (s, 3H); $^{13}$C NMR (75 MHz, $CDCl_3$) δ 144.3, 137.5, 136.8, 129.6, 128.3, 127.7, 127.5, 127.4, 73.0, 68.4, 60.6, 48.9, 44.6, 21.6.

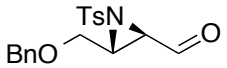


**2.23**

**Preparation of *N*-Ts protected *trans* aziridine-2-carboxaldehyde 2.23.**[14] The aziridine alcohol **2.51** (1.15 g, 2.90 mmol) was dissolved in dry DCM (30 mL) and cooled to 0 °C. $Et_3N$ (3.4 g, 33.64 mmol) was added followed by drop wise addition of $SO_3$.Py complex reagent (1.37 g, 8.70 mmol) dissolved in dry DMSO (14 mL). The reaction was stirred for 30 min and diluted with a 2:1 mixture of Hex/$Et_2O$ (25 mL). The organic layers were washed with sat. $NaHCO_3$ (5 mL) and the aqueous layer was back-extracted with more Hex/diethyl ether. Combined organic layers were then washed with a 1 M solution of sodium phosphate monobasic (5 mL), then brine (5 mL) and dried over

sodium sulfate. The organic solvent was removed via rotary evaporation. The crude compound was purified via column chromatography (4:1 Hex:EtOAc) to give aldehyde **2.23** (0.61 g, 53%) as a white solid. $R_F$ = 0.27 (3:1 Hex:EtOAc). Spectral data: $^1$H NMR (300 MHz, $CDCl_3$) δ 9.5 (d, 1H, *J* = 6.6), 7.8 (d, 2H, *J* = 8.2), 7.4 – 7.1 (m, 7H), 4.4 (s, 2H), 3.75 (m, 2H), 3.6 (m, 1H), 3.25 (dd, 1H, *J* = 10.5, 4.1 Hz), 2.4 (s, 3H); $^{13}$C NMR (75 MHz, $CDCl_3$) δ 193.5, 144.9, 137.1, 135.3, 129.6, 128.2, 127.7, 127.6, 127.4, 73.0, 67.3, 49.4, 44.9, 21.5.

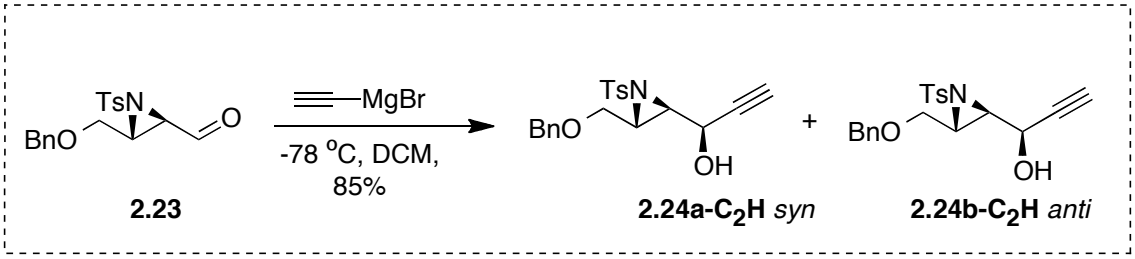


**2.23** **2.24a-$C_2$H** *syn* **2.24b-$C_2$H** *anti*

**Alkylation of *N*-Ts protected *trans* aziridine-2-carboxaldehyde 2.23 by addition of Grignard reagent**: Refer to the procedure as described previously.

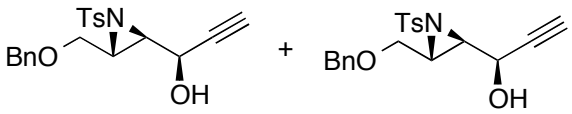


**2.24a-$C_2$H** *syn* **2.24b-$C_2$H** *anti*

Spectral data of **2.24a-$C_2$H** *syn* and **2.24b-$C_2$H** *anti* compounds match with that of the reported compound in literature.[14]

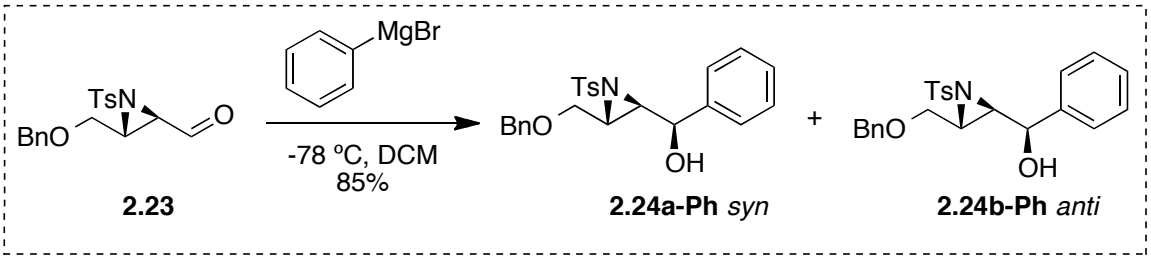


**2.23** **2.24a-Ph** *syn* **2.24b-Ph** *anti*

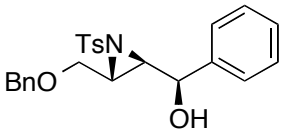


**2.24a-Ph** *syn*

Compound **2.24a-Ph** *syn*: Spectral data: $^{1}$H NMR (500 MHz, $CDCl_3$) δ 7.84 (d, 2H, *J* = 8.4 Hz), 7.41 (d, 2H, *J* = 7.7 Hz), 7.33 (m, 6H), 7.06 (m, 2H), 4.98 (dd, 1H, *J* = 8.0, 2.8 Hz), 4.29 (d, 2H, *J* = 4.9 Hz), 3.58 (dd, 1H, *J* = 11.0, 4.4 Hz), 3.46 (dd, 1H, *J* = 11.0, 0.6 Hz), 3.36 (m, 2H), 3.04 (dd, 1H, *J* = 8.4, 4.7 Hz), 2.41 (s, 3H); $^{13}$C NMR (125 MHz, $CDCl_3$) δ 144.4, 139.8, 137.5, 136.8, 129.6, 128.7, 128.3, 128.2, 127.7, 127.5, 127.4, 125.9, 72.8, 72.3, 68.2, 53.3, 45.6, 21.6; IR (neat, $cm^{-1}$) 3501, 2924, 2858, 1597, 1454, 1317, 1159, 1091; HRMS (ESI) (m/z): $[M + H]^+$ calculated for $[C_{24}H_{26}NO_4S]^+$ 424.1583, found 424.1588.

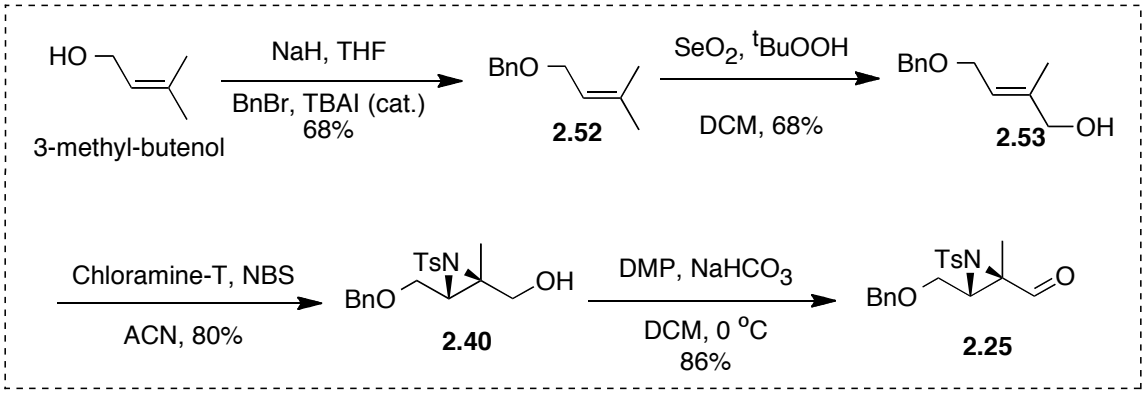


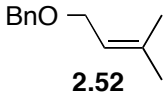


**Preparation of benzyl ether 2.52.**[14] A solution of 3-methyl-2-butenol (1.08 g, 11.6 mmol) in anhydrous THF (50 mL) was added drop wise to a suspension of NaH (0.56 g of 60% dispersion in mineral oil, 13.9 mmol, washed two times with dry pentane) in dry THF (50 mL). The mixture was stirred at room temperature for 30 min, then a solution of benzyl bromide (2.41 g, 11.9 mmol) in dry THF (25 mL) was added drop wise, followed by the addition of tetrabutylammonium iodide (1.43 g, 6 mmol) in one portion. The mixture was heated to 60 ºC overnight. After cooling, water (25 mL) was added and the mixture was extracted with diethyl ether (3 X 20 mL). The combined organics were washed with brine (10 mL), dried over sodium sulfate, and the solvent was removed under reduced pressure to give benzyl ether **2.52** (1.5g, 68%) as a yellow oil. Spectral data: $^{1}$H NMR (300 MHz, $CDCl_3$) $\delta$ 7.4 (m, 5H), 5.5 (m, 1H), 4.6 (s, 2H), 4.1 (d, 2H), 1.8 (s, 3H), 1.7 (s, 3H); $^{13}$C NMR (75 MHz, $CDCl_3$) $\delta$ 138.5, 137.0, 128.2, 127.6, 127.4, 121.0, 72.0, 66.5, 25.7, 18.0.

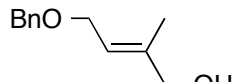


**2.53**

**Preparation of allylic alcohol 2.53.**[14] $SeO_2$ (1.346 g, 12.13 mmol) and $^tBuOOH$ (70% by wt. in water solution) (13.50 ml, 94 mmol) in DCM (45 mL) were stirred for 30 min at room temperature. To this benzyl ether **2.52** (8 g, 44.9 mmol) was added and stirred for 20 h. Reaction after completion was quenched with 10% sodium bisulfite solution (10 mL), extracted with DCM (3 X 20 mL), washed with saturated solution of $NaHCO_3$ (10 mL), brine (5 mL) and dried over sodium sulfate. Solvent was removed under vacuum and the crude compound was further subjected to a reported $NaBH_4$ reduction protocol to give allylic alcohol **2.53** (5.9 g, 68%) as a colorless oil. $R_F$ = 0.4 (2:1 Hex:EtOAc). Spectral data: $^1H$ NMR (300 MHz, $CDCl_3$) $\delta$ 7.33 (m, 5H), 5.67 (t, 1H, $J$ = 7.24 Hz), 4.50 (s, 2H), 4.07 (d, 2H, $J$ = 6.9 Hz), 3.95 (d, 2H, $J$ = 6.9 Hz), 1.66 (s, 3H); $^{13}C$ NMR (75 MHz, $CDCl_3$) $\delta$ 139.3, 138.0, 128.1, 127.6, 127.4, 120.6, 72.0, 67.3, 66.0, 13.6.

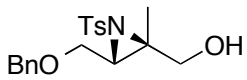


**2.40**

**Preparation of aziridine alcohol 2.40.**[14] The allylic alcohol **2.53** (1.184 g, 6.2 mmol) was dissolved in acetonitrile (30 mL). Anhydrous chloramine-T (1.4 g, 6.2 mmol) and *N*-bromosuccinimide (0.22 g, 1.24 mmol) were added successively and the light yellow slurry was stirred overnight. The reaction mixture was quenched with water (10 mL)

and extracted with EtOAc (3 X 15 mL). The combined organic layers were washed with brine (5 mL) and dried over sodium sulfate. The crude product was purified via column chromatography (4:1 Hex:EtOAc) to give aziridine alcohol **2.40** (1.91 g, 80%) as a white solid (mp = 54 – 56 ºC). $R_F$ = 0.29 (3:1 Hex:EtOAc). Spectral data: $^1$H NMR (300 MHz, $CDCl_3$) δ 7.8 (d, 2H, *J* = 8.2 Hz), 7.45 - 7.40 (m, 7H), 4.4 (s, 2H), 4.0 (d, 2H, *J* = 6.7 Hz), 3.6 (dd, 1H, *J* = 10.4, 4.9 Hz), 3.45 (t, 1H, *J* = 7.0 Hz), 3.35 (t, 1H, *J* = 4.9 Hz), 3.2 (t, 1H, *J* = 7.0 Hz), 2.4 (s, 3H), 1.4 (s, 3H); $^{13}$C NMR (75 MHz, $CDCl_3$) δ 143.9, 137.5, 137.1, 129.4, 129.3, 128.2, 127.6, 127.4, 72.9, 67.0, 65.2, 56.2, 48.4, 21.4, 16.1.

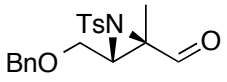


**2.25**

**Preparation of *N*-Ts protected aziridine-2-carboxaldehyde 2.25.**[14] The alcohol **2.40** (0.5 g, 1.39 mmol) was dissolved in dry DCM (15 mL) and cooled to 0 °C. The solution was treated with sodium bicarbonate (0.15 g, 1.81 mmol) and DMP (0.7 g, 1.66 mmol) and stirred for 3 h. The reaction mixture was quenched with a mixture of 1:1:1 sat. $NaHCO_3$/sodium *m*-bisulfite/water (5 mL each) and extracted with DCM (3 X 5 mL). Combined organic layers were washed with 10% aqueous sodium carbonate solution (4 X 5 mL), brine (5 mL) and dried over sodium sulfate. The crude product was purified via column chromatography (4:1 Hex:EtOAc) to give the aldehyde **2.25** (0.43 g, 86%) as a white solid (mp = 54 – 56 ºC). Spectral data: $^1$H NMR (300 MHz, $CDCl_3$) δ 9.5 (s, 1H), 7.8 (d, 2H, *J* = 8.4 Hz), 7.1-7.4 (m, 7H), 4.4 (s, 2H), 3.8 (dd, 1H, *J* = 6.8, 5.1 Hz), 3.6

(dd, 1H, *J* = 10.8, 5.1 Hz), 3.5 (dd, 1H, *J* = 10.8, 6.9 Hz), 2.4 (s, 3H), 1.4 (s, 3H); $^{13}$C NMR (75 MHz, $CDCl_3$) δ 194.3, 144.7, 137.3, 136.1, 129.7, 128.4,127.9, 127.57, 127.52, 126.43, 73.2, 66.5, 56.6, 48.9, 21.6, 11.9.

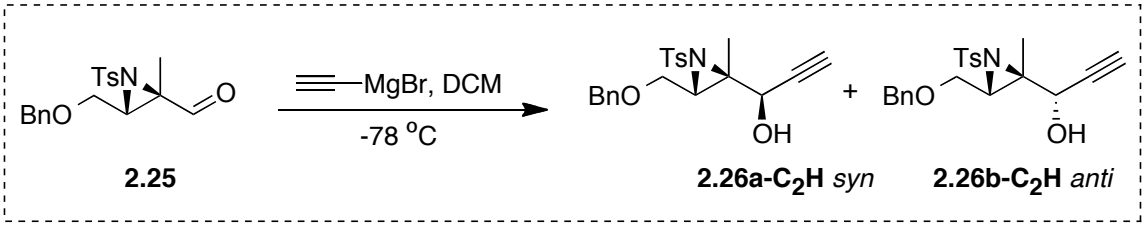


**2.25** **2.26a-$C_2$H** *syn* **2.26b-$C_2$H** *anti*

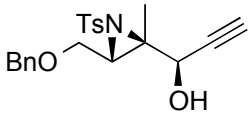


**2.26a-$C_2$H** *syn*

**Alkylation of *N*-Ts protected aziridine-2-carboxaldehyde 2.25**: Refer to the procedure as described previously. Compound **2.26a-$C_2$H** *syn*:[14] Spectral data: $^1$H NMR (300 MHz, $CDCl_3$): δ 7.82 (d, 2H, *J* = 8.0 Hz), 7.3 – 7.1 (m, 7H), 4.9 (dd, 1H, *J* = 2.5, 2.4 Hz), 4.45 (d, 1H, *J* = 11.8 Hz), 4.35 (d, 1H, *J* = 11.8 Hz), 3.66 (m, 2H), 3.41 (m, 2H), 2.55 (d, 1H, *J* = 0.9 Hz), 2.43 (s, 3H), 1.50 (s, 3H); $^{13}$C NMR (75 MHz, $CDCl_3$):δ 144.2, 137.2, 137.5, 136.8, 129.6, 129.4, 128.2, 127.6, 127.3, 127.1, 80.2, 74.5, 72.7, 66.7, 64.9, 57.8, 48.8, 21.5, 12.9

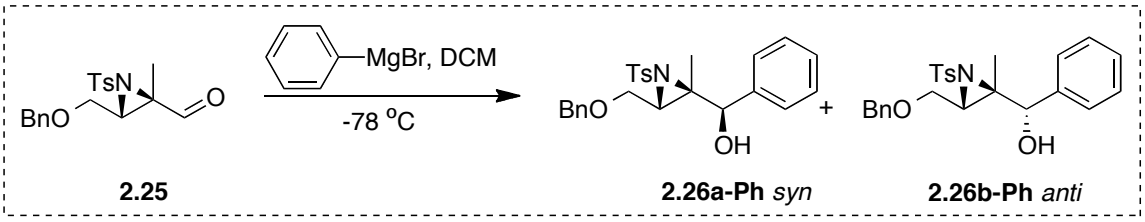


**2.25** **2.26a-Ph** *syn* **2.26b-Ph** *anti*

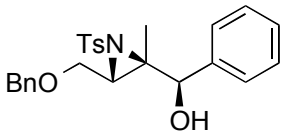


**2.26a-Ph** *syn*

Compound **2.26a-Ph** *syn*: Spectral data: $^{1}$H NMR (500 MHz, $CDCl_3$) δ 7.91 (d, 2H, *J* = 8.19 Hz), 7.54 (d, 2H, *J* = 7.7 Hz), 7.38 (t, 2H, *J* = 7.3 Hz), 7.31 (m, 6H), 7.16 (m, 2H), 5.28 (d, 1H, *J* = 2.7 Hz), 4.40 (s, 2H), 3.97 (d, 1H, *J* = 2.7 Hz), 3.71 (dd, 1H, *J* = 7.0, 5.2 Hz), 3.56 (dd, 1H, *J* = 11, 5.1 Hz), 3.43 (dd, 1H, *J* = 10.7, 7.1 Hz), 2.45 (s, 3H), 1.21 (s, 3H); $^{13}$C NMR (125 MHz, $CDCl_3$) δ 144.1, 139.7, 137.6, 137.6, 129.5, 128.3, 127.7, 127.6, 127.3, 127.2, 126.0, 74.7, 72.9, 67.1, 60.2, 49.9, 21.6, 12.7 IR (neat, $cm^{-1}$) 3420, 2363, 1653, 1319, 1157; HRMS (ESI) (m/z): $[M + H]^+$ calculated for $[C_{25}H_{27}NO_4SH]^+$ 438.1739, found 438.1740.

# REFERENCES

## REFERENCES


1. Cardillo, G.; Gentilucci, L.; Tolomelli, A. *Aldrichimica Acta,* **2003**, *36*, 39-50.
2. Dahanukar, V. H.; Zavialov, I. A. *Curr. Opin. Drug Discovery Dev.,* **2002**, *5*, 918-927.
3. Tanner, D. *Angew. Chemie., Intl. Ed.,* **1994**, *33*, 599-619.
4. Li, A. H.; Dai, L. X.; Aggarwal, V. K. *Chem. Rev.,* **1997**, *97*, 2341-2372.
5. McCoull, W.; Davis, F. A. *Synthesis-Stuttgart,* **2000**, 1347-1365.
6. Sweeney, J. B. *Chem. Soc. Rev.,* **2002**, *31*, 247-258.
7. Antilla, J. C.; Wulff, W. D. *J. Am. Chem. Soc.,* **1999**, *121*, 5099-5100.
8. Antilla, J. C.; Wulff, W. D. *Angew. Chem. Int. Ed.,* **2000**, *39*, 4518-4521.
9. Bisol, T. B.; Sa, M. M. *Quim. Nova,* **2007**, *30*, 106-115.
10. Olsen, C. A.; Franzyk, H.; Jaroszewski, J. W. *Eur. J. Org. Chem.,* **2007**, 1717-1724.
11. Osborn, H. M. I.; Sweeney, J. *Tetrahedron: Asymmetry,* **1997**, *8*, 1693-1715.
12. Vesely, J.; Ibrahem, I.; Zhao, G. L.; Rios, R.; Córdova, A. *Angew. Chem. Int. Ed.,* **2007**, *46*, 778-781.
13. Desai, A. A.; Wulff, W. D. *J. Am. Chem. Soc.,* **2010**, *132*, 13100-13103.
14. Schomaker, J. M.; Geiser, A. R.; Huang, R.; Borhan, B. *J. Am. Chem. Soc.,* **2007**.
15. Ryoji Noyori, M. K. *Angew. Chemie., Intl. Ed.,* **1991**, *30*, 49-69.
16. Urabe, H.; Evin, O. O.; Sato, F. *J. Org. Chem.,* **1995**, *60*, 2660-2661.
17. Manfred, T. R. *Angew. Chemie., Intl. Ed.,* **1984**, *23*, 556-569.
18. Anh, N. In *Organic Chemistry Syntheses and Reactivity* 1980, p 145-162.
19. Giuliana Righi, S. R. C. B. *Eur. J. Org. Chem.,* **2002**, *2002*, 1573-1577.
20. Urabe, H.; Sato, F. *J. Org. Chem. Jpn.,* **1993**, *51*, 14.
21. Escudier, J.-M.; Baltas, M.; Gorrichon, L. *Tetrahedron Lett.,* **1991**, *32*, 5345-5348.
22. Escudier, J.-M.; Baltas, M.; Gorrichon, L. *Tetrahedron,* **1993**, *49*, 5253-5266.

23. Howe, G. P.; Wang, S.; Procter, G. *Tetrahedron Lett.,* **1987**, *28*, 2629-2632.

24. Righi, G.; Spirito, F.; Bonini, C. *Tetrahedron Lett.,* **2002**, *43*, 4737-4740.

25. Ipaktschi, J.; Heydari, A.; Kalinowski, H.-O. *Chem. Ber.,* **1994**, *127*, 905-909.

26. Walsh, A. D. *Nature (London, U. K.),* **1947**, *159*, 712-713.

27. Wilcox, C. F.; Loew, L. M.; Hoffmann, R. *J. Am. Chem. Soc.,* **1973**, *95*, 8192-8193.

28. Kazuta, Y.; Abe, H.; Matsuda, A.; Shuto, S. *J. Org. Chem.,* **2004**, *69*, 9143-9150.

29. Delanghe, P. H. M.; Lautens, M. *Tetrahedron Lett.,* **1994**, *35*, 9513-9516.

30. Mioskowski, C.; Manna, S.; Falck, J. R. *Tetrahedron Lett.,* **1983**, *24*, 5521-5524.

31. Ono, S.; Shuto, S.; Matsuda, A. *Tetrahedron Lett.,* **1996**, *37*, 221-224.

32. Kazuta, Y.; Abe, H.; Yamamoto, T.; Matsuda, A.; Shuto, S. *Tetrahedron,* **2004**, *60*, 6689-6703.

33. Righi, G.; Ciambrone, S. *Tetrahedron Lett.,* **2004**, *45*, 2103-2106.

34. Kim, B. C.; Lee, W. K. *Tetrahedron,* **1996**, *52*, 12117-12124.

35. Park, C. S.; Choi, H. G.; Lee, H.; Lee, W. K.; Ha*, H.-J. *Tetrahedron: Asymmetry,* **2000**, *11*, 3283-3292.

36. Pierre, J. L.; Handel, H.; Baret, P. *Tetrahedron,* **1974**, *30*, 3213-3223.

37. Righi, G.; Pietrantonio, S.; Bonini, C. *Tetrahedron,* **2001**, *57*, 10039-10046.

38. Andres, J.; de Elena, N.; Pedrosa, R.; Perez-Encabo, A. *Tetrahedron,* **1999**, *55*, 14137-14144.

39. Barlet, R.; Baret, P.; Handel, H.; Pierre, J. L. *Spectrochimica Acta Part a-Molecular and Biomolecular Spectroscopy,* **1974**, *A 30*, 1471-1485.

40. Shao, Y.; Molnar, L. F.; Jung, Y.; Kussmann, J.; Ochsenfeld, C.; Brown, S. T.; Gilbert, A. T. B.; Slipchenko, L. V.; Levchenko, S. V.; O'Neill, D. P.; DiStasio, R. A.; Lochan, R. C.; Wang, T.; Beran, G. J. O.; Besley, N. A.; Herbert, J. M.; Lin, C. Y.; Van Voorhis, T.; Chien, S. H.; Sodt, A.; Steele, R. P.; Rassolov, V. A.; Maslen, P. E.; Korambath, P. P.; Adamson, R. D.; Austin, B.; Baker, J.; Byrd, E. F. C.; Dachsel, H.; Doerksen, R. J.; Dreuw, A.; Dunietz, B. D.; Dutoi, A. D.; Furlani, T. R.; Gwaltney, S. R.; Heyden, A.; Hirata, S.; Hsu, C. P.; Kedziora, G.; Khalliulin, R. Z.; Klunzinger, P.; Lee, A. M.; Lee, M. S.; Liang, W.; Lotan, I.; Nair, N.; Peters, B.; Proynov, E. I.; Pieniazek, P. A.; Rhee, Y. M.; Ritchie, J.; Rosta, E.; Sherrill, C. D.;

Simmonett, A. C.; Subotnik, J. E.; Woodcock, H. L.; Zhang, W.; Bell, A. T.; Chakraborty, A. K.; Chipman, D. M.; Keil, F. J.; Warshel, A.; Hehre, W. J.; Schaefer, H. F.; Kong, J.; Krylov, A. I.; Gill, P. M. W.; Head-Gordon, M. *PCCP,* **2006**, *8*, 3172-3191.

41. Becke, A. D. *J. Chem. Phys.,* **1993**, *98*, 1372-1377.

42. Harihara, P. C.; Pople, J. A. *Theor. Chim. Acta,* **1973**, *28*, 213-222.

43. Marenich, A. V.; Olson, R. M.; Kelly, C. P.; Cramer, C. J.; Truhlar, D. G. *Journal of Chemical Theory and Computation,* **2007**, *3*, 2011-2033.

44. Curtiss, L. A.; Redfern, P. C.; Raghavachari, K.; Rassolov, V.; Pople, J. A. *J. Chem. Phys.,* **1999**, *110*, 4703-4709.

45. Aroney, M. J.; Calderbank, K. E.; Stootman, H. J. *J. Chem. Soc., Perk. Trans. 2,* **1973**, 1365-1368.

46. Pelissier, M.; Serafini, A.; Devanneaux, J.; Labarre, J. F.; Tocanne, J. F. *Tetrahedron,* **1971**, *27*, 3271-3284.

47. Chelation of the Boc carbonyl with divalent magnesium has been invoked previously in a number of publications. For example of such see; Merino P.; Lanaspa, A.; Merchan, F. L.; Tejero, M., *Tetrahedron Lett.*, **1997**, *38*, 1813-1816. To our knowledge these authors have not reported confirmatory experiments using e.g. TMEDA or other complexants to address the chelation possibility.

48. Pierre, J. L.; Handel, H.; Baret, P. *Org. Mag. Res.,* **1972**, *4*, 703-707.

49. Handel, H.; Baret, P.; Pierre, J. L. *Comptes Rendus Hebdomadaires Des Seances De L Academie Des Sciences Serie C,* **1973**, *276*, 511-514.

50. Durig, J. R.; Shen, S. Y. *Spectrochimica Acta Part a-Molecular and Biomolecular Spectroscopy,* **2000**, *56*, 2545-2561.

51. Noh, H.-Y.; Kim, S.-W.; Paek, S. I.; Ha, H.-J.; Yun, H.; Lee, W. K. *Tetrahedron,* **2005**, *61*, 9281-9290.

52. Li, B.-F.; Zhang, M.-J.; Hou, X.-L.; Dai, L.-X. *J. Org. Chem.,* **2002**, *67*, 2902-2906.

53. Eliel, E. L., Wilen, S. H., & Doyle, M. P. **2001**.

54. Bartnik, R.; Lesniak, S.; Laurent, A. *Tetrahedron Lett.,* **1981**, *22*, 4811-4812.

55. Spectroscopic data of the alcohol matches with that of the syn compound as reported by Righi and coworkers in their previous study.

56. Kessler, H.; Zimmermann, G.; Forster, H.; Engel, J.; Oepen, G.; Sheldrick, W. S. *Angewandte Chemie-International Edition in English,* **1981**, *20*, 1053-1055.

57. Burgi, H. B.; Dunitz, J. D. *Acc. Chem. Res.,* **1983**, *16*, 153-161.

58. Bhupathy, M.; Cohen, T. *Tetrahedron Lett.,* **1985**, *26*, 2619-2622.

59. Anet, F. A. L.; Trepka, R. D.; Cram, D. J. *J. Am. Chem. Soc.,* **1967**, *89*, 357-362.

60. Horst, K. *Angew. Chemie., Intl. Ed.,* **1970**, *9*, 219-235.

61. Eric, R. J. *Mag. Res. Chem.,* **1995**, *33*, 664-668.

62. Nakanishi, H.; Yamamoto, O. *Tetrahedron,* **1974**, *30*, 2115-2121.

63. Andose, J. D.; Lehn, J. M.; Mislow, K.; Wagner, J. *J. Am. Chem. Soc.,* **1970**, *92*, 4050-4056.

64. Brois, S. J. *J. Am. Chem. Soc.,* **1967**, *89*, 4242-4243.

65. Lambert, J. B.; Packard, B. S.; Oliver, W. L. *J. Org. Chem.,* **1971**, *36*, 1309-1310.

66. Dabbagh, H. A.; Modarresi-Alam, A. R. *J. Chem. Res.,* **2000**, *2000*, 190-192.

67. The calculated Gibbs energy of activation is a measure of all processes that contribute to the observed line broadening of the aldehyde resonances and, thus, is not solely a measure of the nitrogen inversion. In fact, it is anticipated that rotation about the C3-CO bond of **2.21** contributes to the calculated barrier.

68. Armarego, W. L. F. C., C. L. L. *Purification of laboratory chemicals*; 5th ed.; Butterworth-Heinemann: Amsterdam ; Boston,, 2003.

69. Davoli, P.; Forni, A.; Moretti, I.; Prati, F.; Torre, G. *Tetrahedron,* **2001**, *57*, 1801-1812.

70. Boivin, S. O., F.; Paulmier, C. *Tetrahedron Lett.,* **2000**, *41*, 663-666.

71. Alhamadsheh, M. M. P., N.; DasChouduri, S.; Reynolds, K. A. *J. Am. Chem. Soc.,* **2007**, *129*, 1910-1911.

72. Curini, M.; Epifano, F.; Marcotullio, Maria C.; Rosati, O. *Eur. J. Org. Chem.,* **2002**, *2002*, 1562-1565.

73. Righi, G.; Ciambrone, S.; Pompili, A.; Caruso, F. *Tetrahedron Lett.,* **2007**, *48*, 7713-7716.

74. Dodge, J. A. T., J. I.; Presnell, M. *J. Org. Chem.,* **1994**, *59*, 234-236.

75. Motamed, M. B., E. M.; Singaram, S. W.; Sarpong *Org. Lett.,* **2007**, *9*, 2167-2170.

76. Corey, E. J. V., A. *J. Am. Chem. Soc.,* **1972**, *94*, 6190-6191.

77. Schwab, J. M.; Ho, C. K.; Li, W. B.; Townsend, C. A.; Salituro, G. M. *J. Am. Chem. Soc.,* **1986**, *108*, 5309-5316.

78. Ley, S. V. N., J.; Griffith, W. P.; Marsden, S. P. *Synthesis-Stuttgart,* **1994**, *1994*, 639-666.

79. Kumar, P. N., S. V. *J. Org. Chem.,* **2005**, *70*, 4207-4210.

80. Svenja Röttger, H. W. *Eur. J. Org. Chem.,* **2006**, *2006*, 2093-2099.

81. Schomaker, J. M. P., V. R.; Borhan, B. *J. Am. Chem. Soc.,* **2004**, *126*, 13600-13601.

# Chapter 3

## Elaboration Of The Tetrasubstituted Pyrrolidine Moieties, Obtained Via Tandem Aza-Payne/Hydroamination Methodology.

### 3.1 Introduction to hydroamination chemistry.

Addition of an N–H bond either to a carbon-carbon double or a triple bond is referred to as hydroamination (Scheme 3.1).[1] This process involves a reaction between two species, both of which usually behave as nucleophiles; thus this represents an example of umpolung reaction. These reactions lead to the formation of synthetically and pharmaceutically valuable nitrogen containing compounds such as amines, imines and enamines.

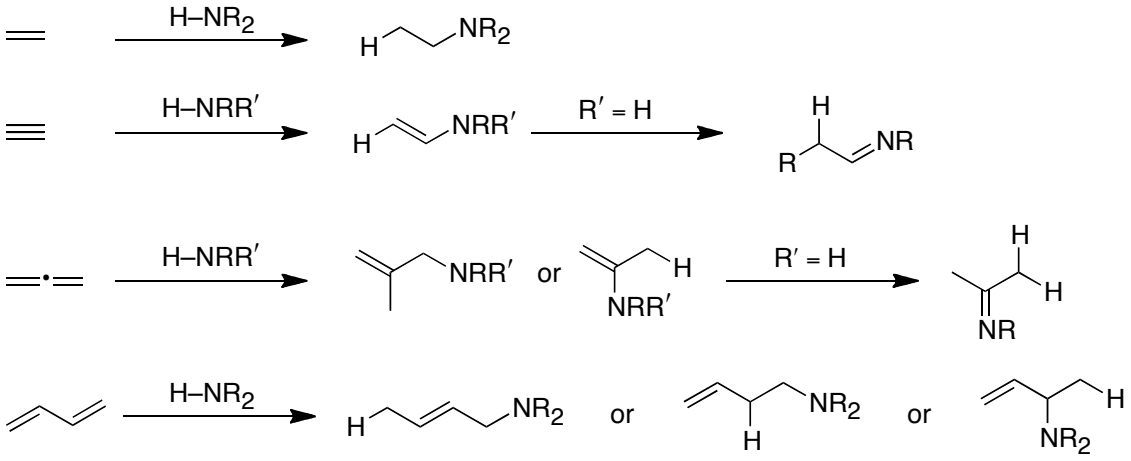


**Scheme 3.1** Hydroamination process.

These transformations are clean and highly efficient in terms of atom economy. Hydroamination of alkynes, catalyzed by metals are easier than that of alkenes due to the higher electron density and reactivity associated with the triple bond towards coordination with the metal. Although the reactions are often considered thermo neutral (very slightly exothermic), high electron repulsion between electron rich substrate and negatively charged nitrogen nucleophile imparts a high activation barrier, thus making it a challenging process.[2] Development of catalysis becomes all the more important in the case of intermolecular reactions due to high entropy encountered during the reactions. And very often these demand low temperature since conversion is limited by the equilibrium of the reaction. Over the past decade the catalytic versions of these reactions have received a lot of attention. As a result innumerable reactions catalyzed by both early and late transition metals have been reported.

Mechanistic aspects of hydroamination of both alkenes and alkynes have been extensively investigated.[3] It has been established that catalytic hydroaminations of C–C multiple bonds take place via formation of M-amido intermediates. Organolanthanide-catalyzed reaction of aminoalkenes is known to occur by intramolecular insertion of olefins into lanthanide amides (Scheme 3.2a).[4] An alternative approach involves the ability of metals such as zirconium (IV) and titanium (IV) to complex with amines forming M–N multiple bonds.

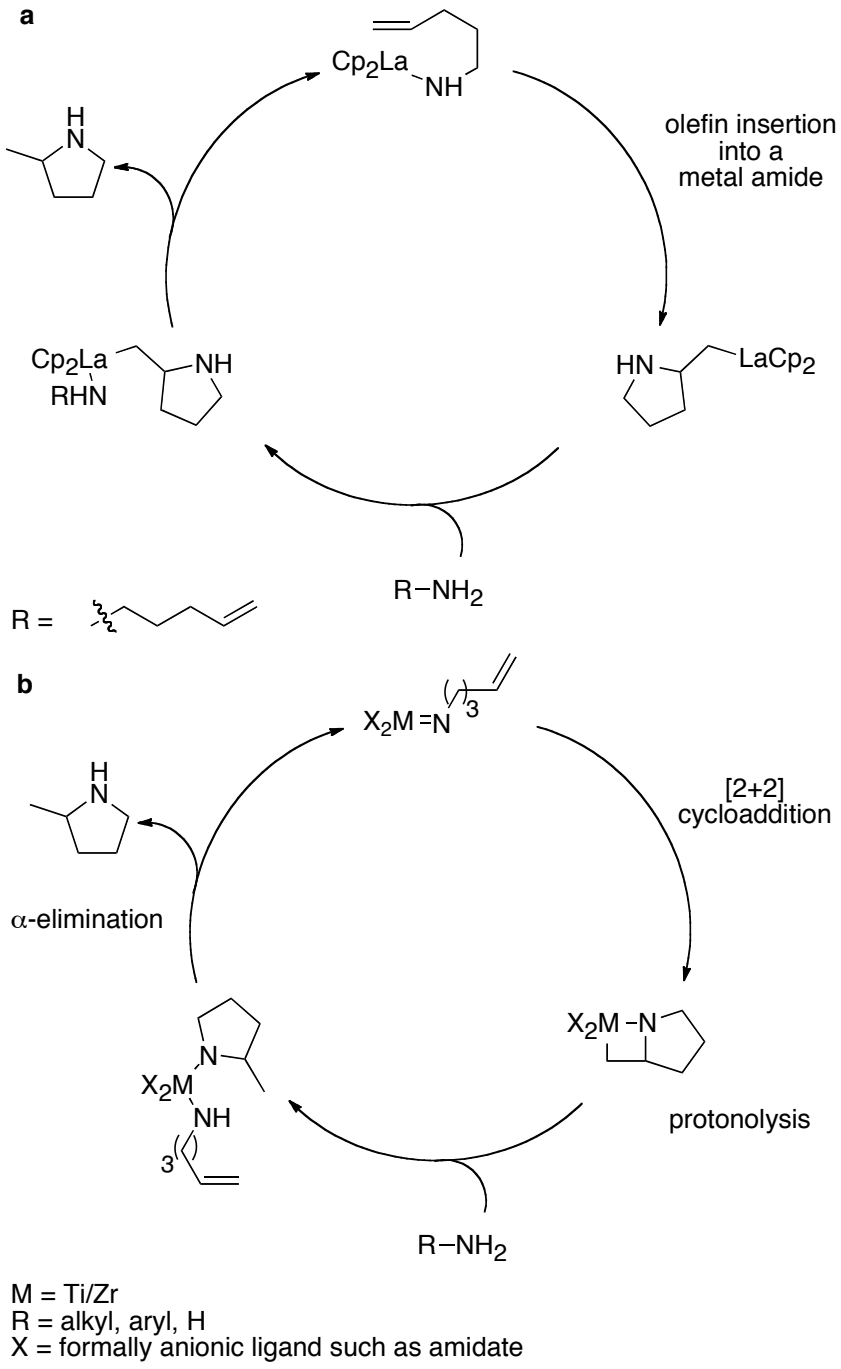


**Scheme 3.2** a) Hydroamination of olefins catalyzed by lanthanide–amides via intramolecular insertions of alkenes into an M–amide bond. b) Catalyzed by group IV complexes via [2 + 2] cycloaddition.

These undergo [2+2] cycloadditions with substrates containing C–C multiple bonds (Figure 3.2b).[5] Hydroamination reactions, which do not employ transition metals, are comparatively less developed. There are some reports that involve the use of combination of very strong bases and metal salts. Deprotonation of an amine with an alkali base generates an alkali amide species **I** (Scheme 3.3). This nucleophilic species adds very slowly to the substrate to give a highly reactive organometallic species **II**, which then immediately deprotonates the amine to give the hydroaminated product. Suginome and coworkers first reported base-catalyzed hydroamination of non-activated alkene.[6] Later several such reactions were reported which involve the catalytic use of butyllithium bases.[7,8] However, functional groups present in these cases have to be carefully chosen and have to be compatible under highly basic conditions.

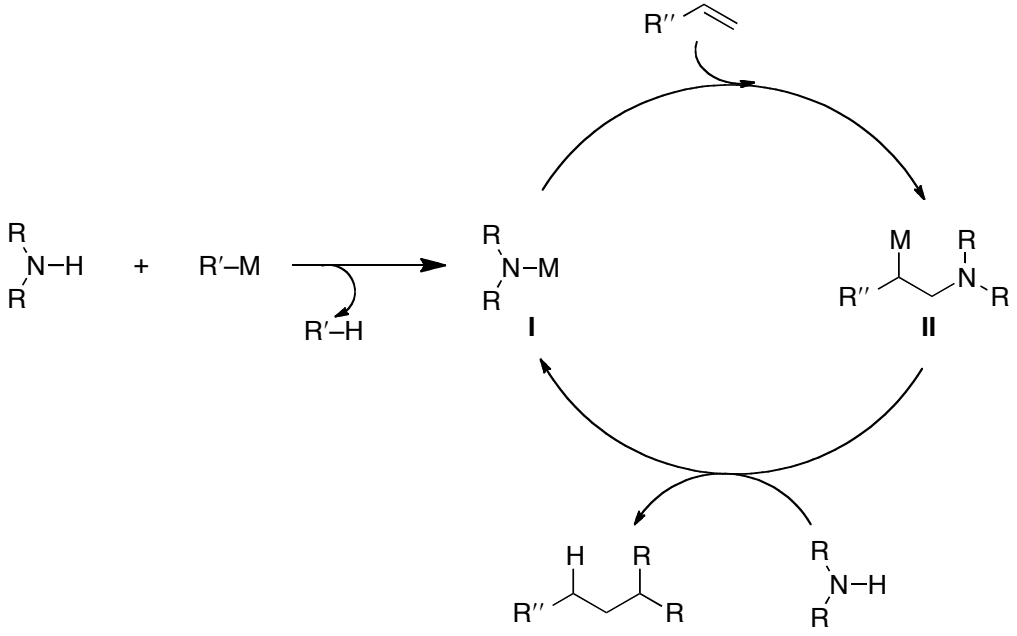


**Scheme 3.3** Base catalyzed hydroamination of alkenes.

### 3.2 Introduction to aza-Payne rearrangement.

Aza-Payne is a variation of the Payne rearrangement where the epoxide oxygen or hydroxide oxygen is replaced by nitrogen.[9] For the discussion here, "forward" aza-Payne rearrangement would refer to the direction of the reaction leading from oxirane to aziridine. And reverse would mean leading to oxirane from aziridine. Unlike the Payne rearrangement, here the equilibrium depends significantly on the substituent present on nitrogen (Table 3.1).

**Table 3.1** Effect of substituents present on nitrogen and oxygen on the aza-Payne equilibrium.

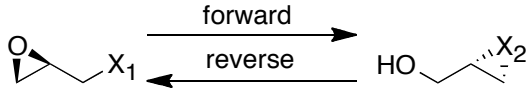


| $X_1$ | $X_2$ | direction favored |
|---|---|---|
| $NH_2$ | NH | reverse |
| NHR | NR | forward |
| NHBoc | NBoc | forward |
| $NR_2$ | $NR_2^+$ | neither |
| NHMs, NHTs | NMs, NTs | neither |

Theoretical calculations predict that for the neutral aziridine substrate **3.1**, oxirane **3.1a** is favored over the corresponding aziridine isomer by 5 Kcal/mol (Figure 3.1). However, when deprotonated, aza-anion **3.2a** is 15 Kcal/mol higher in energy than the corresponding oxy-anion **3.2**. Noticeably, in the presence of Lewis acids such as boron

trifluoride, titanium (IV), trimethylaluminum etc., the equilibrium is completely driven towards aziridine (Scheme 3.4). Although not much mechanistic investigation has been carried out in this area, it is alleged that complexation with oxygen drives the reaction to the aziridine isomer.

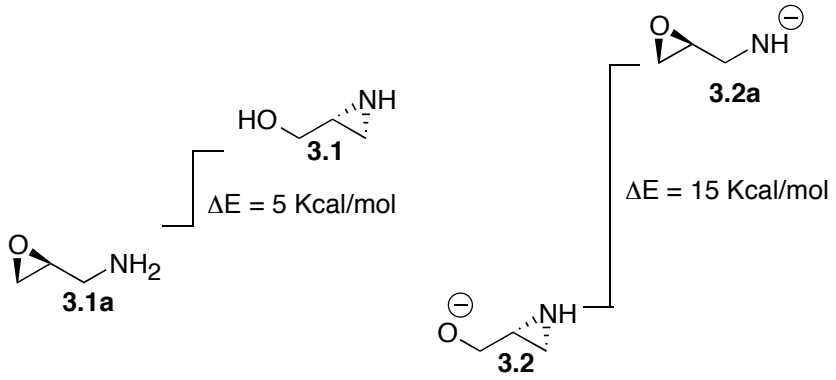


**Figure 3.1** Thermodynamics of aza-Payne chemistry of unprotected aziridinol.

The picture is completely different in case of activated nitrogen aziridines (bearing electron withdrawing groups such as sulfonamides).[10] While under neutral conditions epoxide is slightly energetically favored, aza-anion **3.4a** is highly favored (19 kcal/mol) over the corresponding oxy-anion **3.4** (Figure **3.2**).

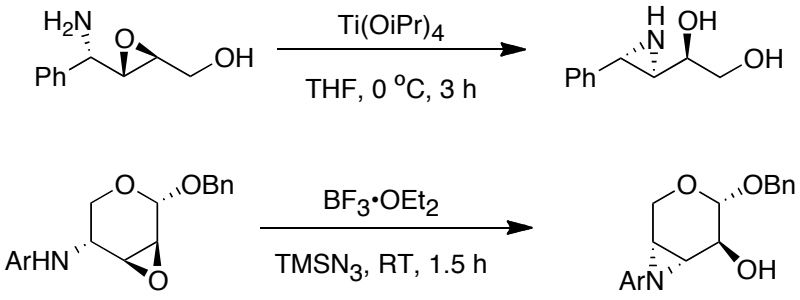


**Scheme 3.4** Thermodynamic equilibrium of aza-Payne under Lewis acidic conditions.

Use of irreversible bases such as NaH, KH in polar aprotic solvents such as DCM, THF or HMPA favors the formation of the oxirane species. On the other hand, under the presence of reversible bases in aqueous conditions the direction of equilibrium depends on the nature of the substrate.

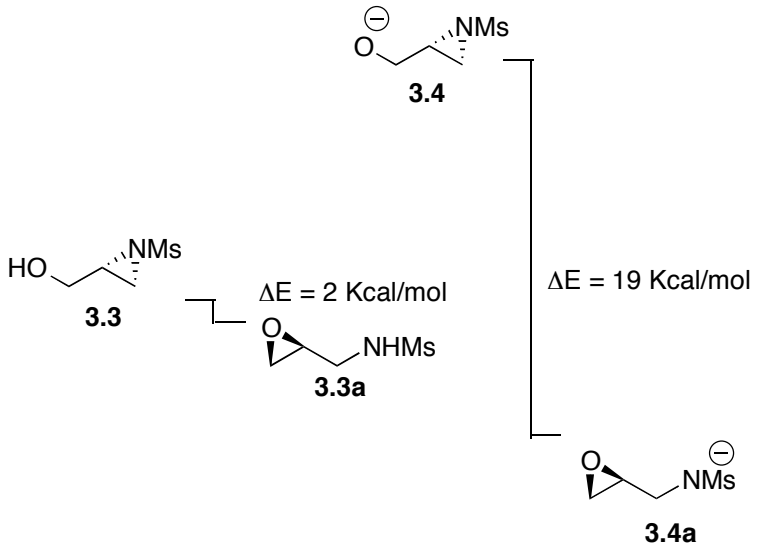


**Figure 3.2** Thermodynamics of aza-Payne chemistry of activated aziridines.

**3.3 From one carbon homologative relay ring expansion of 2,3-aziridin-1-ols to tandem aza-Payne/hydroamination methodology.**

In our group, we have taken advantage of aza-Payne chemistry where 2,3-aziridin-1-ols **3.5**, under basic conditions (in-situ generated ylide), undergo aza-Payne rearrangement to generate epoxy amide intermediates **3.6** (Scheme 3.5). Attack at the terminal position of the epoxide by the ylide leads to the formation of highly reactive intermediate **3.7**, which readily undergoes *5-exo-tet* cyclization to yield 2,3-disubstituted pyrrolidines.[11]

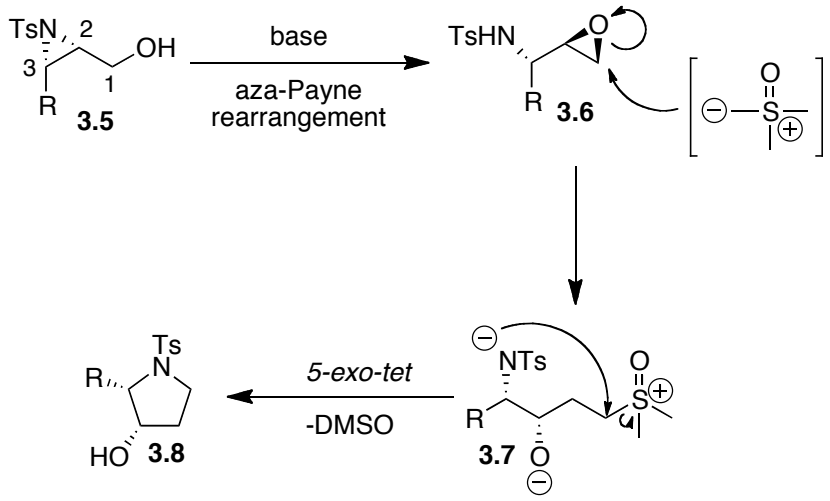


**Scheme 3.5** Ylide mediated one carbon homologative ring expansion of 2,3-aziridin-1-ols to 2,3-disubstituted pyrrolidines.

This method allows access to highly functionalized pyrrolidine rings. Table 3.2 highlights some of the examples, which demonstrate that pyrrolidines can be successfully obtained via this methodology with moderate to high yield and excellent diastereoselectivity. 2,3-Disubstituted, 2,2,3-, 2,3,3-, and 2,2,3,3-tetrasubstituted pyrrolidines can be obtained following this protocol.

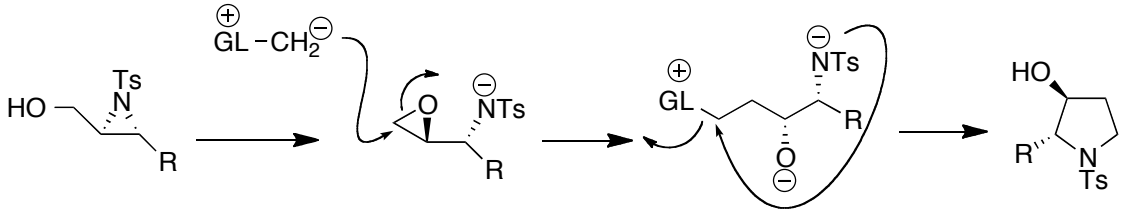


**Scheme 3.6**. Use of ylide as a latent electrophile limits the scope of funtionalization at C-5.

Notably, the absolute stereochemistry present in the starting material is completely translated to the product, which makes this transformation synthetically valuable. Efforts were later made in our group to improve the scope of these reactions, for instance, ways to functionalize other positions of the resulting pyrrolidine products. This methodology relies on the use of the ylide as a latent electrophile. The ylide initially serves as a nucleophile and later reveals electrophilicity undergoing attack by the amide nitrogen. However, once the ylide performs homologation at C-5, it leaves and therefore leaves C-5 unsubsbstituted (Scheme 3.6). This strategy was later revised to incorporate the use of a modified latent electrophile in order to gain functionalization at C-5. The revised strategy incorporated use of an alkyne, which could serve as an electron sink to allow further functionalization (Scheme 3.7). Indeed, when alkyne substituted aziridinols **3.9** were subjected to similar conditions; tetrasubstituted pyrrolidines **3.11** were obtained as products (Scheme 3.8).

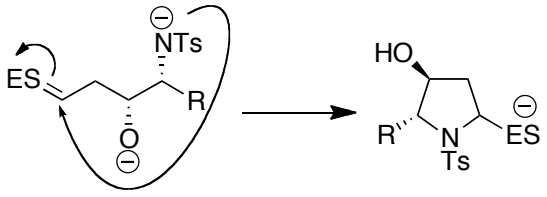


**Scheme 3.7**. Use of an electron sink would allow room to achieve further functionalization at C-5.

**Table 3.2** Diastereoselective 2,3-disubstituted pyrrolidines obtained via tandem aza-Payne/hydroamination.[11]

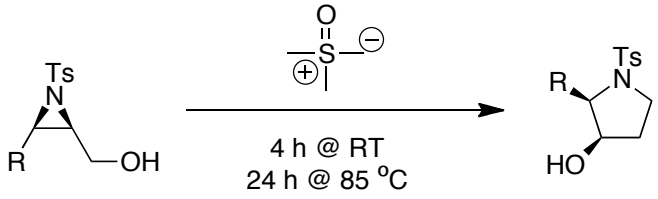


| epoxy amine | pyrrolidine | yield |
|---|---|---|
| 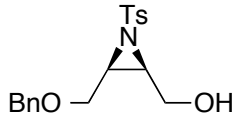 | 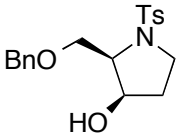 | 82% |
| 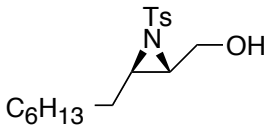 | 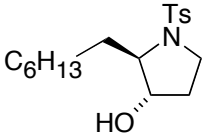 | 71% |
| 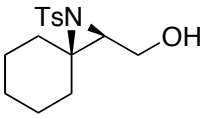 | 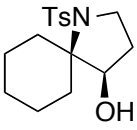 | 79% |
| 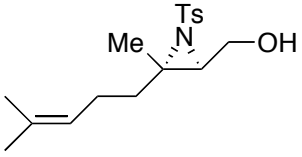 | 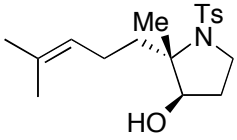 | 70% |
| 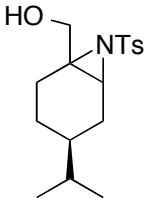 | 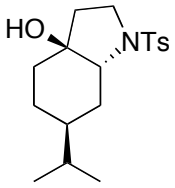 | 50% |
| 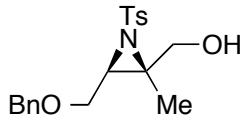 | 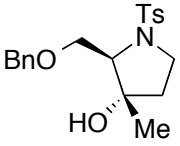 | 76% |
| 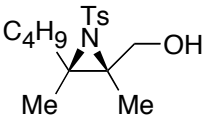 | 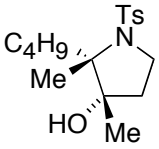 | 67% |

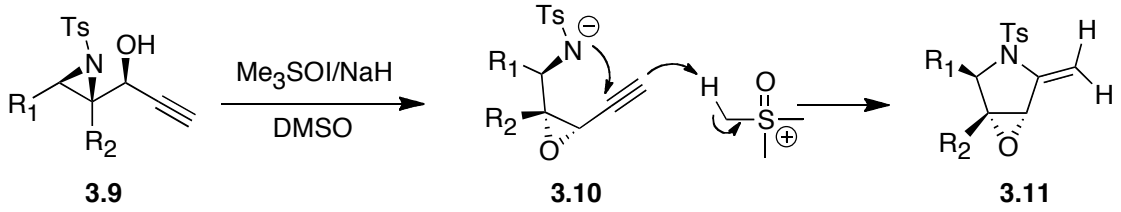


**3.9** **3.10** **3.11**

**Scheme 3.8** Tandem aza-Payne/hydroamination of *syn* aziridinols yield highly functionalized pyrrolidines.

Following the revised approach, synthesis of highly functionalized pyrrolidine motifs was achieved and reported by our group in 2007.[11] This one-pot aza-Payne/hydroamination process involves two steps: 1) generation of *N*-Ts amide epoxide intermediate **3.10** via aza-Payne rearrangement and 2) cyclization via *5-exo-dig* attack of the subsequently generated nitrogen nucleophile at the terminal carbon to yield *N*-Ts enamide tetrasubstituted pyrrolidine **3.11** (Scheme 3.8). Unlike most of the reported metal-catalyzed hydroamination reactions, this methodology requires comparatively milder conditions. This route strictly relies on the use of diastereomerically pure aziridinols **3.9** as starting materials. Synthesis of *syn* aziridinols has already been discussed in Chapter 1.

### 3.3.1 **Significance of *syn* v *anti* isomer on hydroamination reactions.**

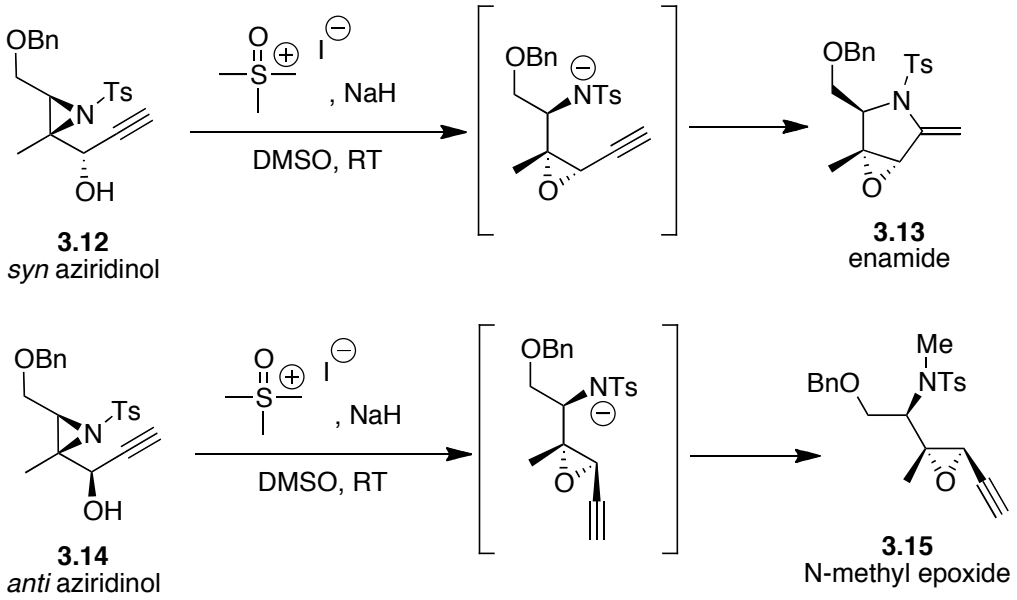


**Scheme 3.9** Fate of *syn* vs *anti* isomer in tandem aza-Payne/hydroamination reactions.

Diastereomeric purity of starting material is highly essential for the accomplishment of these transformations. Thus *syn* aziridinol **3.12** undergoes aza-Payne rearrangement to give epoxy amide intermediate, which then cyclizes to yield the hydroaminated pyrrolidine product **3.13**. On the other hand, aza-Payne rearrangement of the corresponding *anti* isomer **3.14** only affords *N*-methyl epoxide **3.15** and does not yield the desired cyclized product. In the case of the *syn* isomer, both the anionic nitrogen and the alkyne are placed on the same side of the epoxide, which allows the cyclization to occur, whereas the *anti* isomers lacks this arrangement (Scheme 3.9). Table 3.3 illustrates substrate scope of this reaction.

**Table 3.3** Substrate scope of tandem aza-Payne/hydroamination chemistry.[11]

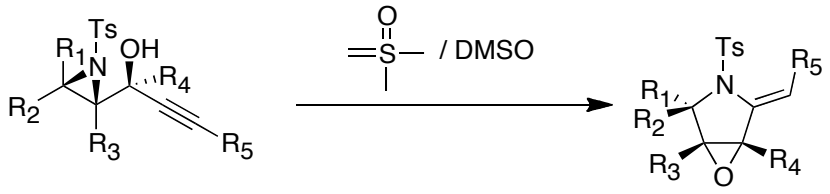


| entry | $R_1$ | $R_2$ | $R_3$ | $R_4$ | $R_5$ | Yield (%) |
|---|---|---|---|---|---|---|
| 1 | Me | $CH_2OBn$ | H | H | H | 72 |
| 2 | H | n-$C_7H_{15}$ | H | H | H | 82 |
| 3 | H | $CH_2OBn$ | H | H | H | 73 |
| 4 | H | $CH_2OBn$ | Me | H | H | 76 |
| 5 | H | Ph | Me | H | H | 71 |
| 6 | H | *p*-$MeOC_6H_5$ | Me | H | H | 71 |
| 7 | H | $CH_2OBn$ | Me | H | Me | 0 |
| 8 | H | $CH_2OBn$ | Me | H | Ph | 63 (*Z*/*E* = 14.5/1) |
| 9 | H | $CH_2OBn$ | Me | Me | H | 64 |
| 10 | H | $CH_2OBn$ | Me | Me | Ph | 63 (*Z*/*E* = 14/1) |

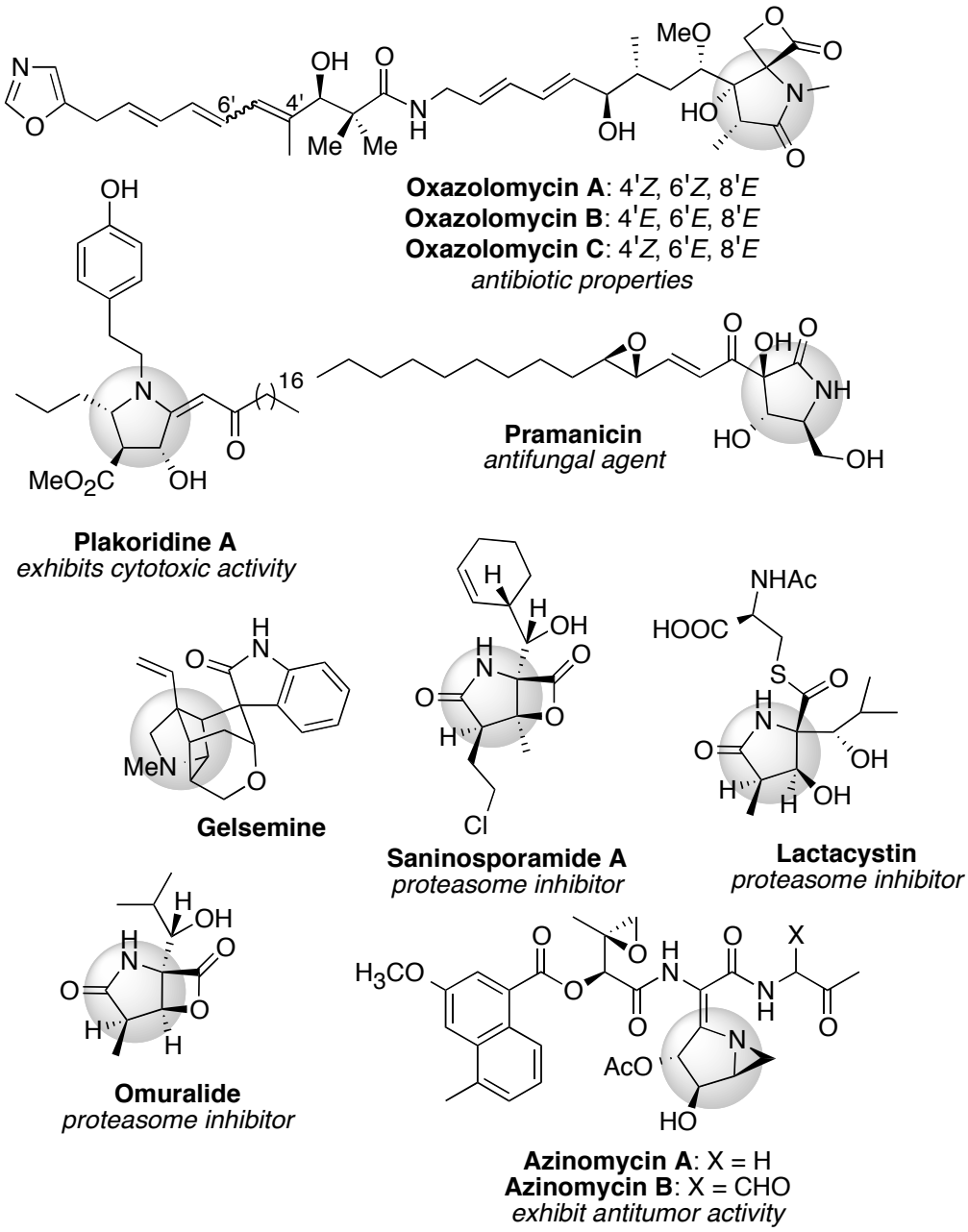


**Figure 3.3** Natural products with highly functionalized pyrrolidine nuclei in skeletal frameworks.

### 3.4 Synthetic potential of the *N*-Ts enamide nucleus and its elaboration.

The tetrasubstituted *N*-Ts enamide **3.13** resulting from tandem aza-Payne/hydroamination reaction (Scheme 3.8) possesses attractive functionalities, which can be manipulated in several possible ways. Clearly this emerges as a very promising and interesting motif, which can be exploited to derive scaffolds with higher complexities.

Thus we aimed at examining a number of useful transformations on the resulting pyrrolidine that would be of interest to us for future total synthetic endeavors. Figure 3.3 summarizes a list of several natural products, which are both biologically and structurally interesting compounds, which possess highly functionalized pyrrolidine nuclei. The sections discussed below would emphasize on the exploitation of various functional groups present in the enamide moiety and several reactions attempted in order to derive a diverse range of interesting scaffolds, which can be used as higher stage intermediates toward the synthesis of such natural products. In order to carry out elaboration studies, pyrrolidine **3.13** was synthesized from *syn* aziridinol **3.12** following the one-pot aza-Payne/hydroamination procedure reported by our group (Scheme 3.10).[11]

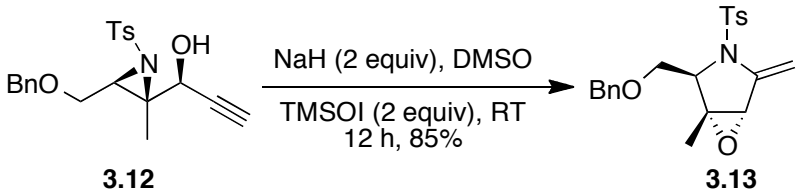


**3.12** **3.13**

**Scheme 3.10** Synthesis of tetrasubstituted pyrrolidine.

### 3.4.1 Challenges and preliminary attempts on the ring opening reactions of the epoxide present in *N*-Ts enamide.

Upon a cursory examination of *N*-Ts enamide compound **3.13,** the epoxide comes across as a highly exploitable functionality. Ring strain (worth 27 Kcal/mol) associated with the three-member heterocycle ring has been known to provide sufficient driving force to carry out ring opening reactions. Regioselectivity achieved in the opening of the epoxides generally depends upon the conditions employed in the reactions. Such a transformation in this case would allow functionalization to occur at either C-3 and C-4 positions (Figure 3.4). Under basic conditions one would expect nucleophilic attack predominantly at C-3 position. On the other hand presence of acidic conditions would primarily yield functionalized C-4 ring opened products. Contrary to the general belief in moderate reactivity exhibited by epoxides, several efforts previously made in our lab either met with failure or lead to the generation of undesired isomerized products.[12,13]

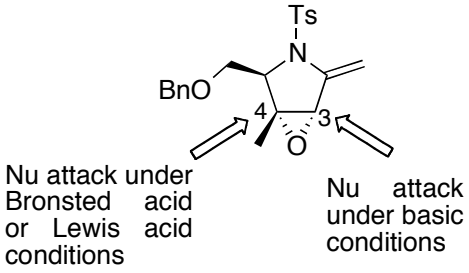


**Figure 3.4** Potential functionalization feasible at C-3 and C-4 under various conditions.

Surprisingly, no reaction occurred when the epoxide compound **3.13** was treated with allylmagnesium bromide in THF at -78 $^{o}$C. Warming to room temperature also failed to

induce any reactivity. Lewis acids are known to activate the epoxide towards ring opening reactions. Thus next, reaction was planned where opening was carried out in the presence of trimethylchlorosilane (Scheme 3.11). To our disappointment, no transformation was observed even after heating the reaction. This points out the unusual unreactivity exhibited by the epoxide, although consumption of Lewis acid in the presence of basic species such as Grignard reagent cannot be ruled out in latter case.

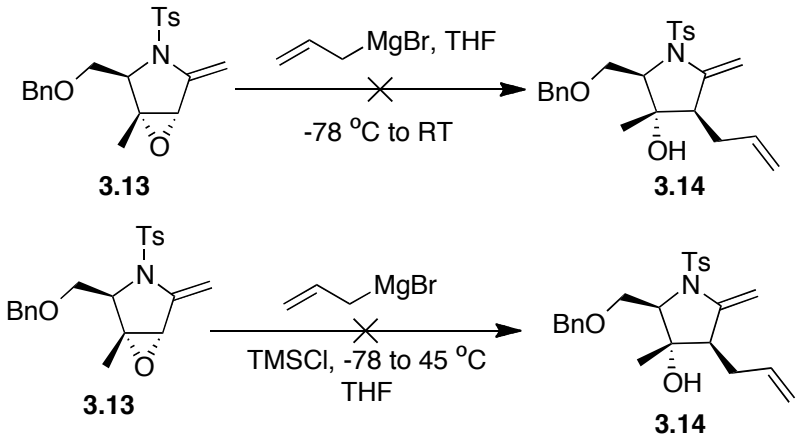


**Scheme 3.11** Grignard addition to the *N*-Ts enamide epoxide.

Finally forced conditions with the use of excess of Grignard reagent along with heating at 40 °C only lead to an undesired pyrrole compound **3.15** (Scheme 3.12).

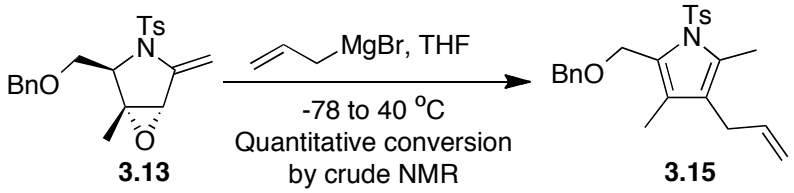


**Scheme 3.12** Excess of Grignard reagent leads to undesired product.

Presence of allyl substituent at C-3 in the aromatic product suggests that epoxide might initially react with allyl magnesium bromide to yield the magnesium alkoxide intermediate **3.13a**. The elimination of $MgBrO^-$ would lead to the formation of olefin intermediate **3.14c**. Stability conferred by aromatization would assist internalization of *exo* olefin, and thus isomerization would give rise to undesired aromatic compound **3.15** (Scheme 3.13).

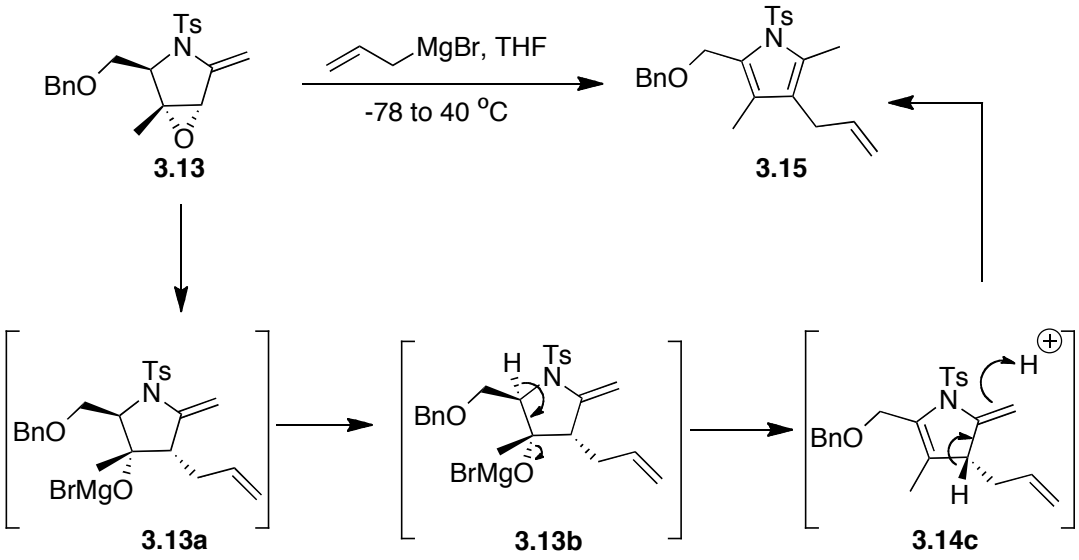


**Scheme 3.13**. Proposed elimination and isomerization generates undesired pyrrole compound.

Also, elimination of the alkoxymagnesiumhydroxide upon aqueous work-up cannot be completely ruled out at this point. Thus *exo* olefin was found to be highly vulnerable towards isomerization process and lead to internalization, yielding undesired aromatic compound **3.15**. Treatment with organo-copper reagent (Scheme 3.14) also resulted in the isolation of the same undesired aromatic compound.

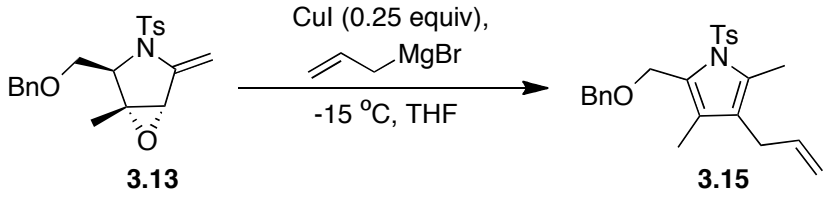


**Scheme 3.14** Addition of organo-copper leads to isomerized product.

Since elimination during the aqueous step was also speculated, several work-up procedures were also tried in order to avoid competing isomerization. Unfortunately, all such attempts led to failure and only returned undesired aromatic products.

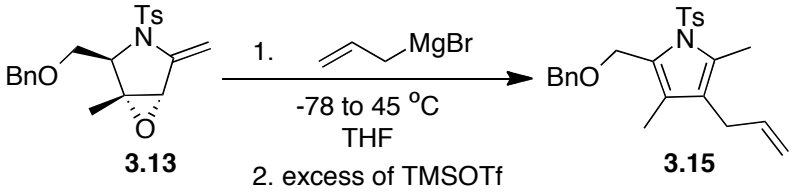


**Scheme 3.15** Attempt to protect the in-situ generated tertiary alcohol also leads to undesired aromatic compound.

Aware of the fact that isomerization is instigated by the elimination of the tertiary alcohol, we also tried to trap the in-situ generated tertiary alcohol during the reaction using a reactive source of electrophile. Thus excess of TMSOTf was added in order to quench the reaction at the end during the addition of Grignard reagent (Scheme 3.15), which also afforded only isomerized product. Nonetheless, masked alcohol being a better leaving group, might even promote such undesired elimination. We also reasoned that elimination of the alcohol leads to the formation of very stable tertiary

carbocation, which would promote such isomerization process. To test this hypothesis, substrate **3.16** was prepared, which would instead lead to the generation of comparatively less stable carbocation. However, treatment of compound with organo-copper only afforded isomerized aromatic product (Scheme 3.16). Thus at this stage it was evident that nucleophilic addition to enamine containing epoxide compound would only result into isomerized aromatic compounds. This nevertheless provided an evidence for the base-catalyzed rearrangement observed for the elimination and isomerization observed during the addition of nucleophiles to the *N*-Ts enamide epoxide.

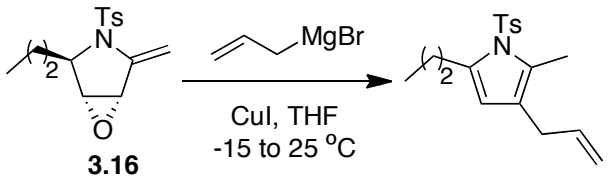


**Scheme 3.16** Addition of organo-copper to *N*-Ts enamide containing di-substituted epoxide also lead to isomerization.

Palladium mediated ring opening of epoxide has also been frequently reported in literature. Tsuji-Shimizu and coworkers reported selective hydrogenolysis of alkenyloxiranes using formic acid, catalyzed by palladium-phosphine catalysts.[14] The selectivity of the reaction depends on both the nature and the amount of phosphine ligands. Later Takemura et al. reported a modified version of the site-selective reduction of vinyl epoxides.[15] Upon subjection of epoxide **3.17** to 1.1 equivalent of

$Bu_3SnH$, site-selective desired reduced product **3.18a** was obtained in excellent yield (entry 4, Table 3.3).

**Table 3.3** Site-selective reduction of vinyl epoxides

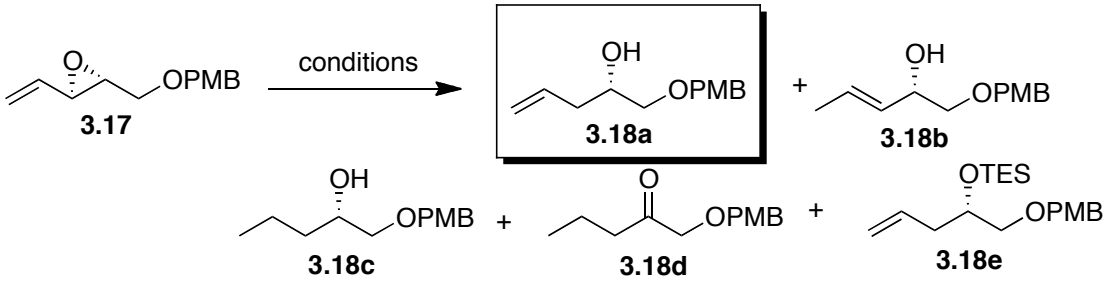


| entry | conditions | products |
|---|---|---|
| 1 | $Pd(dba)_3.CHCl_3$ (0.1 equiv), n-$Bu_3P$ (0.1 equiv), $HCO_2H$ (5 equiv), $NEt_3$ (2 equiv), THF, 24 $^oC$, 2.5 h | **3.18d** (83%), **3.18e** (13%) |
| 2 | $Pd(PPh_3)_4$ (0.1 equiv), $Me_2NH.BH_3$ (1.1 equiv), AcOH (3 equiv), DCM, 23 $^oC$, 1.5 h | **3.18a**:**3.18c** 5.6:1 (97%) |
| 3 | $Pd(PPh_3)_4$ (0.1 equiv), $Et_3SiH$ (1.1 equiv), DCM, 24 $^oC$, 1 h | **3.18e** (75%) |
| 4 | $Pd(PPh_3)_4$ (0.1 equiv), $Bu_3SiH$ (1.1 equiv), DCM, 24 $^oC$, 20 min | **3.18a** (95%) |

Interestingly, upon usage of $Et_3SiH$, the corresponding silylated product was obtained (entry 3). Thus we planned to carry out ring opening of the vinyl epoxide in *N*-Ts enamide moiety following similar strategy. Initially we planned to apply the conditions reported by Takemura's protocol using $Bu_3SnH$ (a, Scheme 3.17) as control experiment. If successful, this would later be modified employing an alkyl radical source (b, Figure 3.17), which would hopefully allow alkylation to occur at C-3 position. However,

subjection of vinyl epoxide compound **3.13** under the above conditions afforded an unexpected compound **3.19** with 75% conversion (Scheme 3.18).

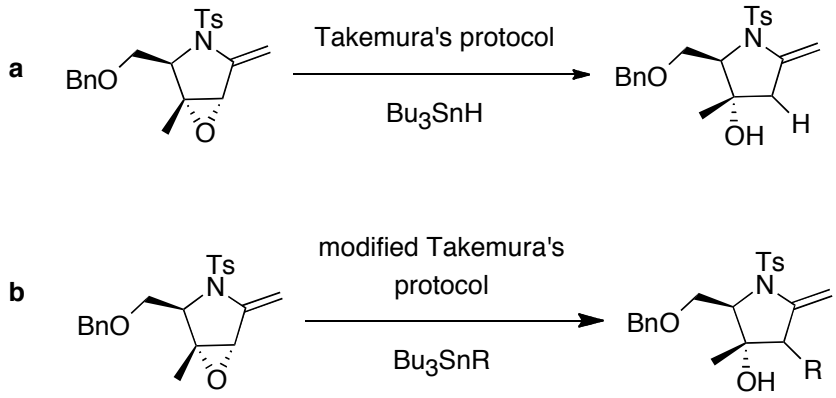


**Scheme 3.17** Palladium mediated ring opening of vinyl epoxide. a) Takemura's protocol. b) Modified conditions.

Formation of compound **3.19** suggests that reduction via hydride occur in desired regioselective fashion although later this undergoes both the epoxide and pyrrolidine ring-opening reactions. Notably our substrate is sterically more demanding than that used by Takemura's report, which might make both metal insertion and transmetallation processes challenging, giving low conversion under similar reaction periods.

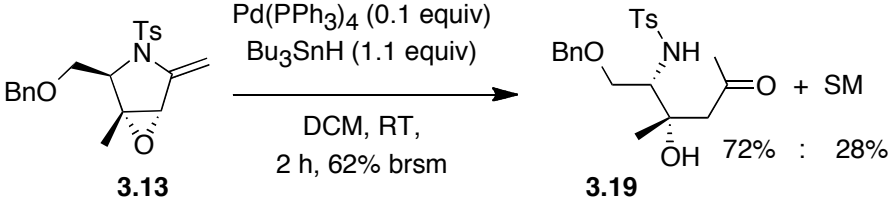


**Scheme 3.18** Palladium mediated vinyl epoxide opening reaction yields an unexpected ring opened product.

Nucleophilic attack by Pd(0) would initially lead to the formation of π-allyl palladium cation species **3.20a**. At this stage transmetallation with $Bu_3SnH$ and reductive elimination of the palladium would have yielded the desired product. However, it seems that the enamine **3.20c** generated upon proto-stannylation leads to iminium upon work-up. The resulting iminium is very likely to undergo hydrolysis upon column purification to provide the ring-opened product **3.19** (Scheme 3.19).

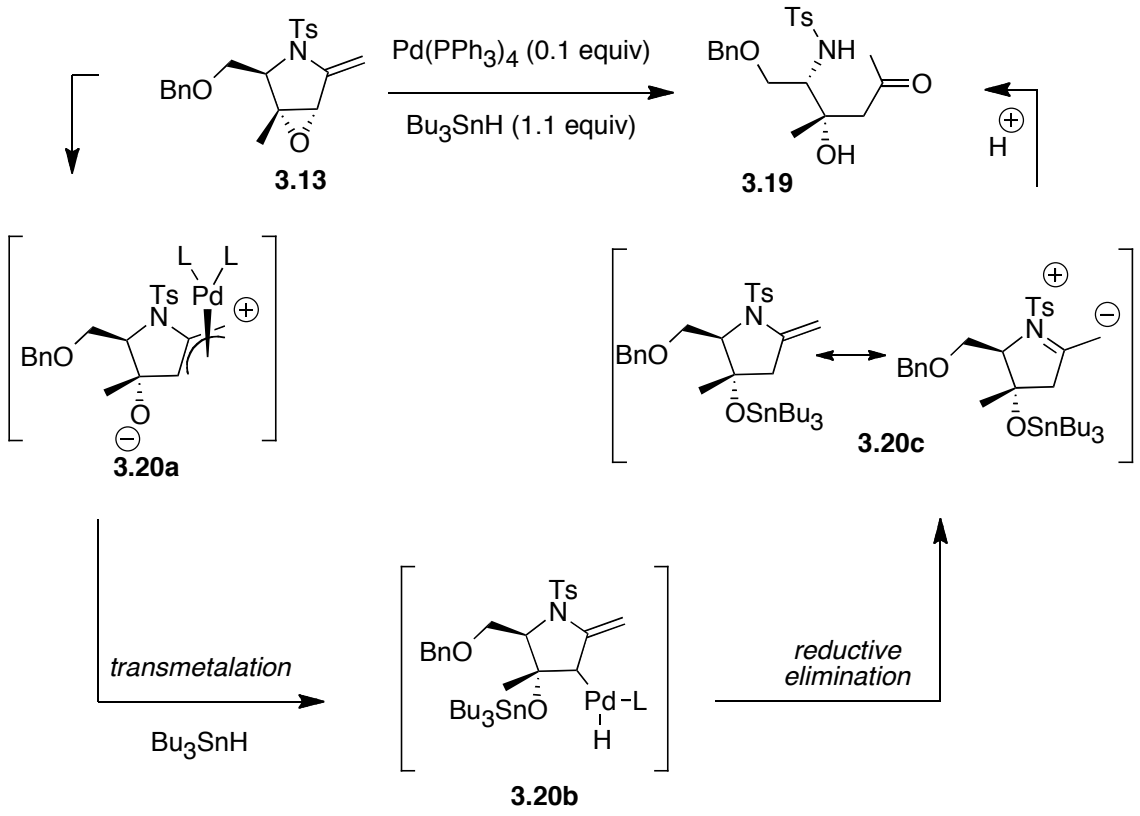


**Scheme 3.19** Mechanistic hypothesis for the unexpected product observed during Pd mediated reductive ring opening reaction.

Although, presence of a base at this stage might have avoided such isomerization, clear reason as to why the generated enamine undergoes isomerization, which later hydrolyzes to give the observed ring opened product, has not been understood.

### 3.4.2 Elaboration of enamine functionality in *N*-Ts enamide motif:

Several reactions such as oxidation, reduction and alkylation were also attempted to take advantage of and exploit the reactivity of enamine functionality present in the molecule.

#### 3.4.2.1 Stereoselective access to *E* and *Z* vinyl bromide intermediates.

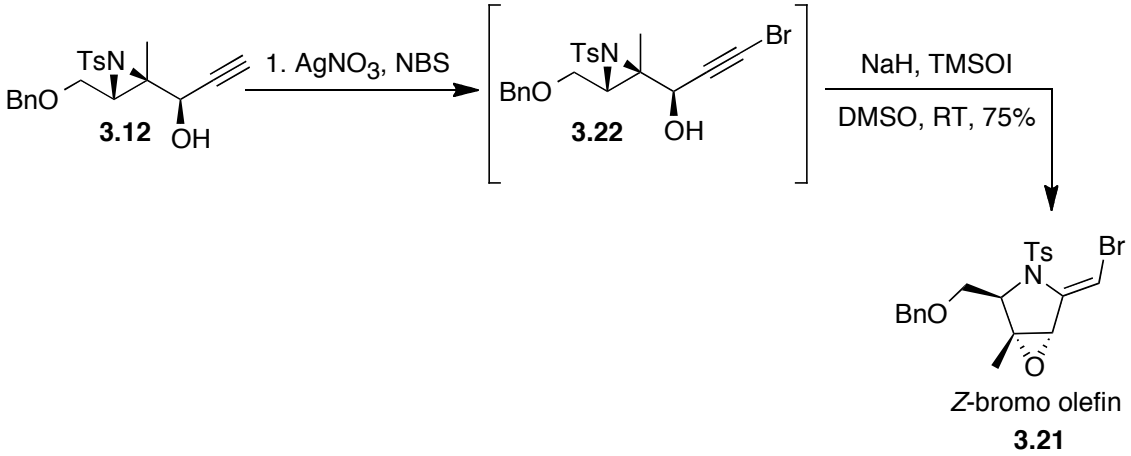


**Scheme 3.20** Two step-protocol to obtain *Z*-bromoolefin.

Formation of vinyl halide **3.21** was reported in our lab following a two-step protocol starting from aziridinol **3.12** (Scheme 3.20).[13] The structural identity of the bromo-olefin compound was determined by X-ray crystallography (Figure 3.5). This clearly revealed that the two-step protocol led to the formation of *Z*-vinyl bromide **3.21** exclusively.

When *N*-Ts enamide compound **3.13** was treated with $Br_2$/N-bromosuccinimide in ether at low temperature vinyl bromide **3.23** was obtained (Scheme 3.21). Careful analysis of NMR spectrum clearly indicated the existence of strictly one geometric isomer. A comparison of the spectroscopic data obtained for the compound **3.23** with that of the known *Z* isomer **3.21** deduced that *E* isomer was exclusively obtained in the later one-step bromination conditions. Scheme 3.21 also illustrates a mechanism that explains the formation of bromo olefin **3.23**, where opening of the initially formed bromonium intermediate by the adjacent lone pair of electrons on nitrogen would lead to the formation of iminium intermediate **3.23a**. The latter upon elimination would deliver the bromoolefin compound.

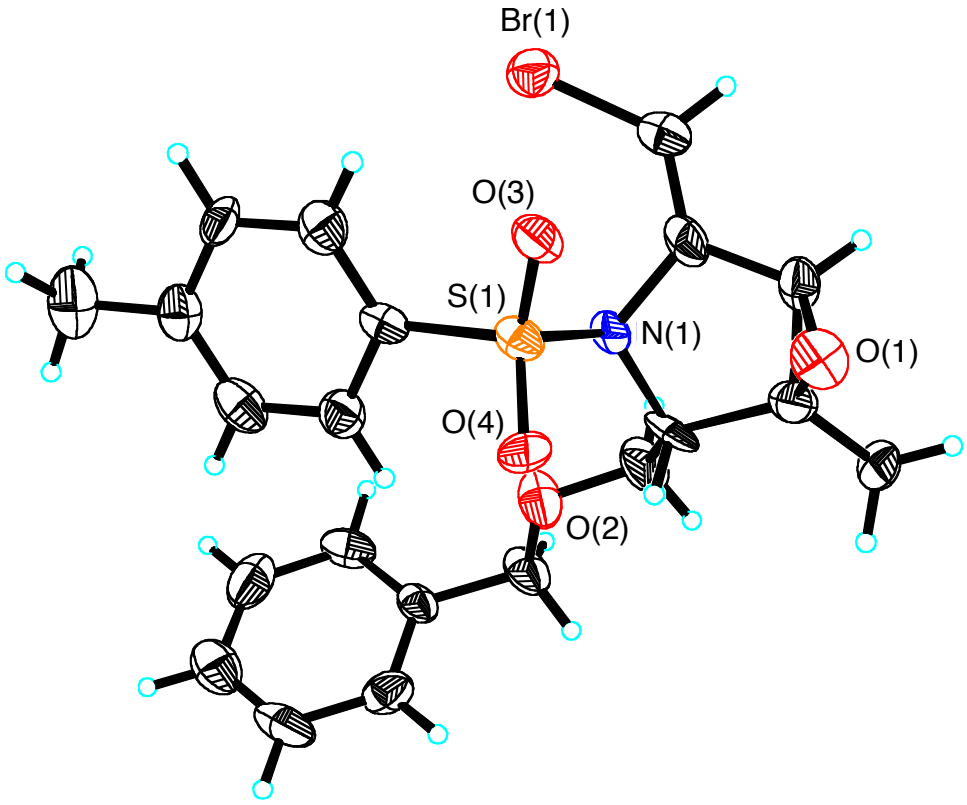


**Figure 3.5** X-ray structure of *Z*-bromo olefin **3.21**.

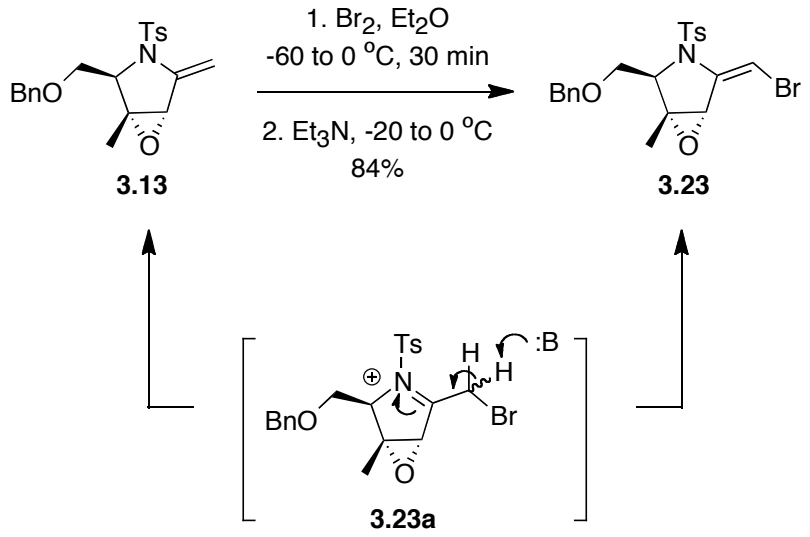


**Scheme 3.21** Synthesis of (*E*)-vinyl bromide **3.23** and its mechanistic rationalization.

Geometric constraints in the iminium ion intermediate would determine the resulting stereochemistry set in the olefin product. Stereoselectivity observed in this reaction can be understood by carefully analyzing the Newman conformations for the iminium intermediate **3.23a**.

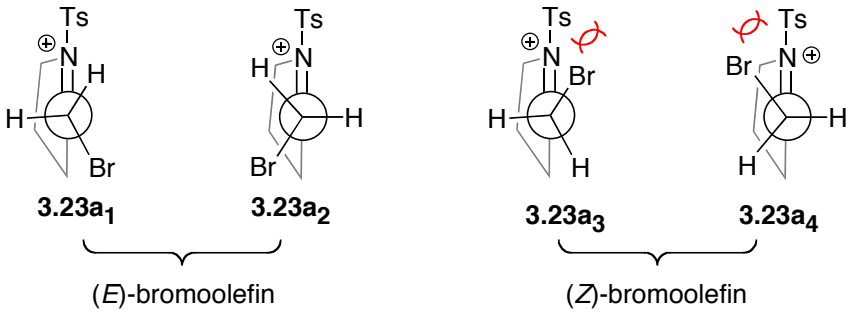


**Figure 3.6** Sterically less demanding conformations lead to the formation of *E*-bromo olefin **3.23**.

Although, **3.23a** may exist in several different conformations, the ones that will assist effective elimination are shown in Figure 3.6 (**3.23a$_1$ to 3.23a$_4$**). Both conformers **3.23a$_3$** and **3.23a$_4$** suffer from $A^{1,3}$ strain. Thus conformers **3.23a$_1$** and **3.23a$_2$** would predominate, thereby prevailing the *E*-selectivity as observed in the experiment.

In order to gain insight on the stereochemical bias and mechanism of the two-step halogenation process, we took note of an observation made during tandem aza-Payne/hydroamination previously reported in our lab on a substituted alkyne substrate. Phenyl substituted propargyllic alcohol **3.24** was reported to undergo aza-Payne/hydroamination reaction which gave *N*-Ts enamide compound **3.25** with high *Z*-selectivity (Scheme 3.22).[12]

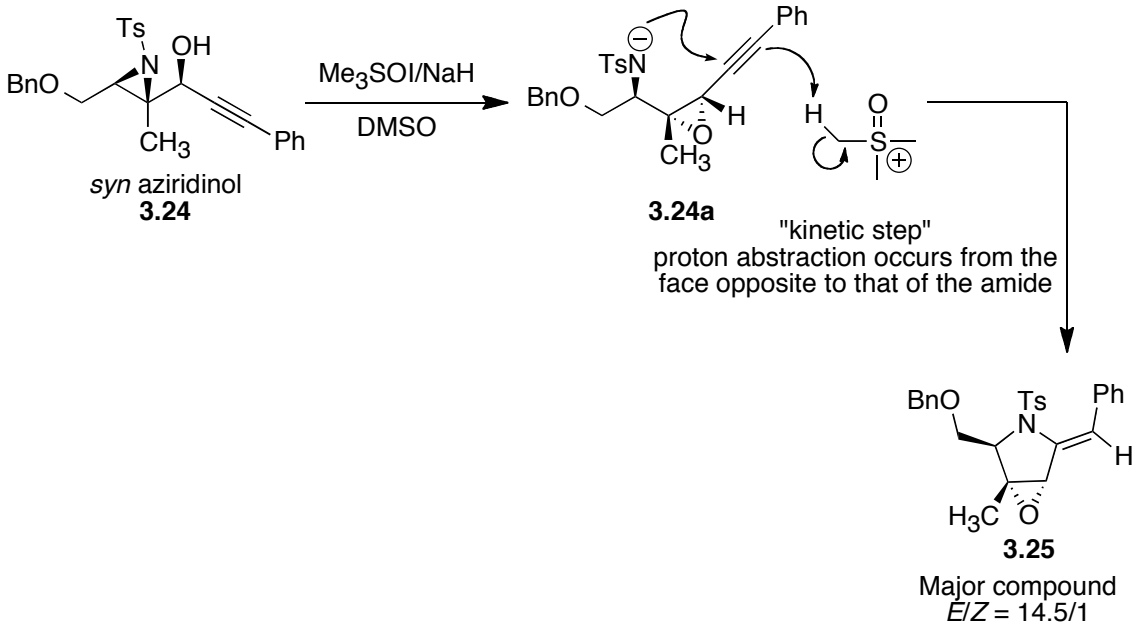


**Scheme 3.22** Tandem aza-Payne/hydroamination yields *Z*-isomer selectively.

It was hypothesized that aza-Payne rearrangement furnishes *N*-Ts amide intermediate **3.24a**, which undergoes *5-exo-dig* cyclization. It seems likely that protonation is a kinetic step, since fast protonation would efficiently occur from the face opposite to that of the attacking nucleophilic amide. This would explain the observed *Z*-selectivity encountered in these reactions. Analogous scenario would explain the observed selectivity obtained in the case where the halogenated alkyne undergoes the hydroamination reaction (Scheme 3.23). Thus at this point we were gratified by accessibility of methods to synthesize bromo-olefin compounds in complete stereocontrolled fashion.

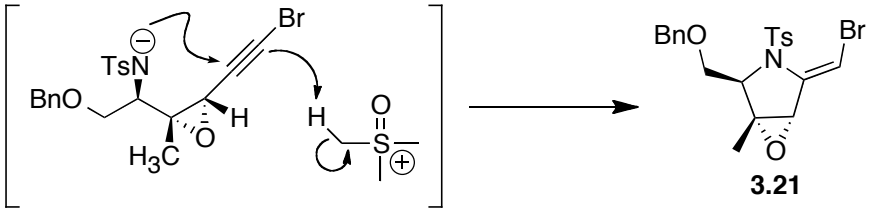


**Scheme 3.23** Mechanistic explanation for the generation of *Z*-bromo olefin.

We also explored the possibility of realizing bis-halogenation of the enamine. Several coupling reactions are precedent in literature where oxidative addition selectively occurs on the *trans* substituted alkenyl halide on a bis-halogenated system.[16-18] Such a route would allow us to functionalize selectively each of the *cis* and *trans* substituted alkenyl halides and would offer an advantage while developing a synthetic route in the future to the natural products in the azinomycin family. For this purpose, *Z*-vinylbromide compound **3.21** was treated with excess of bromine following the similar protocol as

used previously to perform the monobromination of the enamine. Unfortunately when forced, several undesired products were observed, as indicated by analysis of crude NMR (Scheme 3.24).

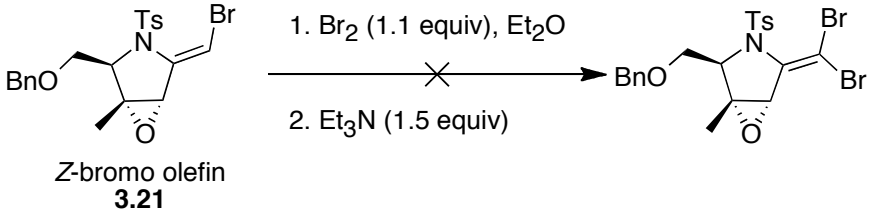


*Z*-bromo olefin
**3.21**

**Scheme 3.24** Failed attempt at dibromination.

### 3.4.2.2 Functionalization of vinylbromide compounds via Suzuki cross coupling reactions.

Vinyl halide compounds have been intensely utilized as starting materials in various coupling reactions, which encouraged us to investigate the scope of vinyl bromide pyrrolidine compounds. Such reactions would enable the functionalization of the olefin in desired fashion, starting with a stereodefined compound.

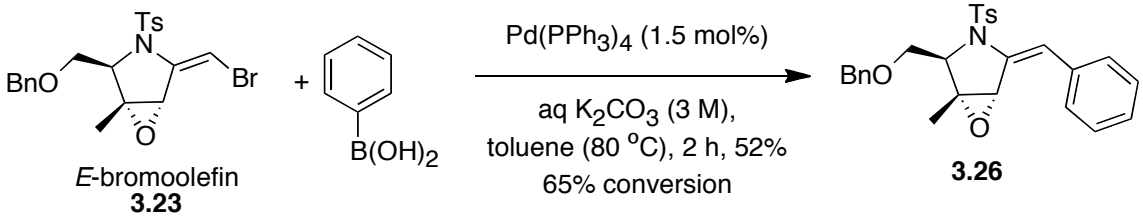


*E*-bromoolefin
**3.23**

**3.26**

**Scheme 3.25** *E*-vinylbromide successfully participates in Suzuki reaction.

Although, some of these compounds could also be synthesized with high *Z* selectivity via tandem aza-Payne/hydroamination chemistry, substrate scope is limited.[11].

Thus *E*-bromo olefin **3.23** was subjected to Suzuki reaction in presence of a base, Pd(0) and phenylboronic acid following a reported procedure (Scheme 3.25).[19] Desired coupled product **3.26** was isolated with 52% yield (80% brsm). The corresponding *Z*-bromo compound **3.21**, on the other hand, afforded the coupled product with low yield (26%, 39% brsm) along with 13% the de-halogenated species (Scheme 3.26).

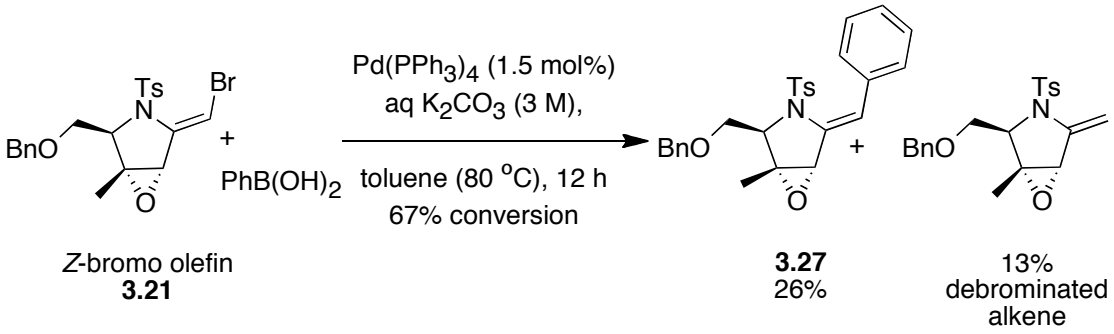


**Scheme 3.26** *Z*-vinylbromide shows poor reactivity in coupling reaction.

This clearly underscores the difference in reactivity of *E* vs *Z* halide compounds toward coupling reactions. The inefficiency of these reaction in case of *Z*-bromo olefin is likely due the fact that palladium insertion is required on a comparatively challenging and sterically encumbered position in the first step (Figure 3.7). Reversibility in the oxidative addition and short-lived organopalladium species might hamper the transmetallation step, which would justify both the de-halogenation and low conversion observed during the transformation.

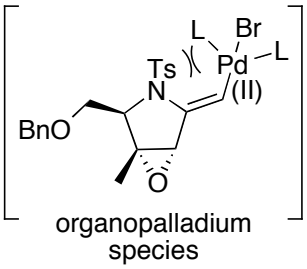


**Figure 3.7** Challenging oxidative addition step in case of sterically demanding *Z*-olefin.

Screening of various conditions such as different ligands for palladium catalyst, bases and solvents and thus optimization will be required especially in the case of Z-vinyl halides. Nevertheless this provides us an efficient way to couple *N*-Ts enamide compounds with different functional groups. The encouraging preliminary results encourage us to explore related coupling reactions to accomplish further bond formations reactions, which will be examined in the future.

**3.4.2.3 Functionalization of vinylbromide compounds via carbonylation reactions:**

Vinyl halide compounds were further subjected to carbonylation reactions. Such transformations, if successful, would provide an access to useful compounds, which would serve as valuable synthetic intermediates for the synthesis of natural products. This would also add both azinomycin A and B (Figure 3.3) as possible targets for total syntheses, since they possess highly branched enamine functionality in their skeletal framework.

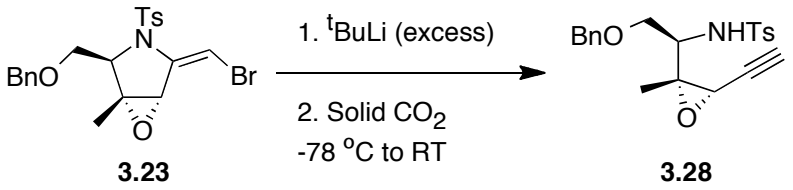


**3.23** **3.28**

**Scheme 3.27** Attempt at the carbonylation via lithium-halogen exchange leads to β-elimination.

Thus vinyl bromide **3.23** was subjected to lithium halogen exchange conditions at -78 $^{o}$C, the in-situ generated lithium species was then treated with $CO_2$. However, no reaction was observed at lowered temperature, slow warming to room temperature afforded ring-opened product **3.28** as one of the identifiable major product (Scheme 3.27). Thus it seems, rate of β-elimination predominates in this case and competes with the desired carbonylation.

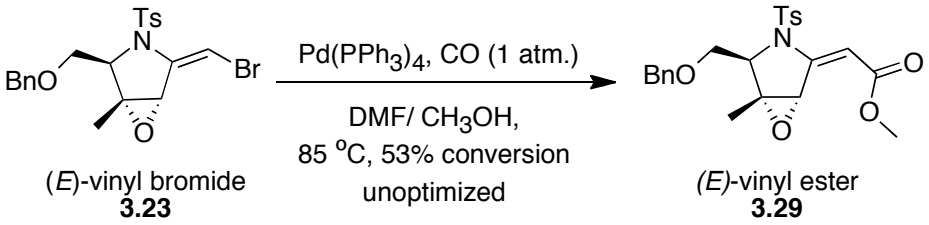


(*E*)-vinyl bromide **3.23**

*(E)*-vinyl ester **3.29**

**Scheme 3.28** Palladium mediated carbonylation of vinyl bromide.

Metal mediated carbonylation reactions are also well precedent in literature.[20,21] Following one of such reported protocols vinyl bromide **3.23** was subjected to CO gas

(atmospheric pressure) in the presence of catalytic Pd(0). Gratifyingly, this reaction afforded the desired ester compound **3.29** with the anticipated *E* stereochemistry of the olefin (Scheme 3.28).

### 3.4.3 Elaboration to lactam and its functionalization.

Epoxide ring opening at enamine stage presented a challenge due to competing isomerization of the *exo*-olefin, therefore masking of the terminal olefin became essential before carrying out such reactions. For this purpose we planned to elaborate the enamine into a lactam.

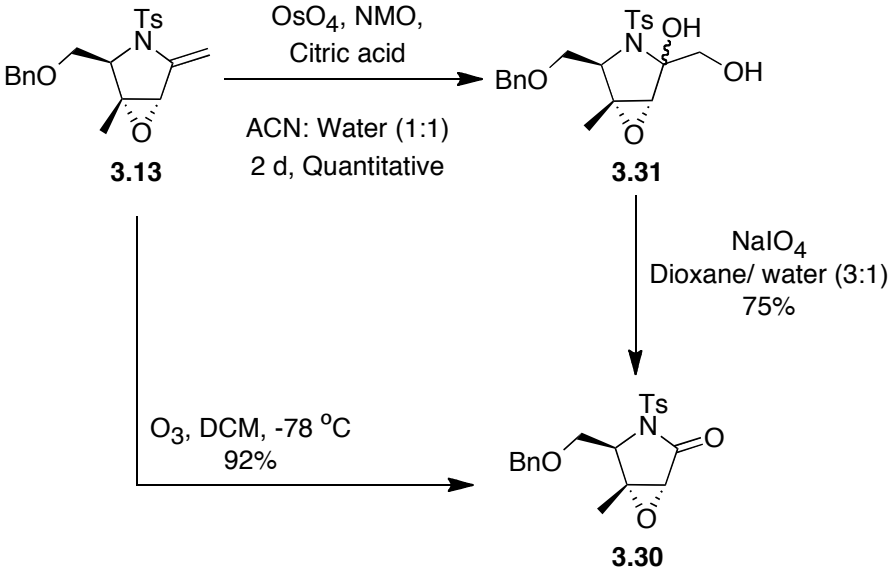


**Scheme 3.29** Oxidation of enamine to lactam **3.30**.

Such a transformation would also be beneficial, keeping in mind these compounds would serve as advanced stage intermediates during the development of a route for the total synthesis of salinosporamide A (see chapter 4). Thus enamine **3.13** was oxidized

to lactam **3.30** via a two-step protocol. Dihydroxylation under modified Upjohn conditions followed by periodate mediated double bond cleavage afforded the lactam **3.30** in good yield.[22,23] Delightfully, the lactam could also be obtained via ozonolysis with excellent yield in one-step (Scheme 3.29).

### 3.4.3.1 Attempts at epoxide opening reactions at lactam stage.

Once masking of the reactive enamine was accomplished, epoxide ring opening was attempted on the lactam species using various nucleophiles. Since, the electrophilic nature of a lactam carbonyl is well precedent in literature,[24] copper based nucleophiles (softer) were examined for the ring opening reactions.

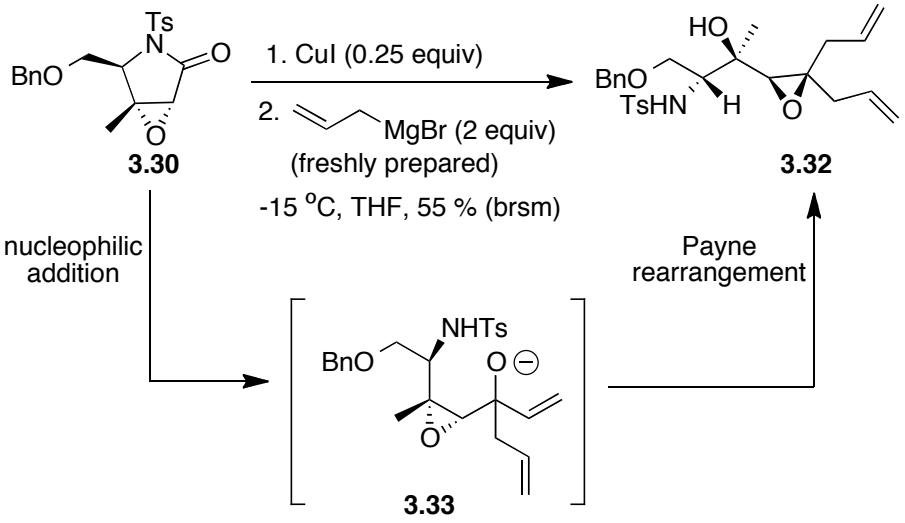


**Scheme 3.30** Epoxide ring opening at lactam stage.

The high Lewis acidity of the latter also makes them highly employed nucleophiles in ring opening reactions of epoxides. Nonetheless when lactam **3.30** was subjected to

addition of organo-copper reagent, ring opened product **3.32** was obtained. It appears that nucleophile attacks the lactam carbonyl twice which leads to the ring opening of the pyrrolidine ring via a putative tetrahedral intermediate. Although at this point, the intermediate alkoxy epoxide **3.33**, appears to undergo Payne rearrangement, which would rationalize the observed product isolated during this transformation. Although the reason for the latter rearrangement is not understood, the high electrophilic character of *N*-Ts lactam carbonyl and release of ring strain explain the formation of the ring opened product observed in this transformation. We were intrigued by the unusual reactivity exhibited by the carbonyl of a purportedly less reactive amide functionality, although the presence of an electron withdrawing group on nitrogen might make it behave more like a ketone. Addition of cuprate was also carried out using a literature protocol.[25] However, several competing reactions were observed as analyzed by crude NMR under these conditions (Scheme 3.30).

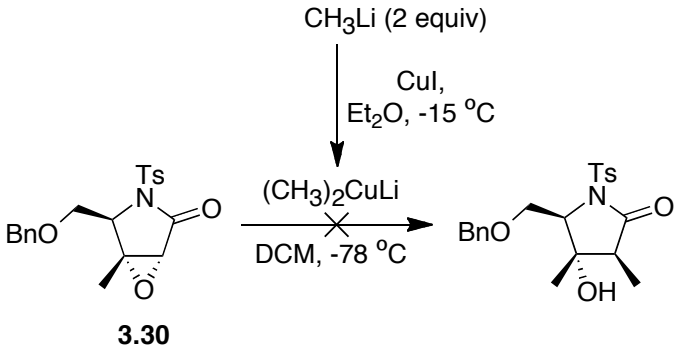


**3.30**

**Scheme 3.31** Addition of lithiumcuprate to lactam.

lactam **3.30** was also treated with cyanocuprate reagent, prepared by a known protocol.[26] The epoxide was further activated using $BF_3$•$OEt_2$. Disappointingly, TLC analysis revealed no reaction under these conditions (Scheme 3.32).

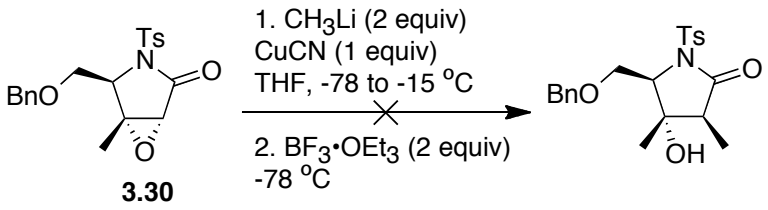


**Scheme 3.32** Attempt at epoxide opening via addition of cyanocuprate under Lewis acidic conditions.

Thus we turned our attention towards the use of other non-carbon based nucleophiles. Sodium acetate and perchloric acid mediated ring opening reactions are very well precedent in the literature.[27,28] Unfortunately no reaction was observed upon treatment of the lactam **3.30** either with aqueous solution of sodium acetate or aqueous solution of perchloric acid at 0 ºC (Scheme 3.33). Regrettably no reaction was observed even upon warming the reaction to room temperature. The un-reactivity that our epoxide exhibited under acidic conditions is not completely understood at this point.

Epoxide ring opening has also been achieved via metal halides which consequently offer access to useful halohydrins compounds.[29,30] Such halohydrin compounds are synthetically valuable since they can be transformed into higher advanced intermediates.

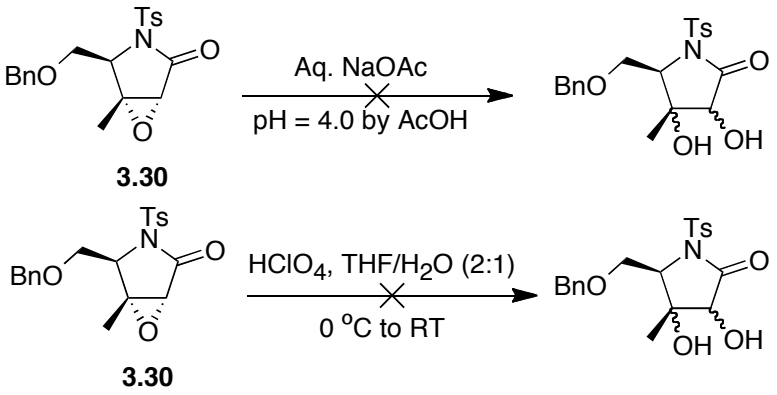


**Scheme 3.33** Failed attempts at epoxide ring opening via non-carbon based nucleophiles.

Bonini and coworkers reported the stereodivergent opening of *trans*-1,2-diphenyloxiranes using $MgBr_2 \cdot OEt_2$ and the effect under the presence of various additives such as NaBr, KBr and Amberlyst 15.[29]

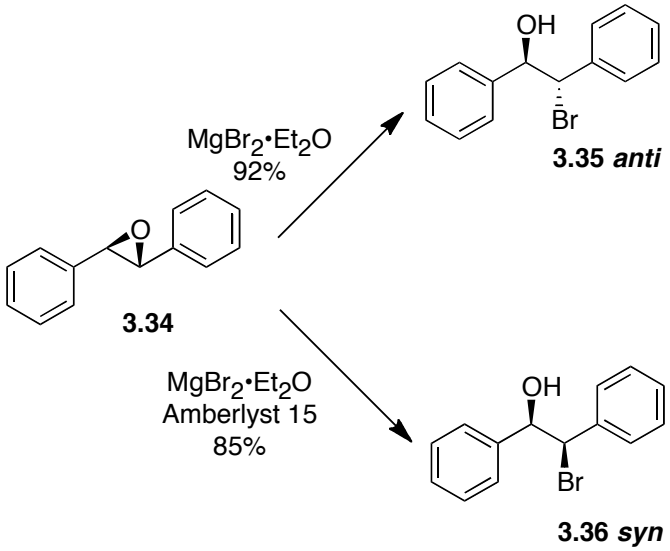


**Scheme 3.34** Reported opening of oxiranes by Bonini and coworkers.

Oxirane ring opening of **3.34** with $MgBr_2$ afforded *anti* ring opened product **3.35** ***anti*** with complete inversion, whereas presence of Amberlyst 15 gave the corresponding *syn* halohydrin compound **3.36** ***syn*** (Scheme 3.34). When lactam **3.30** was subjected under similar conditions, we were delighted to observe the much awaited epoxide ring opened product bromolactam **3.37** with excellent yield. Remarkably, reaction proceeded with both high regio- and stereoselectivity (Scheme 3.35). The identity of the compound was confirmed by X-ray crystallography (Figure 3.8). The structure clearly reveals the *trans* disposition of the bromine and the tertiary alcohol.

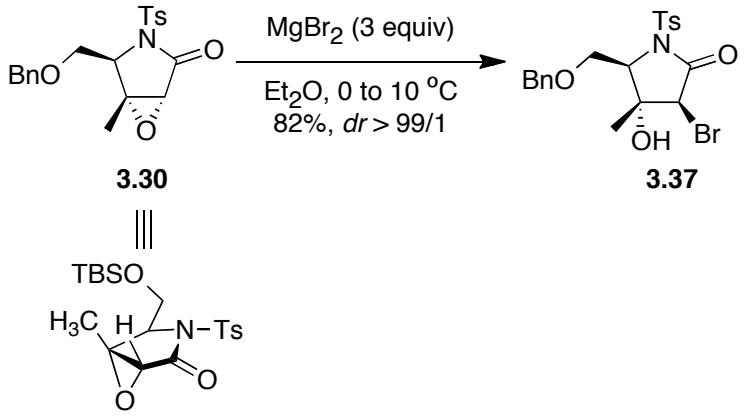


**Scheme 3.35** Regio and stereocontrolled opening of the epoxide.

It is not surprising that bromide attack occurs exclusively at the sterically more available C-3 position. And stereoselectivity seems to be completely governed by the attack in an $S_N2$ fashion, from the top face of the molecule, which leads to the inversion at C-3 position (Scheme 3.35).

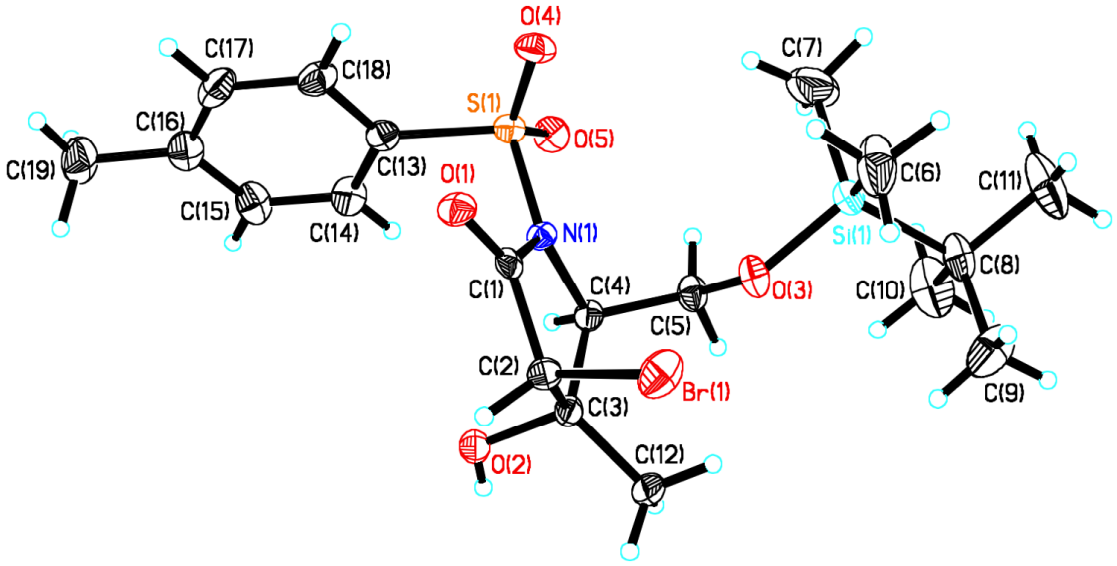


**Figure 3.8** X-ray structure of bromolactam **3.37**.

Epoxide opening was also carried out using Amberlyst 15 as an additive. Unlike in the case of Bonini and coworkers, we did not observe any difference in the strereochemical outcome of the product under these conditions (Scheme 3.36).

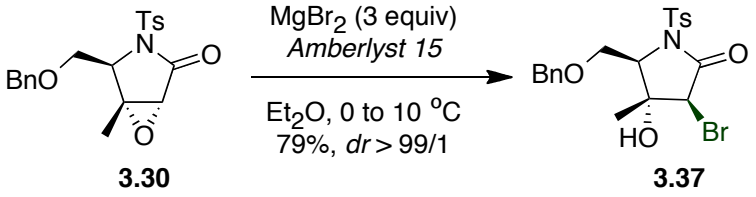


**3.30** **3.37**

**Scheme 3.36** Epoxide ring opening using amberlyst 15 as an additive.

We were nevertheless delighted by the success achieved in the opening of the epoxide by metal halides. This also encouraged us to examine conditions for the direct alkylative opening of the epoxide, since that would shorten the route to achieve C-C

bond formation at C-3 position. Direct C-3 alkylation would also help us to advance our route for the total synthesis of salinosporamide A. Dialkylaluminium reagents have also been used to carry out regioselective opening of the epoxide.[31,32] Although in most of the cases epoxide substrates carry a coordinating group such as an alcohol, which chelate with the aluminum realizing both activation and thus establishing regioselectivity in ring opened products.[33] We presume that C-2 carbonyl might offer a coordinating position in our case. Thus allyldimethylaluminum reagent was generated *in-situ* by treating allylmagnesium chloride with dimethylaluminum chloride. However, a mixture of both C-3 and C-4 regio and stereo isomeric ring-opened products were observed as analyzed by crude NMR.

#### 3.4.3.1.1 Intramolecular epoxide ring opening in lactam: Future Direction

The question whether it's sterics or electronics, which is accountable for the un-reactivity of the epoxide observed in the ring opening reactions, has not been understood clearly.

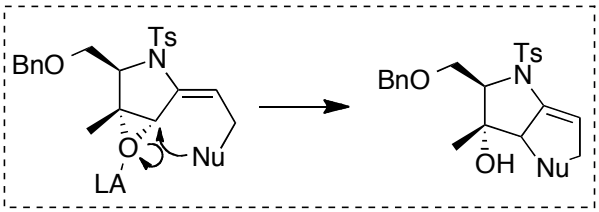


**Scheme 3.37** Proposed activation of the epoxide and intramolecular opening.

It was apparent from the experimental results that the epoxide suffered from low reactivity towards nucleophilic attack, however, upon forced conditions, intended opening suffered from the competing reactivity exhibited by other functional groups present in *N*-Ts enamide moiety. One of the ways to improve such reactivity would be to carry out ring opening in an intramolecular fashion. Scheme 3.37 illustrates a latent nucleophile tethered in the side chain, which would hopefully then execute the ring opening, upon activation. Thus for this purpose we planned to tether the enamine with an appropriate nucleophile. Some of the ways by which the enamine can be functionalized have already been discussed in previous sections. Alternatively, condensation chemistry on the amide carbonyl can also be used to generate nucleophiles such as carboxylic acid derivatives.

**3.5 Attempts toward screening alternative protecting groups on nitrogen.**

Aromatic sulfonic acid derivatives have been used for a long time as efficient protecting groups on nitrogen. Tosyl is one of the most commonly used protecting groups. This makes nitrogen electron deficient and at the same time in many cases provides crystalline nature to the compounds. For the cleavage of *N*-tosyl group, several harsh conditions such as sodium in liquid ammonia and refluxing in a strong acid such as HBr are required. The electron-withdrawing nature of the protecting group on nitrogen favors the aza-Payne rearrangement in favor of the epoxy amide intermediate under basic conditions. Since the formation of this intermediate is required for the subsequent hydroamination to occur in tandem aza-Payne/hydroamination methodology, use of

electron withdrawing groups such as tosyl is crucial. Unfortunately other typical nitrogen protecting groups such as acetyl, tert butoxy carbonyl and benzyl did not facilitate aza-Payne rearrangement.[12] Tert-butoxy sulfonamide group (Bus) has been shown to be an alternative choice. Although Bus group can be easily cleaved under acidic conditions; yield of aza-Payne rearrangement seems to suffer.[12] This has been reasoned either due to the sterics or less stabilization offered by relatively electron rich t-butyl group disfavoring the formation of the intermediate epoxy amide. Thus we became interested in screening other electron withdrawing protecting groups, which would enable participation of the nitrogen efficiently toward aza-Payne rearrangement.

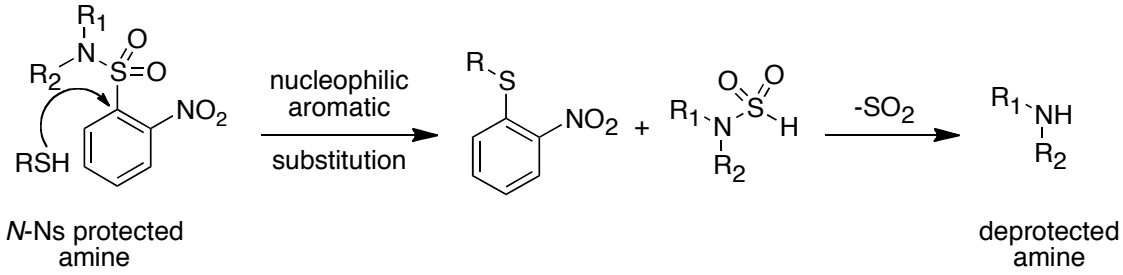


**Scheme 3.38** De-nosylation occurs in the presence of strong nucleophiles.

Groups such as Tces (trichloroethylsulfonate), Ns (o/p nitrobenzene sulfonates) make an appealing choice of an electron withdrawing protecting group and unlike other sulfonamides can be easily removable under strong nucleophlic conditions (Scheme 3.38).[34] We were aware of the requirement of the presence of an appropriate C-2 stereocenter in the course of hydroamination pathway (Section 3.3.1). Our previous study has underscored the significance of Ts as an appropriate choice of protecting

group in order to gain exclusive *syn* selectivity in case of 2,2,3 trisubstituted cases (discussed in Chapter 2).

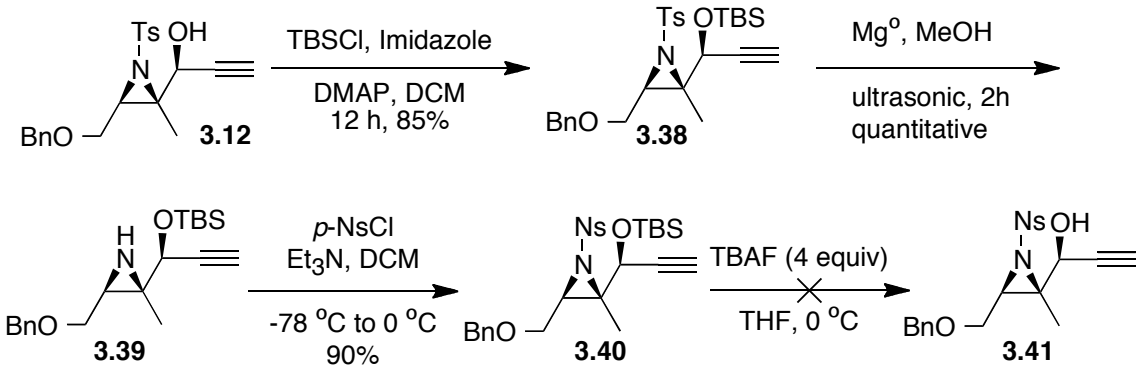


**Scheme 3.39** Synthesis of *N*-Ns protected aziridinol.

Thus we planned to swap Ts protecting group with nosyl once *syn*-selective Grignard addition reaction was accomplished. *Syn* aziridine alcohol **3.12** was first masked as TBS ether **3.38**. Detosylation upon subjection to magnesium in methanol under sonication provided detosylated compound **3.39** quantitatively. The un-protected aziridine was then treated with *p*-nitrobenzenesulfonylchloride to derive *N*-Ns protected aziridine **3.40**. Unfortunately denosylation was observed while attempting TBS removal (Scheme 3.39). Desilylation was then carried out using HF-pyridine, which afforded a mixture of denosylated and an unexpected rearranged aldehyde product **3.43**.Later both *N*-Ts and *N*-Ns protected aziridine alcohols were found to be vulnerable toward such rearrangement.

**Table 3.5** Desilylation of TBS ether of aziridine alcohol.

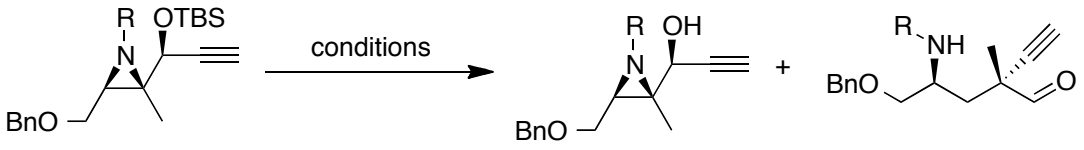


**3.38**: R = Ts
**3.40**: R = Ns

**3.12**: R = Ts
**3.41**: R= Ns

**3.42:** R = Ts
**3.43:** R = Ns

| entry | R | conditions | result alcohol/aldehyde |
|---|---|---|---|
| 1 | Ts | TBAF, RT, 6 h | 35/65 (**3.12**:**3.42**) |
| 2 | Ns | HF-pyridine, ACN, 1 h | 45/55 (**3.41**:**3.43**) |
| 3 | Ts | $BF_3$•$OEt_2$, DCM, RT, 1.5 h | 0/100 (**3.12**:**3.42**) |
| 4 | Ns | 1N HCl, 12 h | n.r. |
| 5 | Ns | 6N HCl, mw (120 $^oC$) | degradation |
| 6 | Ns | THF/$HCO_2H$/$H_2O$ (6:3:1), RT, 3 h | n.r. |
| 7 | Ns | MeOH, $CCl_4$, ultrasonication | n.r. |
| 8 | Ns | 1M $HIO_4$, THF | n.r. |
| 9 | Ns | 1M $HIO_4$, THF, mw (125 $^oC$) | 0/100 |

Table 3.5 lists several conditions under which desilylation was attempted on the TBS ether of both *N*-Ts and *N*-Ns protected aziridine alcohols. Rearranged products were observed in many cases, predominantly under acidic conditions (entry 3 and 9). We found such transformations were well precedent in the literature. Analogous rearrangements have been extensively studied in case of epoxy alcohols. Activation of the epoxide facilitates the ring opening, which promotes the migration of the adjacent

group.[35] Such transformations are observed under Lewis acidic conditions and are referred to as semi-Pinacol type rearrangements.

In fact these rearrangements have been applied at various advanced stages in natural product syntheses. Vleggaar postulated an epoxide-mediated 1,2 alkyl shift (semi pinacol rearrangement) as part of the biosynthesis of asteltoxin.[36] Later Cha and coworkers utilized this transformation in their planned enantioselective synthesis of asteltoxin in close parallel with the proposed synthesis (Scheme 3.40).[37]

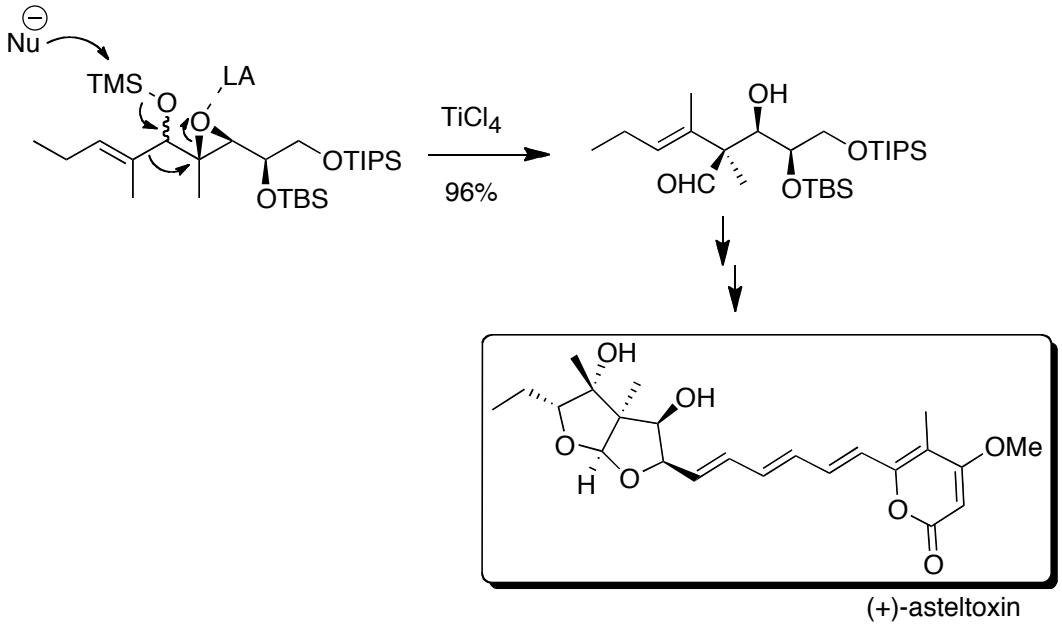


**Scheme 3.40** Semi-pinacol rearragement utilized by Cha and coworkers during the synthesis of asteltoxin.

On the other hand, Tu et al. have reported such rearrangements on 2,3-aziridino alcohol in the presence of $ZnBr_2$.[38] Synthetic value of these transformations involves derivation of two adjacent stereocenters, with one being quaternary (Scheme 3.41).

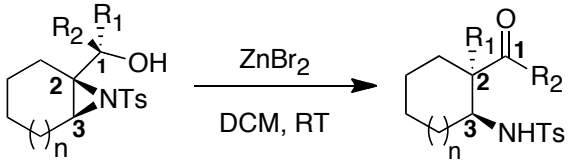


n = 0,1 $R_1$, $R_2$ = H, alkyl, aryl

**Scheme 3.41** Lewis acid promoted rearrangement of 2,3-aziridino alcohols.

These transformations provide an alternative efficient method for the synthesis of $\alpha$-amino ketone and aldehydes, which are particularly versatile synthetic intermediates and find use in medicinal chemistry. It has been proposed that Lewis acid first coordinates to the nitrogen of the aziridine and hydroxyl oxygen. The cleavage of the activated C-N bond occurs simultaneously along with the 1,2 migration of the group in the transition state geometry resembling that of nucleophilic substitution and thus involves inversion. The five-member ring structure due to the coordination of the Lewis acid to both the heteroatom hinders the free rotation of the C1-C2 bond. Thus the group $R_1$ that is *anti* to the C-N bond migrates (Scheme 3.42). This explains the stereoselective rearrangement of the reaction. Different Lewis acids were also screened and $SmI_2$ was reported to be the most efficient whereas $AlCl_3$ was found to be too reactive affecting the yield for such rearrangements (Table 3.6).

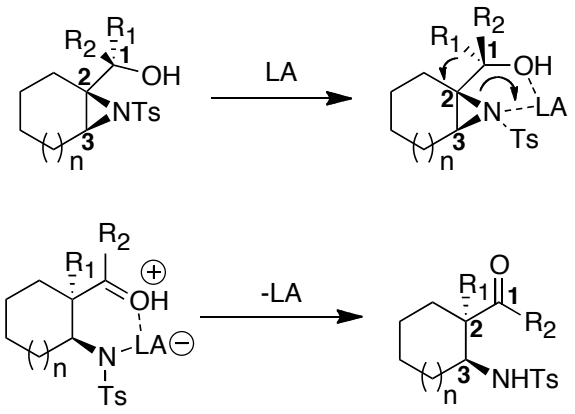


**Scheme 3.42** Mechanistic insight to the semi-Pinacol rearrangement.

On the other hand, similar rearrangements have not been reported for the corresponding TBS ethers of such aziridino alcohols. In this case we also speculate that a similar mechanism is in play, where fluoride attack on silicon would develop a negative charge which would assist in C=O bond formation along with C-N bond cleavage and subsequent migration of the alkyne substituent (Figure 3.9).

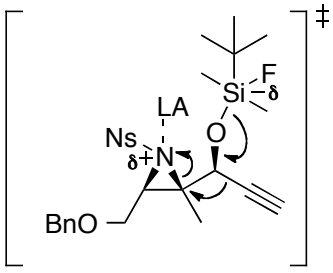


**Figure 3.9** Hypothesized transition state involved in the semi-pinacol rearrangement of TBS ether of aziridinols.

More importantly in presence of a Lewis acid, partial development of positive charge on nitrogen would further promote aziridine ring opening. The latter point is clearly manifested when $BF_3$•$OEt_2$ was used; in this case exclusive formation of such rearranged products was observed.

**Table 3.6** Effective Lewis acids for the rearrangement of 2,3-aziridinols.[38]

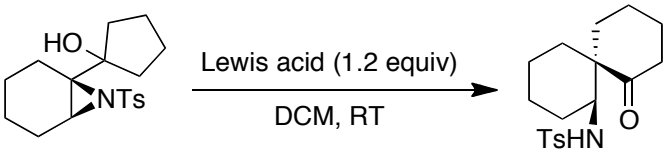


| entry | Lewis acid | yield (%) | time (min) |
|---|---|---|---|
| 1 | $AlCl_3$ | 40 | 30 |
| 2 | $ZnCl_2$ | 74 | 60 |
| 3 | $Sn(OTf)_2$ | 80 | 60 |
| 4 | $BF_3$•$OEt_2$ | 82 | 10 |
| 5 | $SnCl_4$ | 86 | 10 |
| 6 | $SmI_2$ | 93 | 40 |
| 7 | $ZnI_2$ | 82 | 60 |
| 8 | $TiCl_4$ | 55 | 10 |
| 9 | $Sc(OTf)_3$ | 74 | 60 |
| 10 | $ZrCl_4$ | 76 | 20 |

Nevertheless it was evident that desilylation of the masked alcohol was either inefficient or was impeded by semi-pinacol rearrangements. Thus we turned our attention towards selective N-nosylation, which would not require the problematic un-masking of the alcohol. Detosylated aziridine alcohol **3.39** was directly subjected to TBAF assisted desilylation reaction. Unlike in case of *N*-Ts or *N*-Ns protected aziridinol, no semi-pinacol rearrangement was observed in this case. This clearly implies that such rearrangements require the activation of the aziridine nitrogen. Subsequent selective N-nosylation was examined under different conditions. N-tosylation of aziridine nitrogen in the presence of free hydroxyl has been reported in our lab (Scheme 3.43).[11]

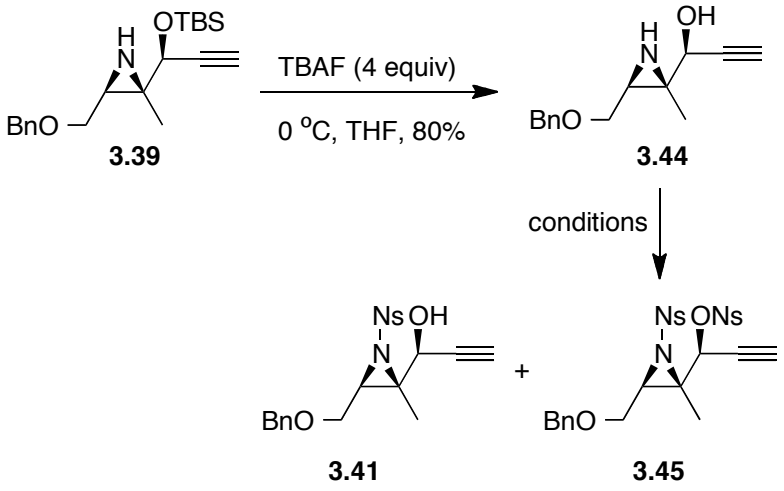


**Scheme 3.43** Synthesis of *N*-Ns protected aziridine alcohol.

Thus we tested the scope of selective N-nosylation under similar conditions. It was found that when temperature was lowered, poor conversion but better selectivity was

achieved (Table 3.7). This observation clearly underscores the higher reactivity of the *p*-NsCl as opposed to that of *p*-TsCl.

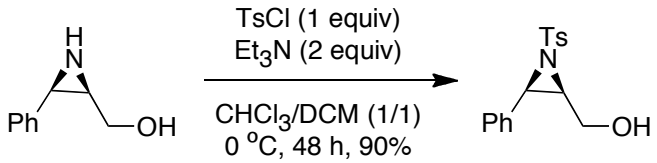


**Scheme 3.44** Reported selective *N*-tosylation.

When *N*-Ns aziridinol substrate **3.41** was subjected to tandem aza-Payne/hydroamination conditions, an unexpected product was obtained. Figure 3.10 illustrates some of the possible structures of the unexpected product, though the exact identity of the structure could not be confirmed.

**Table 3.7** Nosylation of aziridine alcohol.

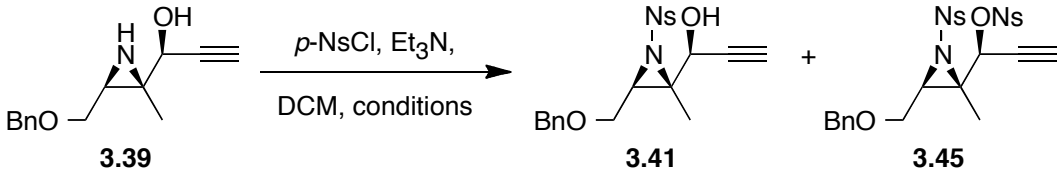


| entry | temperature | time | overall yield | ratio (**3.41**/**3.45**) |
|---|---|---|---|---|
| 1 | -78 to -45 °C | 12 h | 26% | 77/23 |
| 2 | -78 °C | 4 h | 18% | 91/9 |

We also investigated the scope of N-Tces (trichloroethylsulfonate) protected substrate in aza-Payne/hydroamination methodology. For this purpose trichloroethylsulfonate was

prepared in one step starting from trichloroethanol according to a known procedure (Scheme 3.46).[39]

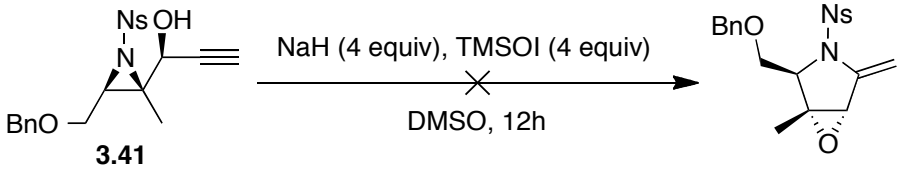


**Scheme 3.45** Tandem aza-Payne/hydroamination reaction of *N*-Ns protected substrate.

Being aware of complications associated with O-protecting group removal, we tried to introduce the Tces group on nitrogen selectively in the presence of free hydroxyl group. Nitrogen is generally assumed to exhibit higher nucleophilicity under neutral conditions, although in the presence of $NaHCO_3$ no reaction was observed as analyzed by TLC (Scheme 3.47).

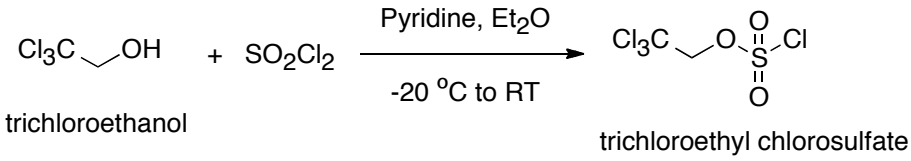


**Scheme 3.46** Synthesis of trichloroethyl chlorosulfate reagent.

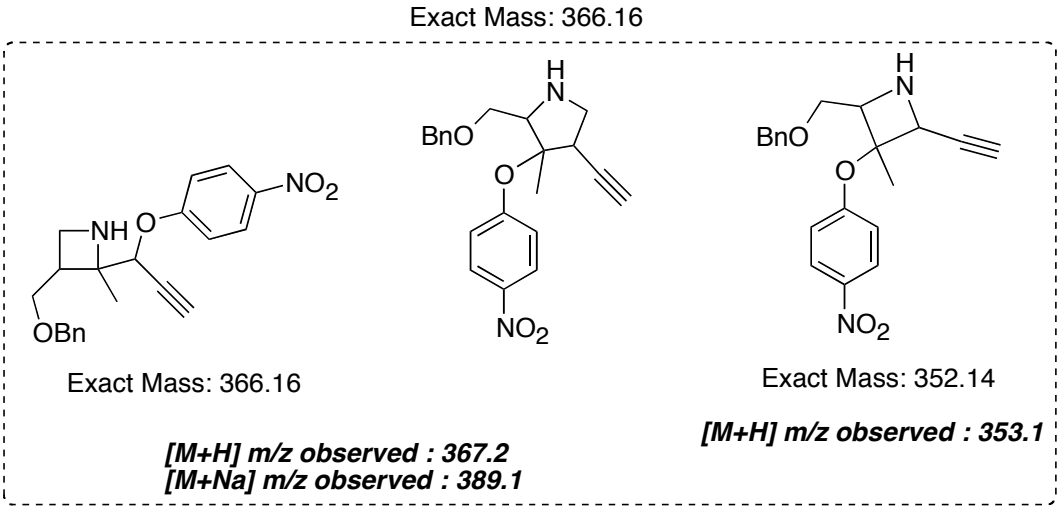


**Figure 3.10** Possible products of the tandem aza-Payne/hydroamination reaction of N-*Ns* aziridinol.

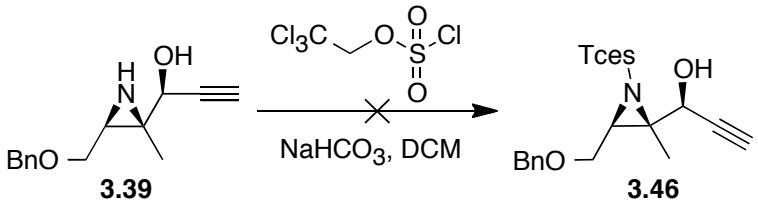


**Scheme 3.47** Failed attempt at the synthesis of N-*Tces* protected aziridinol.

On the other hand when compound **3.39** was treated with TcesCl (Scheme 3.48) in the presence of DABCO, protected aziridinol **3.46** was obtained with 65% yield (Scheme 3.38).[40] Tces protected aziridinol **3.46** was then treated with NaH, in order to test its scope towards aza-Payne rearrangement. After 12 h, starting material was consumed totally and yielded an unexpected cyclic sulfamate product **3.47**.

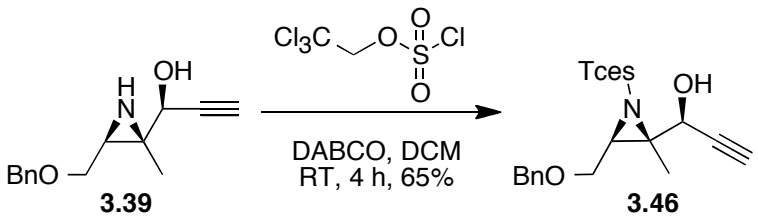


**Scheme 3.48** Successful protection of aziridinol.

Scheme 3.49 outlines a plausible mechanistic explanation for the formation of the unexpected sulfamate product. The alkoxide **3.46a** generated under basic conditions might undergo intramolecular sulfonation via attack on the trichlorethyl sulfate group. Expulsion of trichloroethoxide anion would result in the generation of a fused sulfamate intermediate **3.48**. Deprotonation and aziridine ring opening on this highly strained intermediate would then yield sterically less encumbered 6-member cyclic sulfamate **3.47** (Scheme 3.49).

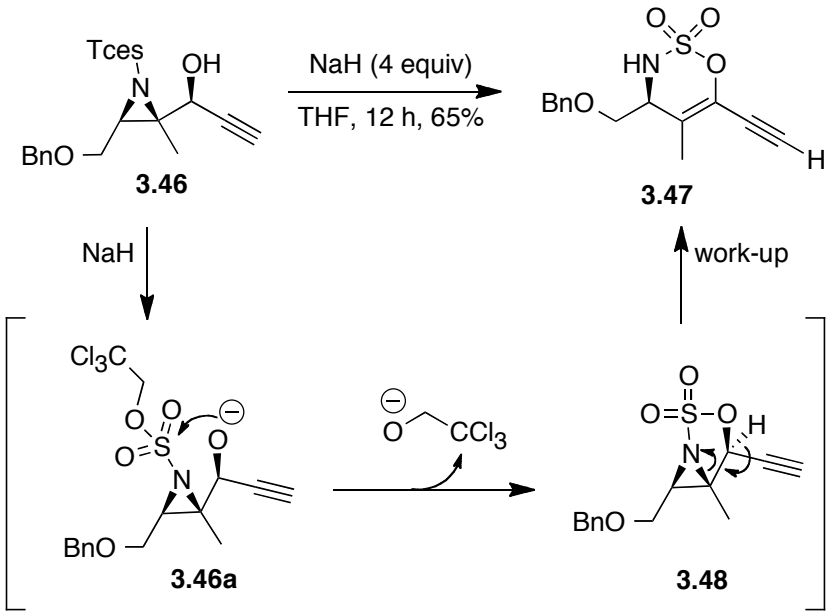


**Scheme 3.49** Subjection of aziridinol **3.46** to basic conditions.

Thus it was inferred that the presence of the trichloroethylsulfate group was incompatible with the strong basic conditions required for aza-Payne rearrangement.

### 3.6 Attempts toward detosylation of the pyrrolidine.

Frustrated by the failed attempts at finding alternative N-protecting groups, at this point we also turned our focus toward examining conditions to carry out detosylation of the *N*-Ts enamide compounds.

**Table 3.8** Attempts at detosylation of N-Ts enamide substrate.

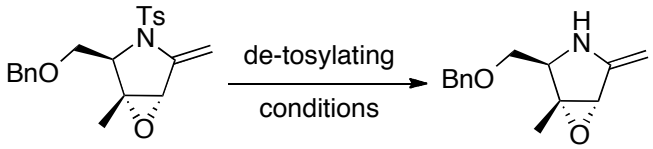


**3.13** **3.49**

| entry | conditions | result |
|---|---|---|
| 1 | $Mg^{o}$, MeOH, sonication, 1- 6 h | n.r. |
| 2 | $SmI_2$, THF, -15 $^{o}$C | degradation |
| 3 | Na, $NH_3$, THF, -78 $^{o}$C | degradation |

Harsher conditions such Na, liquid $NH_3$ resulted into degradation of both pyrrolidine enamide and lactam substrates (Tables 3.8 and 3.9). Interestingly, milder conditions such as magnesium and methanol returned enamine unreacted whereas the lactam substrate was found too reactive, under these conditions.

**Table 3.9** Attempts at detosylation of lactam.

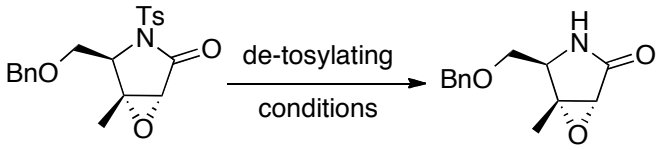


**3.30** **3.50**

| entry | conditions | result |
|---|---|---|
| 1 | $Mg^{o}$, MeOH, sonication, 1-6 h | degradation |
| 2 | $SmI_2$, THF, -15 $^{o}$C | degradation |
| 3 | Na, $NH_3$, THF, -78 $^{o}$C | degradation |

### 3.7 Experimental procedures.

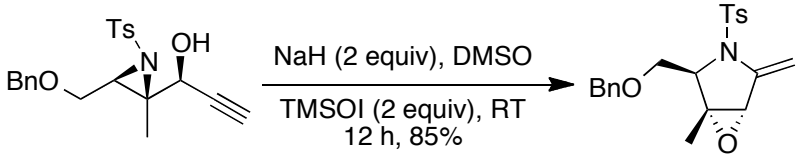


**3.12** **3.13**

**Preparation of *N*-Ts enamide 3.13**. NaH (0.20 g, 5.08 mmol) was suspended in anhydrous freshly distilled DMSO (25 mL). Dried trimethylsulfoxonium iodide (1.12 g, 5.08 mmol) was crushed into fine powder, gradually added in 4 portions over 20 min. The reaction was stirred at room temperature for 30 min, till all the bubbles ceased. Aziridinol **3.12**[3] (0.98 g, 2.54 mmol) dissolved in small amount of anhydrous DMSO (~0.5 mL) was added drop wise to the above solution. The reaction was stirred at room temperature over night. After completion upon TLC analysis, the reaction was quenched with sat. $NH_4Cl$ (5 mL). The aqueous phase was extracted with EtOAc (3 X 10 mL). The combined organic layer was washed with brine (5 mL) and dried over anhydrous sodium sulfate. After rotary evaporation and upon purification with silica gel chromatography (4:1 Hex:EtOAc) compound **3.13** (0.8 g, 82%) was obtained as an oil.[11] Spectral data: $^1$H-NMR (500 MHz, $CDCl_3$) $\delta$ 7.70 (d, 2H, $J$ = 8.2 Hz), 7.38 - 7.29 (m, 8H), 5.48 (s, 1H), 4.85 (s, 1H), 4.67 (d, 1H, $J$ = 12.1 Hz), 4.59 (d, 1H, $J$ = 12.1 Hz), 4.07 (m, 1H), 3.89 (m, 1H), 3.48 (m, 1H), 2.42 (s, 3H), 1.49 (s, 3H); $^{13}$C-NMR (125 MHz, $CDCl_3$) $\delta$ 143.9, 142.5, 137.8, 134.4, 129.2, 128.3, 127.6, 127.5, 98.8, 73.7, 70.6, 65.3, 62.5, 62.2, 21.5, 14.2.

[3] Synthetic procedure and spectroscopy data are discussed in Chapter 1.

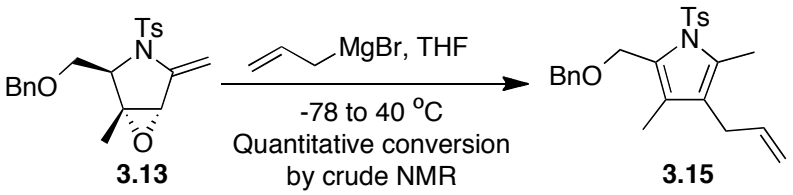


**Procedure for the addition of Grignard reagent to *N*-Ts enamide 3.13**. *N*-Ts enamide **3.13** (0.10 g, 0.26 mmol) was dissolved in anhydrous THF (1 mL). At -78 °C commercially available allylmagnesium bromide (1.3 mL, 1.3 mmol, 1.0 M solution in THF) was added drop wise to the above solution. At this point no reaction was observed. Thus extra allylmagnesium bromide was added (1.3 mL, 1.3 mmol) at -78 °C. The reaction was then heated at 45 °C for 4 h. The reaction after completion was quenched with sat. $NH_4Cl$ (0.5 mL). Following extraction with EtOAc and rotary evaporation pyrrole **3.15** was obtained in quantitative yield.[12] Spectral data: $^1$H-NMR (300 MHz, $CDCl_3$) $\delta$ 7.72 (d, 2H, $J$ = 8.7 Hz), 7.34 - 7.20 (m, 5H), 7.09 (d, 2H, $J$ = 8.1 Hz), 5.78 - 5.64 (m, 1H), 4.92 - 4.76 (m, 2H), 4.72 (s, 2H), 4.51 (s, 2H), 2.99 (s, 3H), 2.31 (s, 3H), 2.21 (s, 3H), 1.89 (s, 3H); $^{13}$C-NMR (75 MHz, $CDCl_3$) $\delta$ 143.9, 138.5, 135.9, 129.5, 128.2, 128.0, 127.7, 126.8, 124.8, 121.9, 114.7, 72.1, 61.8, 28.4, 21.5, 12.3, 9.5.

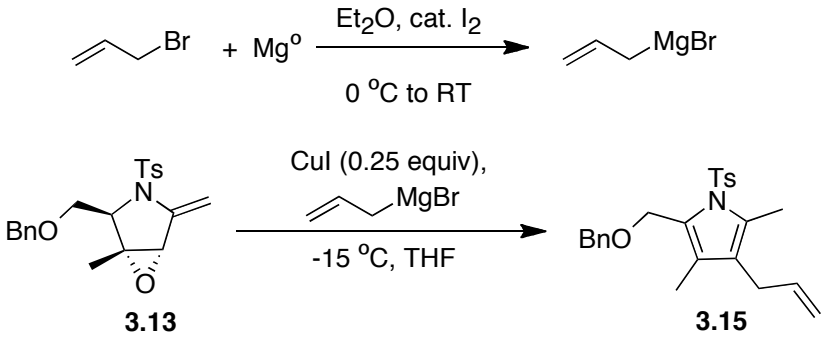


**Procedure for the addition of organo-copper reagent to the *N*-Ts enamide 3.13**. To a flame dried flask was charged magnesium turnings (1.0 g, 41.7 mmol) and anhydrous $Et_2O$ (24 mL) was added under nitrogen. Allylmagnesium bromide (2.5 mL, 29.8 mmol) was added drop wise at 0 °C. Catalytic amount of $I_2$ crystal was added to the above reaction flask. The reaction was slowly warmed to room temperature. The solution (0.44 mL) thus obtained was added drop wise to the enamine epoxide **3.13** (0.01 g, 0.26 mmol) and dried CuI (12.4 mg, 0.06 mmol) dissolved in anhydrous THF (1 mL) at -15 °C. After 2 h extra CuI (12.4 mg, 0.06 mmol) and allylmagnesium bromide solution (0.44 mL, 0.52 mmol) was again added. The reaction was stirred to afford a mixture of starting material and pyrrole compound **3.15**.

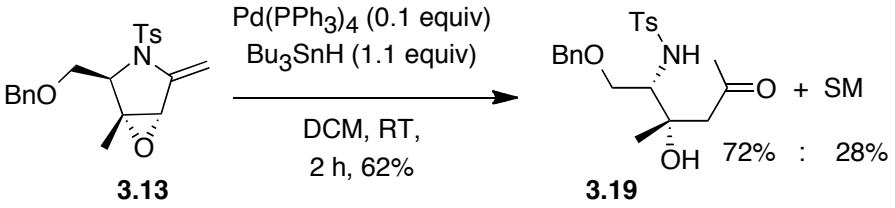


**Palladium mediated vinyl epoxide ring opening reaction.**[15] To a solution of $Pd(PPh_3)_4$ (15 mg, 0.01 mmol) in anhydrous DCM (1.1 mL) was added $Bu_3SnH$ (41.6

mg, 0.14 mmol) at room temperature. To the mixture was then added enamine compound **3.13** (50 mg, 0.13 mmol) dissolved in DCM (2.3 mL) drop wise. The mixture was stirred at room temperature for overnight. Solvent was removed under vacuum to afford epoxide compound **3.19** (33 mg, 62%) with 72% conversion. Spectral data: $^{1}$H-NMR (500 MHz, $CDCl_3$) $\delta$ 7.62 (d, 2H, $J$ = 8.2 Hz), 7.31 - 7.14 (m, 8H), 5.25 (d, 1H, $J$ = 8.7 Hz), 4.38 (s, 1H), 4.29 (d, 1H, $J$ = 12 Hz), 4.14 (dd, 1H, $J$ = 12.1, 2.1 Hz), 3.66 (dd, 1H, $J$ = 9.7, 1.9 Hz), 3.38 (m, 1H), 3.21 (d, 1H, $J$ = 18.3 Hz), 2.84 (m, 1H), 2.45 (dd, 1H, $J$ = 18.2, 1.9 Hz), 2.38 (s, 3H), 2.17 (s, 3H), 1.07 (s, 3H); $^{13}$C-NMR (125 MHz, $CDCl_3$) $\delta$ 212.0, 143.5, 137.2, 129.7, 128.5, 127.9, 127.8, 127.1, 73.4, 66.4, 57.1, 50.0, 31.2, 29.7, 23.3, 21.5; IR (neat) 3283, 2922, 2853, 1702, 1598, 1452, 1362, 1333, 1091; HRMS (ESI) (m/z): $[M+Na]^+$ calculated for $[C_{21}H_{27}NNaO_5S]^+$ 428.1508, found 428.1499.

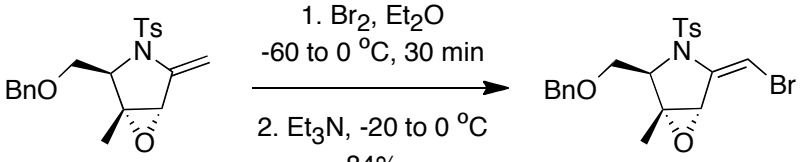


**3.13** **3.23**

**Preparation of *E*-vinyl bromide compound**. Bromine (25 mL, 0.49 mmol) was added under stirring to a solution of enamine **3.13** (170 mg, 0.44 mmol) dissolved in anhydrous $Et_2O$ (3.9 mL) maintained at -60 °C. Stirring was continued at this temperature for 30 min, after which yellow suspension was allowed to warm to 0 °C. Then $Et_3N$ (92 μL, 0.66 mol) in anhydrous $Et_2O$ (0.2 mL) was added at -20 °C, stirring was continued at the same temperature. The resulting colorless suspension was warmed to room

temperature and then stored in a refrigerator (~ -20 $^{o}$C) overnight. In the morning precipitated $Et_3N^+Br^-$ salt was filtered and the solvent was removed under reduced pressure, which was then subjected to silica gel purification (4:1 Hex: EtOAc) to give vinyl bromide compound **3.23** (160 mg, 84 %) as an oil. Spectral data: $^1$H-NMR (500 MHz, $CDCl_3$) δ 7.60 (d, 2H, *J* = 8.4 Hz), 7.35 - 7.27 (m, 8H), 6.67 (s, 1H), 4.61 (d, 1H, *J* = 12.0 Hz), 4.53 (d, 1H, *J* = 12.0 Hz), 4.04 (m, 1H), 3.94 (s, 1H), 3.80 (d, 2H, *J* = 3.4 Hz), 2.41 (s, 3H), 1.43 (s, 3H); $^{13}$C-NMR (125 MHz, $CDCl_3$) δ 144.3, 139.5, 137.6, 134.1, 129.5, 128.4, 127.7, 127.6, 127.5, 94.1, 76.7, 73.7, 70.3, 65.7, 62.1, 61.1, 21.6, 14.1; IR (neat) 3071, 2922, 2863, 1597, 1452, 1357, 1088, 751, 664; HRMS (ESI) (m/z): $[M+H]^+$ calculated for $[C_{21}H_{23}NO_4BrS]^+$ 462.0531, found 462.0535.

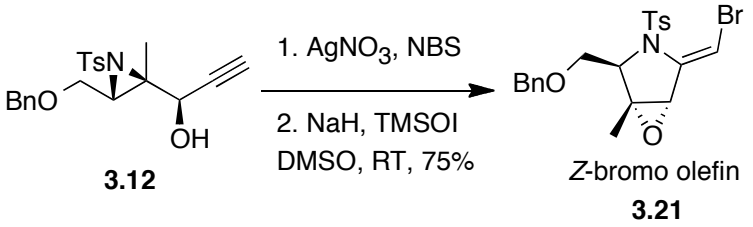


**Preparation of *Z*-vinyl bromide 3.21**. Aziridinol **3.12** (200 mg, 0.52 mmol), silver nitrate (8.8 mg, 0.1 mol%) and NBS (100.2 mg, 0.57 mmol) were dissolved in acetone (8 mL). The solution was stirred at room temperature for 3 h. The solution was filtered through a silica gel plug and the solvent was removed under reduced pressure. The residue was dissolved in dry DMSO (1 mL) and added to *in-situ* generated dimethylsulfoxonium methylide via the addition of NaH (60% as dispersion in oil) (82.8 mg, 2.07 mmol), TMSOI (455.8 mg, 2.06 mmol) in anhydrous DMSO (2.5 mL) for 30

min. The solution was stirred overnight at room temperature under an inert atmosphere of nitrogen. The solution was quenched with sat. $NH_4Cl$ (1 mL). The aqueous phase was extracted with EtOAc (3 X 10 mL). The combined organic layer was washed with brine (5 mL) dried over anhydrous sodium sulfate. After rotary evaporation and upon purification with silica gel chromatography (5:1 Hex:EtOAc) *Z*-bromo olefin **3.21** (165 mg, 68%) was obtained as white solid (m. pt = 125 – 127 $^oC$ ) along with recovered starting material (62 mg, 31%).[13] Spectral data: $^1H$-NMR (500 MHz, $CDCl_3$) $\delta$ 7.70 (d, 2H, *J* = 8.2 Hz), 7.32 - 7.25 (m, 7H), 6.15 (s, 1H), 4.50 (d, 2H, *J* = 12.5 Hz), 4.08 (t, 1H, *J* = 6.5, 3.5 Hz), 3.71 (d, 2H, *J* = 3.5 Hz), 3.52 (s, 1H), 2.35 (s, 3H), 1.43 (s, 3H); $^{13}C$-NMR (125 MHz, $CDCl_3$) $\delta$ 144.0, 141.4, 137.7, 135.4, 129.2, 128.4, 128.2, 127.7, 127.5, 109.7, 95.9, 73.8, 70.1, 65.6, 62.8, 61.6, 21.6, 14.0.

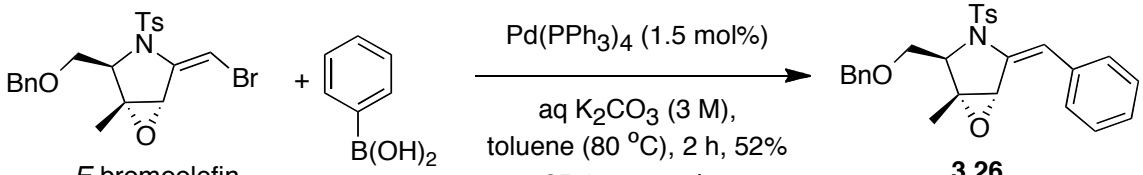


*E*-bromoolefin **3.23**

**3.26**

**Preparation of Suzuki-coupled product 3.26**.[19] Aqueous solution of $K_2CO_3$ (0.13 mL, 3M) and $PhB(OH)_2$ (19 mg, 0.16 mmol) was added to the solution of vinyl bromide **3.23** (59.6 mg, 0.13 mmol) in toluene (1.3 mL). The solution was degassed by allowing it to freeze at -78 $^oC$, vacuum subjection, followed by warming to room temperature and nitrogen flushing. This process was repeated three times in order to de-gas the solution completely. $Pd(PPh_3)_4$ (2.3 mg, 0.01 mmol) was added under nitrogen environment to

the above solution. The solution was heated in a sealed tube for 2 h. After completion [TLC] the solution was filtered through a pad of silica gel and was removed under reduced pressure. The crude was purified via column chromatography (100 % Hex to 3:1 Hex:EtOAc) to afford the *E*-Olefin **3.26** (30 mg, 52 %) as oil. Rest of the material was recovered as the starting material. Spectral data: $^{1}$H-NMR (500 MHz, $CDCl_3$) δ 7.88 (d, 2H, *J* = 8.9 Hz), 7.29 (m, 8H), 4.53 (d, 2H, *J* = 3.9 Hz), 4.34 (m, 1H), 3.98 (m, 3H), 2.39 (s, 3H), 1.56 (s, 3H); $^{13}$C-NMR (125 MHz, $CDCl_3$) δ 144.0, 137.9, 137.4, 135.9, 134.6, 129.3, 128.5, 128.4, 128.3, 127.7, 127.6, 127.1, 118.3, 73.8, 70.9, 64.5, 63.6, 60.6, 21.6, 14.4; IR (neat) 2924, 2860, 1452, 1357, 1088, 998; HRMS (ESI) (m/z): $[M+H]^+$ calculated for $[C_{27}H_{28}SO_4N]^+$ 462.1739, found 462.1734.

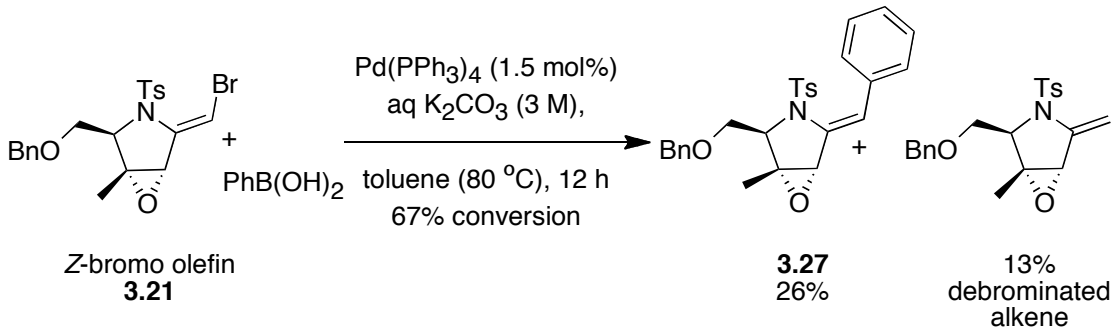


**Preparation of Suzuki-coupled product 3.27**. Aqueous solution of $K_2CO_3$ (0.12 mL, 3M) and $PhB(OH)_2$ (17 mg, 0.14 mmol) was added to the solution of *Z*-vinyl bromide **3.21** (53.7 mg, 0.12 mmol) in toluene (1.2 mL). The solution was degassed by allowing it to freeze at -78 °C, vacuum subjection, followed by warming to room temperature and nitrogen flushing. This process was repeated three times in order to de-gas the solution

completely. $Pd(PPh_3)_4$ (2.0 mg, 0.01 mmol) was added under nitrogen environment to the above solution. The solution was heated in a sealed tube for 12 h. After completion [TLC] the solution was filtered through a pad of silica gel and was removed under reduced pressure. The crude was purified by column chromatography (100 % Hex to 3:1 Hex:EtOAc) to afford the *Z*-Olefin **3.27** (13.5 mg, 26 %) as a yellow oil, along with the mixture of the debrominated alkene and starting material. Spectral data: $^1$H-NMR (500 MHz, $CDCl_3$) δ 7.70 (d, 2H, *J* = 7.2 Hz), 7.60 (d, 2H, *J* = 8.4 Hz), 7.42 - 7.26 (m, 10H), 6.41 (s, 1H), 4.70 (d, 1H, *J* = 12 Hz), 4.63 (d, 1H, *J* = 12 Hz), 4.11 (m, 1H), 4.03 (dd, 1H, *J* = 9.9, 4.5 Hz), 3.90 (dd, 1H, *J* = 9.9, 2.9 Hz), 3.60 (s, 1H), 2.43 (s, 3H), 1.43 (s, 3H); $^{13}$C-NMR (125 MHz, $CDCl_3$) δ 143.6, 137.6, 135.6, 135.4, 132.0, 129.1, 129.0, 128.3, 128.1, 127.8, 127.7, 127.4, 120.6, 73.8, 70.7, 64.9, 63.6, 61.9, 21.6, 14.1.

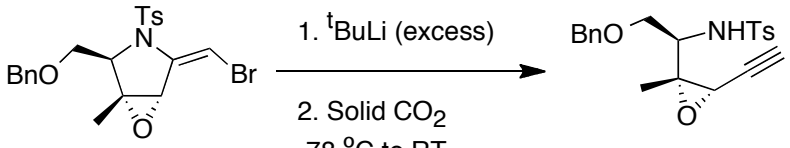


**3.23** **3.28**

**Procedure for carbonylation of the vinyl bromide 3.23.** To a solution of vinyl bromide **3.23** (25 mg, 0.05 mmol) in anhydrous $Et_2O$ (0.54 mL) was added $^t$BuLi (0.3 mL, 0.5 mmol, 1.7 M solution in THF) drop wise, maintained in a dry ice bath at -78 °C. After half an hour, dry ice was added to the above solution. The bath was then gradually warmed to room temperature. After 2 h the reaction was quenched with sat. $NH_4Cl$ (2 mL). Extraction with EtOAc, drying over sodium sulfate and rotary evaporation

gave a mixture of epoxy amine **3.28** along with starting material and impurities.

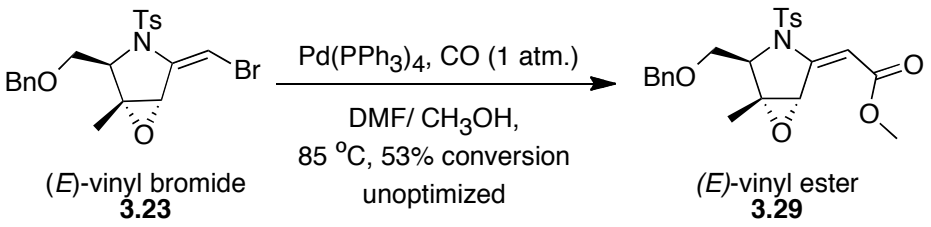


(*E*)-vinyl bromide
**3.23**

*(E)*-vinyl ester
**3.29**

**Preparation of *E*-vinyl ester 3.29**. Methanol (2 mL), anhydrous DMF (4 mL) and $Et_3N$ (0.06 mL) were added under to a flask maintained under nitrogen atmosphere. Solution was cooled to -78 $^oC$, when frozen subjected to vacuum and gradually warmed to room temperature. The flask was later filled with nitrogen. This was repeated two more times. Vinyl bromide **3.23** (18.4 mg, 0.04 mmol) and $Pd(PPh_3)_4$ were added to a V-shaped flask. The flask was evacuated and filled with CO (1 atm) using a balloon filled with CO gas. The above-prepared de-gassed mixture of solvents was added via a syringe. The flask was immersed into a preheated oil bath maintained at 80 $^oC$. The mixture was cooled to room temperature after 4 h. The solution was then poured into brine solution (15 mL) and extracted three times with EtOAc (30 mL each). The organic layer was dried over sodium sulfate. Rotary evaporation and silica gel column purification (Hex:EtOAc 4:1) yielded vinyl ester **3.29** (33 mg, 54%) as a colorless oil. Spectral data: $^1$H-NMR (500 MHz, $CDCl_3$) $\delta$ 7.61 (d, 2H, $J$ = 8.7 Hz), 7.32 - 7.25 (m, 8H), 6.31 (s, 1H), 4.76 (s, 1H), 4.60 (d, 1H, $J$ = 12.8 Hz), 4.52 (d, 1H, $J$ = 12.8 Hz), 4.12 (m, 1H), 3.86 (dd, 1H, $J$ = 10.9, 4.1 Hz), 3.81 (dd, 1H, $J$ = 10.6, 2.0 Hz), 3.70 (s, 3H), 2.39 (s, 3H), 1.48 (s, 3H); $^{13}$C-NMR (125 MHz, $CDCl_3$) 167.0, 137.5, 134.0, 129.7,

129.5, 127.8, 127.5, 103.5, 73.8, 69.9, 65.7, 59.4, 51.5, 14.1; IR (neat) 2924, 2854, 1710, 1642, 1353, 1168, 1085, 1028; HRMS (ESI) (m/z): $[M+H]^+$ calculated for $[C_{23}H_{26}NO_6S]^+$ 444.1481, found 444.1480.

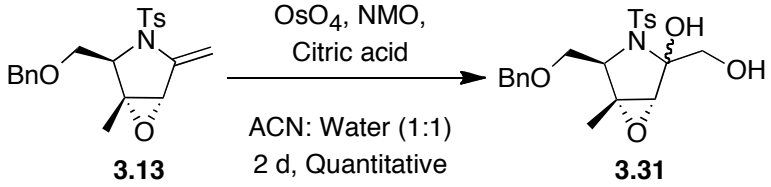


**Preparation of diol 3.31.** The alkene **3.13** (0.43 g, 1.12 mmol) was dissolved in a 1:1 mixture of ACN/water (11.2 mL each). The mixture was then treated with NMO (0.15 g, 1.23 mmol), citric acid (0.18 g, 0.84 mmol) and $OsO_4$ (11 μL, 0.02 mol, 2M in toluene). The reaction mixture was stirred till complete conversion was observed as analyzed by TLC. Upon completion the aqueous layer was extracted three times with EtOAc (15 mL each). The organic layers were washed with brine (20 mL), dried over sodium sulfate and evaporated under reduced pressure to afford diol **3.31** as a white oil with quantitative conversion, which was taken to next step without any purification.

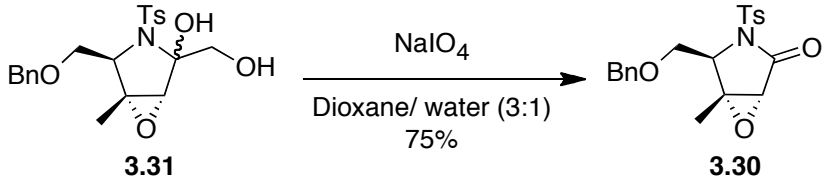


**Preparation of lactam 3.30**. The crude diol **3.31** (0.47 g, 1.11 mmol) was dissolved in dioxane (16.5 mL) and water (5.5 mL). The reaction mixture was treated with $NaIO_4$

(1.19 g, 5.57 mmol), stirred at room temperature overnight. After completion the reaction was quenched with water (10 mL). The aqueous layer was extracted four times with EtOAc (30 mL). The combined organic layers were dried over sodium sulfate and evaporated under reduced pressure. The crude was purified via column chromatography (9:1 Hex:EtOAc to 1:1 Hex:EtOAc) to yield lactam **3.30** (0.35 g, 75%) as a white solid.[12] Spectral data: $^{1}$H-NMR (500 MHz, $CDCl_3$) $\delta$ 7.84 (d, 2H, $J$ = 8.5 Hz), 7.27 (m, 5H), 7.12 (m, 2H), 4.36 (d, 1H, $J$ = 12.1 Hz), 4.32 (d, 1H, $J$ = 12.1 Hz), 3.94 (dd, 1H, $J$ = 11.1, 3.1 Hz), 3.71 (dd, 1H, $J$ = 10.8, 1.54 Hz), 3.35 (d, 1H, $J$ = 1.27 Hz), 2.36 (s, 3H), 1.50 (s, 3H); $^{13}$C-NMR (125 MHz, $CDCl_3$) $\delta$ 169.0, 144.9, 136.8, 135.1, 129.3, 128.1, 127.6, 127.5, 127.4, 127.2, 73.1, 67.1, 62.7, 59.4, 57.0, 21.3, 13.2.

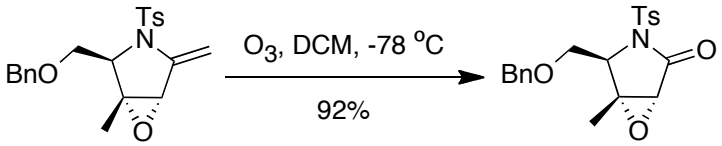


**3.13** **3.30**

**Preparation of lactam 3.30 directly via ozonolysis.** A solution of pyrrolidine **3.13** (100 mg, 0.26 mmol) in anhydrous DCM (9 mL) was treated with Ozone gas maintained at -78 °C using a dry-ice bath. After complete conversion (20 min, reaction turned blue), excess amount of ozone was removed by flushing nitrogen through the reaction mixture. The blue solution turned colorless and was then treated with zinc metal dust (34 mg) and a few drops of acetic acid. The reaction was diluted with water (2 mL) upon completion. Aqueous layer was extracted with DCM (3 X 5 mL). The combined organic layers were dried over anhydrous sodium sulfate and subjected to rotary evaporation.

Upon purification by column chrmatography (4:1 Hex: EtOAc) lactam **3.30** (98 mg, 98%) was obtained as a white solid.[12] Spectral data: $^{1}$H-NMR (500 MHz, $CDCl_3$) $\delta$ 7.84 (d, 2H, *J* = 8.5 Hz), 7.27 (m, 5H), 7.12 (m, 2H), 4.36 (d, 1H, *J* = 12.1 Hz), 4.32 (d, 1H, *J* = 12.1 Hz), 3.94 (dd, 1H, *J* = 11.1, 3.1 Hz), 3.71 (dd, 1H, *J* = 10.8, 1.54 Hz), 3.35 (d, 1H, *J* = 1.27 Hz), 2.36 (s, 3H), 1.50 (s, 3H); $^{13}$C-NMR (125 MHz, $CDCl_3$) $\delta$ 169.0, 144.9, 136.8, 135.1, 129.3, 128.1, 127.6, 127.5, 127.4, 127.2, 73.1, 67.1, 62.7, 59.4, 57.0, 21.3, 13.2.

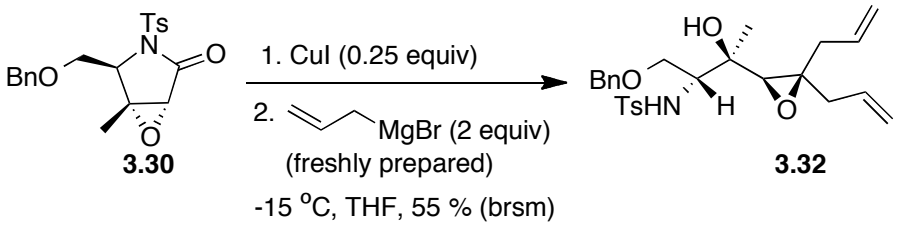


**3.30** **3.32**

**Procedure for the addition of organo-copper reagent to lactam 3.30.** To a solution of lactam **3.30** (67 mg, 0.17 mmol) in anhydrous THF (0.6 mL) maintained at -15 °C, was added purified CuI (8.2 mg, 0.04 mmol). After 5 min, freshly prepared 1.24 M solution of allyl magnesium bromide (0.3 mL, 0.35 mmol) was added drop wise under inert atmosphere at -15 °C. The reaction was quenched with sat. $NH_4Cl$ (0.1 mL). The aqueous phase was extracted with EtOAc (3 X 5 mL), dried over anhydrous sodium sulfate and after rotary evaporation gave the undesired product epoxide **3.32** (32 mg, 80%) along as a colorless oil, along with some recovered starting material (7 mg). Spectral data: $^{1}$H-NMR (500 MHz, $CDCl_3$) $\delta$ 7.67 (d, 2H, *J* = 8.2 Hz), 7.31 (m, 4H), 7.20 (d, 2H, *J* = 8.5 Hz), 7.15 (d, 2H, *J* = 7.4 Hz), 5.87 (m, 2H), 5.18 (m, 4H), 4.68 (bs, 1H),

4.34 (m, 1H), 4.29 (d, 1H, *J* = 11.2 Hz), 4.14 (d, 1H, *J* = 11.2 Hz), 3.51 (dd, 1H, *J* = 9.9, 2.4 Hz), 2.92 (dd, 1H, *J* = 9.5, 4.3 Hz), 2.66 (s, 1H), 2.52 (m, 1H), 2.52 (m, 1H), 2.38 (s, 3H); $^{13}$C-NMR (125 MHz, $CDCl_3$) δ 143.5, 137.6, 137.3, 132.8, 132.3, 129.6, 128.5, 128.4, 127.9, 127.6, 127.1, 119.5, 119.3, 73.3, 71.8, 70.1, 68.7, 63.0, 51.3, 44.0, 41.5, 21.5, 21.0; IR (neat) 3492, 3281, 2924, 1451, 1331, 1091; HRMS (ESI) (m/z): $[M+H]^+$ calculated for $[C_{26}H_{34}SO_5N]^+$ 472.2158, found 471.2150.

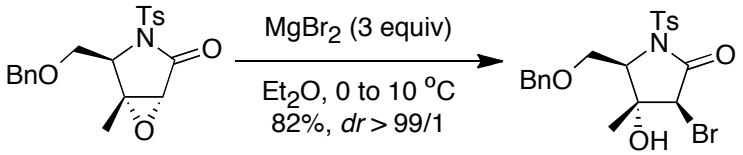


**3.30** **3.37**

**Preparation of bromo lactam 3.37**.[29] To a solution of lactam **3.30** (52.3 mg, 0.14 mmol) in anhydrous $Et_2O$ (3 mL) at 0 °C was added commercially available solid anhydrous $MgBr_2$ (75 mg, 0.41 mmol). Amberlyst 15 (34 mg), if required was added to the solution. The solution was stirred at -10 °C till all the starting material was consumed as analyzed by TLC. Upon completion the solution was filtered and washed with $Et_2O$ (5 mL) and DCM (10 mL). The ether was removed under vacuum. Purification with column chromatography (4:1 Hex:EtOAc) afforded the compound **14** (52.0 mg, 82%) as white solid (89 – 91 °C). Spectral data: $^1$H-NMR (500 MHz, $CDCl_3$) δ 7.88 (d, 2H, *J* = 8.9 Hz), 7.29 (m, 8H), 4.53 (d, 2H, *J* = 3.9 Hz), 4.34 (m, 1H), 3.98 (m, 3H), 2.39 (s, 3H), 1.56 (s, 3H); $^{13}$C-NMR (125 MHz, $CDCl_3$) δ 168.8, 145.5, 137.2,

134.6, 129.5, 128.5, 128.4, 128.0, 127.9, 75.7, 73.3, 69.2, 68.7, 49.8, 21.8; IR (neat) 3491, 2871, 1743, 1363, 1171; HRMS (ESI) (m/z): $[M+H]^+$ calculated for $[C_{20}H_{23}SO_5NBr]^+$ 468.0480, found 468.0475.

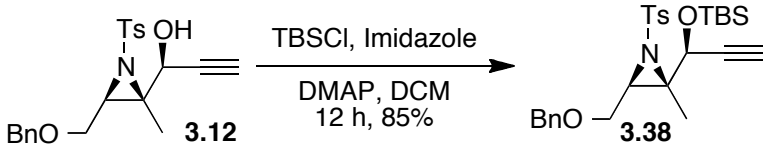


**Preparation of TBS ether 3.38**. Aziridine alcohol **3.12** (1.83 g, 4.75 mmol) was placed in anhydrous DCM (24 mL). To this imidazole (0.31 g, 4.75 mmol), TBDMSCl (0.9 g, 5.7 mmol) and DMAP (61 mg, 0.5 mmol) were added. The reaction was stirred at room temperature overnight and upon completion was quenched with sat. $NaHCO_3$ (5 mL). The aqueous layer was extracted with DCM (3 x 20 mL) and combined organic layers were washed with brine and dried over anhydrous sodium sulfate. The solvent was removed via rotary evaporation and the crude compound was purified by column chromatography (5:1 Hex:EtOAc) to give TBS ether **3.38** (2.0 g, 86%) as a white solid (m. pt. = 76 – 78 ºC). Spectral data: $^1$H-NMR (300 MHz, $CDCl_3$) $\delta$ 7.82 (d, 2H, $J$ = 8.4 Hz), 7.29 - 7.13 (m, 8H), 5.02 (d, 1H, $J$ = 2.18 Hz), 4.40 (d, 2H, $J$ = 11.9 Hz), 4.33 (d, 1H, $J$ = 11.9 Hz), 3.58 (dd, 1H, $J$ = 11.1, 5.2 Hz), 3.41 (dd, 1H, $J$ = 11.2, 6.5 Hz), 3.07 (dd, 1H, $J$ = 6.4, 5.3 Hz), 2.44 (d, 1H, $J$ = 2.2 Hz), 2.36 (s, 3H), 0.92 (s, 12H), 0.18 (d, 6H, $J$ = 3.3 Hz); $^{13}$C-NMR (125 MHz, $CDCl_3$) $\delta$ 143.7, 137.7, 129.2, 128.2, 127.5, 127.4, 127.3, 82.7, 73.9, 72.6, 66.5, 64.3, 58.2, 47.0, 25.7, 21.4, 18.0, 12.7, -4.6, -4.9; IR (neat) 3277, 2931, 2857, 1599, 1330, 1255, 1160, 1098, 1073, 931; HRMS (ESI) (m/z):

$[M+H]^+$ calculated for $[C_{27}H_{38}SO_4SSi]^+$ 500.2291, found 500.2298.

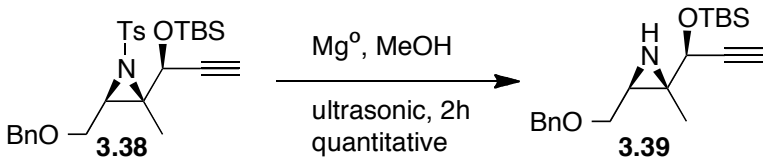


**Preparation of unprotected aziridinol 3.39**. To a solution of *N*-Ts aziridinol **3.38** (1.26 g, 2.52 mmol) in methanol (10 mL) was added powdered magnesium metal (0.4 g, 15.12 mmol). The solution was subjected to ultrasonication for 2 h. Upon completion sat. $NH_4Cl$ (15 mL) was added. The aqueous layer was extracted with EtOAc (3 x 10 mL), the combined organic layers were washed with brine and dried over sodium sulfate. The solvent was removed via rotary evaporation to afford the detosylated compound **3.39** in quantitative yield (61.4 mg) as a white solid (m. pt. = 68 – 70 ºC). Spectral data: $^1$H-NMR (300 MHz, $CDCl_3$) $\delta$ 7.34 - 7.27 (m, 5H), 4.59 (d, 1H, *J* = 12.07 Hz), 4.53 (d, 1H, *J* = 12.07 Hz), 4.38 (m, 1H), 3.59 (dd, 1H, *J* = 10.7, 6.3 Hz), 3.53 (dd, 1H, *J* = 10.7, 6.3 Hz), 2.42 (d, 1H, *J* = 2.1 Hz), 2.38 (t, 1H, *J* = 6.15 Hz), 1.23 (s, 3H), 0.92 (s, 9H), 0.15 (d, 6H, *J* = 16.5 Hz); $^{13}$C NMR (125 MHz, $CDCl_3$) $\delta$ 138.1, 128.2, 127.6, 127.5, 82.1, 73.6, 72.8, 69.6, 66.0, 40.9, 36.0, 25.6, 18.0, 15.0, -4.7, -5.3; IR (neat) 3291, 2954, 2930, 2857, 1599, 1253, 837, 779; HRMS (ESI) (m/z): $[M+H]^+$ calculated for $[C_{20}H_{31}NO2Si]^+$ 341.2124, found 341.2119.

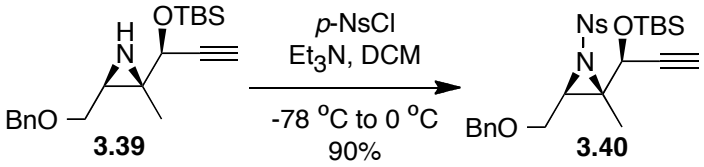


**Preparation of *N*-Ns protected aziridinol 3.40**. *p*-NsCl (47 mg, 0.2 mmol) was added to the solution of aziridine **3.39** (59 mg, 0.17 mmol) and $Et_3N$ (34.4 mg, 0.34 mmol) in anhydrous DCM (0.5 mL) maintained at -78 ºC. After 5 min the reaction was gradually warmed to 0 ºC over 20 min. After completion the reaction was diluted with DCM (2 mL). Organic phase was washed with 1M HCl (2 mL), sat. $NaHCO_3$ (2 mL) and dried over anhydrous magnesium sulfate. The crude was purified by column chromatography (6:1 Hex: EtOAc) to afford N-*Ns* protected aziridinol **3.40** (82 mg, 90%) as a colorless oil. Spectral data: $^1$H-NMR (300 MHz, $CDCl_3$) $\delta$ 8.12 (d, 2H, $J$ = 9 Hz), 8.08 (d, 2H, $J$ = 9Hz), 7.29 (m, 3H), 7.11 (m, 2H), 4.91 (s, 1H), 4.41 (d, 1H, $J$ = 11.6 Hz), 4.30 (d, 1H, $J$ = 11.6 Hz), 3.70 (dd, 1H, $J$ = 10.9, 4.3 Hz), 3.4 (dd, 1H, $J$ = 10.8, 8.1 Hz), 3.18 (dd, 1H, $J$ = 7.8, 4.2 Hz), 2.48 (d, 1H, $J$ = 2.19 Hz), 1.53 (s, 3H), 0.93 (s, 12H), 0.19 (d, 6H, $J$ = 8.4 Hz); $^{13}$C NMR (125 MHz, $CDCl_3$) $\delta$ 150.1, 145.9, 137.3, 128.8, 128.4, 128.0, 127.6, 123.8, 82.3, 74.3, 73.2, 66.8, 64.8, 59.2, 48.4, 25.7, 18.1, 12.9, -4.5; IR (neat) 3287, 3105, 2936, 1606, 1452, 1312, 1167, 1093, 1024, 738; HRMS (ESI) (m/z): $[M+H]^+$ calculated for $[C_{26}H_{35}N_2O_6SSi]^+$ 531.1985, found 531.1990.

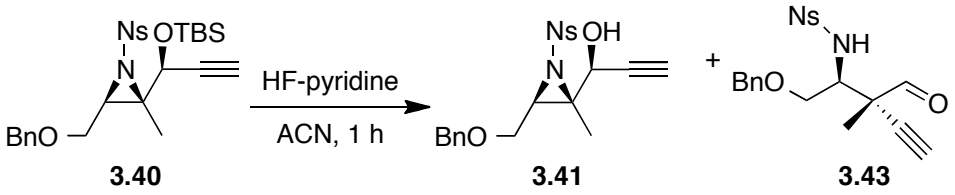


**3.40** **3.41** **3.43**

**Desilylation using HF-pyridine reagent.**[41] To a solution of TBS ether **3.40** (100 mg, 0.19 mmol) in anhydrous ACN (1.3 mL) at room temperature was added HF-pyridine (70% HF) (65 μL, 2.47 mmol) under nitrogen atmosphere. After stirring for 1 h, sat $NaHCO_3$ (13 mL) was added drop wise to the above flask. The solution was extracted with DCM (3 X 15 mL). The organic layers were dried over anhydrous sodium sulfate and evaporated under reduced pressure. Silica gel chromatography (4:1 Hex:EtOAc) afforded a 45:55 mixture of desilylated alcohol **3.41** (22.5 mg, 34%) and aldehyde **3.43** (35.2 mg, 45%) respectively as an oil. Spectral data: desilylated alcohol **3.41**: $^1$H-NMR (300 MHz, $CDCl_3$) δ 8.15 (d, 2H, *J* = 9.3 Hz), 8.08 (d, 2H, *J* = 9Hz), 7.32 (m, 3H), 7.19 (m, 2H), 4.82 (m, 1H), 4.49 (d, 1H, *J* = 11.4 Hz), 4.38 (d, 1H, *J* = 11.4 Hz), 3.74 (dd, 1H, *J* = 10.1, 3.7 Hz), 3.44 (dd, 1H, *J* = 8.5, 3.9 Hz), 3.36 (m, 2H), 2.55 (d, 1H, *J* = 2.36 Hz), 1.54 (s, 3H); $^{13}$C NMR (125 MHz, $CDCl_3$) δ 150.3, 145.2, 137.2, 128.6, 128.5, 128.1, 127.7, 124.0, 75.0, 73.4, 66.9, 65.3, 59.4, 49.7, 25.7, 13.1; IR (neat) 3287, 2926, 2857, 1607, 1591, 1514, 1299, 1248, 1112, 751; HRMS (ESI) (m/z): $[M+H]^+$ calculated for $[C_{20}H_{21}N_2O_6S]^+$ 417.1120, found 417.1125; Spectral data: aldehyde **3.43**: $^1$H-NMR (300 MHz, $CDCl_3$) δ 9.44 (s, 1H), 8.13 (d, 2H, *J* = 9.1 Hz), 7.95 (d, 2H, *J* = 9.1 Hz), 7.26 (m, 3H), 7.07 (m, 1H), 5.05 (d, 1H, *J* = 9.9 Hz), 4.26 (d, 1H, *J* = 11.5 Hz), 4.21 (d, 1H, *J* =

11.5 Hz), 3.90 (dt, 1H, *J* = 10.1, 6.1 Hz), 3.39 (dd, 1H, *J* = 6.5, 3.8 Hz), 2.41 (s, 1H), 1.36 (s, 3H).

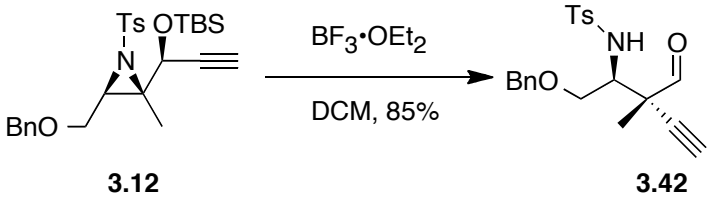


**3.12** **3.42**

**Preparation of aldehyde 3.42 by semi-Pinacol rearrangement**. To the TBS aziridinol **3.12** (92 mg, 0.18 mmol) in anhydrous DCM (5 mL) under nitrogen atmosphere was added $BF_3$•$OEt_2$ (0.21 mL, 1.7 mmol) drop wise. The solution was stirred at room temperature for 2 h. After completion the reaction was poured into 6% $NaHCO_3$ (6 mL) and ice. Organic phase was separated and extracted with DCM (3 X 15 mL). The organics were washed with 6% $NaHCO_3$ (30 mL), water (30 L) and brine (5 mL). Drying over anhydrous sodium sulfate, rotary evaporation followed by purification via silica gel chromatography (3:1 Hex:EtOAc) yielded aldehyde **3.42** (60.4 mg, 85 %) as a colorless oil. Spectral data: $^1$H-NMR (500 MHz, $CDCl_3$) $\delta$ 9.38 (s, 1H), 7.71 (d, 2H, *J* = 8.3 Hz), 7.24 - 7.14 (m, 8H), 4.90 (d, 1H, J = 9.9 Hz), 4.27 (s, 2H), 3.79 (dd, 1H, *J* = 8.2, 4.3 Hz), 3.77 (dd, 1H, *J* = 8.2, 4.2 Hz), 3.40 (dd, 1H, *J* = 9.8, 4.2 Hz), 3.35 (dd, 1H, J = 9.8, 8.2 Hz), 2.39 (s, 3H), 2.37 (s, 1H), 1.25 (s, 3H); $^{13}$C NMR (125 MHz, $CDCl_3$) $\delta$ 195.4, 143.7, 137.5, 136.9, 129.7, 128.3, 127.7, 127.0, 80.6, 75.9, 73.2, 69.3, 56.7, 51.0, 21.5, 19.8; IR (neat) 3275, 2954, 2924, 2855, 1728, 1453, 1334, 1091, 666; HRMS (ESI) (m/z): $[M+H]^+$ calculated for $[C_{21}H_{24}SO_4N]^+$ 386.1426, found 386.1432.

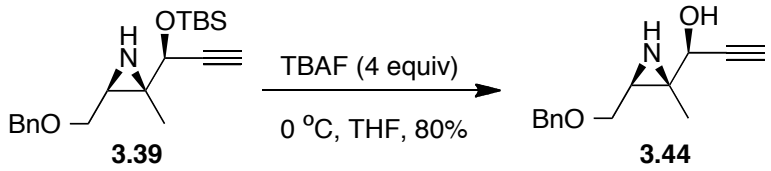


**Preparation of desilylated alcohol 3.44**. To a solution of *N*-Ts aziridinol **3.39** (85 mg, 0.17 mmol) in anhydrous methanol (1 mL) was added magnesium powder (20.4 mg, 0.85 mmol) (finely crushed using mortar and pestle). The solution was subjected to ultra sonication for 1 h. Upon completion the reaction was quenched by addition of sat. $NH_4Cl$ (1 mL). The solution was extracted with EtOAc (3 X 10 mL) to give a crude compound **3.44** (50 mg, 98%), which was taken to next step without any purification. Spectral data: $^1$H-NMR (300 MHz, $CDCl_3$) $\delta$ 7.36 (m, 5H), 4.60 (d, 1H, *J* = 12 Hz), 4.53 (d, 1H, *J* = 11.9 Hz), 3.60 (m, 1H), 3.53 (s, 2H), 2.37 (t, 1H, *J* = 6.2 Hz), 1.20 (s, 3H); $^{13}$C NMR (125 MHz, $CDCl_3$) $\delta$ 137.7, 128.2, 127.6, 127.5, 126.0, 74.1, 73.1, 68.6, 66.2, 37.1, 14.3; IR (neat, $cm^{-1}$) 3289, 2924, 2862, 1728, 1652, 1601, 1454, 1074; HRMS (ESI) (m/z): $[M + H]^+$ calculated for $[C_{12}H_{18}NO_2]^+$ 208.1338, found 208.1334.

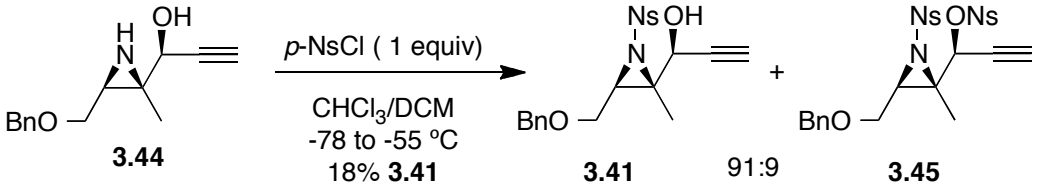


**Preparation of *N*-Ns protected aziridinol 3.41** $Et_3N$ (50 μL, 0.36 mmol) was added drop wise to a stirred suspension of aziridinol **3.44** (41.9 mg, 0.18 mmol) and *p*-NsCl (40 mg, 0.18 mmol) in solution of $CHCl_3$/DCM (0.25 mL each) at -78 °C. The conversion

was found incomplete after 2 h, temperature was warmed to -55 ºC. The solution was diluted with DCM (10 mL), washed with 1M HCl (1 mL) and sat. $NaHCO_3$ (1 mL). The organic layers were dried over anhydrous sodium sulfate and subjected to rotary evaporation. The crude compound was purified using column chromatography (4:1 Hex:EtOAc) to give a mixture of *N*-Ns and bis protected compounds **3.41** (12.4 mg, 18%) and **3.45** with a ratio of 91/9 (by crude NMR) as an oil. Spectral data: **3.41**: $^1$H-NMR (300 MHz, $CDCl_3$) δ 8.15 (d, 2H, *J* = 9.3 Hz), 8.08 (d, 2H, *J* = 9Hz), 7.32 (m, 3H), 7.19 (m, 2H), 4.82 (m, 1H), 4.49 (d, 1H, *J* = 11.4 Hz), 4.38 (d, 1H, *J* = 11.4 Hz), 3.74 (dd, 1H, *J* = 10.1, 3.7 Hz), 3.44 (dd, 1H, *J* = 8.5, 3.9 Hz), 3.36 (m, 2H), 2.55 (d, 1H, *J* = 2.36 Hz), 1.54 (s, 3H); $^{13}$C NMR (125 MHz, $CDCl_3$) δ 150.3, 145.2, 137.2, 128.6, 128.5, 128.1, 127.7, 124.0, 75.0, 73.4, 66.9, 65.3, 59.4, 49.7, 25.7, 13.1; IR (neat) 3287, 2926, 2857, 1607, 1591, 1514, 1299, 1248, 1112, 751; HRMS (ESI) (m/z): $[M+H]^+$ calculated for $[C_{20}H_{21}N_2O_6S]^+$ 417.1120, found 417.1125

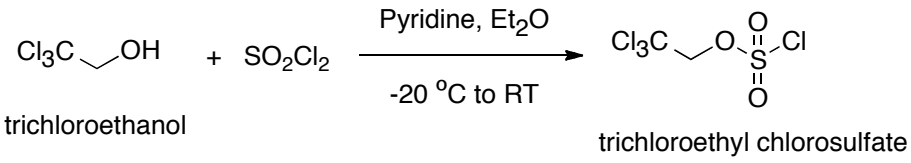

trichloroethanol

trichloroethyl chlorosulfate

**Praparation of trichloroethyl chlorosulfate**. $SO_2Cl_2$ (5 mL, 62 mmol) was added drop wise to a stirred solution of trichloroethanol (6 mL, 62 mmol) and pyridine (15 mL, 62 mmol) in anhydrous $Et_2O$ (120 mL) at -20 ºC. Once the addition was complete the mixture was warmed to room temperature and stirring was continued for 1 h. The

mixture was warmed to room temperature and carefully quenched with water (20 mL), layers were separated, and organic layers were dried and evaporated. Crude product was distilled to afford trichloroethyl chlorosulfate (5.11 g, 90%) as an oil (b. pt. 38 ºC/0.04 mbar). Spectroscopic data matches with the reported compound.[39] Spectral data: $^1$H-NMR (300 MHz, $CDCl_3$) δ 4.89 (s, 2H).

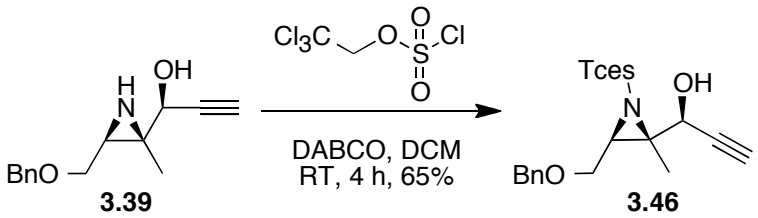


**3.39** **3.46**

A solution of 2,2,2-trichloroethylethylsulfate (112 mg, 0.45 mmol) in anhydrous DCM (1.2 mL) was added in a portion to a stirred solution of aziridinol **3.39** (70 mg, 0.3 mmol) and DABCO (50.5 mg, 0.45 mmol) in anhydrous DCM (30 mL) at room temperature. Extra amount of 2,2,2-trichloroethylethylsulfate (47 mg) was added in order to push the reaction to completion. After completion of the reaction, sat. $NH_4Cl$ (5 mL) was added. The solution was washed with brine and dried over anhydrous sodium sulfate. Rotary evaporation followed by purification by column chromatography (3:1 Hex:EtOAc to 1:1 Hex:EtOAc) afforded *N*-Tces protected aziridinol compound **3.46** (83.3 mg, 65%) as an oil (inseparable with some TCesCl reagent). $^1$H-NMR (300 MHz, $CDCl_3$) δ 7.32 (m, 5H), 5.56 (d, 1H, *J* = 2.3 Hz), 4.77 (d, 1H, *J* = 10.8 Hz), 4.70 (d, 1H, *J* = 10.9 Hz), 4.57 (d, 2H, *J* = 4.3 Hz), 3.68 (dd, 1H, *J* = 7.4, 6.5 Hz), 3.22 (dd, 1H, *J* = 6.6, 5.3 Hz), 2.55 (dd, 1H, *J* = 2.3, 0.5 Hz), 2.12 (s, 3H), 1.60 (s, 3H); $^{13}$CNMR (125 MHz, $CDCl_3$) δ 136.5,

128.7, 128.4, 128.1, 121.0.

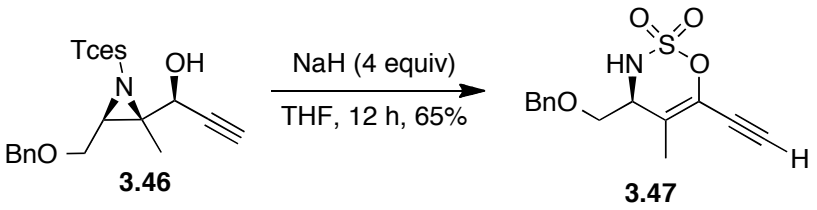


**3.46** **3.47**

**Praparation of sulfamate 3.47**. NaH (24 mg, 0.6 mmol) was suspended in anhydrous freshly distilled THF (0.6 mL). Aziridinol **3.46** (65 mg, 0.15 mmol) dissolved in small amount of anhydrous THF (~ 0.2 mL) was added drop wise to the above stirred suspension. The reaction was stirred at room temperature over night. After completion the reaction was quenched with sat. $NH_4Cl$ (2 mL). The aqueous phase was extracted with EtOAc (3 X 10 mL). The combined organic layers were washed with brine (5 mL) and dried over anhydrous sodium sulfate. After rotary evaporation and upon purification with silica gel chromatography (3:1 Hex:EtOAc) undesired compound **3.47** (42 mg, 65%) was obtained as a an oil. Spectral data: $^1$H-NMR (500 MHz, $CDCl_3$) $\delta$ 7.40 - 7.26 (m, 5H), 4.90 (d, 1H, *J* = 9.5 Hz), 4.58 (d, 1H, *J* = 12), 4.48 (d, 1H, *J* = 12.1 Hz), 4.14 (bm, 1H), 4.07 (m, 1H), 3.80 (dd, 1H, *J* = 10, 3 Hz), 3.59 (dd, 1H, J = 10, 3 Hz), 3.31 (s, 1H), 1.80 (s, 3H); $^{13}$C-NMR (125 MHz, $CDCl_3$) $\delta$ 136.5, 132.3, 128.7, 128.4, 128.1, 121.0, 83.0, 77.2, 76.7, 74.6, 73.6, 66.6, 58.9, 58.8, 15.2; IR (neat) 3283 (s), 2922 (m), 1653 (m), 1419 (s), 1201 (s), 1150 (w), 1070 (s); HRMS (ESI) (m/z): $[M+H]^+$ calculated for $[C_{14}H_{15}NO_4SNa]^+$ 316.0619, found 316.0625.

**Experimental procedures for the de-tosylation reactions:**

**Magnesium, methanol mediated de-tosylation.**[42] To enamine **3.13** (36.7 mg, 0.09 mmol), dissolved in methanol (1 mL) was added powdered magnesium metal (14 mg, 0.57 mmol) in a vial. The vial was sonicated for 3 h in an ultra sonic bath. No conversion was detected on TLC, later the solution was stirred at room temperature for 2 days. Only starting material was recovered.

**$SmI_2$ mediated de-tosylation.**[43] To a solution of enamine **3.13** (49 mg, 0.13 mmol) in anhydrous THF (3 mL) was added commercially available 0.1 M solution of $SmI_2$ in THF (4 mL, 0.39 mmol). The blue reaction mixture was stirred at ambient temperature for 10 minutes and was then quenched with sat. $NaHCO_3$ solution (2 mL), extracted with EtOAc (3 X 10 mL). Several spots were detected on TLC. Desired product was not obtained.

**Sodium napthalenide mediated de-tosylation.** Method I.[44] A flame dried 3N flask was equipped with a glass stir bar, 2 rubber septa, and cold finger under nitrogen. The condenser and the round bottom flask were cooled to -78 ºC and ammonia gas was condensed into 3N flask. To this solution was added at -78 ºC, Na metal (0.22 g, 9.6 mmol), washed with HPLC grade hexane three times. The resulting deep blue solution was stirred at -78 ºC for 5 min and then the solution of enamine **3.13** (0.12 g, 0.31 mmol) in anhydrous THF (62 mL) was added drop wise. The reaction was stirred at -78 ºC for 15 min, quenched with the slow addition of methanol (42 mL) drop wise until

reaction became clear, followed by addition of sat. $NH_4Cl$ (50 mL). The resulting mixture was warmed to room temperature overnight open to atmosphere. Aqueous solution was extracted with DCM (3 X 50 mL). Organic layer was washed with brine and dried over anhydrous $MgSO_4$. Several spots were seen on the TLC, which were then separated by column chromatography. Desired product was not obtained.

Method II.[45] To a flame dried flask containing naphthalene (79.4 mg, 0.62 mmol) under nitrogen was added sodium (12.5 mg, 0.54 mmol, washed three times with HPLC grade hexane) and anhydrous DME (0.5 mL). The mixture was stirred at room temperature for 2 h to give a green black solution. To a flame dried flask containing lactam **3.30** equipped with an additional funnel was added anhydrous THF (0.3 mL). The stirred solution was cooled to -78 ºC, and the solution of sodium naphthalenide was cannulated into an additional funnel. The sodium naphthalenide solution was titrated into the solution of *N*-Ts lactam **3.30** to give a deep green black solution. At this point TLC indicated several spots. Sat. $NH_4Cl$ solution (0.05 mL) was added carefully and the stirred mixture was allowed to warm to room temperature. Aqueous pH 7.0 phosphate buffer (0.2 M, 0.01 mL) was added followed by the dilution with DCM (0.01 mL). The layers were separated and the aqueous phase was extracted with DCM (3 X 5 mL). Combined organic layers were washed with brine, dried over anhydrous sodium sulfate. Desired product was not obtained.

# REFERENCES

## REFERENCES


1. Fukumoto, Y. *J. Syn. Org. Chem. Japan* **2009**, *67*, 735-750.
2. MuÃàller, T. E.; Hultzsch, K. C.; Yus, M.; Foubelo, F.; Tada, M. *Chem. Rev.* **2008**, *108*, 3795-3892.
3. Hartwig, J. F. *Nature* **2008**, *455*, 314-322.
4. Gagne, M. R.; Stern, C. L.; Marks, T. J. *J. Am. Chem. Soc.* **1992**, *114*, 275-294.
5. Walsh, P. J.; Baranger, A. M.; Bergman, R. G. *J. Am. Chem. Soc.* **1992**, *114*, 1708-1719.
6. Fujita, H.; Tokuda, M.; Nitta, M.; Suginome, H. *Tetrahedron Lett.* **1992**, *33*, 6359-6362.
7. Tzalis, D.; Koradin, C.; Knochel, P. *Tetrahedron Lett.* **1999**, *40*, 6193-6195.
8. Quinet, C.; Sampoux, L.; Markó, I. E. *Eur. J. Org. Chem.* **2009**, *2009*, 1806-1811.
9. Ibuka, T. *Chem. Soc. Rev.* **1998**, *27*, 145-154.
10. Ibuka, T.; Nakai, K.; Habashita, H.; Hotta, Y.; Otaka, A.; Tamamura, H.; Fujii, N.; Mimura, N.; Miwa, Y.; Chounan, Y.; Yamamoto, Y. *J. Org. Chem.* **1995**, *60*, 2044-2058.
11. Schomaker, J. M.; Geiser, A. R.; Huang, R.; Borhan, B. *J. Am. Chem. Soc.* **2007**, *129*, 3794-3795.
12. Schomaker, J., Michigan State University, 2006.
13. Hart, S., Michigan State University, 2009.
14. Oshima, M. Y., H.; Shimizu, I.; Nisar, M.; Tsuji, J. *J. Am. Chem. Soc.* **1989**, *111*, 6280-6287.
15. Takemura, A. F., K.; Shimawaki, K.; Murai, A.; Kawai, H.; Suzuki, T. *Tetrahedron* **2005**, *61*, 7392-7419.
16. Rahn, N.; Kalesse, M. *Angew. Chem. Int. Ed.* **2008**, *47*, 597-599.
17. Miller, N. A.; Willis, A. C.; Paddon-Row, M. N.; Sherburn, M. S. *Angew. Chem. Int. Ed.* **2007**, *46*, 937-940.
18. Roush, W. R.; Brown, B. B. *J. Am. Chem. Soc.* **1993**, *115*, 2268-2278.

19. Wakioka, M.; Nagao, M.; Ozawa, F. *Organometallics* **2008**, *27*, 602-608.

20. Martinelli, J. R.; Watson, D. A.; Freckmann, D. M. M.; Barder, T. E.; Buchwald, S. L. *J. Org. Chem.* **2008**, *73*, 7102-7107.

21. Kaganovsky, L.; Gelman, D.; Rueck-Braun, K. *J. Organomet. Chem.*, *695*, 260-266.

22. Eames, J.; J. Mitchell, H.; Nelson, A.; O'Brien, P.; Warren, S.; Wyatt, P. *J. Chem. Soc., Perkin Trans. 1* **1999**, 1095-1104.

23. Schroeder, M. *Chem. Rev.* **1980**, *80*, 187-213.

24. Macdonald, S. J. F.; Inglis, G. G. A.; Bentley, D.; Dowle, M. D. *Tetrahedron Lett.* **2002**, *43*, 5057-5060.

25. Cowans, B. A.; Haltiwanger, R. C.; DuBois, M. R. *Organometallics* **1987**, *6*, 995-1004.

26. Casalnuovo, J. A.; Scott, R. W.; Harwood, E. A.; Schore, N. E. *Tetrahedron Lett.* **1994**, *35*, 1153-1156.

27. Blair, M.; Andrews, P. C.; Fraser, B. H.; Forsyth, C. M.; Junk, P. C.; Massi, M.; Tuck, K. L. *Synthesis* **2007**, *2007*, 1523,1527.

28. Jin, Q.; Williams, D. C.; Hezari, M.; Croteau, R.; Coates, R. M. *J. Org. Chem.* **2005**, *70*, 4667-4675.

29. Lupattelli, P. B., C.; Caruso, L.; Gambacorta, A. *J. Org. Chem.* **2003**, *68*, 3360-3362.

30. Bonini, C. R., G. *Synthesis* **1994**, *1994*, 225-238.

31. von Zezschwitz, P. *Synthesis* **2008**, *2008*, 1809-1831.

32. Uemura, M.; Iwasaki, M.; Morita, E.; Yorimitsu, H.; Oshima, K. *Bull. Chem. Soc. Jpn.* **2007**, *80*, 2400-2405.

33. Sasaki, M.; Tanino, K.; Miyashita, M. *Org. Lett.* **2001**, *3*, 1765-1767.

34. Cardullo, F.; Donati, D.; Merlo, G.; Paio, A.; Salaris, M.; Taddei, M. *Synlett* **2005**, *2005*, 2996,2998.

35. Snape, T. J. *Chem. Soc. Rev.* **2007**, *36*, 1823-1842.

36. Kruger, G. J.; Steyn, P. S.; Vleggaar, R.; Rabie, C. J. *J. Chem. Soc., Chem. Commun.* **1979**, 441-442.

37. Eom, K. D.; Raman, J. V.; Kim, H.; Cha, J. K. *J. Am. Chem. Soc.* **2003**, *125*, 5415-5421.

38. Wang, B. M. S., Z. L.; Fan, C. A.; Tu, Y. Q.; Shi, Y. *Org. Lett.* **2002**, *4*, 363-366.

39. Liu, Y.; Lien, I. F. F.; Ruttgaizer, S.; Dove, P.; Taylor, S. D. *Org. Lett.* **2003**, *6*, 209-212.

40. F√ºrstner, A.; Domostoj, M. M.; Scheiper, B. *J. Am. Chem. Soc.* **2005**, *127*, 11620-11621.

41. Vedejs, E.; Naidu, B. N.; Klapars, A.; Warner, D. L.; Li, V.-s.; Na, Y.; Kohn, H. *J. Am. Chem. Soc.* **2003**, *125*, 15796-15806.

42. Motamed, M.; Bunnelle, E. M.; Singaram, S. W.; Sarpong, R. *Org. Lett.* **2007**, *9*, 2167-2170.

43. Wang, S.; Dilley, A. S.; Poullennec, K. G.; Romo, D. *Tetrahedron* **2006**, *62*, 7155-7161.

44. Nilsson, B. L.; Overman, L. E.; Read de Alaniz, J.; Rohde, J. M. *J. Am. Chem. Soc.* **2008**, *130*, 11297-11299.

45. Abbotto, A.; Bradamante, S.; Pagani, G. A. *J. Org. Chem.* **1993**, *58*, 444-448.

# Chapter 4

## Progress Towards The Total Synthesis Of Salinosporamide A Via Tandem Aza-Payne/Hydroamination Methodology

### 4.1 Introduction:

Salinosporamide A **4.1** was isolated from the culture extracts of novel microbial source, *salinispora* strains, a marine actinomycete *S tropica* which was discovered in 2003 by Fenical and co-workers.[1] This compound belongs to a class of newly described genus *Salinispora*.[2]

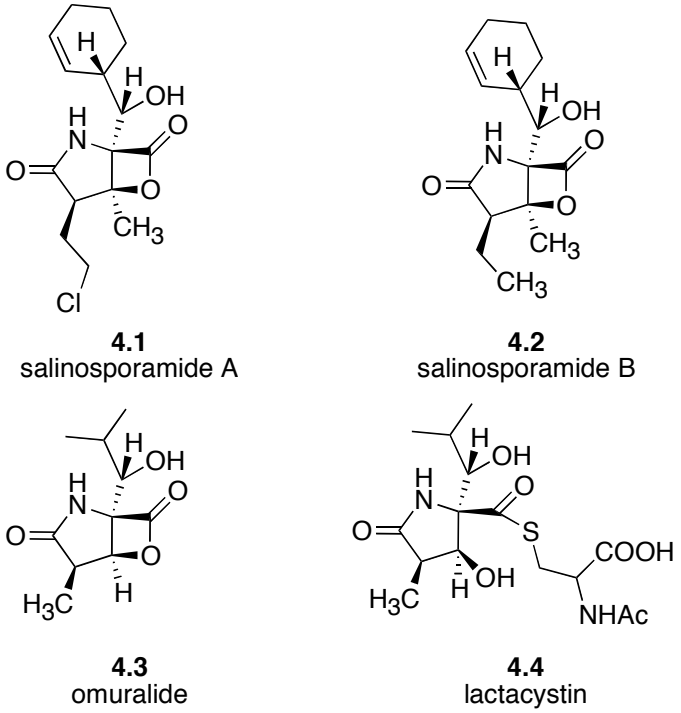


**Figure 4.1** Salinosporamide A and structurally related proteasome inhibitors.

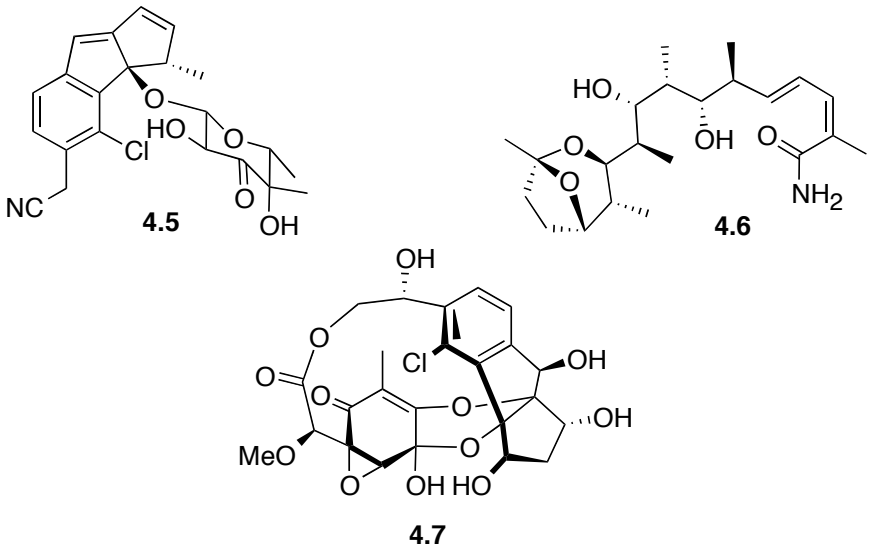


**Figure 4.2** Novel natural products isolated from marine actinomycetes of the genus *Salinispora*: cyanosporamide A **4.5**, saliniketal **4.6** and sporolide A **4.7**.

Further investigation of this newly discovered class of marine bacteria has led to the discovery of various new secondary metabolites such as cyanosporaside A **4.5** from *S. pacifica*,[3] saliniketal A **4.6** from *S. aerenicola* ,[4] sporolide A **4.7** from *S. tropica* (Figure 4.2).[5] Salinosporamide A **4.1** is structurally related to β-lactone pyrrolidinone-based terrestrial natural products omuralide **4.3** and lactacystin **4.4** (Figure 4.1). More recently, the homologues **4.8-4.14** designated cinnabaramide A-G, have been also isolated from the terrestrial streptomycete *S. cinnabarinus.*[6] The compounds that belong to this family are characterized by the presence of densely functionalized γ-lactam cores. Omuralide is known to specifically inhibit the proteolytic activity of the proteasome 20S subunit.

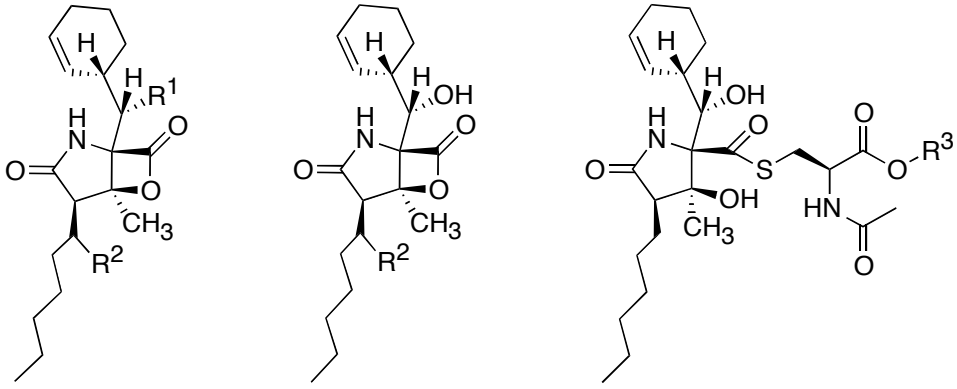


**4.8** $R^1$ = OH, $R^2$ = H
**4.9** $R^1$ = $R^2$ = OH
**4.10** $R^1$ = $R^2$ = H

**4.11** $R^2$ = OH
**4.12** $R^2$ = H

**4.13** $R^3$ = H
**4.14** $R^3$ = $CH_3$

**Figure 4.3** Homologues of salinosporamide and lactacystin.

Salinosporamide A **4.1** is a more effective proteasome inhibitor than Omuralide **4.3** and exhibits cytotoxicity against many tumor cell lines, and particularly, against Velcade ® resistant multiple myeloma cells.

### 4.2 The Proteasome: Target in Cancer Chemotherapy

Proteins constitute the basic building elements of living organisms. They are characterized by a limited lifetime in a cell. This lifetime varies and lasts from several minutes to several days in some cases. Regulatory proteins appear for a definite time and are short-lived as compared to those responsible for basic cell functions. Once their functions are fulfilled or because they have aged these proteins are eliminated by degradation. The degradation of proteins known as proteolysis is carried out by two systems: lysosome and proteasome. The lysosome functions in far simpler and transparent manner.[7] They are membrane bound vesicles and contain hydrolytic

enzymes with the help of which they degrade the products of ingestion, worn out organelles. They are frequently named as “suicidal bags” by cell biologists because of their role in autolysis. On the other hand proteasome involves a large ATP-dependent proteolytic complex which catalyzes the rapid degradation of ubiquitinated proteins.[8] This is involved in the control of many crucial cellular processes, such as cell-cycle, signal transduction, transcription, stress signaling, cell differentiation, and apoptosis. The proteasome breaks down proteins acquired through endocytosis and are targeted for degradation by ligation to ubiquitin, a 76 amino-acid residue protein. The biochemical steps involved are well investigated and are illustrated in Scheme 4.1. The proteasome requires sequential action of three enzymes E1-E3. The cysteine residue of the ubiquitin-activating enzyme E1 binds ubiquitin through a thioester bond, which consumes ATP.[9] The substrate is then transferred to a ubiquitin conjugating enzyme E2, which facilitates transfer of ubiquitin either directly onto a ubiquitin-ligase E3 bound protein substrate or to an active-site cysteine residue on the E3 with subsequent attachment to the protein. Ubiquitin is in most cases conjugated to an $\varepsilon$-$NH_2$ function of a lysine residue of the target protein, or sometimes to its N-terminal group. The polyubiquitinated substrate is then recognized by the down stream 26S proteasome, which is a large multi-subunit complex consisting of one or two 19S caps and a 20S core unit.

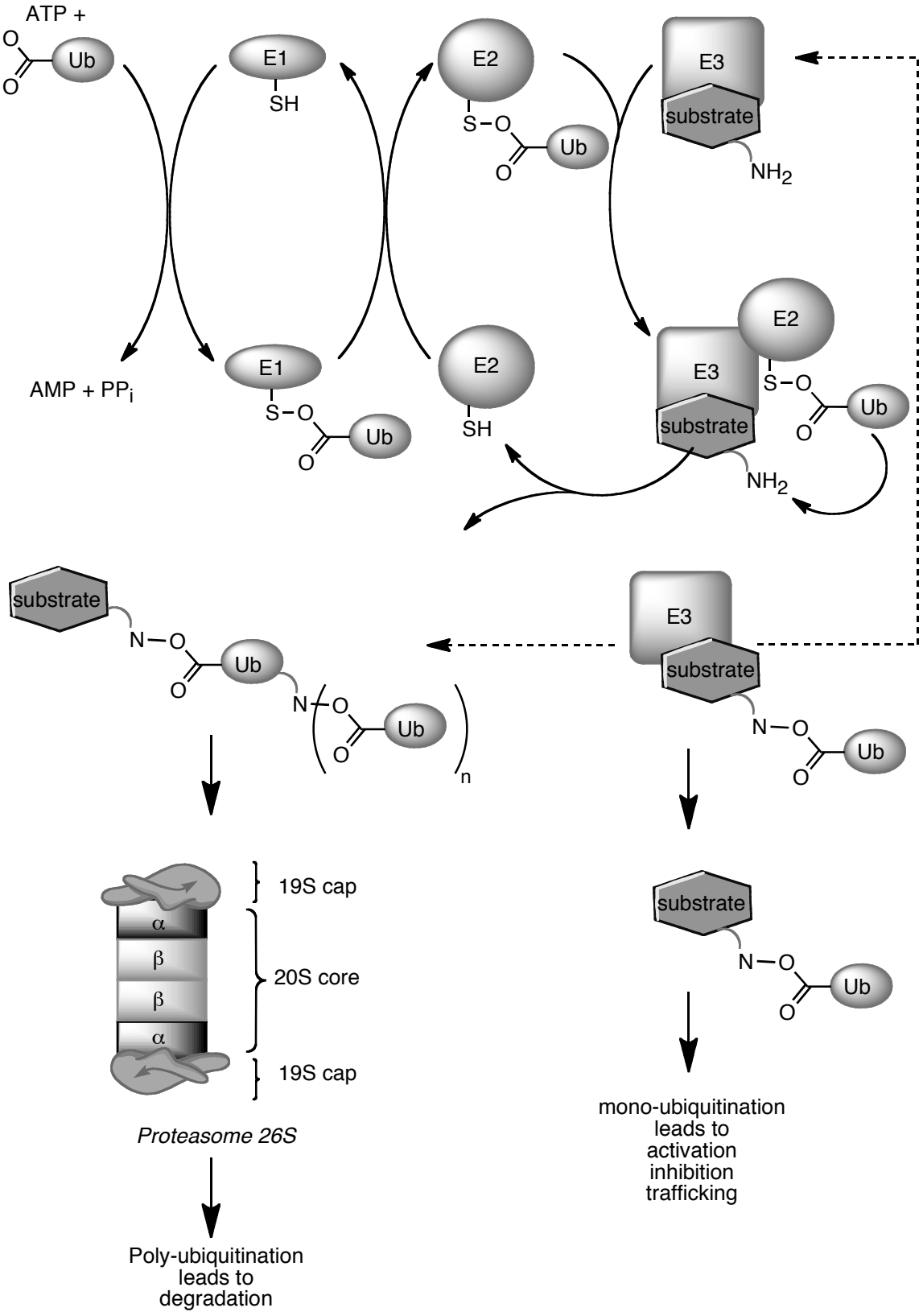


**Scheme 4.1** Mechanism of protein degradation by ubiquitin-proteasome system.

Protein degradation is catalyzed by three β subunits per β7 ring. The proteolytic activities can be categorized as caspase-(β1 CA-L), trypsin-(β2, T-L), and chymotrypsin-like (β5, CT-L), and the selectivity of the subunits is dictated by the composition of their respective binding pockets.[10] There are strong indications that the ubiquitin system is involved in development and apoptosis, although the target proteins involved in these cases have not been identified. Abberations in the ubiquitin-proteasome system are implicated in the pathogenesis of human diseases, such a malignancies and neurodegenerative disorders. Thus the proteasome has recently emerged as a new avenue for the development of mechanism based drugs that can potentially treat those diseases. Proteasome-inhibitors can make effective anticancer drugs because these compounds can cause the accumulation of proteasome substrates, including cyclins and transcription factors, and induce cell-cycle arrest with apoptotic program activation.

### 4.3 Anti cancer activity of salinosporamide A *vs* other lactam based proteasome inhibitors.

Understanding of the molecular mechanism of this catalytic machinery has evolved from detailed studies of the yeast 20S proteasome core particle in complex with salinosporamide A **4.1**, enabled by the availability of the crystal structure, reported by Groll and coworkers in 2006.[11] In the first step of inhibition, Thr1Oγ cleaves the lactone ring of **4.1** thereby forming an inhibitor-proteasome adduct (Scheme 4.2). This resembles the mode of action by covalent attachment of similar inhibitors to the protein as previously proposed for other molecules such as omuralide **5.3**.[10]

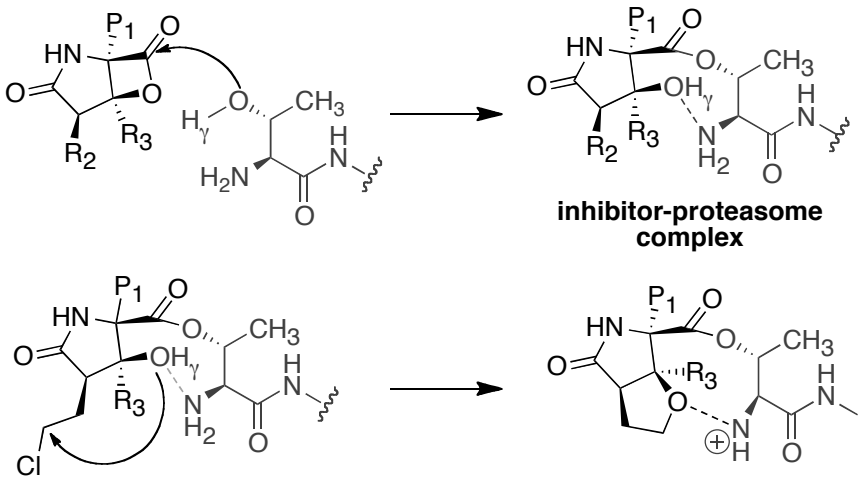


**Scheme 4.2** Proposed mechanism of action in proteolytic sites.

**Table 4.1** Lactam-based inhibitors and their bioactivity.[10]

| compound | inhibition of proteasomal active sites [$K_{ass}$ ($M^{-1}s^{-1}$)] | | | other than proteasome intracellular targets ($IC_{50}$) |
|---|---|---|---|---|
| | chymotrypsin like | trypsin like | caspase like | |
| Lactacystin **4.4** | 194 | 10 | 4.2 | cathepsin A, TPPII |
| β-lactone (omuralide) **4.3** | $IC_{50}$: 57 | 540 | 10000 | cathepsin A, TPPII |
| salinosporamide A **4.1** | $IC_{50}$: 2.6 | 4.1 | 430 | |
| salinosporamide B **4.2** | $IC_{50}$: 27 | 640 | 1200 | |

Table 4.1 summarizes the inhibitory activities of various lactam-based inhibitors. Lactacystin **4.4** was the first non-peptidic inhibitor isolated from *Streptomyces sp*. OM-6519.[12] Later *in-vitro* studies proved that this compound by itself was not active against proteasomes. In aqueous conditions (pH = 8), the reactive compound hydrolyzes into clasto-lactacystin (β-lactone also known as omuralide **4.3**).[13] In case of omuralide **4.3**,

once the β-lactone is cleaved, the released tertiary alcohol displaces the water molecules situated in the active site of the proteasome, thus preventing undesired saponification of the ester of the inhibitor-protein ester linkage. However, presence of unique structural features in salinosporamide A makes it an outstanding drug molecule. Catalyzed by deprotonation of the tertiary hydroxyl group by Thr1, nucleophilic displacement of the side chain chlorine atom by the respective alcoholate leads to intramolecular formation of a THF ring (Scheme 5.2). Generation of this cyclic ether further prevents reformation of the β-lactone and any catalytic cleavage of the inhibitor-proteasome ester linkage.

### 4.4 A glance through previous total syntheses.

Biological properties such as high cytotoxicity against several cell lines make salinosporamide A very attractive natural product and of high interest to synthetic community. The presence of five contiguous stereocenters and a densely functionalized bicyclic framework makes it a challenging target. Not surprisingly, many formal and total, racemic and enantioselective syntheses have been reported till date. This section will concisely describe some of these efforts.

#### 4.4.1 Total synthesis of salinosporamide A by Corey and coworkers.

After its isolation in 2003, the first enantiospecific synthesis was accomplished by Corey's group in 2004.[14] The synthesis was achieved in 17 total steps starting from (*S*)-threonine methyl ester **4.15** A key early step in the synthesis was a Baylis-Hillman

cyclization, which afforded γ-lactam **4.21b** with moderate diastereoselectivity. An alternate route was offered later in 2005, where the Kulinchovik reaction[15] (Scheme 4.4) was used instead to install the lactam **4.21b** in >99:1 diastereoselectivity (Scheme 4.4).[16] Radical mediated cyclization of silylated alcohol **4.22** afforded bicyclic γ lactam **4.23** in good yield and excellent selectivity. Development of a crucial key step that involved the application of cyclohexenyl zinc reagent with an appropriately installed aldehyde intermediate **4.24**, providing complete stereocontrol at C-5 and C-6 positions, was one of the major contributions made by the synthetic report. The stereochemical outcome of this reaction has been explained by invoking a cyclic 6-member chair like transition state that involves the addition of organozinc reagent to the sterically more accessible face of the formyl group. Overall this synthetic route provided access to salinosporamide A with an impressive 16.5% yield starting from **4.15**. The synthesis also stands out because of the minimum use of protecting group manipulative steps. More importantly development of the protocol for installation of the cyclohexenyl moiety and late stage delivery of the chlorine atom, is evidenced by their recurring use in later syntheses.

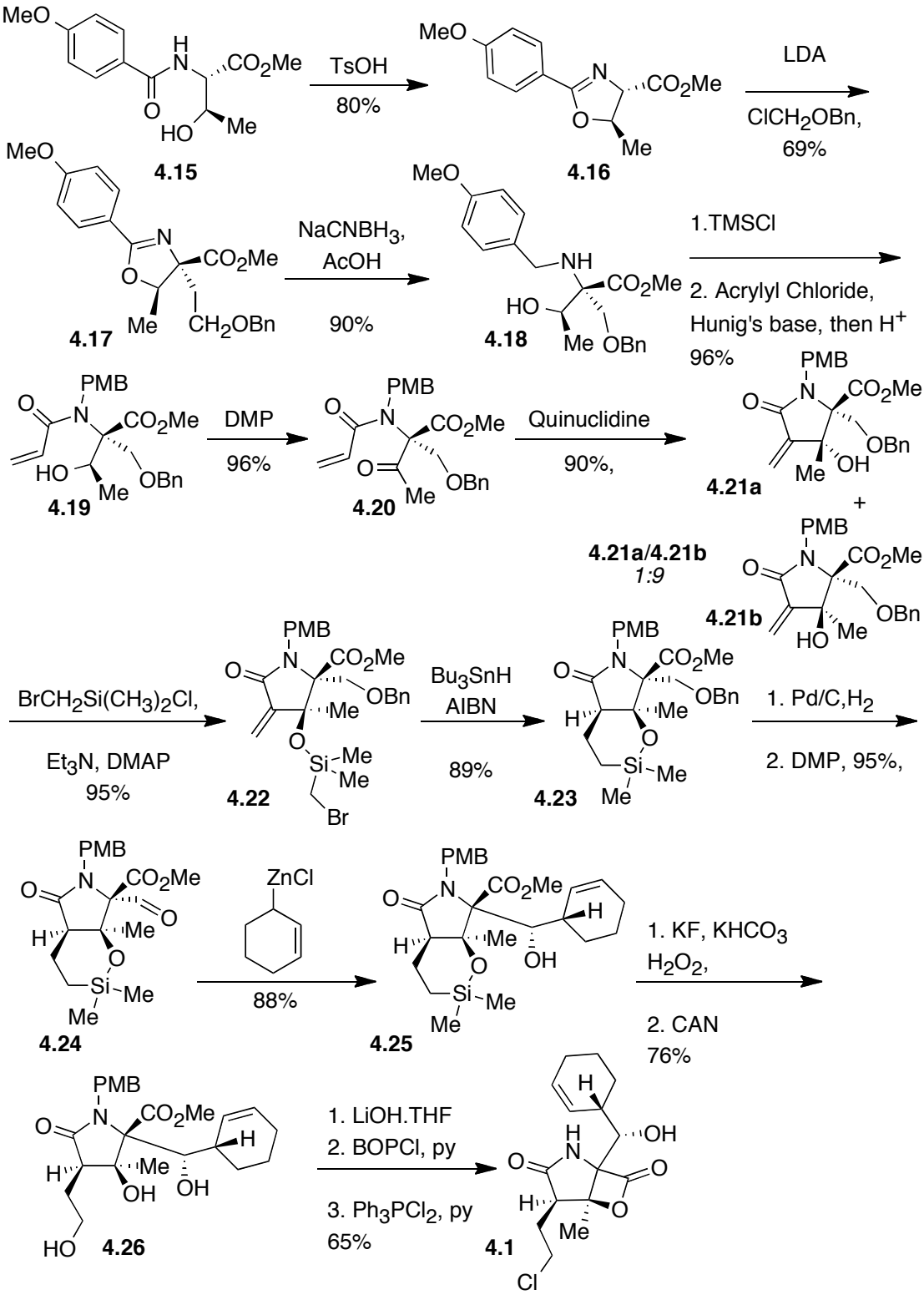


**Scheme 4.3** Total synthesis of salinosporamide by Corey et al.

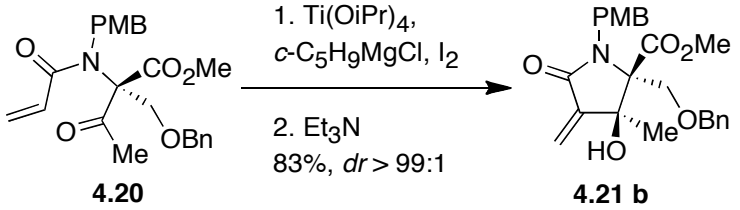


**Scheme 4.4** Kulinchovik reaction: An alternative route to install γ-lactam.

### 4.4.2 Synthesis by Endo and Danishefsky's group.

A second synthesis of salinosporamide was reported by Danishefsky's group in 2005.[17] Stereocenters were appropriately installed by taking advantage of the facial bias of the pyroglutamate derivative **4.27** (Scheme 4.5). Thus, vinyl cuprate addition at C-3 selectively occurred from α-face followed by C-2 alkylation, which proceeded with high diastereoselectivity. Following a few more steps, N-O acetal was then transformed into lactam **4.30**. Oxidation, esterification and treatment with Meerwein salt yielded imidate ester **4.31**. Subjection to base generated an enolate that underwent intramolecular acylation to afford lactone **4.32** with a stereo-defined quaternary C-4 center. Hydrolysis of the imidate, N-protection and hydrogenolytic cleavage of Bn ether furnished alcohol intermediate **4.33**. Subjection to *in-situ* generated phenyl selenide, masking of the released acid as a benzyl ester, oxidation/elimination and DMP oxidation of the alcohol afforded aldehyde intermediate **4.35**. Acetal mediated cationic cyclization upon treatment with phenyl selenyl bromide and $AgBF_4$ allowed lactonization, with complete facial selectivity on the *exo*-olefin to yield bicyclic compound **4.36** along with the generation of C-4 quaternary center. Radical deselenylation, chemoselective reduction of the ester and oxidation then furnished advanced intermediate **4.37**. The synthesis of

salinosporamide was then achieved in 7 additional steps employing the same protocol as developed by Corey's group to install cyclohexenyl group.

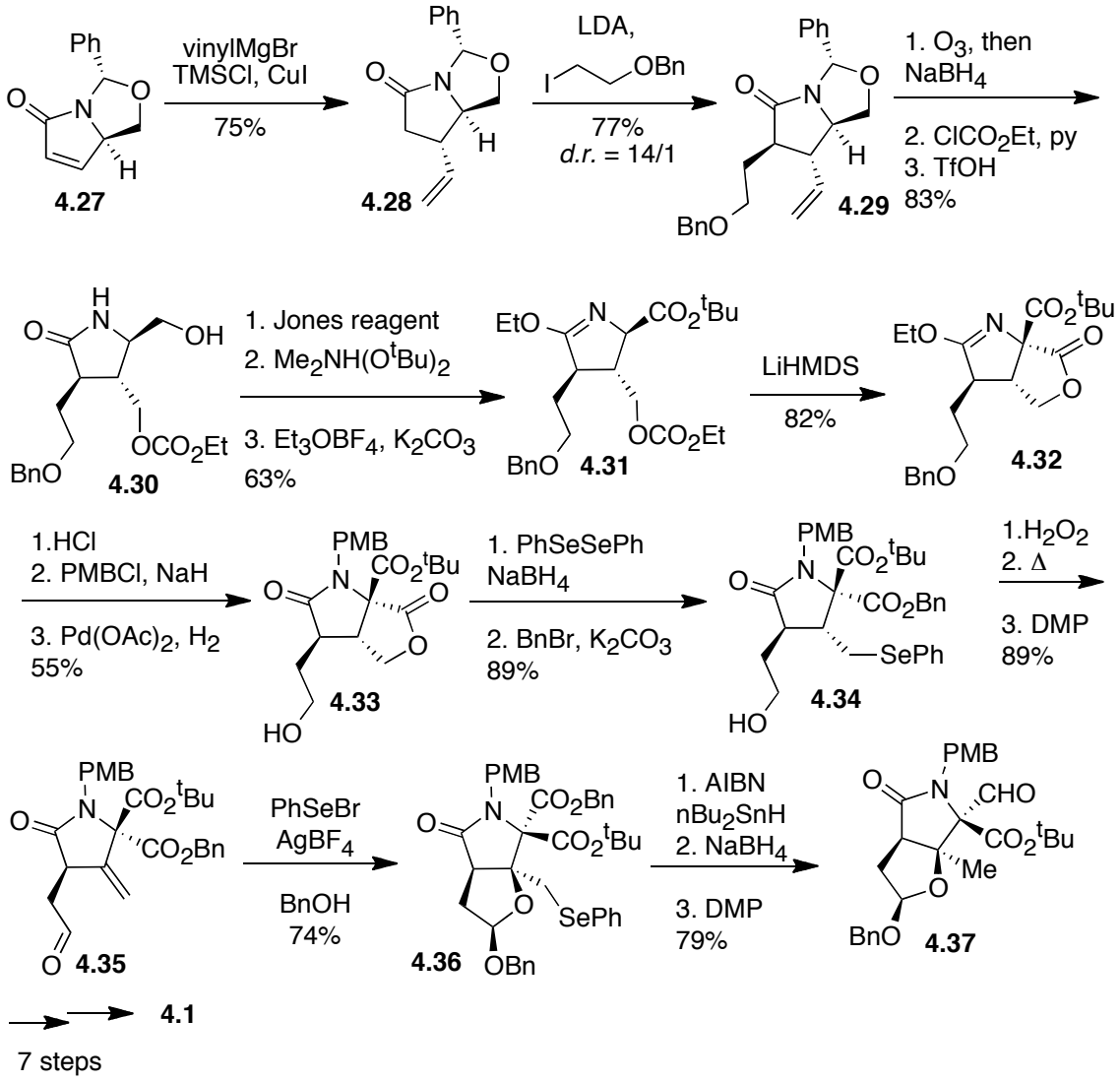


**Scheme 4.5** Synthesis by Endo and Danishefsky.

### 4.4.3 Pattenden's synthesis.

A biosynthetically inspired approach was first presented by Pattenden and coworkers in 2006 (Scheme 4.6).[18] The starting material is the α-substituted β-keto ester **4.38** and is structurally highly related to that in the polyketide synthase pathway (PKS), as proposed for the biosynthesis, reported for salinosporamide A.[19] Ketal formation, saponification of methyl ester and coupling of the acid with dimethyl 2-aminomalonate delivered amide **4.40**.

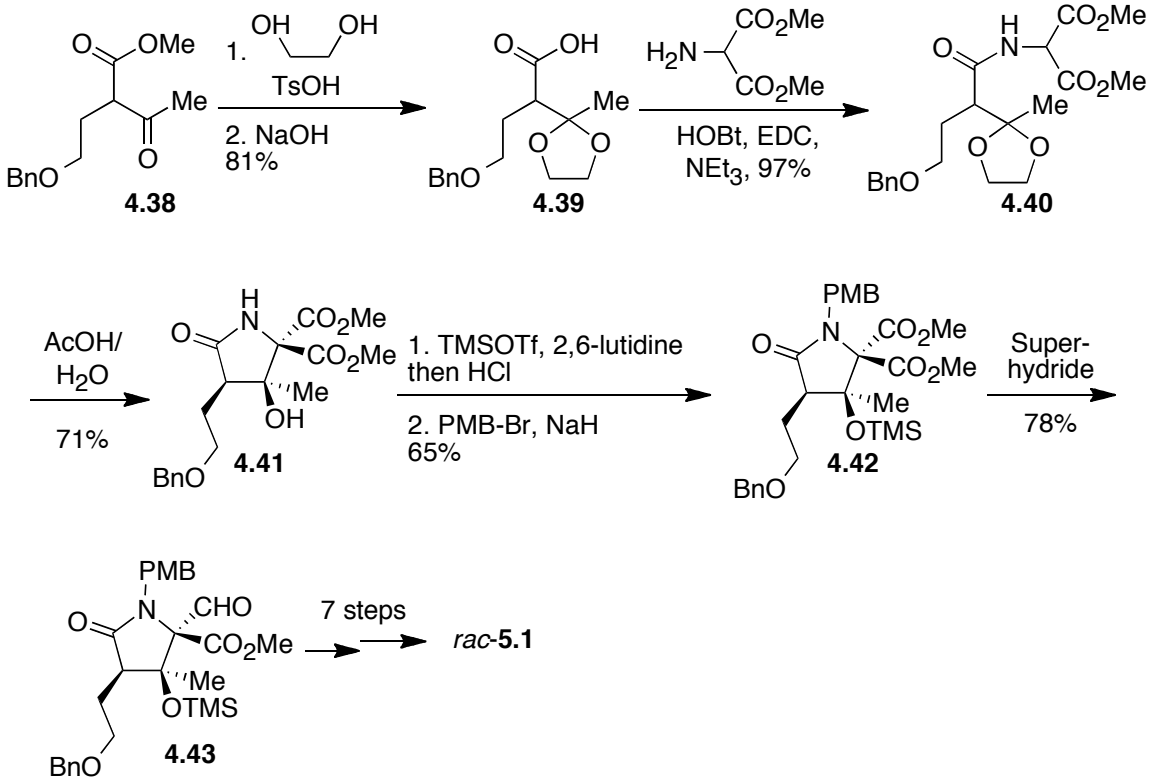


**Scheme 4.6** Pattenden's biosynthetically inspired synthesis of *rac*-salinosporamide A.

This intermediate resembles the proposed linear PKS-NRPKS intermediate of the biosynthetic pathway.[20] Removal of dioxolane under acidic condition leads to the biomimetic intramolecular cyclization of the methyl ketone to furnish γ-lactam **4.41** as a single diastereomer. Routine protection steps and chemoselective reduction of the methyl ester, afforded advanced intermediate compound **4.43**. The racemic synthesis of salinosporamide A **4.1** was then carried out in 7 additional steps, which also included Corey's protocol to install the cyclohexenyl group.

### 4.4.4 Biomimetic synthesis by Romo and coworkers.

A racemic and biomimetic synthesis was reported by Romo and coworkers in 2007.[21] Later an enantioselective concise route was developed by the same group in 2010 which involved development of an enantioselective version of a previously proposed key bis-cyclization step of a β-keto tertiary amide.[22] In this step, optical purity was retained, which is proposed to be controlled via $A^{1,3}$-strain which renders epimerization slow with respect to the rate of bis-cyclization process in intermediate **4.44** (Scheme 4.7).

The synthesis began with commercially available (*R*)-serine derivative **4.46**, which was subjected to reductive amination and subsequent esterification to provide allyl ester **4.47** with minimal racemization (98% *ee*) (Scheme 4.8). Acylation with unsymmetric ketene dimer **4.48** under microwave conditions yielded diastereomeric mixture of β-ketoamides **4.49**/**4.49'** (*dr* 1/1) in 80% yield. Separation by MPLC then provided isolation of the desired diastereomer (*R, R*)-β-ketoamide **4.49**. Under acidic conditions the undesired epimer could also be transformed into a 1:1 mixture of diastereomers via epimerization

of the C-2 but not the C-4 stereocenter, as confirmed by chiral HPLC. Pd(0) mediated deallylation delivered β-keto acid **4.50** with negligible erosion of stereochemistry. Nucleophile catalyzed aldol cyclization (NCAL) upon treatment with MsCl and 4-PPY (4-pyrrolidinopyridine) afforded bicyclic β-lactone **4.51**. This reaction was also done on multigram scale with comparable diasteroselectivity and retention of enantiopurity (52% over two steps, *dr* 5:1, 90% *ee*).

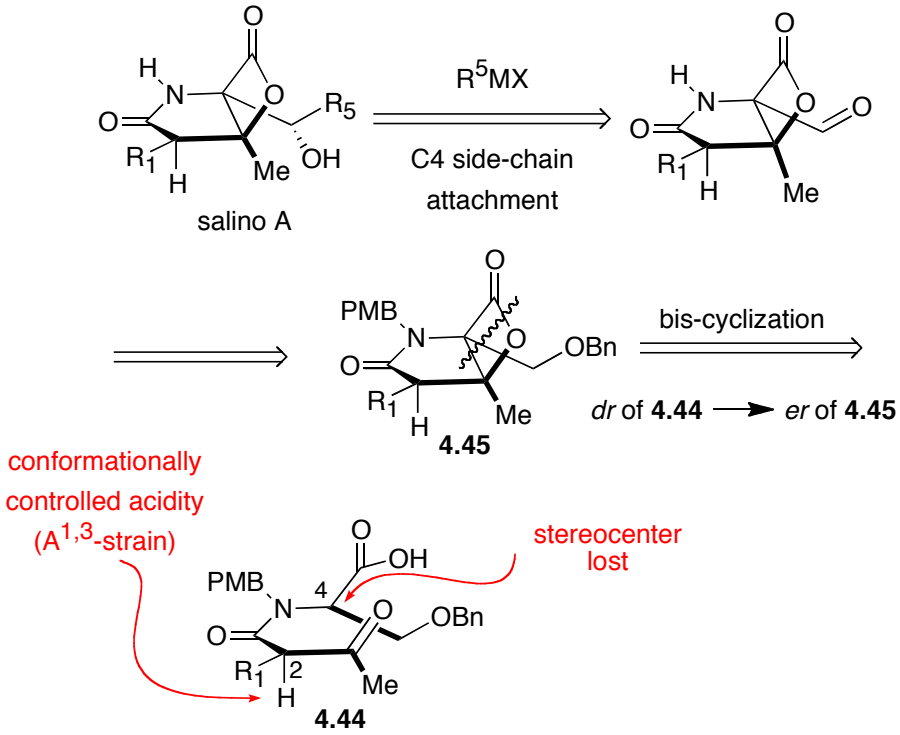


**Scheme 4.7** $A^{1,3}$-strain in β-keto tertiary amide leads to optically defined bis-cyclized product.

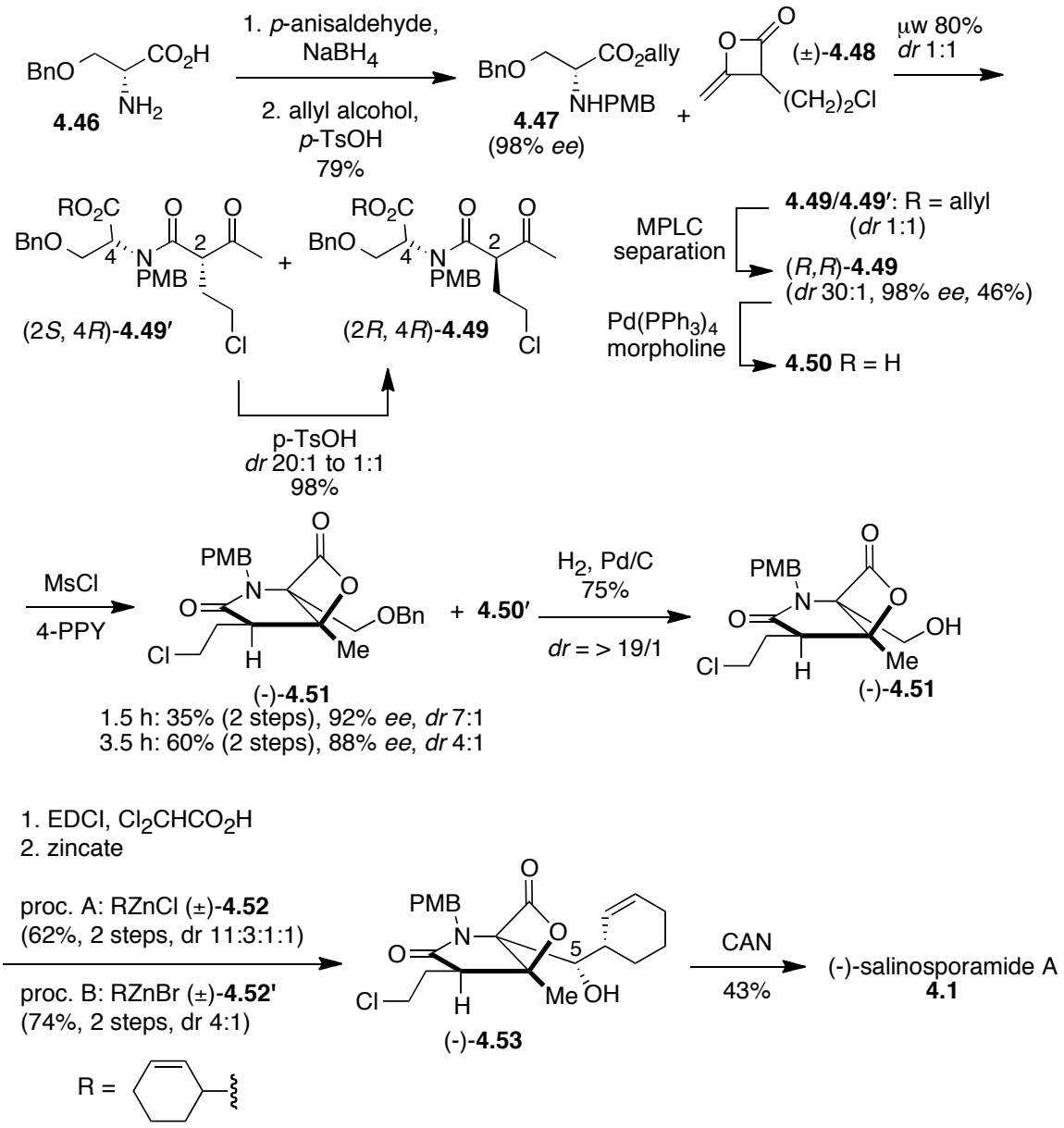


**Scheme 4.8** Enantioselective synthesis of salinosporamide A by Romo et al.

Hydrogenolysis, modified Moffat oxidation and following Corey's protocol a C5-C6 diastereomeric mixture of alcohols was obtained (*dr* 11:3:1:1) in 62% yield (Procedure A) affording the desired compound **4.53** as the major product. Following Procedure B both diastereoselectivity and yield could be enhanced. Finally PMB deprotection

afforded pure (-) salinosporamide A **4.1**.

### 4.4.5 Total synthesis toward salinosporamide A by Nereus pharmaceuticals.

The enantioselective route presented by Nereus pharmaceuticals relied on a protocol other than that developed by Corey's group for the installation of the cyclohexenyl moiety.[23] The key precursor, β-keto amide **4.54** (Scheme 4.9) was subjected to intramolecular Aldol condensation exploiting the concept of self-regeneration of chirality developed by Seebach et al.[24] Thus following this strategy oxazolidine-γ-lactam **4.55** was obtained with 17:3 *dr* containing all the required stereogenic elements. This step could also be scaled up to generate 100 g of **4.55**. A Few routine group transformations afforded tricyclic intermediate **4.56**. Unfortunately when subjected to Corey's protocol to install the cyclohexenyl group the undesired *anti* addition product (undesired configurations at C5 and C6) was obtained. Finally Brown's allylboration chemistry allowed them to prepare *syn* addition adduct **4.58**. After a series of oxidation-reduction steps and protective group alterations, the undesired C-5 *epi* salinosporamide A *epi*-**4.1** was obtained. In order to correct the C-5 stereocenter, it was subjected to oxidation to deliver keto salinosporamide A. Although stereoselective reduction seemed very challenging initially, use of enzymatic reaction employing NADH-dependent ketoglutarase KRED-EXP-B1Y and glucose dehydrogenase (GDH) for *in-situ* generation of the cofactor successfully delivered the required stereocenter.

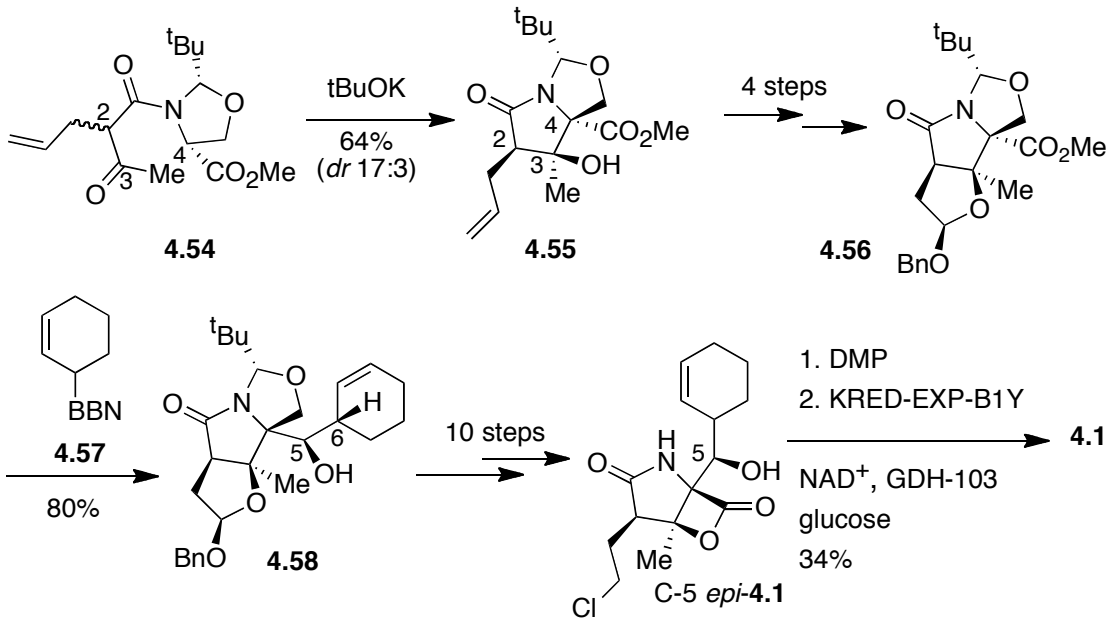


**Scheme 4.9** Synthetic route reported by Nereus Pharmaceuticals.

### 4.4.6 Indium catalyzed Conia-ene approach towards the synthesis of salinosporamide A.

Another route to salinosporamide A was reported by Hatakeyama and coworkers, where a Conia-ene reaction was utilized as a key step to build the pyrrolidinone framework.[25] Chiral propargyl alcohol **4.59** was converted into diol **4.60** following few transformations (Scheme 4.10). Oxidation to a carboxylic acid and then amidation via activation of the acid afforded amide intermediate **4.61**, the precursor for the key Conia-ene reaction step. Column chromatography led to the partial conversion of this precursor into an inseparable mixture of both the starting material and desired pyrrolidinone **4.62**. However, upon treatment with $In(OTf)_3$, complete conversion into Conia-ene product lactam **4.62** took place without any epimerization. Due to the labile nature of acetate **4.62**, deacetylation was carried out under very mild conditions using lipase. Oxidation

with DMP then afforded aldehyde **4.63**, which is similar to the advanced intermediate used by Danishefsky.[17] The only difference is the presence of the bis methyl ester instead of the bis t-butyl ester used in Danishefsky's synthesis, which was subsequently converted into natural product **4.1** using similar synthetic steps.

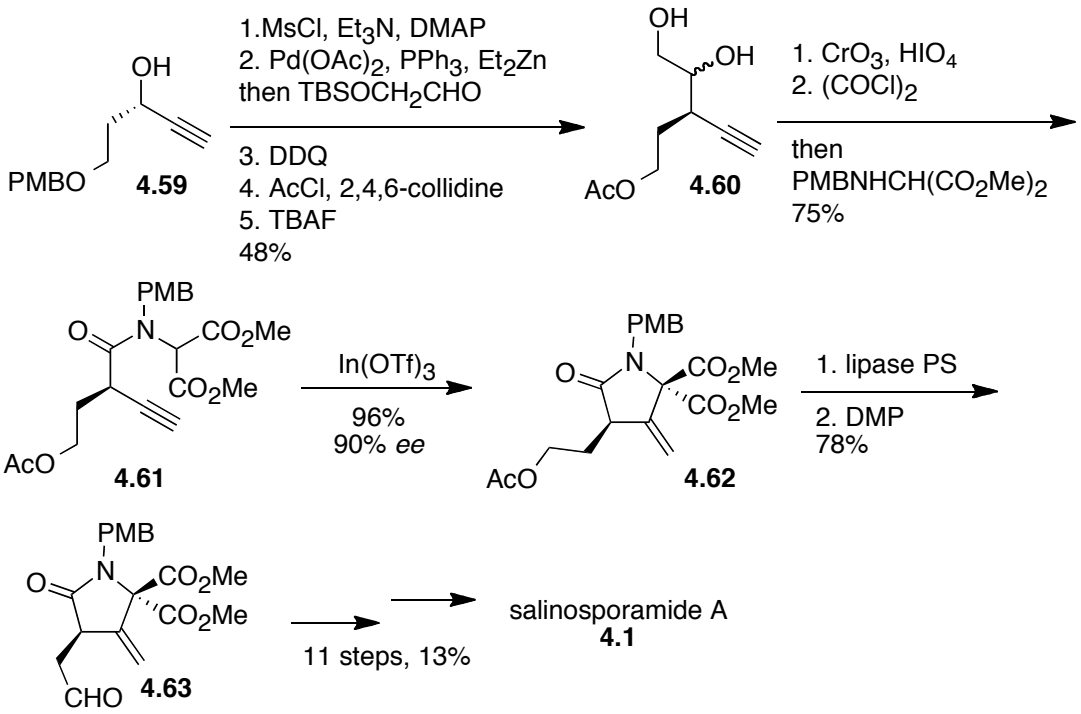


**Scheme 4.10** Total synthesis of salinosporamide A by Hatakeyama and coworkers.

### 4.4.7 Synthesis by Omura and coworkers.

Omura and coworkers reported another interesting route that involved earlier construction of the cyclohexenyl ring.[26] Achiral **4.64** aldehyde was transformed into chiral acetate **4.66** following Wittig olefination, acetonide deprotection, lipase catalyzed desymmetrization and O-silylation. Deacetylation, reprotection of the unmasked alcohol with MEM group, desilylation, intramolecular carbamation and finally PMB protection

afforded oxazolidinone intermediate **4.67**. Oxidation of the alkene to diol and $NaIO_4$ mediated cleavage then delivered aldehyde **4.68**. Addition of cyclohexenone was achieved by chelation controlled Aldol reaction, benzoylation of the then generated secondary alcohol afforded cyclohexanone intermediate **4.69** with 20:1 diastereoselectivity. This intermediate was then elaborated into cyclohexene derivative **4.72** via generation of sulfate intermediate **4.70**, and then DBU promoted elimination and hydrolysis by TsOH. Intramolecular transcarbamation and oxidation then delivered aldehyde **4.73**. Installation of the lactam unit then proceeded by generation of ketone **4.74**, which when subjected to N-acetylation, followed by intramolecular Aldol reaction afforded pyrollidinone **4.75** as a single diastereomer. C-2 side chain was installed by $SmI_2$ mediated Reformatsky type reaction with benzyloxyacetaldehyde. Deoxygenation in the side chain was carried out by O-mesylation, elimination to yield alkene, which was then subjected to hydride addition to yield advanced precursor **4.77**. The latter was then elaborated into the final product following 9 steps, similar to the one used by Corey's group to install chloride in the side chain.

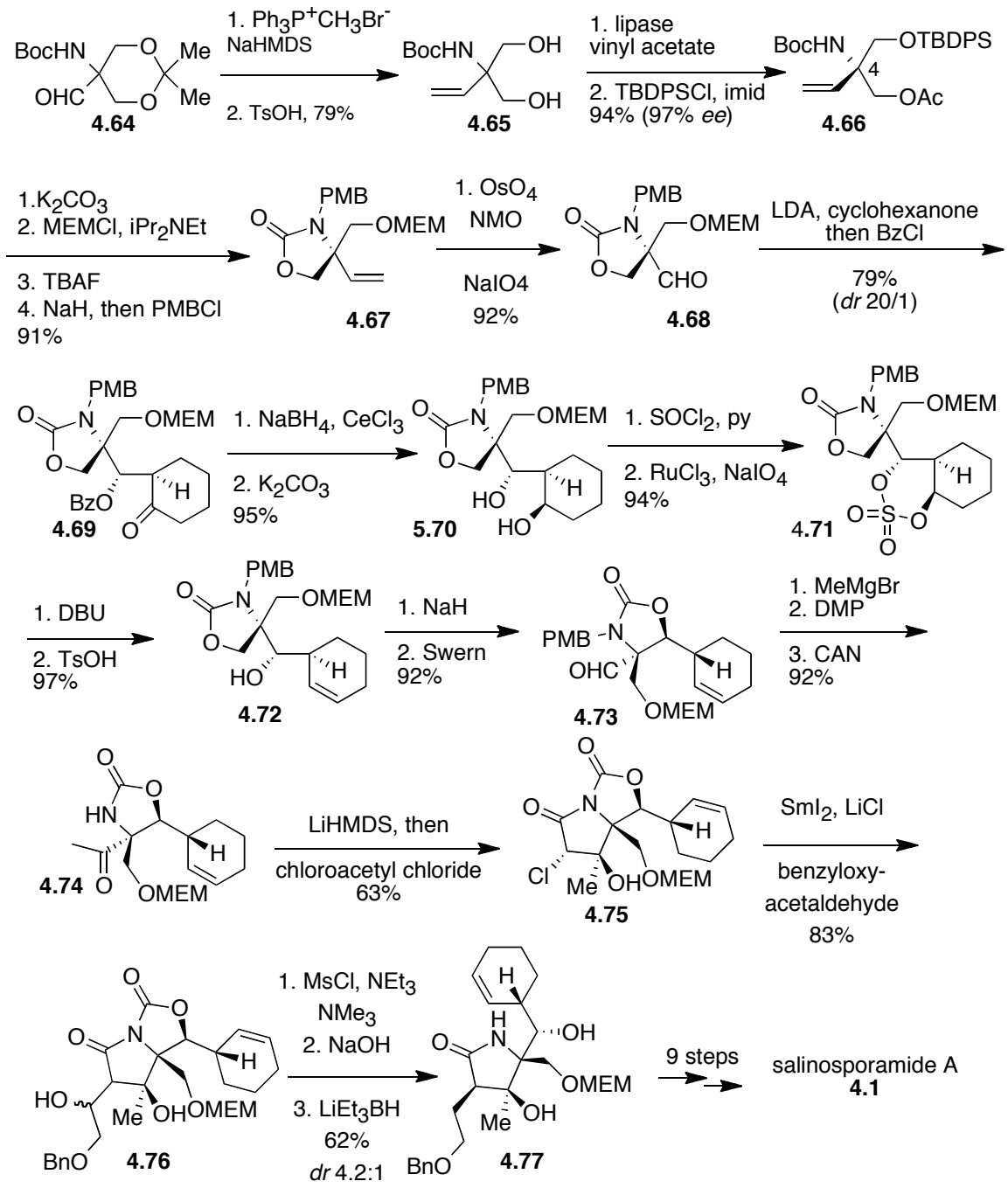


**Scheme 4.11** Total synthesis by Omura and coworkers.

### 4.4.8 Discussion of other formal syntheses reported in the literature.

Several studies have been reported for the formal synthesis of salinosporamide A. Chida and coworkers illustrated one starting from chiral furanose derivative **4.78**.[27] Routine functional group manipulations and protecting group alterations of the starting material resulted in elaboratation into lactam **4.79** in 22 steps (Scheme 4.12). The C4 quaternary center was installed by the use of a stereoselective Overman rearrangement.[28]

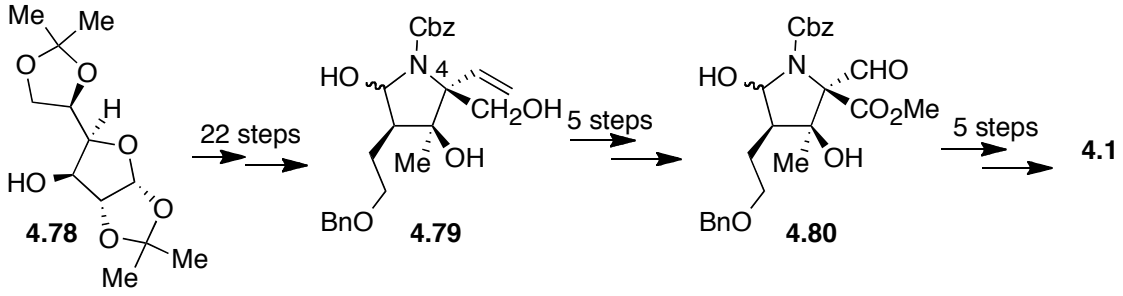


**Scheme 4.12** Formal synthesis by Chida and coworkers

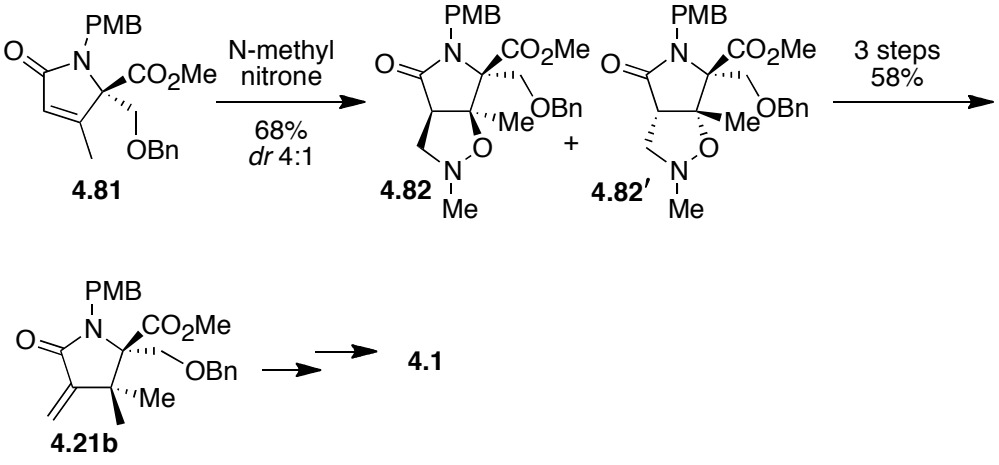


**Scheme 4.13** Formal synthesis presented by Langlois et al.

Following 5 steps, the latter intermediate was taken to an advanced intermediate **4.80** which could be transformed into the natural product in 5 steps. In another formal synthesis reported by Laglois and coworkers (Scheme 4.13), regioselective N-methylnitrone cycloaddition was used as a key step in order to produce the γ-lactam adducts **4.82/4.82'** with 4:1 diasteroselectivity.[29] The desired cycloadduct was transformed into the known advanced lactam intermediate **4.21** as used by Corey's group. Tepe and coworkers have utilized an ene-type reaction in order to elaborate oxazoline **4.83** into racemic β-amino alcohol **4.84**.[30]

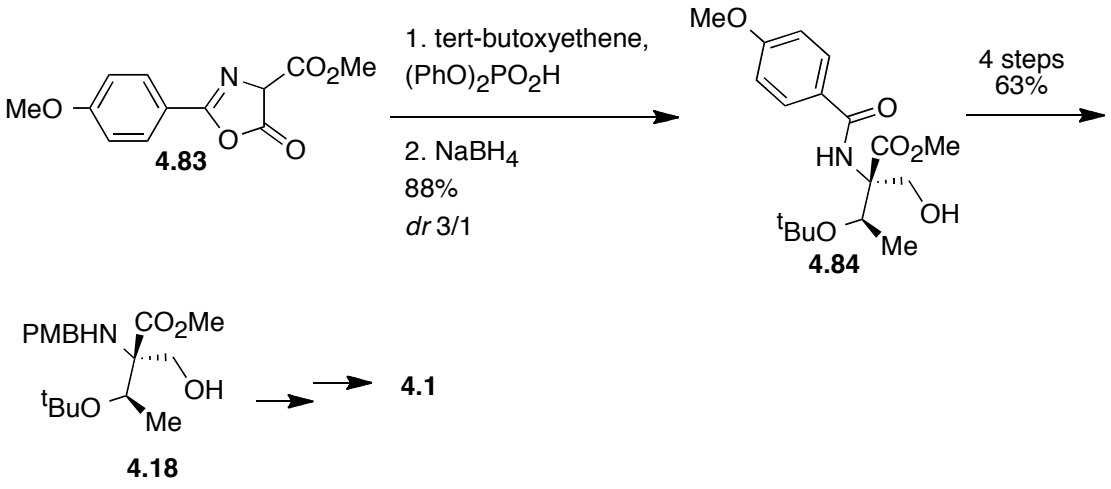


**Scheme 4.14** Formal synthesis reported by Tepe and coworkers.

Known alcohol intermediate **4.18** can be derived in four steps which can be further taken to the target molecule following route developed by Corey's group. Lam and coworkers utilized a strategy similar to that employed by Corey's group to install the lactam **4.85** (Scheme 4.15).[31] Nickel catalyzed reductive Aldol cyclization/lactonization

led to the formation of bicyclic lactam **4.86** with moderate selectivity.[32] The latter can be transformed into intermediate **4.87** in 4 steps, which is the N-PMB protected form of a known intermediate utilized in Corey's synthesis.

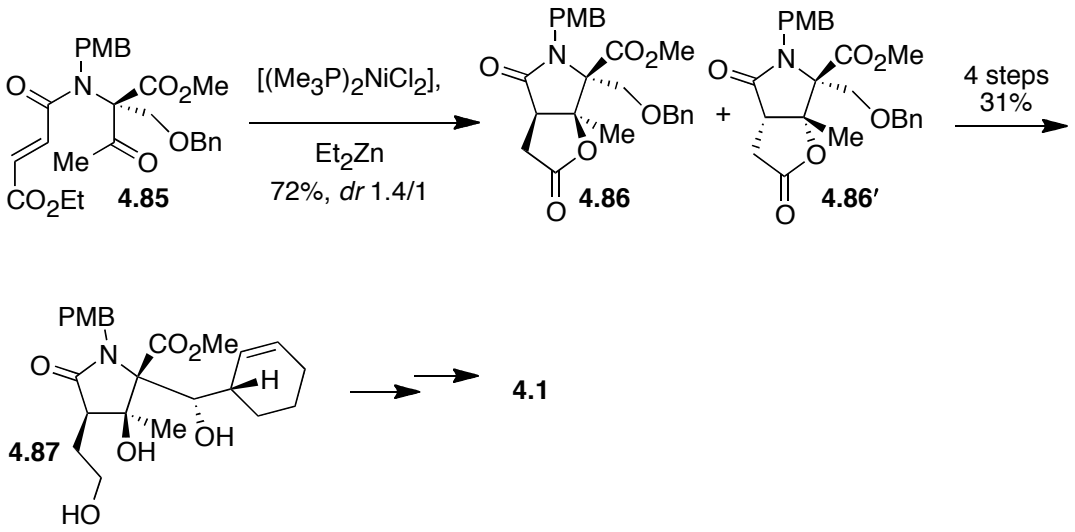


**Scheme 4.15** Formal synthesis reported by Lam et al.

Bode et al. developed a N-heterocycle carbene **4.88** catalyzed intramolecular lactamization method to produce a 1:1.1 mixture of bicyclic γ-lactams, more in favor of the undesired isomer which was subjected to conditions similar to the ones developed by Lam and coworkers (Scheme 4.16).[33]

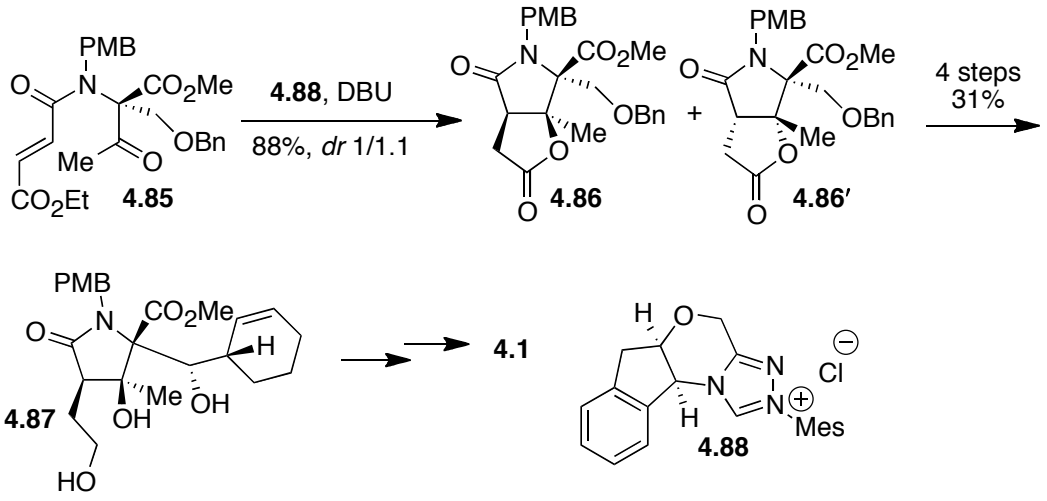


**Scheme 4.16** Formal synthesis by Bode et al.

## 4.5 Retrosynthetic analysis using the tandem aza-Payne/hydroamination methodology.

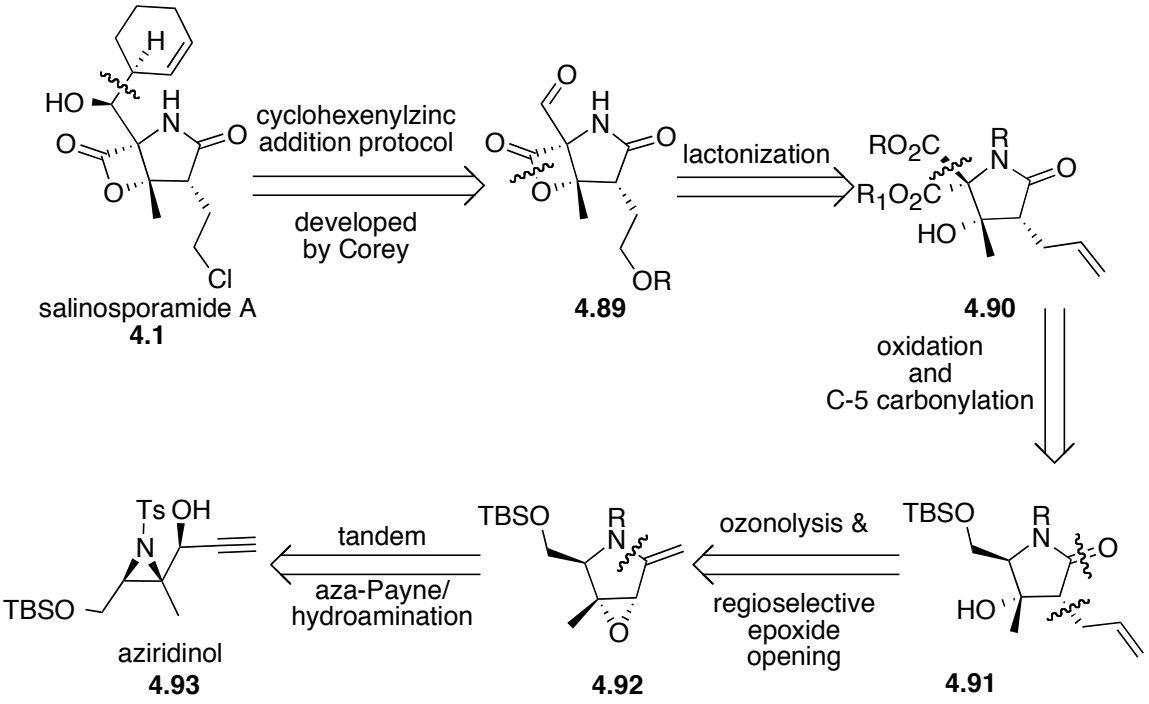


**Scheme 4.17** Disconnective approach for the synthesis of salinosporamide A.

Scheme 4.17 illustrates our strategy for the major disconnective approach planned for the synthesis of salinosporamide A. Advanced aldehyde precursor **4.89** will be subjected to the organozinc addition protocol as developed by Corey to install the cyclohexenyl group to yield salinosporamide A. Alternatively other approaches that involve the use of other reagents such as cyclohexenyl-9BBN adduct **4.57**, as employed by Nereus pharmaceuticals can also be examined, in order to establish both C-5 and C-6 stereocenters. β-Lactonization would be achieved via intramolecular esterification in intermediate **4.90** between the ester moiety and tertiary alcohol arranged in the *cis* fashion. The C5 ester would be installed by the oxidation and C-5 carbonylation starting from alcohol intermediate **4.91**. The latter in turn would be derived from a lactam elaborated from the intermediate **4.92** via olefin- ozonolysis followed by opening of the epoxide in both regio- and stereocontrolled fashion. Tetrasubstituted pyrrolidine **4.92** would be assembled via the tandem aza-Payne/hydroamination methodology starting from diastereomerically pure aziridinol **4.93**.[34]

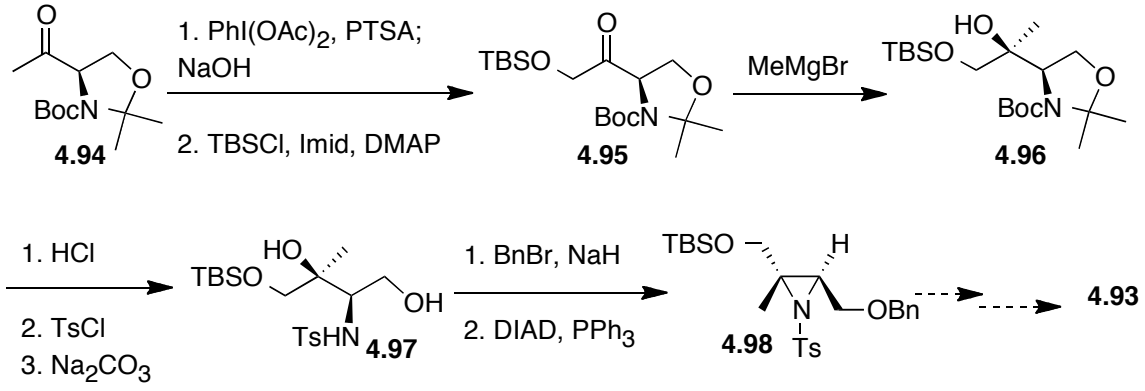


**Scheme 4.18** Proposed route for the synthesis of chiral trisubstituted aziridinol.

Chiral aziridination protocols such as those utilized in Wullf's VAPOL/VANOL based,[35-37] Cardova's proline based,[38] or Dubois's N transfer via rhodium based catalysts would be examined in order to install optically pure trisubstituted aziridinols for the enantioselective route.[39] An alternate approach would rely on the use of a ketone derived from a commercially available chiral aldehyde[4] precursor **4.94**, which can be alpha hydroxylated using a reported literature protocol.[40] Silylated alcohol **4.95** can be subjected to a series of transformations following a similar route that has been well developed by Joullie and coworkers to derive aziridinol **4.98**.[41] Required chiral aziridinal **4.93** can be prepared in few steps following routine protective group alterations and oxidation step. This method thus efficiently allows us to obtain the highly functionalized pyrrolidine nucleus, which can be built in one pot starting from aziridinol precursor **4.93**. Gratifyingly, the *N*-Ts enamide at this stage in intermediate **4.92** contains most of the stereogenic elements as required in skeletal framework of the lactam nucleus in the target molecule.

## 4.6 Racemic route toward the synthesis of salinosporamide A

### 4.6.1 Diastereoselective synthesis of trisubstituted aziridinol 4.93 and construction of *N*-Ts enamide intermediate 4.105.

Our synthesis began with the use of commercially available 3-methyl-2-butenol **4.99**, which was protected as the silyl ether **4.100** using DMF as the solvent (Scheme 4.19).[42]

[4] Corresponding methyl ester is also available and sold by Aldrich.

Interestingly, no conversion was observed as analyzed by TLC upon employing DCM as solvent, a usual choice for the silyl protection reactions. The silylether was then subjected to $SeO_2$ and $^tBuOOH$ mediated allylic hydroxylation, which gave a 3:1 mixture of desired allylic alcohol **4.102** and over oxidized aldehyde **4.101** in moderate yield. Treatment of the aldehyde with sodium borohydride in methanol afforded the required allylic alcohol in 72% yield.

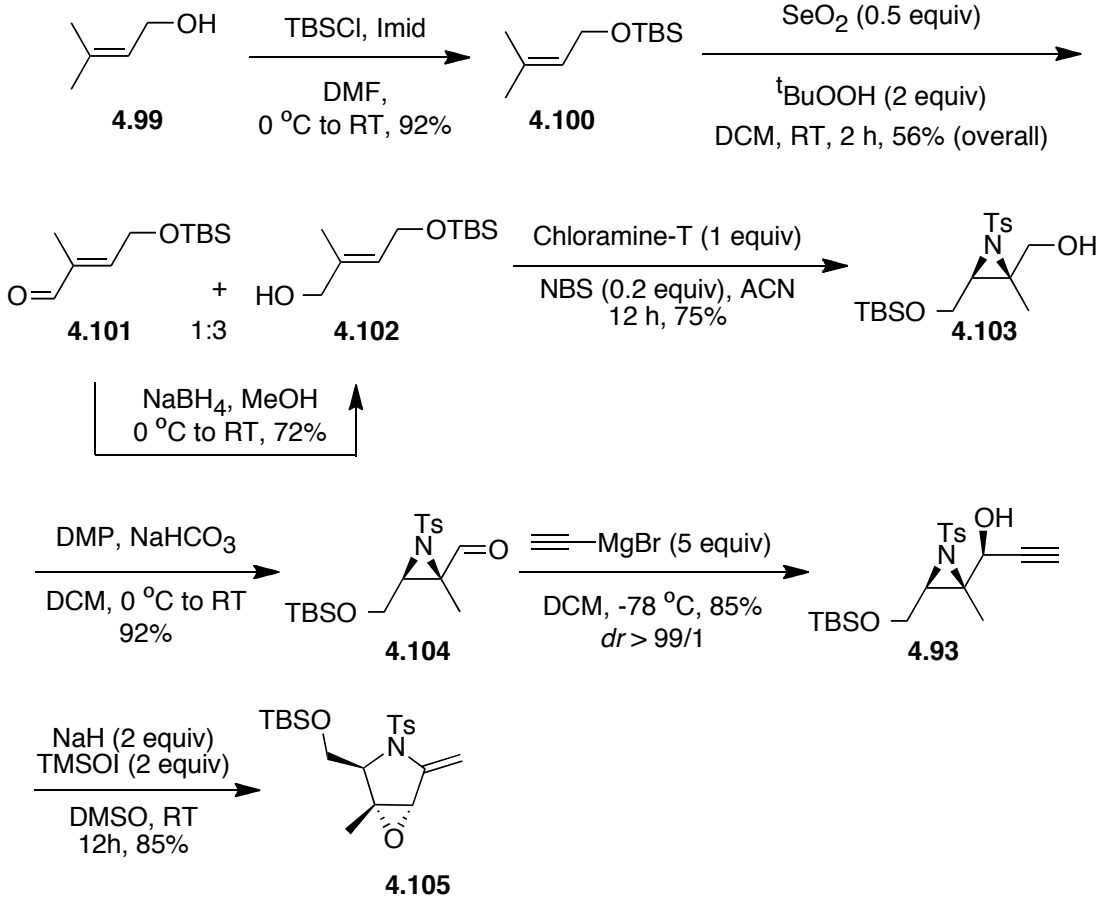


**Scheme 4.19** Schematic route for the construction of *N*-Ts enamide **4.105**.

Aziridination of the allylic alcohol was achieved using catalytic amount of NBS and Chloramine-T following a reported procedure.[43] Unfortunately oxidation to aziridinal in the next step could not take place when PCC or Swern oxidations were attempted. Nonetheless the reaction proceeded smoothly under Moffat oxidation or buffered DMP conditions, consistent with results reported previously from our lab.[44] Addition of ethynyl Grignard was accomplished to yield propargyl alcohol **4.93** with both excellent yield and diastereoselectivity (>99/1). As reported in Chapter 1, 5 equivalents of Grignard reagent had to be used to push the conversion toward completion. The one pot aza-Payne/hydroamination reaction provided *N*-Ts enamide intermediate **4.105** in high yield.

### 4.6.2 Ring opening of the epoxide and elaboration to α-bromo hydroxylactam intermediate.

The *exo* methylene was found to be highly vulnerable towards internalization, when epoxide opening was carried out on *N*-Ts enamide **4.105** under nucleophilic conditions. As discussed in chapter 3, any attempt at this course led to the generation of undesired aromatic pyrrole products. Thus masking of the *exo* olefin was critical before carrying out epoxide ring opening. Since elaboration to lactam would be required at a later stage for the proposed synthetic route, the pyrrolidine compound was successfully ozonolized to reveal the pyrrolidinone intermediate, **4.106** in excellent yield.

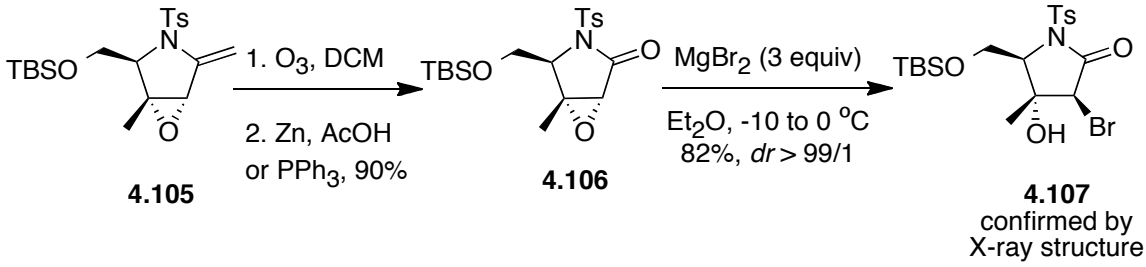


**Scheme 4.20** Elaboration of *N*-Ts enamide to 3-bromo hydroxylactam **4.107**.

Once the *exo* olefin was removed, several attempts to perform ring opening under various well precedent conditions in literature met with failure (discussed in chapter 3). Gratifyingly, treatment of *N*-Ts pyrrolidinone **4.106** with $MgBr_2$ afforded the $\alpha$-bromo hydroxylactam **4.107** in high yield (Scheme 4.20). The identity of the ring-opened product was confirmed by X-ray crystallography (Figure 4.1).

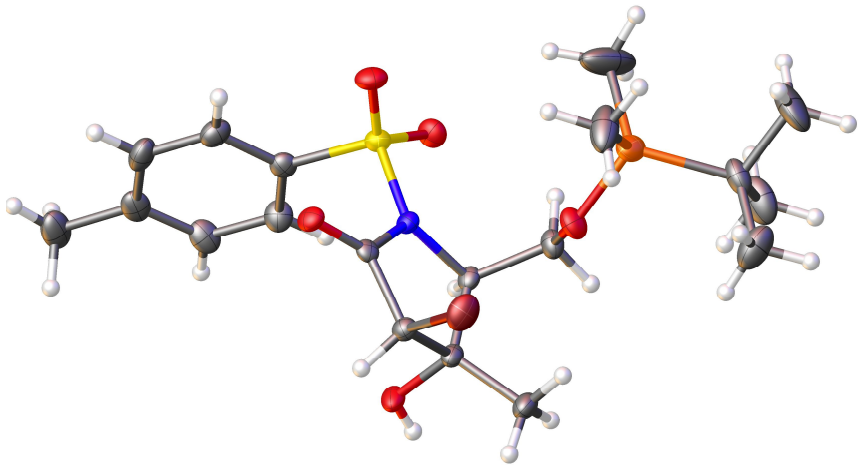

**Figure 4.4** X-Ray structure of $\alpha$-bromo hydroxylactam intermediate **4.107**.

The structure clearly reveals the *anti* disposition of the released tertiary alcohol and the bromide moiety. As anticipated attack exclusively occurred at sterically available C-3 position in an $S_N2$ fashion in order to deliver the product with the anticipated stereochemistry (Figure 4.5).

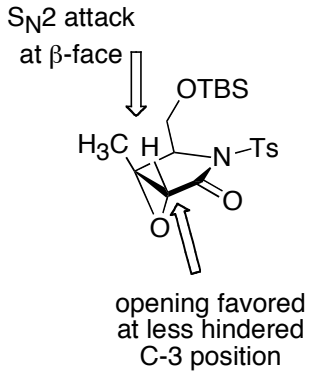


**Figure 4.5** Origin of regio- and stereoselectivity established during epoxide ring opening reaction.

A small amount of moisture, if present in the powdered $MgBr_2$, was found detrimental to the efficiency of the reaction. When powdered $MgBr_2$ was replaced by freshly prepared $MgB_2 \cdot OEt_2$,[45] a competing elimination of the tertiary alcohol was observed (Scheme 4.21). The observed elimination is not well understood, but apparently Lewis acidity of the reagent might be higher in the presence of DCM as the solvent, which might facilitate the elimination of the tertiary alcohol during the course of the reaction. Since a biphasic system was observed upon addition of $MgB_2 \cdot OEt_2$ to the solution of lactam in $Et_2O$, DCM had to be added in order to make it a homogenous solution. Thus use of

powdered $MgBr_2$ dried under vacuum in ether seemed be the optimum condition for the ring opening reaction. Alternatively when highly reactive bromonium was generated using $PPh_3$ and $CBr_4$, same $\alpha$-bromo hydroxylactam compound **4.107** was isolated albeit in low yield (Scheme 4.22).

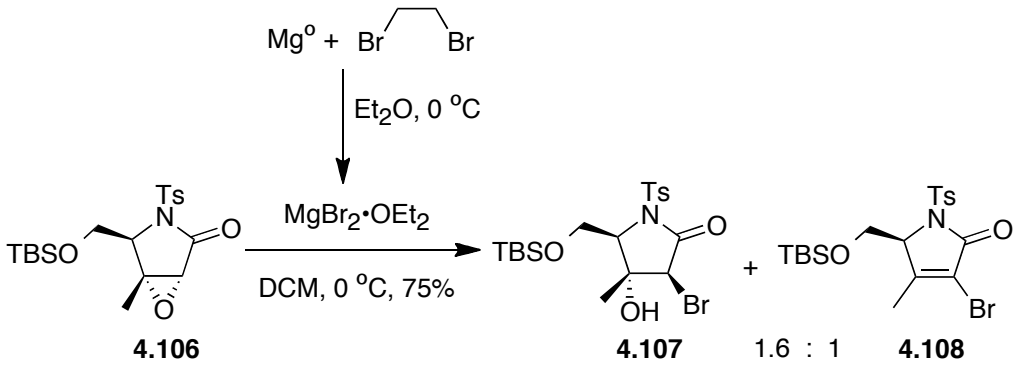


**Scheme 4.21** Competing dehydration upon treatment with freshly generated $MgBr_2 \cdot OEt_2$.

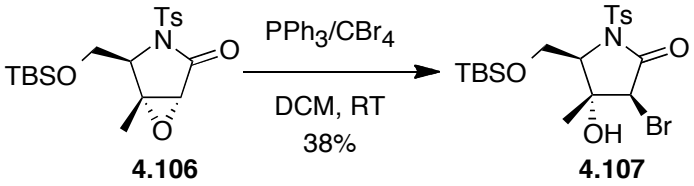


**Scheme 4.22** Alternative procedure to perform ring opening of the epoxide.

### 4.6.3 Attempts at C-3 alkylation of $\alpha$-bromo hydroxylactam.

Once epoxide opening was successfully accomplished, attention was then brought to C-3 alkylation of the bromo hydroxylactam, as required for the proposed synthetic plan. This was attempted via intermolecular enolate mediated alkylation reaction under basic

condition (Scheme 4.23). Thus the α-bromo hydroxylactam **4.107** was treated with $^{t}$BuLi at low temperature, the *in-situ* generated lithium enolate was allowed to react with allyl iodide. Unfortunately only epoxide material along with starting material was observed through NMR analysis of the crude product. It has been known that metal-halogen exchange involves electron transfer and can compete with deprotonation. The latter process requires atom transfer and thus may slow down especially at low temperatures. This has been implemented successfully in several cases reported in the literature.[46-48]

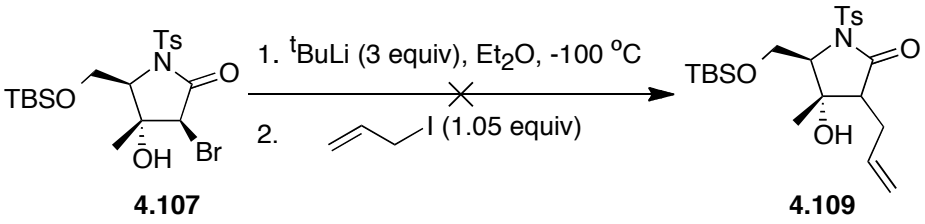


**4.107** **4.109**

**Scheme 4.23** Attempt at enolate mediated intermolecular alkylation reaction.

However, rate of such deprotonation in our case, seemed much faster, which led to the generation of the undesired epoxide (Scheme 4.23). Since competing intramolecular epoxidation pathway seemed unavoidable, we revised our strategy and resorted to an intramolecular version to perform the alkylation. Thus, tethering the tertiary alcohol to a group was planned, which upon employing the appropriate radical or ionic conditions, would facilitate transfer of the alkyl group to replace the reactive C-Br bond. This route would not only offer a reaction at much faster rate (intramolecular nature), but would also help to relay the chirality in the desired fashion from C-4 to C-3 position (Figure

4.6). Siloxy ethers when subjected under appropriate radical conditions are known to undergo cyclic siloxane formation.[49] Subsequent oxidation of siloxanes reveals the alcohol moiety. Thus hydroxy lactam **4.107** was treated with dimethylvinylsilylchloride under basic conditions. Unfortunately this also led in poor conversion to the generation of the undesired epoxide compound (Scheme 4.24). O-allylation was also attempted, since if accessible, would be examined for the allyl transfer reactions under basic conditions (Scheme 4.25). Compound **4.107** was treated with allyl bromide in the presence of calcium sulfate and freshly prepared silver oxide (Scheme 4.26).

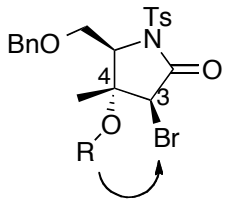


transfer of the chirality from C-4 to C-3 during transfer of R intramolecularly

**Figure 4.6** Intramolecular transfer of R would lead to the desired stereochemistry at C-3 position.

Under such conditions silver oxide is known to ionize allyl bromide activating it towards the attack by the alcohol, and the precipitation of silver bromide drives the equilibrium.[50,51] Further it was thought that the bromide present in the starting material, would lead to electronically less favored carbocation ($\alpha$ to carbonyl). However, not surprisingly the reaction was extremely slow and epoxide **4.106** was identified as the only major compound identified via analysis of the crude NMR (Scheme 4.26).

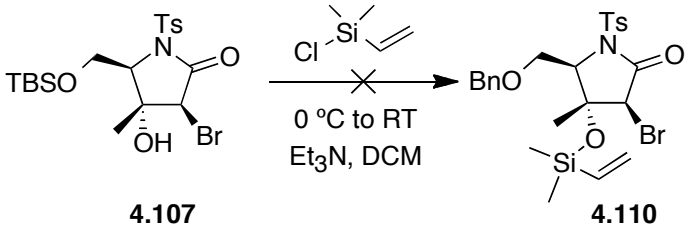


**Scheme 4.24** An attempt at O-silylation of the tertiary alcohol.

Alternatively the allylation reaction was also attempted under milder conditions. For this purpose allyltrichloro acetimidate was freshly prepared and subjected to bromolactam **4.107** in the presence of *p*-TSA. Unfortunately O-allyl product was not observed and only undesired epoxide compound was detected along with the starting material as confirmed by the analysis of the crude NMR spectrum (Scheme 4.26).

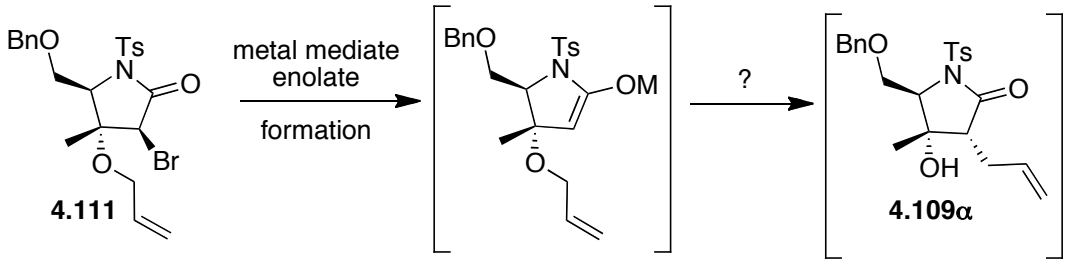


**Scheme 4.25** Proposed plan to execute allyl transfer intramolecularly.

Guibe and coworkers reported another method, which allows preparation of allyl ethers under palladium conditions from the corresponding allyloxycarbonyl compounds (Scheme 4.27).[52] Notably these allyloxy carbonyl compounds can in turn be prepared under very mild basic conditions. These compounds are known to undergo

decarboxylation when subjected to Pd(0) conditions following a catalytic cycle illustrated in Scheme 4.28.

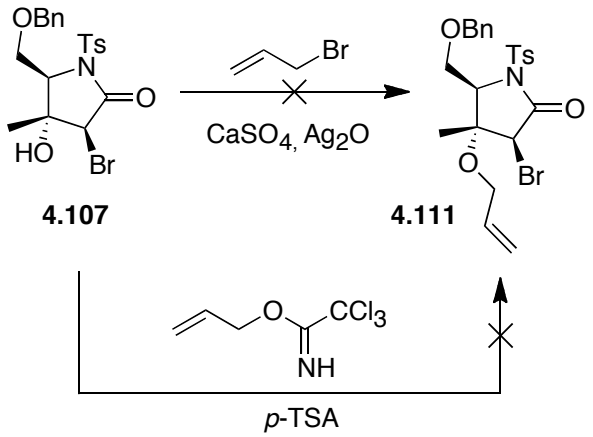


**Scheme 4.26** Attempts at O-allylation.

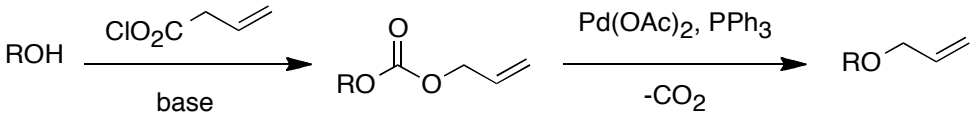


**Scheme 4.27** Palladium mediated conversion of allyloxycarbonyls to allylether.

Unfortunately formation of epoxide could not be avoided even under mildly basic conditions (Scheme 4.29a). This thwarted our attempt to prepare the allyloxycarbonyl derivative of the bromolactam **4.107**. Several other attempts were made to mask the tertiary alcohol in order to perform alkylation of the bromide compound (Scheme 4.29b,c).

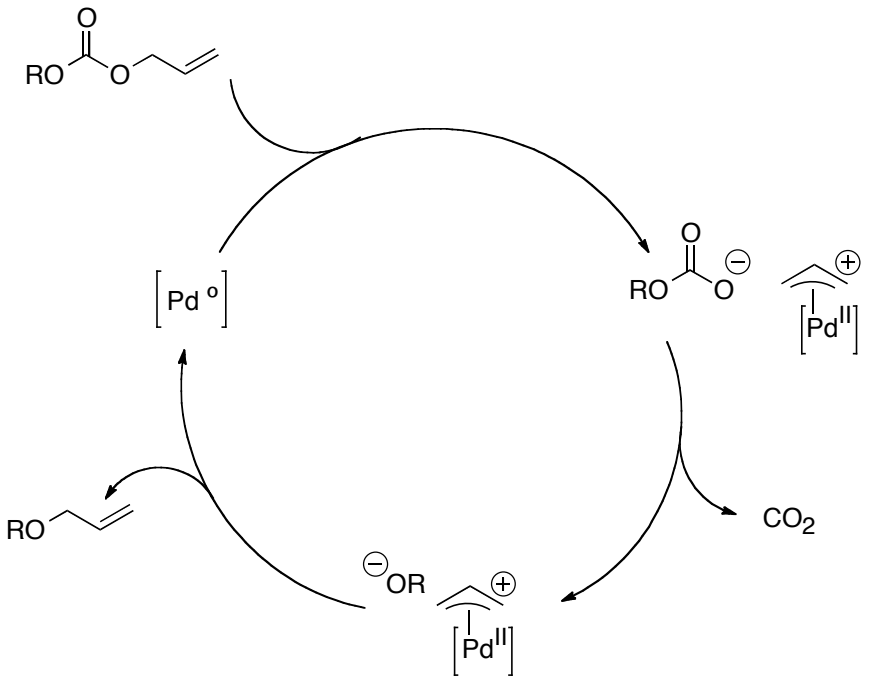


**Scheme 4.28** Palladium mediated decarboxlyation and generation of allyl ether from allyloxycarbonyl compounds.

Upon treatment with acetic anhydride under basic condition, a mixture of epoxide **4.106** and bis dihydroxy compound (structure not confirmed) was observed by NMR analysis of the crude product. The highly reactive electrophile N-trichlorocarbonyl isocyanate was also examined. Unfortunately workup conditions (Scheme 4.29c) which was very basic and nucleophilic, led to both the epoxidation and methanolysis of the lactam. Thus sadly, all our attempts to carry out either alkylations or O-protection either met with failure or only produced the undesired epoxide. Suffering from dominating competing $S_N2$ attack and facing unsuccessful attempts at alkylation under basic or acidic conditions, we then turned our attention to the radical mediated Keck allylation.[53]

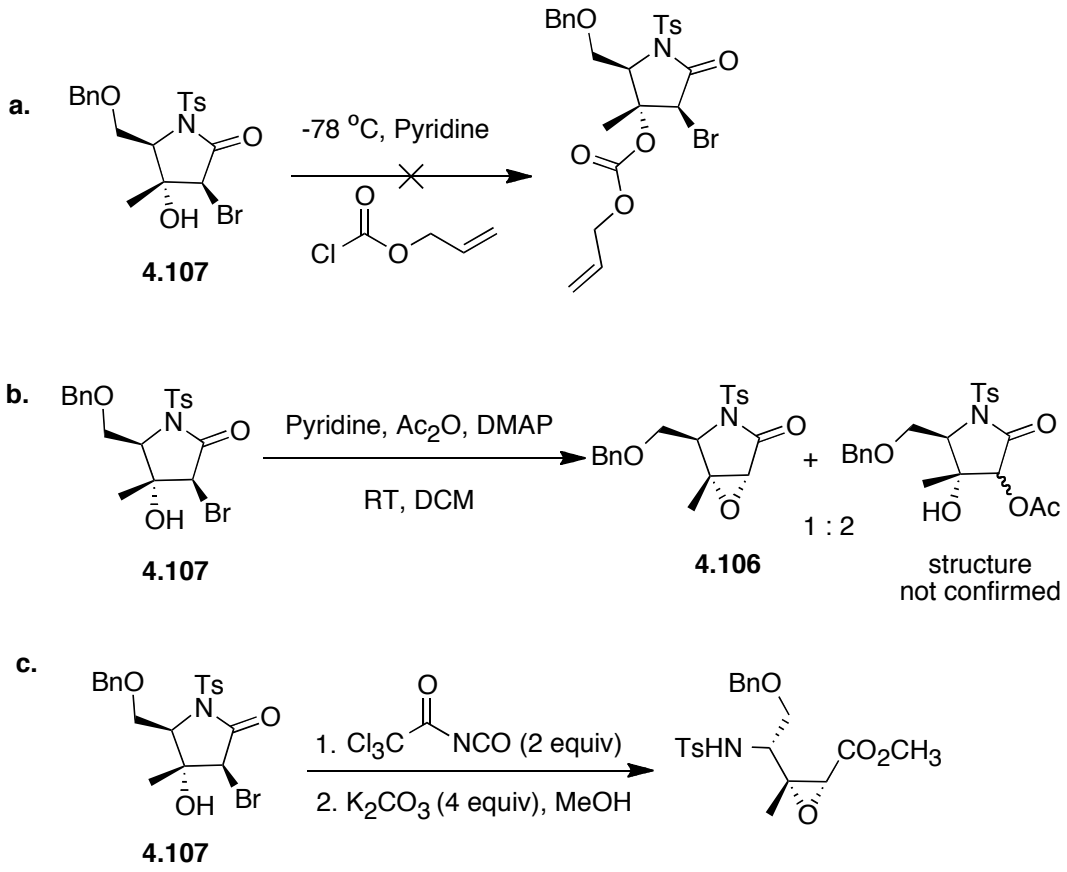


**Scheme 4.29** Various attempts at O-protection.

Keck allylation allows the construction of C-C bond utilizing the reaction of allyltri-n-butylsilane with halides, which are good precursors to radical formations in the presence of a suitable initiator. This has been exploited often for C-C bond formation reactions and has been applied in various stages in total syntheses.[54-56]

Hydroxy bromide **4.107** was refluxed with allyltributyl tin in toluene in the presence of AIBN as the radical initiator to provide the C-3 alkylated products as a mixture of two diastereomers (**4.112α**/ **4.112β**, *dr* 75/25). We were delighted to find that the reaction provided the desired diastereomer **4.112α** (alpha addition at C-3) as the major isomer

(Scheme 4.30). The stereochemistry at C-3 position was identified with the help of 1D NOE experiments.

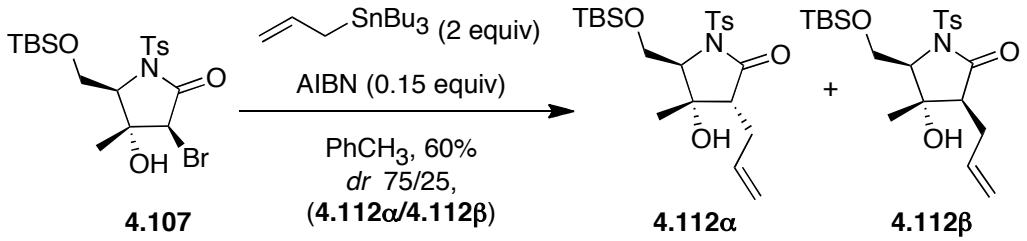


**Scheme 4.30** Radical mediated C-3 alkylation of bromo hydroxylactam **4.107**.

Several conditions were tried in order to optimize both the yield and the diastereoselectivity of the radical mediated reaction. Table 5.2 lists various conditions that were tried for the optimization for the radical-mediated C-3 alkylative reactions. The toluene and benzene seemed to be equally good choices as solvent. The $\alpha$-adduct was found to be the favored isomer obtained under these conditions with 75/25 as the best selectivity achieved under these conditions. Although, heating is required for the homolytic cleavage of the radical initiator AIBN, UV light could be employed for initiation in order to test the effect of the temperature on this transformation. However, at lower temperature, either extremely low conversion or no reaction was observed (entry 3 and 4). Upon employing Lewis acidic conditions (entry 5) selectivity was completely switched in favor of the $\beta$-adduct.

**Table 4.2** Radical mediated alkylation under various conditions.

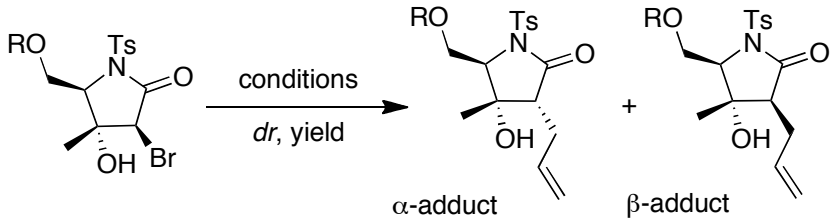


| entry | R | conditions | product (α/β) *dr* (α/β)[5] | yield[6] |
|---|---|---|---|---|
| 1 | TBS | allyltributyltin, AIBN, benzene, 80 °C, 6 h | **5.112** (2.5-2.8:1) | 60 |
| 2 | TBS | allyltributyltin, AIBN, toluene, 110 °C, 3 h | **5.112** (2.4:1) | 75 |
| 3[7] | TBS | allyltributyltin, AIBN, uv, 0 °C (initial), 6 h | **5.112** (1:1) | - |
| 4[8] | TBS | allyltributyltin, AIBN, uv, 0 °C (initial to 4 °C), 6 h | - | - |
| 5 | TBS | allyltributyltin, $ZnCl_2$, $Et_3B$, $O_2$, DCM/THF, -78 °C, 6 h | **5.112** (1:3.5-4.5) | 50% |
| 6 | Bn | allyltributyltin, AIBN, benzene, 80 °C, 6 h | **5.109** (1.5:1) | 62% |

Interestingly, when the O-*Bn* analog was subjected under standard optimized conditions (entry 6), deteriorated selectivity was obtained. This clearly suggested the influence of the nature of the substrate on the selectivity obtained for the reaction and helped us to understand the mechanism and streochemical outcome of the reaction under different

[5] Ratios of α and β adducts were determined by the analysis of the crude NMR spectra.

[6] Isolated yields are reported.

[7] Low conversion was observed.

[8] Only starting material was recovered.

conditions. Based on the difference in the nature of the reagents, radical mediated reactions can be divided into two groups:

A. Non-Lewis acid mediated conditions

B. Lewis acid mediated conditions

#### 4.6.3.1 Rationale for the selectivity achieved under non-Lewis acid radical conditions.

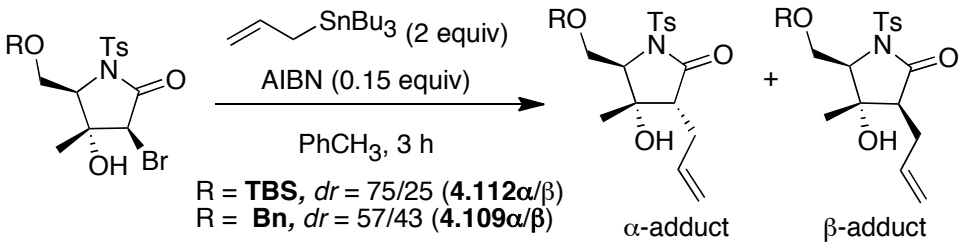


**Scheme 4.31** Allylation under non-Lewis acid conditions.

Upon treatment with non-Lewis acid conditions, a higher selectivity was achieved in the case of the substrate with TBS ether at C-5. Structures illustrated in Figure 4.7 depict the intermediates that would be generated from the TBS and Bn ether substrates via radical cleavage of the reactive C-Br bond. In the case when a sterically burdened protecting group i.e. TBS is used, the attack occurs to predominantly alkylate the more available $\alpha$-face leading to the formation of the $\alpha$-adduct (a, Figure 4.7). Whereas in the case when oxygen is masked with the smaller benzyl group, this stereo-differentiation is not that strong, thus lowering the selectivity (b, Figure 4.7). The presence of two

comparatively large groups at both C-4 and C-5 positions mask the β-face, thus delivering the α-isomer as the slightly favored adduct in both cases.

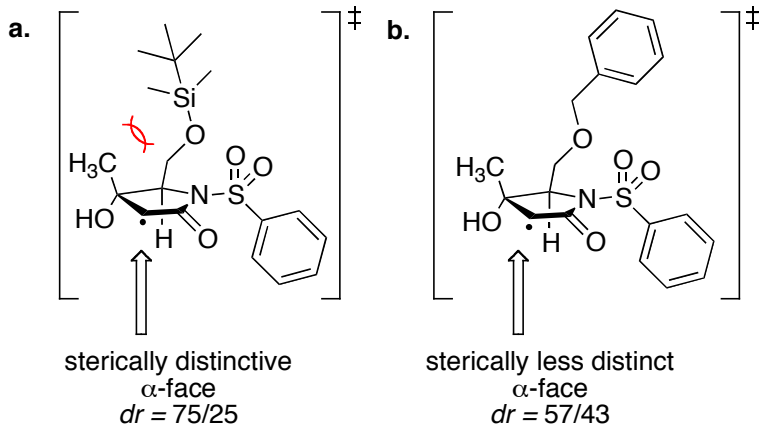


**Figure 4.7** Radical intermediates for TBS and Bn ether substrates.

### 4.6.3.2 Rationale for the selectivity observed under Lewis acid radical conditions.

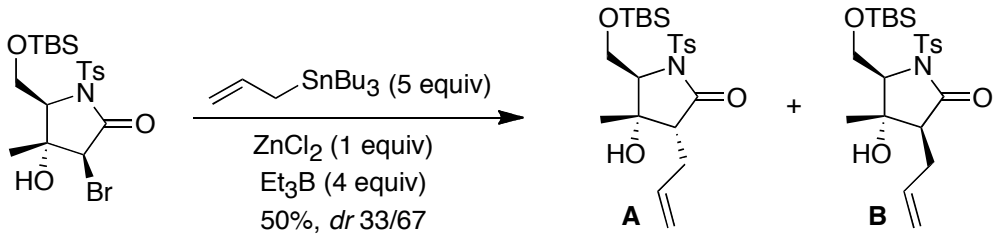


**Scheme 4.32** Allylation achieved under Lewis acid type conditions.

On the other hand, when Lewis acidic $ZnCl_2$ was employed as the reagent, diastereoselectivity switched in favor of the β-adduct. Initially this result stands in contrast with that obtained under non-Lewis acidic conditions. But careful analysis of

the intermediate, which incorporates the Lewis acid in the picture, can justify the observed diastereoselectivity. The structure presented in Figure 4.8 illustrates that the tertiary alcohol forms a complex with the Lewis acid ($ZnCl_2$) thus making the α-face sterically encumbered. As anticipated under this condition, attack from the β-face dominates delivering the β-adduct as the major isomer.

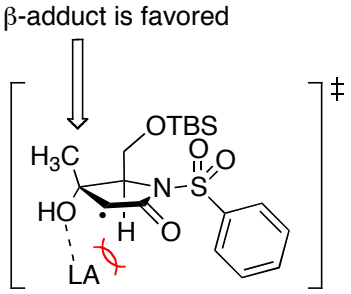


**Figure 4.8** Stereochemical explanation of favored attack at β-face under Lewis acid conditions.

Thus non-Lewis acid conditions seem suitable for the synthetic plan, where the desired α-isomer at C-3 position is desired. Nonetheless, we were delighted to find the appropriate conditions that allow the preparation of the C-3 alkylated products with stereochemical control. In future we would like to probe conditions by varying the sterics at C-4 and C-5 position in order to establish quaternary stereocenter at C-3 position. Scheme 4.33 illustrates one such hypothesized mnemonic, which can predict the stereochemistry established under such radical mediated alkylation reactions, based on steric discrimination between different substituents.

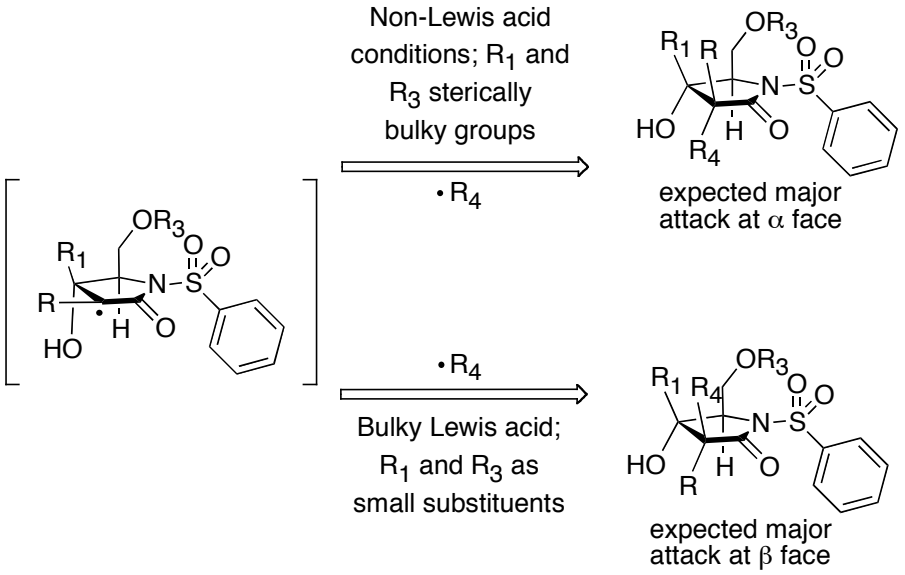


**Scheme 4.33** Hypothesized mnemonic to predict stereochemical outcome at C-3 position in radical mediated alkylation reactions.

### 4.6.4 Epimerization: Thermodynamic equilibrium towards the desired C-3 epimer.

Analysis of the two isomers (**4.112α** and **4.112β**) obtained during radical mediated allylation reaction, clearly shows that β-adduct **4.112β** suffers from severe stric clash between the two large alkyl groups substituted at C-4 and C-5 positions (Scheme 4.34).

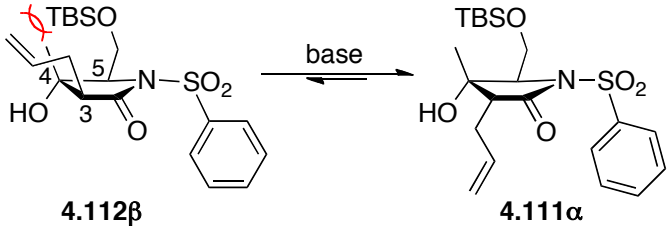


**Scheme 4.34** Thermodynamic equilibrium towards the desired C-3 epimer.

If the energy difference between two diastereomers is substantial, under reversible basic conditions should be viable to epimerization at C-3 position. This would proceed via abstraction of the acidic proton at the C-3 position favoring the equilibrium to thermodynamically more stable and desired $\alpha$-adduct **5.111a**. Indeed when a mixture of isomers was treated with catalytic amount of DBU in DCM at room temperature epimerization to the desired compound proceeded with excellent diastereoselectivity (Scheme 4.35).

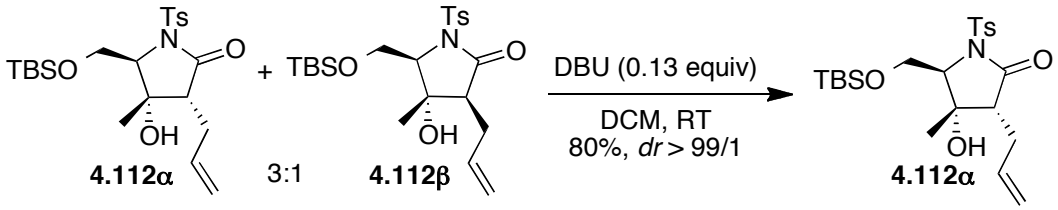


**Scheme 4.35** Epimerization of the C-3 center.

### 4.6.5 Successful attempt at Detosylation.

Benzenesulfonamide is one of the most commonly used N-protective groups. Because most of these compounds are robust and are crystalline in nature this also facilitates their isolation. This group also amends the polarity of these compounds thus allowing convenience while performing purification. There are a number of procedures reported in the literature to cleave Ts group such as dissolving metals ($Li^o/Na^o$) in liquid ammonia,[57] HMPA or alcohol,[58] sodium naphthelene or anthracene, sodium amalgam,[59] $Bu_3SnH$, $SmI_2$,[60,61] alkali metals in silica gel,[62] refluxing in strong bases

such as NaOH, KOH, $CsCO_3$,[63] $NaO^tBu$ or refluxing in TBAF. Most of the latter conditions are harsh; therefore it often is not suitable for complex molecules. With every step, higher complexity is built up and thus one has to be cautious to carry out reactions like these at a late-stage of the synthesis. Keeping this our mind, a number of attempts were made at each stage in order to remove the tosyl group. Chapter 3 summarizes the details of some of the challenges faced during detosylation of various pyrrolidine substrates.

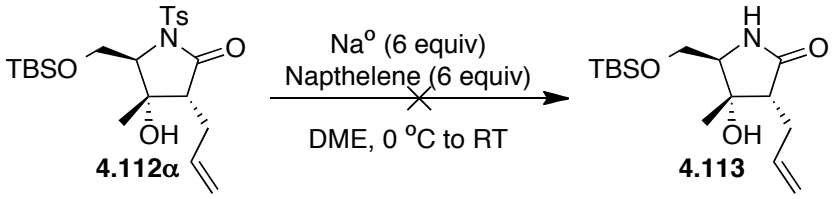


**Scheme 4.36** Detosylation under sodium-naphthlenide conditions.

Upon treatment of compound **4.112α** with sodium and naphthalene at 0 °C in DME, no reaction was observed. However upon warming the reaction mixture to room temperature, several undesired products were observed as analyzed by TLC (Scheme 4.36). Magnesium-MeOH mediated detosylation reaction was reported by Nyasse and coworlers and a number of successful attempts have been reported in literature.[64] To our delight, when compound **4.112α** was treated with powdered magnesium metal in methanol, and sonication for 1 h, the detosylated compound **4.113** was delivered with excellent yield (Scheme 4.37).

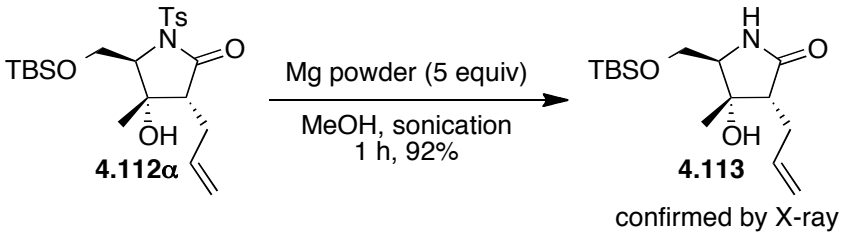


**Scheme 4.37** Mg-MeOH mediated detosylation reaction.

The identity of the de-tosylated product was further confirmed by X-ray structure analysis (Figure 4.9). This structure further confirms the stereochemistry at C-3 position, which was established previously on the basis of coupling constants, NOE results and clearly reveals the *anti* disposition of C-3 methyl and allyl substituent at C-4 position.

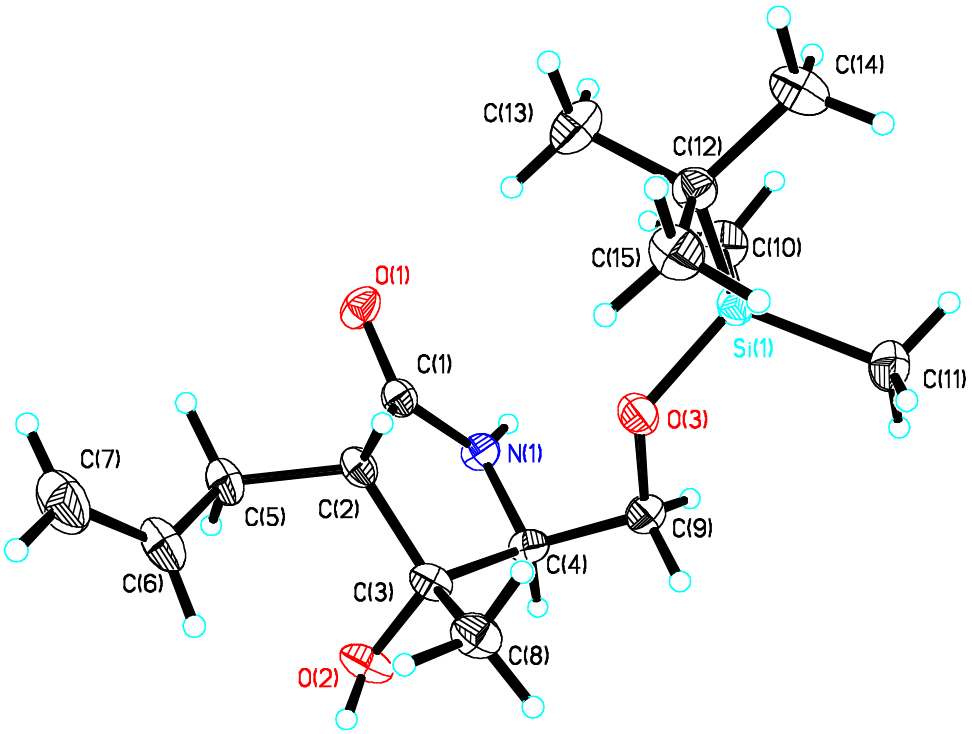


**Figure 4.9** X-ray structure of detosylated lactam **4.113**.

### 4.6.6 Attempts at C-5 alkylation and β-lactonization.

Having access to detosylated intermediate **4.113** in hands, we then turned our attention toward constructing the C-5 quaternary stereocenter. At this point, we required both C-5 functionalization and β-lactonization in order for this intermediate to progress towards our immediate advanced precursor to salinosporamide A (Scheme 4.38).

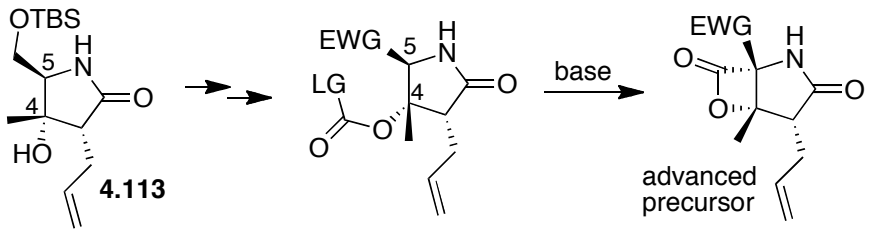


**Scheme 4.38** Strategy to install β-lactone via O-carbonylation.

Our synthetic route demanded installation of carboxylic acid derivative at C-5, which would be able to lactonize with the hydroxyl group present at C-4 in order to assemble β-lactone with the appropriate stereochemistry. Thus we proceeded with our plan where carboxylic acid derivative would be revealed via oxidation of the primary alcohol at C-5. This would render alkylation possible at this position using enol/enolate chemistry. Considering the requirement to install carboxylic acid derivative at α-face (*syn* to C-4 alcohol), we decided to incorporate a carbonylating reagent intramolecularly tethered to the tertiary alcohol at C-4. It was hoped that treatment under acid/ basic conditions would lead to the intramolecular alkylation at C-5, in turn delivering the β-lactone with the required stereochemistry (Scheme 4.39). Alternately, a bis-carboxylate

intermediate[9] can also be revealed (Scheme 4.39), where only the *cis* substituted ester with respect to the C-4 tertiary alcohol would participate in the lactonization.

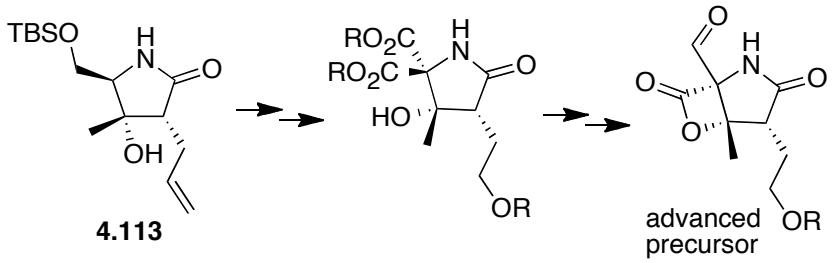


**Scheme 4.39** C-5 alkylation and β-lactonization required to proceed to the advanced precursor to salinosporamide A.

### 4.6.6.1 Attempts at O-carbonylation.

We investigated the scope of C-4 hydroxyl group in de-tosylated lactam **4.113** towards carbonate formation. Alcohol **4.113** was treated with triphosgene, in the presence of DMAP.

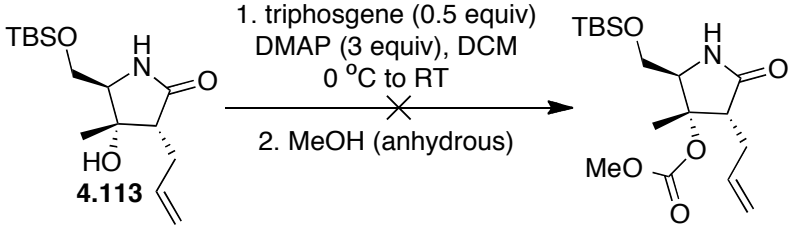


**Scheme 4.40** An attempt at O-carbonate formation via treatment with phosgene.

[9] Two identical alkyl/aryl esters would be installed at C-5 that would simplify the stereochemical issues during its installation.

Labile alkoxycarbonyl chloride generated in-situ was then treated with anhydrous methanol in order to generate methyl carbonate. However, several products were observed when analyzed by TLC and NMR. Desilylation was identified as one of the side reactions. In another attempt triphosgene was replaced with sterically less encumbered and more reactive reagent phosgene.

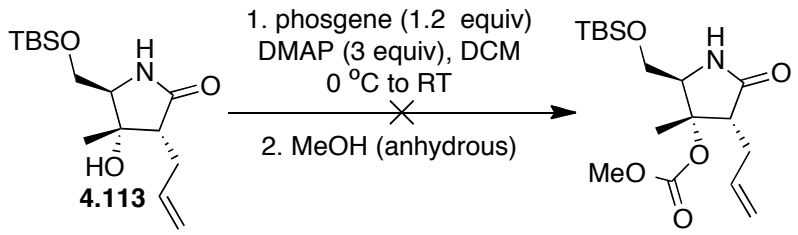


**Scheme 4.41** An attempt at carbonate formation at C-4 hydroxyl group.

However, a messy crude NMR spectrum in this case also indicated the occurrence of several undesired products. Desilylation was also seen in this case. A more reactive primary alcohol, if revealed, would compete towards O-carbonate formation. The methyl carbonate if formed at primary alcohol, might lead to intramolecular carbonate formation with the assistance of the tertiary alcohol. Participation of the amide towards carbamate formation or carbonylation of the imidate cannot be ruled out either. As a result, we decided to carry out formation of methylcarbonate by treatment of *in-situ* generated lithium alkoxide followed by quenching with carbonylating electrophiles. Thus alcohol **4.113** was treated with LiHMDS to generate the alkoxide and later quenched with methylchloroformate to afford a 1:3 mixture of mono-protected (N-carabamate) and bis protected (O-carbonate + N-carbamate) products (Scheme 4.42). Mono-protected

O-carbonate compound was never observed under these conditions. This may suggest that N protection might occur faster than O-carbonate formation.[10]

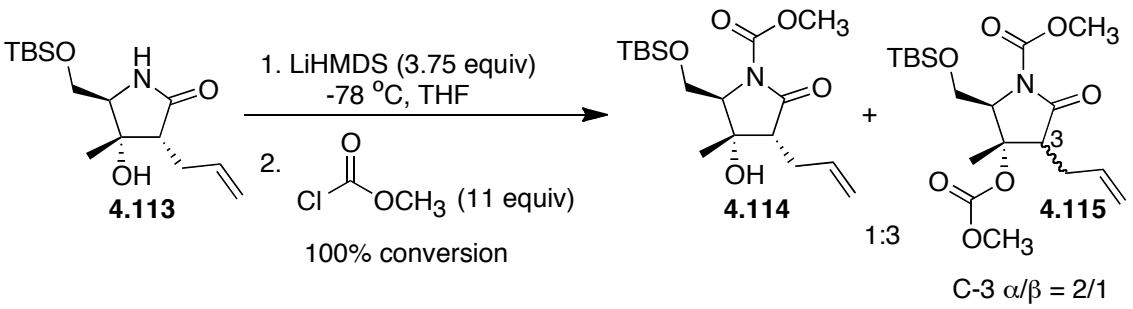


**Scheme 4.42** Carbonate and carbamate formation.

Also the electrophilic attack at the tertiary alcohol might be sluggish as compared to that on the $sp^2$ hybridized nitrogen. Thus reaction proceeds initially to giving *N*-carbamate **4.114**, which undergoes successive trap on the tertiary alcohol to form the bis-protected compound **4.115** (Scheme 4.43). When the amount of LiHMDS and methylchloroformate reagent was lowered to 1.2 and 1.5 equivalent, respectively, only *N*-carbamate **4.114** was observed which proceeded with 100% conversion. We were initially startled by the epimerization exclusively observed in the case of the bis-protected **4.115** compound. When C-4 hydroxyl gets protected as carbonate, it leads to steric repulsion between two large groups at C-4 and C-3 disposed on the same side.

[10] The pKa of a tertiary alcohol is approximately 29.4 (DMSO) whereas that of a 5-member lactam is 24.1 (DMSO).

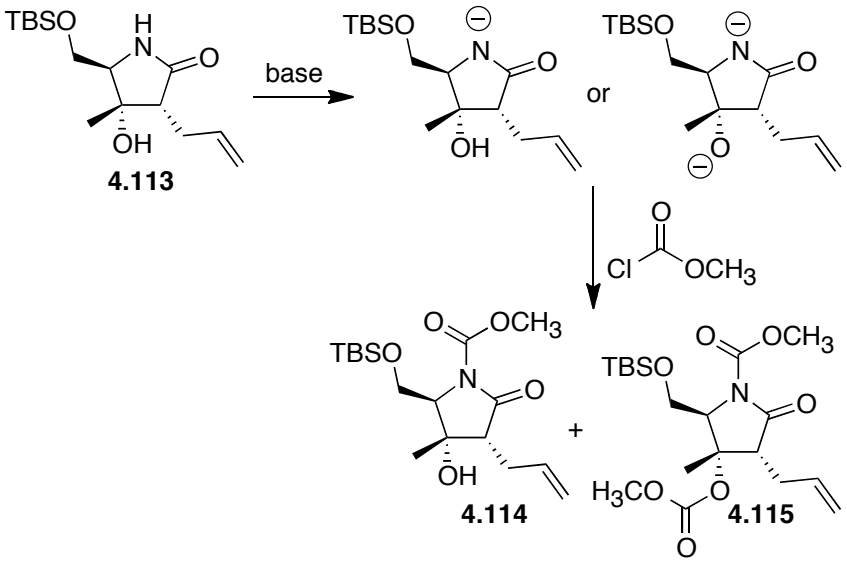


**Scheme 4.43** Acylation leads to both mono and bis protected compounds.

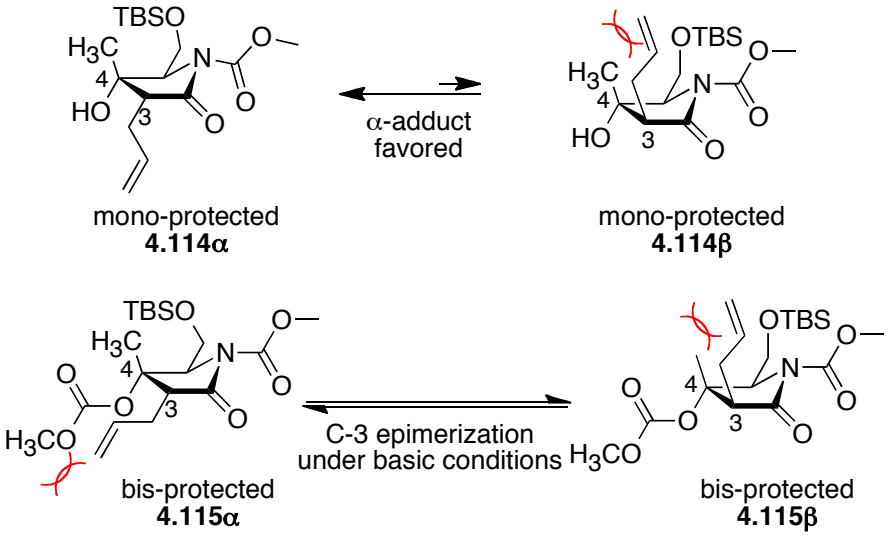


**Figure 4.10** Severe steric clash between groups substituted at C-3 and C-4 leads to epimerization in bis-protected **4.115** only.

This interaction favors the β-isomer **4.115 β** unlike that observed in the case of mono-protected **4.114** compound (Figure 4.10). This explains the fact that only bis-protected

compound suffers from C-3 epimerization, since mono-protected compound **4.114** does not experience any change in steric clash between substituents at C-3 and C-4 positions.

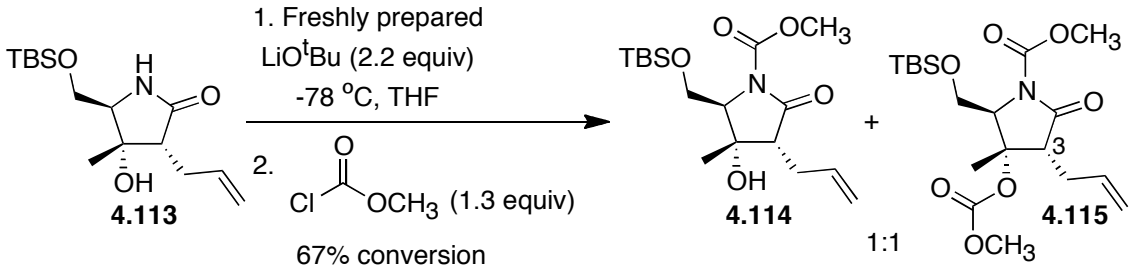


**Scheme 4.44** LiO$^t$Bu mediated acylation.

We realized that use of strong basic conditions employed in the reaction might cause this epimerization. Thus, our primary focus became the tuning of the basicity of the reaction while carrying out carbonate formation. LiO$^t$Bu has been reported in literature as a weak basic and nucleophilic metal alkoxide.[65,66] When LiO$^t$Bu was employed and reaction was carried out on alcohol **4.113**, an equimolar mixture of mono- and bis-protected compound was obtained. Although under these conditions, low conversion was achieved, no epimerization was observed in case of di-protected compound **4.115**. Table 4.3 summarizes the conversion and ratios of mono and bis-protected compound, obtained in case of both of the reagents.

**Table 4.3** Mono and bis-protection achieved under different conditions.

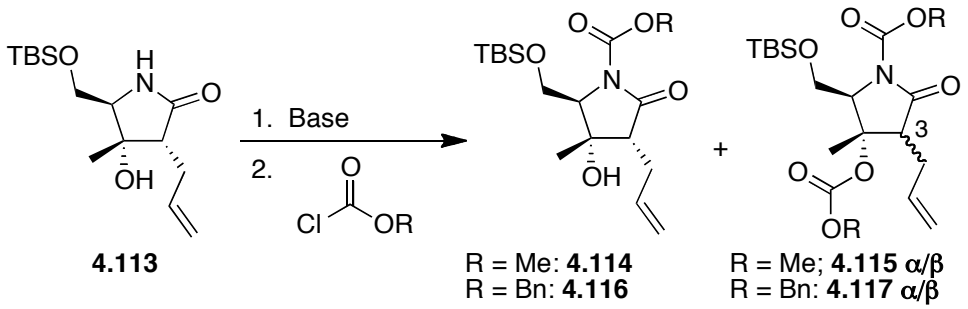


**4.113**

R = Me: **4.114**
R = Bn: **4.116**

R = Me; **4.115** α/β
R = Bn: **4.117** α/β

| entry | base (equiv) | *R* (equiv) | conditions | products ratio ($\alpha$:$\beta$)[11] | conv. (%) |
|---|---|---|---|---|---|
| 1 | LiHMDS (3.75) | *Me* (11) | THF, -78 to 0 °C | **4.114**:**4.115** =1:3 (2:1)[8] | 100 |
| 2 | LiHMDS (1.2) | *Me* (1.5) | THF, -78 to 0 °C | **4.114**:**4.115** =1:0 | 35 |
| 3 | LiO$^t$Bu[12] (2.2) | *Me* (1.3) | EtOAc, DMF $^t$BuOH, -40 to 0 °C | **4.114**:**4.115** =1:1 | 67 |
| 4 | LiO$^t$Bu[9] (3.75) | *Bn* (4) | EtOAc, DMF $^t$BuOH, -40 to 0 °C | **4.116**:**4.117** =0:1 | 100 |

Upon escalating the equivalents of both the reagents and using benzylchloroformate (entry 4) only bis-protected compound **4.116** was obtained without any epimerization, along with complete conversion. Thus we decided to incorporate these conditions in our route, where we had an access to O-carbonate compound having nitrogen masked as carbonate (Scheme 4.45). Next desilylation of the primary alcohol was required in order to elaborate it into a carboxylic acid derivative.

[11] Ratio of the α and β epimers at C-3.

[12] Reagent was freshly prepared. See experimental section for the procedure.

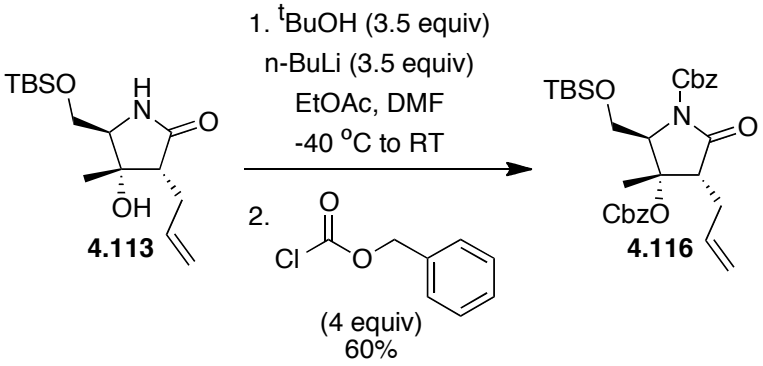


**Scheme 4.45** Successful protection of both N and O.

The TBS ether **4.116** was treated with TBAF but unfortunately that lead to an inseparable mixture of compounds, some of which were identified as elimination products (Scheme 4.46). Several conditions for removal of the silyl protecting group were tried but all led to the elimination of either one or both the alcohols at C-4 and C-5 (Table 4.4).

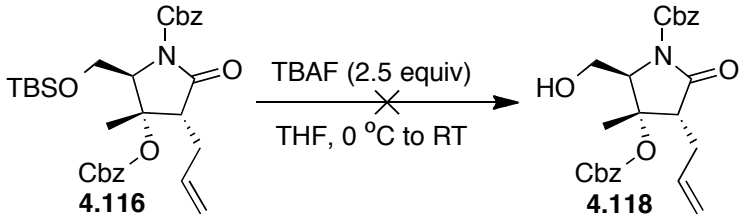


**Scheme 4.46** Failed silyl deprotection of the TBS ether.

Although due to characteristic NMR resonances, these compounds could be identified, in the absence of separation and isolation of pure materials, their identity could not be completely confirmed. Clearly TBAF appeared to be harsher leading to the elimination of both the alcohols. Mild acidic conditions (entry 3 and 4) either returned starting

material or afforded mono elimination product **4.119**. Lewis acid treatment also gave a mixture of mono and bis-elimination products (entry 5).

**Table 4.4** Different de-silylating conditions tried on TBS ether.

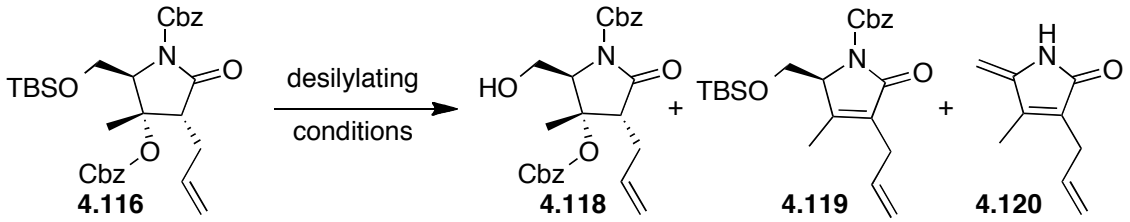


| entry | desilylating conditions | products[13] |
|---|---|---|
| 1 | TBAF, THF, 0 °C | **4.119** + **4.120** (major) |
| 2 | TBAF, DMF, 0 °C | **4.119** + **4.120** (major) |
| 3 | AcOH, $H_2O$, THF (3/1/1) | n.r. |
| 4 | TsOH (cat) + THF/$H_2O$ (20/1) | **4.119** + **4.116** |
| 5 | $BF_3$•$OEt_2$ | **4.119** + **4.120** |
| 6 | $Bu_4N^+Si^-F_2Ph_3$ | **4.119 (major)** + **4.116** |

Unfortunately, even use of milder reagents such as tetrabutylammonium difluorotriphenylsilicate could not prevent these eliminations.[67] The tertiary alcohol is likely to be transformed into a leaving group under the reaction conditions and further location at a position β to a carbonyl, might facilitate its elimination. Although at this point elimination of the primary alcohol was not anticipated. Under basic conditions

[13] The ratios were determined by the analysis of crude NMR spectra.

elimination of the benzyloxycarbonate in **4.116** is likely to proceed via $E_{1CB}$, due to the stabilization of the carbanion via the C-2 carbonyl. This leads to the generation of $\alpha,\beta$-unsaturated $\gamma$-lactam **4.119** in mono elimination product. Elimination of the primary alcohol might proceed via an intramolecular acyl transfer, facilitating its removal that leads to a conjugated system (Scheme 4.47).

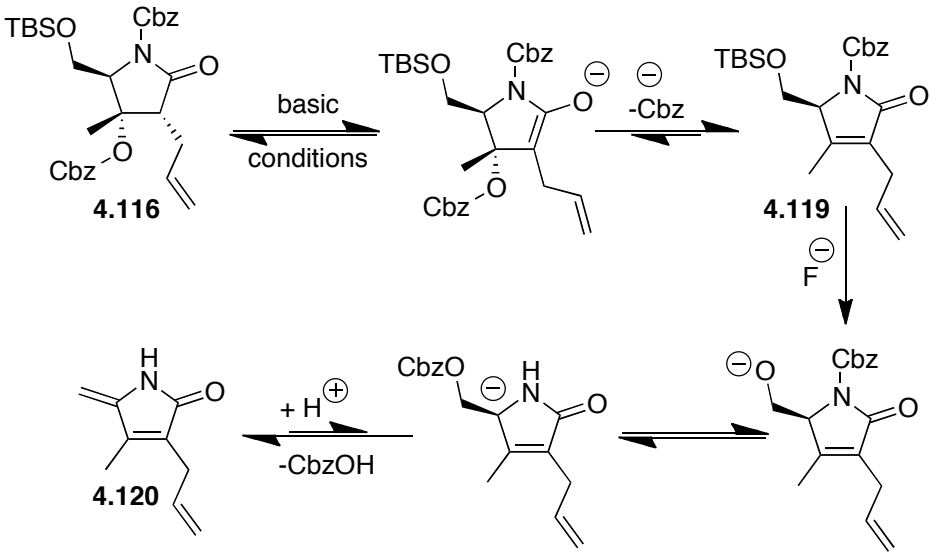


**Scheme 4.47** Mechanistic hypothesis for the elimination reaction observed during de-silylation conditions.

Thus it seems that the presence of the O-carbonate activates the alcohol toward elimination, and N-protected amide further assists the elimination of the primary alcohol. Figure 4.11 illustrates some of the identified problems associated with the structure of the intermediates, which makes elimination a competing and unavoidable problem during the de-silylation process. Thus we decided to switch the sequence of the O-

carbonylation and desilylation reactions. It was envisaged that the generation of a naked tertiary alkoxide under basic conditions would dissuade the undesired elimination pathway.

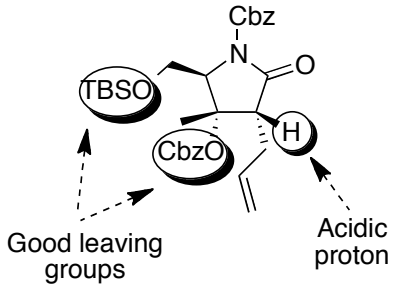


**Figure 4.11** Structural features responsible for the undesired elimination pathways.

Indeed when lactam **4.113** was treated with TBAF at low temperature, desilylation took place smoothly to afford the desired unmasked alcohol **4.121** with excellent yield (Scheme 4.48). This further corroborates our hypothesis proposed for the competing elimination during de-silylation reactions (Scheme 4.47).

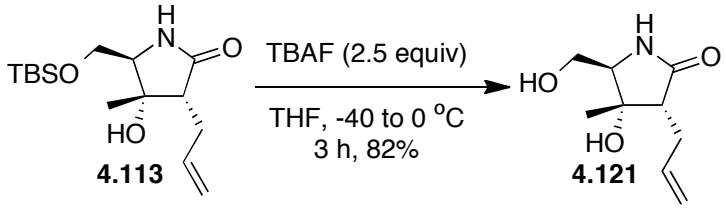


**Scheme 4.48** TBAF mediated desilylation of TBS ether.

Lactam **4.121** was then treated with Boc anhydride in order to mask it as a carbamate. Since selective N-protection had to be achieved, initially mild conditions were applied under sonication, but no reaction occurred (Scheme 4.49).

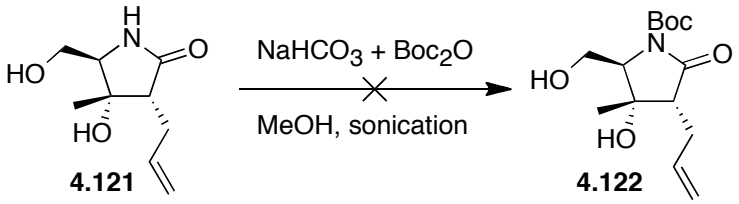


**Scheme 4.49** Failed N-carbamate formation under mild conditions.

Later lactam **4.121** was treated with Boc anhydride but in the presence of stronger base and ACN as solvent, which lead to a mixture of N-Boc and O-Boc compounds. Interestingly, under these conditions, intramolecular acylation of oxygen might assist via the neighboring nitrogen atom consistent with the reported migration of Boc in case of pyroglutamate compounds (Scheme 4.50).[68]

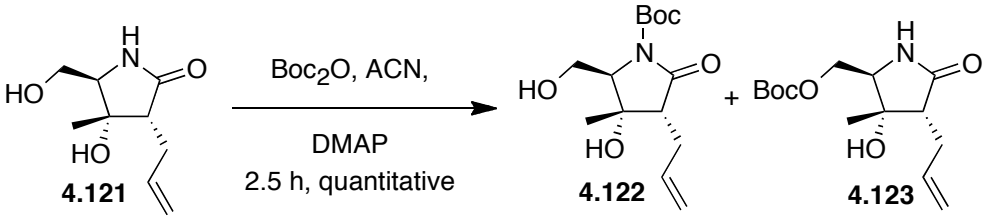


**Scheme 4.50** *N*-Boc migration observed in lactam.

Thus, we again decided to switch the order of the steps and carried out Boc protection of the lactam **4.113** first, which occurred efficiently to provide the carbamate **4.124** in

quantitative yield (Scheme 4.51). Unfortunately desilylation of the carbamate again led to a mixture of both N and O-Boc protected compounds.[69]

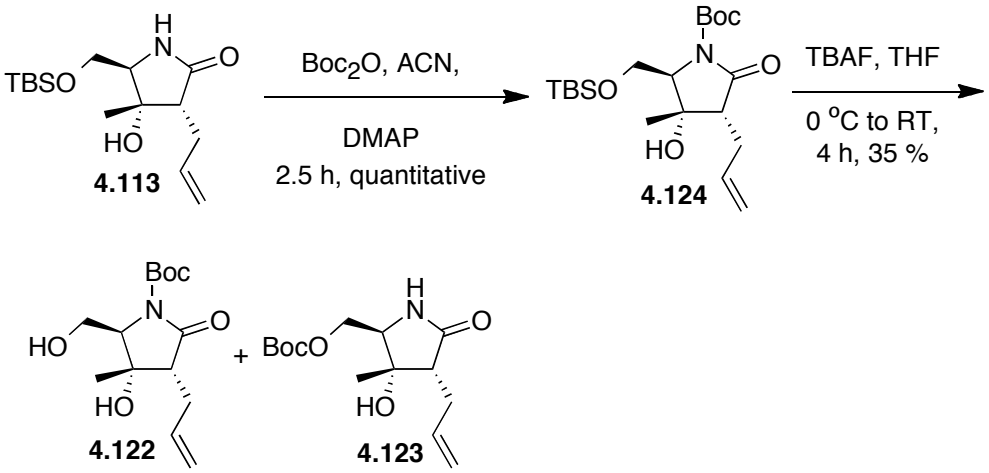


**Scheme 4.51** *N*-Boc protection and desilylation.

At this point we were aware of the challenges associated with acyl type protecting groups on nitrogen, suffering from migration problems, as observed in case of Boc and Cbz protecting groups. An alternative would be to leave nitrogen unmasked or keep tosyl on and explore a suitable detosylation stage later. Also, we were unsuccessful in our attempt to probe a system to perform intramolecular alkylation via tethering a carbonylating electrophile in tertiary alcohol, as a result of the dominating β-elimination pathways. These competing elimination problems were also manifested when TBS removal was attempted while O, N were masked as carbonate and carbamates.

Based on this information, we decided to probe oxidation of the C-5 primary alcohol and put efforts toward functionalization of the C-5 alcohol, leaving the C-4 tertiary alcohol unmasked (this would make it least favorable leaving group under basic conditions). At

this point we also chose to retain to Ts as the protecting group on nitrogen to first examine conditions for C-5 functionalization. If necessary or demanded later, we had identified this stage suitable to perform de-tosylation and substitute it with a more labile protecting group. Further late-stage detosylation could also be explored. Thus *N*-Ts lactam **4.112α** was chosen as a model substrate to perform all the studies required in order to investigate C-5 alkylation.

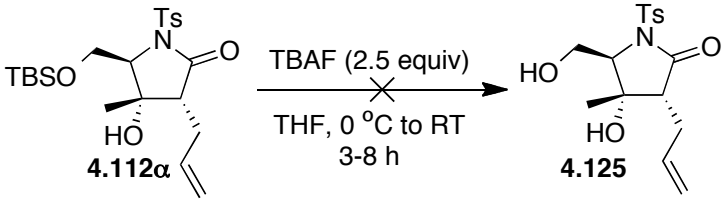


**Scheme 4.52** Failed de-silylation with TBAF.

When TBS ether was treated with TBAF, no de-silylation was observed (Scheme 4.52). On the other hand treatment with HF-pyridine yielded TBS deprotected lactam **4.125α** in excellent yield along with 15% of C-3 epimer **4.125β** (Scheme 4.53).

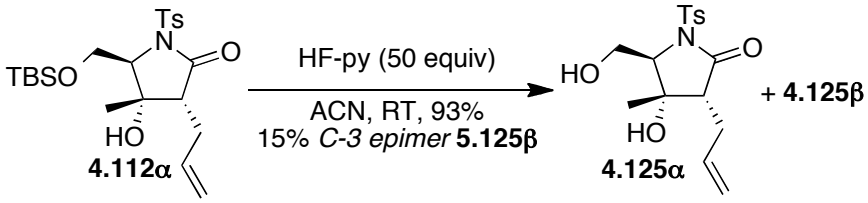


**Scheme 4.53** HF-pyridine assisted de-silylation of TBS ether.

The observed epimerization observed can be reasoned due to the perturbed equilibrium since TBS removal makes the primary alcohol sterically less encumbered (Scheme 4.34). The revealed primary alcohol was subjected to DMP oxidation under buffered conditions, which yielded aldehyde **4.126** in good yield (Scheme 4.54).

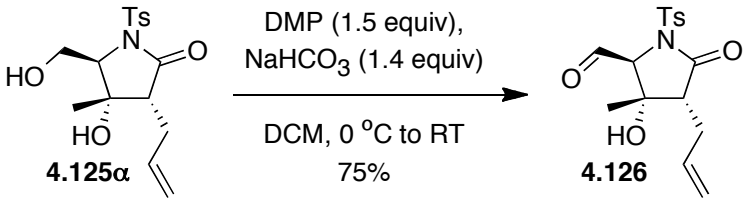


**Scheme 4.54** DMP oxidation to yield aldehyde.

We required a reactive electrophile which could chemoselectively perform C-alkylation and later could participate in C-4 O-acylation intramolecularly. Methylcyanoformate (Mander's reagent) is a commonly employed reagent, which has been reported to yield β-ketoesters regioselectiviely through C-acylation of preformed lithium enolates.[70,71] It is considered a better choice than other acylating agents such as acyl chloride, anhydrides and carbon dioxide that could also lead to several un-desired O-acylated products.

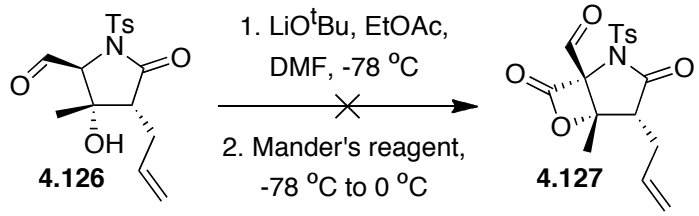


**Scheme 4.55** Enolate mediated C-5 alkylation and β-lactonization attempt.

The aldehyde precursor **4.126** was treated with freshly prepared LiO$^t$Bu (milder conditions as established previously) followed by addition of Mander's reagent. Unfortunately a mixture of several un-identified products was observed as analyzed by both TLC and NMR spectroscopy (Scheme 4.55).

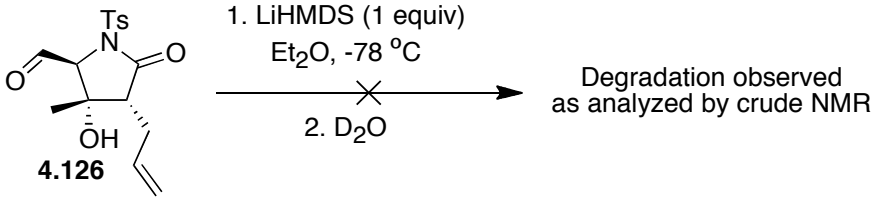


**Scheme 4.56** Aldehyde exhibited instability under basic conditions.

Although, formation of O-acylated, C-3 and C-5 acylated products cannot be ruled out, possibility of retro-Aldol might further add complications. In order to test the latter supposition, the stability of the aldehyde intermediate was examined under basic conditions. LiHMDS was added to the solution of aldehyde in ether at -78 °C followed by quenching with deuterated water to probe the efficiency of the deprotonation.

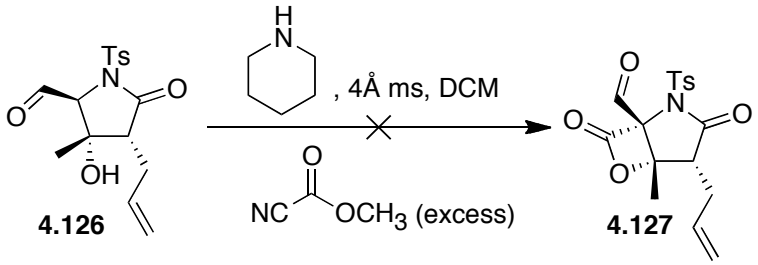


**Scheme 4.57** Cyclization attempted via enamine-catalysis.

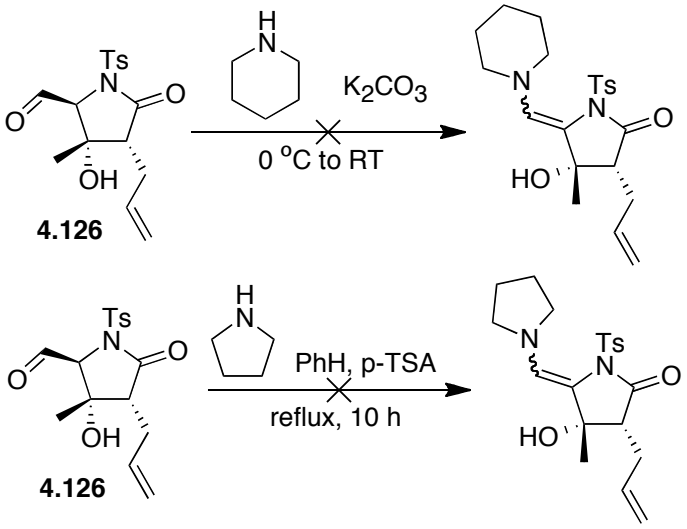


**Scheme 4.58** Attempts to form enamine.

Unfortunately degradation was observed under these conditions. We also examined the scope of this aldehyde intermediate towards C-5 functionalization under acidic conditions. For this purpose, aldehyde **4.126** was treated with piperidine and molecular sieves. Mander's reagent was added in the same pot in hope to carry out C-5 acylation via enamine (Scheme 4.57). Unfortunately no reaction took place in this case. We then looked at other conditions required for the enamine formation (Scheme 4.58). Conditions employing both piperidine and pyrrolidine rings were investigated.

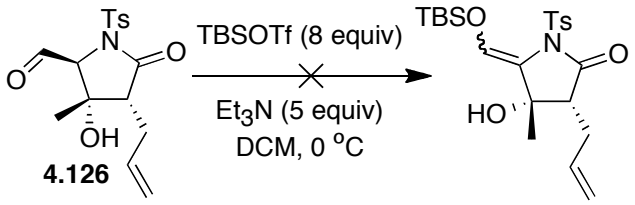


**Scheme 4.59** Cyclization attempted via enol ether-catalysis.

Further both basic and acidic conditions were attempted, but no enamine formation was observed when analyzed by TLC or NMR spectroscopy of the crude reaction mixture. Formation of silyl enol ether was also attempted using reactive silylating reagents such as TBSOTf, but this led to a mixture of several un-identified compounds along with some recovered starting material (Scheme 4.59). However, lability of either enamine or enol ether cannot be ruled out. For the cases when a one-pot alkylation was attempted via *in-situ* generated enamine/enol intermediates, alkylation might be a challenging task bearing in mind the sterically hindered nature of the C-5 carbon (tertiary carbon). Proximity to the C-4 center, adds to the steric demands imposed by the substrate. Further, elimination of the tertiary alcohol might be feasible under acidic conditions, which would add to the complications associated with these reactions.

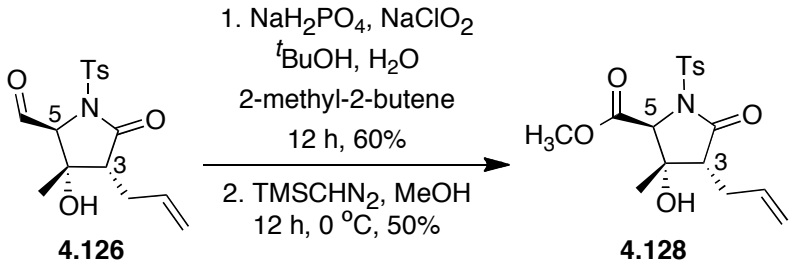


**4.126** **4.128**

**Scheme 4.60** Synthesis of the ester intermediate.

Keeping this information in mind, we turned our attention back towards functionalization under basic conditions. Lability of the aldehyde precursor was also known at this point (Scheme 4.56). Thus reactive aldehyde precursor **4.126** was taken to the next oxidation

state by subjecting it to Pinnick oxidation followed by TMS diazomethane mediated esterification to yield ester **4.128** (Scheme 4.60).

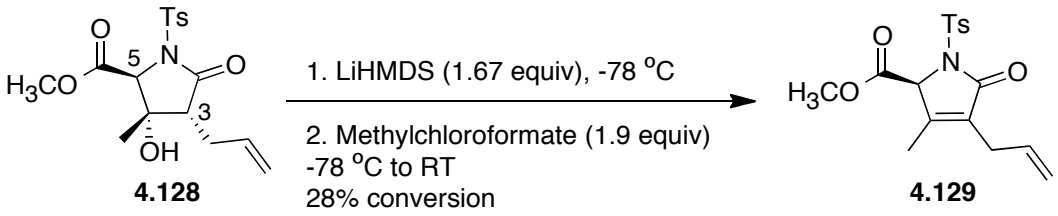


**Scheme 4.61** C-5 alkylation suffered by β-elimination pathway.

Lithium enolate of ester **4.128** was generated at -78 °C and methylchloroformate was added while keeping the temperature strictly at -78 °C. No reaction was observed when analyzed by TLC at this temperature. However, gradual warming to room temperature yielded only undesired β-elimination product **4.129**, this transformation proceeded with only 28 % conversion. Scheme 4.62 outlines both desired (pathway a) and the undesired pathway (pathway b) originating from *in-situ* generated O-carbonate ester **4.128-carbonate** (Scheme 4.62). Pathway a represents the desired approach, where a lithium enolate would attack the carbonyl of the methyl carbonate generated *in-situ* on C-4 alcohol. Elimination of methoxide would then occur via the tetrahedral intermediate to install the β-lactone. Pathway b outlines the undesired β-elimination process, where deprotonation at C-3 along with elimination of methylcarbonate would lead to the α,β-unsaturated γ-lactam **4.129**. Although initial deprotonation might occur at C-5, isomerization to the observed α,β-unsaturated lactam can not be ruled out, the *anti*

disposition of the C-4 carbonate (leaving group) and that of the proton at the C-3 might also facilitate the elimination leading to the observed product.

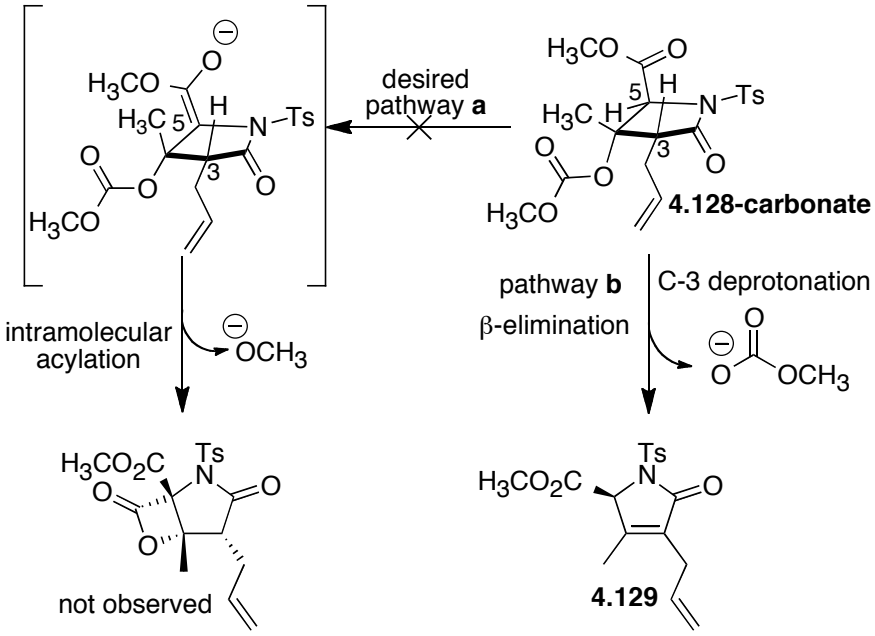


**Scheme 4.62** β-elimination predominates during C-5 alkylation conditions.

From the experimental observation, it is evident that pathway b predominates and competes with the β-lactonization. Thus, the intended alkylation seemed challenging in the presence of acidic proton at C-3. We became interested in lowering the acidity of the C-3 proton, and thus avoiding deprotonation at C-3. We decided to elaborate the allyl substituent into a group, which could be tethered to the C-4 alcohol, while achieving its oxidation at the same time. This would transform the current lactam compound into a *cis* 5,5 fused system. We had anticipated that this would lower the acidity of C-3 proton, since its deprotonation would lead to a less conjugated system involving the C-2 carbonyl due to the strain associated with the fused rings.

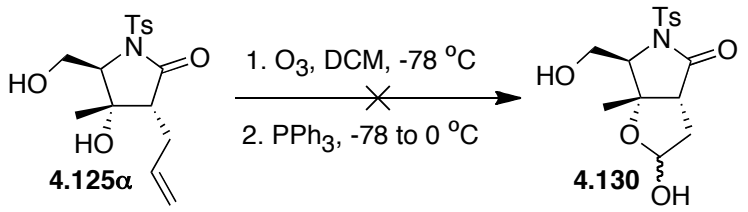


**Scheme 4.63** Failed synthesis of lactol with exposed C-5 primary alcohol.

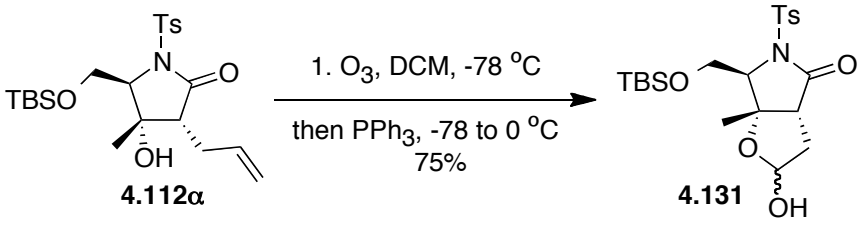


**Scheme 4.64** Ozonolysis of the TBS ether compound.

Ozonolysis of **4.125α** at -78 ºC followed by reductive work-up only returned the starting material. Notice, polarity of the starting material might create solubility issues and could prevent the reaction in dichloromethane (Scheme 4.63). However, ozonolysis of the corresponding TBS ether **4.112α** afforded lactol **4.131** as 1:1 mixture of diastereomers (epimers at acetal carbon) (Scheme 4.64), which was then oxidized by PCC in presence of molecular sieves. Both lactone formation and TBS removal (unmasking of C-5 primary alcohol) in one pot gave compound **4.132** with only 30% yield (Scheme 4.65).

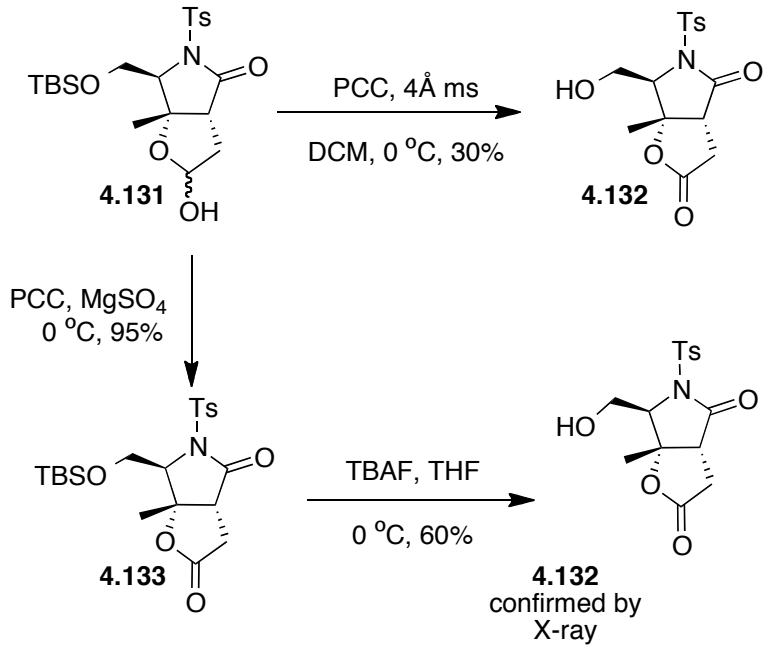


**Scheme 4.65** Formation of lactone and TBS removal to reveal alcohol.

Surprisingly when PCC was used in the presence of dehydrating reagent $MgSO_4$, excellent yield of the lactone **4.133** was obtained (Scheme 4.65). Notice, the latter conditions were found to be milder since no de-silylation was observed during this reaction. Later TBS ether **4.133** was treated with TBAF in order to obtain the primary alcohol **4.132** in moderate yield (Scheme 5.65). The structural identity of this lactone was confirmed by X-ray crystallography (Figure 4.12).

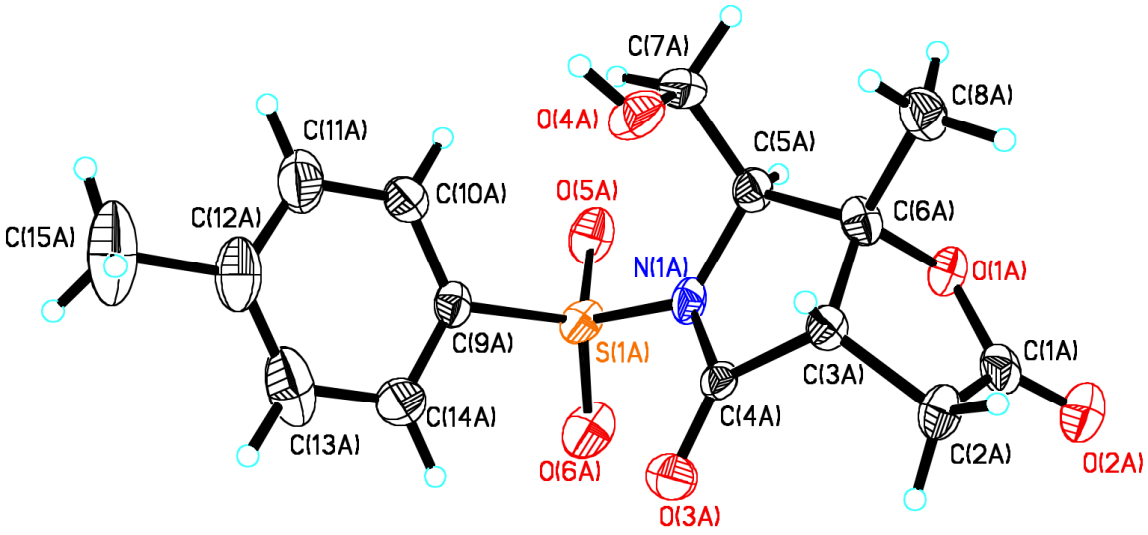


**Figure 4.12** X-ray structure of lactone **4.132**.

Initial attempts at oxidation of primary alcohol **4.132** were challenging. Treatment of alcohol with DMP under usual conditions only delivered un-reacted starting material back (Scheme 4.66). Later several attempts were made to investigate conditions to convert the alcohol into the desired aldehyde **4.134**. Table 4.5 lists various conditions where the oxidation to the aldehyde was carried out. PCC oxidation with $MgSO_4$, which proved very efficient in case of lactol oxidation, only delivered starting material in this case.

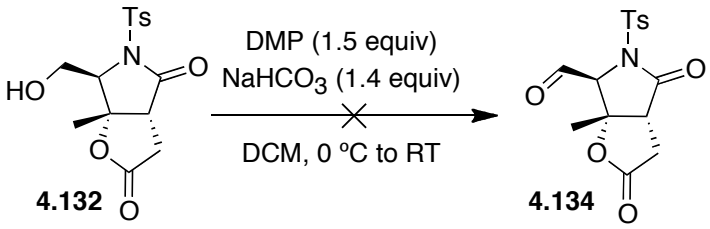


**Scheme 4.66** Failed oxidation of alcohol by DMP.

TPAP has been a popular catalytic room temperature stable oxidizing reagent reported in literature, but no reaction was observed in our case.[72] Swern oxidation upon employing DMSO and TFAA and a base also returned starting material.[73] Interestingly, TEMPO based oxidation under both buffered and non-buffered systems gave an isomeric mixture of aldehydes along with a mixture of other unidentified products. Perhaps due to instability, these aldehydes could not be purified and therefore remained unidentified. This unreactivity displayed by the primary alcohol was unexpected and came as a surprise. Proximity to sterically encumbered C-4 quaternary center might make it challenging yet, one cannot completely rule out the influence of electronics. Disheartened by all these efforts, we then chose to transform the alcohol into the carboxylic acid functionality. Catalytic ruthenium in the presence of stoichiometric amount of oxidant ($NaIO_4$) is a well established mild way to oxidize primary alcohols to carboxylic acid, via an intermediancy of *in-situ* generated aldehyde.[74] This again, was found unreactive when employed for our substrate (Scheme 4.67). With the unreactive nature of the primary alcohol we chose to experiment with the harsher Jones oxidation conditions. To our delight, when alcohol **4.132** was treated with excess of Cr(VI) and sulfuric acid the desired carboxylic acid **4.135** was obtained with quantitative conversion (Scheme 4.68). Notably, the reaction time was long even after using an excess amount of reagents at room temperature.

**Table 4.5** Various oxidation methods to obtain the aldehyde intermediate.

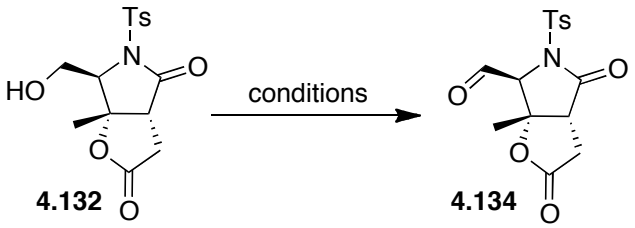


| entry | conditions | products |
|---|---|---|
| 1 | DMP, $NaHCO_3$, DCM, 0 ºC to RT | n.r. |
| 2 | PCC, $MgSO_4$ DCM, RT | n.r. |
| 3 | TPAP, NMO ACN, RT | n.r. |
| 4 | DMSO, TFAA, TEA DCM, -78 ºC to RT | n.r. |
| 5 | TEMPO, KBr, $NaClO_2$ DCM, 0 ºC to RT | 2 aldehydic compounds + other impurities (inseparable) |
| 6 | TEMPO, KBr, $NaHCO_3$, $NaClO_2$, DCM, 0 ºC to RT | 2 aldehydic compounds + other impurities (inseparable) |

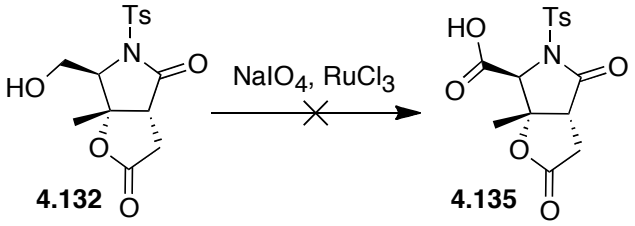


**Scheme 4.67** An attempt at ruthenium mediated oxidation of alcohol.

Due to the polar nature of the substrate, the crude carboxylic acid product was esterified without purification. Treatment with TMS diazomethane afforded ester **4.136** with low yield. However, Lewis acid mediated esterification provided the desired ester in high

yield. This clearly suggested the sensitivity of this compound under basic conditions (Scheme 4.69).

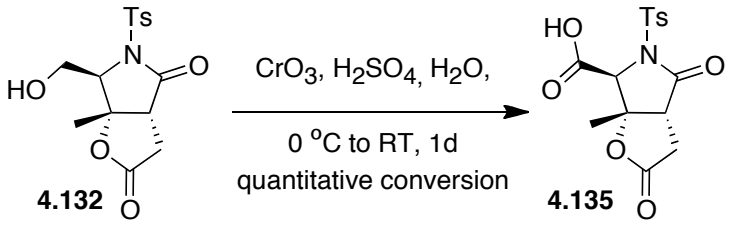


**Scheme 4.68** Jones oxidation yields carboxylic acid.

With the ester in hand, we could explore alkylation conditions. Previously we had examined the scope of different electrophiles such as methylchloroformate and Mander's reagent. Unfortunately neither provided the desired alkylation. At this point we became interested in screening other reactive electrophiles for C-5 alkylation. N-methylmethoxycarbonyl imidazole is used to regioselectively perform C-alkylation (instead of O-alkylation).[75] Thus the reagent **4.137** was prepared in one step starting from imidazole according to a reported procedure, with an excellent yield (Scheme 4.70).[75] The lithium enolate of **4.136** was generated using excess amount of LiHMDS at low temperature followed by the treated with freshly prepared N-methoxycarbonyl imidazole **4.137**. No reaction was observed when the temperature was held at -78 °C (Scheme 4.71). To our disappointment, upon gradual warming, the reaction gave a mixture of different compounds, which was dominated by elimination products (signature peak in the crude NMR spectrum).

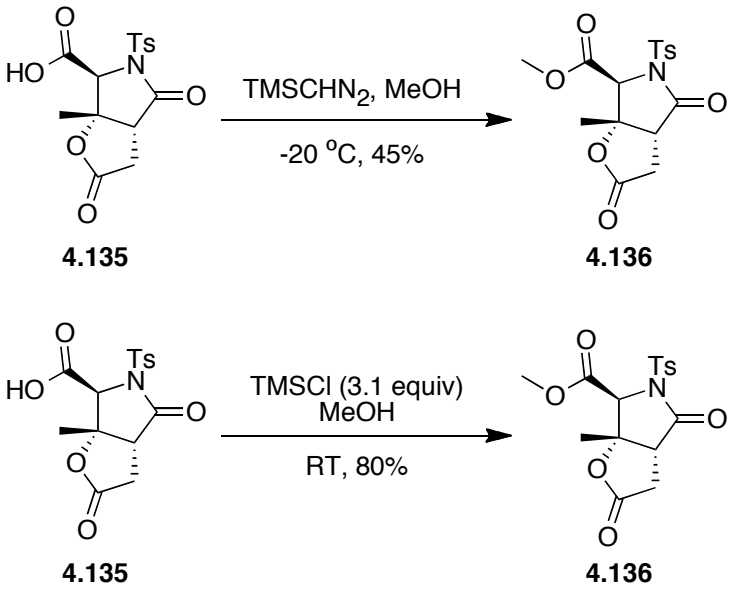


**Scheme 4.69** Esterification of the lactam acid.

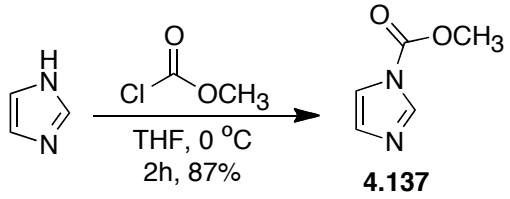


**Scheme 4.70** Synthesis of *N*-methoxycarbonyl imdizaole.

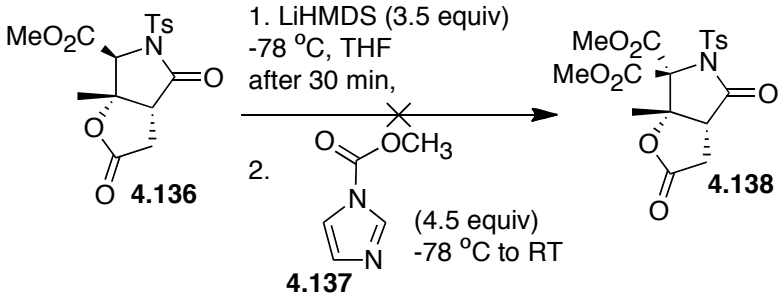


**Scheme 4.71** Failed attempt at C-5 alkylation.

We also investigated the scope of the highly reactive electrophile HCHO. The gas was generated *in-situ* by thermally cracking the polymeric formaldehyde reagent. The excess of this reagent was passed through the solution containing pre-generated lithium enolate of ester **4.136**. To our surprise, this reaction also afforded an inseparable mixture of three compounds (Scheme 4.72). Based on some of the signature peaks in crude NMR spectrum that an equimolar mixture of C-3 and C-5 alkylated compounds **4.139** and **4.140** was obtained. The C-3 alkylated compound appeared to exist as 1/1 mixture of both epimers at the C-5 position. C-5 alkylation was accompanied by elimination to form the $\alpha,\beta$-unsaturated lactam **4.140**.

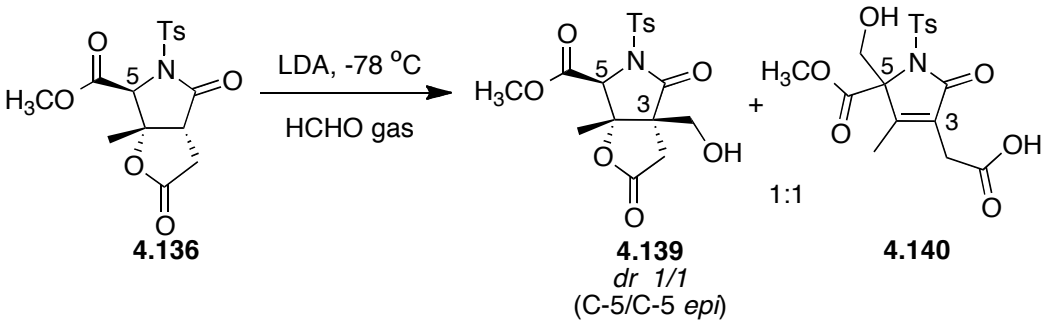


**4.136** **4.139** *dr 1/1* (C-5/C-5 *epi*) **4.140**

**Scheme 4.72** C-5 alkylation with $H_2CO$ electrophile gave mixture of undesired products.

## 4.67 Re-visiting previous C-5 alkylation strategies; challenges associated, solution and future endeavors.

At this point we wanted to analyze the problems associated with our previous strategies to carry out C-5 alkylation and carefully revise them. Scheme 5.73 illustrates our first strategy where C-5 alkylation and $\beta$-lactonization was attempted in one pot. Initially O-acylation was anticipated to occur which later would intramolecularly acylate the C-5

enolate formed under basic conditions. This would execute both construction of quaternary center at C-5 and β-lactone formation in one step. However, such efforts were impeded by the dominating β-elimination of O-acylated species. We also tried to employ various electrophilic reagents to carry out C-alkylation selectively. Thus, if C-alkylation occurs first, elimination of tertiary alkoxide would be un-favored which would dissuade un-desired elimination pathway. Unfortunately in our case, selective C-alkylation did not occur. All the eliminations lead to the formation of the α,β-unsaturated lactam (product with double bond between C-4 and C-5 and α,β-unsaturated ester was never observed).[76]

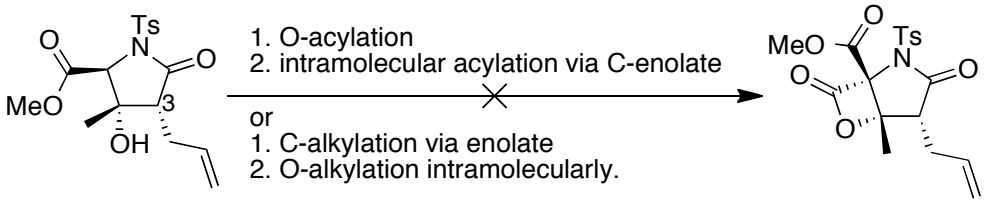


**Scheme 4.73** β-elimination foils attempt at one-pot C-5 alkylation and β-lactonization under various conditions.

This suggested two possibilities: 1) most probably $E_{1CB}$ (or $E_1$) elimination assisted by C-5 enolate to give rise to kinetic elimination product initially, which might isomerize to give the observed thermodynamic product. 2) Internal deprotonation can lead directly to the formation of observed α,β-unsaturated lactam (Scheme 4.74).

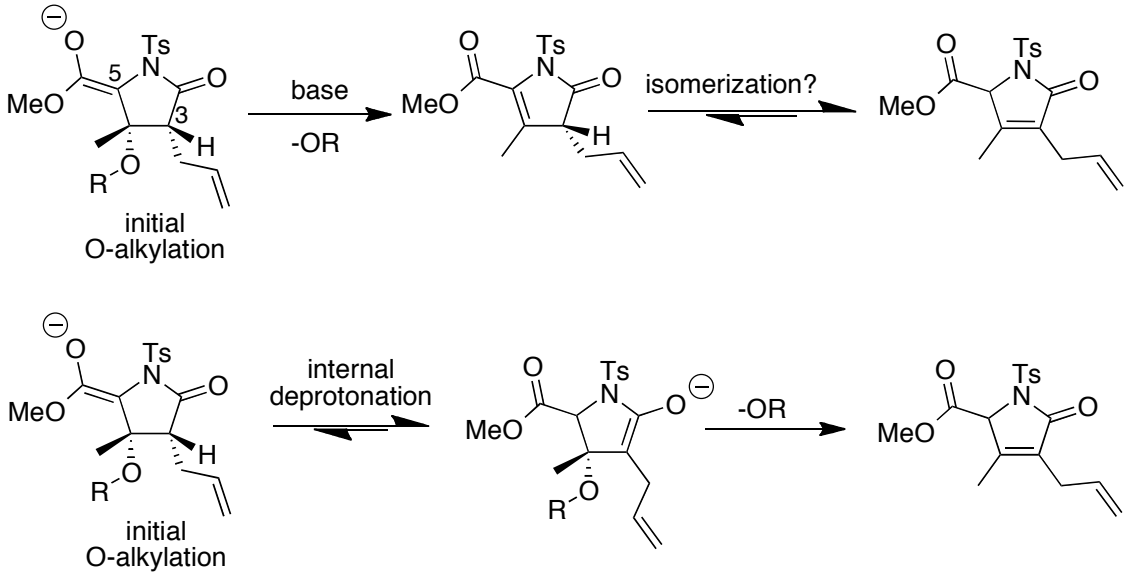


**Scheme 4.74** Proposed pathways for elimination.

Notice, *anti* arrangement of C-4 alkoxide and that of C-3 proton could also assist in the E2 elimination. Although it was difficult to rule out either of those two pathways, we decided to lower the acidity of C-3 proton and to study its influence on the alkylation reaction. Thus C-3 substituent was elaborated and tied to the C-4 hydroxyl group, which afforded a *cis* 5,5 fused system. It was anticipated that the latter would substantially lower the $pK_a$ of C-3 proton, since conjugation would be less favored for the C-3 enolate due to the ring strain. To our disappointment such an implementation did not help us over come elimination pathways (Scheme 4.72). Notice even after employing reactive electrophiles, both elimination to $\alpha,\beta$-unsaturated lactam and some C-3 alkylation was observed. Figure 4.13 outlines the structural features of both the precursors exploited in C-5 alkylation studies. On one hand, $pK_a$s of both C-3 and C-5 protons could be similar in case of intermediate **4.128** however, release of carboxylate

anion might still play a role in assisting elimination in case of **4.136** ester. This also indicates that enolate alkylation at sterically demanding C-5 position might be challenging and slow, thus leading to elimination processes.

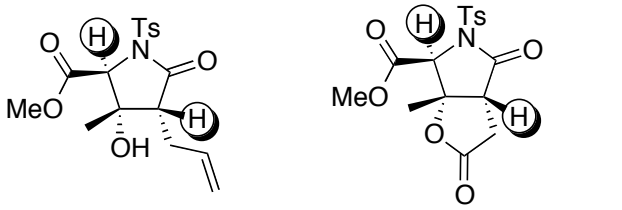


ester intermediate **4.128** bicyclic ester intermediate **4.136**

**Figure 4.13** Structural analysis of precursors to perform the C-5 alkylation.

#### 4.6.7.1 C-5 alkylation on masked C-2 carbonyl intermediates.

Higher acidity at C-3 facilitated the formation of the $\alpha,\beta$-unsaturated lactam assisting the elimination pathways. Thus the next step was to look at systems with the masked C-2 carbonyls and see if that would prevent such undesired elimination reactions. Lactam carbonyls can be protected as cyclic-imidates and are well precedent in the literature.[77-80] Table 4.6 outlines several such efforts where O-imidate formation was carried out. Notice, treatment with dimethylsulfate, one of the most reliable methods to protect lactams, either returned the starting material or if pushed too hard under microwave conditions led to degradation of the starting material (entry 1 and 2). Treatment with reactive halides such as allyl bromide in presence of freshly prepared silver oxide turned out to be a messy reaction, although when treated with methyl iodide O-imidate **A**, O

and N-alkylated products **B** and **D** were formed as analyzed by crude NMR (entry 3 and 4).

**Table 4.6** Attempts at imidate synthesis.

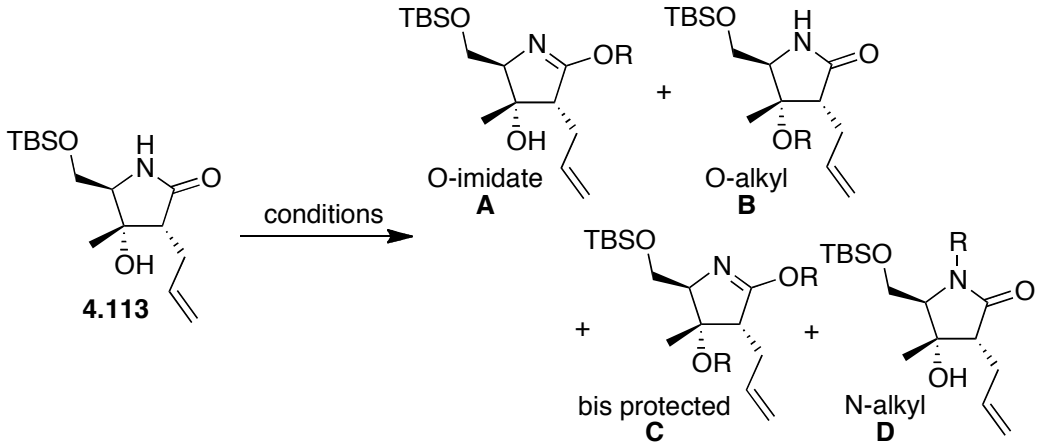


| entry | conditions | R | product |
|---|---|---|---|
| 1 | dimethylsulfate, PhH, 60 °C | Me | *n.r.* |
| 2 | dimethylsulfate, mw[14] | Me | degradation |
| 3 | $Ag_2O$[15], allylbromide | allyl | several spots on TLC |
| 4 | $Ag_2O$[12], MeI, ACN, dark | Me | A+B+C |
| 5 | TMSCl, $Et_3N$, cold room, 16 h[16] | TMS | Only B (**4.141**) |
| 6 | TMSCl, $Et_3N$, cold room, 24 h[13] | TMS | B (**4.141**) + C (**1.142**) |

[14] Compound was subjected to heating neat in a microwave from 60 to 180 °C. No reaction occurred at low temperature and degradation was observed at higher temperature.

[15] Freshly prepared silver oxide was used.

[16] Freshly distilled TMSCl and $Et_3N$ were used.

Reaction with trimethylsilyl chloride was sensitive to the duration. Although, initial protection solely lead to O- protected **4.141** (entry 5), bis-protected compound **1.142** was gradually observed as time progressed (entry 6).

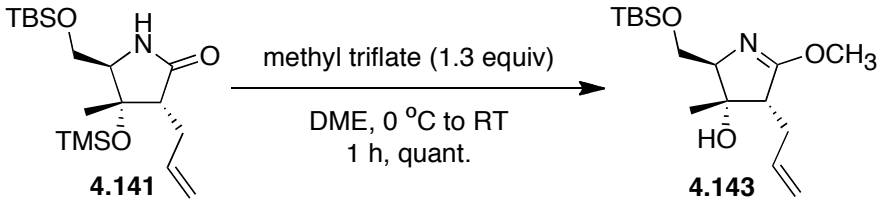


**Scheme 4.75** Synthesis of O-methyl imidate.

Finally treatment of O-TMS protected **4.141** with reactive methyl triflate exclusively afforded desired O-methyl imidate **4.143** with quantitative conversion, although concomitant desilylation of the C-4 alcohol was also observed (Scheme 4.75).[17] Following few functional group manipulations, compatible with the imidate functional group, TBS ether can be transformed into the corresponding ester. Scope of alkylation on such imidate intermediate would be explored in future (Scheme 4.76). This should deter the elimination pathways by increasing the $pK_a$ of the C-3 proton (compared to that of carbonyl lactam species).

[17] Bis-protected compound **1.142** will also be used for the similar purpose in future.

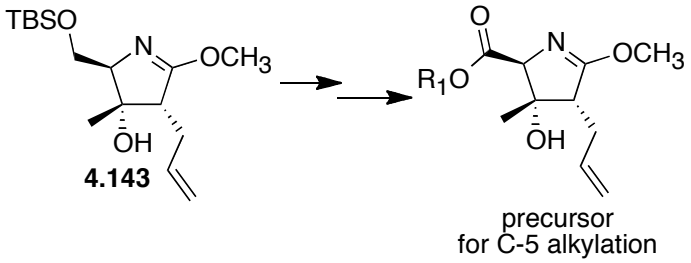


**Scheme 4.76** Planned precursor for future C-5 alkylation studies.

Nonetheless, such an approach does not completely shut down the acidity of C-2 proton. Retrosynthetic approach outlined in scheme 4.77 illustrates another approach where one may certainly rule out the possibility of elimination via C-3 deprotonation. This approach relies on masking the C-2 lactam as an acetonide.

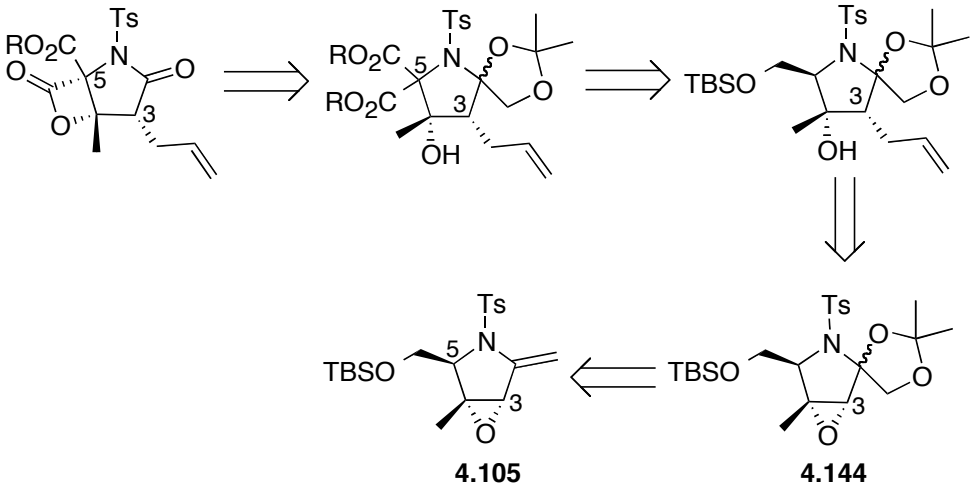


**Scheme 4.77** Disconnective approach proposed with C-2 masked carbonyl intermediates.

Previous studies in our lab have shown that enamine present in tandem aza-Payne/hydromination product **4.105** can be dihydroxylated to give an equimolar mixture

of diols (discussed in Chapter 3). Resulting diol when reacted with acetone in the presence of a Bronsted acid would deliver acetonide **4.144** (Scheme 4.77). Efforts will be made in future to investigate the influence of acetonide (instead of carbonyl at C-2) on the epoxide ring opening reaction. If successful, C-2 carbonyl would be revealed, once C-5 alkylation under basic condition is effectively achieved.

### 4.6.7.2 Scope of C-5 alkylation at earlier stages during synthesis.

Elimination of tertiary alcohol is the dominating process, which thwarts our efforts toward C-5 functionalization. Thus construction of C-5 quaternary stereocenter should be examined at an earlier stage before the tertiary alcohol is revealed. Scheme 4.78 highlights one such approach. Prospect of C-5 alkylation should be examined before carrying out epoxide ring opening. However, one cannot certainly rule out the possibility epoxide opening during the course of C-5 alkylation under basic conditions.

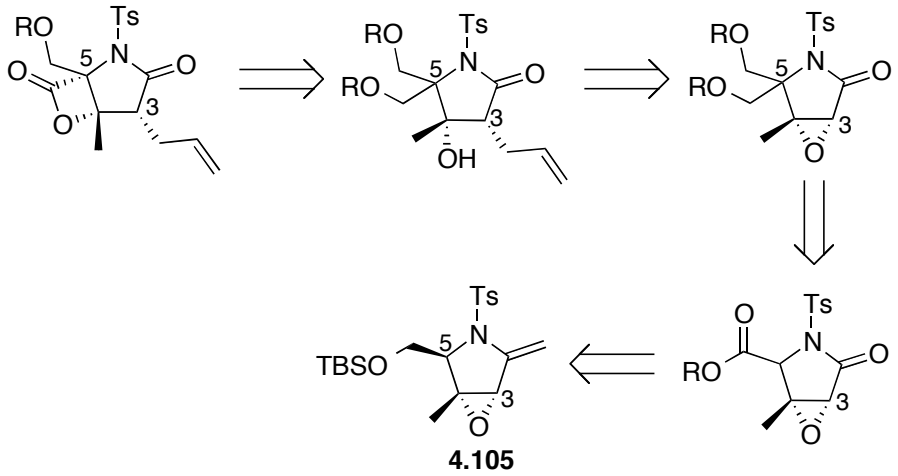


**4.105**

**Scheme 4.78** Schematic outline for early stage C-5 functionalization.

There are other possibilities such as installation of quaternary C-5 stereocenter before carrying out tandem aza-Payne/hydroamination step. Although, a challenging synthesis of a stereo-defined tetrasubstituted aziridine ring is required, this would offer a direct access to pyrrolidine compound with a pre-established C-5 quaternary stereocenter. One would also have to analyze the effect of the di-substituted C-5 stereocenter on the stereochemical outcome of the epoxide opening and allylation reactions.

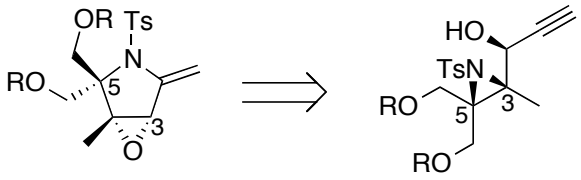


**Scheme 4.79** Tandem aza-Payne/hydroamination on precursor with pre-installed C-5 quaternary center.

### 4.6.7.3 Scope of C-5 alkylation via palladium chemistry.

Huang et al. have reported palladium-catalyzed $\alpha$-vinylation of carbonyl compounds using LiHMDS as base and vinyl bromides.[81] Substrate scope of such chemistry is pretty broad and enables vinylation of esters substituted on tertiary position (a, Scheme 4.80).

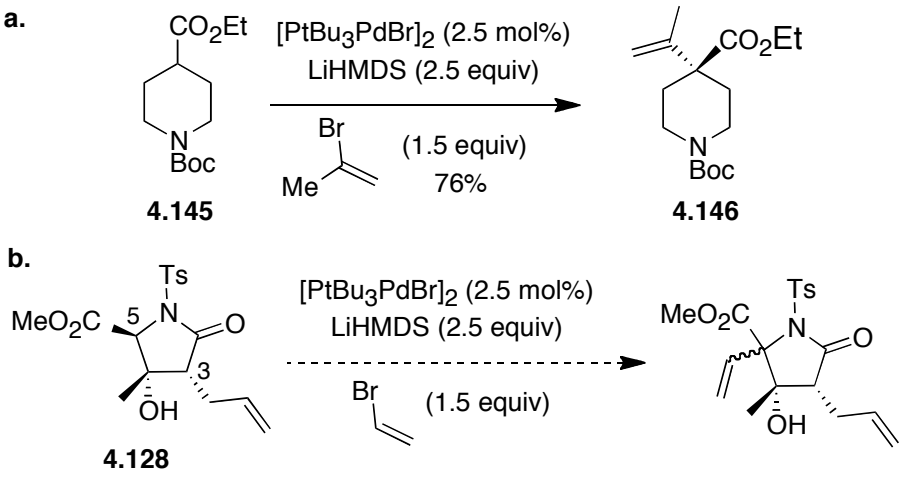


**Scheme 4.80** Pd catalyzed $\alpha$-vinylation of ketones. **a.** Literature precedence **b.** proposed plan.

Generation of a similar palladium enolate at a sterically demanding position in case of the pyrrolidine ester **4.128** might be challenging, if feasible, will provide access to $\alpha$-vinylated compound (b, Scheme 4.80). The latter upon ozonolysis would be elaborated into the desired carbonyl functionality.

#### 4.6.7.4 Scope of C-5 alkylation via radical chemistry.

Santamaria and coworkers have developed a selective method for generating an iminium cation via photoinduced single electron transfer process.[82] Thus using this protocol, irradiation of 3-piperideines **4.146** in the presence of catalytic amount of 9,10-dicyanoanthracene (DCA as electron acceptor) under oxygen bubbling, affords the endocyclic $\alpha$-amino nitriles in fair yields (Scheme 4.81). This method has also been applied in the synthesis of alkaloids.[83] Although generation of iminium cation in this

case, is assisted by the stabilization of the allylic position, proximity to nitrogen is likely to deliver regioselectivity obtained for C-2 cyanation. In case of pyrrolidine, α-carbonyl arrangement adjacent to the pyrrolidine nitrogen may simulate a similar role.

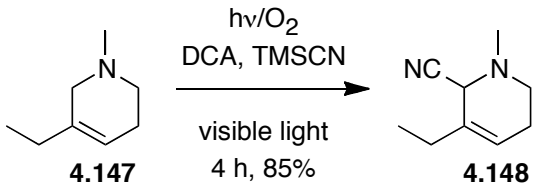


**4.147** **4.148**

**Scheme 4.81** Endocyclic α-aminonitriles resulting from DCA-photosensitization of alkylpiperideines.

Pandey and coworkers have also shown the generation of iminium cation by photosensitized single electron transfer and intramolecular cyclization by oxygen and carbon nucleophiles.[84]

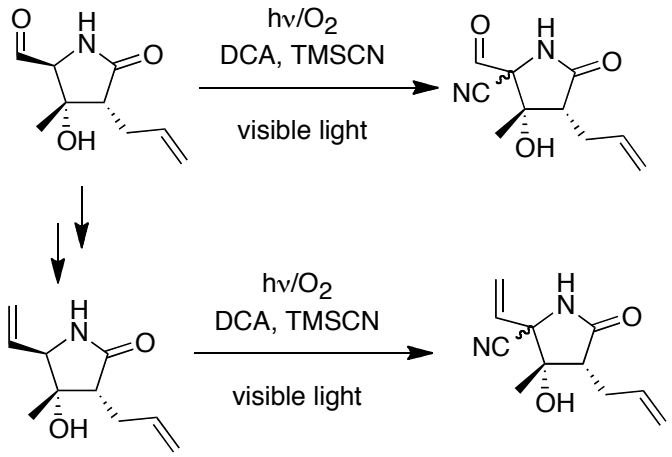


**Scheme 4.82** Proposition of α-cyanation to pyrrolidine using photoinduced electron transfer.

This certainly highlights the possibility of generating an iminium ion without the assistance of a stabilizing neighboring group participation, unlike in the previous case (Scheme 4.83 *vs* 4.82). Thus in case of pyrrolidine, with the absence of allylic stabilization, such chemistry might still be able to effect formation of an iminium ion. We are however, aware of competing cyanation at C-3 or the allylic position of the C-3 substituent. Nonetheless, if required, aldehyde carbonyl can be elaborated into an olefin by routine functional group manipulations in order to boost regioselectivity at C-5 (Scheme 4.82).

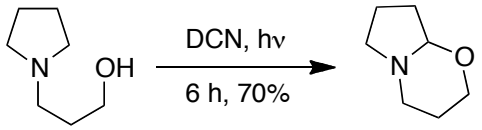


**4.149** **4.150**

**Scheme 4.83** Intramolecular cyclization of iminium generated via SET by oxygen nucleophile.

### 4.6.7.5 Scope of C-5 alkylation via Steven's rearrangement.

Smith and coworker's have shown the utility of Steven's rearrangement for $\alpha$-alkylation next to the nitrogen on pyrrolidine compounds.[85] Treatment of *N*-allyl pyrrolidine compound with iodomethane in the presence of base and upon reflux afforded the Steven's rearranged product with quaternary stereocenter adjacent to nitrogen (Scheme 4.84). Allylation of the pyrrolidine nitrogen in our case and a similar rearrangement

would alkylate the C-5 position. The resulting intermediate would require demethylation, although such reactions require harsher conditions, are precedent in the literature.[86,87]

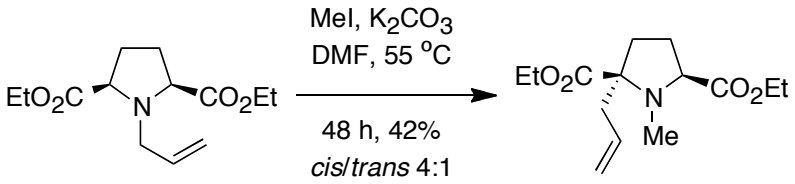


**Scheme 4.84** $\alpha$-allylation to nitrogen via Steven's rearrangement.

### 4.6.8 Conclusion

Tandem aza-Payne/hydroamination methodology allows access to tetrasubstituted stereodefined *N*-Ts enamide pyrrolidines. This approach has been efficiently show cased to assemble a pyrrolidine core **4.105** starting from a diastereomerically pure trisubstituted aziridinol **4.93**. The aziridinol in turn can be derived via highly diastereoselective addition of the Grignard reagent to azirine-2-carboxaldehydes. The latter can be progressed to a complex and advanced aldehyde intermediate **4.126** in only 7 steps (Scheme 4.85). Attempts for C-5 alkylation in the aldehyde or similar precursors were frustrated by the competing elimination pathways.

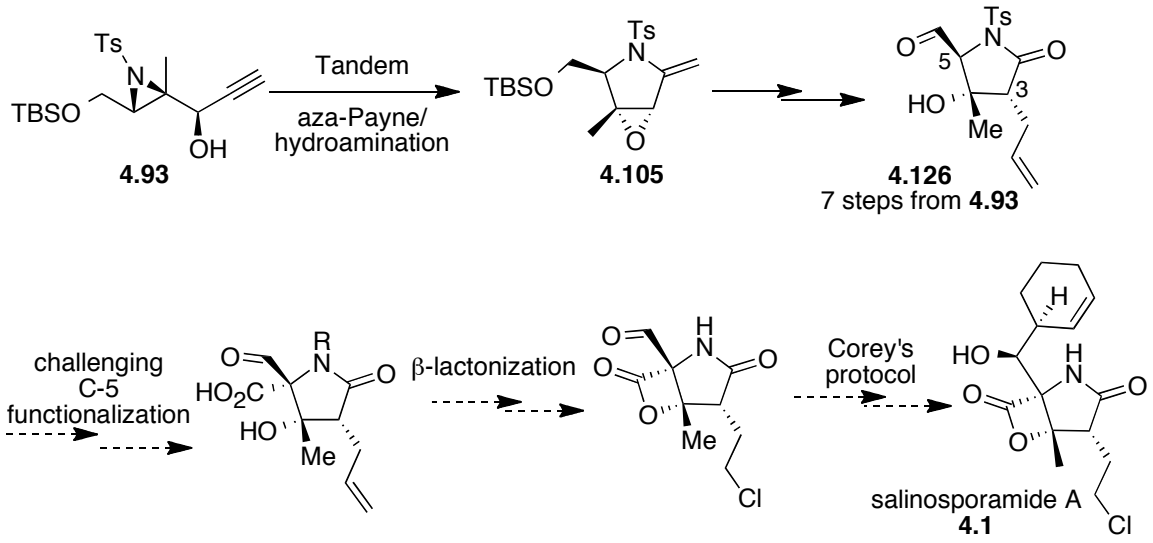


**Scheme 4.85** Elaboration to aldehyde precursor and remaining challenges toward salinosporamide A.

Several alternative routes have been proposed for the purpose, which will be examined in near future. Once bis-carboxylic acid intermediate is accessible, intramolecular esterification would be applied to install the β-lactone. Transformation steps as developed by Corey's group would be examined in order to elaborate the side chain at C-3 to ethyl chloride substituent and installation of the cyclohexenyl group.

## 4.8 Experimental procedures.

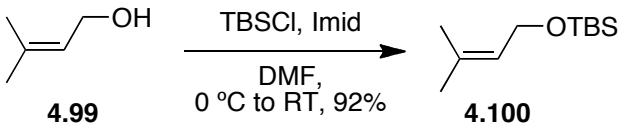


**Preparation of TBS ether 4.100.**[42] To a solution of commercially available 3-methyl-2-butenol (12 g, 139.3 mmol) in DMF (70 mL) was added imidazole (23.7 g, 348.2 mmol) and TBSCl (23.1, 153.2 mmol) at 0 ºC. After stirring for 6 h the mixture was poured into water (50 mL). The aqueous layer was extracted with EtOAc (3 X 50 mL) and washed with brine (45 mL). Organic layers were dried over anhydrous sodium sulfate and evaporated under reduced pressure. The crude compound was purified by column chromatography (3:1 Hex:EtOAc) to yield TBS ether **4.100** (25.7 g, 92%) as a colorless oil. Spectroscopic data matches with that of the reported compound in literature.[88] Spectral data: $^{1}$H-NMR (500 MHz, $CDCl_3$) $\delta$ 5.30 (t, 1H, $J$ = 6.5 Hz), 4.22 (d, 2H, $J$ = 6.5 Hz), 1.68 (s, 3H), 1.60 (s, 3H), 0.90 (s, 9H), 0.07 (s, 6H); $^{13}$C-NMR (125 MHz, $CDCl_3$) $\delta$ 133.9, 124.9, 60.6, 26.4, 26.1, 18.8, 18.2, -4.7.

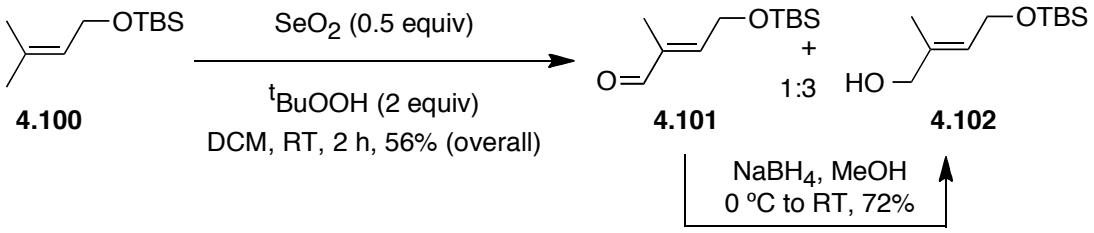


**Preparation of allylic alcohol 5.102**.[42] To a solution of $SeO_2$ (0.57 g, 4.99 mmol) in

DCM (21 mL) was added $^{t}$BuOOH (70% aqueous solution) (2.86 mL, 19.96 mmol) drop wise at 0 ºC. After 30 min a solution of TBS ether **5.101** dissolved in DCM (11 mL) was added to the above solution drop wise at 0 ºC under inert atmosphere. This was then allowed to stir at room temperature for 2 h. The mixture was extracted with EtOAc (3 X 50 mL). Organic layers were washed with 10% KOH (4 X 5 mL), sat. $NaHCO_3$ (1 X 10 mL) and water (1 X 5 mL). The organic solvent was evaporated under reduced pressure. Crude compound obtained was purified by silica gel column (4:1 Hex:EtOAc) to afford a mixture of over-oxidized product aldehyde **4.101** (0.3 g, 14%), the desired alcohol **4.102** (0.92 g, 43%), along with recovered starting material (0.63 g, 31.5%). The aldehyde **4.101** was reduced by $NaBH_4$ reduction protocol reported in the literature to yield the desired alcohol **4.102** (0.22 g, 72 %). Spectral data matches with that of the reported compounds in literature.[34] Spectral data for **4.102**: $^{1}$H-NMR (300 MHz, $CDCl_3$) δ 5.53 (dd, 1H, *J* = 6.0, 5.1 Hz), 4.21 (d, 2H, *J* = 6.3 Hz), 3.96 (d, 2H, *J* = 3.9 Hz), 1.84 (br s, 1H), 1.63 (s, 3H), 0.87 (s, 9H); $^{13}$C-NMR (75 MHz, $CDCl_3$) δ 136.1, 125.2, 68.2, 59.9, 26.0, 18.3, 13.8, -5.2. Spectral data for **4.101**: $^{1}$H-NMR (300 MHz, $CDCl_3$) δ 9.40 (s, 1H), 6.50 (td, 1H, *J* = 5.3, 1.2 Hz), 4.48 (dd, 2H, *J* = 5.7, 0.6 Hz), 1.70 (s, 3H), 0.88 )s, 3H), 0.07 (s, 3H); $^{13}$C-NMR (75 MHz, $CDCl_3$) δ 194.4, 153.0, 137.7, 60.4, 25.8, 25.7, 18.2, 9.3, -5.3.

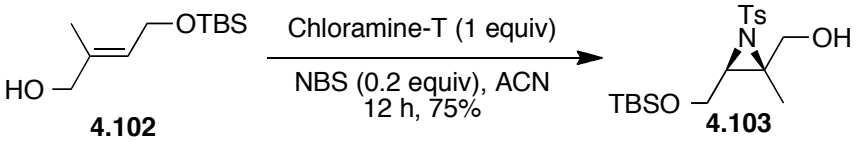

**Preparation of aziridinol 4.103**.[43] To a solution of alcohol **4.102** (3.65 g, 16.9 mmol) in ACN (84 mL) was added NBS (0.6 g, 3.38 mmol) and Chloramine-T (3.85 g, 16.9 mmol). The flask was covered with an aluminum foil and the reaction mixture was stirred under nitrogen overnight. Upon completion as analyzed by TLC, water (50 mL) was added to quench the reaction. The aqueous layer was extracted with EtOAc (3 X 30 mL), organic layers were dried over sodium sulfate and evaporated under low pressure. The purification was done by column chromatography (3:1 Hex:EtOAc) to yield aziridinol **4.103** (4.9 g, 75%) as a syrupy yellow oil. Spectral data for **4.103**: $^{1}$H-NMR (500 MHz, $CDCl_3$) $\delta$ 7.82 (d, 2H, *J* = 8.2 Hz), 7.28 (d, 2H, *J* = 8.2 Hz), 4.00 (overlapping m, 2H), 3.65 (dd, 1H, *J* = 11.3, 5.4 Hz), 3.55 (dd, 1H, *J* = 11.3, 6.8 Hz), 3.20 (dd, 1H, *J* = 6.6, 5.5 Hz), 3.06 (dd, 1H, *J* = 8.9, 6.3 Hz), 2.41 (s, 3H), 1.41 (s, 3H), 0.81 (s, 9H), -0.04 (s, 3H), -0.06 (s, 3H); $^{13}$C-NMR (125 MHz, $CDCl_3$) $\delta$ 143.9, 137.5, 129.4, 127.1, 65.4, 60.7, 56.4, 50.5, 25.7, 21.5, 18.1, 16.2, -5.5, -5.6; IR (neat) 3518, 3315, 2952, 2886, 2859, 1467, 1409, 1320, 156, 1158, 1093, 673; HRMS (ESI) (m/z): [M+H$^+$ calculated for $[C_{18}H_{32}NO_4SSi)^+$ 386.1821, found 386.1817.

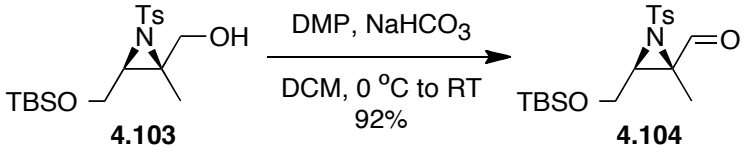

**4.103** **4.104**

**Preparation of aziridinal 4.104**.[34] To a solution of aziridine alcohol **4.103** (3 g, 7.78 mmol) in anhydrous DCM (86 mL) was added DMP (4.6 g, 10.9 mmol) and $NaHCO_3$

(0.98 g, 11.67 mmol) at 0 ºC under inert atmosphere. The reaction was stirred for 3 h over which temperature was gradually warmed to room temperature. Upon completion as analyzed by TLC, the reaction was quenched with the addition of sat. sodium thiosulfate (16 mL), sat. $NaHCO_3$ (16 mL) and water (16 mL). The aqueous phase was extracted with DCM (3 X 20 mL). The organic layers were dried over anhydrous sodium sulfate and subjected to rotary evaporation. Purification was achieved by silica gel chromatography (4:1 Hex:EtOAc) to afford aziridinal **4.104** (2.75 g, 92 %) as an off-white solid (m.pt = 70 - 72 ºC). Spectral data for **4.104**: $^1$H-NMR (500 MHz, $CDCl_3$) δ 9.51 (s, 1H), 7.82 (d, 2H, *J* = 8.2 Hz), 7.30 (d, 2H, *J* = 8.2 Hz), 3.67 (d, 2H, *J* = 2.9 Hz), 2.42 (s, 3H), 1.41 (s, 3H), 0.82 (s, 9H), -0.03 (s, 3H), -0.04 (s, 3H); $^{13}$C-NMR (125 MHz, $CDCl_3$) δ 194.4, 144.6, 136.2, 129.6, 127.5, 60.3, 56.7, 50.9, 25.6, 21.6, 18.1, 11.8, -5.5, -5.6; HRMS (ESI) (m/z): $[M+H]^+$ calculated for $[C_{18}H_{29}NO_4SSiH]^+$ 384.1665, found 384.1662.

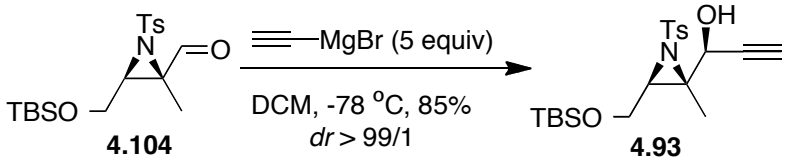


**Preparation of propargylic alcohol 4.93**.[34] Commercially available 0.5 M solution of ethynylmagnesium bromide in THF (11.12 mL, 5.56 mmol) was drop wise added to a solution of aziridinal **4.104** (0.4 g, 1.11 mmol) in anhydrous DCM (41 mL) maintained at -78 ºC using a dry-ice bath. Upon completion as analyzed by TLC, reaction was

quenched by addition of sat. $NH_4Cl$ (15 mL). The aqueous phase was extracted with DCM (2 X 15 mL) and EtOAc (20 mL). The organics were washed with brine (20 mL), dried over anhydrous sodium sulfate, evaporated under reduced pressure. The crude compound was purified by flash chromatography to afford propargylic alcohol **4.93** (0.4 g, 85%) as a white solid (m.pt = 48 – 50 ºC). Spectral data for **4.93**: $^1$H-NMR (500 MHz, $CDCl_3$) δ 7.81(d, 2H, *J* = 8.2 Hz), 7.29 (d, *J* = 8.2 Hz), 4.85 (dd, 1H, *J* = 3.3, 2.1 Hz), 3.67 (dd, 1H, *J* = 11.2, 5.4 Hz), 3.55 (dd, 1H, *J* = 11.2, 6.6 Hz), 3.54 (d, 1H, *J* = 3.7 Hz), 3.22 (dd, 1H, *J* = 6.9, 5.5 Hz), 2.49 (d, 1H, *J* = 2.2 Hz), 2.41 (s, 3H), 1.52 (s, 3H), 0.82 (s, 9H), -0.03 (s, 3H), -0.06 (s, 3H); $^{13}$C-NMR (125 MHz, $CDCl_3$) δ 144.3, 137.2, 129.5, 127.3, 80.4, 74.4, 65.3, 60.4, 58.2, 50.8, 25.7, 18.1, 12.9, -5.5, -5.6; IR (neat) 3496, 3289, 2931, 2858, 1598, 1312, 1158, 1094, 836; HRMS (ESI) (m/z): $[M+Na]^+$ calculated for $[C_{20}H_{32}NO_4SSi]^+$ 410.1821, found 410.1819.

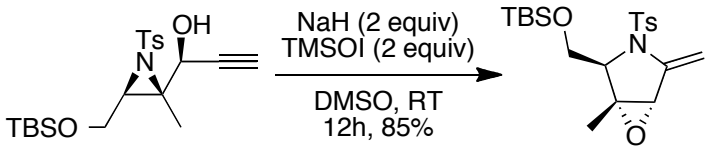


**4.93** **4.105**

**Preparation of *N*-Ts enamide 4.105**.[34] Dried TMSOI (0.2 g, 0.88 mmol) was added (in four portions) to a well-stirred solution of NaH (60% as oil dispersion) (35.2 mg, 0.88 mmol) in anhydrous DMSO (4.4 mL) at room temperature. After stirring for 30 min (when bubbles ceased) propargylic alcohol **4.93** (0.18 g, 0.44 mmol) dissolved in anhydrous DMSO (0.5 mL) was drop-wise added to the above solution at room

temperature. The reaction was stirred for 12 h and was quenched upon analysis with TLC by addition of sat. $NH_4Cl$ (2.5 mL). The aqueous phase was extracted with EtOAc (3 X 5 mL). The organic layers were washed with brine (5 mL), dried over sodium sulfate and evaporated under reduced pressure. The crude upon purification with column chromatography yielded *N*-Ts enamide **4.105** (0.15 g, 85%) as a white solid (m.pt = 58 – 60 ºC). Spectral data for **4.105**: $^1$H-NMR (500 MHz, $CDCl_3$) $\delta$ 7.61 (d, 2H, *J* = 8.3 Hz), 7.24 (d, 2H, *J* = 8.2 Hz), 5.35 (s, 1H), 4.74 (s, 1H), 4.03 (dd, 1H, *J* = 11.1, 3.4 Hz), 3.91 (dd, 1H, *J* = 11.1, 2.2 Hz), 3.89 (bs, 1H), 3.38 (s, 1H), 2.38 (s, 3H), 1.47 (s, 3H), 0.85 (s, 9H), 0.09 (s, 3H), 0.08 (s, 3H). DCM; $^{13}$C-NMR (125 MHz, $CDCl_3$) $\delta$ 143.8, 142.8, 134.7, 129.2, 127.7, 98.4, 66.8, 63.9, 62.7, 62.6, 62.3, 25.7, 21.6, 17.9, 14.2, -5.6, -5.7; IR (neat) 2952, 2859, 1658, 1467, 1348, 1256, 1167, 1099, 661; HRMS (ESI) (m/z): $[M+H]^+$ calculated for $[C_{20}H_{32}NO_4SiS]^+$ 410.1821, found 410.1826.

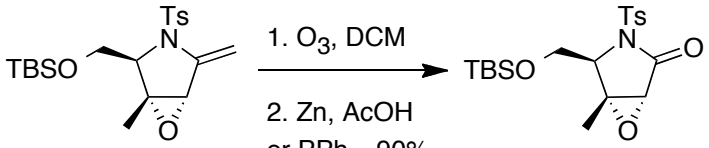

**4.105** **4.106**

**Preparation of lactam 4.106**.[89] Ozone gas was bubbled through a solution of N-Ts enamide **4.105** (0.15 g, 0.36 mmol) dissolved in anhydrous DCM (4 mL) at -78 $^o$C maintained in a dry-ice bath. In 15 min, as the color of the solution turned blue, TLC analysis revealed the completion of the reaction. Excess ozone was removed via bubbling with nitrogen gas. $PPh_3$ (0.11 g, 0.43 mmol) was added to the solution and the

reaction was stirred at room temperature overnight. The solvent was evaporated and the crude was directly subjected to silica gel chromatography to yield lactam 5.108 (0.14 g, 90%) as a white solid (m.pt = 160 – 162 ºC). Spectral data for **4.106**: $^{1}$H-NMR (500 MHz, $CDCl_3$) δ 7.83 (d, 2H, *J* = 8.2 Hz), 7.29 (d, 2H, *J* = 8.2 Hz), 4.33 (m, 1H), 4.13 (dd, 1H, *J* = 11.3, 2.8 Hz), 3.89 (dd, 1H, *J* = 11.3, 1.5 Hz), 3.32 (s, 1H), 2.40 (s, 3H), 1.52 (s, 3H), 1.56 (s, 3H), 0.79 (s, 9H), 0.06 (s, 3H), 0.00 (s, 3H); $^{13}$C-NMR (125 MHz, $CDCl_3$) δ 169.1, 145.1, 135.4, 129.6, 128.1, 64.5, 61.4, 59.4, 57.4, 25.5, 21.6, 17.8, 13.5, -5.8, -6.0; IR (neat) 2931, 2857, 1740, 1349, 1262, 1167, 1132, 564; HRMS (ESI) (m/z): $[M+H]^+$ calculated for $[C_{19}H_{30}NO_5SiS]^+$ 412.1614, found 412.1618.

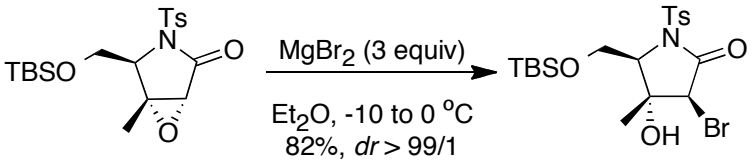


**4.106** **4.107**

**Preparation of hydroxy lactam bromide 4.107**.[90] To a solution of lactam epoxide **4.106** (82.6 mg, 0.2 mmol) in anhydrous $Et_2O$ (4 mL) was added solid commercially available $MgBr_2$ (dried under vacuum overnight) at -10 ºC. The reaction was stirred for 3 h and maintained at 0-10 ºC until all the starting material was observed consumed by TLC. The solution was filtered and washed with $Et_2O$ (2 mL) and DCM (5 mL). The solvent was removed by rotary evaporation and column purification afforded the bromo hydroxylactam **4.107** (81 mg, 82%) as a white solid (m.pt = 118 – 120 ºC). Spectral data for **4.107**: $^{1}$H-NMR (500 MHz, $CDCl_3$) δ 7.90 (d, 2H, *J* = 8.3 Hz), 7.31 (d, 2H, *J* =

8.3 Hz), 4.19 (d, 1H, *J* = 6.5 Hz), 4.14 (3, 1H), 4.13 (d, 1H, *J* = 6.5 Hz), 3.95 (s, 1H), 2.42 (s, 3H), 1.62 (s, 3H), 0.91 (s, 9H), 0.13 (s, 3H), 0.10 (s, 3H); $^{13}$C-NMR (125 MHz, $CDCl_3$) δ 168.7, 145.5, 134.8, 129.6, 128.5, 75.8, 71.1, 62.5, 50.0, 25.8, 22.1, 21.7, 18.2, -5.4, -5.5; IR (neat) 3491, 2925, 1743, 1596, 1363, 1171, 1115, 956; HRMS (ESI) (m/z): $[M+H]^+$ calculated for $[C_{19}H_{30}BrO_5SSiH]^+$ 492.0876, found 492.0875.

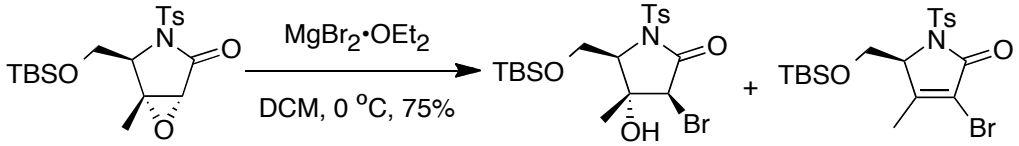


**4.106** **4.107** 1.6 : 1 **4.108**

Spectral data for **4.108**: $^1$H-NMR (500 MHz, $CDCl_3$) δ 7.93 (d, 2H, *J* = 8.4 Hz), 7.27 (d, 2H, *J* = 8.4 Hz), 4.65 (m, 1H), 4.21 (dd, 1H, *J* = 10.7, 3.4 Hz), 4.20 (dd, 1H, *J* = 10.7, 3.4 Hz), 2.38 (s, 3H), 2.03 (s, 3H), 0.68 (s, 9H), -0.02 (s, 3H), -0.06 (s, 3H); $^{13}$C-NMR (125 MHz, $CDCl_3$) δ 164.4, 157.5, 145.1, 135.7, 129.6, 129.5, 128.5, 128.0, 114.1, 67.2, 60.4, 49.8, 25.4, 21.6, 17.7, 14.7, -5.6, -5.8; IR (neat) 3477, 2953, 2930, 2858, 1740, 1363, 1171, 1113, 668; HRMS (ESI) (m/z): $[M+H]^+$ calculated for $[C_{19}H_{29}NBrNO_4SSi]^+$ 474.0770, found 474.0775.

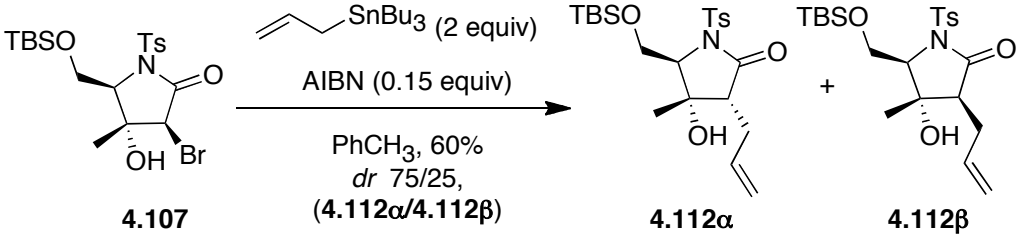


**4.107** **4.112α** **4.112β**

**Preparation of α-allyl lactam 4.112.**[91] Solution of hydroxylactam bromide **4.107** (40.5 mg, 0.08 mmol) in anhydrous toluene (0.5 mL) was degassed and refluxed at 100 ºC under nitrogen.[92] To this was added AIBN (3 mg, 0.02 mmol) and alllyltributyl tin (68 mg, 0.21 mmol). The reaction was stirred at that temperature untill all the starting material was completely consumed upon analysis with TLC. The solvent was evaporated and crude was directly subjected to column purification (5:1 Hex:EtOAc) to yield (23 mg, 60%) as an inseparable 75/25 mixture of α-adduct **4.112α** and β-adduct **4.112β**. Spectral data for **4.112α**: $^{1}$H-NMR (500 MHz, $CDCl_3$) δ 7.88 (d, 2H, *J* = 8.2 Hz), 7.25 (d, 2H, *J* = 8.2 Hz), 5.80 (m, 1H), 5.04 (d, 1H, *J* = 17.2 Hz), 4.96 (d, 1H, *J* = 10.3 Hz), 4.07 (d, 1H, *J* = 12.6 Hz), 3.99 (s, 1H), 3.87 (d, 1H, *J* = 12.6 Hz), 2.81 (dd, 1H, *J* = 7.7, 5.9 Hz), 2.39 (m, 1H), 2.37 (s, 3H), 2.19 (m, 1H), 1.42 (s, 3H), 0.77 (s, 9H), 0.03 (s, 3H), -0.01 (s, 3H); $^{13}$C-NMR (125 MHz, $CDCl_3$) δ 174.3, 144.6, 136.6, 135.9, 129.4, 128.1, 116.3, 70.8, 62.0, 52.2, 27.7, 25.6, 22.1, 21.5, 17.8, -5.8, -6.0; IR (neat) 3515, 2930, 1726, 1597, 1353, 1258, 1170, 1113, 836; HRMS (ESI) (m/z): $[M+H]^+$ calculated for $[C_{22}H_{36}NO_5SSi]^+$ 454.2083, found 454.2079.

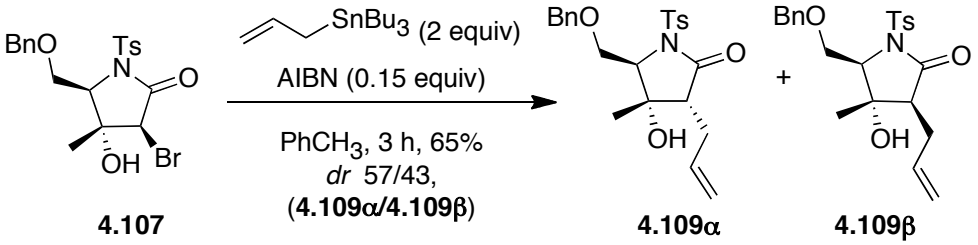


**4.107** **4.109α** **4.109β**

**Preparation of α-allyl lactam 4.109.**[91] Lactam **4.109** was prepared using a procedure

similar to that used for the synthesis of lactam **4.112**. Spectral data for **4.109α**: $^{1}$H-NMR (500 MHz, $CDCl_3$) δ 7.91 (d, 2H, *J* = 8.7 Hz), 7.27 (m, 6H), 7.12 (d, 2H, *J* = 7.7 Hz), 5.82 (m, 1H), 5.07 (d, 1H, *J* = 17.1 Hz), 4.99 (d, 1H, *J* = 9.7 Hz), 4.42 (d, 1H, *J* = 12.3 Hz), 4.35 (d, 1H, *J* = 12.3 Hz), 4.09 (m, 1H), 3.93 (dd, 1H, *J* = 11.1, 3.3 Hz), 3.74 (dd, 1H, *J* = 11.3, 1.4 Hz), 2.80 (dd, 1H, *J* = 8.0, 5.5 Hz), 2.43 (m, 1H), 2.36 (s, 3H), 2.25 (td, *J* = 15, 8.1 Hz), 1.39 (s, 3H); $^{13}$C-NMR (125 MHz, $CDCl_3$) δ 174.0, 144.8, 137.2, 136.5, 135.9, 129.4, 128.4, 128.2, 127.9, 127.5, 116.7, 73.8, 69.5, 68.6, 60.4, 51.8, 28.1, 22.5, 21.6, 21.0, 14.2; IR (neat) 3508, 2921, 2872, 1731, 1356, 1165, 1121; HRMS (ESI) (m/z): $[M+H]^+$ calculated for $[C_{23}H_{28}NO_5S]^+$ 430.1688 found 430.1683. Spectral data for **4.109β**: $^{1}$H-NMR (500 MHz, $CDCl_3$) δ 7.89 (d, 2H, *J* = 8.6 Hz), 7.29 - 7.20 (m, 8H), 5.79 (m, 1H), 4.95 (d, 1H, *J* = 10.1 Hz), 4.92 (d, 1H, *J* = 17.9 Hz), 4.49 (d, 1H, *J* = 11.3 Hz), 4.48 (d, 1H, *J* = 11.3 Hz), 4.09 (dd, 1H, *J* = 6.5, 2.9 Hz), 4.03 (dd, 1H, *J* = 10.3, 2.9 Hz), 3.87 (dd, 1H, *J* = 10.3, 6.5 Hz), 2.39 (s, 3H), 2.37 (m, 1H), 2.23 (m, 1H), 1.53 (s, 3H); HRMS (ESI) (m/z): $[M+H]^+$ calculated for $[C_{23}H_{28}NO_5S]^+$ 430.1688 found 430.1690.

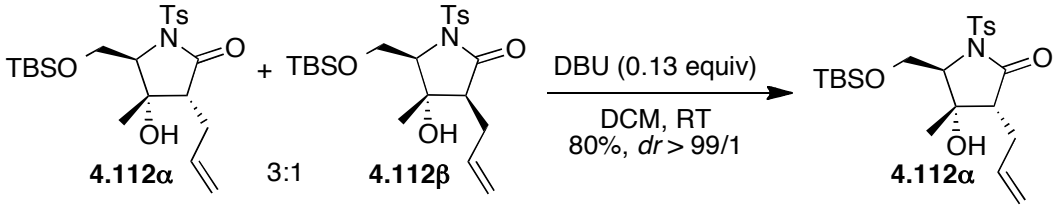


**Procedure for the epimerization of C-3 in the hydroxy lactam 4.112.** The mixture of isomers **4.112α** and **4.112β** (3:1) (40 mg, 0.08 mmol) was placed in anhydrous DCM (1 mL). To this DBU (2 mg, 0.01 mmol) was added and the reaction was allowed to stir for

5 h at room temperature. After the completion as analyzed by the TLC, sat. $NH_4Cl$ (0.5 mL) was added. The aqueous phase was extracted with DCM (3 X 5 mL). The collected organic layers were dried over anhydrous sodium sulfate. The organic solvent was removed via rotary evaporation. The crude compound was purified via column chromatography (4:1 Hex:EtOAc) to yield the pure isomer **4.112α** (32 mg, 80%) as a colorless oil. Spectral data for **4.112α**: $^1$H-NMR (500 MHz, $CDCl_3$) δ 7.88 (d, 2H, *J* = 8.2 Hz), 7.25 (d, 2H, *J* = 8.2 Hz), 5.80 (m, 1H), 5.04 (d, 1H, *J* = 17.2 Hz), 4.96 (d, 1H, *J* = 10.3 Hz), 4.07 (d, 1H, *J* = 12.6 Hz), 3.99 (s, 1H), 3.87 (d, 1H, *J* = 12.6 Hz), 2.81 (dd, 1H, *J* = 7.7, 5.9 Hz), 2.39 (m, 1H), 2.37 (s, 3H), 2.19 (m, 1H), 1.42 (s, 3H), 0.77 (s, 9H), 0.03 (s, 3H), -0.01 (s, 3H); $^{13}$C-NMR (125 MHz, $CDCl_3$) δ 174.3, 144.6, 136.6, 135.9, 129.4, 128.1, 116.3, 70.8, 62.0, 52.2, 27.7, 25.6, 22.1, 21.5, 17.8, -5.8, -6.0; IR (neat) 3515, 2930, 1726, 1597, 1353, 1258, 1170, 1113, 836; HRMS (ESI) (m/z): $[M+H]^+$ calculated for $[C_{23}H_{28}NO_5S]^+$ 430.1688 found 430.1689.

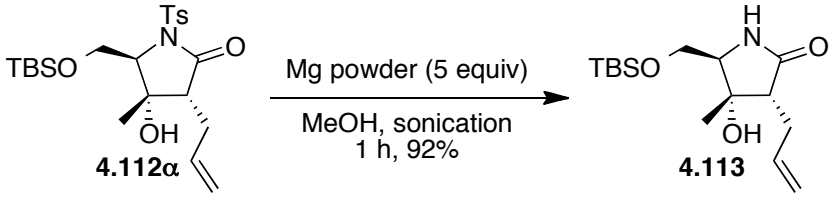


**Preparation of detosylated lactam 4.113**.[93] To a solution of α-allyl lactam **4.112α** (0.33 g, 0.73 mmol) in methanol (3 mL) was added well-crushed magnesium powder (107 mg, 4.36 mmol). The solution was sonicated in an ultra-sonicator bath for 1.5 h to afford detosylated compound **4.112α** (0.2 g, 92%) as a white solid (m.pt = 78 – 80 ºC).

Spectral data for **4.112α**: $^{1}$H-NMR (500 MHz, $CDCl_3$) δ 6.41 (s, 1H), 5.95 (m, 1H), 5.13 (d, 1H, *J* = 17.0 Hz), 5.02 (d, 1H, *J* = 10.2 Hz), 3.61 (d, 2H, *J* = 4.0 Hz), 3.36 (dt, 1H, *J* = 4.2, 1.3 Hz), 2.51 (m, 1H), 2.39 (m, 2H), 1.36 (s, 3H), 0.84 (s, 9H), 0.0.2 (s, 3H), 0.01 (s, 3H); $^{13}$C-NMR (125 MHz, $CDCl_3$) δ 178.2, 137.5, 115.9, 77.5, 65.3, 62.6, 51.1, 28.2, 25.7, 22.5, 18.0, -5.7, -5.8; IR (neat) 3346, 2925, 1687, 1441, 1379, 1217, 1121, 1032, 910; HRMS (ESI) (m/z): $[M+H]^+$ calculated for $[C_{15}H_{30}NO_3Si]^+$ 300.1995, found 300.1971; X-ray structure:

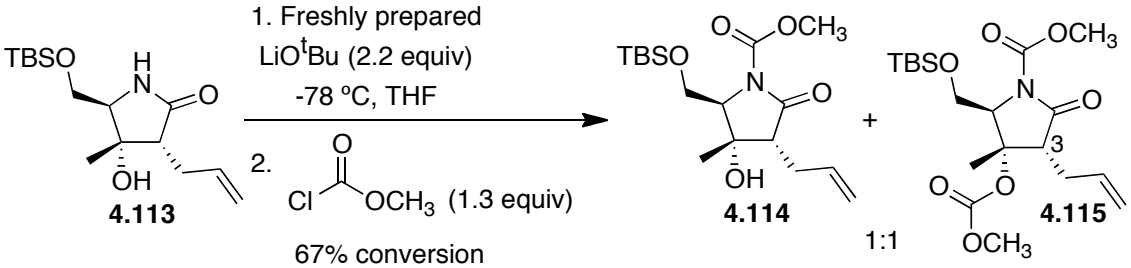


**Preparation of carbamates 4.114 and 4.115**.[94] To a solution of lactam **4.113** (21.7 mg, 0.07 mmol) in anhydrous THF (2.4 mL) at -78 ºC was added commercially available LiHMDS (1M solution in THF) (0.26 mL, 0.26 mmol) under inert atmosphere drop-wise. The reaction mixture was stirred at the same temperature for 10 min. Reaction was removed from bath maintained at -78 ºC and stirred at room temperature for 1 min. It was again transferred to bath maintained at -78 ºC and stirred. After 5 min commercially available methyl chloroformate (52.5 μL, 0.77 mmol) was drop-wise added to the above solution under nitrogen. Reaction was stirred gradually warmed to 0 ºC and stirred till reaction was done as analyzed by TLC. Upon completion, EtOAc (1 mL)

was added to quench the reaction. EtOAc layer was washed with 5% HCl (1 mL), 5% $NaHCO_3$ (1 mL) and water (5 mL), brine (2 mL). At this point the pH was carefully maintained at 7.0. The aqueous phase was extracted with EtOAc (3 X 5 mL) and dried over anhydrous sodium sulfate. Rotary evaporation and subjection to silica gel column afforded an inseparable mixture of mono **4.114** and bis-protected **4.115** compounds. Further a ratio of 2/1 diastereomers **4.115α** ($\alpha$-adduct) and **4.115β** ($\beta$-adduct) was observed in case of bis-protected compound **4.115**. Spectral data for **4.114**: $^1$H-NMR (500 MHz, $CDCl_3$) $\delta$ 5.95 (m, 1H), 5.15 (ddd, 1H, *J* = 17.2, 2.9, 1.7 Hz), 5.05 (ddd, 1H, *J* = 10.1, 2.7, 0.96 Hz), 4.02 (dd, 1H, *J* = 11.2, 2.9 Hz), 3.87 (dd, 1H, *J* = 2.9, 1.3 Hz), 3.84 (s, 3H), 3.85 (s, 3H), 3.80 (dd, 1H, *J* = 11.2, 1.3 Hz), 2.83 (dd, 1H, *J* = 8.3, 5.6 Hz), 2.60 (m, 1H), 2.37 (m, 1H), 1.71 (bs, 1H), 1.48 (s, 3H), 0.83 (s, 9H), 0.00 (s, 3H), -0.03 (s, 3H); $^{13}$C-NMR (125 MHz, $CDCl_3$) $\delta$ 174.2, 152.5, 137.1, 116.5, 85.4, 75.6, 68.7, 60.1, 53.5, 52.8, 28.4, 25.7, 22.5, 18.0, -5.8, -5.9; IR (neat) 2951, 2872, 1734, 1290; HRMS (ESI) (m/z): $[M+H]^+$ calculated for $[C_{17}H_{32}NO_5SSi]^+$ 358.2050, found 358.2054. Spectral data for **4.115**: Major isomer: $^1$H-NMR (500 MHz, $CDCl_3$) $\delta$ 5.92 (m, 1H), 5.11 (m, 1H), 5.02 (m, 1H), 4.67 (dd, 1H, *J* = 2.6, 1.1 Hz), 4.09 (dd, 1H, *J* = 12.0, 3.1 Hz), 3.88 (dd, 1H, J = 12.0, 1.5 Hz), 3.85 (s, 3H), 3.70 (s, 3H), 2.89 (dd, 1H, J = 7.7, 6.2 Hz), 2.61 (m, 1H), 2.38 (m, 1H), 1.77 (s, 3H), 0.82 (s, 9H), 0.00 (s, 3H), -0.04 (s, 3H); Minor isomer: $^1$H-NMR (500 MHz, $CDCl_3$) $\delta$ 5.78 (m, 1H), 5.12 (m, 1H), 5.02 (m, 1H), 4.43 (d, 1H, *J* = 10.1 Hz), 3.86 (s, 3H), 3.82 (d, 1H, *J* = 10.1 Hz), 3.70 (s, 3H), 3.04 (m, 1H, 2.61 (m, 1H), 2.38 (m, 1H), 1.90 (s, 3H), 0.77 (s, 9H), -0.02 (s, 3H), -0.04 (s, 3H).

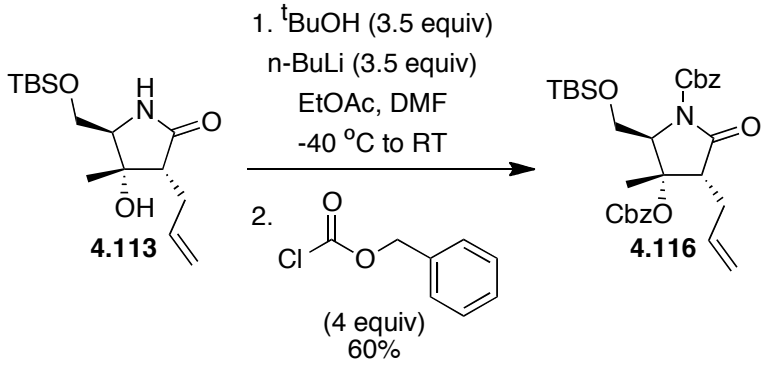


**Preparation of carbamate 4.116**. To a freshly distilled $^{t}$BuOH (1.3 mL, 13.5 mmol) in a flask covered with a condenser was added at 0 ºC commercially available n-BuLi (1.6 M solution in hexane) (8.4 mL, 13.5 mmol) drop-wise under nitrogen pressure.[66] This freshly generated LiO$^{t}$Bu (0.43 mL, 0.69 mmol) was stirred for 15 min and then drop-wise added to lactam **4.113** (59 mg, 0.2 mmol) placed in a mixture of freshly distilled EtOAc (6.6 mL) and DMF (0.12 ML) cooled at -40 ºC. Immediately following the previous step, commercially available benzyl chloroformate (0.12 mL, 0.79 mmol) was added. The reaction was monitored by TLC and quenched with sat. $NH_4Cl$ (10 mL) carefully. Aqueous phase was extracted with EtOAc (3 X 15 mL) and the organic layers were dried over sodium sulfate. Rotary evaporation followed by column chromatography (6:1 Hex:EtOAc) afforded the bis-protected compound **4.116** (90.1 mg, 81%) as an oil. Spectral data for **4.116**: $^{1}$H-NMR (500 MHz, $CDCl_3$) $\delta$ 7.40 - 7.30 (m, 10H), 5.91 (m, 1H), 5.29 (d, 1H, *J* = 12.8 Hz), 5.24 (d, 1H, *J* = 12.8 Hz), 5.11 (ddd, 1H, *J* = 17, 3.1, 1.6 Hz), 5.07 (d, 2H, *J* = 3.3 Hz), 5.02 (d, 1H, *J* = 10.1), 4.68 (m, 1H), 4.04 (dd, 1H, *J* = 12.2, 2.6 Hz), 3.85 (dd, 1H, *J* = 12.1, 0.96), 2.89 (dd, 1H, *J* = 7.3, 6.5 Hz), 2.61 (m, 1H), 2.38 (m, 1H), 1.76 (s, 3H), 0.79 (s, 9H), -0.07 (s, 3H0, -0.14 (s, 3H); $^{13}$C-

NMR (125 MHz, $CDCl_3$) δ 173.0, 153.3, 151.5, 136.6, 135.2, 135.0, 128.6, 128.5, 128.3, 128.1, 128.0, 116.5, 85.7, 69.3, 68.1, 63.5, 60.0, 53.7, 28.3, 25.7, 18.2, 17.9, -5.9, -6.0; IR (neat) 2952, 2857, 1743, 1724, 1295, 1271, 838, 697; HRMS (ESI) (m/z): $[M+H]^+$ calculated for $[C_{31}H_{42}NO_7Si]^+$ 568.2731, found 568.2727.

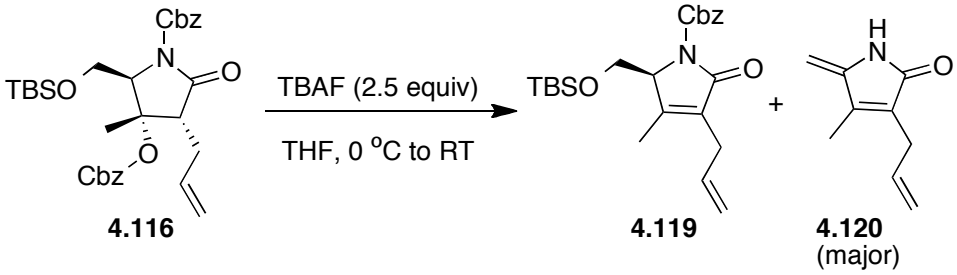


**4.116** **4.119** **4.120** (major)

**Procedure for de-silylation by TBAF**.[95] Commercially available 1M solution of TBAF in THF (0.35 mL, 0.35 mmol) was drop wise added to a solution of lactam **4.116** (85 mg, 0.14 mmol) placed in anhydrous THF (2 mL) at 0 ºC. The reaction was stirred at that temperature till all the starting material was consumed based on TLC analysis. Reaction upon completion was quenched with sat. $NaHCO_3$ (0.5 mL). The aqueous layer was extracted with EtOAc (4 X 5 mL). The organic layers were collected and dried over anhydrous sodium sulfate. Solvent was removed under reduced pressure and column purification (3.5:1 Hex:EtOAc) provided a pure fraction of **4.120** (5 mg) and rest as an inseparable mixture of **4.119** and **4.120** along with some unidentified impurities. Spectral data for **4.120**: $^1$H-NMR (500 MHz, $CDCl_3$) δ 7.52 (bs, 1H), 5.84 (m, 1H), 5.05 - 5.00 (m, 2H), 4.80 (d, 1H, *J* = 7.1 Hz), 4.79 (d, 1H, *J* = 7.1 Hz), 3.07 (d, 1H, *J* = 6.0 Hz), 2.00 (s, 3H); $^{13}$C-NMR (125 MHz, $CDCl_3$) δ 171.7, 144.4, 141.6, 134.0, 131.3, 115.8,

92.7, 27.6, 9.5; IR (neat) 2926, 1761, 1726, 1587, 1279, 1030, 807; HRMS (ESI) (m/z): $[M+H]^+$ calculated for $[C_9H_{12}NO]^+$ 150.0919, found 150.0929.

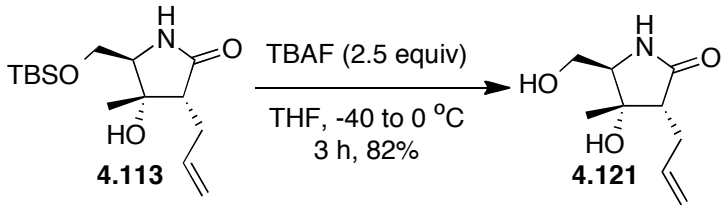


**Preparation of lactam 4.121**. Commercially available 1M solution of TBAF in THF (0.15 mL, 0.15 mmol) was drop wise added to a solution of lactam **4.113** (21 mg, 0.07 mmol) placed in anhydrous THF (1 mL) at -65 ºC. The reaction was stirred at -65 ºC till all the starting material was consumed based on the TLC analysis. Reaction upon completion was quenched with sat. $NaHCO_3$ (2 mL). The aqueous layer was extracted with EtOAc (4 X 10 mL). The organic layers were collected and dried over anhydrous sodium sulfate. Solvent was removed under reduced pressure and purification by silica gel afforded de-silylated compound **4.121** (11 mg, 82%) as an oil. Spectral data for **4.121**: $^1$H-NMR (500 MHz, $CDCl_3$) $\delta$ 7.29 (bs, 1H), 5.94 (m, 1H), 5.08 (d, 1H, $J$ = 16.7 Hz), 4.96 (d, 1H, $J$ = 9.8 Hz), 4.68 (bs, 1H), 4.08 (m, 1H), 3.74 (m, 1H), 3.53 (m, 2H), 2.46 - 2.32 (m, 3H), 1.30 (s, 3H); HRMS (ESI) (m/z): $[M+H]^+$ calculated for $[C_{16}H_{22}NO_5S]^+$ 340.1219, found 340.1222.

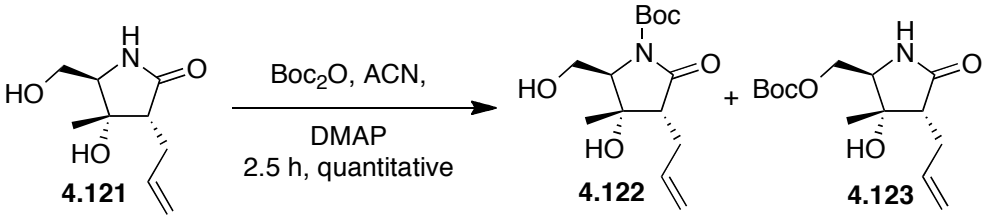


**Preparation of carbamate 4.122 and 4.123**.[96] To a solution of lactam **4.121** (13 mg, 0.07 mmol) in distilled ACN (0.7 mL) was added DMAP (1 mg) and t-butyldicarbonate (19.5 μL, 0.08 mmol). The reaction mixture was stirred and extra t-butyldicarbonate (19.5 μL, 0.08 mmol) was added to push the reaction towards completion. Upon completion as analyzed by TLC, reaction was quenched with sat. $NH_4Cl$ (1 mL) and water (2 mL). The aqueous layer was extracted with DCM (3 X 5 mL). Organic phase was washed with brine (2 mL), dried over sodium sulfate, evaporated under reduced pressure to yield an inseparable mixture of O-Boc (major) and N-Boc protected compounds **4.122** and **4.123** respectively.

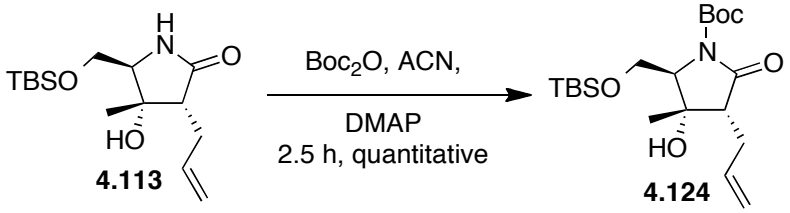


**Preparation of carbamate 4.124**.[96] To a solution of lactam **4.113** (50 mg, 0.17 mmol) in distilled ACN (1.7 mL) was added DMAP (5 mg) and t-butyldicarbonate (50 μL, 0.20 mmol). Upon completion as analyzed by TLC, reaction was quenched with sat. $NH_4Cl$ (5 mL) and water (10 mL). The aqueous layer was extracted with DCM (3 X 15 mL).

Organic phase was washed with brine (5 mL), dried over sodium sulfate, evaporated under reduced pressure to yield compound **4.124** with a quantitative yield, which was taken to the next step without any purification.

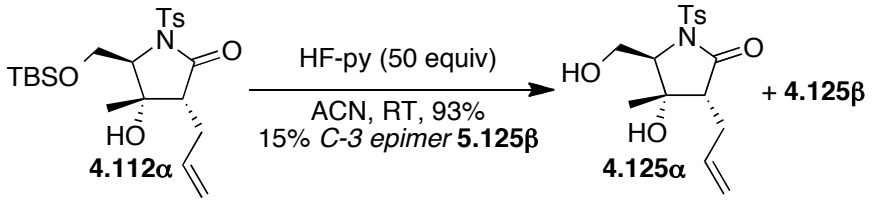


**Preparation of desilylated lactam 4.125α.**[97] To a solution of lactam **4.112α** (0.28 g, 0.61 mmol) in ACN (0.15 mL) in a Teflon-flask at room temperature HF-pyridine (70% HF) (0.42 mL, 15.9 mmol) was added drop-wise under nitrogen atmosphere. After stirring for 2 h, extra amount of HF-pyridine (0.22 mL, 12.2 mmol) was again added. Upon completion as analyzed by TLC, reaction was quenched with addition of sat. $NaHCO_3$ (1 mL) in order to keep the pH maintained at 7.0. The aqueous layers were extracted with DCM (3 X 5 mL) and dried over anhydrous sodium sulfate. The organics were subjected to rotary evaporation and purification via column chromatography to afford a 6/1 mixture of **4.125α** and **4.125β**[18](0.19 g, 93%) as an oil. Spectral data for **4.125α**: $^1$H-NMR (500 MHz, $CDCl_3$) $\delta$ 7.90 (d, 2H, $J$ = 8.4 Hz), 7.29 (d, 2H, $J$ = 8.4 Hz), 5.82 (m, 1H), 5.07 (dd, 1H, $J$ = 17.4, 1.2 Hz), 4.98 (dd, 1H, $J$ = 9.9, 0.7 Hz), 4.18 (ddd, 1H, $J$ = 12.4, 5.0, 3.2 Hz), 4.01 (m, 1H), 3.90 (ddd, 1H, $J$ = 12.6, 6.3, 1.8 Hz), 2.83 (dd, 1H, $J$ = 8.0, 5.7 Hz), 2.40 (s, 3H), 2.24 (m, 2H), 1.47 (s, 3H), EtOAc; $^{13}$C-NMR (125

[18] Column chromatography provided the fraction of **5.125b** contaminated with **5.125a**.

MHz, $CDCl_3$) δ 174.3, 145.0, 136.5, 135.4, 129.5, 128.3, 116.7, 76.9, 71.0, 61.7, 60.4, 51.8, 28.0, 22.6, 21.7, 21.0, 14.2; IR (neat) 3512, 2925, 1726, 1595, 1168, 912; HRMS (ESI) (m/z): $[M+H]^+$ calculated for $[C_{16}H_{22}NO_5S]^+$ 340.1219, found 340.1210

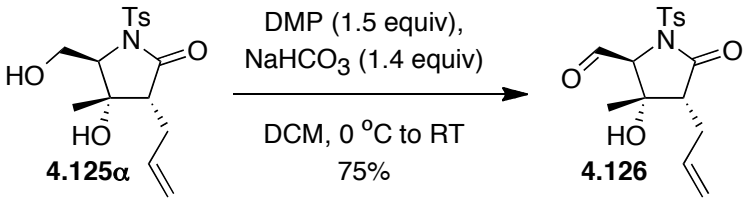


**Preparation of aldehyde 4.126**.[34] To a solution of alcohol **4.125α** (27 mg, 0.07 mmol) in anhydrous DCM (0.75 mL) at 0 ºC was added DMP (40.1 mg, 0.09 mmol) and solid $NaHCO_3$ (9 mg, 0.10 mmol). The reaction was stirred and slowly warmed to room temperature. Upon disappearance of starting material as analyzed by TLC, reaction was quenched by addition of sat. sodium thiosulfate (0.15 mL), sat. $NaHCO_3$ (0.15 mL) and water (0.15 mL). The aqueous layer was extracted with DCM (3 X 2 mL). The organic layers were dried over anhydrous $MgSO_4$ and subjected to rotary evaporation. The crude upon purification via column chromatography yielded aldehyde **4.126** (20 mg, 75%) as a colorless oil. Spectral data for **4.126**: $^1$H-NMR (500 MHz, $CDCl_3$) δ 9.77 (d, 1H, *J* = 1.2 Hz), 7.90 (d, 2H, *J* = 8.1 Hz), 7.32 (d, 2H, *J* = 8.0 Hz), 5.79 (m, 1H), 5.09 (ddd, 1H, *J* = 17.1, 3.0, 1.7 Hz), 5.01 (d, 1H, *J* = 10.1), 4.74 (d, 1H, *J* = 1.2 Hz), 2.48 (m, 1H), 2.43 (m, 1H), 2.42 (s, 3H), 2.32 (m, 1H), 1.48 (s, 3H); $^{13}$C-NMR (125 MHz, $CDCl_3$) δ 196.1, 172.1, 145.6, 135.4, 134.6, 129.5, 128.8, 117.5, 76.1, 75.0, 51.8, 27.6, 23.7, 21.7; IR (neat) 3184, 3084, 2952, 2929, 1702, 1251, 1072, 1005, 838, 772; HRMS (ESI)

(m/z): $[M+H]^+$ calculated for $[C16H20NO_5S]^+$ 338.1062, found 338.1057.

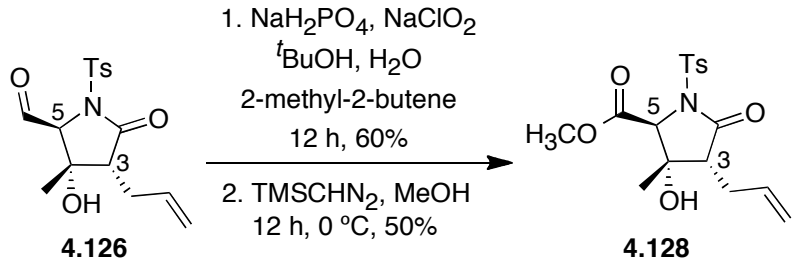


**4.126** **4.128**

**Preparation of ester 4.128**.[98] To a solution of aldehyde **4.126** (65 mg, 0.19 mmol) in $^t$BuOH (1.8 mL) at 0 ºC was added commercially available 2-methyl-2-butene (90%) (0.2 mL, 1.9 mmol), 1M aqueous $NaH_2PO_4$ (0.9 mL, 0.9 mmol) and 0.6M aqueous $NaClO_2$ (80%) (0.9 mL, 0.54 mmol). The reaction when completed upon analysis with TLC was quenched with aqueous $NaHSO_3$ (3 mL, 1M) and extracted with chloroform (3 X 5 mL) and EtOAc (5 mL). The organics were washed with brine (5 mL), evaporated to yield the crude carboxylic acid (27 mg, 60%). The crude acid (21.4 mg, 0.06 mmol) was placed in MeOH (1.2 mL) at 0 ºC. Commercially available TMS protected diazomethane (0.15 mL, 0.3 mmol) was drop-wise added to the above solution maintained at 0 ºC under nitrogen. Upon completion as analyzed by TLC, reaction was quenched by the addition of AcOH (0.2 mL) and sat. $NaHCO_3$ (0.2 mL) and in a way that neutral pH was maintained for the resulting ester. The aqueous phase was extracted with EtOAc (3 X 5 mL). The organics after drying over anhydrous sodium sulfate and rotary evaporation gave in hands crude ester which was purified by silica gel (3:1 Hex:EtOAc) to obtain ester **4.128** (11 mg, 50%) as oil. Spectral data for **4.128**: $^1$H-NMR (500 MHz, $CDCl_3$) $\delta$

7.89 (d, 2H, *J* = 8.3 Hz), 7.31 (d, 2H, *J* = 8.3 Hz), 5.83 (m, 1H), 5.11 (d, 1H, *J* = 17.1 Hz), 5.03 (d, 1H, *J* = 10.0 Hz), 4.61 (s, 1H), 3.80 (s, 3H), 2.59 (dd, 1H, *J* = 7.7, 5.0 Hz), 2.50 (m, 1H), 2.41 (s, 3H), 2.31 (m, 1H), 1.37 (s, 3H); $^{13}$C-NMR (125 MHz, $CDCl_3$) δ 172.4, 169.1, 145.4, 135.8, 134.8, 129.4, 128.7, 117.4, 76.0, 70.3, 52.9, 50.8, 27.8, 23.2, 21.7; IR (neat) 3507, 2980, 2925, 1748, 1361, 1171, 668; HRMS (ESI) (m/z): $[M+Na]^+$ calculated for $[C_{17}H_{22}NO_6S]^+$ 368.1168, found 368.1125.

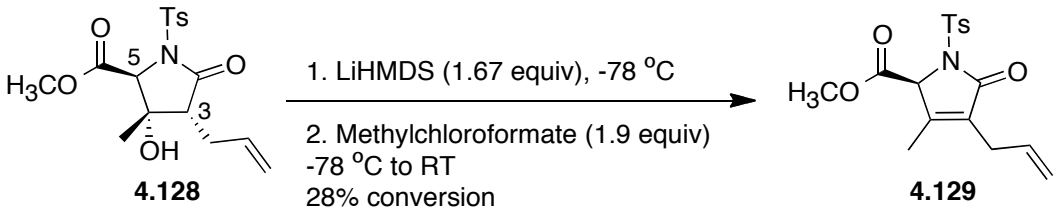

**4.128** **4.129**

**Procedure for C-5 alkylation**. To a solution of ester **4.128** (22 mg, 0.06 mmol) placed in anhydrous THF (2 mL) at -78 ºC was added methyl chloroformate (8 μL, 0.11 mmol) followed by drop-wise addition of LiHMDS (1M solution in THF) (0.1 mL, 0.1 mmol). Analysis with TLC showed no sign of progress of reaction. Reaction was strictly kept between -70 to -78 ºC. Although the reaction was analyzed to be incomplete after 4 h, it then quenched by addition of sat. $NH_4Cl$ (1 mL) and water (0.5 mL). The aqueous layer was extracted with EtOAc (3 X 4 mL). The organics were dried over anhydrous sodium sulfate and subjected to rotary evaporation to yield an inseparable mixture of undesired elimination product **4.129** and starting material with 28% conversion. Spectral data for **5.131**: $^1$H-NMR (500 MHz, $CDCl_3$) δ 7.98 (d, 2H, *J* = 8.4 Hz), 7.31 (d, 2H, *J* = 7.8 Hz), 5.71 (m, 1H), 5.10 (m, 1H), 4.99 - 4.96 (m, 2H), 3.82 (s, 3H), 2.93 (d, 1H, *J* = 6.3 Hz),

2.41 (s, 3H), 1.98 (s, 3H); HRMS (ESI) (m/z): $[M+H]^+$ calculated for $[C_{17}H_{20}NO_5S]^+$ 350.1062, found 350.1070.

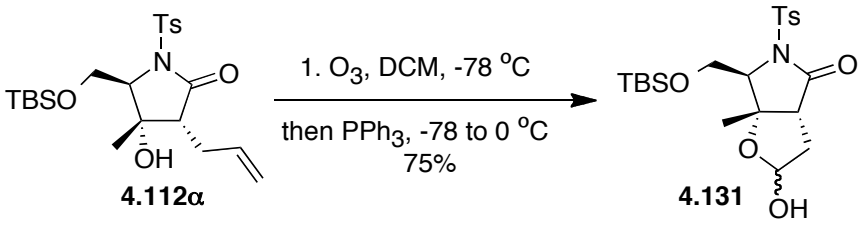

**4.112α** **4.131**

**Preparation of lactol 4.131**.[89] Lactam **4.112α** (0.2 g, 0.59 mmol) was placed in anhydrous DCM (6 mL). The flask was maintained at -78 ºC using dry-ice acetone bath. Ozone gas was bubbled to the above solution till color of the solution turned blue. Upon completion of the reaction, analyzed by TLC, excess of ozone was removed via bubbling with nitrogen till the solution turned colorless, re-crystallized $PPh_3$ (0.31 g, 1.18 mol) was added and the reaction was stirred while gradually warming the reaction to room temperature. The solvent was removed under vacuum and column chromatography (4:1 Hex:EtOAc) provided lactol **4.131** as a 1.1:1 diastereomeric mixture (0.2 g, 75%) as a white solid (m.pt = 148 – 150 ºC). Spectral data for **4.131**: Major diastereomer: $^1$H-NMR (500 MHz, $CDCl_3$): $\delta$ 7.93 (d, 2H, $J$ = 8.3 Hz), 7.28 (m, 2H), 5.28 (d, 1H, $J$ = 4.6 Hz), 4.29 (m, 1H), 4.15 (dd, 1H, $J$ = 11.4, 2.4 Hz), 4.08 (m, 1H), 2.90 (d, 1H, $J$ = 8.7 Hz), 2.15 (m, 1H), 2.07 (m, 1H), 1.32 (s, 3H), 0.78 (s, 9H), 0.05 (s, 3H), 0.00 (s, 3H); $^{13}$C-NMR (125 MHz, $CDCl_3$) $\delta$ 174.9, 144.6, 135.8, 132.9, 129.3, 127.9, 98.0, 86.8, 69.2, 61.9, 53.2, 36.3, 21.5, 20.2, -6.0; IR (neat) 3267, 3057, 2952, 2857, 1738, 1593, 1437, 1190, 1119, 934; HRMS (ESI) (m/z): $[M+Na]^+$ calculated for

$[C_{21}H_{33}NO_6SSi]^+$ 456.1876, found 456.1880. Minor diastereomer: $^1$H-NMR (500 MHz, $CDCl_3$): δ 7.86 (d, 2H, *J* = 8.3 Hz), 7.26 (m, 2H), 5.08 (t, 1H, *J* = 4.63 Hz), 4.21 (m, 1H), 3.85 (ddd, 2H, *J* = 14.0, 11.5, 1.2 Hz), 2.75 (d, 1H, *J* = 7.6 Hz), 2.51 (dd, 1H, *J* = 12.8, 5.7 Hz), 2.27 (d, 1H, *J* = 12.7 Hz), 1.53 (s, 3H), 0.79 (s, 9H), 0.05 (s, 3H), 0.00 (s, 3H); $^{13}$C-NMR (125 MHz, $CDCl_3$)[19] δ 173.8, 144.6, 135.4, 132.8, 129.3, 127.9, 97.0, 85.5, 68.7, 61.8, 51.3, 36.7, 20.3, 17.9, -5.8; HRMS (ESI) (m/z): $[M+H]^+$ calculated for $[C_{21}H_{33}NO_6SSi]^+$ 456.1876, found 456.1880.

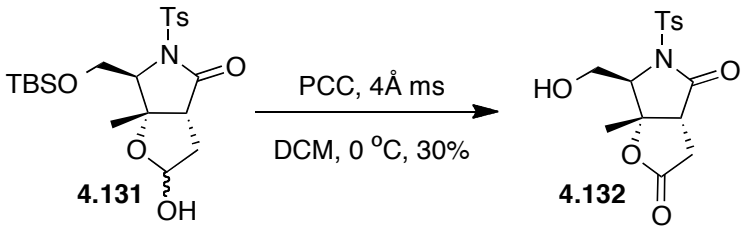


**Preparation of lactone 4.132**.[99] Lactol **4.131** (33.8 mg, 0.07 mmol) was dissolved in anhydrous DCM (1.9 mL) and maintained at 0 ºC using an ice-bath. To this activated 4Å ms (15 mg) was added. PCC (32 mg, 0.15 mmol) dissolved in anhydrous DCM (1.9 mL) was added via an addition funnel to the above solution at 0 ºC. The reaction was stirred and analyzed by TLC. Upon completion the solution was filtered and the solvent was removed under reduced pressure. Purification by flash chromatography (1:1 Hex:EtOAc) furnished lactol **4.132** (7.2 mg, 30%). Desilylated compound **4.132** was also obtained via removal of the TBS group utilizing the standard protocol starting from

[19] Sample was contaminated with $PPh_3$.

lactone **4.133**. Spectral data for **4.132**: $^{1}$H-NMR (600 MHz, $CDCl_3$) δ. 7.84 (d, 2H, J = 8.4 Hz), 7.32 (d, 2H, J = 8.4 Hz), 4.44 (s, 1H), 4.33 (dd, 1H, J = 12.6, 2.4 Hz), 3.97 (dd, 1H, J = 12.6, 1.2 Hz), 3.14 (dd, 1H, J = 9, 0.6 Hz), 2.73 (dd, 1H, J = 18.0, 9.0 Hz), 2.62 (d, 1H, J = 18 Hz), 2.42 (s, 3H), 1.61 (s, 3H); $^{13}$C-NMR (150 MHz, $CDCl_3$) δ 172.4, 172.2, 146.0, 134.4, 129.8, 128.2, 87.2, 67.6, 61.4, 49.2, 30.7, 21.7, 19.4; IR (neat) 3361, 2955, 2926, 1786, 1739, 1596, 1457, 1173, 1090; HRMS (ESI) (m/z): $[M+H]^+$ calculated for $[C_{15}H_{18}NO_6S]^+$ 340.0855, found 340.0891.

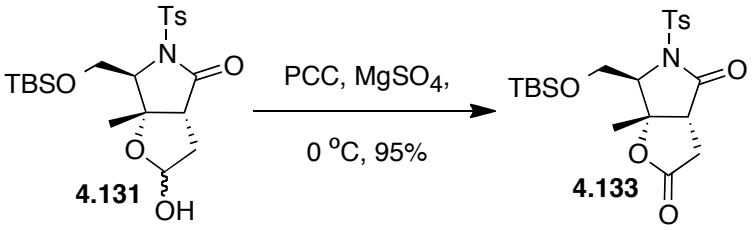


**Preparation of lactone 4.133**.[4] Lactol **4.131** (0.7 g, 1.53 mmol) was placed in anhydrous DCM (38 mL). Anhydrous powdered $MgSO_4$ (4g) was added. To this PCC (98%) (0.75 g, 3.37 mmol) dissolved in anhydrous DCM (42 mL) was added to the above solution at 0 ºC under nitrogen drop-wise via an addition funnel. The reaction was stirred for 5 h and after completion as confirmed by TLC, was filtered. DCM was removed under reduced pressure and column purification (2:1 Hex:EtOAc) yielded lactol **4.133** (0.65 g, 95%) as a wax. Spectral data for **4.133**: $^{1}$H-NMR (500 MHz, $CDCl_3$) δ 7.83 (d, 2H, *J* = 8.0 Hz), 7.29 (d, 2H, *J* = 8.0 Hz), 4.44 (s, 1H), 4.19 (d, 1H, *J* = 11.9 Hz), 3.94 (d, 1H, *J* = 11.9 Hz), 3.02 (d, 1H, *J* = 8.1 Hz), 2.73 (dd, 1H, *J* = 18.2, 8.8 Hz), 2.62 (d, 1H, *J* = 18.2 Hz), 2.40 (s, 3H), 1.58 (s, 3H), 0.83 (s, 9H), 0.09 (s, 3H), 0.06 (s, 3H);

$^{13}$C-NMR (125 MHz, $CDCl_3$) δ 172.3, 171.8, 145.6, 134.9, 129.7, 128.0, 87.3, 67.6, 62.1, 49.4, 30.8, 25.7, 21.7, 19.1, 18.0, -5.7, -6.0; IR (neat) 2953, 1791, 1738, 1559, 1260, 1174, 939; HRMS (ESI) (m/z): $[M+H]^+$ calculated for $[C_{21}H_{32}NO_6SiS]^+$ 454.1720, found 454.1715.

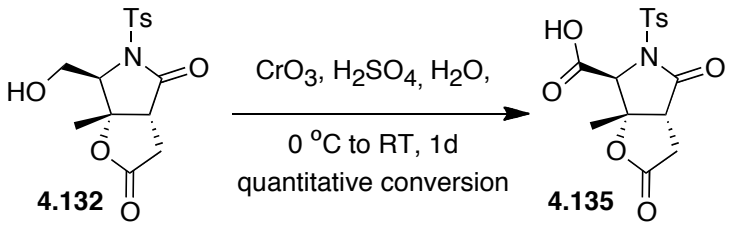


**Preparation of acid 4.135**.[100] Alcohol **4.132** (26.7 mg, 0.08 mmol) was placed in acetone (0.4 mL). The solution was cooled to 0 ºC and $H_2SO_4$ (8.1 μL) was added. A mixture of $CrO_3$ (38 mg, 0.38 mmol) and $H_2SO_4$ (31 μL, 0.57 mmol) dissolved in water (32 μL, 1.75 mmol) was added to the above acidic solution at 0 ºC. Note, sometimes small amount of acetone had to be used in order to transfer the latter mixture completely to the reaction flask maintained at 0 ºC. Slowly reaction was warmed to room temperature. After 8 h upon completion as analyzed by TLC, reaction was quenched by the addition of isopropanol (0.3 mL). The mixture was diluted with DCM and sat. $NaHCO_3$ (0.5 mL). The aqueous layer was separated and acidified with 10% $H_2SO_4$ to maintain pH at 1.0 and extracted with EtOAc (3 X 5 mL). The organics were dried over anhydrous sodium sulfate and evaporated under reduced pressure and was taken to next step without purification.

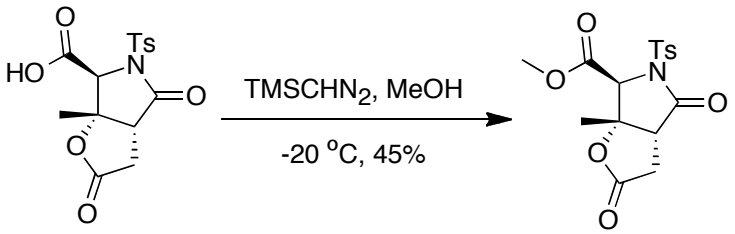


**4.135** **4.136**

**Preparation of ester 4.136**.[101] The crude carboxylic acid **4.135** (0.13 g, 0.37 mmol) was placed in methanol (7.5 mL). The flask was maintained at -20 ºC via a chiller. To this was then added TMS protected diazomethane (2M solution in toluene) (0.93 mL, 1.85 mmol) drop-wise under inert atmosphere. The reaction was warmed to 0 ºC and stirred till all the starting material was consumed as analyzed by TLC. Upon completion, the reaction was quenched by the addition of AcOH (0.2 mL) and sat. $NH_4Cl$ to neutralize the pH. The aqueous layer was extracted with EtOAc (3 X 10 mL). The organics were washed with brine (5 mL) and dried over anhydrous sodium sulfate. Rotary evaporation and column purification furnished ester **4.136** (61 mg, 45%) as a colorless oil. Spectral data for **4.136**: $^1$H-NMR (500 MHz, $CDCl_3$) $\delta$ 7.86 (d, 2H, $J$ = 8.2 Hz), 7.32 (d, 2H, $J$ = 8.2 Hz), 4.95 (s, 1H), 3.87 (s, 3H), 3.08 (dd, 1H, $J$ = 7.5, 2.9 Hz), 2.81 (m, 2H), 2.43 (s, 3H), 1.46 (s, 3H); $^{13}$C-NMR (125 MHz, $CDCl_3$) $\delta$ 171.6, 170.5, 168.2, 146.2, 129.8, 129.7, 128.8, 84.2, 67.4, 53.4, 47.8, 30.4, 21.8, 20.4; IR (neat) 2956, 1797, 1748, 1595, 1364, 1172, 1089, 1004; HRMS (ESI) (m/z): $[M+H]^+$ calculated for $[C_{16}H_{18}NO_4S]^+$ 368.0804, found 368.0811.

**Alternate procedure**:[102] To a solution of carboxylic acid **4.135** (42.3 mg, 0.12 mmol)

dissolved in anhydrous MeOH (1 mL) freshly distilled TMSCl (0.43 mL, 0.37 mmol) was drop-wise added. The reaction was stirred overnight under nitrogen. Upon completion as analyzed by TLC, the solvent was removed under reduced pressure. The crude upon purification with column chromatography (1:1 Hex:EtOAc) afforded ester **4.136** (35.2 mg, 80%) as an oil.

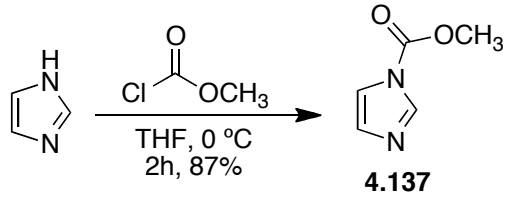

**4.137**

**Preparation of methyl imidazolecarboxylate**.[75] To a solution of imidazole (15 g, 22.03 mmol) in anhydrous THF (26 mL) was added methyl chloroformate (0.95 mL, 12.12 mmol) at 0 ºC. The reaction was stirred under nitrogen for 3 h at the same temperature. The reaction was filtered and the filtrate was concentrated in vacuum to afford N-methoxycarbonyl imidazole **4.137** (24 g, 84%).

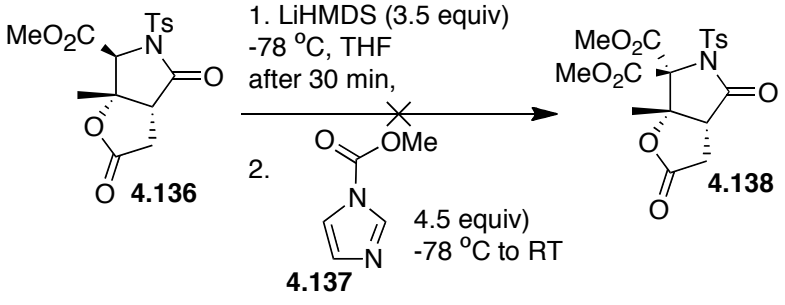


**Procedure for carbamoylation with N-methoxycarbonyl imidazole**:[75] To ester **4.136** (29 mg, 0.08 mmol) dissolved in anhydrous THF (2.6 mL) was added

commercially available LiHMDS (1M solution in THF) (0.12 mL, 0.12 mmol) at -78 $^{o}$C. The solution was stirred for 0.5 h and then N-methoxycarbonyl imidazole **5.139** (20 mg, 0.16 mmol) dissolved in a small amount of THF (0.3 mL) was added under nitrogen. No reaction was observed and thus extra LiHMDS (0.16 mL, 0.16 mmol) and N-methoxycarbonyl imidazole **4.137** (30 mg, 0.24 mmol) was added. TLC analysis revealed several spots, at which point the reaction was quenched with sat. $NH_4Cl$ (3 mL). The aqueous phase was extracted with EtOAc (3 X 5 mL). The organics were washed with brine (5 mL), dried over anhydrous sodium sulfate and subjected to rotary evaporation. The crude NMR showed several in-separable products.

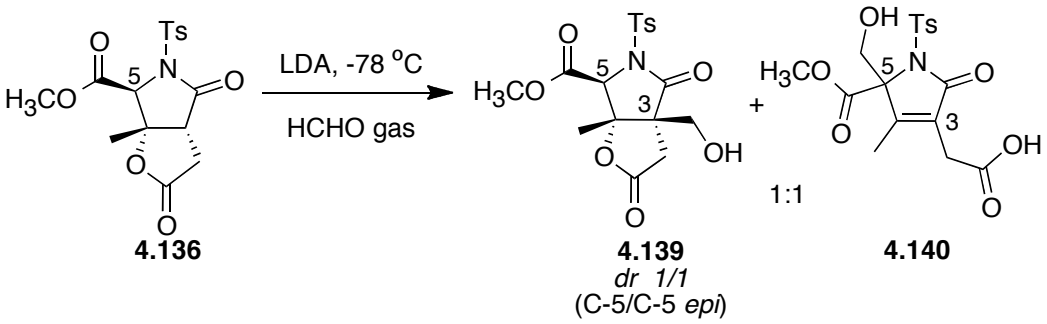


**4.136** | **4.139** *dr 1/1* (C-5/C-5 *epi*) | **4.140**

**Procedure for the alkylation of ester 4.136 with paraformaldehyde**. To a flame dried flask under nitrogen was added DIPA (0.28 mL, 1.98 mmol) and anhydrous THF (10 mL). The solution was cooled to -78 ºC and n-BuLi (1.13 mL, 1.94 mmol) was added via syringe. LDA was stirred at -78 ºC for 15 min and then warmed to 0 ºC for 15 min and brought back to -78 ºC. Generated LDA (0.34 mL, 0.07 mmol) was added drop-wise to the solution of ester **4.136** (21 mg, 0.06 mmol) in anhydrous THF (0.1 mL). Immediately followed by bubbling of excess of in-situ generated HCHO gas. After

stirring for 2 h, reaction was quenched with sat. $NH_4Cl$ (1mL), extracted with EtOAc (2 X 5 mL). The organic layer was dried over anhydrous sodium sulfate and evaporated under vacuum. The crude product upon analysis revealed a 1:1 mixture of **4.139** and **4.140** compounds. Spectral data for **4.139**: $^1$H-NMR (500 MHz, $CDCl_3$) $\delta$ 7.87 (d, 2H, *J* = 8.2 Hz), 7.33 (d, 2H, *J* = 8.2 Hz), 4.96 (s, 1H), 3.89 (s, 3H), 3.84 (d, 1H, *J* = 12.2 Hz), 3.73 (d, 1H, *J* = 12.2 Hz), 2.73 (d, 1H, *J* = 8.9 Hz), 2.44 (m, 1H), 2.43 (s, 3H), 1.51 (s, 3H); $^{13}$C-NMR (125 MHz, $CDCl_3$) $\delta$ 165.6, 146.4, 129.8, 129.6, 129.0, 128.8, 86.3, 67.7, 61.6, 53.5, 35.7, 33.8, 21.8, 19.6, 18.00; IR (neat) 2931, 1784, 1745, 1364, 1172, 949; HRMS (ESI) (m/z): $[M+H]^+$ calculated for $[C_{17}H_{20}NO_8S]^+$ 398.0910, found 398.0907. Spectral data for **4.140**: $^1$H-NMR (500 MHz, $CDCl_3$) $\delta$ 7.99 (d, 2H, *J* = 8.4 Hz), 7.32 (d, 2H, *J* = 8.4 Hz), 4.52 (d, 1H, *J* = 11.3 Hz), 4.34 (m, 1H), 3.83 (s, 3H), 3.31 (m, 2H), 2.41 (s, 3H), 2.39 (m, 1H), 1.95 (s, 3H); $^{13}$C-NMR (125 MHz, $CDCl_3$) $\delta$ 196.1, 180.9, 152.0, 145.6, 132.9, 129.4, 127.5, 125.2, 115.0, 113.1, 110.3, 93.7, 60.4, 53.3, 30.0, 29.7, 22.6, 21.7, 14.2; HRMS (ESI) (m/z): $[M+H]^+$ calculated for $[C_{17}H_{20}NO_8S]^+$ 398.0910, found 398.0902.

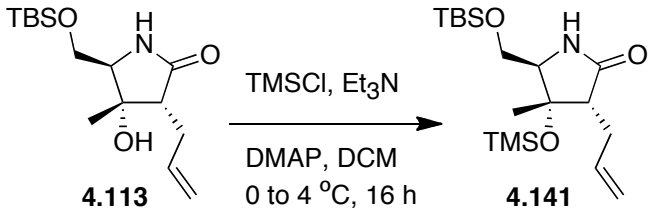


**4.113** **4.141**

**Preparation of TMS ether 4.141**.[20] To a solution of lactam **4.113** (0.37 g, 1.25 mmol)

in anhydrous DCM (5 mL) at 0 ºC was added freshly distilled $Et_3N$ (0.53 mL, 3.75 mmol) and DMAP (15 mg, 0.13 mmol). Freshly distilled TMSCl (0.32 mL, 2.5 mmol) was then added drop-wise under nitrogen to the above solution at 0 ºC. The reaction was left to stir in the cold room (temperature 4 ºC) for overnight. Upon completion as analyzed by TLC, the solvent was removed under reduced pressure. Purification with column chromatography (2:1 Hex:EtOAc) gave O-TMS compound **4.141** with quantitative yield. Spectral data for **4.141**: $^1$H-NMR (500 MHz, $CDCl_3$) $\delta$ 8.18 (bs, 1H), 6.46 (d, 1H, $J$ = 5.3 Hz), 5.94 (m, 1H), 5.11 (d, 1H, $J$ = 16.9 Hz), 5.00 (d, 1H, $J$ = 10.2 Hz), 3.68 (dd, 1H, $J$ = 11.3, 2.7 Hz), 3.55 (dd, 1H, $J$ = 11.3, 3.6), 3.26 (dd, 1H, $J$ = 3.7, 2.5 Hz), 2.98 (s, 3H), 2.59 (dd, 1H, $J$ = 8.3, 5.4 Hz), 2.53 (m, 1H), 2.28 (m, 1H), 1.39 (s, 3H), 0.84 (s, 9H), 0.26 (s, 9H), 0.02 (s, 3H), 0.01 (s, 3H), EtOAc; $^{13}$C-NMR (75 MHz, $CDCl_3$) $\delta$ 177.7, 137.6, 115.7, 79.8, 65.3, 62.9, 52.3, 28.8, 25.8, 23.2, 18.1, 2.2, -5.6; IR (neat) 3187, 2953, 1702, 1381, 1253, 1073, 1006, 839; HRMS (ESI) (m/z): $[M+H]^+$ calculated for $[C_{18}H_{38}NO_3Si_2]^+$ 372.2390, found 372.2398.

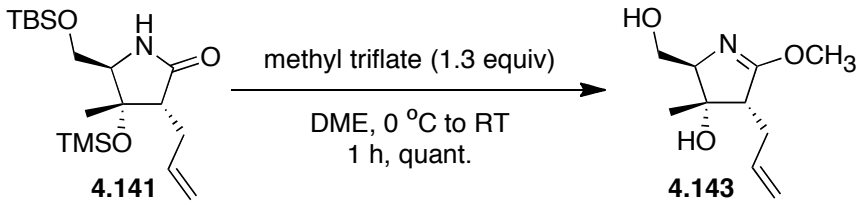


**Preparation of O-methylimidate 4.143**.[103] Lactam **4.141** (14 mg, 0.04 mmol) was dissolved in anhydrous DME (0.75 mL). To this was added methyl trifluorosulfonate (6 μL, 0.05 mmol) under nitrogen. The reaction was stirred for 2 h and upon completion of

the reaction as analyzed by TLC, $Et_3N$ (7 μl) was added and the pH was adjusted to neutral by sat. $NH_4Cl$. Solvent evaporation afforded O-methyl triflate compound **4.143**.

# REFERENCES

## REFERENCES


1. Feling, R. H.; Buchanan, G. O.; Mincer, T. J.; Kauffman, C. A.; Jensen, P. R.; Fenical, W. *Angew. Chem., Int. Ed.* **2003**, *42*, 355-357.

2. Fenical, W.; Jensen, P. R. *Nat. Chem. Biol.* **2006**, *2*, 666-673.

3. Oh, D.-C.; Williams, P. G.; Kauffman, C. A.; Jensen, P. R.; Fenical, W. *Org. Lett.* **2006**, *8*, 1021-1024.

4. Williams, P. G.; Asolkar, R. N.; Kondratyuk, T.; Pezzuto, J. M.; Jensen, P. R.; Fenical, W. *J. Nat. Prod.* **2006**, *70*, 83-88.

5. Buchanan, G. O.; Williams, P. G.; Feling, R. H.; Kauffman, C. A.; Jensen, P. R.; Fenical, W. *Org. Lett.* **2005**, *7*, 2731-2734.

6. Stadler, M.; Bitzer, J.; Mayer-Bartschmid, A.; Muller, H.; Benet-Buchholz, J.; Gantner, F.; Tichy, H. V.; Reinemer, P.; Bacon, K. B. *J. Nat. Prod.* **2007**, *70*, 246-252.

7. Bubko, I.; Gruber, B. M.; Anuszewska, E. L. *Postepy Hig. Med. Dosw.*, *64*, 314-325.

8. Goldberg, A. L. *Biochem. Soc. Trans.* **2007**, *035*, 12-17.

9. Gulder, T. A. M.; Moore, B. S. *Angew. Chem., Int. Ed.* **2010**, *49*, 9346-9367.

10. Borissenko, L.; Groll, M. *Chem. Rev.* **2007**, *107*, 687-717.

11. Groll, M.; Huber, R.; Potts, B. C. M. *J. Am. Chem. Soc.* **2006**, *128*, 5136-5141.

12. S. Ōmura, K. M., T. Fujimoto, K. Kosuge, T. Furuya, S. Fujita, and A. Nakagawa *J. Antibiot.* **1991**, *44*.

13. Dick, L. R. C., A. A.; Grenier, L.; Melandri, F. D.; Nunes,; S. L.; Stein, R. L. *J. Biol. Chem.* **1996**, *271*.

14. Reddy, L. R.; Saravanan, P.; Corey, E. J. *J. Am. Chem. Soc.* **2004**, *126*, 6230-6231.

15. Kulinkovich, O. G.; de Meijere, A. *Chem. Rev.* **2000**, *100*, 2789-2834.

16. Reddy, L. R.; Fournier, J. F.; Reddy, B. V. S.; Corey, E. J. *J. Am. Chem. Soc.* **2005**, *127*, 8974-8976.

17. Endo, A.; Danishefsky, S. J. *J. Am. Chem. Soc.* **2005**, *127*, 8298-8299.

18. Mulholland, N. P.; Pattenden, G.; Walters, L. A. S. *Org. Biomol. Chem.* **2006**, *4*, 2845-2846.

19. Beer, L. L.; Moore, B. S. *Org. Lett.* **2007**, *9*, 845-848.

20. Mulholland, N. P.; Pattenden, G.; Walters, I. A. S. *Org. Biomol. Chem.* **2008**, *6*, 2782-2789.

21. Ma, G.; Nguyen, H.; Romo, D. *Org. Lett.* **2007**, *9*, 2143-2146.

22. Nguyen, H.; Ma, G.; Gladysheva, T.; Fremgen, T.; Romo, D. *J. Org. Chem.* **2010**, *76*, 2-12.

23. Ling, T. T.; Macherla, V. R.; Manam, R. R.; McArthur, K. A.; Potts, B. C. M. *Org. Lett.* **2007**, *9*, 2289-2292.

24. Seebach, D.; Sting, A. R.; Hoffmann, M. *Angew. Chem., Int. Ed. Engl.* **1996**, *35*, 2708-2748.

25. Keisuske Takahashi, M. M., Kei Kawano, Jun Ishihara, Susumi Hatakeyama *Angew. Chem., Int. Ed.* **2008**, *47*, 6244-6246.

26. Fukuda, T.; Sugiyama, K.; Arima, S.; Harigaya, Y.; Nagamitsu, T., Ömura, Satoshi *Org. Lett.* **2008**, *10*, 4239-4242.

27. Momose, T.; Kaiya, Y.; Hasegawa, J.-i.; Sato, T.; Chida, N. *Synthesis* **2009**, *2009*, 2983,2991.

28. Overman, L. E. *J. Am. Chem. Soc.* **1976**, *98*, 2901-2910.

29. Caubert, V.; Masse, J.; Retailleau, P.; Langlois, N. *Tetrahedron Lett.* **2007**, *48*, 381-384.

30. Mosey, R. A.; Tepe, J. J. *Tetrahedron Lett.* **2009**, *50*, 295-297.

31. Villanueva Margalef, I.; Rupnicki, L.; Lam, H. W. *Tetrahedron* **2008**, *64*, 7896-7901.

32. Joensuu, P. M. M., G. J.; Fordyce, E. A. F.; Luebbers, T.; Lam, H. W. *J. Am. Chem. Soc.* **2008**, *130*, 7328-7338.

33. Struble, J. R. B., J. W. *Tetrahedron* **2009**, *65*, 4957-4967.

34. Schomaker, J. M.; Geiser, A. R.; Huang, R.; Borhan, B. *J. Am. Chem. Soc.* **2007**, *129*, 3794-3795.

35. Antilla, J. C. W., W. D. *Angew. Chem., Int. Ed.* **2000**, *39*, 4518-4521.

36. Lu, Z. Z., Y.; Wulff, W. D. *J. Am. Chem. Soc.* **2007**, *129*, 7185-7194.

37. Desai, A. A.; Wulff, W. D. *J. Am. Chem. Soc.* **2010**, *132*, 13100-13103.

38. Vesely, J. I., I.; Zhao, G. L.; Rios, R.; Córdova, A. *Angew. Chem. Int. Ed.* **2007**, *46*, 778-781.

39. Guthikonda, K. D. B., J. *J. Am. Chem. Soc.* **2002**, *124*, 13672-13673.

40. Moriarty, R. M. H., H.; Gupta, S. C. *Tetrahedron Lett.* **1981**, *22*, 1283-1286.

41. Forbeck, E. M. E., C. D.; Gilleran, J. A.; Li, P.; Joullie, M. M. *J. Am. Chem. Soc.* **2007**, *129*, 14463-14469.

42. Liu, H.; Zhang, T.; Li, Y. *Chirality* **2006**, *18*, 223-226.

43. Thakur, V. V.; Sudalai, A. *Tetrahedron Lett.* **2003**, *44*, 989-992.

44. Schomaker, J. Ph.D., Michigan State University, 2006.

45. Wang, T.; Ji, W.-H.; Xu, Z.-Y.; Zeng, B.-B. *Synlett* **2009**, *2009*, 1511,1513.

46. Parham, W. E.; Jones, L. D.; Sayed, Y. *J. Org. Chem.* **1975**, *40*, 2394-2399.

47. Beak, P.; Chen, C.-W. *Tetrahedron Lett.* **1985**, *26*, 4979-4980.

48. Bailey, W. F.; Longstaff, S. C. *Chimica Oggi-Chemistry Today* **2001**, *19*, 27-31.

49. Robertson, J.; O'Connor, G.; Sardharwala, T.; Middleton, D. S. *Tetrahedron* **2000**, *56*, 8309-8320.

50. Shaikh, A. L.; Kale, A. S.; Shaikh, M. A.; Puranik, V. G.; Deshmukh, A. R. A. S. *Tetrahedron* **2007**, *63*, 3380-3388.

51. Molander, G. A.; McKie, J. A. *J. Org. Chem.* **1995**, *60*, 872-882.

52. Guibe, F.; M'Leux, Y. S. *Tetrahedron Lett.* **1981**, *22*, 3591-3594.

53. Keck, G. E.; Yates, J. B. *J. Am. Chem. Soc.* **1982**, *104*, 5829-5831.

54. Keck, G. E.; Enholm, E. J.; Yates, J. B.; Wiley, M. R. *Tetrahedron* **1985**, *41*, 4079-4094.

55. Umehara, M.; Honnami, H.; Hishida, S.; Kawata, T.; Ohba, S.; Zen, S. *Bull. Chem. Soc. Jpn.* **1993**, *66*, 562-567.

56. Bamford, S. J.; Luker, T.; Speckamp, W. N.; Hiemstra, H. *Org. Lett.* **2000**, *2*, 1157-1160.

57. Berkessel, A.; Schr√∂der, M.; Sklorz, C. A.; Tabanella, S.; Vogl, N.; Lex, J.; Neud√∂rfl, J. r. M. *J. Org. Chem.* **2004**, *69*, 3050-3056.

58. Paul, B. J.; Hobbs, E.; Buccino, P.; Hudlicky, T. *Tetrahedron Lett.* **2001**, *42*, 6433-6435.

59. Forshee, P. B.; Sibert, J. W. *Synthesis-Stuttgart* **2006**, 756-758.

60. Moussa, Z.; Romo, D. *Synlett* **2006**, *2006*, 3294,3298.

61. Ritzen, B.; Hoekman, S.; Verdasco, E. D.; van Delft, F. L.; Rutjes, F. *J. Org. Chem.*, *75*, 3461-3464.

62. Nandi, P.; Redko, M. Y.; Petersen, K.; Dye, J. L.; Lefenfeld, M.; Vogt, P. F.; Jackson, J. E. *Org. Lett.* **2008**, *10*, 5441-5444.

63. Bajwa, J. S.; Chen, G. P.; Prasad, K.; Repic, J.; Blacklock, T. J. *Tetrahedron Lett.* **2006**, *47*, 6425-6427.

64. Nyasse, B.; Grehn, L.; Ragnarsson, U. *Chem. Commun.* **1997**, 1017-1018.

65. Kaiser, E. M.; Woodruff, R. A. *J. Org. Chem.* **1970**, *35*, 1198-1199.

66. Crowther, G. P.; Kaiser, E. M.; Woodruff, R. A.; Hauser, C. R. *Org. Synth.* **1971**, *51*.

67. Pilcher, A. S.; Ammon, H. L.; DeShong, P. *J. Am. Chem. Soc.* **1995**, *117*, 5166-5167.

68. Bunch, L.; Norrby, P. O.; Frydenvang, K.; Krogsgaard-Larsen, P.; Madsen, U. *Org. Lett.* **2001**, *3*, 433-435.

69. Lefranc, D.; Ciufolini, M. A. *Angew. Chem. Int. Ed.* **2009**, *48*, 4198-4201.

70. Bissember, A. C. *Synlett* **2009**, *2009*, 681,682.

71. Mander, L. N.; Sethi, S. P. *Tetrahedron Lett.* **1983**, *24*, 5425-5428.

72. Ley, S. V.; Norman, J.; Griffith, W. P.; Marsden, S. P. *Synthesis-Stuttgart* **1994**, 639-666.

73. Mancuso, A. J.; Swern, D. *Synthesis* **1981**, *1981*, 165,185.

74. Carlsen, P. H. J.; Katsuki, T.; Martin, V. S.; Sharpless, K. B. *J. Org. Chem.* **1981**, *46*, 3936-3938.

75. Trost, B. M.; Zhang, Y.; Zhang, T. *J. Org. Chem.* **2009**, *74*, 5115-5117.

76. Becker, J.; Grimme, S.; Fröhlich, R.; Hoppe, D. *Angew. Chem. Int. Ed.* **2007**, *46*, 1645-1649.

77. Khodachenko, A. N.; Shivanyuk, A. N.; Shishkina, S. V.; Shishkin, O. V.; Nazarenko, K. G.; Tolmachev, A. A. *Synthesis*, *2010*, 2588,2598.

78. Noguchi, T.; Tanaka, N.; Nishimata, T.; Goto, R.; Hayakawa, M.; Sugidachi, A.; Ogawa, T.; Niitsu, Y.; Asai, F.; Ishizuka, T.; Fujimoto, K. *Chem. Pharm. Bull.* **2009**, *57*, 22-33.

79. Decker, M.; Kraus, B.; Heilmann, J. *Bioorg. Med. Chem.* **2008**, *16*, 4252-4261.

80. Beckmann, U.; Eichberger, E.; Lindner, M.; Bongartz, M.; Kunz, P. C. *Eur. J. Org. Chem.* **2008**, *2008*, 4139-4147.

81. Huang, J.; Bunel, E.; Faul, M. M. *Org. Lett.* **2007**, *9*, 4343-4346.

82. Santamaria, J.; Kaddachi, M. T. *Synlett* **1991**, *1991*, 739,740.

83. Santamaria, J.; Kaddachi, M. T.; Ferroud, C. *Tetrahedron Lett.* **1992**, *33*, 781-784.

84. Pandey, G.; Kumaraswamy, G. *Tetrahedron Lett.* **1988**, *29*, 4153-4156.

85. Smith, S. C.; Bentley, P. D. *Tetrahedron Lett.* **2002**, *43*, 899-902.

86. Tellitu, I.; Serna, S.; Dominguez, E. *ARKIVOC* **2010**, *3*, 7-14.

87. Pathak, U.; Pandey, L. K.; Tank, R. *J. Org. Chem.* **2008**, *73*, 2890-2893.

88. V√∂lkert, M.; Uwai, K.; Tebbe, A.; Popkirova, B.; Wagner, M.; Kuhlmann, J. r.; Waldmann, H. *J. Am. Chem. Soc.* **2003**, *125*, 12749-12758.

89. Lorenz, O.; Parks, C. R. *J. Org. Chem.* **1965**, *30*, 1976-1981.

90. Lupattelli, P.; Bonini, C.; Caruso, L.; Gambacorta, A. *J. Org. Chem.* **2003**, *68*, 3360-3362.

91. Enholm, E. J.; Gallagher, M. E.; Jiang, S.; Batson, W. A. *Org. Lett.* **2000**, *2*, 3355-3357.

92. Murray, L. M.; O'Brien, P.; Taylor, R. J. K. *Org. Lett.* **2003**, *5*, 1943-1946.

93. Motamed, M.; Bunnelle, E. M.; Singaram, S. W.; Sarpong, R. *Org. Lett.* **2007**, *9*, 2167-2170.

94. Medina, J. R.; Blackledge, C. W.; Erhard, K. F.; Axten, J. M.; Miller, W. H. *J. Org. Chem.* **2008**, *73*, 3946-3949.

95. Cohen, J. L.; Chamberlin, A. R. *J. Org. Chem.* **2007**, *72*, 9240-9247.

96. Leonard, N. M.; Woerpel, K. A. *J. Org. Chem.* **2009**, *74*, 6915-6923.

97. Vedejs, E.; Naidu, B. N.; Klapars, A.; Warner, D. L.; Li, V.-s.; Na, Y.; Kohn, H. *J. Am. Chem. Soc.* **2003**, *125*, 15796-15806.

98. Nicolaou, K. C.; Li, A.; Edmonds, D. J.; Tria, G. S.; Ellery, S. P. *J. Am. Chem. Soc.* **2009**, *131*, 16905-16918.

99. Tadano, K. I., Y.; Minami, M.; Ogawa, S. *J. Org. Chem.* **1993**, *58*, 6266-6279.

100. Surmont, R.; Verniest, G.; Thuring, J. W.; Macdonald, G.; Deroose, F.; De Kimpe, N. *J. Org. Chem.*, *75*, 929-932.

101. Fuller, A. A. C., B.; Minter, A. R.; Mapp, A. K. *J. Am. Chem. Soc.* **2005**, *127*, 5376-5383.

102. Coriani, S. F., C.; Furlan, G.; Nitti, P.; Pitacco, G.; Ringholm, M.; Ruud, K. *Tetrahedron* **2009**, *20*, 1459-1467.

103. Gibbard, A. C. M., C. J.; Rees, C. W. *J. Chem. Soc., Perkin Trans. 1* **1986**, 145-149.

# Chapter 5

## Piperidines Via One-Pot Baylis-Hillman/Aza-Payne/Conjugate Addition Reaction: Novel Entry To Iminosugars.

### 5.1 Introduction to iminosugars and their biological significance:

Iminosugars are polyhydroxylated alkaloids and sugar mimics in which the endocyclic oxygen is replaced by a nitrogen atom. Their biological activity as glycosidase inhibitors have made their way from the laboratory to the clinic. They make one of the most attractive classes of carbohydrate mimics reported so far.[1] Iminosugars can be classified into five structural classes: polyhydroxylated piperidines, pyrrolidines, indolizidines, pyrrolizidines, and nortropanes.

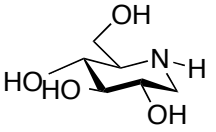


**5.1**
1-deoxynojirimysin (DNJ)

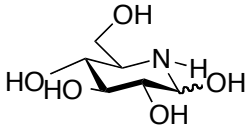


**5.2**
nojirimycin

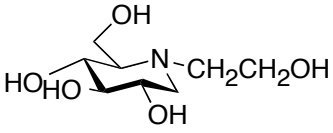


**5.3**
Glyset™

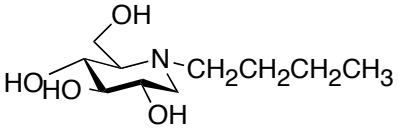


**5.4**
Zavesca™

**Fgure 5.1** Iminosugars compounds.

Scientific history of these compounds dates back to the first synthesis of 1-deoxy-nojirimycin (DNJ) **5.1** reported by Paulsen and coworkers in 1966 (Figure 5.1).[2] Later Inouye et al. reported the isolation of nojirimycin (NJ) **6.2** from bacteria streptomyces *roseochromogenes* R-468 and S. *lavendulae* SF-425 and identification of its antibiotic properties.[3] The scope of the biological activity of iminosugars has been applied to the inhibition of a variety of enzymes of medicinal interest such as glycosyltransferases,[4] glycogen phopshorylases,[5] nucleoside-processing enzymes,[6] a sugar nucleotide mutase and metalloproteins.[7,8]

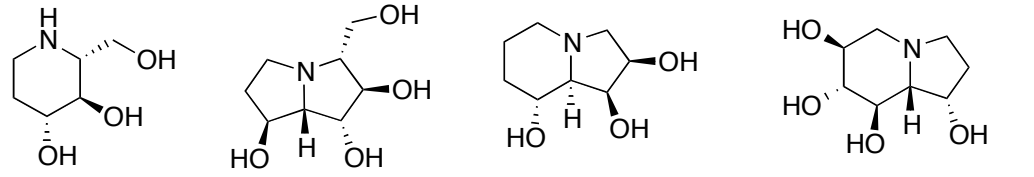


**Figure 5.2** Naturally occurring iminosugars.

Because of the use of iminosugars, significant progress has been made in the field of glycobiology in past 10 years.[9] DNJ **5.1** analogue is being evaluated in clinical phase trials (Phase II) for the treatment of Fabry disease, emphasizing its prospect as a new therapeutic option for lysosomal diseases. Iminosugars C-nucleosides designed as transition state analogues exhibit inhibition values in femtomolar and are among the most powerful inhibitors described for any enzyme to date.[10] Glyset™ was approved in 1996 for the treatment complications associated with type II diabetes, and Zavesca™ in

2003 as the first oral treatment for severe lysosomal disorder disease known as Gaucher. Figure 6.2 illustrates some of the other known iminosugars, which make popular targets for total syntheses because of their biological activity and structural complexity.[11-18] The following sections will primarily summarize the previous syntheses and our methodology to access specifically piperidine containing iminosugar compounds.

## 5.2 Previous approaches for the syntheses of piperidine based iminosugars.

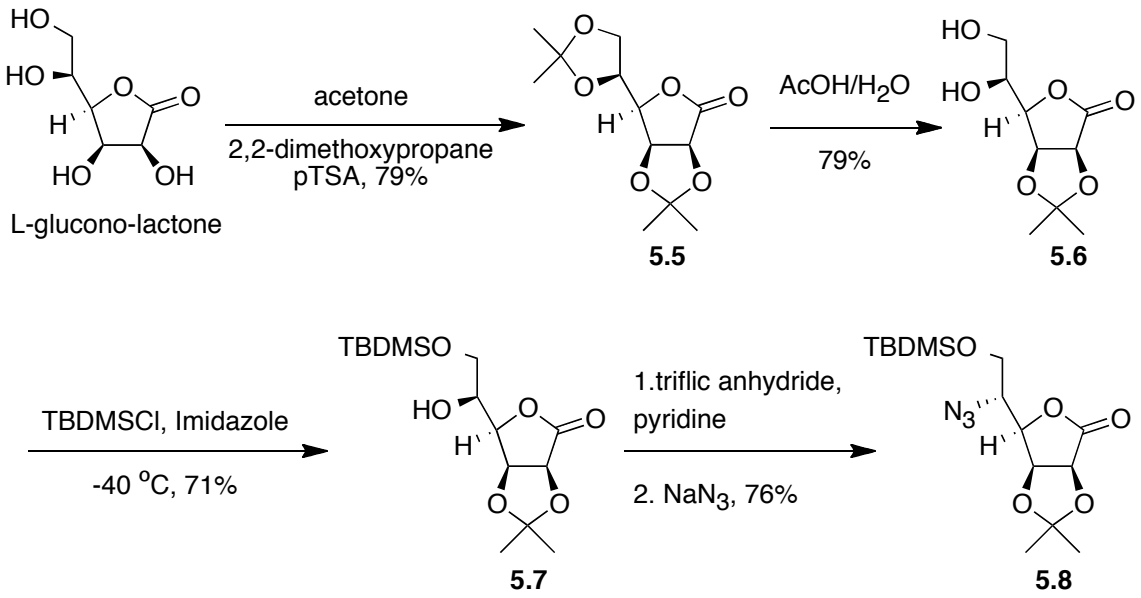


**Scheme 5.1** Synthesis of azido lactone, a common precursor employed in iminosugar syntheses.

Most of the previous strategies demonstrated for the synthesis of iminosugars adopt carbohydrates as the starting material. Although easy availability of the starting materials make these strategies convenient, introduction of nitrogen in the ring is often

achieved via several synthetic steps, often which are, tedious and involve long synthetic sequences.[19] Recently several common synthetic methodologies have been developed for the formation of library of compounds rather than adopting parallel syntheses for individual compounds. The easy availability of both enantiomers of gluconolactone makes them an attractive starting material for such syntheses. Scheme 5.1 illustrates the synthetic steps for the synthesis of azido lactone, an intermediate frequently exploited in various routes reported in the literature. Following few routine protection and deprotection steps, silylated compound **5.7** can be obtained in 3 steps starting from a glucono-lactone with the appropriate chirality.[20] Displacement of the trifluorosulfonated alcohol with sodium azide yielded azido lactone **5.8** in 76% yield. Wong and coworkers have used this precursor as their starting material to synthesize various derivatives of fuconojirimycin (FNJ) **5.10** (Scheme 5.2).[21] Nucleophilic addition of methyllithium to substrate **5.8** and subsequent reductive amination afforded piperidine **5.9** with the desired stereocenter exclusively in moderate yield. Acidic deprotection then produced β-homofunojirimycin **5.10**. A library of analogues, with substituents varied at C-1 has been reported following this strategy.

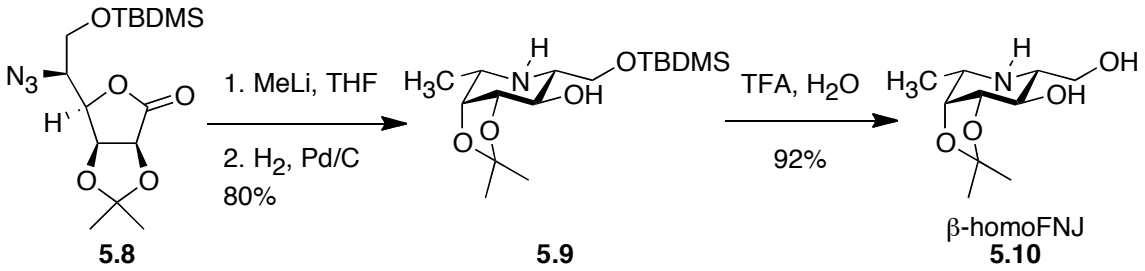


**5.8** **5.9** **5.10**

**Scheme 5.2** Proposed route to synthesize FNJ derivatives.

Alternatively, commercially available glucopyranose has also been utilized as starting material. Ferla and coworkers proposed a strategy that allows the preparation of different N-substituted iminosugars, having both $\alpha$ and $\beta$-structures with both D and L stereochemistry, this in turn offers a combinatorial approach for the design of library for the study of various analogs.[22] For this route aldehyde **5.11** was prepared from commercially available 2,3,4,6-tetra-O-benzyl-D-glucopyranose according to a known procedure in few steps (Scheme 5.3).[23] HWE reaction with phosphorane afforded *trans* olefin **5.12**. Although, Michael addition with allyl amines (other amines can be used in order to prepare different analogs) provided two diastereomers **5.13** and **5.14**, both diastereomers may contribute towards the library. As a result no efforts were made to improve the selectivity at this point. Notably, the predominance of **5.13** (*S)* over **5.14** (*R*) was rationalized invoking a Cram transition state model. In order to perform the cyclization, few manipulations were done. The isopropylidene protecting group was hydrolyzed. Selective silylation of the primary alcohol and protection of the secondary nitrogen with Fmoc afforded amine **5.15**. PCC oxidation to reveal the ketone, unmasking of the Fmoc protected nitrogen and in-situ reductive amination in the same pot afforded iminosugar **5.17**.

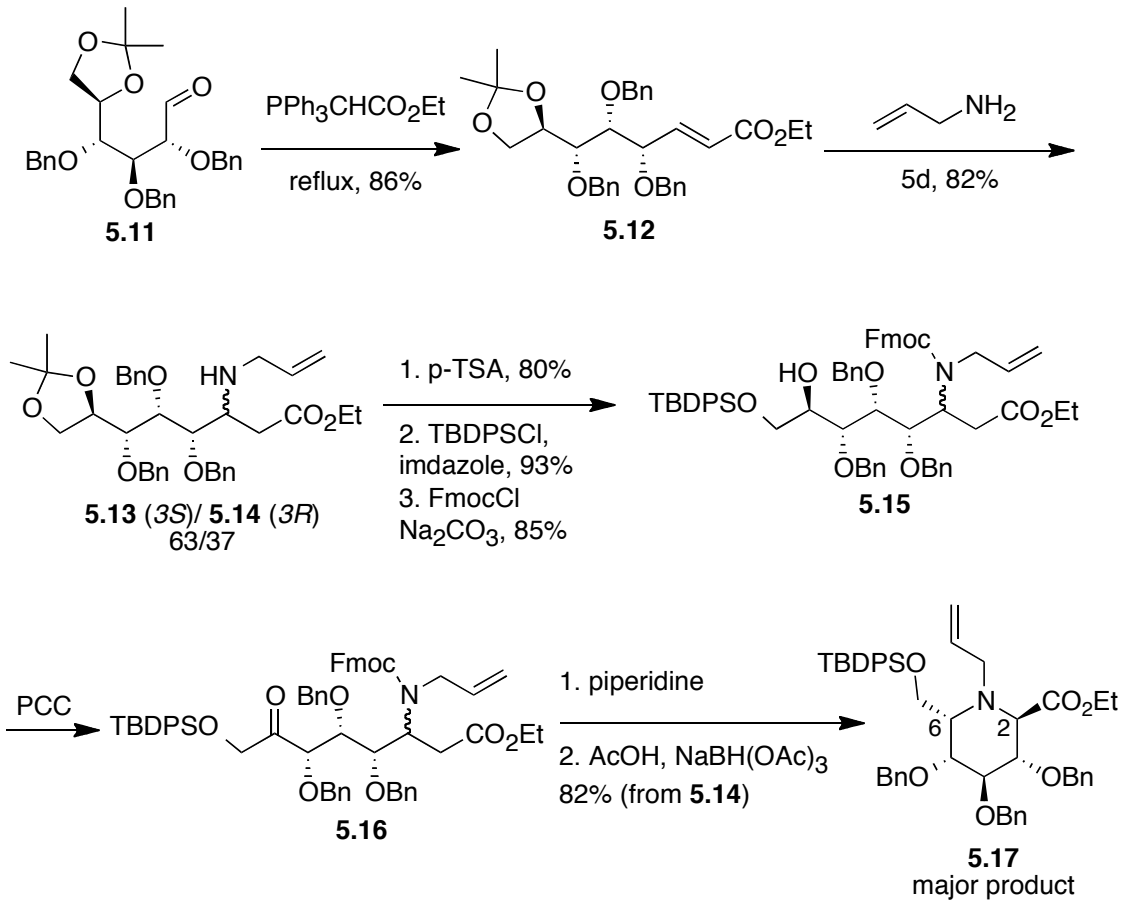


**Scheme 5.3** Route for the synthesis of iminosugars from glucopyranose.

As illustrated for *N*-allyl protected group in the scheme, cyclization was performed on various substituted nitrogen and most of them afforded the major product as the diastereomer having the substituent at C-6 position *trans* with respect to that at C-2 (see compound **5.17**, Scheme 5.3). Using this approach a library of eight iminosugar scaffolds was realized. Other than classis syntheses that involved carbohydrates the starting materials, some other non-carbohydrate based approaches are also reported. First example was illustrated by the synthesis of (±)-deoxymannojirimycin (Scheme 5.4).[24] Palladium catalyzed chemo and regioselective amination of butenediol

dicarbonate, epoxidation, intramolecular aldol for piperidine ring formation and Tamao-Fleming oxidation were some of the key steps involved in the synthesis.

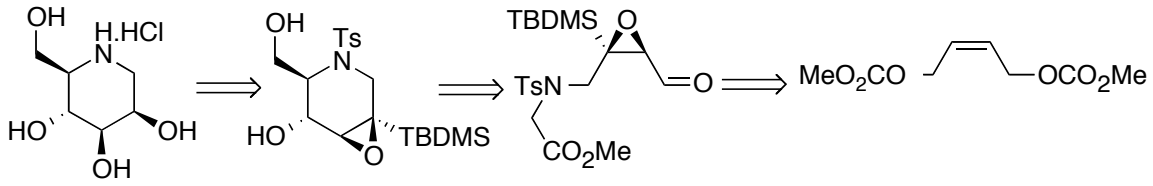


**Scheme 5.4** Retrosynthetic disconnections to access iminosugars starting from non-carbohydrate type starting material.

Cong and Yao reported the synthesis of iminosugars using furan derivatives, which in turn can be prepared starting with amino acids, by manipulating side chain substituents (Scheme 5.5).[25] Several synthetic routes to iminosugars reported so far definitely emphasize the significance of iminosugars. Innumerous potential therapeutic avenues demonstrated by iminosugars over a period of years, has kept interest at a high level in the synthetic community.

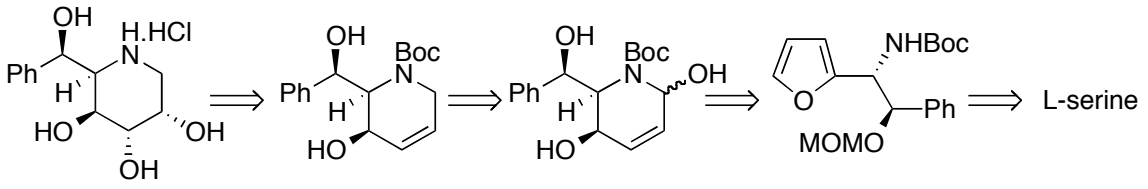


**Scheme 5.5** Route to iminosugars using 2-aminofuran derivatives.

## 5.3 Pyrrolidines to piperidines; via extension of tandem aza-Payne/hydroaminaiton methodology.

Tandem aza-Payne/hydroamination route[20] allows us to prepare 5-member rings exclusively. Pyrrolidine nuclei obtained via this route offer promising scaffolds, and can be elaborated to access iminosugar cores. In future, attempts to develop synthetic routes to access pyrrolidine-based iminosugars will be endeavored (Refer to Part-B for the discussion on some of these efforts toward the synthesis of pyrrolidine containing iminosugars). Higher member analogs; piperidine rings on the other hand, constitute skeletal framework of several important iminosugars and a number of natural products.[26,27] Thus, we aimed to extend the scope of this methodology in order to access 6-member cyclic compounds. The success of our one-pot aza-Payne/hydroamination approach relies on the choice of a suitable latent electrophile. The alkyne moiety serves as a nucleophile during the addition of the Grignard reagents to the aziridine-2-carboxaldehyde **5.18**, and later reveals its electrophilicity under the appropriate conditions in amide intermediate **5.20**, allowing for the cyclization. Notice, under these conditions, electrophilicity at C-1 results into the *5-exo-dig* cyclization, paving the way for the synthesis of 5-member rings exclusively (Scheme 5.6). Modification of this to a route that enables formation of 6-member rings would require the use of a latent electrophile, with altered electronics that provides higher electrophilicity at C-2.

---

[20] Refer to Chapter 3 (Section 3.3) for a detailed discussion on the tandem aza-Payne/hydroamination methodology.

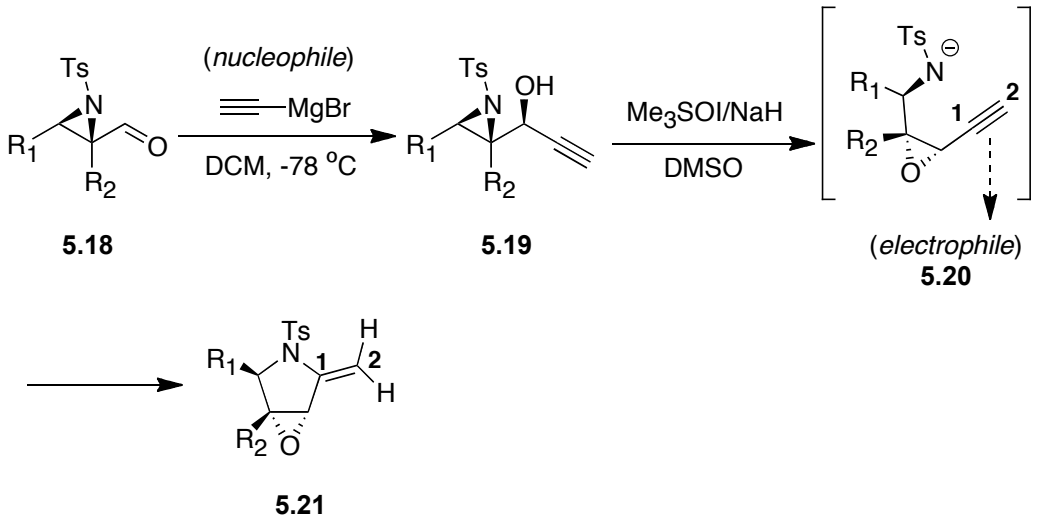


**5.18** **5.19** **5.20** **5.21**

**Scheme 5.6** Alkynes serve as latent electrophiles in tandem aza-Payne/hydroamination.

Olefins tethered to electron withdrawing groups are considered to exhibit higher electrophilicity at the C-2 position (β with respect to the carbonyl or other electron withdrawing substituents) and therefore, would fulfill such a requirement. Scheme 5.7 illustrates our proposed plan for such a strategy. Notice this plan incorporates aziridinol **5.22** tethered with an α,β-unsaturated carbonyl group (or other electron withdrawing groups). This would hopefully lead to epoxy amide intermediate **5.23** via the base-induced aza-Payne rearrangement. Ensuing *5-endo-dig* ring closure would then permit access to piperidine compounds. We were aware of the prerequisite for diastereomeric purity of aziridinol **5.22**, since only the *syn* isomer places both the electrophile and the nucleophile in exact orientation to aid in the cyclization.[21]

[21] Refer to Chapter 3 (Section 3.3.1) for the detailed discussion on the significance of the appropriate isomer in such transformations.

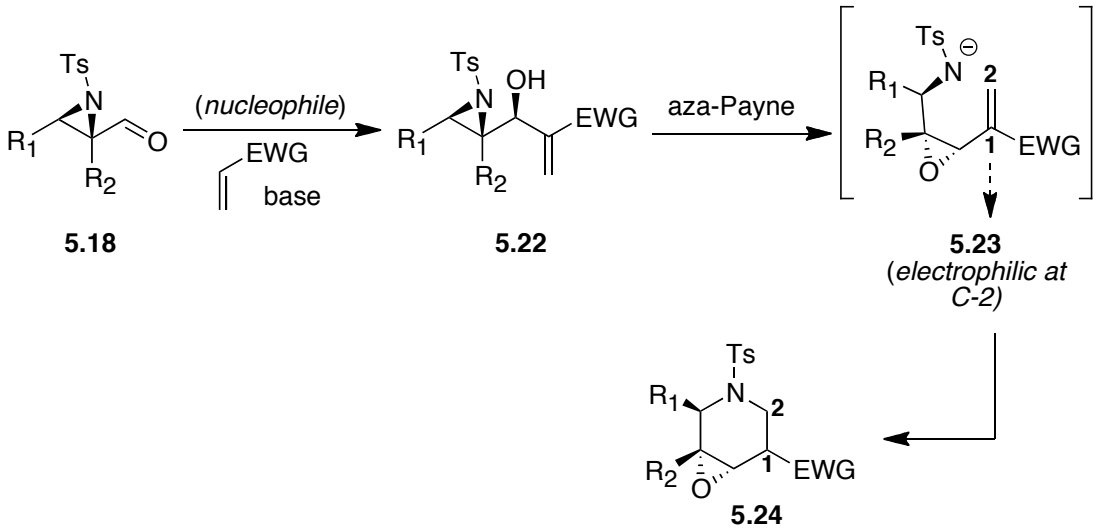


**Scheme 5.7** Proposed plan for the synthesis of piperidine rings.

Thus initial focus of our investigation became the assembly of *syn*-aziridinol compounds substituted with $\alpha,\beta$-unsaturated carbonyl or other electron withdrawing groups.

### 5.3.1 Synthesis of aziridinols substituted with activated olefins.

Synthesis of such aziridinols was envisioned via addition of suitable nucleophiles to form aziridine-2-carboxaldehyde **5.18**. Baylis-Hillman is a well precedent reaction in the literature which allows C-C bond formation between activated olefins and electrophiles.[28] S*yn*-selectivity was also anticipated during these reactions, based on the predominance of a stable bisected *exo* conformer,[22] observed previously in the case of Grignard addition to aziridine-2-carboxaldehydes. Since chelation does not play any role during such additions; replacement of the Grignard nucleophile with a carbon

[22] Refer to Chapter 2 (Section 2.5.2.3) for detailed discussion for the effect of the stable *exo* conformer on the selectivity obtained during such additions.

enolate, in theory, should not affect the resulting stereochemical outcome. Thus, as shown in Scheme 5.7, we planned to carry out Baylis-Hillman addition reactions on aziridine-2-carboxaldehyde **5.18** and commonly employed activated olefin compounds in such transformations.

#### 5.3.1.1 Precedence of Baylis-Hillman (B-H) reactions with aziridine -2-carboxaldehydes.

Krishna and coworkers have demonstrated the utility of epoxy aldehydes as electrophiles and commonly used nucleophiles in Baylis-Hillman reactions.[29] Moderate *anti* selectivity was achieved in case of *trans* substituted epoxy -2-carboxaldehydes (see **a**, Scheme 5.8), curiously in case of *cis*-substituted compounds excellent *syn* selectivity was obtained (see **b**, Scheme 5.8). Cornforth-based working model has been invoked, although its difficult to understand completely the opposite stereochemical outcome observed in case of *cis* and *trans* substituted epoxides substrates employing the same working model. On the other hand, use of *N*-Tr protected aziridine-2-carboxaldehydes has been reported by Zwanenburg and coworkers in a facile Baylis-Hillman reaction using a variety of activated olefins.[30] Catalytic amount of DABCO was used as the base to obtain an almost equimolar mixture of *syn*/*anti* adducts (Table 5.1). Although, reaction times were long (8-10 days), moderate yield of adducts was obtained (entries a-e).

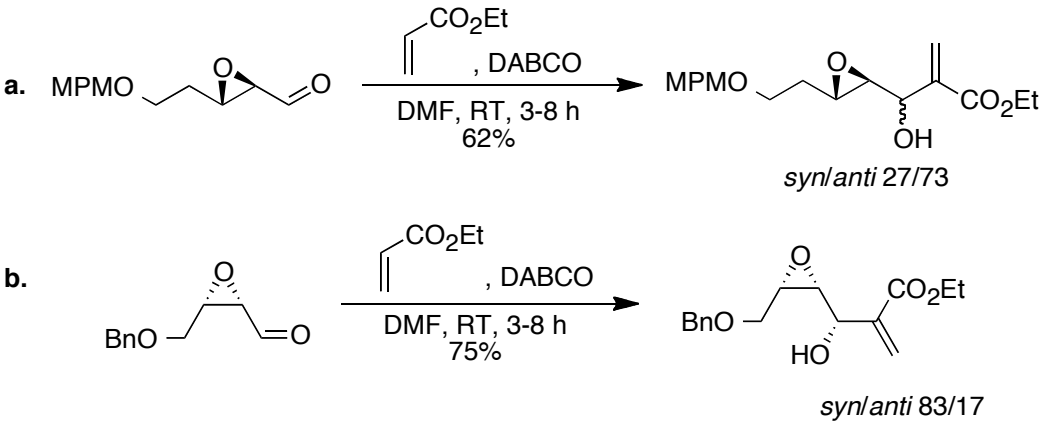


**Scheme 5.8** Epoxy-2-carboxaldehydes as electrophiles in Baylis-Hillman reactions.

Among various nucleophiles used for the reaction, best reactivity and selectivity was demonstrated by acrylonitrile (Table 6.1, entry c). Ketones were found less reactive (entry d) but sulfone exhibited extreme sluggish behavior towards the aldheyde (entry e). Recently, Yudin et al. reported the synthesis of Baylis-Hillman type adducts via the aza-Michael/Aldol pathway.[31] Starting material aziridine aldehyde **5.27** (Scheme 5.9) is known to exist in equilibrium with both the dimeric acyclic and cyclic forms. Cyclic dimer **5.27** was found to be the favored species under various solvents.

**Table 5.1** Substrate scope of *N*-Tr protected aziridine-2-carboxaldehydes in Baylis-Hillman reactions.

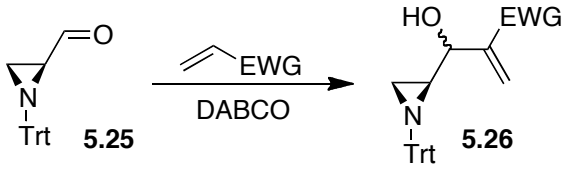


| entry | EWG | yield (%) | *syn*/*anti* [23] | time (days) |
|---|---|---|---|---|
| a | $CO_2Me$ | 82 | 50/50 | 8 |
| b | $CO_2Et$ | 81 | 50/50 | 8 |
| c | CN | 83 | 67/33 | 3 |
| d | COMe | 57 | 40/60 | 10 |
| e | $SO_2Ph$ | 28 | 43/57 | 45 |

In a typical experiment, a mixture of aldehyde **5.25**, methyl acrylate (1.5 equiv) and DABCO (0.15 equiv) were allowed to react at RT until all **5.25** had been consumed. The excess methylacrylate was removed the crude compound was subjected to column purification directly. When aziridine aldehyde dimers were reacted with cinnamaldehyde using a secondary amine/Bronsted acid catalytic system, $\alpha,\beta$-unsaturated aldehydes were isolated in high yields and excellent selectivity (Table 5.2). Particularly important is the judicious choice of the solvent acetonitrile, since dissociation kinetics of the dimer aldehyde is strictly governed by the nature of the solvent. Scheme 5.10 illustrates the

[23] The ratio of *syn* and *anti* adduct was determined by $^1$H-NMR shift of the methine proton H-C-OH; the methane proton of the syn isomers were always at higher field than those of the anti isomers.

mechanism suggested for the aza-Michael/Aldol reaction. The high diastereoselectivity is likely to result from the rigid environment assumed by the dimer intermediate **5.27-II**.

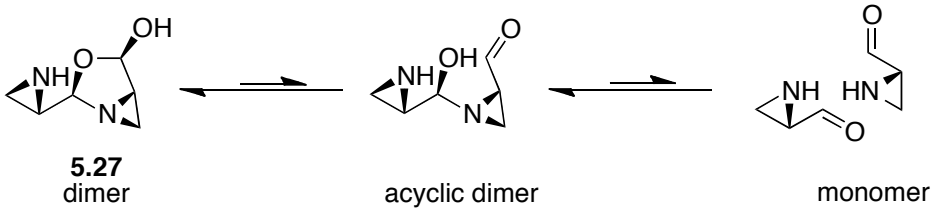


**5.27**
dimer

acyclic dimer

monomer

**Scheme 5.9** Monomer-dimer equilibrium for amphoteric amino-aldehydes.

Theoretical calculations performed on this intermediate supported the involvement of a hydrogen bonding interaction between the aldehydic and the hemi-aminal oxygens to stabilize this intermediate. This rigid environment provides the facial selectivity achieved in the attack of the enamine on the aldehyde and leads to the formation of stereo-defined intermediate **5.27-III**, which gives rise to the product **5.28** along with the regeneration of the catalyst.

**Table 5.2** Aza-Michael/Aldol reactions of aziridine-2-carboxaldehyde dimers.

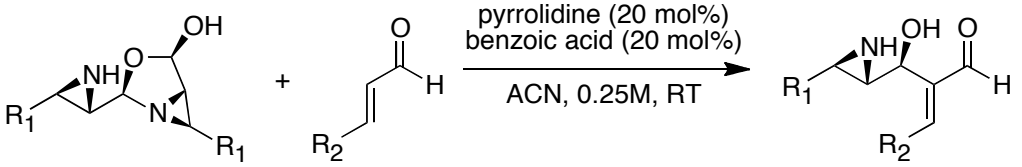


**5.27a**: $R_1 = {}^{i}Bu$
**5.27b**: $R_1 = H$
**5.27c**: $R_1 = CH_2OTBDMS$

**5.28**

| entry | $R_1$ | $R_2$ | product[24] | time | Yield (%) |
|---|---|---|---|---|---|
| 1 | **5.27a** | Ph | 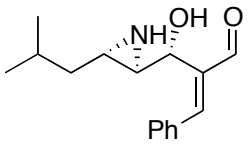 | 5h | 89 (*dr*>20:1) |
| 2 | **5.27c** | Ph | 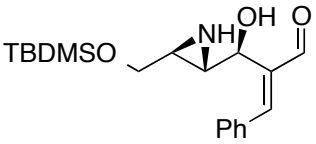 | 5h | 90 (*dr*>20:1) |
| 3 | **5.27b** | Ph | 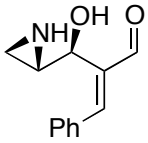 | 4h | 86 (*dr*>20:1) |
| 4 | **5.27a** | *m*-pyridine | 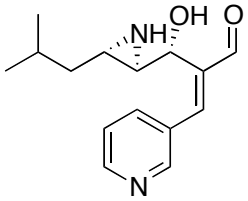 | 8h | 86 (*dr*>20:1) |

For a typical procedure 0.2 mmol of the substrate, 0.4 mmol of 5.28, 20 mol% of pyrrolidine/benzoic acid, 0.25 M ACN, RT.

Although high yield and selectivity are obtained in this case and utilize unprotected aldehydes, scope of products is restricted to aryl substituted $\alpha,\beta$-unsaturated

[24] Product identities were determined using 1D, 2D NMR spectroscopy and HRMS. Diastereomeric and *E/Z* ratios were determined by crude $^{1}$H-NMR analysis.

compounds. In conclusion, literature reports on the use of aziridine aldehydes as electrophiles in Baylis-Hillman reactions are limited.

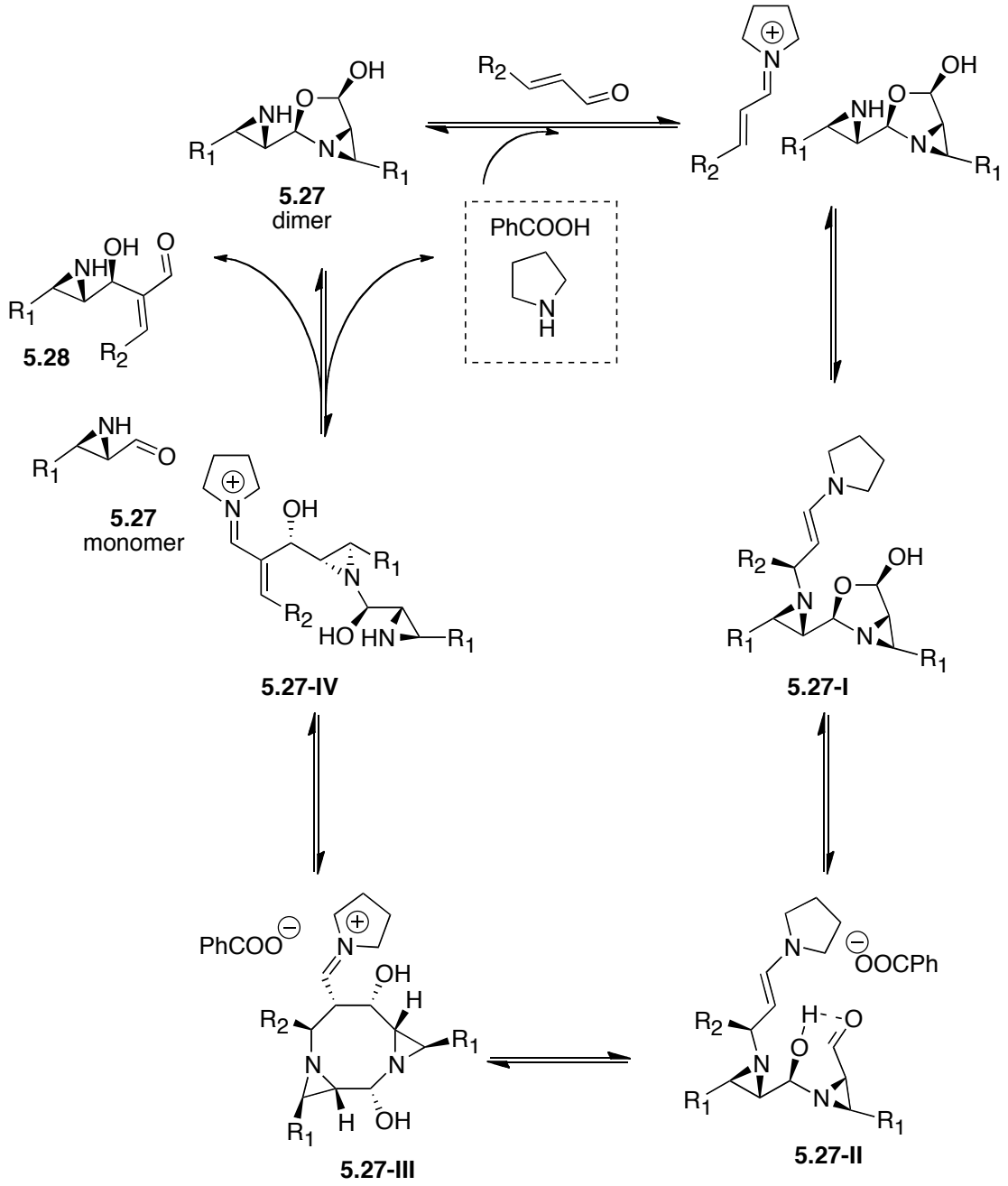


**Scheme 5.10** Mechanistic explanation for domino aza-Michael/Aldol reactions.

### 5.3.1.2 Unprecedented diastereoselective Baylis-Hillman reactions with *N*-Ts protected aziridine-2-carboxaldehydes.

As discussed previously in Section 5.3.1, we planned to investigate the synthesis of aziridinols substituted with activated olefins starting from the aziridine carboxaldehydes. 2,3-disubstituted aziridine-2-carboxaldehyde demonstrated the best *syn* selectivity (*dr*>99/3) along with the highest yield obtained during the addition of Grignard. Similar stereochemical outcome was anticipated, assuming that stability of the *SX* conformer[25] of the substrate would also prevail in the Baylis-Hillman reaction conditions, resulting in high *syn* selectivity, observed previously upon addition of Grignard reagents.

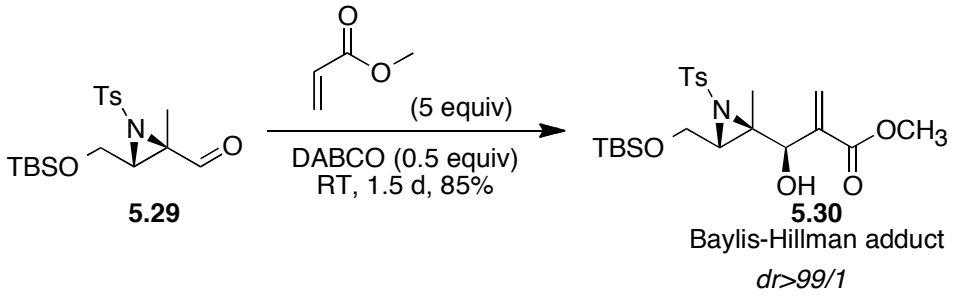


**Scheme 5.11** Highly diastereoselective Baylis-Hillman reactions of aziridine-2-carboxaldehyde.

Aware of precedent ring opening in activated aziridine compounds, initially methyl acrylate was added to a mixture of aziridinal **5.29** in the presence of catalytic amount of DABCO in DCM at -78 $^{o}$C. Unfortunately no reaction was observed as analyzed by

[25] Refer to Chapter 2 (Section 2.5.2.3) for a detailed discussion on the conformational preference observed in case of the substrate similar to **5.29**.

TLC, even when the temperature was raised to 0 $^{o}$C. Indeed when the reaction was carried out at room temperature, while using excess of methyl acrylate neat, starting material was completely consumed in 1.5 days to yield *syn* Baylis-Hillman adduct **5.30**. Remarkably the *anti* adduct was not at all observed by NMR (500 MHz) under these conditions. Identity of the compound **5.30** was further confirmed by X-ray crystallography (Figure 5.3).

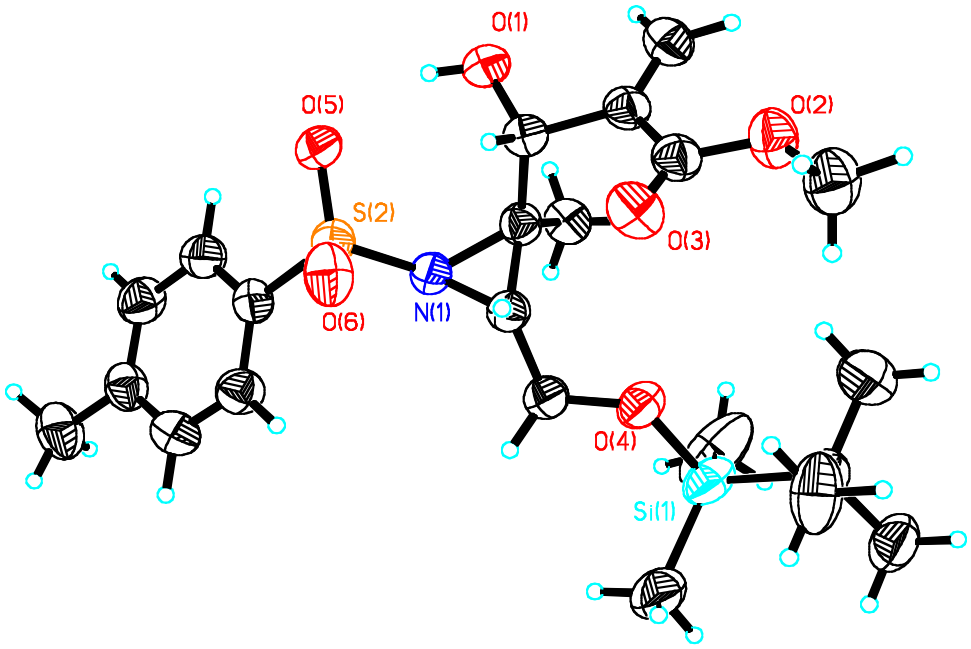


**Figure 5.3** X-ray structure of *syn* Baylis-Hillman adduct **5.30**.

We were encouraged by the observed expected diastereoselectivity, obtained in this case, since this further validates our hypothesis for the predominance and dominating role of the *SX* isomer. Later several other 2,3 di-substituted aziridine-2-

carboxaldehydes were subjected to the Baylis-Hillman reaction and gratifyingly afforded exclusively the *syn* products.

**Table 5.3** Scope of 2,3-disubstituted aziridine-2-carboxaldehydes utilized in Baylis-Hillman reaction with methyl acrylate.

| entry | substrate | time (days) | yield (%) | product *dr* (*syn/anti*) |
|---|---|---|---|---|
| 1[26] | 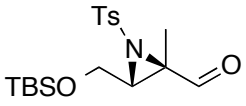 **5.29** | 1.5 | 85 | **5.30**[27] >99/1 |
| 2[28] | 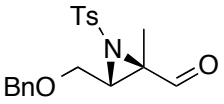 **5.31** | 1.5 | 82 | **5.32** >97/3 |
| 3[29] | 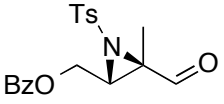 **5.33** | 1.5 | 79 | **5.34** >97/3 |
| 4 | 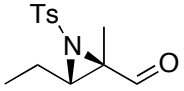 **5.35** | - | - | **5.36** |

General procedure: aldehyde (1 mmol) was stirred neat with methyl acrylate (5 equiv) and DABCO (0.5 equiv) under nitrogen till all the aldehyde was consumed completely.

[26] Refer to Chapter 4 (Section 4.6.1) for the preparation of compound **5.29**.

[27] Stereochemistry was confirmed by X-ray crystallography.

[28] Refer to Chapter 2 (Experimental procedures) for the preparation of compound **5.31**.

[29] Refer to Hart, S. Ph.D., Michigan State University, 2009 for the preparation of compound **5.33**.

Table 5.3 demonstrates the scope of 2,3-di-substituted aziridine-2-carboxaldehde substrates that were utilized in this reaction. Both alkyl ethers and non-ether substituents participated in the reactions successfully in high yield and leading to the product with excellent selectivity.

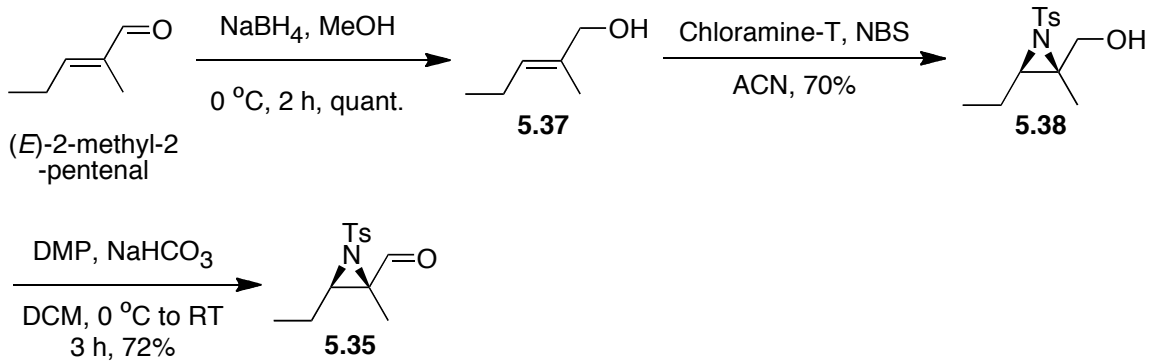


**Scheme 5.12** Synthesis of 2,3-disubstituted aziridine-2-carboxaldehyde.

Scheme 5.12 illustrates our route for the synthesis of substrate **5.35**, mimicking the strategy for the preparation of other 2,3-disubstituted aziridine-2-carboxaldehyde described previously. Thus borohydride reduction of commercially available (*E*)-2-methyl-2-pentenal proceeded in quantitative yield to furnish alcohol **5.37**. NBS/Chloramine-T protocol afforded aziridinol **5.38**, which was then oxidized by buffered DMP to obtain aldehyde **5.35**. Table 5.4 demonstrates the scope of some of the activated olefins, which were allowed to participate in the reaction. Notably, acrylonitrile exhibited the highest reactivity affording the product **5.39** in maximum yield in only 1 day (entry 2). This observation is consistent with that made for the Baylis-Hillman reaction of *N*-Trityl protected aziridine-2-carboxaldehydes.[30]

**Table 5.4** Scope of different activated olefins used in the Baylis-Hillman reaction.

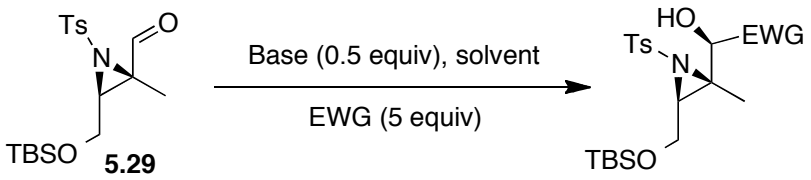


| entry | EWG | time (days) | yield (%) | product *dr* (*syn/anti*) |
|---|---|---|---|---|
| 1 | methyl acrylate | 1.5 | 85 | **5.30** 99/1 |
| 2 | acrylonitrile | 1.0 | 87 | **5.39** 99/1 |
| 3[30] | MVK | 1 | - | - |
| 4 | phenylvinylsulfone | 7 | - | *n.r.* |
| 5 | methylcrotylate | 7 | - | *n.r.* |

#### 5.3.1.2.1 Effects of ring substitution and *N*-protecting group on *syn/anti* ratios of adducts in the Baylis-Hillman reactions.

Both the substitution pattern and the protecting group on nitrogen played an important role in determining the stereochemical outcome observed for addition of Grignard reagents to aziridine-2-carboxaldehydes.[31] In order to probe the persistence of the same behavior, other classes of aziridine-2-carboaxaldehyde were examined. *Trans* substituted aziridine-2-carboxaldehyde substrates were synthesized using a previously described strategy. Aziridine alcohol **5.40** was

[30] Only degradation of the starting material was observed after 1 day.

[31] Refer to Chapter 2.

synthesized starting from commercially available crotyl alcohol using Chloramine-T/NBS protocol followed by oxidation by DMP under buffered conditions afforded aldehyde **5.41** (Scheme 5.13).

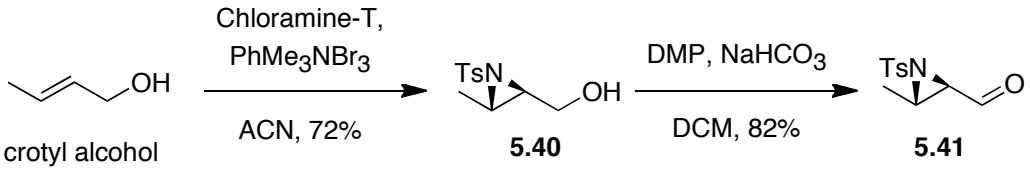


**Scheme 5.13** Synthesis of *N*-Ts protected *trans* aziridine-2-carboxaldehyde **5.41**.

Synthesis of substrate **5.42** was accomplished in four steps starting from commercially available 1,4-butyne diol (Scheme 5.14). Mono protection of the allylic alcohol **5.43** to yield the desired compound **5.44** had to be carried out very carefully. Longer reaction times led to the formation of the *bis*-silylated product **5.45** even in the presence of a half equivalent of TBSCl. Curiously competing reaction of mono-silylated compound for silylation was observed when reaction was kept for longer time, the latter can be reasoned due to the higher solubility of mono-silylated TBS ether; leading to undesired *bis*-silylated compound **5.45**.

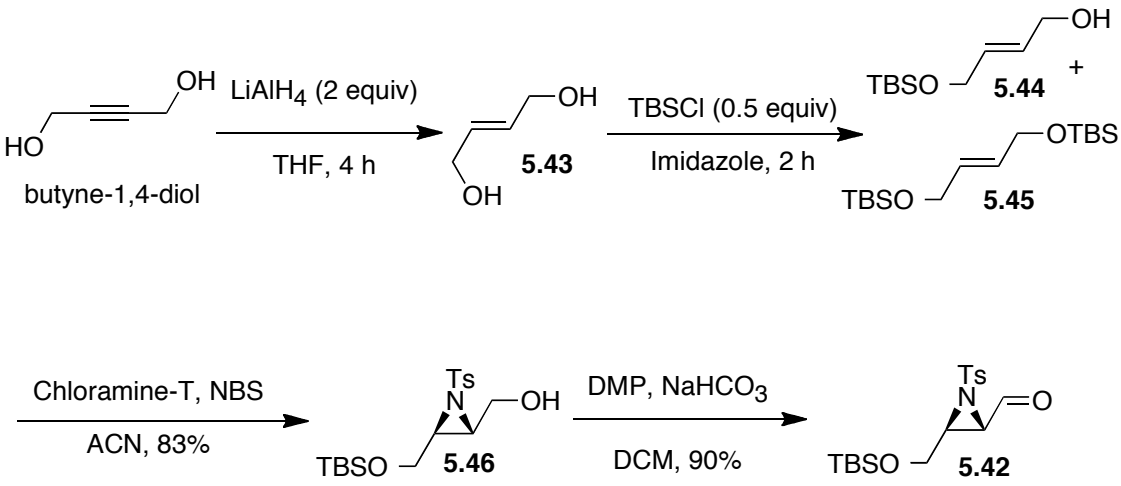


**Scheme 5.14** Synthesis of aziridine-2-carboxaldehyde **5.42**.

Unfortunately when subjected to the Baylis-Hillman reaction the desired products were obtained in low yields and moderate selectivity (Table 5.5). Moderate selectivity observed in these conditions also corroborates with those observed for the addition of Grignard reagents. In the absence of spectroscopic evidence however, the identity of the two isomers could not be revealed in these reactions. Notice in the case of Baylis-Hillman reactions, several competing reactions were also observed by analysis of the crude $^{1}$H-NMR. We were also encouraged by the excellent selectivity exhibited by *N*-Boc *trans* substituted aziridine-2-carboxaldehydes during addition of Grignard reagents.[32] Thus, we aimed to examine the scope of *N*-Boc protected aziridinals in the Baylis-Hillman reactions. Chloramine-T promoted one pot aziridination provides a quick

[32] Refer to Chapter 2 (Section 2.5.2.2) for the discussion on the selectivity obtained during the addition of Grignard reagent to such substrates.

access to install the aziridine functionalities; unfortunately similar protocol to install *N*-Boc protected aziridine rings is not well precedent in the literature.

**Table 5.5** Baylis-Hillman reaction using *trans* substituted aziridine-2-carboaxaldehydes with methyl acrylate.

| entry | substrate | time (days) | yield (%) | product *ratio*[33] |
|---|---|---|---|---|
| 1[32] | 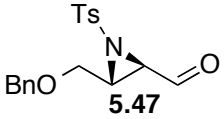 **5.47** | 2 | 35 | **5.48a**/**5.48b** 80/20 |
| 2 | 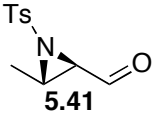 **5.41** | 2 | 37 | **5.49a**/**5.49b** 60/40 |
| 3 | 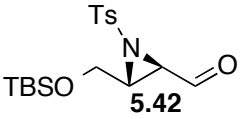 **5.42** | 2 | 24 | **5.50a**/**5.50b** 80/20 |

General procedure: Methyl acrylate (5 equiv), aldehyde (1 equiv) and DABCO (0.5 equiv) were added in a flask (Note in some cases small amount of DCM was added to make a slurry). The reaction was allowed to stir under inert atmosphere until all the starting material was consumed. After completion, excess methyl acrylate was removed and the crude was subjected to purification via column chromatography.

Thus, crotyl alcohol was aziridinated using a reported protocol, to afford aziridinol **5.51** in high yield. Unfortunately magnesium, methanol mediated detosylation led to a mixture of ring-opened products. Interestingly, products are likely to result from the ring

[33] Ratio of two isomers was determined by the analysis of crude $^{1}$H-NMR spectrum and identity of each has not been determined in the absence of sufficient evidence.

opening of the aza-Payne arranged epoxide compound via methanol (Scheme 5.15). This intramolecular opening of the aziridine via terminal alcohol as a of the generation of basic conditions via the formation of $Mg(OMe)_2$. The opening of the resulting epoxide by methanol under sonication conditions also seems viable.

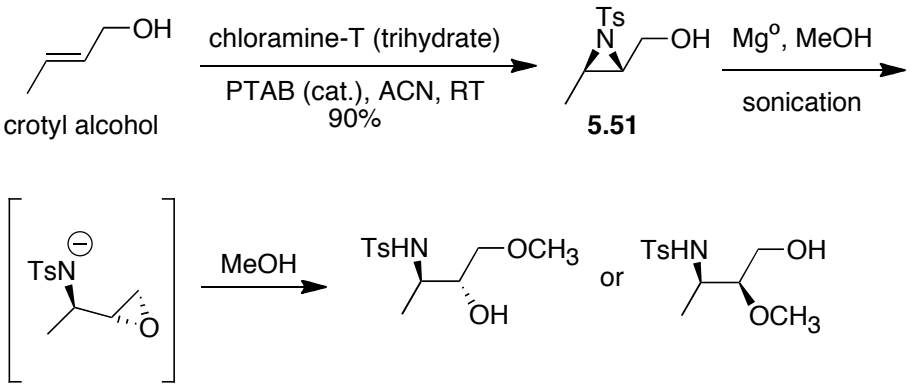


**Scheme 5.15** Failed attempt to detosylate *N*-Ts protected aziridinol.

In order to test the previous supposition, we decided to mask the alcohol as the silyl ether **5.52** and investigated its propensity towards detosylation. Interestingly, when aziridine alcohol **5.51** was subjected to TBSCl and imidazole using DMF as a solvent, a mixture of TBS ether and aza-Payne rearranged product was obtained. This observation further emphasizes the ease of this substrate to undergo such intramolecular ring opening reactions even under mild basic conditions. Instead, use of $Et_3N$ as the base and DCM as the solvent gave rise to the desired TBS ether although with poor conversion after 6 h, addition of catalytic amount of DMAP furnished the TBS ether **5.52** in excellent yield (Scheme 5.16). Satisfyingly, treatment of the TBS ether

under the previously described conditions successfully afforded the desired aziridine alcohol compound **5.53** in good yield.

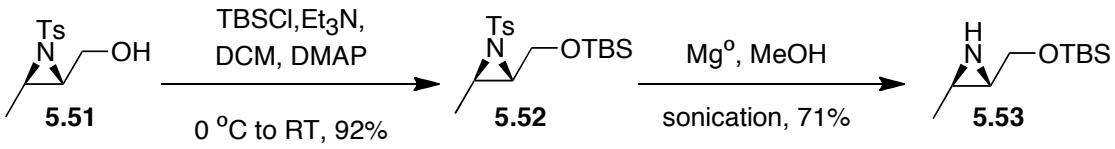


**Scheme 5.16** Successful synthesis of desoylated azirdine alcohol.

Unfortunately upon treatment of the TBS ether **5.53** with TBAF, the desired unprotected compound could not be isolated (Scheme 5.17). Polarity and high volatility associated with the molecule might make isolation of this compound challenging. On the other hand, desilylation of the corresponding *N*-Boc protected compound **5.54** provided the desired desilylated *N*-Boc aziridine alcohol **5.55** in low yield.[33] DMP oxidation under buffered conditions then afforded substrate **5.56** in surprisingly low yield. Scheme 5.18 demonstrates an alternate route by which this compound was also synthesized albeit with further lower overall yield.

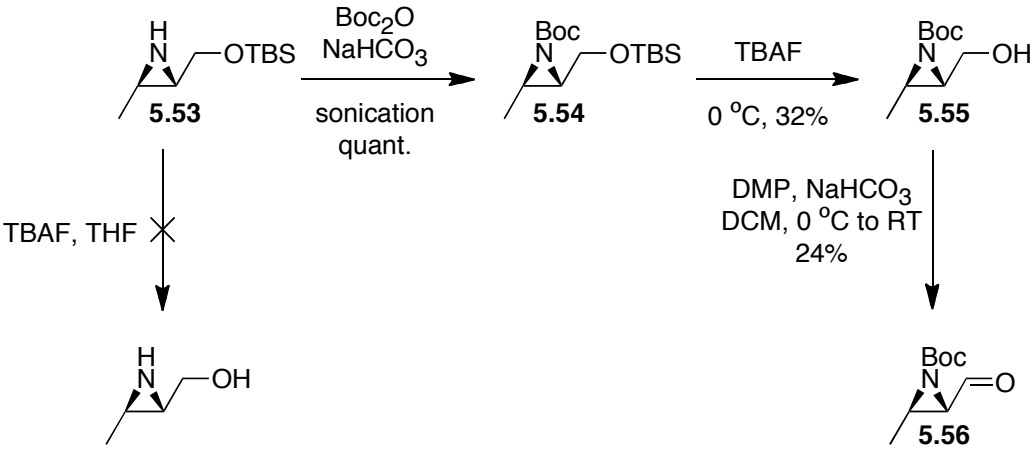


**Scheme 5.17** Synthesis of *N*-Boc protected aziridine-2-carboxaldehyde.

To our disappointment, when *N*-Boc aziridine-2-carboxaldehyde **5.56** was subjected to previously described Baylis-Hillman reaction conditions only starting material was recovered even after increased catalyst loading after 7 days.[34,35] We were intrigued by the success of *N*-Ts protected substrate under the similar conditions. Higher electrophilicity of aldehydic carbonyl due to the inductive effect exerted by electronically deficient tosyl might explicate the higher reactivity observed with *N*-Ts protected substrates. Although participation of the *N*-trityl protected aziridine-2-carboxaldhyde,[30] reported in the literature, does indicate the influence of factors other than just electronics (Scheme 5.19).

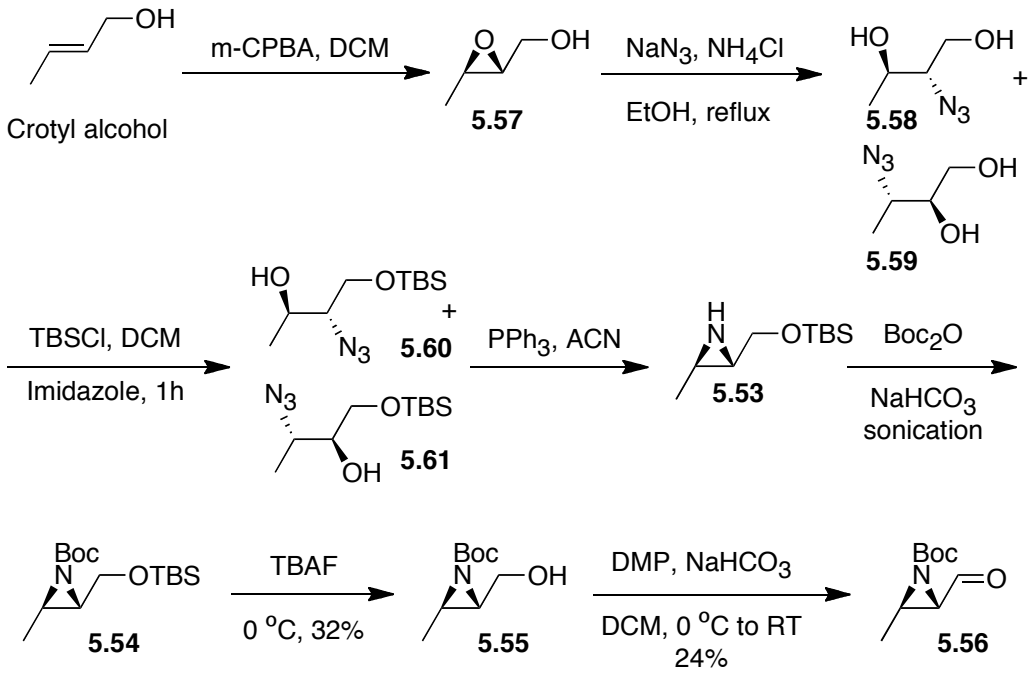


**Scheme 5.18** Alternate route to synthesize *N*-Boc protected aziridine-2-carboxaldehyde.

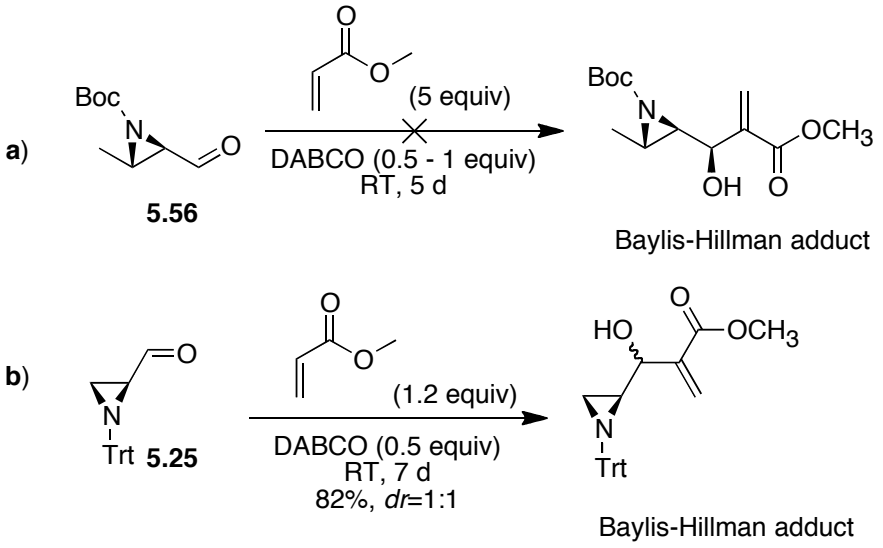


**Scheme 5.19 a**) Unreactive *N*-Boc proctected substrate **b**) *N*-Tr protected azirdine-2-carboxaldehyde yields Baylis-Hillman product successfully.

### 5.3.2 Cyclization of diastereomerically pure Baylis-Hillman products.

With the synthesis of the aziridinols via the Baylis-Hillman route accomplished, appropriate conditions for cyclization were investigated. Efforts were made to perform the cyclization under the conditions that were optimized for tandem aza-Payne/hydroamination reaction. Treatment of *syn* aziridinol compound **5.30** with *in-situ* generated dimethylsulfoxonium methylide in DMSO only led to degradation of the starting material, perhaps due to the harsh conditions (Scheme 5.20). At this point we decided first to probe the appropriate conditions to execute the aza-Payne rearrangement. Previously it was shown that the aza-Payne rearrangement can be carried out in the presence of NaH and DMSO.[36] Thus, we attempted the rearrangement by subjecting the Baylis-Hillman adduct **5.30** to NaH (2 equivalents) and DMSO. Unfortunately the reaction was marred by the presence of several undesired products as evident by crude NMR analysis (Scheme 5.21).

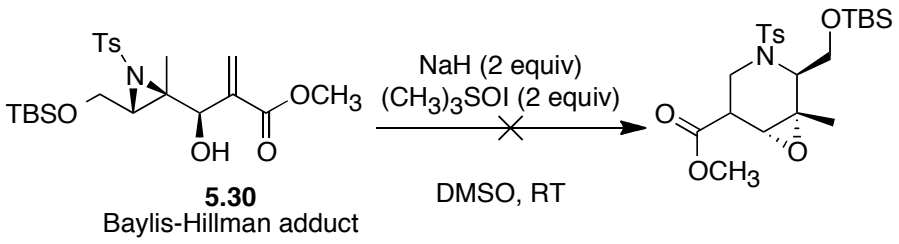


**Scheme 5.20** Failed cyclization under tandem aza-Payne/hydroamination.

However, treatment of adduct **5.30** with catalytic amount of NaH at cooler temperatures successfully afforded the unexpected compound dehydropiperidine compound **5.62**[34] in high yield.

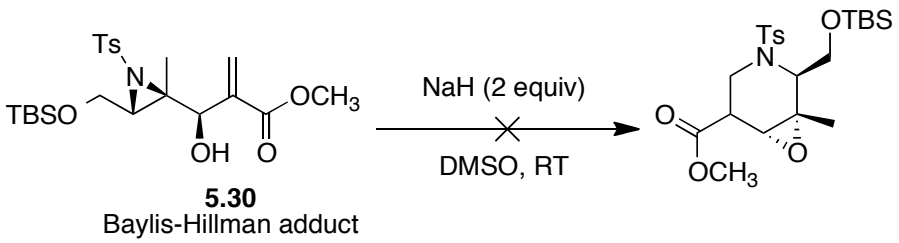


**Scheme 5.21** Baylis-Hillman adduct degrades under the aza-Payne rearrangement conditions.

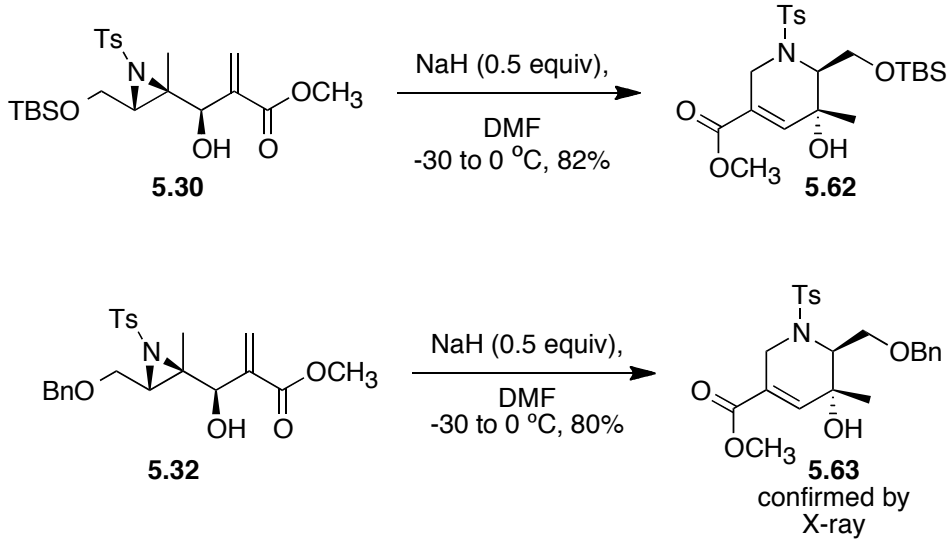


**Scheme 5.22** Successful cyclization of Baylis-Hillman adduct with catalytic base.

[34] Presence of only one isomer was revealed by analysis of both $^{1}$H-NMR and $^{13}$C-NMR spectra.

Treatment of the Baylis-Hillman adduct **5.32** under similar conditions yielded the cyclized product **5.63**, pleasantly whose structural identity was confirmed by X-ray crystallography (Figure 5.2). The mechanistic for the formation of the unexpected product is illustrated in Scheme 5.23. Base instigates the formation of the epoxy amide intermediate via the aza-Payne rearrangement of aziridinol **5.30**, which facilitates the intramolecular conjugate addition. However, at this stage concomitant opening of the epoxide is likely to result via the enolate, which leads to the formation of dehydropiperidine compound **5.62**. Unfortunately, epoxide opening could not be avoided even upon lowering the temperature to -78 ºC. Notably, epoxide opening was observed (TLC monitoring) along with the presence of starting material even at -78 ºC.

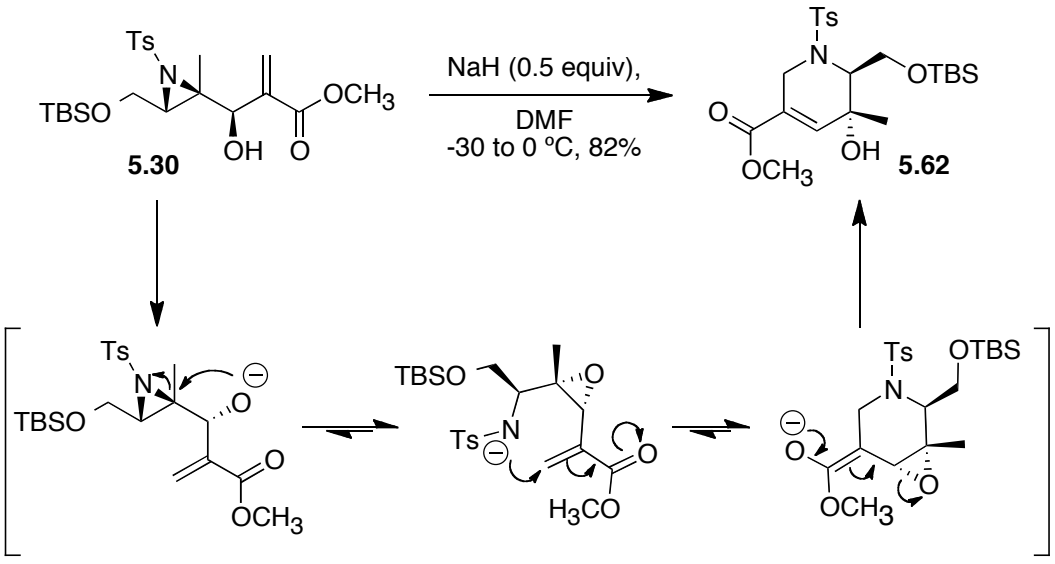


**Scheme 5.23** Postulated mechanism for the tandem aza-Payne/aza-Michael addition reaction.

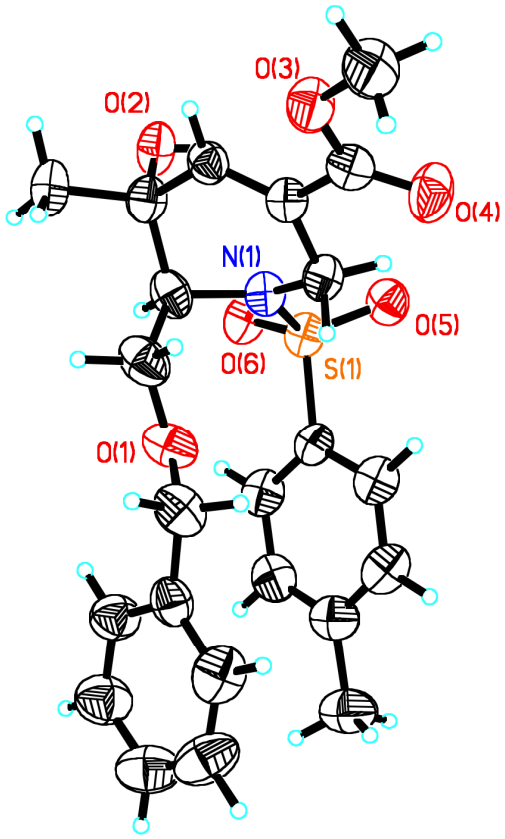


**Figure 5.4** X-ray structure of dehydropiperidine **5.63**.

Thus epoxide opening seems un-avoidable and favored perhaps due to the thermodynamic stability gained via ring strain release. Intramolecular nature of this reaction further makes it a facile process. Nevertheless, we were delighted by the access to the highly stereodefined 6-membered ring, which can be easily obtained via aza-Payne/conjugate addition reaction in one step. The compatibility of other functional groups in this reaction was proven by the successful participation of nitrile compound **5.39**, which also afforded dehydropiperidine adduct **5.64** in very good yield and excellent *syn* selectivity. (Scheme 5.24) The structural identification of this adduct was further confirmed by the X-ray crystal structure obtained for this compound (Figure 5.5).

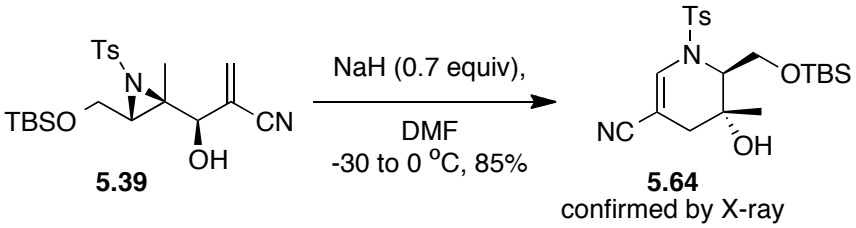


**Scheme 5.24** Successful participation of nitrile compound in tandem aza-Payne/conjugate addition reaction.

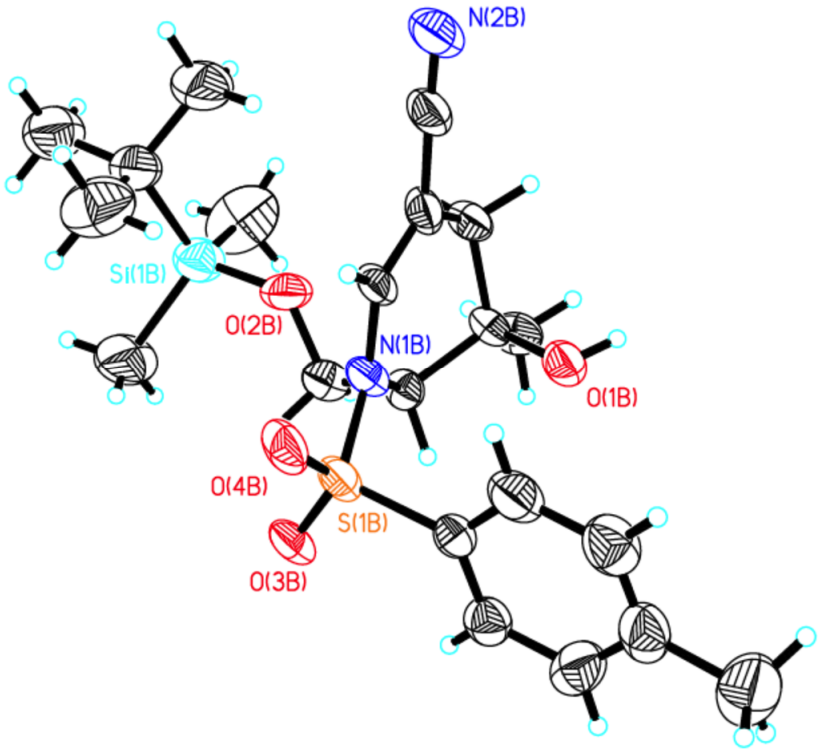


**Figure 5.5** X-ray structure of dehydropiperidine **5.64**.

### 5.3.3 Efforts toward a one-pot Baylis-Hillman/aza-Payne/conjugate addition protocol.

One-pot syntheses are advantageous since they avoid a lengthy separations, and are operationally simpler and less time consuming. This makes the tandem aza-Payne/conjugate addition protocol an attractive route to synthesize piperidine compounds. Although, at this point isolation of the diasteromerically pure Baylis-Hillman adduct was required, before we initated cyclization, we turned our attention towards performing all the three steps in one pot.

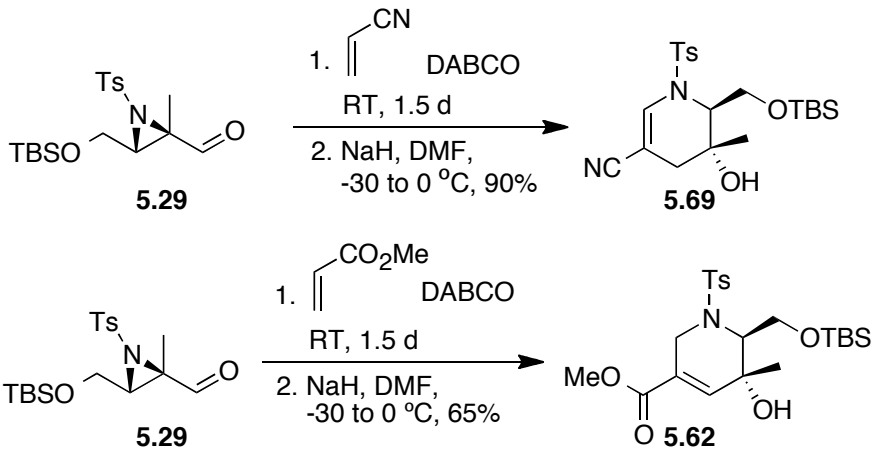


**Scheme 5.25** Synthesis of dehydropiperidines via Baylis-Hillman/aza-Payne/conjugate addition reactions in one pot.

For this purpose aziridine-2-carboxaldehyde **5.29** was first subjected to excess of acrylonitrile in presence of catalytic amount of DABCO to furnish the Baylis-Hillman adduct. This was taken as crude after rotary evaporation of the excess acrylonitrile to the next step, where it was treated in anhydrous DMF with catalytic amount of NaH.

The one-pot protocol of telescoping three reactions efficiently afforded the desired dehydropiperidine compound **5.69** in high yield (Scheme 5.25). Synthesis of another dehydropiperidine compound **6.59** was also shown to proceed very efficiently using this one pot protocol. Thus, dehydropiperidine compounds, with high complexity can be obtained in one pot starting from simple starting materials such as aziridine-2-carboxaldehydes. Solvent free conditions for the Baylis-Hillman reaction and operation of three steps in one pot also makes this reaction environmentally-benign and efficient.

### 5.3.4 Challenges toward elaboration of dehydropiperidines toward iminosugars and future directions.

Our route provides an access to obtain highly functionalized core of dehydropiperidine ring with two well-defined stereocenters. This makes it an attractive scaffold presented with various interesting functional groups, and can be further exploited in order to derive advanced intermediates. For example, transformations known for $\alpha,\beta$-unsaturated olefins can be utilized and new stereocenters can be constructed taking advantage of the inherent stereochemistry of the six-member ring. The only unfunctionalized methylene next to the nitrogen arom can be functionalized taking advantage of both its allylic nature and the $\alpha$-nitrogen placement. Future endeavors would include development of such piperidine cores toward the synthesis of some of the known and biologically active iminosugars or other piperidine containing natural products (Scheme 5.26).

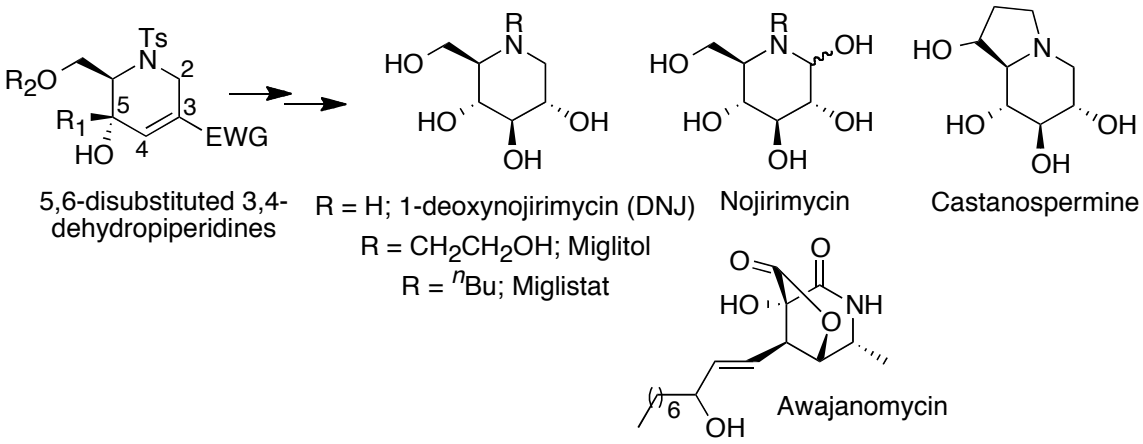


**Scheme 5.26** Planned elaboration of dehydropiperidines toward iminosugars and other piperidine containing natural products.

### 5.3.4.1 Attempts at epoxidation of α,β-unsaturated olefin present in dehydropiperidine.

Most of the iminosugars often bear hydroxyl groups at C-3 and C-4 positions, arranged in *trans* fashion. Thus, we plan to install an epoxide, hopefully directed by the C-5 tertiary hydroxyl group. Opening of the epoxide with nucleophiles such as perchloric acid would introduce the nucleophile at C-4, *anti* with respect to that of C-5 in the desired fashion. [37-39]

**Table 5.6** Efforts at epoxidation.

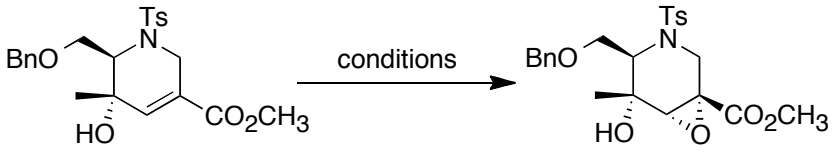


**5.63** **5.65**

| entry | conditions | product |
|---|---|---|
| 1 | TBHP (2 equiv), $Va(acac)_2$ (0.05 equiv) | several undesired products |
| 2 | TBHP (2 equiv), $KO^tBu$ | several undesired products |
| 3 | $H_2O_2$, NaOH, MeOH | *n.r.* |
| 3 | UHP, $Ac_2O$, $Na_2HPO_4$ | *n.r.* |
| 4 | m-CPBA (10 equiv), DCM, reflux | *n.r.* |
| 5 | aq. oxone (1.3 equiv), acetone | several undesired products |
| 6 | DMDO (excess) | SM + benzyl ester[35] + other unknown products |

We embarked on investigation of the required epoxidation. A directed epoxidation was attempted on dehydropiperidine **5.63** using catalytic amount of $Va(acac)_2$ catalyst (Table 5.6, entry1).[40] Several undesired competing reactions were observed as analyzed by crude NMR, although appearance of resonance in NMR spectrum corresponding to the olefin proton at C-4 clearly indicated its un-reactivity towards epoxidation. TBHP in the presence of a base also failed to produce any epoxidized product (entry 2).[41] Both hydrogen peroxide and urea hydrogen peroxide assisted

[35] Benzyl ether was oxidized to the corresponding benzyl ester. However, compound was obtained as a mixture with other impurities, which did not allow for the confirmation of the structure.

epoxidation returned all the starting material back, whereas harsher conditions led to degradation.[42,43] Electron deficient olefins have also been known to undergo epoxidation via excess of m-CPBA reagent under refluxing conditions.[44] Disappointingly in our case, epoxidation was not observed under these conditions either. Reaction with oxone in acetone also gave several undesired products (entry 5). Interestingly reaction with excess of DMDO led to a mixture of starting material, oxidized benzyl ether along with some other unknown impurities (entry 6).[45] Although lack of reactivity of the olefin toward the epoxidation can not be rationalized completely, the steric influence imposed by quaternary center at C-5 might be the source of unreactivity.

#### 5.3.4.2 Epoxide formation via activation of $\alpha,\beta$-unsaturated ester.

Frustrated by our attempts toward epoxidation of $\alpha,\beta$-unsaturated olefin, we then resorted to a different strategy in order to install oxygen at C-4. We planned to utilize C-5 tertiary alcohol to effect an oxa-michael addition step; the *in-situ* generated enolate was planned to be trapped as a ketene acetal under basic conditions. Thus lithium alkoxide was generated to realize conjugate addition and the resulting enolate was allowed to react with TBSCl (Scheme 5.27). However, no reaction was found to occur under these conditions as analyzed by TLC.

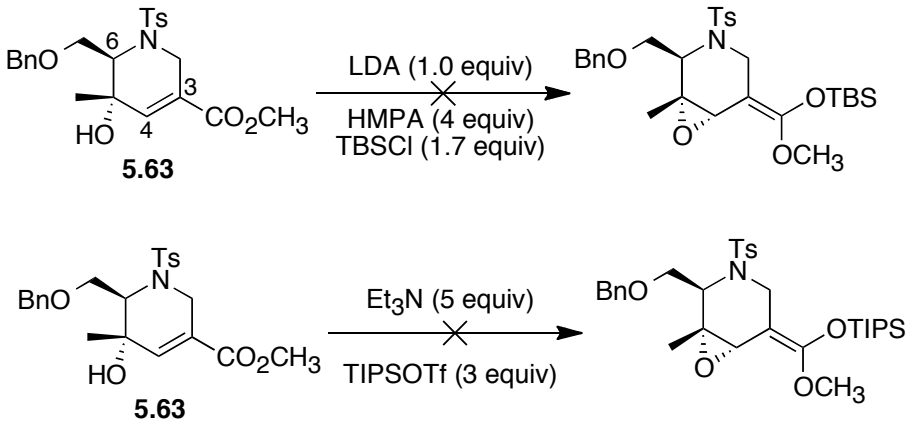


**Scheme 5.27** Attempt at oxa-Michael addition and formation of epoxide.

Use of a different base ($Et_3N$) and the more reactive TIPSOTf also returned starting material only. We then decided to execute the strategy using Lewis acidic conditions, assuming that the presence of a Lewis acid would help to activate the carbonyl, and thus polarize the $\alpha,\beta$-unsaturated olefin to facilitate the 1,4-attack. Boron triflate is commonly employed for the generation of boron enolates in Aldol reactions. Thus excess of this reagent was employed in presence of a base to form an epoxide (Scheme 5.28). Concerned by its lability, the resulting boron ketene acetal was allowed to react with ozone at low temperature to reveal the C-3 carbonyl. Unfortunately analysis of crude NMR spectrum suggested several competing undesired products under these conditions.

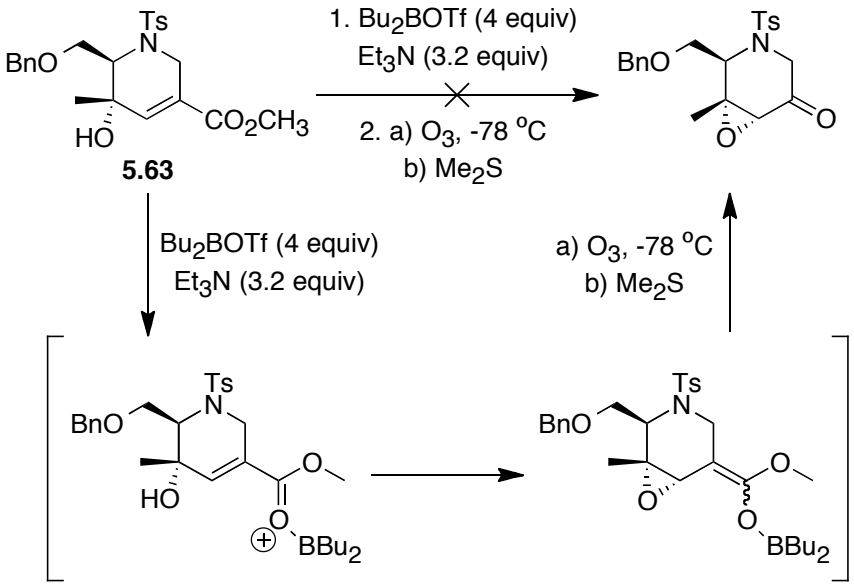


**Scheme 5.28** Attempt at Lewis acid mediated oxa-Michael addition and epoxide formation.

### 5.3.4.3 Attempts at detosylation.

Gratifyingly treatment of *N*-Ts protected dehydropiperidine **5.62** with powdered Mg and methanol under sonication successfully afforded detosylated compound **5.66** in quantitative yield. (Scheme 5.29)

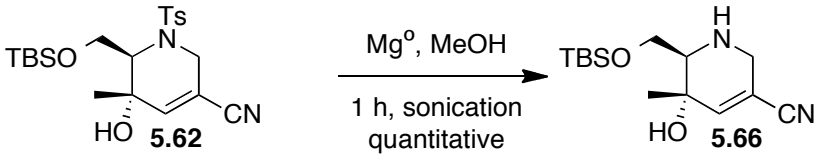


**Scheme 5.29** Detosylation of *N*-Ts dehydropiperidine compound.

This provides us an opportunity to analyze the scope of the unprotected compound towards further elaboration.

#### 5.3.4.4 Future directions toward elaboration of piperidine compounds toward 7-member nitrogen containing rings.

Brechbiel and coworkers have shown that piperidine rings containing primary alcohol alpha to nitrogen can successfully undergo ring expansion reactions to form azepane compounds (Scheme 5.30).[46] Similar transformations utilizing our *N*-alkyl protected dehydropiperidine compounds would provide an efficient route to access azepane compounds.

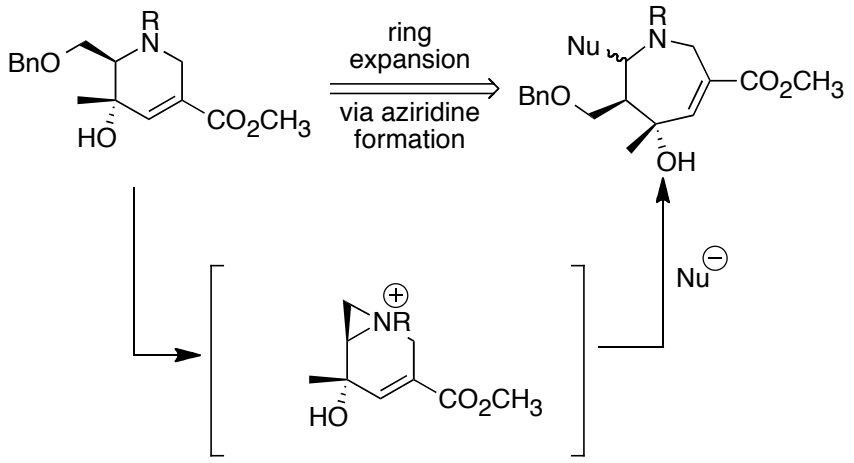


**Scheme 5.30** Ring expansion to azepanes.

Although installing the epoxide to access oxygen functionality at C-4 met with difficulty, dihydroxylation could be another avenue to obtain similarly hydroxylated products. C-5 alcohol can also be protected as a tert-butyl carbonate, which later can be utilized to deliver an oxygen atom intramolecularly via the iodoetherification protocol. Access to the detosylated compound also opens up the possibility to explore its elaboration with the latter chemistry. In conclusion, one-pot Baylis-Hillman/aza-Payne/conjugate

reactions provide a unique and efficient pathway to access highly functionalized dehydropiperidine compounds, which can be further elaborated to advanced intermediates and other useful targets such as iminosugars. Future endeavors would focus to effect such elaborations.

## 5.4 Experimental procedures.

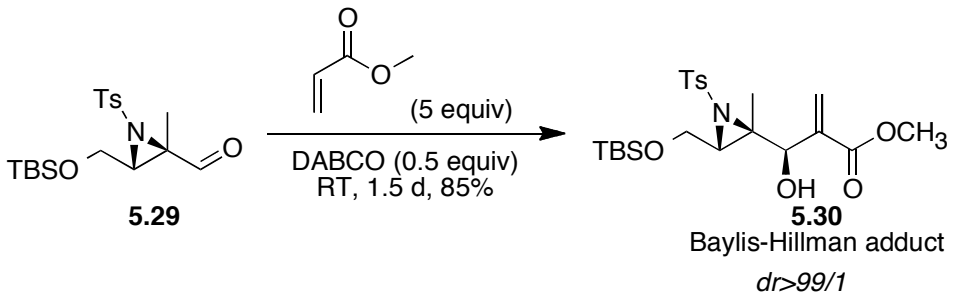


**Preparation of Baylis-Hillman adduct 5.30.** To aziridine-2-carboxaldehyde **5.29** (0.3 g, 0.83 mmol) was added methyl acrylate (0.36 g, 4.17 mmol) and DABCO (46.8 mg, 0.42 mmol) under a nitrogen atmosphere. The reaction was allowed to stir for 1.5 days (till all the starting material was consumed as analyzed by TLC). Upon completion sat. $NH_4Cl$ (1 mL) was added to quench the reaction. The aqueous layer was extracted with EtOAc (3 X 10 mL), organic layers were dried over sodium sulfate and evaporated under low pressure. The purification of the crude compound was accomplished by column chromatography (4:1 Hex:EtOAc) to yield the *syn* adduct **5.30** (0.33 g, 85%) as a white solid (m.pt = 79 – 81 ºC). Spectral data for **5.30**: $^1$H-NMR (500 MHz, $CDCl_3$) $\delta$ 7.82 (d, 2H, *J* = 8.3 Hz), 7.26 (d, 2H, *J* = 8.2 Hz), 6.40 (t, 1H, *J* = 1.4 Hz), 6.18 (t, 1H, *J* = 1.7 Hz), 5.01 (m, 1H), 3.95 (d, 2H, *J* = 3.1 Hz), 3.74 (s, 3H), 3.63 (dd, 1H, *J* = 6.8, 4.8 Hz), 3.55 (dd, 1H, *J* = 11.2, 5.1 Hz), 3.47 (dd, 1H, *J* = 11.0, 7.1 Hz), 2.38 (s, 3H), 1.20 (s, 3H), 0.78 (s, 9H), -0.07 (s, 3H), -0.09 (s, 3H); $^{13}$C-NMR (125 MHz, $CDCl_3$) $\delta$ 165.7, 143.9, 138.6, 137.5, 129.4, 127.6, 127.2, 71.0, 60.6, 57.9, 52.3, 51.7, 25.6, 21.4, 18.1, 12.4, -5.7, -5.6; IR (neat) 3490, 2953, 2930, 2857, 1723, 1440, 1304, 1159, 1091, 836;

HRMS (ESI) (m/z): $[M+H]^+$ calculated for $[C_{22}H_{36}NO_6SSi]^+$ 470.2033, found 470.2030.

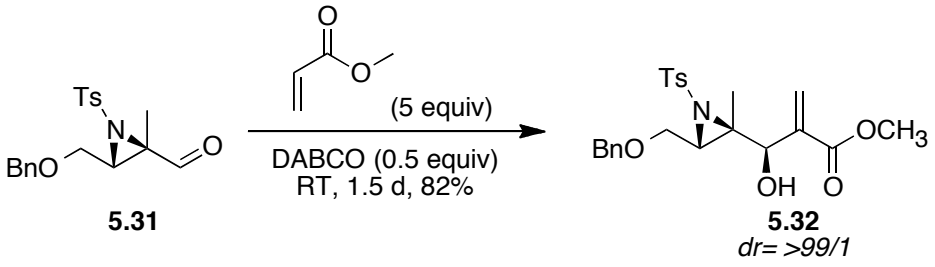


**Preparation of Baylis-Hillman adduct 5.32**. To aziridine-2-carboxaldehyde **5.31** (1.5 g, 4.17 mmol) was added methyl acrylate (1.6 g, 20.8 mmol) and DABCO (0.23 g, 2.1 mmol) under a nitrogen atmosphere. The reaction was allowed to stir for 1.5 days (till all the starting material was consumed as analyzed by TLC). Upon completion sat. $NH_4Cl$ (3 mL) was added to quench the reaction. The aqueous layer was extracted with EtOAc (3 X 15 mL), organic layers were dried over sodium sulfate and evaporated under low pressure. The purification of the crude compound was accomplished by column chromatography (3:1 Hex:EtOAc) to yield the *syn* adduct **5.32** (1.5 g, 82%) as an oil. Spectral data for **5.32**: $^1$H-NMR (500 MHz, $CDCl_3$) $\delta$ 7.83 (d, 2H, *J* = 8.2 Hz), 7.35-7.26 (m, 3H), 7.22 (d, 2H, *J* = 8.4 Hz), 7.14 (d, 2H, *J* = 7.6 Hz), 6.42 (t, 1H, *J* = 1.5), 6.22 (t, 1H, *J* = 1.7 Hz), 5.03 (m, 1H), 4.38 (dd, 1H, *J* = 11.8 Hz), 4.35 (dd, 1H, *J* = 11.8 Hz), 3.97 (d, 1H, *J* = 2.9 Hz), 3.78 (dd, 1H, *J* = 7.5, 5.1 Hz), 3.70 (s, 3H), 3.48 (dd, 1H, J = 10.7, 5.0 Hz), 3.33 (dd, 1H, *J* = 10.7, 7.4 Hz), 2.39 (s, 3H), 1.22 (s, 3H); $^{13}$C-NMR (125 MHz, $CDCl_3$) $\delta$ 165.9, 144.1, 138.6, 137.7, 129.7, 129.2, 128.5, 128.1, 127.4, 127.2, 126.9, 72.8, 71.5, 70.8, 67.0, 58.1, 51.9, 50.6, 21.5.; IR (neat) 3525, 2953, 2929,

2857, 1559, 1472, 1091, 1044; HRMS (ESI) (m/z): $[M+Na]^+$ calculated for $[C_{23}H_{27}NO_6SNa]^+$ 468.1457 found 468.1451.

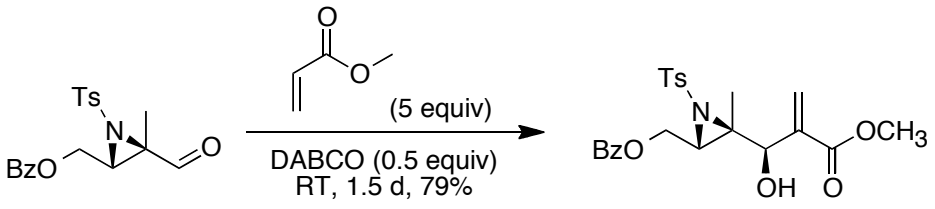


**5.33** **5.34** *dr= >99/1*

**Preparation of Baylis-Hillman adduct 5.34**. To aziridine-2-carboxaldehyde **5.33** (0.5 g, 1.34 mmol) was added methyl acrylate (0.58 g, 6.70 mmol) and DABCO (75 mg, 0.67 mmol) under a nitrogen atmosphere. The reaction was allowed to stir for 1.5 days (till all the starting material was consumed as analyzed by TLC). Upon completion sat. $NH_4Cl$ (3 mL) was added to quench the reaction. The aqueous layer was extracted with EtOAc (3 X 25 mL), organic layers were dried over sodium sulfate and evaporated under low pressure. The purification of the crude compound was accomplished by column chromatography (5:1 Hex:EtOAc) to yield the *syn* adduct **5.34** (0.48 g, 79%) as an oil. Spectral data for **5.34**: $^1$H-NMR (500 MHz, $CDCl_3$) $\delta$ 7.84 – 7.80 (m, 4H), 7.56 (t, 1H, J = 7.6 Hz), 7.39 (t, 2H, J = 7.8 Hz), 7.15 (d, 2H, J = 8.0 Hz), 6.48 (t, 1H, J = 1.5 Hz), 6.27 (t, 1H, J = 1.8 Hz), 5.05 (m, 1H), 4.27 (dd, 1H, J = 11.8, 5.3 Hz), 4.18 (dd, 1H, J = 11.8, 7.4 Hz), 3.95 (d, 1H, J = 2.7 Hz), 3.92 (dd, 1H, J = 7.6, 5.1 Hz), 3.66 (s, 3H), 2.33 (s, 3H), 1.33 (s, 3H); $^{13}$C-NMR (125 MHz, $CDCl_3$) $\delta$ 165.8, 144.3, 138.2, 136.9, 133.2, 129.6, 129.5, 129.4, 128.3, 128.2, 127.3, 71.0, 61.6, 58.5, 51.9, 49.3, 21.6, 12.9;

IR (neat) 3535, 2853, 1563, 1472, 1091, 1050; HRMS (ESI) (m/z): $[M+H]^+$ calculated for $[C_{23}H_{26}NO_7S]^+$ 460.1430, found 460.1437.

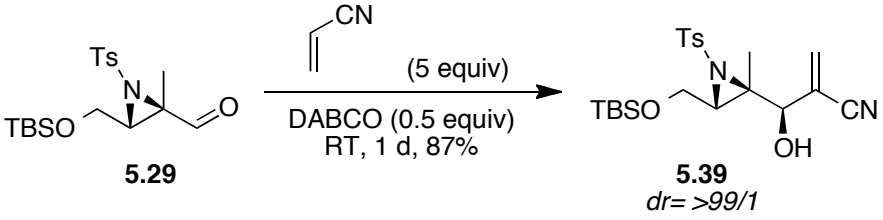


**5.29** **5.39** *dr= >99/1*

**Preparation of Baylis-Hillman adduct 5.39**. To aziridine-2-carboxaldehyde **5.29** (90 mg, 0.24 mmol) was added methyl acrylate (64 mg, 1.2 mmol) and DABCO (13 mg, 0.12 mmol) under a nitrogen atmosphere. The reaction was allowed to stir for 1 d (till all the starting material was consumed as analyzed by TLC). Upon completion sat. $NH_4Cl$ (2 mL) was added to quench the reaction. The aqueous layer was extracted with EtOAc (3 X 10 mL), organic layers were dried over sodium sulfate and evaporated under low pressure. The purification of the crude compound was accomplished by column chromatography (4:1 Hex:EtOAc) to yield the *syn* adduct **5.39** (89 mg, 87%) as a white solid (m.pt = 74 – 76 ºC). Spectral data for **5.39**: $^1$H-NMR (500 MHz, $CDCl_3$) $\delta$ 7.85 (d, 2H, J = 8.2 Hz), 7.29 (d, 2H, J = 8.2 Hz), 6.36 (d, 1H, J = 2.2 Hz), 6.15 (d, 1H, J = 2.3 Hz), 4.69 (dd, 1H, J = 4.9, 2.3 Hz), 4.03 (d, 1H, J = 2.9 Hz), 3.93 (dd, 1H, J = 10.6, 2.8 Hz), 3.46 – 3.41 (m, 2H), 2.42 (s, 3H), 1.28 (s, 3H), 0.80 (s, 9H), -0.03 (s, 3H), -0.07 (s, 3H); $^{13}$C-NMR (125 MHz, $CDCl_3$) $\delta$ 144.3, 136.9, 132.2, 129.5, 127.3, 121.4, 116.8, 72.6, 60.5, 56.1, 52.4, 25.7, 21.5, 18.1, 12.3, -5.6, -5.7; IR (neat) 3490, 2959, 2929, 2229, 1473, 1318, 1160, 1100, 1064; HRMS (ESI) (m/z): $[M+H]^+$ calculated for

$[C_{21}H_{33}N_2O_4SSi]^+$ 437.1930, found 437.1938.

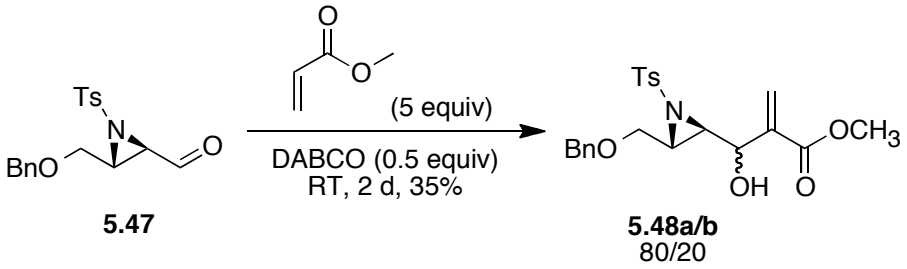


**5.47** **5.48a/b** 80/20

**Preparation of Baylis-Hillman adduct 5.48**. To aziridine-2-carboxaldehyde **5.47** (0.15 g, 0.43 mmol) was added methyl acrylate (0.19 g, 2.17 mmol) and DABCO (24 mg, 0.21 mmol) under a nitrogen atmosphere. The reaction was allowed to stir for 1.5 days (till all the starting material was consumed as analyzed by TLC). Upon completion sat. $NH_4Cl$ (2 mL) was added to quench the reaction. The aqueous layer was extracted with EtOAc (3 X 20 mL), organic layers were dried over sodium sulfate and evaporated under low pressure. The purification of the crude compound was accomplished by column chromatography (6:1 Hex:EtOAc) to yield a 4:1 mixture of isomers of Baylis-Hillman adduct **5.48** (0.33 g, 85%) as an oil.

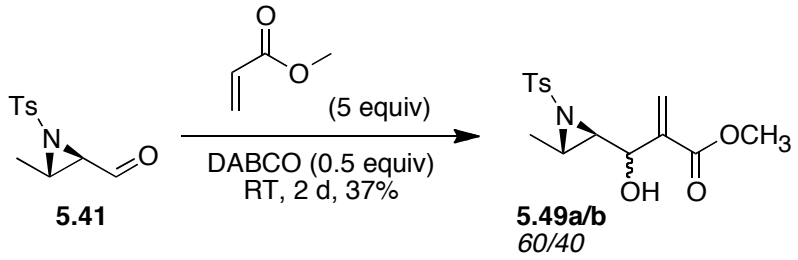


**5.41** **5.49a/b** *60/40*

**Preparation of Baylis-Hillman adduct 5.49**. To aziridine-2-carboxaldehyde **5.41** (0.24 mg, 0.99 mmol) was added methyl acrylate (0.43 g, 4.97 mmol) and DABCO (56 mg,

0.5 mmol) under a nitrogen atmosphere. The reaction was allowed to stir for 2 days (till all the starting material was consumed as analyzed by TLC). Upon completion sat. $NH_4Cl$ (3 mL) was added to quench the reaction. The aqueous layer was extracted with EtOAc (3 X 25 mL), organic layers were dried over sodium sulfate and evaporated under low pressure. The purification of the crude compound was accomplished by column chromatography (4:1 Hex:EtOAc) to yield a 3:2 mixture of isomers of Baylis-Hillman adduct **5.49** (0.12 g, 37%) as an oil as an inseparable mixture of isomers. Spectral data for **5.49a**: $^1$H-NMR (300 MHz, $CDCl_3$) $\delta$ 7.79 (d, 2H, J = 8.5 Hz), 7.29 (d, 2H, J = 8.5 Hz), 6.18 (m, 1H), 5.81 (m, 1H), 4.49 (m, 1H), 3.75 (s, 3H), 3.05 (m, 1H), 2.94 (dd, 1H, J = 6.1, 4.6 Hz), 2.64 (d, 1H, J = 5.8 Hz), 2.41 (s, 3H), 1.51 (d, 3H, J = 5.9 Hz); IR (neat) 3491, 2927, 1717, 1439, 1321, 1160, 1091, 816. Spectral data for **5.49b**: $^1$H-NMR (300 MHz, $CDCl_3$) $\delta$ 7.79 (d, 2H, J = 8.5 Hz), 7.29 (d, 2H, J = 8.5 Hz), 6.09 (m, 1H), 5.69 (t, 1H, J = 1 Hz), 4.29 (t, 1H, J = 5.7 Hz), 3.76 (s, 3H), 3.21 (t, 1H, J = 4.8 Hz), 2.87 (dd, 1H, J = 6.0, 4.6 Hz), 2.81 (d, 1H, J = 6.2 Hz), 2.42 (s, 3H), 1.64 (d, 3H, J = 6.1 Hz); $^{13}$C-NMR (125 MHz, $CDCl_3$) 165.9, 144.3, 139.0, 137.2, 129.7, 129.3, 126.8, 126.2, 68.5, 68.5, 52.7, 44.2, 21.5, 14.2; HRMS (ESI) (m/z): $[M+H]^+$ calculated for $[C_{15}H_{20}NO_5S]^+$ 326.1062, found 326.1066.

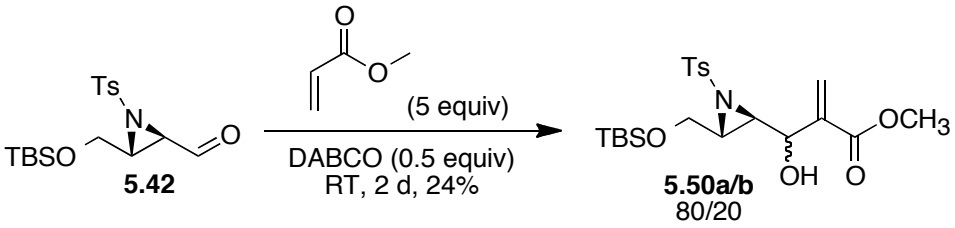

**Preparation of Baylis-Hillman adduct 5.50**. To aziridine-2-carboxaldehyde **5.42** (0.23 g, 0.62 mmol) was added methyl acrylate (0.3 g, 3.1 mmol) and DABCO (36 mg, 0.31 mmol) under a nitrogen atmosphere. The reaction was allowed to stir for 2 d (till all the starting material was consumed as analyzed by TLC). Upon completion sat. $NH_4Cl$ (0.5 mL) was added to quench the reaction. The aqueous layer was extracted with EtOAc (3 X 10 mL), organic layers were dried over sodium sulfate and evaporated under low pressure. The purification of the crude compound was accomplished by column chromatography (5:1 Hex:EtOAc) to yield a 4:1 mixture of two isomers of Baylis-Hillman adduct **5.50** (68 mg, 24%) as a yellow oil as an inseparable mixture. Spectral data for **5.50**: $^1$H-NMR (500 MHz, $CDCl_3$) $\delta$ 7.84 (d, 2H, J = 8.5 Hz), 7.29 (d, 2H, J = 8.1 Hz), 6.32 (s, 1H), 6.04 (s, 1H), 4.76 (dd, 1H, J = 7.7, 4.6 Hz), 3.76 (s, 3H), 3.73 (m, 1H), 3.32 (d, 1H, J = 4.4 Hz), 3.29 (dd, 1H, J = 9.8, 5.3 Hz), 2.93 (dd, 1H, J = 7.6, 4.4 Hz), 2.41 (s, 3H), 0.79 (s, 9H), -0.06 (s, 3H), -0.08 (s, 3H); $^{13}$C-NMR (125 MHz, $CDCl_3$) $\delta$ 167, 144.3, 138.9, 129.7, 129.3, 127.9, 127.2, 69.0, 61.2, 52.0, 51.0, 48.1, 25.8, 25.6, -5.7; IR (neat) 2953, 2857, 1723, 1598, 1441, 1326, 1161, 1096;–HRMS (ESI) (m/z): $[M+Na]^+$ calculated for $[C_{22}H_{25}NNaO_6S]^+$ 454.1300, found 454.1310.

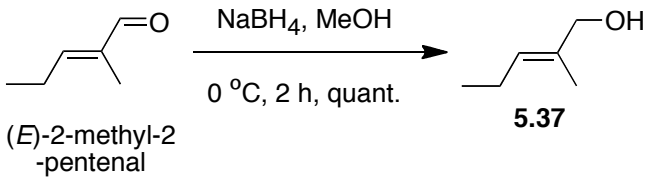


**Preparation of allylic alcohol 5.37.**[47] To a solution of commercially available (*E*)-2-

methyl-2-pentenal (5 g 52.5 mmol), in methanol (438 mL) at 0 $^{o}$C was added $NaBH_4$ (5.36 g, 141.8 mmol) in small portions under inert atmosphere. Reaction was allowed to stir at 0 $^{o}$C for 2 h. After completion (monitored by TLC), the reaction was diluted with ether and quenched with sat. $NaHCO_3$ (25 mL). Excess of methanol was removed via rotary evaporation. The aqueous phase was extracted with EtOAc (3 X 80 mL). The organic layers were dried over anhydrous sodium sulfate and the solvent was removed under reduced pressure to give alcohol **5.37** as a yellow oil, which was taken to the next step without any purification. Spectral data for **6.35**: $^{1}$H-NMR (300 MHz, $CDCl_3$) $\delta$ 5.37 (m, 1H), 3.96 (s, 2H), 2.01 (m, 2H), 1.63 (s, 3H), 0.94 (t, 3H, $J$ = 7.5 Hz); $^{13}$C-NMR (75 MHz, $CDCl_3$) $\delta$ 134.0, 127.9, 68.7, 60.4, 20.7, 14.0, 13.4.

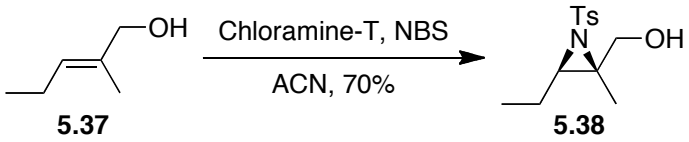


**5.37** **5.38**

**Preparation of aziridinol 5.38.** To the solution of allylic alcohol (4.1 g, 40.9 mmol) in ACN (207 mL) was added chloramine-T (9.32 g, 40.9 mmol) and NBS (1.5 g, 8.20 mmol). The reaction mixture was allowed to stir overnight till all the starting material was consumed as analyzed by TLC. The reaction was then diluted with water (150 mL). The aqueous layer was extracted with EtOAc (3 X 50 mL), organic layers were dried over anhydrous sodium sulfate and evaporated under reduced pressure. The crude was purified by column chromatography (4:1 EtOAc/Hex) to yield aziridinol **5.38** (7.7 g, 70%) as a yellow syrup. Spectral data for **5.38**: $^{1}$H-NMR (300 MHz, $CDCl_3$) $\delta$ 7.84 (d,

2H, J = 7.8 Hz), 7.30 (d, 2H, J = 7.8 Hz), 3.99 (m, 2H), 3.11 (m, 1H), 2.96 (dd, 1H, J = 8.1, 5.7 Hz), 2.41 (s, 3H), 1.49 (m, 1H), 1.39 (s, 3H), 1.37 (m, 1H), 0.81 (t, 3H, J = 7.5 Hz); $^{13}$C-NMR (75 MHz, $CDCl_3$) δ 143.9, 137.5, 129.5, 127.1, 65.6, 57.8, 51.9, 21.5, 20.6, 16.0, 14.1, 11.6.

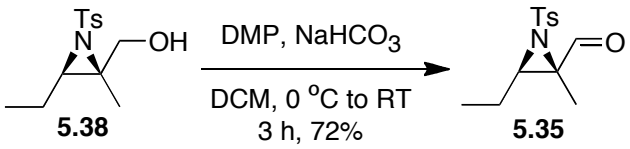

**5.38** **5.35**

**Preparation of aziridine-2-carboxaldehyde 5.35.** To a solution of aziridinol **5.38** in anhydrous DCM (305 mL) at 0 ºC was added DMP (16.3 g, 38.5 mmol) and $NaHCO_3$ (3.5 g, 41.2 mmol) under a nitrogen atmosphere. The reaction mixture was allowed to stir for 3 h and upon completion (as analyzed by TLC) was quenched with sat. $Na_2S_2O_3$ (50 mL), sat. $NaHCO_3$ (50 mL) and water (50 mL). The aqueous layer was extracted with DCM (3 X 75 mL). The organic layers were dried over anhydrous sodium sulfate and subjected to rotary evaporation. The crude obtained was purified by column chromatography (3:1 Hex:EtOAc) to furnish aziridine-2-carboxaldehyde **5.35** (5.3 g, 72%) as an off-white solid (m.pt = 94 – 96 ºC). Spectral data for **5.35**: $^1$H-NMR (500 MHz, $CDCl_3$) δ 9.50 (s, 1H), 7.81 (d, 2H, *J* = 8.3 Hz), 7.32 (d, 2H, *J* = 8.3 Hz), 3.43 (dd, 1H, *J* = 7.8, 5.5 Hz), 2.43 (s, 3H), 1.57 – 1.47 (m, 2H), 1.37 (s, 3H), 0.90 (t, 3H, *J* = 7.7 Hz); $^{13}$C-NMR (125 MHz, $CDCl_3$) δ 195.1, 144.6, 136.3, 129.7, 127.5, 58.1, 52.4, 21.6, 20.8, 11.7, 11.5; IR (neat) 2974. 1727, 1598, 1306, 1090, 900; HRMS (ESI) (m/z):

$[M+H]^+$ calculated for $[C_{13}H_{18}NO_3S]^+$ 268.1007 found 268.1000.

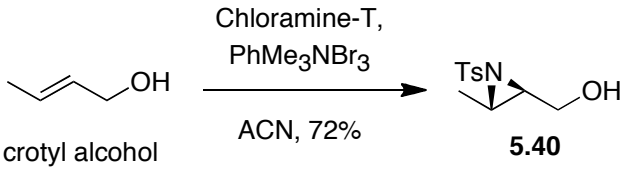


**Preparation of aziridinol 5.40.**[48] To a solution of commercially available crotyl alcohol (3 g, 42.0 mmol) in acetonitrile (200 mL) was added chloramine-T (10.4 g, 45.8 mmol) and phenyltrimethyl ammoniumtribromide (1.57 g, 4.16 mmol). The reaction was stirred for few hours till all the starting material was consumed as analyzed by TLC. After completion, water (100 mL) was added to the reaction flask. The reaction mixture was extracted with EtOAc (3 X 100 mL). The organic layers were dried over sodium sulfate and evaporated under low pressure. The product was purified by column chromatography (3:1 Hex:EtOAc) to yield aziridinol **5.40** (7.2 g, 72%) as a yellow syrup. Spectral data for **5.40**: $^1$H-NMR (500 MHz, $CDCl_3$) $\delta$ 7.81 (d, 2H, $J$ = 8.5 Hz), 7.31 (d, 2H, $J$ = 8.5 Hz), 3.99 (m, 1H), 3.75 (m, 1H), 2.96 (m, 2H), 2.42 (s, 3H), 2.34 (m, 1H), 1.41 (d, 3H, $J$ = 5.2 Hz.)

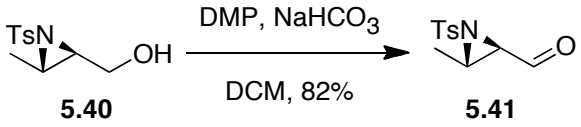


**Preparation of aziridine-2-carboxaldehyde 5.41.**[49] To a solution of aziridinol **5.40** (6.3 g, 26.2 mmol) in anhydrous DCM (345 mL) under an inert atmosphere was added

DMP (15.5 g, 36.6 mmol) and $NaHCO_3$ (3.3 g, 39.2 mmol). The reaction mixture was stirred for 3.5 h. Upon completion of the reaction as determined by TLC, sat. $Na_2S_2O_3$ (50 mL), sat. $NaHCO_3$ (50 mL) and water (50 mL) was added. The mixture was stirred for another 0.5 h and extracted with DCM (3 X 50 mL). The organics were dried over anhydrous sodium sulfate and the organic solvent was evaporated under reduced pressure. The crude compound upon purification by column chromatography (2:1 Hex:EtOAc) afforded aziridine-2-carboxaldehyde **5.41** (5.1 g, 82%) as an oil. Spectral data for **5.41**: $^1$H-NMR (500 MHz, $CDCl_3$) $\delta$ 7.82 (d, 2H, J = 8.5 Hz), 7.31 (d, 2H, J = 8.5 Hz), 3.99 (m, 1H), 3.75 (m, 1H), 2.95 (m, 2H), 2.42 (s, 3H), 2.41 (m, 1H), 2.33 (m, 1H), 1.41 (d, 3H, J = 5.8 Hz); $^{13}$C-NMR (125 MHz, $CDCl_3$) $\delta$ 194.6, 144.9, 136.1, 129.8, 127.9, 127.4, 52.1, 42.5, 21.6, 14.8.

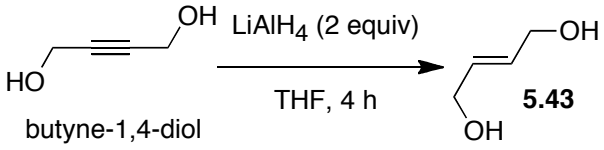


**Preparation of 1,4-butene-diol 5.43.**[50] To $LiAlH_4$ (9.3 g, 232.3 mmol) in anhydrous THF (230 mL) at 0 ºC was slowly added recrystallized commercially available butyne-1,4-diol (10 g, 116 mmol) dissolved in anhydrous THF (350 mL) via cannula under a nitrogen atmosphere. When addition was complete, the reaction mixture was refluxed for an additional 3.5 h. The reaction was quenched with the addition of water (10 mL), 3N NaOH (10 mL) and water (30 mL). The white precipitates were filtered and the filtrate was subjected under reduced pressure to yield diol **5.43** with quantitative

conversion and taken to next step without any purification.

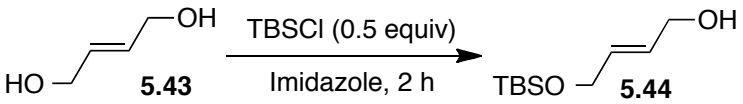


**Preparation of TBS ether 5.44.**[51] To a solution of diol **5.43** (6.24 g, 70.8 mmol), imidazole (6.0 g, 88.5 mmol) in anhydrous DMF (40 mL) was added TBSCl (5.34 g, 35.41 mmol) in several portions over 10 min. The resulting mixture was warmed to room temperature and stirred for 2 h, after which was poured into water (140 mL). The aqueous layer was extracted with EtOAc (2 X 100 mL). The organics were dried over anhydrous sodium sulfate and the solvent was removed under vacuum. The crude was purified via column chromatography to furnish the mono protected alcohol **5.44** (4.61 g, 32%) with the balance of material isolated as a mixture of *bis* protected compound **5.45** and starting material.

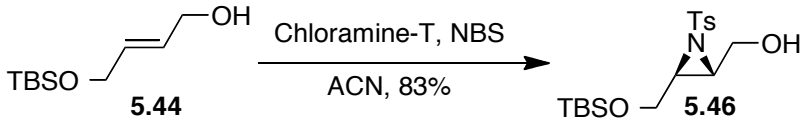


**Preparation of aziridine alcohol 5.44.**[52] To a solution of TBS alcohol **5.46** (2.23 g, 11.04 mmol) in ACN (55 mL) was added Chloramine-T (2.51 g, 11.04 mmol) and NBS (0.39 g, 2.21 mmol). The reaction mixture was stirred overnight under nitrogen in a flask covered with aluminum foil. Upon completion, as analyzed by TLC, the reaction was quenched with water (50 mL). The aqueous layer was extracted with EtOAc (3 X 25 mL). The organic layers were dried over anhydrous sodium sulfate and the solvent

was removed under vacuum. The crude product was purified via column chromatography (4:1 Hex:EtOAc) to yield aziridine alcohol **5.44** (3.4 g, 83%) as a white syrup.

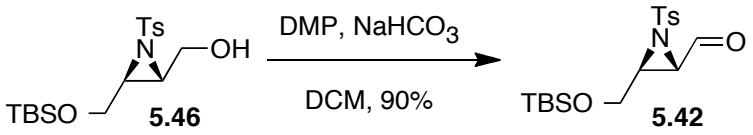


**Preparation of aziridine-2-carboxaldehyde 5.42.** To a solution of aziridine alcohol **5.46** (2.89 g, 7.77 mmol) in anhydrous DCM (86 mL) was added DMP (4.62 g, 10.91 mmol) and $NaHCO_3$ (0.98 g, 11.65 mmol) at 0 ºC under nitrogen. The temperature was allowed to warm to room temperature and the reaction was stirred till no starting material was observed, as analyzed by TLC. Reaction was then quenched with sat. $Na_2S_2O_3$ (14 mL), sat. $NaHCO_3$ (14 mL) and water (14 mL). The aqueous phase was extracted with DCM (2 X 25 mL). The organic solvent was dried over anhydrous sodium solvent and the solvent was then removed under reduced pressure. The crude compound was purified by column chromatography (4:1 Hex:EtOAc) to furnish aziridine-2-carboxaldehyde **5.42** (1.91 g, 67%) as an oil. Spectral data for **5.42**: $^{1}$H-NMR (500 MHz, $CDCl_3$) $\delta$ 9.54 (d, 1H, J = 6.8 Hz), 7.84 (d, 2H, J = 8.1 Hz), 7.32 (d, 2H, J = 8.1 Hz), 3.82 (dd, 1H, J = 11.6, 3.8 Hz), 3.70 (dd, 1H, J = 11.5, 5.2 Hz), 3.59 (dt, 1H, J = 5.1, 3.8, 3.18 (dd, 1H, J = 6.9, 3.7 Hz), 2.43 (s, 3H), 0.79 (s, 9H), -0.08 (s, 3H), -0.09 (s, 3H); $^{13}$C-NMR (125 MHz, $CDCl_3$) $\delta$ 193.8, 144.9, 135.7, 129.8, 129.5, 127.7, 60.9, 60.3, 49.5, 46.9, 25.8, 25.6, 21.6, 21.0, 18.2, 14.2, -5.6, -5.7; IR (neat) 2951, 2872, 1657,

1344, 1165, 1032; HRMS (ESI) (m/z): $[M+H]^+$ calculated for $[C_{17}H_{28}NO_4SSi]^+$ 370.1508, found 370.1500.

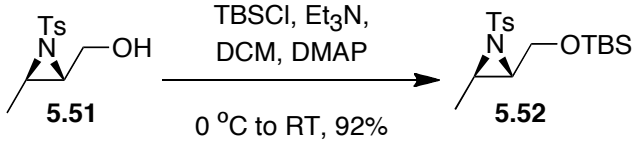


**Preparation of TBS ether 5.52.**[48] To a solution of aziridine alcohol **5.51** (2 g, 8.3 mmol) in anhydrous DCM (14 mL) was added a solution of TBSCl (1.38 g, 9.13 mmol) in anhydrous DCM (9 mL) under a nitrogen atmosphere. The reaction mixture was stirred at 0 ºC for 1 h and then later at room temperature for 5 h. Incomplete conversion was observed by TLC, thus DMAP (10.1 mg, 0.08 mmol) was added to the reaction and allowed to stir for an additional 3 h. Upon completion of the reaction as analyzed by TLC, sat. $NaHCO_3$ (10 mL) was added. The aqueous phase was extracted with DCM (2 X 25 mL). The organic layers were dried over anhydrous sodium sulfate and later removed under rotary evaporation to give a crude compound. The purification of the latter afforded TBS ether **5.52** (2.7 g, 92%) as a white syrup. Spectral data for **5.52**: $^1$H-NMR (500 MHz, $CDCl_3$) $\delta$ 7.81 (d, 2H, J = 8.6 Hz), 7.27 (d, 2H, J = 8.6 Hz), 3.70 (dd, 1H, J = 11.2, 4.6 Hz), 3.63 (dd, 1H, J = 11.3, 5.4 Hz), 2.90 (dd, 1H, J = 10.1, 5.0 Hz), 2.77 (m, 1H), 2.40 (s, 3H), 1.60 (d, 3H, J = 5.9 Hz), 0.79 (s, 9H), -0.07 (s, 3H), -0.10 (s, 3H).

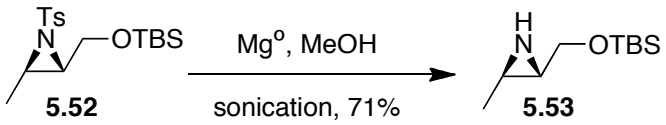


**Preparation of detosylated aziridine 5.53.** To a solution of *N*-Ts aziridinol **5.52** (1 g, 2.81 mmol) in reagent grade methanol (11 mL) was added crushed magnesium powder (0.34 g, 14.06 mmol). The solution was sonicated till all the starting material was consumed as analyzed by TLC (2 h). The reaction was then quenched with sat. $NH_4Cl$ (1 mL) and extracted with EtOAc (3 X 15 mL). The solvent was evaporated under reduced pressure to give detosylated aziridine **6.49** (0.40 g, 71%) as an oil, which was taken to next step without any purification. Spectral data for **5.53**: $^1$H-NMR (500 MHz, $CDCl_3$) $\delta$ 3.69 (m, 2H), 1.83 (m, 1H), 1.73 (m, 1H), 1.15 (d, 3H, J = 5.3 Hz), 0.84 (s, 9H), 0.01 (s, 6H); $^{13}$C-NMR (125 MHz, $CDCl_3$) $\delta$ 62.6, 39.0, 28.9, 25.9, 25.8, 18.5, 18.2, 13.8, -5.4; IR (neat) 3852, 2954, 2857, 1678, 1471, 1254, 1092, 838; HRMS (ESI) (m/z): $[M+H]^+$ calculated for $[C_{10}H_{24}NOSi]^+$ 202.1627, found 202.1630.

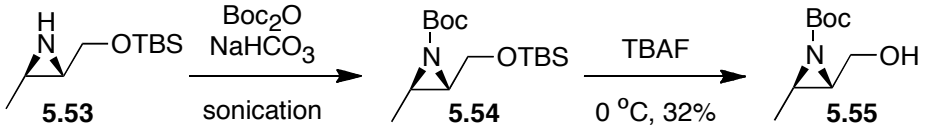


**Preparation of *N*-Boc protected aziridinol 5.55.**[34] To a solution of aziridinol **5.53** (59.3 mg, 0.29 mmol) in MeOH (1.7 mL) was added $NaHCO_3$ (73 mg, 0.87 mmol) and ditertbutyl dicarbonate (95 mg, 0.43 mmol). The solution was sonicated for 2 h till no more starting material was observed when analyzed by TLC. The crude was placed in

anhydrous THF (1.7 mL). To this, 1M solution of TBAF in THF (0.73 mL, 0.73 mmol) was added at 0 $^{o}$C drop wise under nitrogen. The reaction mixture was stirred for 3 h. Upon completion, as analyzed by TLC, the reaction was quenched with sat. $NaHCO_3$ (2 mL). The aqueous layer was extracted with EtOAc (3 X 10 mL). After drying the organics with anhydrous sodium sulfate, rotary evaporation of the solvent afforded desilylated aziridine alcohol **6.51** (16.9 mg, 32%, two steps) as an oil. Spectral data for **5.55**: $^{1}$H-NMR (500 MHz, $CDCl_3$) $\delta$ 3.94 (d, 1H, J = 12.3 Hz), 3.46 (dd, 1H, J = 12.2, 6.1 Hz), 2.41 (m, 2H), 1.45 (s, 9H), 1.26 (d, 3H, J = 5.2 Hz); HRMS (ESI) (m/z): $[M+H]^+$ calculated for $[C_9H_{18}NO_3]^+$ 188.1287, found 188.1280.

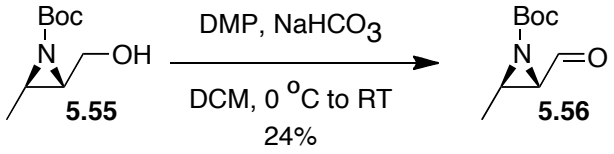


**Preparation of *N*-Boc protected aziridine-2-carboxaldehyde 5.56.**[35] To a solution of aziridine alcohol **5.55** (17 mg, 0.08 mmol) in anhydrous DCM (1 mL) at 0 $^{o}$C was added DMP (50 mg, 0.11 mmol) and $NaHCO_3$ (10 mg, 0.13 mmol). The reaction was slowly warmed to room temperature and allowed to stir for 3 h. Upon completion, as analyzed by TLC, the reaction was quenched with sat. $Na_2S_2O_3$ (0.2 mL), sat. $NaHCO_3$ (0.2 mL) and water (0.2 mL). The aqueous phase was extracted with DCM (2 X 5 mL) and the organics were dried over anhydrous sodium sulfate. The organic solvent was removed via rotary evaporation and the resulting crude was purified via column chromatography

(2:1 Hex:EtOAc) to yield aziridine aldehyde **5.56** (4 mg, 24%) as a colorless oil. Spectral data for **5.56**: $^{1}$H-NMR (500 MHz, $CDCl_3$) $\delta$ 9.08 (d, 1H, J = 5.2Hz), 2.86 (d, 2H, J = 4.8 Hz), 1.46 (s, 9H), 1.37 (d, 3H, J = 6.4 Hz; $^{13}$C-NMR (125 MHz, $CDCl_3$) $\delta$ 198.4, 160.6, 82.63, 48.0, 39.9, 28.04, 16.2, 14.3.

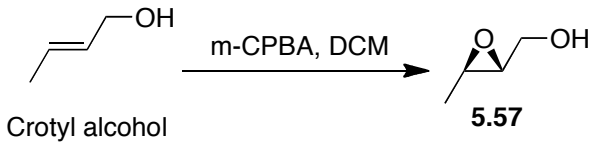


**Preparation of epoxy alcohol 5.57.**[53] Commercially available crotyl alcohol (2 g, 28.0 mmol) was placed in anhydrous DCM (270 mL), to which m-CPBA (77%, 6.5 g, 29.1 mmol) was added. The reaction mixture was stirred under nitrogen and the reaction upon completion as analyzed by TLC was quenched by the addition of water (50 mL) and sat. $Na_2CO_3$ (50 mL). The aqueous phase was extracted with DCM (3 X 80 mL). The organics were dried over anhydrous sodium sulfate, evaporated under reduced pressure and the crude compound was purified via column chromatography (4:1 Hex:$Et_2O$) to furnish epoxide **5.57** (2 g, 82%) as a colorless oil. Spectroscopic data matches with that of the reported compound.

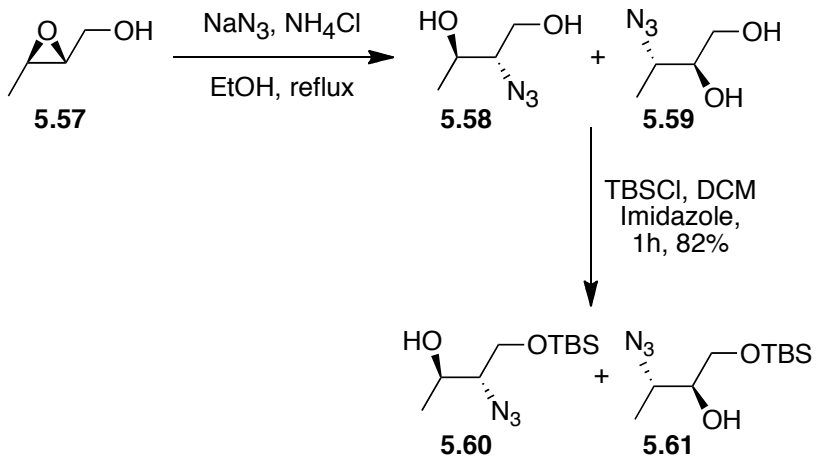


**Preparation of TBS ethers 5.60 and 5.61**.[54] Epoxide **5.57** (2g, 22.7 mmol) was dissolved in a solution of MeOH (200 mL) and water (25 mL). $NaN_3$ (7.5 g, 11.3 mmol) and $NH_4Cl$ (2.7 g, 49.9 mmol) were added to the solution. The mixture was allowed to stir at room temperature initially for 10 min and then refluxed at 80 ºC for 16 h. Upon completion, as analyzed by TLC, the reaction mixture was cooled and methanol was evaporated. The aqueous phase was extracted with EtOAc (3 X 100 mL). The organic solvent was removed via rotary evaporation to yield a regioisomeric mixture of azido alcohol **5.58** and **5.59**. The mixture was placed in anhydrous DCM (120 mL). To this TBSCl (1.92 g, 12.7 mmol) and Imidazole (2.0 g, 29.4 mmol) was added at 0 ºC. The mixture was allowed to stir in a nitrogen atmosphere for 2 h. Upon completion, as analyzed by TLC, sat. $NaHCO_3$ (20 mL) was added. The aqueous phase was extracted with DCM (3 X 65 mL). The collected organic layers were dried over anhydrous sodium sulfate. The solvent was removed via rotary evaporation to yield a regioisomeric mixture of TBS ethers **5.60** and **5.61** (4.5 g, 82%) as a white syrup. The crude was taken to next step without further purification.

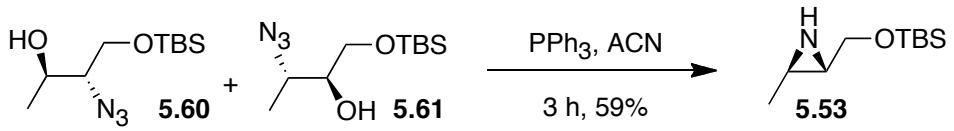


**Preparation of aziridine 5.53.** Mixture of isomeric TBS ethers **5.60** and **5.61** (1.96 g, 7.99 mmol) was placed in ACN (35 mL). To this $PPh_3$ (2.28 g, 8.71 mmol) was added in small portions over 20 min. The mixture was allowed to stir at room temperature for 1 h and then refluxed for 3 h. Upon completion of the reaction, as analyzed by TLC, the solvent was removed by rotary evaporation. The crude compound was purified by column chromatography (5:1 Hex:EtOAc) to yield the aziridine **5.53** (0.95 g, 59%) as a yellow oil. Spectral data for **5.53**: $^{1}$H-NMR (500 MHz, $CDCl_3$) $\delta$ 3.69 (m, 2H), 1.83 (m, 1H), 1.73 (m, 1H), 1.15 (d, 3H, J = 5.3 Hz), 0.84 (s, 9H), 0.01 (s, 6H); $^{13}$C-NMR (125 MHz, $CDCl_3$) $\delta$ 62.6, 39.0, 28.9, 25.9, 25.8, 18.5, 18.2, 13.8, -5.4; IR (neat) 3852, 2954, 2857, 1678, 1471, 1254, 1092, 838; HRMS (ESI) (m/z): $[M+H]^+$ calculated for $[C_{10}H_{24}NOSi]^+$ 202.1627, found 202.1630.

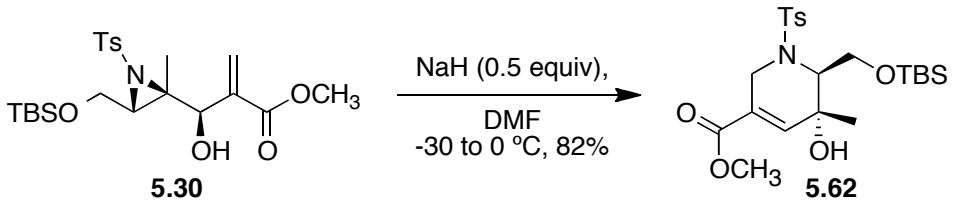


**Preparation of piperidine 5.62.** To a dispersion of NaH (60% as oil dispersion), (2.5 mg, 0.06 mmol) under nitrogen Baylis-Hillman adduct **5.30** (50 mg, 0.11 mmol) dissolved in anhydrous DMF (0.5 mL). The solution was cooled to -30 ºC. The mixture

was allowed to stir, while gradually warming the temperature to 0 ºC. After 45 min, when all the starting material was completely consumed as analyzed TLC, sat. $NH_4Cl$ (0.2 mL) was added followed by addition of water (2 mL). The aqueous phase was extracted (3 X 2 mL). The collected organics were dried over anhydrous sodium sulfate. The organic solvent was removed via rotary evaporation. The crude compound was purified via column chromatography (3:1 Hex:EtOAc) to furnish pirperidine **5.62** as an oil. Spectral data for **5.62**: $^1$H-NMR (500 MHz, $CDCl_3$) $\delta$ 7.77 (d, 2H, J = 8.6 Hz), 7.29 (d, 2H, J = 8.6 Hz), 6.77 (s, 1H), 4.34 (dd, 1H, J = 17.2, 1.8 Hz), 4.03 (t, 1H, J = 3.7 Hz), 3.74 (m, 1H), 3.73 (s, 3H), 3.71 (m, 1H), 3.48 (m, 1H), 2.41 (s, 3H), 1.35 (s, 3H), 0.74 (s, 9H), -0.14 (s, 3H), -0.18 (s, 3H); $^{13}$C-NMR (125 MHz, $CDCl_3$) $\delta$ 165.3, 141.1, 136.8, 129.9, 127.7, 127.3, 68.0, 62.6, 61.4, 60.3, 52.0, 41.6, 36.5, 25.5, 23.4, 21.4, 17.8, 14.1; IR (neat) 2953, 2857, 1721, 1665, 1338, 1257, 1163, 1092, 838, 778; HRMS (ESI) (m/z): $[M+H]^+$ calculated for $[C_{22}H_{36}NO_6SSi]^+$ 470.2033, found 470.2031.

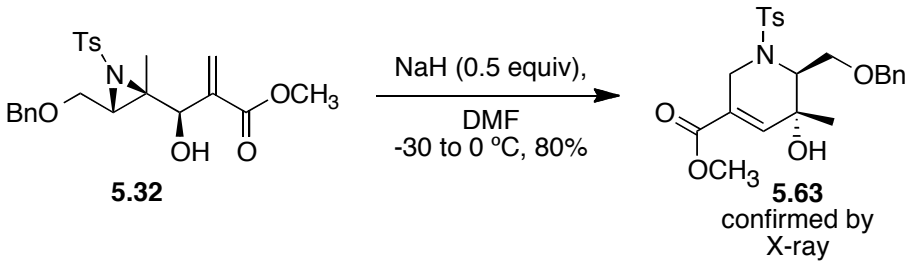


**Preparation of piperidine 5.63.** To a dispersion of NaH (60% as oil dispersion), (36 mg, 0.86 mmol) under nitrogen Baylis-Hillman adduct **5.32** (0.77 g, 1.73 mmol) dissolved in anhydrous DMF (18 mL). The solution was cooled to -30 ºC. The mixture was allowed to stir, while gradually warming the temperature to 0 ºC. After 45 min,

when all the starting material was completely consumed as analyzed TLC, sat. $NH_4Cl$ (3 mL) was added followed by addition of water (20 mL). The aqueous phase was extracted (3 X 25 mL). The collected organics were dried over anhydrous sodium sulfate. The organic solvent was removed via rotary evaporation. The crude compound was purified via column chromatography (3:1 Hex:EtOAc) to furnish pirperidine **5.63** (0.61 g, 80%) as a wax. Spectral data for **5.63**: $^1$H-NMR (500 MHz, $CDCl_3$) $\delta$ 7.74 (d, 2H, J = 8.4 Hz), 7.27 (m, 3H), 7.19 (d, 2H, J = 8.4 Hz), 7.08 (m, 2H), 6.74 (m, 1H), 4.36 (dd, 1H, J = 18.0, 1.9 Hz), 4.26 (t, 1H, J = 5.4 Hz), 4.23 (d, 1H, J = 12.1 Hz), 4.17 (d, 1H, J = 12.1 Hz), 3.73 (s, 3H), 3.57 (dd, 1H, J = 18.1, 2.9 Hz), 3.31 (dd, 1H, J = 10.5, 5.1 Hz), 3.17 (dd, 1H, J = 10.2, 6.4 Hz), 2.41 (s, 1H), 2.37 (s, 3H), 1.30 (s, 3H); $^{13}$C-NMR (125 MHz, $CDCl_3$) $\delta$. 165.2, 143.6, 140.9, 137.4, 136.6, 129.6, 128.3, 128.1, 127.7, 127.6, 127.5, 73.1, 67.8, 67.0, 61.1, 52.1, 40.6, 23.5, 21.5; IR (neat) 3502, 2952, 2863, 1717, 1339, 1272, 1162, 744; HRMS (ESI) (m/z): $[M+H]^+$ calculated for $[C_{23}H_{28}NO_6S]^+$ 446.1637 found 446.1633.

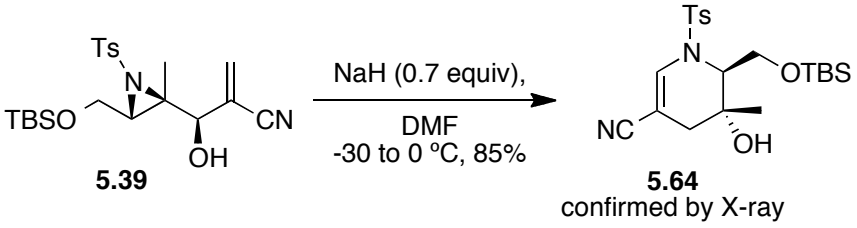


**Preparation of piperidine 5.64**. To a dispersion of NaH (60% as oil dispersion), (4 mg, 0.10 mmol) under nitrogen Baylis-Hillman adduct **5.39** (66 mg, 0.15 mmol) dissolved in anhydrous DMF (0.8 mL). The solution was cooled to -30 ºC. The mixture was allowed

to stir, while gradually warming the temperature to 0 ºC. After 30 min, when all the starting material was completely consumed as analyzed TLC, sat. $NH_4Cl$ (0.5 mL) was added followed by addition of water (1 mL). The aqueous phase was extracted (3 X 5 mL). The collected organics were dried over anhydrous sodium sulfate. The organic solvent was removed via rotary evaporation. The crude compound was purified via column chromatography (4:1 Hex:EtOAc) to furnish pirperidine **5.64** (57 mg, 85%) as a white solid (mp = 163 – 165 ºC). Spectral data for **5.64**: $^1$H-NMR (500 MHz, $CDCl_3$) δ 7.68 (d, 2H, J = 8.5 Hz), 7.57 (m, 1H), 7.31 (d, 2H, J = 8.5 Hz), 3.86 (dd, 1H, J = 11.7, 4.0 Hz), 3.77 (dd, 1H, J = 11.6, 2.3 Hz), 3.59 (m, 1H), 2.55 (dd, 1H, J = 16.7, 1.8 Hz), 2.40 (s, 3H), 2.00 (d, 1H, J = 17.0 Hz), 1.32 (s, 3H), 0.85 (s, 9H), 0.03 (s, 3H), 0.02 (s, 3H); $^{13}$C-NMR (125 MHz, $CDCl_3$) δ 145.0, 137.6, 130.1, 127.2, 119.3, 86.7, 67.0, 64.1, 63.6, 35.7, 26.2, 25.7, 21.6, 18.0, -5.7,-5.8; IR (neat) 3455, 2953, 2858, 2210, 1637, 1377, 1351, 1252, 1164, 1129, 993, 838; HRMS (ESI) (m/z): $[M+H]^+$ calculated for $[C_{21}H_{33}N_2O_4SiS]^+$ 437.1930 found 437.1938.

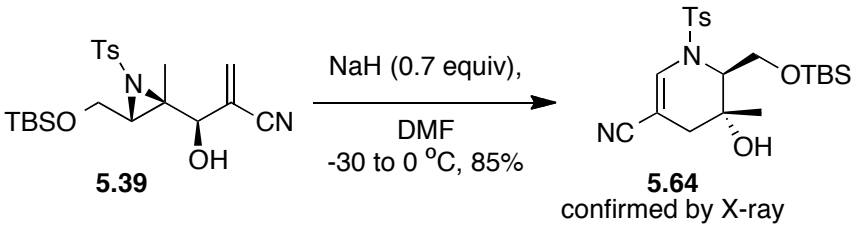


**Preparation of piperidine 5.64 via a one pot procedure**. To aziridine-2-carboxaldehyde **5.29** (0.25 g, 0.65 mmol) was added acrylonitrile (0.3 mL, 4.6 mmol). A few drops of anhydrous DCM (0.2 mL) were added at this point, in order to make a

homogenous solution. The reaction mixture was allowed to stir at room temperature under nitrogen for 1.5 d. Once all the starting material was consumed as analyzed by TLC, the solvent was removed by rotary evaporation. The flask containing the crude compound was put under nitrogen atmosphere and anhydrous DMF (3.3 ML) was added. NaH (60% as oil dispersion) (13 mg, 0.32 mmol) was added to the above solution maintained at -30 ºC. Starting material was consumed as the reaction mixture was allowed to warm to 0 ºC in 20 min. The reaction was quenched by sat. $NH_4Cl$ (0.5 mL). The aqueous phase was extracted with EtOAc (3 X 5 mL). The organics were dried over anhydrous sodium sulfate and the solvent was removed under reduced pressure. The crude compound was then purified via flash chromatography to yield the piperidine compound **5.64** (0.26 g, 90%) as a white solid. Spectral data for **5.64**: $^1$H-NMR (500 MHz, $CDCl_3$) $\delta$ 7.68 (d, 2H, J = 8.5 Hz), 7.57 (m, 1H), 7.31 (d, 2H, J = 8.5 Hz), 3.86 (dd, 1H, J = 11.7, 4.0 Hz), 3.77 (dd, 1H, J = 11.6, 2.3 Hz), 3.59 (m, 1H), 2.55 (dd, 1H, J = 16.7, 1.8 Hz), 2.40 (s, 3H), 2.00 (d, 1H, J = 17.0 Hz), 1.32 (s, 3H), 0.85 (s, 9H), 0.03 (s, 3H), 0.02 (s, 3H); $^{13}$C-NMR (125 MHz, $CDCl_3$) $\delta$ 145.0, 137.6, 130.1, 127.2, 119.3, 86.7, 67.0, 64.1, 63.6, 35.7, 26.2, 25.7, 21.6, 18.0, -5.7,-5.8; IR (neat) 3455, 2953, 2858, 2210, 1637, 1377, 1351, 1252, 1164, 1129, 993, 838; HRMS (ESI) (m/z): $[M+H]^+$ calculated for $[C_{21}H_{33}N_2O_4SiS]^+$ 437.1930 found 437.1938.

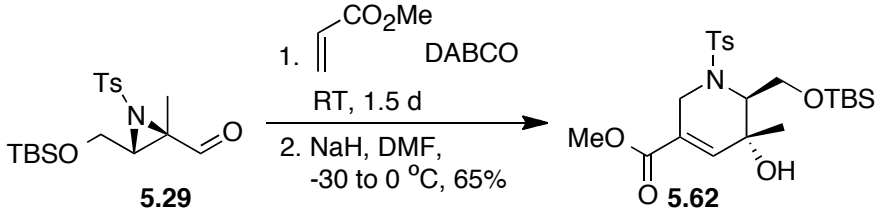

**Preparation of piperidine 5.62 via a one-pot reaction.** To aziridine-2-carboxaldehyde **5.29** (0.25 g, 0.65 mmol) was added methyl acrylate (0.3 mL, 3.25 mmol). The reaction mixture was allowed to stir at room temperature under nitrogen for 1.5 d. Once all the starting material was consumed as analyzed by TLC, the solvent was removed by rotary evaporation. The flask containing the crude compound was put under nitrogen atmosphere and anhydrous DMF (3.3 ML) was added. NaH (60 % as oil dispersion) (13 mg, 0.32 mmol) was added to the above solution maintained at -30 ºC. Starting material was consumed as the reaction mixture was allowed to warm to 0 ºC in 30 min. The reaction was quenched by sat. $NH_4Cl$ (0.5 mL). The aqueous phase was extracted with EtOAc (3 X 5 mL). The organics were dried over anhydrous sodium sulfate and the solvent was removed under reduced pressure. The crude compound was then purified via flash chromatography to yield the piperidine compound **5.62** (0.19 g, 65%) as an oil. Spectral data for **5.62**: $^1$H-NMR (500 MHz, $CDCl_3$) $\delta$ 7.77 (d, 2H, J = 8.6 Hz), 7.29 (d, 2H, J = 8.6 Hz), 6.77 (s, 1H), 4.34 (dd, 1H, J = 17.2, 1.8 Hz), 4.03 (t, 1H, J = 3.7 Hz), 3.74 (m, 1H), 3.73 (s, 3H), 3.71 (m, 1H), 3.48 (m, 1H), 2.41 (s, 3H), 1.35 (s, 3H), 0.74 (s, 9H), -0.14 (s, 3H), -0.18 (s, 3H); $^{13}$C-NMR (125 MHz, $CDCl_3$) $\delta$ 165.3, 141.1, 136.9, 129.9, 127.3, 68.1, 62.6, 61.4, 60.4, 52.0, 41.6, 36.5, 31.5, 26.1, 25.5, 23.4, 21.4, 17.8; IR (neat) 2953, 2857, 1721, 1665, 1338, 1257, 1163, 1092, 838, 778; HRMS (ESI) (m/z): $[M+H]^+$ calculated for $[C_{22}H_{36}NO_6SSi]^+$ 470.2033, found 470.2031.

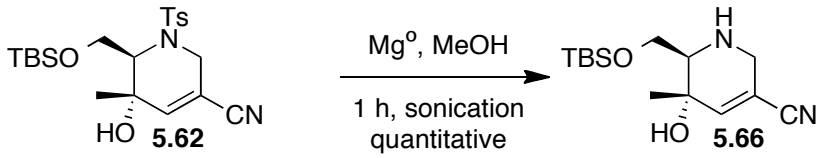


**Preparation of detosylated piperidine 5.66.** To a solution of piperidine **5.62** (50 mg, 0.11 mmol) in MeOH (0.42 mL) was added well-grounded magnesium powder (14 mg, 0.55 mmol). The solution was sonicated for 2 h till no more starting material was found upon TLC analysis. Sat. $NH_4Cl$ (0.5 mL) was added followed by addition of water (1 mL). The aqueous phase was extracted with EtOAc (5 X 5 mL). The organics were dried over anhydrous sodium sulfate and the solvent was removed under rotary evaporation. The crude product did not require any further purification. Spectral data for **5.66**: $^1$H-NMR (500 MHz, $CDCl_3$) $\delta$ 6.90 (d, 1H, $J$ = 6.1 Hz), 4.81 (d, 1H, $J$ = 5.0 Hz), 3.76 (dd, 1H, $J$ = 9.9, 4.6 Hz), 3.44 (dd, 1H, $J$ = 9.8, 8.5 Hz), 3.17 (m, 1H), 2.29 (d, 1H, $J$ = 16.0 Hz), 2.20 (d, 1H, $J$ = 16.0 Hz), 1.20 (s, 3H), 0.87 (s, 9H), 0.04 (s, 6H); $^{13}$C-NMR (125 MHz, $CDCl_3$) $\delta$ 171.1, 143.0, 122.1, 66.4, 62.6, 60.4, 37.3, 25.8, 23.3, 21.0, 18.1, 14.1, -5.5, -5.4; IR (neat) 3380, 2928, 2190, 1629, 1103, 1065, 839; HRMS (ESI) (m/z): $[M+H]^+$ calculated for $[C_{14}H_{27}N_2O_2Si]^+$ 283.1842, found 283.1838.

# REFERENCES

## REFERENCES


1. Asano, N.; Nash, R. J.; Molyneux, R. J.; Fleet, G. W. J. *Tetrahedron: Asymmetry* **2000**, *11*, 1645-1680.

2. Paulsen, H. *Angew. Chem., Int. Ed. Engl.* **1962**, *1*, 597-597.

3. Inouye, S.; Tsuruoka, T.; Ito, T.; Niida, T. *Tetrahedron* **1968**, *24*, 2125-2144.

4. Wong, C. H.; Dumas, D. P.; Ichikawa, Y.; Koseki, K.; Danishefsky, S. J.; Weston, B. W.; Lowe, J. B. *J. Am. Chem. Soc.* **1992**, *114*, 7321-7322.

5. Bols, M.; Hazell, R. G.; Thomsen, I. B. *Chem. Eur. J.* **1997**, *3*, 940-947.

6. Horenstein, B. A.; Zabinski, R. F.; Schramm, V. L. *Tetrahedron Lett.* **1993**, *34*, 7213-7216.

7. Lee, R. E.; Smith, M. D.; Nash, R. J.; Griffiths, R. C.; McNeil, M.; Grewal, R. K.; Yan, W.; Besra, G. S.; Brennan, P. J.; Fleet, G. W. J. *Tetrahedron Lett.* **1997**, *38*, 6733-6736.

8. Moriyama, H.; Tsukida, T.; Inoue, Y.; Yokota, K.; Yoshino, K.; Kondo, H.; Miura, N.; Nishimura, S.-I. *J. Med. Chem.* **2004**, *47*, 1930-1938.

9. Compain, P.; Martin, O. R. *Iminosugars: Past, Present and Future*; John Wiley & Sons, Ltd, 2008.

10. Singh, V.; Evans, G. B.; Lenz, D. H.; Mason, J. M.; Clinch, K.; Mee, S.; Painter, G. F.; Tyler, P. C.; Furneaux, R. H.; Lee, J. E.; Howell, P. L.; Schramm, V. L. *J. Biol. Chem.* **2005**, *280*, 18265-18273.

11. Takahashi, M.; Maehara, T.; Sengoku, T.; Fujita, N.; Takabe, K.; Yoda, H. *Tetrahedron* **2008**, *64*, 5254-5261.

12. Dressel, M.; Restorp, P.; Somfai, P. *Chem. Eur. J.* **2008**, *14*, 3072-3077.

13. Yoda, H.; Katoh, H.; Takabe, K. *Tetrahedron Lett.* **2000**, *41*, 7661-7665.

14. Tian, Y. S.; Joo, J. E.; Kong, B. S.; Pham, V. T.; Lee, K. Y.; Ham, W. H. *J. Org. Chem.* **2009**, *74*, 3962-3965.

15. Alam, M. A.; Kumar, A.; Vankar, Y. D. *Eur. J. Org. Chem.* **2008**, 4972-4980.

16. Shi, G. F.; Li, J. Q.; Jiang, X. P.; Cheng, Y. *Tetrahedron* **2008**, *64*, 5005-5012.

17. Bowen, E. G.; Wardrop, D. J. *Org. Lett.*, *12*, 5330-5333.

18. Ceccon, J.; Greene, A. E.; Poisson, J. F. *Org. Lett.* **2006**, *8*, 4739-4742.

19. Ferla, B. L.; Cipolla, L.; Nicotra, F. *General Strategies for the Synthesis of Iminosugars and New Approaches Towards Iminosugar Libraries*; John Wiley & Sons, Ltd, 2008.

20. Fleet, G. W. J.; Ramsden, N. G.; Witty, D. R. *Tetrahedron* **1989**, *45*, 319-326.

21. Wu, C.-Y.; Chang, C.-F.; Chen, J. S.-Y.; Wong, C.-H.; Lin, C.-H. *Angew. Chem., Int. Ed.* **2003**, *42*, 4661-4664.

22. La Ferla, B.; Bugada, P.; Cipolla, L.; Peri, F.; Nicotra, F. *Eur. J. Org. Chem.* **2004**, *2004*, 2451-2470.

23. Paulsen, H.; von Deyn, W. *Liebigs Ann. Chem.* **1987**, *1987*, 125-131.

24. Boglio, C. c.; Stahlke, S.; Thorimbert, S.; Malacria, M. *Org. Lett.* **2005**, *7*, 4851-4854.

25. Cong, X.; Liu, K.-G.; Liao, Q.-J.; Yao, Z.-J. *Tetrahedron Lett.* **2005**, *46*, 8567-8571.

26. Pearson, M. S. M.; Mathe-Allainmat, M.; Fargeas, V.; Lebreton, J. *Eur. J. Org. Chem.* **2005**, 2159-2191.

27. Weintraub, P. M.; Sabol, J. S.; Kane, J. M.; Borcherding, D. R. *Tetrahedron* **2003**, *59*, 2953-2989.

28. Basavaiah, D.; Reddy, B. S.; Badsara, S. S. *Chem. Rev.*, *110*, 5447-5674.

29. Krishna, P. R.; Lopinti, K. R.; Kannan, V. *Tetrahedron Lett.* **2004**, *45*, 7847-7850.

30. Nayak, S. K.; Thijs, L.; Zwanenburg, B. *Tetrahedron Lett.* **1999**, *40*, 981-984.

31. Hili, R.; Yudin, A. K. *J. Am. Chem. Soc.* **2009**, *131*, 16404-16406.

32. Schomaker, J. M.; Geiser, A. R.; Huang, R.; Borhan, B. *J. Am. Chem. Soc.* **2007**, *129*, 3794-3795.

33. Wipf, P.; Fritch, P. C. *J. Org. Chem.* **1994**, *59*, 4875-4886.

34. Arai, H.; Sugaya, N.; Sasaki, N.; Makino, K.; Lectard, S.; Hamada, Y. *Tetrahedron Lett.* **2009**, *50*, 3329-3332.

35. Vesely, J.; Ibrahem, I.; Zhao, G.-L.; Rios, R.; Córdova, A. *Angew. Chem., Int. Ed.* **2007**, *46*, 778-781.

36. Schomaker, J., Michigan State University, 2006.

37. Mulholland, N. P.; Pattenden, G.; Walters, I. A. S. *Org. Biomol. Chem.* **2008**, *6*, 2782-2789.

38. Crimmins, M. T.; Ellis, J. M.; Emmitte, K. A.; Haile, P. A.; McDougall, P. J.; Parrish, J. D.; Zuccarello, J. L. *Chem. Eur. J.* **2009**, *15*, 9223-9234.

39. Lautens, M.; Colucci, J. T.; Hiebert, S.; Smith, N. D.; Bouchain, G. *Org. Lett.* **2002**, *4*, 1879-1882.

40. Tavassoli, A.; Duffy, J. E. S.; Young, D. W. *Org. Biomol. Chem.* **2006**, *4*, 569-580.

41. SÃåvenda, J.; Myers, A. G. *Org. Lett.* **2009**, *11*, 2437-2440.

42. Churruca, F.; Fousteris, M.; Ishikawa, Y.; von Wantoch Rekowski, M.; Hounsou, C.; Surrey, T.; Giannis, A. *Org. Lett.*, *12*, 2096-2099.

43. Cooper, M. S.; Heaney, H.; Newbold, A. J.; Sanderson, W. R. *Synlett* **1990**, *1990*, 533,535.

44. Orrling, K. M.; Marzahn, M. R.; GutiÈrrez-de-Ter·n, H.; ≈qvist, J.; Dunn, B. M.; Larhed, M. *Bioorg. Med. Chem.* **2009**, *17*, 5933-5949.

45. Hanessian, S.; Boyer, N.; Reddy, G. J.; Deschenes-Simard, B. *Org. Lett.* **2009**, *11*, 4640-4643.

46. Chong, H.-s.; Ganguly, B.; Broker, G. A.; Rogers, R. D.; Brechbiel, M. W. *Chem. Commun. Perkin Trans. 1* **2002**, 2080-2086.

47. Yadav, J. S.; Pratap, T. V.; Rajender, V. *J. Org. Chem.* **2007**, *72*, 5882-5885.

48. Nobutaka, F. K., Nakai; Hiromu, Habashita; Yuka, Hotta; Hirokazu, Tamamura; Akira, Otaka ; Toshiro, Ibuka *Chem. Pharm. Bull.* **1994**, *42*, 2241.

49. Funaki, I.; Bell, R. P. L.; Thijs, L.; Zwanenburg, B. *Tetrahedron* **1996**, *52*, 12253-12274.

50. Crimmins, M. T.; DeBaillie, A. C. *J. Am. Chem. Soc.* **2006**, *128*, 4936-4937.

51. Liu, F.; Park, J.-E.; Lee, K. S.; Burke Jr, T. R. *Tetrahedron* **2009**, *65*, 9673-9679.

52. Tanner, D.; He, H. M.; Somfai, P. *Tetrahedron* **1992**, *48*, 6069-6078.

53. White, J. D.; Theramongkol, P.; Kuroda, C.; Engebrecht, J. R. *J. Org. Chem.* **1988**, *53*, 5909-5921.

54. Pu, J.; Franck, R. W. *Tetrahedron* **2008**, *64*, 8618-8629.

# Chapter 6

## Polyhydroxylated Alkaloids Via Modification of the Tandem Aza-Payne/Hydroamination Reaction

### 6.1 Polyhydroxylated alkaloids and their biological significance:

Alkaloids mimicking the structures of monosaccharides are prevalent in both plants and microorganisms.[1] Due to the structural resemblance with the sugar moiety in nature, these compounds inhibit glycosidases. Significance of these compounds and especially that of piperidine containing iminosgars has already been discussed in Chapter 5 (Section 5.1).

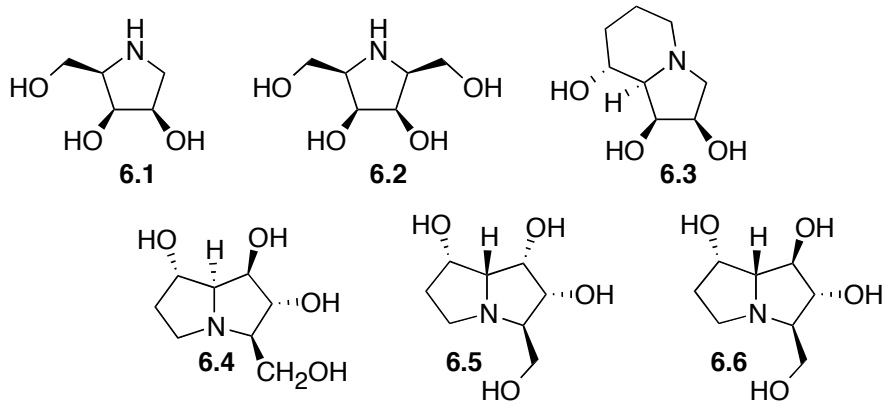


**Scheme 6.1** Polyhydroxylated alkaloids with significant biological activity.

This chapter will focus briefly on the chemistry developed for the preparation of polyhydroxylated pyrrolidine and pyrrolizidines in the literature and later describe the

modification of our tandem aza-Payne/hydroamination methodology to access similarly functionalized compounds.

Fleet and coworkers have reported the synthesis of 1,4-dideoxy-1,4-imino-D-lyxitol (DIL) **6.1** from D-mannose in 1985 (Scheme 7.1). The compound is found to be a strong inhibitor of coffee bean $\alpha$-galactosidase, with an $IC_{50}$ value of 0.2 $\mu$M.[2] Later 2,5-dideoxy-2,5-imino-D-galactitol **6.2** was synthesized by introducing a hydroxymethyl group at C-1$\beta$, and was shown to have higher inhibitory potency towards the same enzyme, with an $IC_{50}$ value of 0.05 $\mu$M.[3] Another indolizidine alkaloid swainsonine **6.3** isolated from the legumes of *swainsona canescens* was the first identified toxin, responsible for the syndrome "pea struck". Swainsonine is a potent inhibitor of acidic or lysosomal $\alpha$-mannosidase and golgi-mannosidase II.[4,5] Alexine **6.4** is another pyrrolidizine compound, which was isolated from the pods and seeds of *C. australe* and *A. leiopetala*.[6] After its isolation in 1987, several other tetrahydroxypyrrolidizine compounds were isolated from *C. australe*. Alexine, although a poor inhibitor of mammalian glucosidases, displays amyloglucosidase inhibition and is also an effective thioglucosidase inhibitor. Stereoisomer of alexine **6.5** also displays amyloglucosidase inhibitory properties.[7,8] Australine **6.6** is another specific inhibitor of fungal amyloglucosidase and glycoprotein-processing glucosidase 1.[9] Nonetheless chiral polyhydroxylated pyrrolidines have also been utilized both as catalysts and ligands in asymmetric synthesis.[10]

**6.2 General approaches to install polyhydroxylated pyrrolidines.**

As discussed for the case of piperidine containing iminosugars (Chapter 5, Section 5.2), most of the syntheses utilize commercially available monosaccharides as starting material. Scheme 6.2 illustrates one of the common approaches used for the synthesis of imino-D-galactitol derivative **6.8** starting from the protected heptonolactone **6.7**. Introduction of nitrogen is often achieved later via displacement reactions.

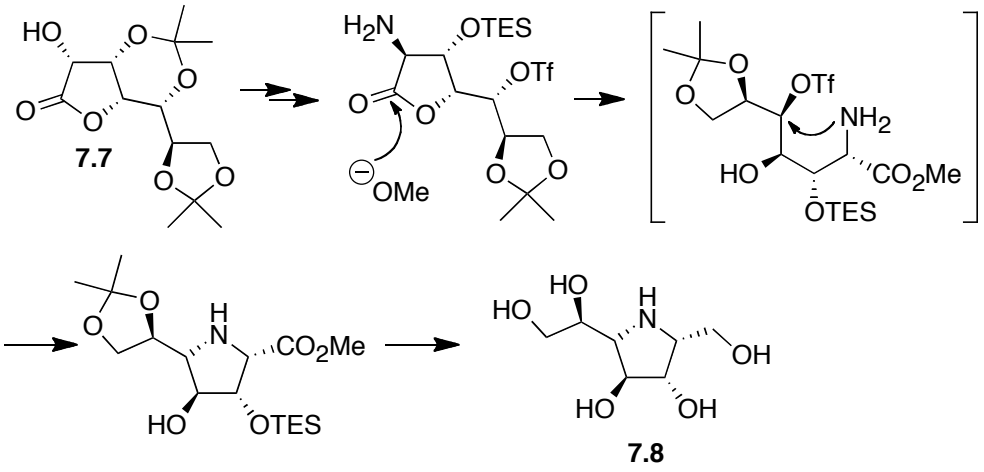


**Scheme 6.2** General approach towards the synthesis of imino-D-galactitol derivatives.

In this strategy, triflated lactone is subjected to methanolysis, which then undergoes ring closure via intramolecular nucleophilic displacement by the amine group to yield the iminosugar ring. This strategy has been used to design a library of galactofuranose mimics in order to search for potential inhibitors of mycobacterial cell wall biosynthesis.[11] Similarly, galactitol derivatives **6.9** - **6.11** with different substituted amino groups were synthesized via performing lactone ring opening with different primary amines instead of methoxide for this case. (Scheme 6.3)

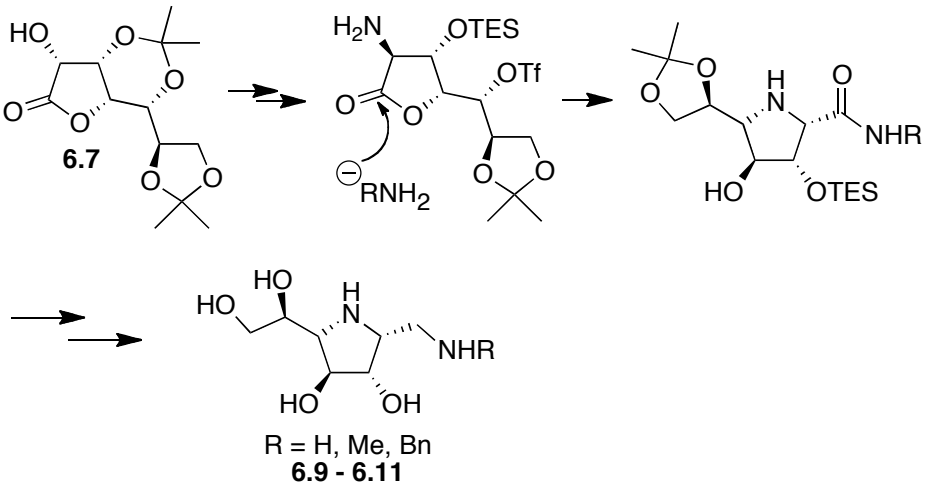


**Scheme 6.3** Synthesis of imino-D-galactitol derivatives.

Han et al., on the other hand, have demonstrated the asymmetric synthesis of such compounds starting from an olefin starting material, utilizing the regioselective aminohydroxylation reaction and the tandem epoxidation-intramolecular cyclization cascade reactions (Scheme 6.4).[12] Notably, asymmetric synthesis relies on both the enantiopurity and regioselectivity accomplished via the aminohydroxylation reaction on the olefin precursor, unlike the availability of the chiral starting material as utilized in previous cases. Directed epoxidation using $VO(acac)_2$/tBuOOH, followed by an intramolecular cyclization of the resulting γ-epoxycarbamate, provides a general route starting from non-monosaccharide type starting material. Recently, similar routes based on non-carbohydrate starting materials have been investigated. Several syntheses of polyhydroxylated compounds such as alexine, swainsonine and other pyrrolizidine alkaloids have been reported.[13-21]

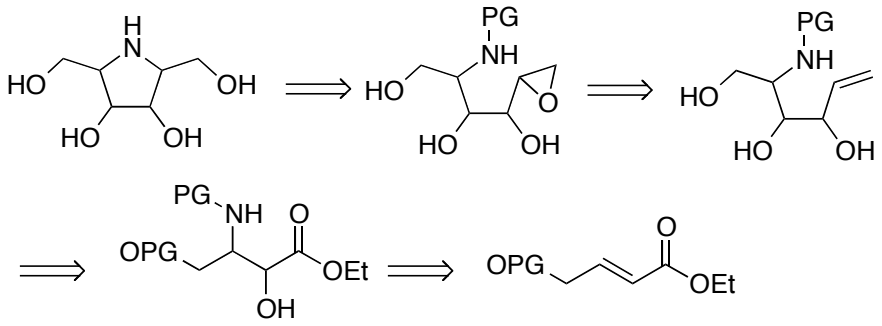


**Scheme 6.4** Retrosynthetic approach for the synthesis of polyhydroxylated pyrrolidines.

## 6.3 Modification of the tandem aza-Payne/hydroamination reaction towards functionalized pyrrolidines.

The tandem aza-Payne/hydroamination methodology yields tetrasubstituted pyrrolidines that are densely decorated. The resulting pyrrolidine products bear interesting functional groups, which can be exploited in several ways to derive compounds of elaborated nature. Some of these studies have already been discussed in Chapters 3 and 4. We became interested in examining, at this point, the scope of the aza-Payne/hydroamination reaction and its modification to access pyrrolidine scaffolds, however with increased complexity. Scheme 6.5 outlines the synthesis of conventional enamides via the tandem aza-Payne/hydroamination protocol.[22] Once the *syn* aziridine alcohol **6.12** is deprotonated, the alkoxide intermediate **6.12a** executes an intramolecular aziridine ring opening (aza-Payne rearrangement). The resulting epoxy *N*-Ts amide intermediate **6.12b** then readily undergoes the *5-exo-dig* ring closure to yield enamide **6.13**. Notably the success of this protocol relies significantly on the ease of the aza-Payne equilibrium towards the epoxy amide intermediate. The resulting

epoxy amide intermediate **6.12b** bears both the electrophile and the nucleophile, and if orients correctly (*syn* isomer), an efficiently ring closure ensues.

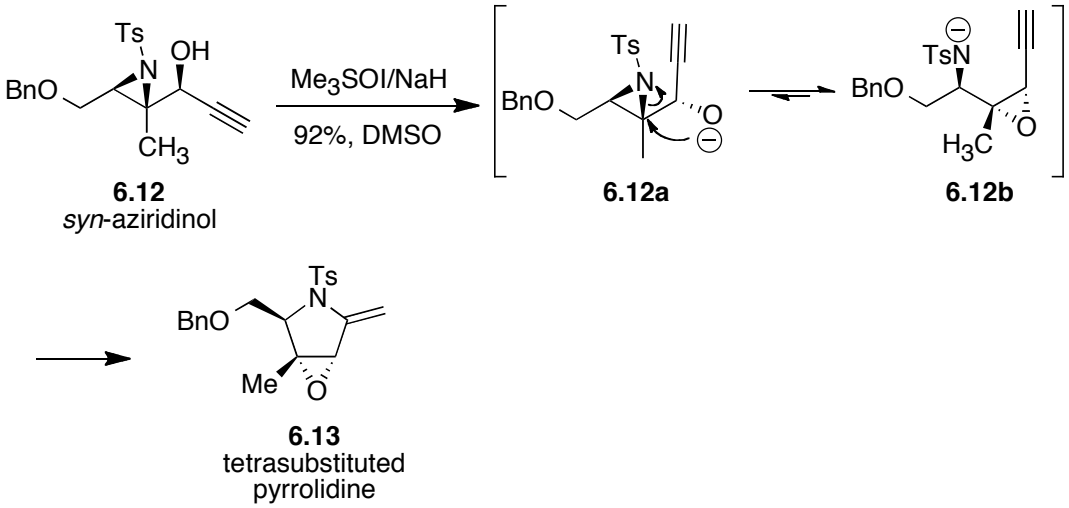


**6.12**
*syn*-aziridinol

**6.12a**

**6.12b**

**6.13**
tetrasubstituted
pyrrolidine

**Scheme 6.5** Tandem aza-Payne/hydroamination yields tetrasubstituted pyrrolidines.

Thus, one way to affect the fate of the hydroamination pathway would be by interrupting the alkoxide intermediate **6.12a** with a latent nucleophile, before it executes the aza-Payne rearrangement. Aziridine ring opening with a modified nucleophile, would then lead to enamide compounds embellished with functionalities of different nature. Scheme 6.7 illustrates the latter proposal that relies on the use of $CO_2$ as a latent nucleophile. We anticipated that this would initially serve as an electrophile to affect the acylation of the alkoxide intermediate, thereby introducing instead a carbonate nucleophile to carry out the aziridine ring opening. Ensuing *5-exo-ring* closure should hopefully deliver the functionalized enamide carbonate product. The intramolecular aza-Payne process is efficient and therefore makes the attempt to interrupt this path via an

external electrophile a challenging task. This modified route would demand the generation of a long-lived **6.12a** alkoxide species capable of intermolecular trapping, since it would most likely perform the intramolecular ring opening, without allowing it to react with an external electrophile. Evidence for obtaining a long-lived alkoxide intermediate came from a desilylation experiment carried out with the TBS ether **6.14** (Scheme 6.6). Participation of the latter in the observed semi-Pinacol rearrangement[36] to aldehyde **6.15**, required the migration of an alkyl group, suggesting the higher stability of the alkoxide **6.14a** in this case. This encouraged us to pursue our interest towards probing the reactivity of the alkoxide intermediate and its potential to react with a suitable latent nucleophile *in-situ*.

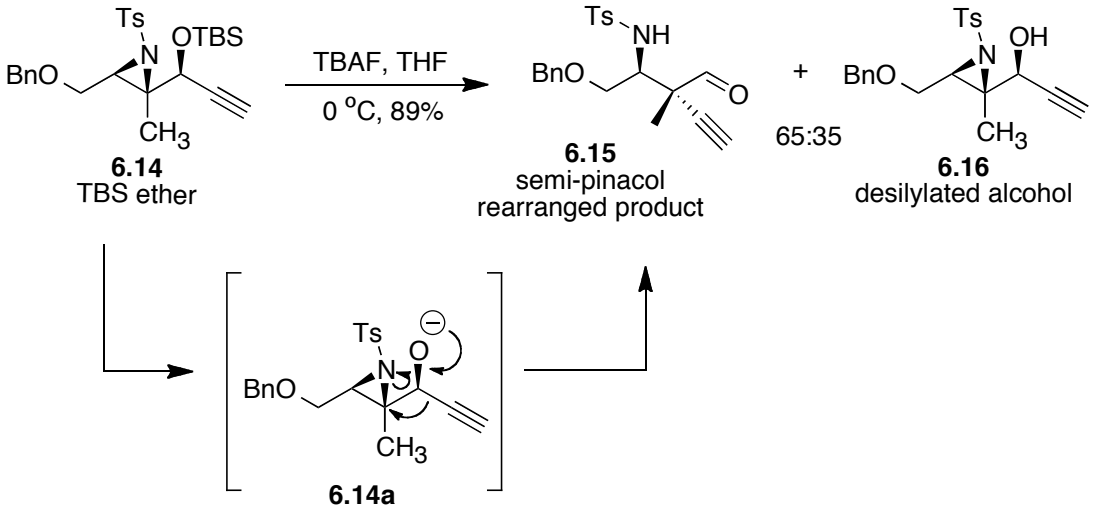


**Scheme 6.6** Comparatively long-lived alkoxide intermediate leads to the semi-Pinacol rearranged aldehyde product.

[36] Unexpected semi-Pinacol rearrangement resulted during desilylation reaction has been discussed in detail in Chapter 3, Section 3.5.

Having demonstrated that the alkoxide **6.14a**, generated under conditions demonstrated in Scheme 6.6, does not readily aza-Payne, we used the similar conditions to introduce $CO_2$ functioning as an electrophile, which upon reaction with the alkoxide would reveal itself as a potential nucleophile (Scheme 6.7). TBS ether **6.14** was subjected to desilylation and allowed to react with $CO_2$, generated via dissolving excess of $NaHCO_3$ in a polar solvent such as DMF. Scheme 6.8 illustrates various products obtained during this reaction at 0 ºC for 2 h.

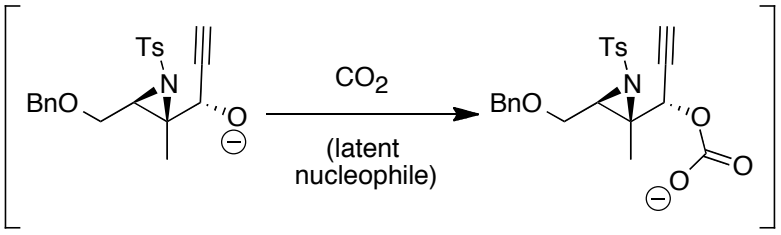


**Scheme 6.7** Trapping latent nucleophile such as $CO_2$ by alkoxide intermediate would deliver functionalized enamides.

Interestingly, a mixture (18:22:26:34) of desylilated alcohol **6.16**, aza-Payne rearranged epoxide **6.17**, the conventional tandem aza-Payne/hydroamination product **6.18** along with a carbonate trapped enamide compound **6.19** was obtained. This indicated that the generated alkoxide, after desilylation undergoes the expected intramolecular aziridine ring opening reaction leading to the formation of the epoxy amine **6.17**. The latter then undergoes *5-exo-dig* ring closure, as observed previously under ylide/DMSO conditions, providing *N*-Ts enamide compound **6.18**.

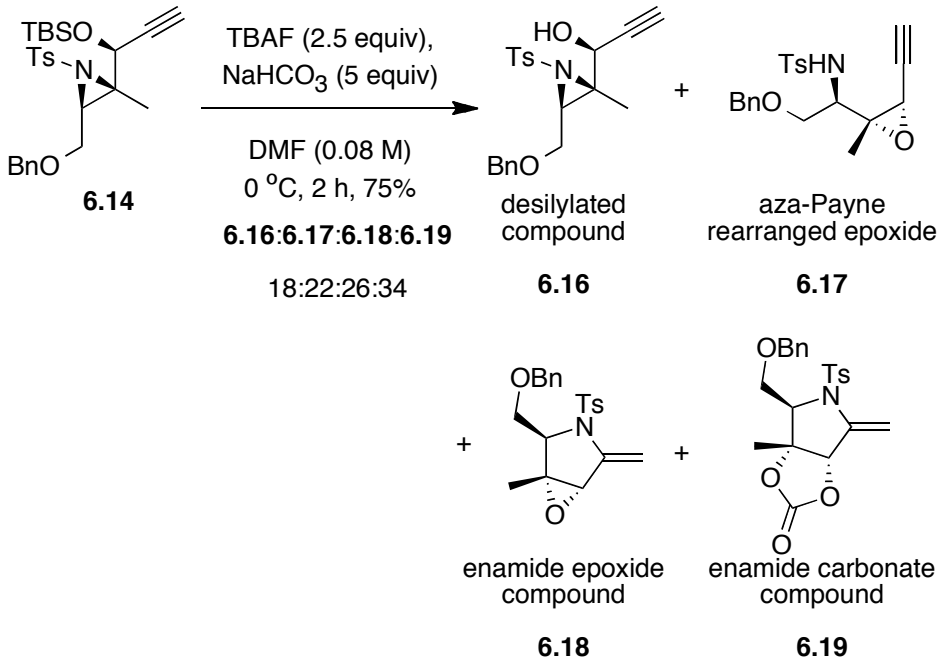


**Scheme 6.8** Initial attempt to trap *in-situ* generated alkoxide with $CO_2$.

The desired and significant result however, was revealed via the formation of the carbonate enamide compound **6.19** thereby indicating the fruitful attempt at intercepting the generated alkoxide with $CO_2$. The reaction gave a mixture of products, nevertheless provided encouraging results to continue efforts to optimize the reaction toward the synthesis of the desired *N*-Ts carbonate enamide compound **6.19**[37]. Table 6.1 demonstrates various conditions that were examined in order to optimize the reaction to maximize the production of the desired carbonate compound.

[37] Structure of compound **6.19** was determined by the analysis of 1D, 2D NMR experiments and HRMS data. Efforts will be made in future to obtain the X-ray structure for further structural confirmation and validation of the proposed relative stereochemistry at C-3 and C-4 positions.

**Table 6.1** Optimization of reaction towards the synthesis of *N*-Ts enamide carbonate compound **6.19**.

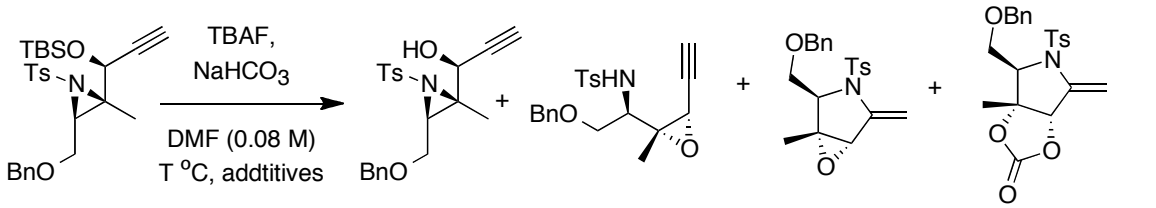


**6.14** | desilylated compound **6.16** | aza-Payne rearranged epoxide **6.17** | enamide epoxide compound **6.18** | enamide carbonate compound **6.19**

| entry | TBAF (equiv) | $NaHCO_3$ (equiv) | T °C | additives (equiv) | ratios (**6.16**/**6.17**/**6.18**/**6.19**) | time (h) |
|---|---|---|---|---|---|---|
| 1 | 5 | 10 | 0 | - | 18/22/26/34 | 2 |
| 2 | 5 | 10 | 0 to RT | - | 0/0/20/80 | 6 |
| 3 | 2.5 | 10 | 0 to RT | - | 0/0/38/62 | 12 |
| 4 | 5[a] | 10 | RT | 4 Å ms | 0/0/100/0 | 12 |
| 5 | 2 | 20 | -10 to RT | - | 0/0/18/82 | 8 |
| 6 | 2 | 20 | -30 to 60 | - | 0/0/30/70 | 12[b] |
| 7[c] | 2 | 20 | 0 to RT | $Cs_2CO_3$ (10 equiv) | 0/0/62/38 | 2 |
| 8 | 2 | 20 | 0 to RT | $Cs_2CO_3$ (10 equiv) | 0/0/90/10 | 2 |
| 9 | 2 | 20 | 0 to RT | $CO_2$ bubbling | 0/0/5/95[c] | 5 |
| 10 | 5+6 | 20 | 0 to RT | $CO_2$ bubbling | 0/0/0/100 | 8 |

[a.]TBAF was stirred over 4 Å ms for 1 h before its was added to the reaction. [b]polar and unidentified impurities were observed, as analyzed by NMR of crude mixture, at elevated temperature. [c]TBAF was added at 0 °C then reaction was warmed to RT

followed by sonication. [d]only 38% conversion was observed by NMR analysis of crude reaction mixture.

The initial reaction conditions (entry 2) implied that longer reaction times were critical for the conversion of the intermediates into final products. The alkoxide might rapidly undergo aza-Payne rearrangement or form the carbonate intermediate although reversibly; the latter seems likely to require longer time to execute the hydroamination process. The starting material, i.e. the TBS ether **6.14** was consumed fast as analyzed by TLC, but earlier quenching only resulted in the formation of the desilylated alcohol **6.16** and the epoxy amine **6.17**. Temperature was also found to play an important role. Initial reaction was performed by maintaining the temperature at 0 ºC, which did not allow for the complete consumption of presumably the initially generated intermediates into the final products. This was also verified by the fact that later, when the reaction was allowed to warm to room temperature, no desilylated alcohol **6.16** or epoxy amine **6.17** was obtained (entries 2-10). Curiously, complete anhydrous conditions (where TBAF reagent was dried by stirring over 4 Å ms) lead to the exclusive generation of the enamide epoxide compound **6.18** (entry 4). The reason for the formation of latter compound under these conditions is not understood. Nonetheless, we were gratified to find an alternative route for the synthesis of *N*-Ts enamide compound **6.18**, which requires the generation of an ylide according to the original tandem aza-Payne/hydromination conditions. Initiation of the reaction at lowered temperature did not lead to any considerable change of the product ratios (entry 5, 6). Nonetheless,

heating of the reaction solution led to the generation of some polar un-identified impurities (entry 6). Higher ratio of *N*-Ts enamide epoxide **6.18** was observed when $Cs_2CO_3$ was added as an additive and sonication was performed in an attempt to maximize the solubility of $CO_2$ in the solution (entry 7). Lack of sonication, however, resulted in a further improvement in favor of the *N*-Ts enamide epoxide **6.18** (entry 8). This also contrasted our belief that the presence of $Cs_2CO_3$ reagent could enhance the amount of $CO_2$ in the reaction solution. Next, we turned our attention to enhance the availability of $CO_2$ by bubbling the latter as a gas, in order to improve the amount of dissolved reagent present in the reaction mixture. Indeed, when TBAF was added to the solution of the TBS alcohol **6.14**, bubbled with $CO_2$ gas, 95% of the desired carbonate enamide compound **6.19** was obtained (entry 9). The reaction suffered for poor conversion however, upon treatment with excess TBAF, the desired carbonate compound **6.19** was obtained with complete conversion, as confirmed by the analysis of the crude NMR spectrum (entry 10).

**6.4 Evidence of Intermediates and mechanistic studies.**

Information obtained during the optimization studies provided clues for the mechanism of the reaction (Scheme 6.9). An experiment was carried out at this stage to analyze the necessity to have a protected alcohol in this transformation, since presumably, the alcohol would also lead to the required alkoxide under basic conditions. Alcohol **6.16**, upon treatment with excess of $NaHCO_3$ in DMF, returned only the starting material,

demonstrating that masking of the alcohol as a silyl ether is critical for the reaction (Scheme 6.9).

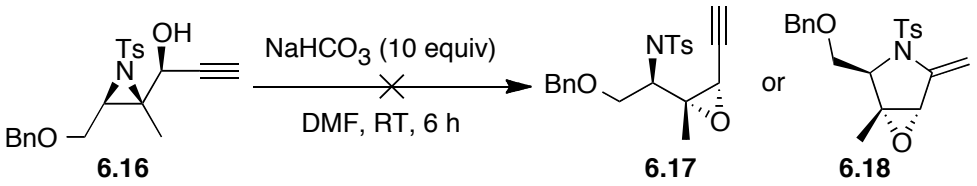


**Scheme 6.9** The unmasked alcohol does not undergo aza-Payne/hydroamination reaction.

This could also mean that generation of an alkoxide intermediate in an irreversible manner is crucial for the transformation, since the corresponding TBS ether upon treatment with fluoride would satisfy the latter condition.

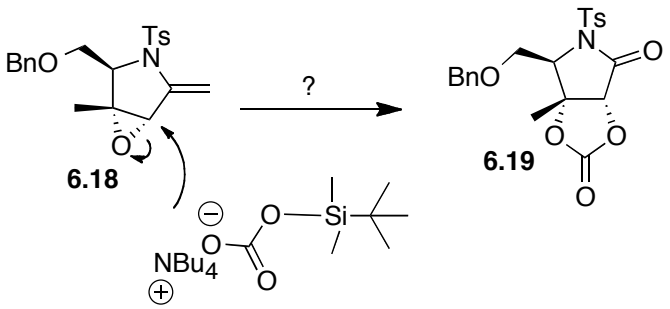


**Scheme 6.10** Putative mechanism for the formation of *N*-Ts enamide carbonate **6.19**.

Mechanistically, one could also suspect that the epoxide compound **6.18** resulting under these conditions could also react thereby converting into the desired carbonate compound **6.19** (Scheme 6.10). To analyze the latter possibility, the *N*-Ts enamide

epoxide compound **6.18** was treated with excess of both TBAF, $NaHCO_3$ in DMF. No reaction was observed even after 8 h, therefore implying against the possibility that the original enamide epoxide product could lead to the observed carbonate **6.19** (Scheme 6.11). This suggests that reaction is likely to proceed via two independent paths. One of the paths dominates in the absence and the other in the presence of dissolved $CO_2$ in the solution.

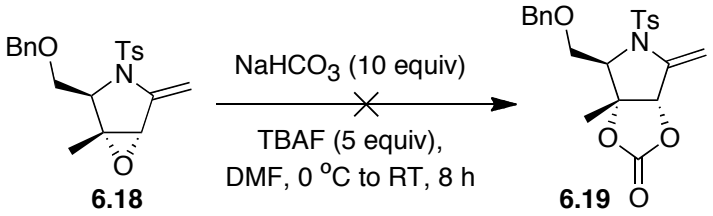


**Scheme 6.11** Treatment of *N*-Ts enamide epoxide under conditions that lead to the carbonate product does not yield the *N*-Ts carbonate **6.19**.

Treatment of the TBS compound **6.14** with TBAF, initiates the formation of desilylated alkoxide **6.14a**, which then traps the dissolved $CO_2$ to form the carbonate intermediate **6.20**. Intramolecular aziridine ring opening of **6.20** yields the carbonate amide intermediate **6.20a**. Ensuing *5-exo-dig* cyclization of the amide intermediate completes the formation of the *N*-Ts enamide carbonate compound **6.19** (Scheme 6.12).

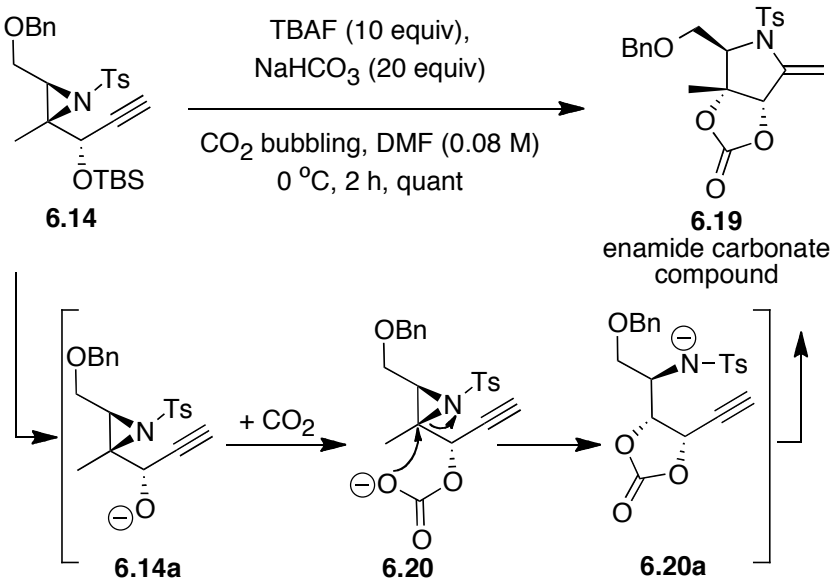


**Scheme 6.12** Postulated mechanism for the formation of *N*-Ts enamide carbonate compound.

Both intermediate **6.14a** (which is equivalent to desilylated alcohol **6.16**) and epoxy amine **6.17** (obtained via aza-Payne rearrangement) were observed and isolated a number of times. We presumed that hydromination on the latter led to the *N*-Ts enamide **6.18,** based on the mechanism of aza-Payne/hydromination process. Curiously, **6.20a** was never isolated under different conditions screened during the optimization procedure (entries 1-10, Table 6.1) leaving room for doubt regarding its intermediacy in the proposed mechanism. Possibility of formation of this intermediate could however not be completely ruled out in the absence of its isolation, since the latter depends on the stability of an intermediate during the reactions. Thus one possibility could be that the higher reactivity of **6.20a** intermediate would favor hydromination yielding the carbonate compound **6.19**. In order to test this supposition and to trap the

putative carbonate intermediate, we chose a substrate **6.22** which was incapable of undergoing the hydroamination process according to studies previously done in our lab.[23]

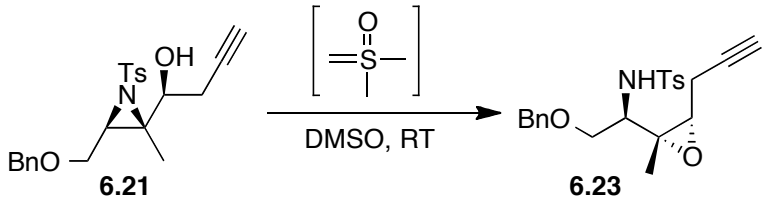


**Scheme 6.13** Hydroamination of aziridinol **6.21** does not yield the hydroaminated product.

Notice, the unmasked alcohol **6.21** bears an extra methylene between the carbinol and the alkyne position. The flexibility afforded by the extra methylene does not allow for the formation of the required constrained conformation, required for cyclization, yielding the aza-Payne product only (Scheme 6.13). The substrate **6.22** was prepared by treating the aziridinol **6.21**[38] with TBSOTf in the presence of 2,6-lutidine (Scheme 6.14).

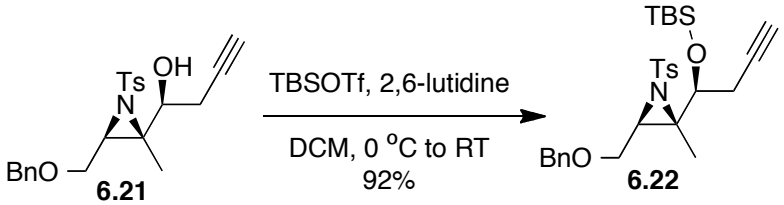


**Scheme 6.14** Silylation of aziridine alcohol.

[38] Alcohol was prepared according to the procedure describe in the thesis submitted by Dr. Stewart Hart in our lab. (see Ref 23)

Notably the silylation procedure with TBSCl and Imidazole only returned the starting material. The prepared TBS ether **6.22** was treated under initial conditions that lead to the isolation of various intermediates (See Scheme 6.8). Gratifyngly, *syn* aziridinol **6.22** upon treatment with excess of TBAF and $NaHCO_3$ under previously established conditions yielded a mixture of both the aza-Payne epoxide **6.23** and the much anticipated carbonate amide **6.24** in a ratio of 31:69 (Scheme 6.15). This provides evidence that the carbonate intermediate **6.20a** (akin to **6.24**) is most probably produced however, is not isolable once it proceeds to the final hydroamination product **6.19**.

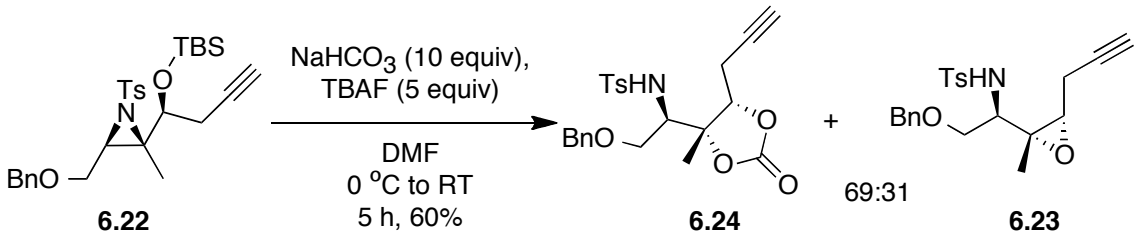


**Scheme 6.15** Substrate incapable of undergoing the hydroamination reaction yields the elusive carbonate amide intermediate.

With this information in hand, we had evidence in support of all the intermediates involved in the transformation illustrated (Scheme 6.12) although, a better understanding at the competing intermolecular reaction (intercepting the alkoxide species with electrophiles) with that of the intramolecular transformation (aza-Payne) was required. Scheme 6.16 illustrates the detailed mechanistic outline proposed for the reaction. Desilylation of aziridinol **6.25** generates the alkoxide intermediate **6.26**, which in the absence of $CO_2$ would exist in equilibrium with the aza-Payne intermediate

**6.27**[39]. Noticeably, such equilibrium is known to be favored towards the aza-Payne rearranged epoxy amide species for the cases where the nitrogen is stabilized by an electron withdrawing group such as Ts. The latter in turn would undergo ring closure, generating the reactive vinyl anion intermediate **6.28**, and which upon rapid protonation would yield the *N*-Ts enamide epoxide **6.29**. Thus, the rate constant $k_{-1}$ would govern the extent of the reversibility of the *N*-Ts enamide vinyl anion back to the ring opened amide intermediate **6.27** in the reaction.

On the other hand in the presence of enough soluble $CO_2$ the alkoxide intermediate **6.26** would trap the electrophile leading to the formation of the carbonate intermediate **6.30**. The latter would execute the intramolecular aziridine ring opening, thus allowing an equilibrium between the carbonate **6.30** and the amide **6.31**. Cyclization of **6.31** would yield the vinyl anion 6.32 which would also rapidly protonate. The rate constant $k_{-2}$ would govern the rate of ring opening of the enamide vinyl species back to the carbonate amide intermediate **6.31**. Thus, the path of the reaction leading to a specific product would be predominantly controlled via the magnitude of both rate constants $k_1$ and $k_2$ and the respective rates for the back reactions. The failure at the isolation of the carbonate intermediate **6.31** (similar to **6.20a**) during the reaction condition could reasonably imply that **6.31** in comparison to **6.27** enjoys a faster rate of cyclization. In order to understand for the possibility for the back reaction governed by $k_{-1}$, a substrate

[39] Refer to Chapter 3 for discussion on the aza-Payne equilibrium.

**6.34**[40] was synthesized. The vinyl anion generated upon lithium-halogen exchange of **6.34** (leading to the mimic of **6.27**) failed to react with $CO_2$ and instead underwent ring opening to afford only the β-elimination product **6.35**. The conditions used in the hydroamination reactions are irreversible unlike in the case of lithium-halogen exchange conditions. Nevertheless the experiment proves unequivocally that reversion of the vinyl anion **6.28** is feasible. Combining the results from the last two evidences observed for both the reactions, one could conclude that $K_{-1} > K_{-2}$. This implies that the rate of ring opening of the vinyl epoxide intermediate **6.28** is much faster than that in case of vinyl carbonate **6.32**. A careful examination of the computationally calculated ground state conformation[41] for the two intermediates revealed that the dihedral angle $\theta_1$ in case of epoxy amide **6.28** is slightly larger than that ($\theta_2$) in the carbonate amide **6.32**.

[40] Synthetic procedure for compound **6.34** has been discussed in Chapter 3 (Section 3.4.2.1).

[41] Calculations were performed on SPARTAN using semiempirical theory (AM1).

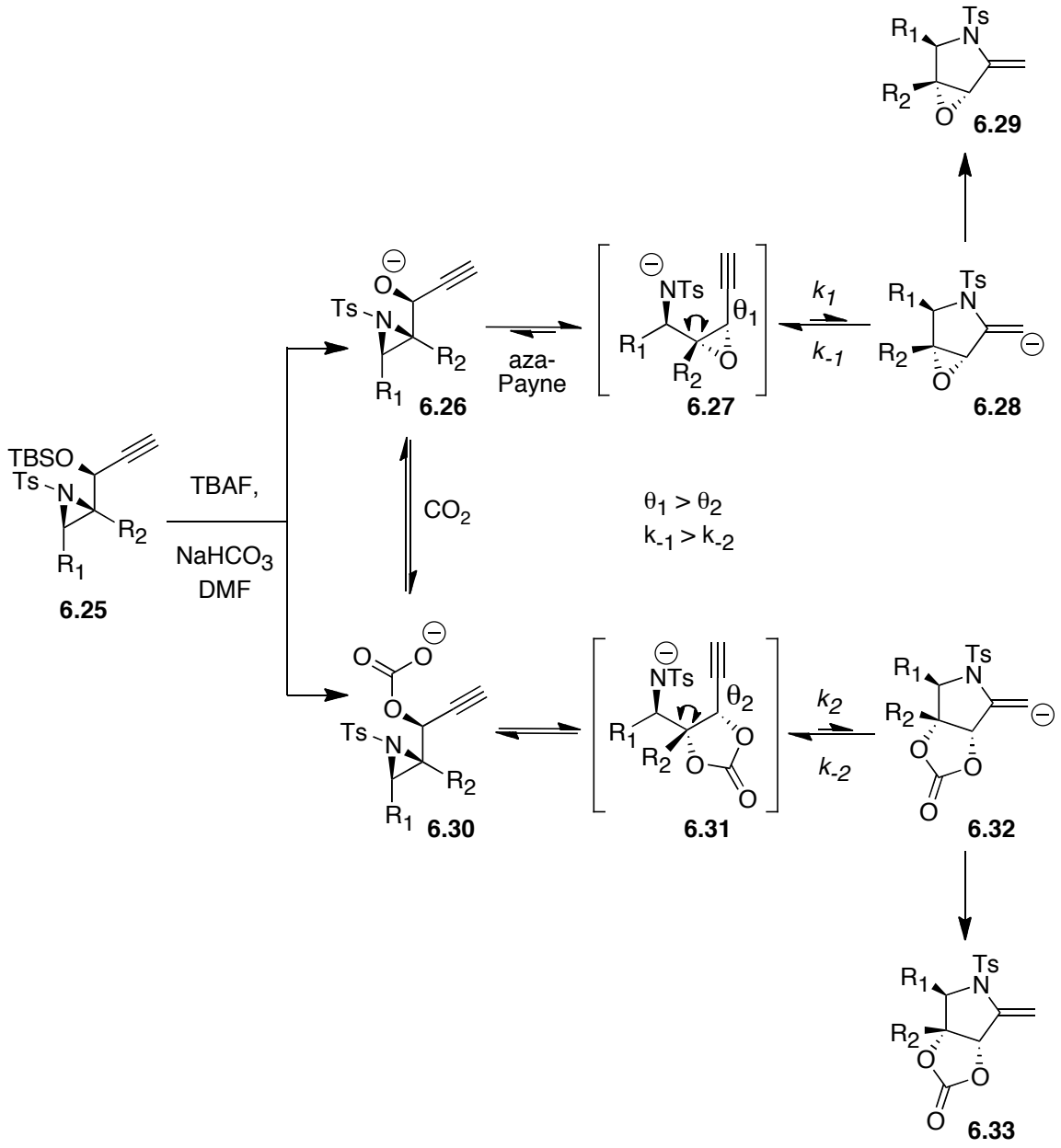


**Scheme 6.16** Mechanistic rationale for the synthesis of enamide epoxide and carbonate compounds.

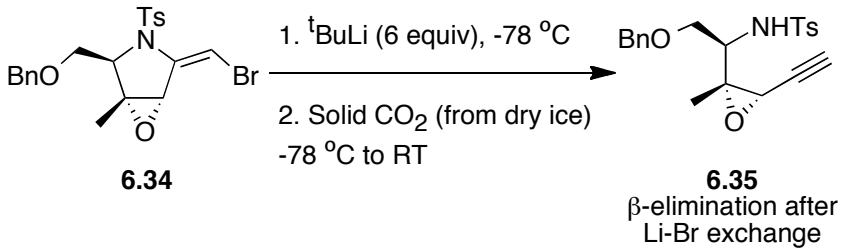


**Scheme 6.17** Failed attempt at trapping the vinyl lithium with $CO_2$.

Noticeably even a small difference in dihedral angles would effect the rate of the cyclization, since proximity and the right conformation is crucial for the success of the hydroamination reaction. Note, the intermolecular trap of $CO_2$ by the alkoxide could be slower which might limit the production of carbonate intermediate **6.30** with respect to **6.26**. However, once generated, both of these intermediates would execute the intramolecular aziridine ring opening to generate the epoxy amide **6.27** and the carbonate amide **6.31**, both of which in turn would undergo *5-exo-dig* ring closure. Higher rate of reversibility in case of the vinyl anion **6.28** (higher $k_{-1}$) (compared to that of the cyclized carbonate vinyl anion **6.32)** to the ring opened form **6.27** would prevent the generation of this intermediate. Further closer proximity between the electrophile and the nucleophile in case of the carbonate amide **6.31** would maximize the generation of carbonate vinyl anion **6.32**. Alternately, strain involved in the [3.1.0] system (**6.28** intermediate) as compared to [3.3.0] system (**6.32** intermediate) can be further invoked to explain the higher reversibility displayed by the former intermediate. Thus, under the appropriate conditions, the system is set to siphon all the intermediates toward the formation of the desired carbonate product **6.33**.

### 6.5 Elaboration of *N*-Ts enamide carbonates toward Iminosugars.

Modification of aza-Payne/hydroamination conditions in presence of the latent nucleophile $CO_2$, allowed for the preparation of the *N*-Ts enamide carbonate compounds. Such compounds are potential intermediates toward the synthesis of iminosugars, as the hydrolysis of the carbonate moiety would install the *bis* hydroxy functionality at C-3 and C-4 positions.

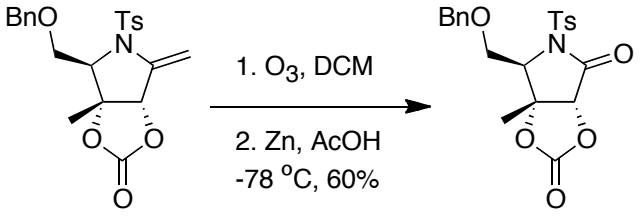


**6.19** **6.36**

**Scheme 6.18** Elaboration of the *N*-Ts enamide carbonate to lactam.

For this purpose, the reactive *N*-Ts enamide carbonate compound **6.19** was first oxidized to reveal lactam compound **6.36** in a quantitative conversion and 60 % yield (Scheme 6.18).

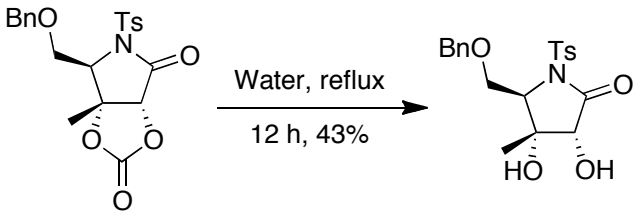


**6.19** **6.37**

**Scheme 6.19** Hydrolysis of the lactam carbonate to 3,4-dihydoxylactam.

The latter, when refluxed in water for 12 h furnished 3,4-dihydroxylactam **6.37** with moderate yield (Scheme 6.19).

## 6.6 Prospect of other latent nucleophiles in modified tandem aza-Payne chemistry.

The current transformation relies on the use of $CO_2$ as a latent nucleophile. Initially it serves as an electrophile thereby undergoing an attack with the *in-situ* generated alkoxide intermediate. Later, functioning as a nucleophile, it executes the ring opening of the aziridine to form the enamide carbonate. Thus, this transformation provides useful carbonate pyrrolidines. Noticeably, the corresponding epoxide pyrrolidines obtained via the conventional tandem aza-Payne/hydroamination, have proved to be challenging substrates for the epoxide ring opening reactions.[42] In future similar reactions will be examined on the carbonate compounds.

It would also be interesting to examine the prospect of other latent nucleophiles in this transformation. The modified nucleophiles would enable access to pyrrolidines with different functionalities established at C-3 and C-4 positions. For instance, use of $CS_2$ would deliver pyrrolidine **6.38** with a fused cyclic xanthate group (Scheme 6.20). Further availability of the reagent in liquid form might also improve the efficiency of this transformation. The latter would serve as an interesting compound for further elaborations, since treatment with a radical initiator would putatively generate C-4

[42] Challenges presented by the ring opening of the epoxide in such scaffolds and various attempts in this direction have been discussed in detail in Chapter 3 (Section 3.4.1 and 3.4.3.1)

stabilized radical and in turn would enable the functionalization at this relatively hindered position. Note, so far, we have been able to show C-3 functionalization via limited epoxide ring opening reactions on the tandem aza-Payne/hydroamination product.[43]

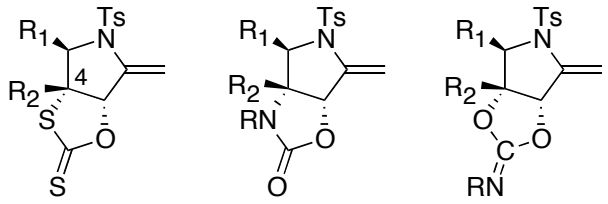


**6.38** **6.39** **6.40**

**Scheme 6.20** Potential exploitable latent nucleophiles.

Use of isocyanates (RNCO) as latent nucleophiles would be another appealing choice; this azacarbonate intermediate could potentially lead to either carbamate **6.39** or carbonate **6.40** (Scheme 6.21). Choice of R group would be important to tune the path of the reaction to the desired product. Product **6.39** would be of higher synthetic interest, since it establishes C-N bond at C-4 position. Another choice to ensure C-N bond formation would be to employ a latent nucleophile such as DCC (dicyclohexylcarbodiimide). Thus an extensive investigation of such latent nucleophiles would allow formation of pyrrolidine scaffolds embellished with functionalities of varying nature.

[43] Refer to Chapter 4 (Section 4.6.3) for a detailed discussion on such transformations.

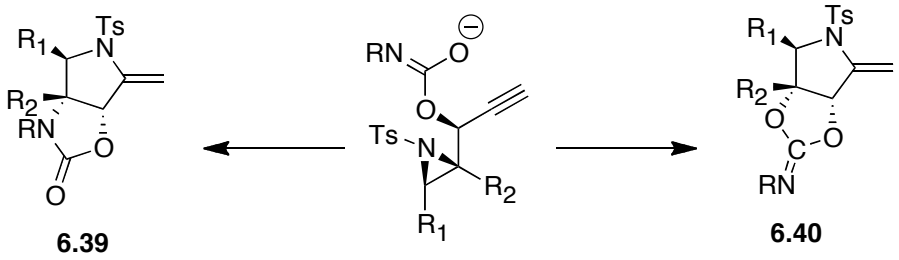


**Scheme 6.21** Potential products via intramolecular aziridine ring opening via azacarbonate intermediate.

## 6.7 Experimental procedures.

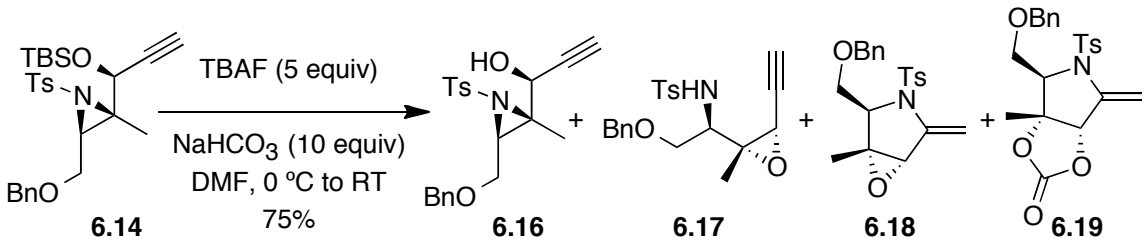


**Procedure for modified aza-Payne/hydroamination using $NaHCO_3$ as source of $CO_2$** (Table 7.1, entry 1). To a solution of aziridinol **6.14**[44] (0.18 g, 0.46 mmol) in anhydrous DMF (6 mL) maintained at 0 ºC, was drop wise added 1.0 M solution of TBAF in THF (2.3 mL, 2.3 mmol) under nitrogen. The reaction was allowed to stir while gradually warming it to room temperature over 20 min. After 2 h when starting material was completely consumed as analyzed by TLC, the reaction was quenched by addition of water (2 mL). The aqueous phase was extracted with EtOAc (3 X 10 mL). The organics were dried over anhydrous sodium sulfate and the solvent was removed under reduced pressure. The crude compound was purified by column chromatography (4:1 Hex:EtOAc) to yield a mixture of desilylated aziridinol **6.16**,[45] epoxy amine **6.17**,[24] *N*-Ts enamide **6.18**[b] and *N*-Ts enamide carbonate **6.19** as an oil with overall 75% yield. Spectral data for **6.19**: $^1$H-NMR (500 MHz, $CDCl_3$) $\delta$ 7.68 (d, 2H, J = 8.5 Hz), 7.33 – 7.24 (m, 7 H), 5.48 (dd, 1H, J = 1.9, 1.3 Hz), 4.82 (dd, 1H, J = 1.2, 0.96 Hz), 4.72 (m,

[44] Synthetic procedure for compound **6.14** has been discussed in Chapter 3 (Section 3.5).

[45] Refer to Chapter 1 (Experimental procedure) for compound **6.16**.

1H), 4.59 (d, 1H, J = 11.7 Hz), 4.46 (d, 1H, J = 11.7 Hz), 4.38 (t, 1H, J = 2.2 Hz), 3.86 (dd, 1H, J = 10.7, 2.8 Hz), 3.78 (dd, 1H, J = 10.6, 1.8 Hz), 2.39 (s, 3H), 1.52 (s, 3H); $^{13}$C-NMR (125 MHz, $CDCl_3$) δ 152.0, 145.1, 141.4, 137.1, 134.3, 129.8, 128.5, 128.0, 127.6, 127.1, 98.5, 87.7, 85.4, 74.1, 70.4, 68.8, 60.3, 22.6, 21.6, 21.0, 18.3, 14.2; IR (neat) 2960, 2874, 1812, 1671, 1470, 1164, 1043, 884; HRMS (ESI) (m/z): $[M+H]^+$ calculated for $[C_{22}H_{24}NO_6S]^+$ 430.1324, found 430.1329.

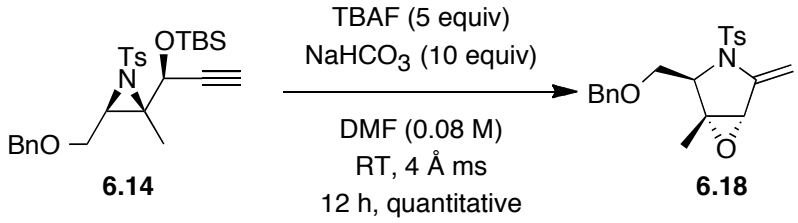


**Preparation of *N*-Ts enamide epoxide 6.18 under modified conditions** (Table 7.1, entry 4)**.** A 1.0 M solution of TBAF in THF (1 mL) was stirred over activated 4 Å ms (250 mg) under nitrogen for 2 h.[25] This dried reagent (0.5 mL, 0.5 mmol) was then added drop wise to the solution of aziridinol **6.14** (50 mg, 0.1 mmol) in DMF (1.3 mL) stirred over activated powdered 4 Å ms (25 mg) under nitrogen at room temperature. The reaction was allowed to stir for 12 h (no more starting material was observed at this point, as analyzed by TLC). Reaction was quenched by the addition of water (2 mL). The aqueous phase was extracted with EtOAc (3 X 6 mL). The organics were dried over anhydrous sodium sulfate. The solvent was removed under reduced pressure to yield the crude product in quantitative amount of the enamide epoxide compound **6.18**[22]

(analyzed by crude NMR spectra).[46] Spectral data for **6.18**: Spectral data: $^{1}$H-NMR (500 MHz, $CDCl_3$) δ 7.70 (d, 2H, *J* = 8.2 Hz), 7.38 - 7.29 (m, 8H), 5.48 (s, 1H), 4.85 (s, 1H), 4.67 (d, 1H, *J* = 12.1 Hz), 4.59 (d, 1H, *J* = 12.1 Hz), 4.07 (m, 1H), 3.89 (m, 1H), 3.48 (m, 1H), 2.42 (s, 3H), 1.49 (s, 3H); $^{13}$C-NMR (125 MHz, $CDCl_3$) δ 143.9, 142.5, 137.8, 134.4, 129.2, 128.3, 127.6, 127.5, 98.8, 73.7, 70.6, 65.3, 62.5, 62.2, 21.5, 14.2.

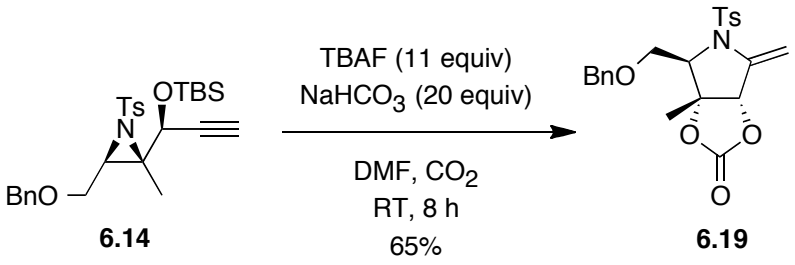


**Preparation of *N*-Ts enamide carbonate product 6.19** (Table 7.1, entry 10)**.** Dry ice was placed in an Erlenmeyer flask at room temperature and the generated $CO_2$ gas was bubbled into the solution of aziridinol **6.14** (13 mg, 0.03 mmol) in anhydrous DMF (0.33 mL) via a drierite-containing tube. The reaction solution was cooled to 0 °C and a 1.0 M solution of TBAF (0.13 mL, 0.13 mmol) was added drop wise to the above solution. After stirring for 3 h, TLC analysis revealed incomplete conversion. At this point extra 1.0 M solution of TBAF in THF (0.15 mL, 0.15 mmol) was added to the reaction mixture. The reaction was allowed to stir for 2 h. The reaction was quenched by addition of water (1 mL). The aqueous layer was extracted with EtOAc (3 X 2 mL). The collected organics were dried over anhydrous sodium sulfate. The organic solvent

[46] The product was obtained along with some contamination with tetrabutyl ammonium salt. The NMR spectra were found completely identical with that of the previously synthesized and reported compound.

was subjected to rotary evaporation to provide carbonate compound **6.19** as a single product as an oil (quantitative by crude NMR). Spectral data for **6.19**: $^{1}$H-NMR (500 MHz, $CDCl_3$) $\delta$ 7.68 (d, 2H, J = 7.9 Hz), 7.33 – 7.26 (m, 7H), 5.48 (dd, 1H, J = 1.9, 1.5 Hz), 4.82 (m, 1H), 4.72 (m, 1H), 4.59 (d, 1H, J = 12.0 Hz), 4.46 (d, 1H, J = 12.0 Hz), 4.38 (m, 1H), 3.86 (dd, 1H, J = 10.7, 2.6 Hz), 3.78 (dd, 1H, J = 10.7, 1.7 Hz), 2.39 (s, 3H), 1.52 (s, 3H); $^{13}$C-NMR (125 MHz, $CDCl_3$) $\delta$ 171.1, 152.0, 145.1, 141.1, 137.1, 134.3, 129.8, 128.5, 128.0, 127.6, 127.1, 98.5, 87.7, 85.4, 74.1, 70.4, 68.8, 60.3, 31.5, 22.6, 21.6, 21.0, 18.3, 14.2; IR (neat) 2960, 2874, 1812, 1671, 1470, 1164, 1043, 884; HRMS (ESI) (m/z): $[M+H]^+$ calculated for $[C_{22}H_{24}NO_6S]^+$ 430.1324, found 430.1329.

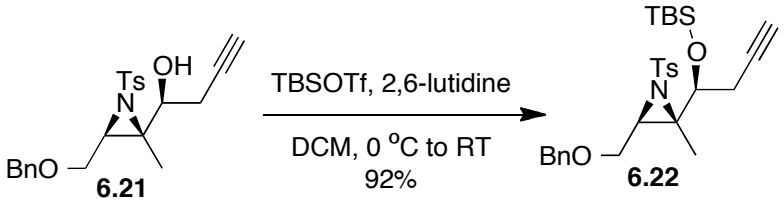


**Preparation of TBS ether 6.22.** Aziridine alcohol **6.21**[23] (100 mg, 0.25 mmol) was placed in anhydrous DCM (2.5 mL) and the solution was cooled down to 0 ºC. TBSOTf (99.1 mg, 0.38 mmol) and 2,6-lutidine (60 μL, 0.50 mmol) were added to the above solution at 0 ºC. The reaction was allowed to stir at room temperature for 2.5 h. TLC analysis revealed incomplete conversion at this point. Extra TBSOTf (0.03 mL, 0.13 mmol) was added. Reaction was found complete after stirring for another 2 h and quenched with sat. $NaHCO_3$ (2 mL). The aqueous phase was extracted with DCM (3 X 10 mL). The organics were dried over anhydrous sodium sulfate and the solvent was

removed via rotary evaporation to yield TBS ether **6.22** (118 mg, 92%) as a colorless oil, which was taken to next step without purification. Spectral data for **6.22**: $^{1}$H-NMR (500 MHz, $CDCl_3$) δ 7.82 (d, 2H, J = 8.4 Hz), 7.25 (m, 3H), 7.16 (d, 2H, J = 8.4 Hz), 7.09 (d, 2H, J = 7.7 Hz), 4.34 (dd, 1H, J = 8.9, 5.6 Hz), 4.30 (s, 2H), 3.72 (dd, 1H, J = 10.8, 3.8 Hz), 3.45 (m, 1H), 3.19 (dd, 1H, J = 7.8, 3.8 Hz), 2.49 (ddd, 1H, J = 17.0, 5.5, 2.8 Hz), 2.39 (ddd, 1H, J = 16.7, 8.5, 2.6 Hz), 2.33 (s, 3H), 1.95 (m, 1H), 1.41 (s, 3H), 0.89 (s, 9H), 0.18 (s, 3H), 0.10 (s, 3H); $^{13}$C-NMR (125 MHz, $CDCl_3$) δ 143.5, 138.1, 137.9, 129.1, 128.2, 127.6, 127.5, 127.3, 80.1, 72.8, 72.7, 71.3, 66.7, 60.3, 57.5, 48.8, 26.1, 25.9, 21.5, 18.1, 14.1, 12.0, -4.3, -4.5.

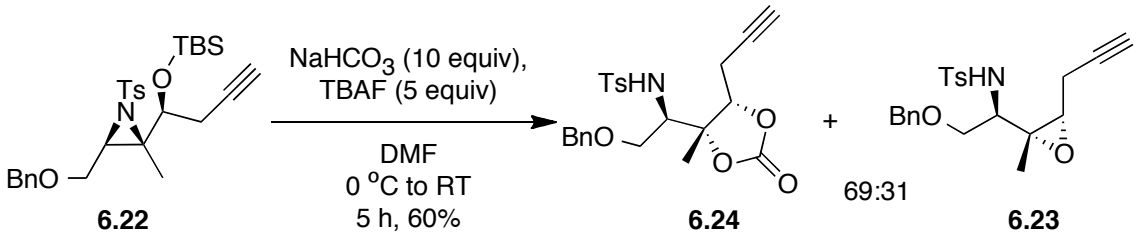


**6.22** **6.24** **6.23**

**Preparation of carbonate amine 6.24 and epoxy amine 6.23.** To a solution of aziridinol **6.22** (0.11 g, 0.21 mmol) in anhydrous DMF (3 mL) maintained at 0 ºC, was drop wise added 1.0 M solution of TBAF in THF (1.1 mL, 1.07 mmol) under nitrogen. The reaction was allowed to stir while gradually warming it to room temperature over 20 min. After 5 h when starting material was completely consumed as analyzed by TLC, the reaction was quenched by addition of water (5 mL). The aqueous phase was extracted with EtOAc (3 X 15 mL). The organics were dried over anhydrous sodium sulfate and the solvent was removed under reduced pressure. The crude compound

was purified by column chromatography (4:1 Hex:EtOAc) to yield a 69:31 mixture of carbonate amine **6.24** (65 mg, 68%), epoxy amine **6.23** (37 mg, 43%), respectively, as an oil. Spectral data for **6.24**: $^{1}$H-NMR (500 MHz, $CDCl_3$) $\delta$ 7.73 (d, 2H, J = 8.3 Hz), 7.32 – 7.29 (m, 5H), 7.11 (d, 1H, J = 7.5 Hz), 7.10 (d, 1H, J = 7.5 Hz), 5.17 (d, 1H, J = 11.0 Hz), 4.42 (t, 1H, J = 5.0 Hz), 4.17 (d, 1H, J = 11.0 Hz), 4.07 (m, 1H), 3.97 (d, 1H, J = 11.0 Hz), 3.55 (dd, 1H, J = 10.1, 1.5 Hz), 3.12 (ddd, 1H, J = 17.7, 4.7, 2.7 Hz), 2.89 (ddd, 1H, J = 17.5, 5.1, 2.8 Hz), 2.80 (dd, 1H, J = 10.3, 4.6 Hz), 2.44 (s, 3H), 1.55 (s, 3H); $^{13}$C-NMR (125 MHz, $CDCl_3$) $\delta$ 171.1, 152.9, 144.4, 137.2, 136.6, 130.0, 128.6, 128.2, 127.8, 127.1, 84.8, 82.7, 77.3, 73.5, 72.7, 66.3, 60.4, 52.8, 22.2, 21.6, 19.9, 14.2; IR (neat) 3285, 2958, 2923, 1807, 1453, 1340, 1163, 1089, 1037, 817; HRMS (ESI) (m/z): $[M+H]^+$ calculated for $[C_{23}H_{26}NO_6S]^+$ 444.1481, found 444.1486. Spectral data for **6.23**:[23] $^{1}$H-NMR (500 MHz, $CDCl_3$) $\delta$ 7.67 (d, 2H, J = 8.4 Hz), 7.34 – 7.30 (m, 3H), 7.23 (d, 2H, J = 8.2 Hz), 7.18 (d, 1H, J = 8.0), 7.17 (d, 1H, J = 8.1 Hz), 5.14 (d, 1H, J = 6.3 Hz), 4.37 (d, 1H, J = 11.7 Hz), 4.28 (d, 1H, J = 11.7 Hz), 3.59 (dd, 1H, J = 9.7, 4.9 Hz), 3.30 (dd, 1H, J = 9.6, 4.7 Hz), 3.09 (m, 1H), 2.98 (dd, 1H, J = 7.6, 4.0 Hz), 2.76 (ddd, 1H, J = 17.6, 4.1, 2.6 Hz), 2.40 (s, 3H), 2.27 (ddd, 1H, J = 17.5, 7.6, 2.6 Hz), 2.03 (t, 1H, J = 2.6 Hz), 1.34 (s, 3H); HRMS (ESI) (m/z): $[M+H]^+$ calculated for $[C_{22}H_{26}NO_4S]^+$ 400.1583 found 400.1582.

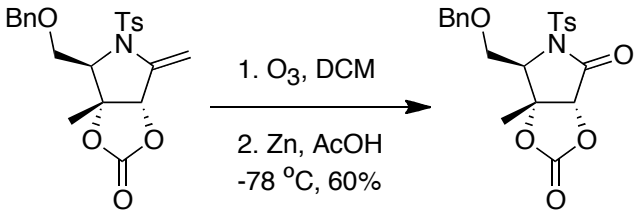


**6.19** **6.36**

**Preparation of carbonate lactam 6.36.** To a solution of *N*-Ts enamide **6.19** (24 mg, 0.06 mmol) in DCM (1 mL) maintained at -78 °C was passed ozone till the color of the reaction turned blue. Nitrogen gas was bubbled through the solution to get rid of excess ozone gas. At this point the reaction turned colorless. Zinc dust (5 mg, 0.07 mmol) and a few drops of acetic acid were added. The reaction was allowed to stir for 5 h while gradually warming to room temperature. The aqueous phase was diluted with water (1 mL) and extracted with DCM (3 X 5 mL). The organic phase was dried over anhydrous sodium sulfate and was later subjected to rotary evaporation to yield lactam **6.36** (15 mg, 60%) as an oil. Spectral data for **6.36**: $^{1}$H-NMR (500 MHz, $CDCl_3$) $\delta$ 7.91 (d, 2H, J = 8.4 Hz), 7.32 (m, 5H), 7.11 (m, 2H), 5.27 (s, 1H), 4.58 (s, 2H), 4.43 (d, 1H, J = 11.6 Hz), 4.34 (d, 1H, J = 11.6 Hz), 3.94 (dd, 1H, J = 10.9, 2.0 Hz), 3.74 (d, 1H, J = 11.0 Hz), 2.41 (s, 3H), 1.58 (s, 3H); $^{13}$C-NMR (125 MHz, $CDCl_3$) $\delta$ 164.8, 151.5, 146.3, 136.1, 134.2, 129.9, 128.7, 128.4, 127.9, 85.1, 80.1, 74.3, 67.2, 64.7, 21.7, 18.2; IR (neat) 2922, 1736, 1717, 1652, 1558, 1171, 1091.

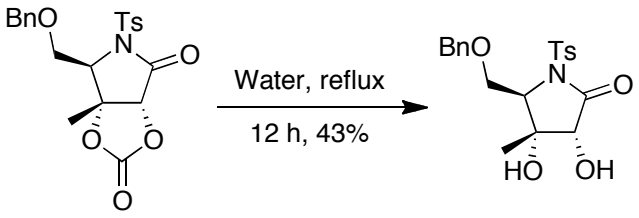


**6.19** **6.37**

**Preparation of 3,4-dihydroxy lactam 6.37.** Carbonate lactam **6.19** (12 mg, 0.03 mmol) was dissolved in water (1 mL). The solution was allowed to reflux for 12 h till no more starting material was observed as analyzed by TLC. Upon completion the reaction was cooled and extracted with $CHCl_3$ (3 X 5 mL) to yield crude 3,4-dihydroxy compound **6.36** (5 mg, 43%) as an oil as the only product. Spectral data for **6.36**: $^1$H-NMR (500 MHz, $CDCl_3$) $\delta$ 7.89 (d, 2H, J = 8.8 Hz), 7.30 – 7.14 (m, 8H), 4.49 (d, 1H, J = 11.2 Hz), 4.40 (d, 1H, J = 11.0 Hz), 4.30 (m, 1H), 4.15 (m, 1H), 3.98 (dd, 1H, J = 11.5, 3.1 Hz), 3.74 (d, 1H, J = 11.2 Hz), 2.38 (s, 3H), 1.37 (s, 3H); $^{13}$C-NMR (125 MHz, $CDCl_3$) $\delta$ 173.1, 145.3, 137.0, 135.1, 129.5, 128.5, 128.2, 128.0, 127.8, 75.5, 74.8, 74.0, 68.4, 67.8, 21.7, 20.5; IR (neat) 3477, 2924, 1740, 1597, 1360, 1171, 1104, 815; HRMS (ESI) (m/z): $[M+H]^+$ calculated for $[C_{20}H_{24}NO_6S]^+$ 406.1324, found 406.1322.

# REFERENCES

## REFERENCES


1. Asano, N.; Nash, R. J.; Molyneux, R. J.; Fleet, G. W. J. *Tetrahedron: Asymmetry,* **2000**, *11*, 1645-1680.

2. Rhinehart, B. L.; Robinson, K. M.; Liu, P. S.; Payne, A. J.; Wheatley, M. E.; Wagner, S. R. *J. Pharmacol. Exp. Ther.,* **1987**, *241*, 915-920.

3. Kite, G. C.; Horn, J. M.; Romeo, J. T.; Fellows, L. E.; Leest, D. C.; Scofield, A. M.; Smith, N. G. *Phytochemistry,* **1990**, *29*, 103-105.

4. Stegelmeier, B. L.; Molyneux, R. J.; Elbein, A. D.; James, L. F. *Veterinary Pathology Online,* **1995**, *32*, 289-298.

5. Fuhrmann, U.; Bause, E.; Legler, G.; Ploegh, H. *Nature,* **1984**, *307*, 755-758.

6. Nash, R. J.; Fellows, L. E.; Dring, J. V.; Fleet, G. W. J.; Derome, A. E.; Hamor, T. A.; Scofield, A. M.; Watkin, D. J. *Tetrahedron Lett.,* **1988**, *29*, 2487-2490.

7. Simmonds, M. S. J.; Blaney, W. M.; Fellows, L. E. *J. Chem. Ecol.,* **1990**, *16*, 3167-3196.

8. Scofield, A. M.; Rossiter, J. T.; Witham, P.; Kite, G. C.; Nash, R. J.; Fellows, L. E. *Phytochemistry,* **1990**, *29*, 107-109.

9. Fleet, G. W. J.; Haraldsson, M.; Nash, R. J.; Fellows, L. E. *Tetrahedron Lett.,* **1988**, *29*, 5441-5444.

10. Ikegami, S.; Uchiyama, H.; Hayama, T.; Katsuki, T.; Yamaguchi, M. *Tetrahedron,* **1988**, *44*, 5333-5342.

11. Lee, R. E.; Smith, M. D.; Pickering, L.; Fleet, G. W. J. *Tetrahedron Lett.,* **1999**, *40*, 8689-8692.

12. Singh, S.; Han, H. *Tetrahedron Lett.,* **2004**, *45*, 6349-6352.

13. Donohoe, T. J.; Thomas, R. E.; Cheeseman, M. D.; Rigby, C. L.; Bhalay, G.; Linney, I. D. *Org. Lett.,* **2008**, *10*, 3615-3618.

14. Takahashi, M.; Maehara, T.; Sengoku, T.; Fujita, N.; Takabe, K.; Yoda, H. *Tetrahedron,* **2008**, *64*, 5254-5261.

15. Chikkanna, D.; Singh, O. V.; Kong, S. B.; Han, H. *Tetrahedron Lett.,* **2005**, *46*, 8865-8868.

16. Tang, M. Y.; Pyne, S. G. *Tetrahedron,* **2004**, *60*, 5759-5767.

17. Yoda, H.; Katoh, H.; Takabe, K. *Tetrahedron Lett.,* **2000**, *41*, 7661-7665.

18. Pearson, W. H.; Hines, J. V. *J. Org. Chem.,* **2000**, *65*, 5785-5793.

19. Ikota, N.; Nakagawa, H.; Ohno, S.; Noguchi, K.; Okuyama, K. *Tetrahedron,* **1998**, *54*, 8985-8998.

20. Tian, Y. S.; Joo, J. E.; Kong, B. S.; Pham, V. T.; Lee, K. Y.; Ham, W. H. *J. Org. Chem.,* **2009**, *74*, 3962-3965.

21. Alam, M. A.; Kumar, A.; Vankar, Y. D. *Eur. J. Org. Chem.,* **2008**, 4972-4980.

22. Schomaker, J. M.; Geiser, A. R.; Huang, R.; Borhan, B. *J. Am. Chem. Soc.,* **2007**, *129*, 3794-3795.

23. Hart, S. Ph.D., Michigan State University, 2009.

24. Schomaker, J. M.; Bhattacharjee, S.; Yan, J.; Borhan, B. *J. Am. Chem. Soc.,* **2007**, *129*, 1996-2003.

25. Westmanu, E.; Stromberg, R. *Nucleic Acids Res.,* **1994**, *22*, 2430-2431.